The Getty Conservation Institute

Color Science in the Examination of Museum Objects

Nondestructive Procedures

TOOLS FOR CONSERVATION

Ruth Johnston-Feller

Tools for Conservation

Color Science in the Examination of Museum Objects

Nondestructive Procedures

Ruth Johnston-Feller

The Getty Conservation Institute Los Angeles

Tevvy Ball: *Project Editor*
Elizabeth Maggio: *Copy Editor*
Anita Keys: *Production Coordinator*
Hespenheide Design: *Designer*

Printed in the United States of America
10 9 8 7 6 5 4 3 2 1

The Getty Conservation Institute works internationally to advance conservation in the visual arts. The Institute serves the conservation community through scientific research, education and training, model field projects, and the dissemination of information. The Institute is a program of the J. Paul Getty Trust, an international cultural and philanthropic institution devoted to the visual arts and the humanities.

The Institute's Tools for Conservation series provides practical scientific procedures and methodologies for the practice of conservation. The series is specifically directed to conservation scientists, conservators, and technical experts in related fields. Previously published in the series are *Infrared Spectroscopy in Conservation Science* (1999) by Michele R. Derrick, Dusan Stulik, and James M. Landry, and *Thin-Layer Chromatography for Binding Media Analysis* (1996) by Mary F. Striegel and Jo Hill.

"The Colors Live," from *Hailstones and Halibut Bones,* by Mary O'Neill and Leonard Weisgard, Ill. Copyright ©1961 by Mary LeDuc O'Neill. Used by permission of Doubleday, a division of Random House, Inc.

Library of Congress Cataloging-in-Publication Data
Johnston-Feller, Ruth, 1923–2000.
Color science in the examination of museum objects : nondestructive procedures / Ruth Johnston-Feller
p. cm.—(Tools for conservation)
Includes bibliographical references and index.
ISBN 0-89236-586-2
1. Art—Conservation and restoration. 2. Spectrophotometry.
3. Colorimetry. 4. Pigments. 5. Color in art. I. Title. II. Series.
N8560.J64 2001
702'.8'7—dc21 2001-031449
CIP

The colors live
Between black and white
In a land that we
Know best by sight.
But knowing best
Isn't everything,
For colors dance
And colors sing,
And colors laugh
And colors cry—
Turn off the light
And colors die.

—Mary O'Neill, "The Colors Live"

Contents

This page intentionally left blank

Foreword

One of the principal objectives of the Getty Conservation Institute is to advance the application of scientific principles and methods in the study and care of museum collections. This book has been prepared to assist conservators and color scientists in the measurement, description, and investigation of the color and appearance of works of art. We are pleased that, over the decade of her semiretirement, Ruth Johnston-Feller undertook this project, which she was able to bring to completion in spite of her steadily declining health. We deeply regret that she did not live to see the present volume into print.

Fortunate is the individual who finds satisfaction in the work that each day brings. The joy that conservators experience in their chosen profession informs the myriad tasks that they perform in caring for the irreplaceable materials in their charge. Ruth Johnston-Feller, a scientist trained in chemistry, enjoyed the world of color with similar passion. She also enjoyed the privilege of being present at the beginning of a new and growing field—the field of color instrumentation and color science. Over the years she taught numerous courses and generously shared her experience and expertise, serving as a mentor for many colleagues and students. In this monograph, she looked forward to the opportunity to make accessible a body of knowledge gained over the course of a lifetime.

During the years of preparation of this book, several authoritative texts on color science have appeared, including Anni Berger-Shunn's *Practical Color Measurement* (1994) and a classic work that has recently appeared in a third edition under the title *Billmeyer and Saltzman's Principles of Color Technology*, ably revised and updated by Roy S. Berns (2000). Each of these volumes, as well as the present monograph, emphasizes somewhat different facets of color science application. However, these distinguished authors, who worked together on a number of projects, all emphasize the overriding importance of the fundamental principles of color measurement and appearance.

Today technology rushes ahead at an ever-accelerating pace. The cumbersome Leres spectrophotometer that was used to record many of the spectrophotometric curves in this book, for example, has been replaced by a variety of handheld devices that rapidly yield sets of numbers representing both colorimetric and color-difference values. Instead of unquestioningly accepting the numbers thus obtained, however, these authors recommend that conservators make every effort to understand the principles behind such data. Indeed, as this monograph demonstrates, a solid grasp of the principles of colorimetry and spectrophotometry provides a powerful tool for conservators and conservation scientists to better understand a wide range of color-related problems, such as the characterization and identification of pigments; changes in the gloss, color, and translucency of paints; and the discoloration of binding media that can occur with age. No other book on color science and measurement, in fact, focuses as directly as the present volume on issues pertinent to the conservator. There are sections that will be useful for the analysis and treatment of traditional materials as well as of materials used in contemporary art. Other topics covered include the color measurement of fluorescent materials, the effects of whitening agents, and the weak fluorescence of binder resins. The book also treats subjects not commonly found in the conservation literature, including the color of metals and of pearlescent, iridescent, and metallic flake pigments.

We hope that this volume will assume a place among the standard references in the conservation field. Ruth Johnston-Feller's lifelong enthusiasm for her work and her many insights into color science constitute a distinguished legacy, one that the Getty Conservation Institute is privileged to place on record.

Timothy P. Whalen
Director
The Getty Conservation Institute

Preface

Many fine books have been written about the science of color, about the origin of color, about the techniques of its measurement and description, about the interrelationship of color with other aspects of appearance, and about sensation and perception. Some of these books are listed as recommended reading in appendix E, and the reader is urged to consult them. However, few books have been written that describe the application of color science to the solution of practical problems. It is the purpose of this book to present some examples illustrating how the basic principles of color science can contribute to an understanding of the color and appearance of materials. Emphasis is placed on nondestructive analytical methods based on measurement and computation, and on how the resultant information can be interpreted.

My experience in industrial applications necessarily forms the basis for many of the discussions presented. I was employed by a number of corporations with diverse interests in color science, and this experience provided me with a varied background of knowledge. These corporations included the Coatings and Resins Division of PPG Industries, manufacturer of paints and plastics; the Macbeth Division of Kollmorgen Corporation, manufacturer of color-measuring instruments and originator of computer software for color matching; and the Pigments Division of Ciba-Geigy Corporation (now the Colors Division of Ciba Specialty Chemicals), manufacturer of pigments. Many of the examples presented in this volume had their origins in my experience with one or more of these employers. I wish to express my thanks to these corporations for their permission to use their equipment in my spare time, to work with Robert Feller on a number of challenging conservation-science problems.

Because of this industrial background, many of my examples as well as the materials I describe are taken from problems encountered while performing day-to-day work. However, my introduction to conservation-science problems provided an additional opportunity to look at color science and its potential applications from a different point of view. Beginning in 1975, I have worked on a consulting basis in conservation science with Robert Feller at the Research Center on the Materials of the Artist and Conservator, Carnegie Mellon Research Institute, Carnegie Mellon University. Throughout my years of interest in the problems of conservation, I have encountered many diverse applications for color science, some of which are described here.

In the pages that follow, emphasis is placed on the appropriate use of spectrophotometry, which is the analytical tool for defining the characteristics of color, and on the complementary use of colorimetry, which is the numerical, three-dimensional specification of the visual stimulus for the sensation of color. The examples presented are interpreted in terms that utilize information from both types of approaches, emphasizing the complementary values of these two types of study.

The successful use of the methods described here depends on the knowledge and skill of the persons using the instruments and interpreting the measurements. All of the important aspects of good analytical science techniques are as basic to the application of color science as to any other analytical procedure. At the very heart of all reliable analytical work are proper instrument calibration; a thorough knowledge of instrument limitations; multiple samplings and measurements to provide for statistically reliable results; recognition of the effect of sample characteristics on the method of analysis; and the need for reference information. A plea is made here for the start of an ongoing program to build an atlas of the spectral curves of colorants, both pigments and dyes. The need is not only for colorants used in the past but also for those currently used; such data would be of inestimable value for the future.

Because my experience has been most extensive in studying pigmented systems, the reader will find that most of the examples presented are for those materials. However, many of the principles described apply equally to dyed materials.

The list of references for this monograph is not as comprehensive as it could be. I wish to apologize to the many authors of valuable articles not specifically mentioned. However, many excellent supplementary articles can be found in the references cited throughout and in the recommended reading in appendix E. Hopefully, some older and very valuable references to the basic work done many years ago will be consulted by interested readers. We must never forget that we all stand on the shoulders of the giants who came before us.

Ruth Johnston-Feller

Acknowledgments

This project was undertaken with the help and support of the Getty Conservation Institute. Frank Preusser, former associate director of programs, arranged for the task to be undertaken; James R. Druzik gave advice and encouragement throughout; and Eric Hansen made many helpful comments.

The Center on the Materials of the Artist and Conservator at the Carnegie Mellon Research Institute, headed by Paul Whitmore, spent a large amount of time and effort on carrying out measurements and calculations. The author appreciates the interest and help provided by Paul Whitmore and his staff. Thanks are expressed to John Bogaard for helping with references to the literature on the color of paper and on TAPPI testing methods. Catherine Bailie is especially thanked for her laboratory work, much of which is represented here; for her organization of the vast collection of measurements, calculations, and spectral curves; and for her liaison with the Photo and Graphic Services of Carnegie Mellon University. Gary Thomas, head of Photo and Graphic Services, and Kelly Young, who reproduced the spectrophotometric curves to a common scale and produced the diagrams, played a most significant role in creating the illustrations so necessary in explaining the text. Thanks are also given to Lynn Labun, librarian at the Carnegie Mellon Research Institute, and to her staff for their assistance in locating many of the articles and patents referenced in this monograph.

The help of Hugh Davidson of Davidson Colleagues in supplying many of the computer programs, as well as in giving helpful suggestions, is especially appreciated.

The valued criticisms, comments, and suggestions made by Fred W. Billmeyer Jr. are acknowledged and greatly appreciated.

Many thanks are expressed to Max Saltzman for his interest, help, and encouragement. And to Dennis Osmer, of Ciba Vision Corporation, the author wishes to express her thanks for his continuing interest and many helpful discussions.

The author would also like to acknowledge the help of Leon Greenstein in preparing the section on pearlescence and iridescence.

The author is grateful to the many copyright holders for their kind permission to utilize and reproduce graphs and drawings that were considered especially useful in illustrating particular ideas in the text.

To Sandra Melzer, secretary at the Carnegie Mellon Research Institute, the author expresses her gratitude for her continued help in typing, correcting, and organizing the many drafts, all of which was done with great skill, speed, and patience.

Most of all, the author wishes to acknowledge the continuing interest and help of her husband, Robert L. Feller, with whom she has worked on, discussed, and studied much of the material presented. His aid in the organization and logistics, and his continuing support, have been invaluable.

In the end, it is the editorial and design work of Getty Trust Publications that, in cooperation with the author, has produced the present volume.

Introduction

Care of the art and artifacts produced by civilizations past and present is a responsibility owed to posterity—to our children, to their children, to their children's children. To carry out this trust, every effort must be made to preserve cultural materials with the best possible knowledge and skill. To a great extent, their proper care depends on identification of the materials used in their creation. Of the many analytical techniques that can be employed for colorant identification, those that do not require the taking of samples should be used first. One such noninvasive technique is *spectrophotometry,* which measures the amount of light reflected or transmitted by a material at individual wavelengths of the spectrum. A graph of the relative percent of electromagnetic power reflected or transmitted at each wavelength is called a *spectrophotometric curve* or simply a *spectral curve.* The shapes of such curves are often unique for various colorants—pigments or dyes—and thus can be helpful in identifying the colorants present in the object. The discussion in these pages is limited to the spectral curves measured in the visible spectral region. These are the curves responsible for the color we see. Although positive identification may not always be possible with spectral curves, information concerning what is *not* present can also be of considerable value.

We do not see spectral curves, however. Our eyes are not analytical instruments—they are integrative. We *hear* analytically, that is, we hear the single frequencies (or wavelengths) of sounds in chords and as harmonies. On the other hand, we do not see individual wavelengths (or frequencies) of light, only their summation. (Frequency of radiant power is the inverse of the wavelength, so the two terms are inexorably related.) This integration, or summation, of radiant power over all wavelengths of visible radiation results in a single color response: blue or green, light or dark, brilliant or dull.

There are many factors, in addition to the pigments and dyes present, that affect our perception of an object's color. It is first of all affected by the light source—a red object looks black in green light, for example, because all of the incident green light is absorbed. Moreover, each observer may see colors somewhat differently because humans differ in their responses to wavelength, and people with the condition popularly referred to as color blindness may vary radically in their responses from those with so-called normal color vision. The science of *colorimetry* includes the wavelength intensities of a number of standard illuminants—

selected by the Commission Internationale de l'Eclairage, or the International Commission on Illumination (CIE)—and the wavelength sensitivities of two average observers. One standard observer represents distance viewing, and one represents arm's-length viewing. By suitable measurement of the reflectance of an object (or transmittance of a transparent material) followed by calculations incorporating the data for one of the CIE standard illuminants and a standard observer, three figures can be obtained that can be used to describe any color. This science of colorimetry, under the aegis of the CIE, is accepted worldwide. The CIE system provides a standard procedure for describing a color stimulus in terms of defined illuminants and a defined standard observer.

The sensation of color is complex. Perception of a scene involves many variables. Considered analytically, color sensation incorporates not just the factors of object coloration but also surface gloss or matteness, illuminant directionality or diffuseness (which affects our evaluation of surface characteristics), and size and shape. Perceptually, viewing a complex scene further depends on other factors difficult to characterize, such as the contrast between neighboring colors and the adaptation of the eye to the total surroundings. These factors make it difficult to match any single color in a complex composition on the basis of our visual impression. It is physical measurement, made under defined geometrical conditions, that can provide an unambiguous description of an object's reflectance or transmittance. This objective measurement, by its revealing wavelength characteristics, can aid in the identification of the colorants involved.

It is therefore necessary that the study of colored objects utilize both the analytical approach of spectral analysis and the colorimetric data obtainable by use of the methods described by the CIE. Both approaches are used in the descriptions and applications of color science discussed in this monograph.

Spectrophotometry in the visible wavelengths and the science of colorimetry can be useful in many important ways in objective analysis and research. These include monitoring changes in materials following exposure to light or other deleterious conditions; measuring the degree of yellowing of a vehicle, varnish, or substrate; documenting changes in gloss and the resulting effect on color; determining the degree and rate of colorant fading or darkening; and measuring the colors of metals and their change upon exposure. One of the chief purposes of the remarks that follow is to describe how these particular problems can be approached.

Fascinating new pigmentary materials, such as microvoids and vesiculated beads, came into use following World War II. Many of these new materials—fluorescent pigments, metallic pigments, and iridescent pigments—present special spectral measurement problems and are discussed in chapters 5 and 6.

It is not the purpose of this monograph to provide another textbook on color and spectrophotometry. In the initial sections a few basic principles are reviewed so that the reader will be reminded of the fundamentals used in the various applications described in subsequent chapters. The primary emphasis, however, is on the description of methods of approach for studying a variety of problems and materials and on understanding the principles involved so that, even without elaborate equipment, valuable information can be obtained. It is hoped that the guidelines presented will help prevent the occasional misinterpretation of the results of spectrophotometric and colorimetric measurements and the drawing of erroneous conclusions from them. As with any analytical technique, reference materials of defined composition are the first essential; so it is with using spectrophotometric curves. In the discussions that follow, it should become evident that an atlas of curves of known colorants is a necessity.

It is assumed that the reader has some technical background but is not a specialist in color science and its applications. A certain knowledge of basic mathematics is necessary. This monograph has been prepared primarily for museum laboratory personnel. Nonetheless, it is hoped that others also may find some of the ideas, discussions, and applications helpful.

This page intentionally left blank

Chapter 1

Spectrophotometry

The optical instrument used to measure how materials reflect or transmit light is called a spectrophotometer. Such instruments measure the relative amount of electromagnetic power reflected or transmitted at individual wavelengths of the spectrum. When the amount of power reflected or transmitted by a material is scanned across a particular region of the spectrum, a curve may be plotted showing reflection or transmission as a function of wavelength. Such a curve is called a *spectral curve* or a *spectrophotometric curve*. The shape of this measured curve is often specific, providing a type of fingerprint characteristic of the chemical nature of the material. This fingerprinting and objective characterization of colored materials in the visible spectral region is one of the subjects of this monograph.

The unit of wavelength used in the visible region is the *nanometer,* which is equal to 10^{-9} meters and is abbreviated nm. (Older literature used the term *millimicron,* abbreviated mμ, for the same size.) In plotting graphs of reflectance or transmittance versus wavelength, the x (horizontal) axis is the wavelength, often indicated by the symbol λ, and the y (vertical) axis is conventionally the reflectance or transmittance, generally expressed as a percentage on a scale of 0 to 100. The inverse of the wavelength, $1/\lambda$, is the frequency, which is often used in the infrared region. The CIE currently recommends using the term *reflectance factor* for the ratio of the light reflected by a sample relative to that reflected by a reference standard. This is described in Standard E 284 of the American Society for Testing and Materials (ASTM). For convenience, however, the older term *percent reflectance* (or simply *reflectance*) is used throughout this monograph, even though, in modern CIE terms, reflectance factor is being measured. In these pages there is an additional word modifying reflectance: either *diffuse,* meaning "specular reflectance excluded," or *total,* meaning "specular reflectance included." To describe color in CIE terms, diffuse reflectance must be used. To analyze the intensity of the light beam, the total reflectance has to be considered. Illustrations of spectrophotometric reflectance curves for various pigments in glossy paints are presented in appendix A and in chapter 7. They are used frequently as examples throughout this book.

Spectrophotometers

All spectrophotometers consist of three essential parts: (1) a light source, (2) a monochromator to select the individual wavelength, and (3) a photodetector. The light source for visible wavelengths is generally either a tungsten lamp, a tungsten-halogen lamp, or a xenon flash-tube lamp. The monochromator is either a grating or a prism, suitably equipped with a slit mechanism to isolate a narrow band of wavelengths. The detector is a device that is sensitive to radiation in the desired visible spectral region, such as a silicon photodiode or a photomultiplier tube. A photodiode array is often used today. Additional essential parts of a spectrophotometer are arrangements for mounting and illuminating the sample, a reference standard, and a geometric arrangement for selecting or collecting the light that falls on the detector. The measurement made with a spectrophotometer is the ratio of the light reflected, or transmitted, by the sample to that reflected, or transmitted, by a reference standard. This ratio can be described as I/I_0, where I is the light intensity from the sample and I_0 is the intensity from the reference material. It may be recorded by a plotter as a continuous (analog) curve or printed in digital (numerical) form. The advantage of the digital output is that any corrections to the data can be made to correct for instrument calibration deviations or to calculate the measured ratio to a different reference standard. Such corrections are desirable to achieve maximum precision or accuracy. Color-measuring instruments available today are equipped with computers to make such corrections.

Most modern instruments do not measure continuous (analog) curves, such as those illustrated in appendix A and chapter 7. For example, color-measuring instruments produced for industrial color control measure at 10 nm intervals, or even just 20 nm intervals. Such digital instruments are now popularly called spectrophotometers, but they are only "abridged" spectrophotometers, as they were formerly described. Data from such instruments cannot provide a continuous analog curve. Their advantage for use in industry is the speed of measurement. With the use of diode-array detectors, 33 wavelength measurements can be made in a few seconds and entered into a computer for calculations, such as color differences or colorant formulations, which are then printed out. In addition, corrections for instrument deviations in calibration can be calculated before the measurements are utilized. Often, however, the operator does not even see the spectrophotometric data on which the derived calculations were based and thus has no idea of the value of the spectral information being missed. Berger-Schunn (1994) expressed the present author's views: "While the reflectance curves in the early days of color measurement had to be drawn by hand or, when automatically measured, at least had to be looked at for further use, with modern color measurement systems the curves are measured but often neither printed nor recorded. The user today therefore may miss a large amount of information."

Modern instruments that measure the reflectance or transmittance in digital terms but at 2 nm or less wavelength intervals can properly be called spectrophotometers. Graphs made of the percent reflectance or transmittance of such digital data are very similar in curve shape to the older analog continuous curves measured on the best spectrophotometers that were used to record the spectral curve characteristics of many colorants in the post–World War II period until the late 1970s. Many of these valuable curves still exist and should be accumulated in an atlas for future reference.

The characteristics of the sample to be measured will determine the selection of a spectrophotometer's essential components and their most suitable arrangement. The cost and availability of the equipment must also be considered. Throughout the discussions that follow, reference is made to the instrument requirements for various types of samples and to the measurement tasks. Chapter 9 is devoted to a discussion of defining the problem to be solved and selecting the proper instrument to meet its needs. ASTM Standard E 805 presents a concise summary of the features of spectrophotometers, as well as of colorimeters, that need to be considered when making measurements of the color or color difference of materials.

Two basic differences in instrument design should be noted here at the start. The first involves the location of the light source and the monochromator relative to the location of the sample. In some spectrophotometers, light from the source is first passed through the monochromator to isolate narrow wavelength regions. The resulting monochromatic light then illuminates the sample in the sequence: lamp → monochromator → sample → detector. However, if the sample exhibits any fluorescence, the measurements made with this arrangement cannot accurately represent its visual appearance. This is because any emitted fluorescence is registered by the detector at the excitation wavelength rather than at the emission wavelength. (See discussion of fluorescence in chap. 6.)

An arrangement whereby the locations of the sample and the monochromator are interchanged is now more commonly used in color-measuring instruments in the sequence: lamp → sample → monochromator → detector. This arrangement provides measurements agreeing with what a human observer sees. With this interchange of the sample and monochromator positions, the light reflected or transmitted by the sample passes through the monochromator *after* being reflected or transmitted by the sample. The sample is illuminated by the polychromatic light from the source. The spectral distribution of this polychromatic source is critical when measuring fluorescent samples; the power distribution of the excitation wavelengths influences the amount of the fluorescence emitted. When measuring nonfluorescent samples, either arrangement of sample and monochromator is satisfactory.

The second important aspect of spectrophotometer design relates to the geometric arrangement for illuminating the sample and for collecting the reflected light. Reflection at the air–sample interface always occurs because of a change in the refractive index. (Objects would be nearly invisible if this were not true.) On highly polished or very glossy materials, the surface reflection is mirrorlike, that is, light will be reflected at an angle equal and opposite to the incident angle. This type of mirrorlike reflection is called *specular* or *Fresnel* reflection. When surfaces are matte (nonglossy), all of the surface reflection is diffuse—that is, the light is scattered in all directions. Between these two extremes there are all degrees of glossiness or matteness. In dielectric materials (nonmetals), the surface reflection is simply the character of the illuminant. Color is produced from the internal absorption and scattering of the incident light inside the material. Therefore, to describe the color as observed, it is desirable to *exclude* the specular reflection on glossy samples. This is what human observers do; they ignore the very bright highlights. On matte samples, the diffusely reflected surface light with the spectral character of the illuminant is mixed with the internally reflected light so that the observer sees the object color as desaturated or less pure. Metals (nondielectrics), on the other hand, reflect only at the surface. Light does not significantly penetrate into a metal. The color of copper and gold, for example, comes from the surface reflection alone. (See discussion of metal color in chap. 5.)

For collecting reflected light, three basic types of optical design are used in spectrophotometers: (1) bidirectional geometry, generally 0° (perpendicular) illumination, 45° viewing (written as 0°/45°, or the reverse, 45°/0°); (2) integrating sphere geometry with either 0° illumination and diffuse viewing (0°/d) or near-normal incidence, such as 8°, and diffuse viewing (8°/d); and (3) variable angle geometry in which the incident and viewing angles may be changed.

The first type, bidirectional geometry, measures only diffusely reflected light; the specularly reflected light is reflected back into the instrument. Such an instrument is unsuitable for measuring the color of metals and, often, is not designed to measure the transmission of light by transparent materials. Its only purpose is to measure the diffusely reflected light—the color—of dielectric materials.

The second type, integrating sphere geometry, is more versatile. However, if the angle of illumination is normal (perpendicular, or 0°) to the surface of the sample, the specular surface reflection is also excluded and reflected back into the instrument. This type of integrating sphere with its rejection of the specular reflection is inappropriate for measuring the color of metals. In the most commonly used type of integrating sphere geometry, however, the angle of illumination is about 8° off the normal, or perpendicular (0°), so that light reflected specularly at −8° (that is, at 8° but on the opposite side of the perpendicular, as indicated by the minus sign) strikes the integrating sphere wall and is included in the measurement. Such instruments are appropriate for measuring the color of metals and also for making transmission measurements. They are generally equipped to exclude the specular reflection, if desired. For example, at the angle equal and opposite to the incident angle of illumination, a piece of the sphere wall can be removed, and a black port (or light trap) inserted in place of the white port. With the black port in place, the specularly reflected light will be absorbed, and only the diffusely reflected light is recorded (see fig. 6.9b).

Variable angle geometry, the third type of optical design, utilizes variable angles of illumination and view. Such an arrangement is extremely valuable for measuring materials that change color when the viewing angle or the illumination angle is changed. Some materials that exhibit such color changes are those containing metallic flake pigments or iridescent pigments (see chap. 5). Several recent commercial instruments use this design. Two basic types of instruments that measure color as a function of the angles of illumination and view can be distinguished. In one optical arrangement, the reflection is measured as a function of the angles of illumination and view, keeping the wavelength of illumination constant. Such an instrument, a *goniophotometer,* can be called a *spectrogoniophotometer* if provision is made for changing the wavelengths of the incident light across the spectrum (FSCT 1995; ASTM Standard E 284). Reducing the measurements made by such instruments to color terms requires the use of many wavelengths of incident light across the spectrum. A computer, which is an essential part of such instruments, can carry out these calculations for each wavelength of illumination and angle of view. Any variable angle measurement can be invaluable in characterizing the nature of surfaces as well as of internal structures. However, if one is interested primarily in the differences in color as a function of the viewing angle, an instrument that measures the spectrophotometric curves at specified angles of illumination and view is more convenient. Such an instrument is called a *goniospectrophotometer* (FSCT 1995; ASTM Standard E 284).

The instrument referred to throughout this monograph is a goniospectrophotometer, specifically the Trilac manufactured by Leres in France. This is the instrument used for the variable angle measurements described in chapters 5 and 6. The Trilac also has the more common mode of optical arrangement utilizing an integrating sphere for measuring diffuse and total reflectance in the conventional manner. It is no longer manufactured.

In its goniospectrophotometer mode (hereafter referred to as the "gonio mode"), the instrument does not have high resolution; the incident beam is nearly collimated (parallel beam), with about 4° aperture angle. In contrast to a number of more modern gonio instruments, however, the viewing angle is relatively wide, with an aperture angle of about 15°. This angle of view is close to visually subtended angles, with the result that the measured color agrees moderately well with visual observations. In all current commercial gonio instruments, including the Trilac, the angles of illumination and view lie in the same plane, as illustrated in figure 1.1. With gonio measurements, it is easiest to interpret the results if one angle, either that of illumination or view, is kept constant as a reference point. More complicated gonio measurements usually result in large numbers of measurements and are challenging to interpret.

The notation used in this monograph to describe the angles of illumination and view is the following: The angle of illumination is given first, designated as negative if on the side of the perpendicular opposite to the angle of view. This is followed by a slash, and then by

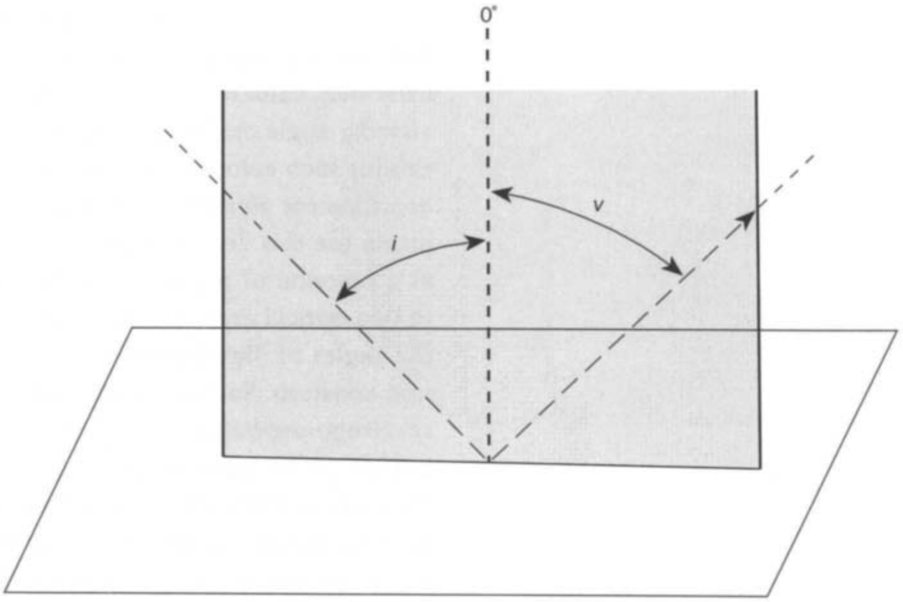

Figure 1.1
The two planes as used in the Trilac goniospectrophotometer. The shaded plane represents the incident and viewing plane, perpendicular and at right angles to the sample plane (in white). The viewing angle (*v*) is positive. The incident angle (*i*) is negative when on the opposite side of the normal (0°) line, or positive when on the same side as the viewing angle. On the instrument, the viewing-angle dial is labeled α, and the dial representing the total subtended angle, $i + v$, is labeled β.

the angle of view, which is always positive. One further convention used here is to give the aspecular angle (that is, the angular degrees of viewing off the specular angle) in parentheses. Thus a typical notation to describe the geometric conditions used in a measurement is: –30°/10° (20°). This describes an angle of illumination of –30° and an angle of view of 10°, which is 20° off the specular angle of 30°.

For all of the measurements so described, the reference white standard was pressed barium sulfate ($BaSO_4$). This was also used for the gonio measurements. When making variable angle measurements, only perfectly diffuse samples measure the same reflectance at any angle of illumination and view. Measurements on any other type of sample are not absolute and so are designated as relative. Thus, for all of the curves illustrated in chapter 5 (under "Bronzing," "Pearlescence and Iridescence," and "Other Flake Pigments"), the ordinate is designated as *relative reflectance*. On nondiffuse samples, as the measurements at the viewing angle approach the specular angle, the measured reflectance rises sharply and can surpass 100% relative to the diffusely reflecting white standard. To make measurements at the specular angle as described for the pearlescent and interference pigments, a neutral-density filter is required in the sample beam of the instrument to decrease the specular reflectance to 10% or 20% of the true value. In this way the response will stay on the instrument scale. It should be noted also that the CIE notations calculated for such relative reflectance gonio measurements, when converted into color-difference data, do not have the same meaning as true absolute reflectance data measured on conventional nondirectional samples with conventional color-measuring instruments. Corrections can be made for the absorption of the neutral-density filters used, however. Without such corrections, and assuming that the neutral-density filter transmission curve is very close to neutral, the derived CIE *chromaticity coordinates*—*x* and *y*—provide useful information for comparison with similar samples measured in similar fashion. In summary, such relative gonio measurements are not absolute in the normal sense, as are measurements made with conventional color-measuring instruments intended to measure diffuse or total reflectance.

Note that transfer standards (defined below) for the diffusing reference white, such as white glass, should not be used unless they have been calibrated for the particular angular conditions used or fully described for comparison purposes.

Reference Standards

Regardless of the type of instrument used to measure transmittance or reflectance, all measure the ratio of the light flux transmitted or reflected by the sample relative to the flux transmitted or reflected by a reference standard. In measuring transmittance, the reference standard may be air or, in the case of solutions, an identical cell containing the solvent used to dissolve the sample material. Correspondingly, when measuring reflectance, a reference standard that *reflects* 100% at all angles over the entire spectral range being studied is desirable. This material would be a *perfect reflecting diffuser.* No such material has been found to exist, although many materials come close to this ideal. The CIE has recommended it as the official white reference to use for measurements made to describe color. Since no such material exists, a *transfer standard* (Johnston 1971a) is used. This is a white material that has been calibrated in absolute terms, compared to the perfect diffuser, by a national standardizing laboratory, such as the National Institute of Standards and Technology (NIST), formerly the National Bureau of Standards. Such calibrated physical standards are generally supplied with an instrument when it is purchased, but they may also be purchased separately. They are frequently made from white opal glass or other white materials and are in general relatively permanent. Other standards may be used as working standards for everyday use. Diffuse white materials, such as pressed $BaSO_4$ and pressed poly(tetrafluoroethylene) (Halon G-50), have been recommended. These "working standards" may be calibrated against the transfer standard, and the results stored in the computer for corrections, if desired. (See ASTM Standard E 259.) A stack of Millipore filters with a pore size of 0.025 μm (for example, VSWP 293-25) can also be recommended, particularly for use where pressed powders are inappropriate. These materials owe their whiteness to entrapped air spaces. Many operators simply use their calibrated transfer standard as a working standard.

In considering what to use for a working standard, there is one major characteristic of a working standard that, in the author's experience, is paramount: its surface characteristics. Although relative whiteness is important when making the most precise measurements, the diffuseness—or lack of gloss—of the working standard can be even more important. This is especially true when making measurements on materials that exhibit color in the specular or mirrorlike reflectance, such as bronzed paints or inks, or interference pigments (see chap. 5).

If one wishes to make very precise measurements, all care must be taken to use the best white reference available. However, one may question how significant this is for everyday practical work of curve-shape identification. All of the above-mentioned powder transfer standards, that is, all transfer standards except the ceramic materials, reflect about 97% or more on an absolute scale (relative to the perfect diffuser). Thus, if a pressed $BaSO_4$ standard has an absolute reflectance of 98%, the maximum error is 2% of the measured reflectances. At the 40% reflectance level, instead of measuring 40.0%, one will measure 40.8%. Does it really matter? No. Since the whole measurement scale is displaced, this is of little consequence. When spectrophotometry is used to analyze the relative shapes of curves, the absorption ratios at various wavelengths, which create the characteristic fingerprints, are the important aspect.

Finally, it must be pointed out that there are, in reality, no "absolute" measurements in spectrophotometry or in colorimetry. All measurements depend ultimately on both the geometric and spectral design of the instrument. For example, one will not obtain exactly the same measurements on sphere instruments as on bidirectional (0°/45° or 45°/0°) instruments (Raggi and Barbiroli 1993). Reference curves used for identification need to be made on instruments on which similar curves can be measured. In the pages to follow, continuous curves recorded with the General Electric Recording Spectrophotometer or with the Trilac are presented. The white reference was a diffuse pressed white powder, $BaSO_4$. Except for the variable angle measurements, all of the reflectance curves were measured using one of these two spectrophotometers, both equipped with integrating spheres. Agreement between these two instruments was excellent on all reflectance measurements. Today other instruments will be used. They should be identified and described.

Instrument Calibration and Measurement Reproducibility

When it is desired to make color and color-difference measurements with the reproducibility over time that approaches the sensitivity of the human observer to see small color differences, the measurements must be made with the utmost care. Instruments must be accurately calibrated. The samples being measured must be handled carefully. Repetitive measurements need to be made. Additionally, in using any particular instrument, the precision attainable should be known in order to interpret the measured results. Regardless of the color-measuring instrument used, a procedure for regularly calibrating it should be followed. Hemmendinger (1983) gives an extensive review of spectrophotometer calibration procedures. Basically, measurements of selected stable reference standards are necessary for determining photometric and wavelength scale accuracies. Also, an understanding of the means for adjustment and correction, if necessary, is required.

From repetitive measurements of the stable reference standards, the reproducibility with which measurements can be made can be determined. The process of operating color-measuring instruments reliably has been described in ASTM Standards E 1164, E 1331, E 1345, E 1348, and E 1349. Most of the modern color-measuring instruments are interfaced to a computer so that corrections are automatically applied to the measured data. It is important that the results on the reference standards be studied and interpreted over periods of time if measurements are going to be made over such periods of time. Obviously, studying fading is one such application for which the reliability of the measurements must be known. The latest instruments are very reliable, but people are not always so. If I use an instrument, I want to know how well I can operate it. How significant are my data?

Periodically in these pages sample characteristics and their effect on color measurement are discussed. But it is not simply the nature of the sample that is important; the condition of the sample and of the reference white standard are vital. Too often fingerprints appear and scratches occur. Dirt accumulates. Such happenings are most likely to occur when measurements are made over an extended period of time. They can be responsible for unwanted errors. Every student of statistics learns the importance of making multiple measurements. Measuring color is no different. Multiple measurements are important. Treating them statistically is discussed in chapter 8.

Spectrophotometric Curves

The value of the spectrophotometric curves presented throughout these pages lies with the skill of the person interpreting the measurements. Ultimately, the most important, and generally the most expensive, part of the successful application of spectrophotometry as a tool in material analysis is the person behind the instrument. With practice, operators can learn to read spectral curves like another language; they may not necessarily be able to interpret every word or nuance, but they can understand the implications and limitations.

Spectrophotometric curves in the visible spectrum are generally plotted as percent reflectance or transmittance on the vertical axis (y) versus wavelength on the horizontal axis (x) at a scale of 400–700 nm. The color of the wavelength regions is indicated at the top of the spectrophotometric curves in this monograph, from violet at the left through the spectrum to red at the right. If a sample reflects more blue wavelengths than those in other regions, one soon comes to realize that the material will look blue to an observer (see figs. A.8 and A.10). If the sample reflects both blue and red (both ends of the visible spectrum), it looks purple (see figs. A.25 and A.27). Yellows reflect green, yellow, orange, and red, which visually mix additively to make yellow (see chap. 2, "Additive Color Mixture"). Neutrals and near neutrals, such as whites and grays, reflect all wavelengths, approaching a flat reflectance curve. The closer a curve comes to this flat shape, the more it resembles a neutral color, and the lower is its saturation or *Chroma,* which is the Munsell designation that corresponds closely to saturation. (See chap. 2, "Other Color Notation Systems.") An illustration of the effect of adding black to any chromatic color is shown in figures A.9, A.11, A.13, A.15, A.17, A.19, A.21, A.23, and A.26. Conversely, the more contrast there is between the minimum and maximum reflectance, the higher is the saturation (Chroma). Another indicator of saturation is the steepness of the curve between lowest and highest reflectance: the steeper the curve, the higher the saturation will be. This is particularly evident in yellows, oranges, and reds, where the steepness of the curves is most obvious.

Thus, the three dimensions of color—hue, saturation, and lightness—can be inferred roughly from an examination of the spectral reflectance curve measured on a specimen. Hue can be visualized approximately from the reflectance maximum; saturation (or its opposite, grayness) from the contrast between the reflectance minimum and maximum; and lightness from the amount of the reflectance.

For analytical identification purposes, however, it is not the nature of the spectral reflection but the character of the *absorption* (low reflection region) that is definitive. It is the region of low reflection where the chemical structure of the colorant has its effect on the curve shape. So it is in this low reflection region where we look for a fingerprint. To see the characteristic absorption of pigments, they have to be diluted with white pigment or applied as incomplete hiding over a reflecting substrate; to see the absorption of textile dyes, they have to be diluted with solvent (when in solution) or applied thinly on a reflective substrate such as a light textile fabric. Throughout this monograph pigments are used as examples and are mixed with white. The author is most familiar with pigments as colorants. An examination of the curves in appendix A and in chapter 7 illustrates how some of the pigments have distinctive absorption curve shapes in mixture with white, whereas others have very little distinctive shape or clue to identify them. Many yellows, for example, are not easily distinguished from one another, although there are subtle differences that can provide some help, such as the wavelength at which the reflectance increases (or the absorption decreases).

Many topics are discussed in the pages that follow. Most concern the use of spectral curves as aids in the identification of colored materials. Of great help, however, is simply *looking at the material!* Our eyes are very sensitive instruments, and they are basic to an intelligent study of colorant composition. On the wall of every color-measurement laboratory there should be a sign that says: LOOK: THINK. (This is opposite in order to the admonition given by Billmeyer and Saltzman [1981] in their *Principles of Color Technology*.) Look at the samples. Look at the spectral curves. Then think about what they tell you.

In the end, every nondestructive tool available for chemical analysis should be used before taking samples of valuable materials. Our visual impressions can be characterized with considerable objectivity by calculating colorimetric descriptions from spectral curves using the science of colorimetry, which is the subject of chapter 2.

Chapter 2

Colorimetry

Wyszecki and Stiles (1982) define colorimetry as the "branch of color science concerned with specifying numerically the color of a physically defined visual stimulus." Thus a system of colorimetry is basically a "language" with which an observer may describe a color unambiguously and uniquely to distinguish it from all others. Although the basic techniques for determining colorimetric data are described in this chapter, the reader is also referred for additional details to the recognized textbooks on color science listed in appendix E.

Regardless of their basic type, all systems of colorimetry are required to be three-dimensional because of the nature of human vision. This means that the specification of three independent variables is required to describe colors uniquely. A *perceptual system* of colorimetry is based on visual appearance, with the three dimensions of hue, saturation (distance from neutral), and lightness; a *psychophysical system* is based on *additive* color mixture of three primary *colors;* and a *physical system* is based on *subtractive* colorant mixture of three primary *colorants*. Most of the commonly used systems are based on one of the first two types: perceptual or psychophysical. The last type, a physical system, is exemplified by many commercial color atlases based on a limited number of colorants mixed systematically.

Additive Color Mixture, Subtractive Colorant Mixture

In the preceding paragraph, two common but confusing concepts that require clarification were introduced: (1) color and colorant mixture, and (2) primary colors and primary colorants. As children, we learned that the three primary colors are red, blue, and yellow. This appeared to be confirmed when, using little pans of watercolor, we mixed yellow and blue and made green. However, we were not mixing color but rather *colorants,* that is, pigments or dyes. This type of colorant mixture is called *subtractive colorant mixture* because the individual colorants absorb—that is, subtract—portions of the incident light in certain spectral regions, leaving only the light from the nonabsorbed spectral regions to be reflected or transmitted, and observed. Thus, in the case of the mixture of yellow and blue watercolors, the yellow absorbs the violet and blue regions of the spectrum, and the blue absorbs the orange and red regions. As a result, only green is left to be reflected. Subtractive mixture is of major concern when identifying colorants and is discussed in chapter 4.

In contrast to the term *colorant,* the term *color* involves the human response to light reaching the eye. Each of three color-vision receptors in our eyes adds light of all the visible wavelengths into a single response, hence the term *additive color mixture.* Thus vision is an integrative process, and not an analytical one, in terms of the individual wavelengths of light reaching the eye. (Conversely, as mentioned earlier, hearing is an analytical process because it recognizes individual frequencies of sound reaching the ear.)

Returning to the watercolor paints, if we painted very tiny squares of yellow and blue, and looked at this array at such a distance that we could not distinguish the individual squares, we would see the additive mixture of the light reaching our eyes from the blue squares and from the yellow squares. The color observed can be calculated by averaging the spectral reflectance curves for the yellow and the blue since each occupies half of the area. The spectral curve for the *subtractive* colorant mixture of yellow iron oxide, phthalocyanine blue (hereafter abbreviated "phthalo blue"), and white (TiO_2) is shown as curve 1 in figure 2.1, and

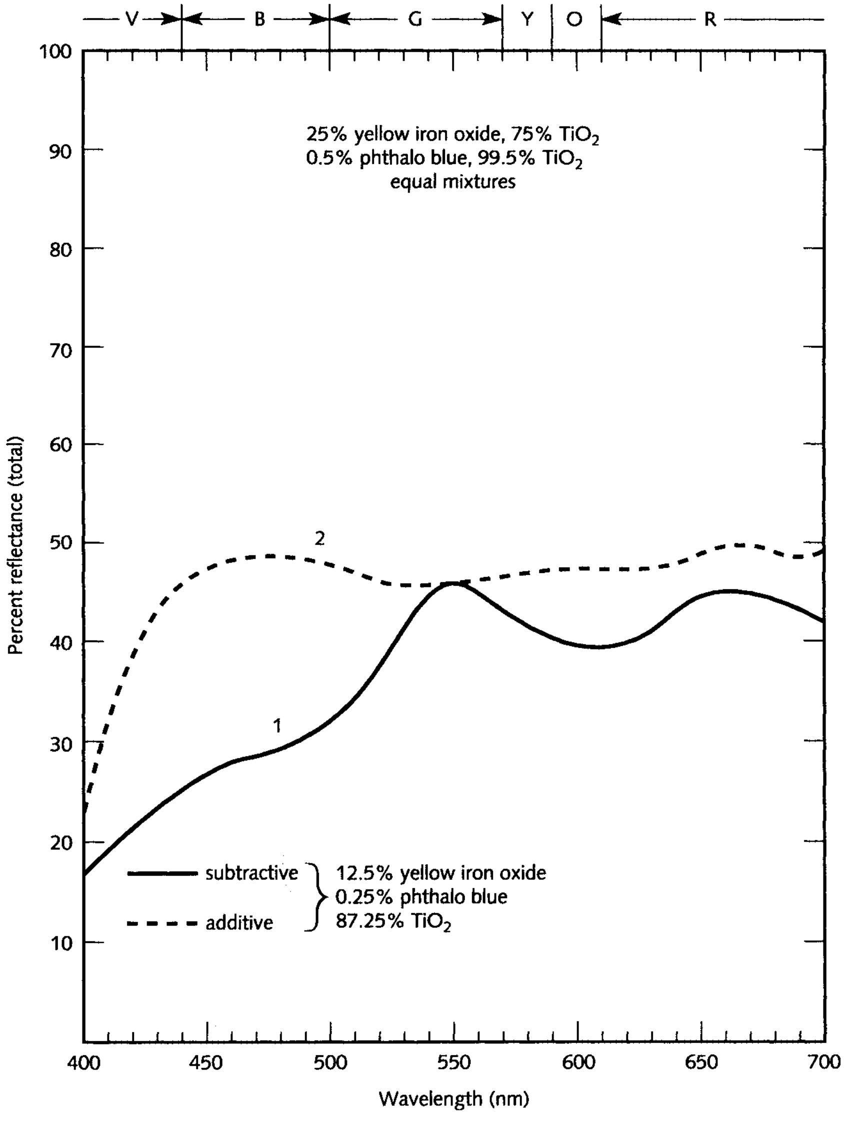

Figure 2.1

Spectrophotometric curves calculated for equal mixtures of yellow, blue, and white colorants mixed subtractively (a physical mixture) and additively (a visual mixture). The subtractive mixture (curve 1) is a green; the additive mixture (curve 2) is a near-neutral color.

the *additive* color mixture of the same materials applied as little squares is shown as curve 2. Examination of curve 2 indicates that the resultant color is a nearly neutral gray and is lighter than the subtractive green mixture. Spectral curves for the individual colorants—phthalo blue and white, and yellow iron oxide and white—are illustrated in figures A.10 and A.18, respectively.

An additive mixture does not necessarily result in colors that are nearly gray. The curves illustrated in figure 2.2 for the subtractive and additive mixtures of red oxide and white, and phthalo blue and white illustrate this in an interesting way. Red oxide is a very orange red (see fig. A.12). When it is mixed subtractively with phthalo blue, a near-neutral, rather muddy color results. However, the additive mixture is a beautiful purple.

Additive mixtures are often demonstrated by means of a disk that can be rotated rapidly. It consists of color segments that can be changed in size to alter the relative amounts of colors to be mixed as the disk is rotated. When it is rotated rapidly so that the individual

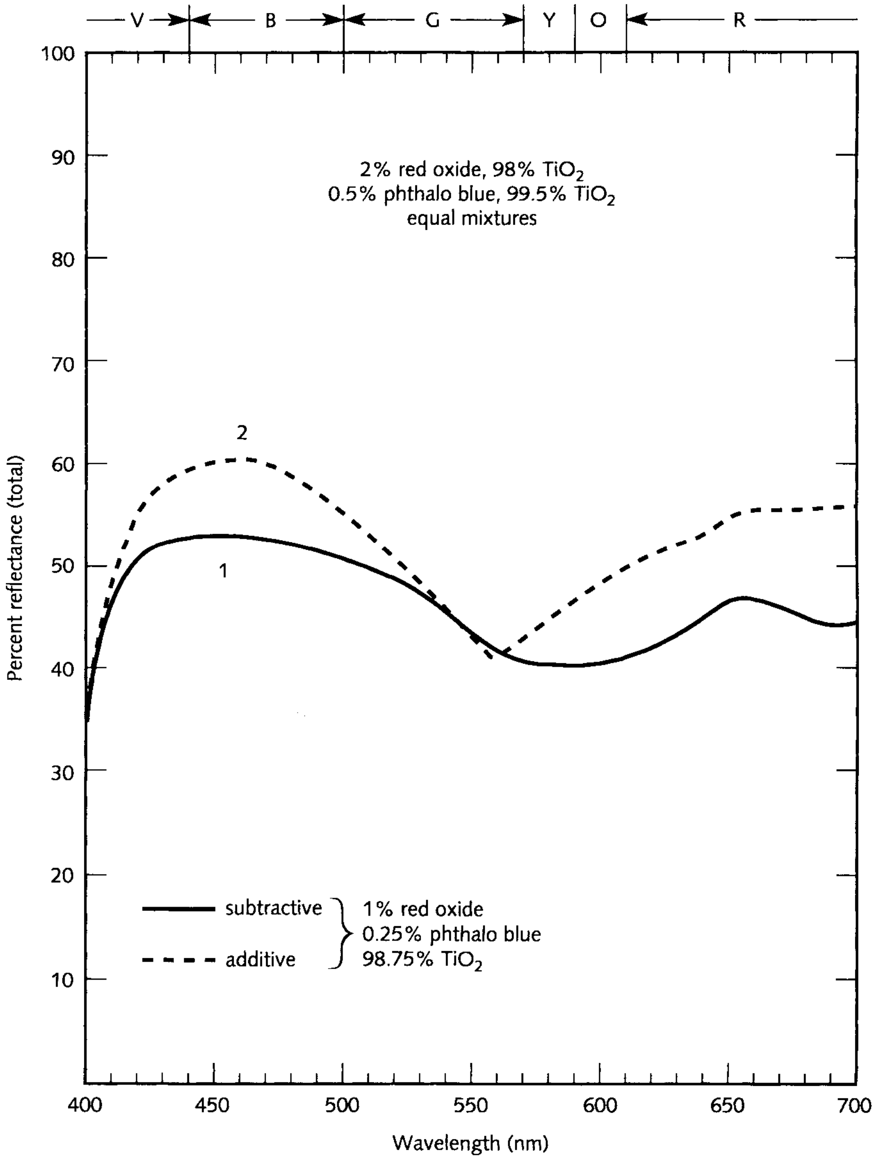

Figure 2.2

Spectral curves calculated for equal mixtures of an orange-red (2% red oxide and 98% TiO_2) with a blue (0.5% phthalocyanine blue and 99.5% TiO_2). The subtractive mixture (curve 1) is a near neutral; the additive mixture is a purple (from Johnston 1973. Copyright © 1973 John Wiley & Sons, Inc. Reprinted by permission).

colors cannot be discerned, the observer sees the additive mixture. Such an instrument with a disk that has segmented color sections is called a Maxwell disk, after James Clerk Maxwell, the scientist who demonstrated the usefulness of the tool in studying color matching (Maxwell 1860; Judd and Wyszecki 1975). If the spectrophotometric curves of the individual colors on the disk are known, and if the relative areas of each are also known, then the spectral curve of the additive mixture can be calculated, and the color notation also calculated.

Primary colors

We can define primary colors as sets of three specified colors from which large numbers of colors and a neutral can be made by suitable mixture. Primary colors for additive color mixture are not the same as the primary colors of the dyes or pigments used in subtractive colorant mixture. For additive color mixture, the three most useful primary colors are an orange-red, a green, and a violet-blue, which are generally described simply as red, green, and blue. We can observe how these colors mix by illuminating a white wall or a projection screen with light from three identical slide projectors, each equipped with a different colored filter transmitting the color of one of the additive primaries. When the proper amount of filtered light from each of the projectors is focused on the same area of the white wall or screen, the resultant color is white light. If the green light and the red light are focused on the same area, yellow light results; green and violet mixed additively result in a greenish blue (cyan); violet-blue and red mixed additively make a bluish red (magenta). These colors (yellow, cyan, and magenta), which are the common *secondary additive* colors, are found to be the most useful primary colors in *subtractive* colorant mixture. (In popular terminology, magenta, yellow, and cyan are also referred to as red, yellow, and blue.) Thus in color printing, the three primary colors of ink required for use in subtractive colorant mixture are magenta, yellow, and cyan. We find the most familiar use of the additive primaries in the orange-red, green, and violet-blue phosphors in our television tubes.

These relationships are described in figure 2.3, which illustrates a Hue Circle of colors with primaries indicated on the circumference of the circle. The additive primaries are marked with a plus sign (+), the subtractive primaries with a minus sign (–). The center, N, marks neutral. A similar diagram is presented in Billmeyer and Saltzman (1981). From this diagram one can see that there is no fundamental reason to select a specific set of primary colors, either for additive color mixture or for subtractive colorant mixture. For example, for additive mixture, the three primary lights used for color matching may be obtained by filtering white light through three appropriate filters as described earlier for additive mixture, or they may even be three monochromatic lights, that is, three lights each of a single wavelength. Similarly, the subtractive primaries may be any of a number of pigments or dyes in the hue ranges of magenta, yellow, and cyan.

Two colors that result in a neutral color when mixed in proper amounts are said to be *complementary*. In the next section, which

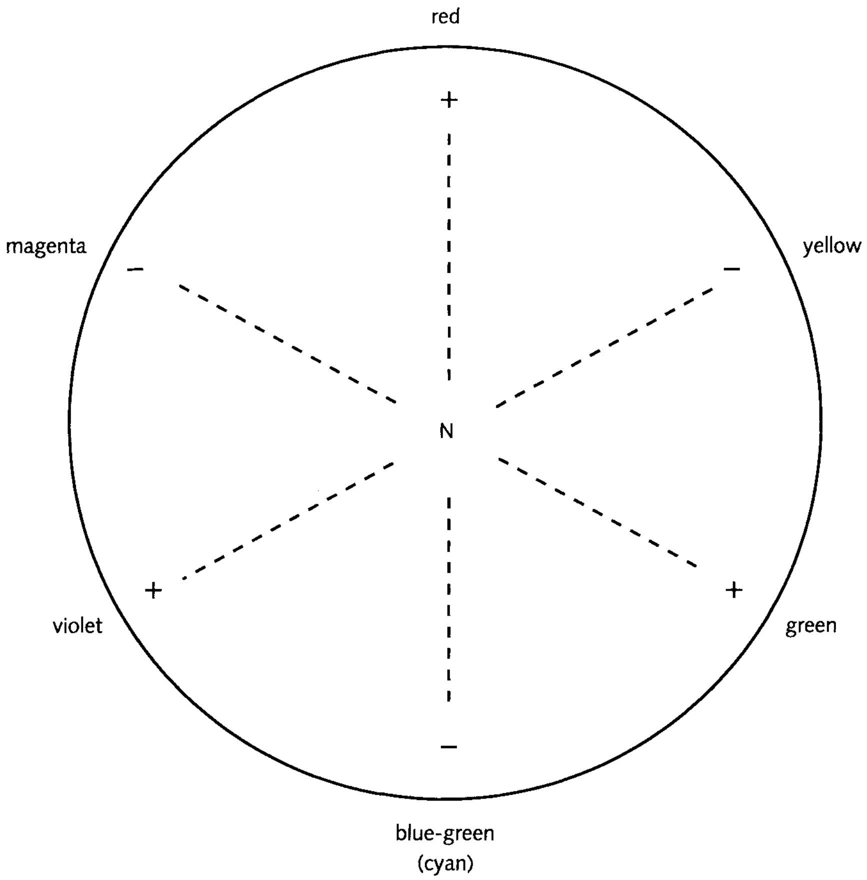

Figure 2.3
A color circle illustrating the relationships of the additive color primaries, marked with a plus sign (+), and the subtractive primaries, marked with a minus sign (–). Note that the additive and subtractive primaries are complementary—i.e., 180° opposite on the color circle.

deals with the CIE system for describing color, the method for determining the exact hue of complementary colors in additive color mixture is described. There is, however, no comparable, precise method for describing colorants that are complementary when mixed subtractively. In the practical world of colorant mixture, the absorption *and* scattering of light by colorants and by the color of the substrate affect the resultant color of the admixture. That some colorants are essentially complementary is well known to the artist: mixing red paint with blue-green (cyan) paint will result in a muddy gray paint; red and cyan are complementary.

These concepts of additive and subtractive color mixture and of complementary colors in both types of mixture have importance beyond the fact that each is the basis for a different type of colorimetry system, that is, for an essentially different language for describing color. When attempting to describe or identify the colors of objects, an understanding of these concepts is vital. If all objects were of uniform color, the problem of measurement would be relatively straightforward. But when the object is multicolored or patterned, the problem is not so easily solved, and the analyst must be aware of the possibilities inherent in the principles just described and of the pitfalls that may be encountered.

The little squares of yellow and blue described previously are akin to the technique of the pointillists, the late-nineteenth-century painters who discovered scientific additive mixture theory and, using this principle, painted dots of relatively pure color to define their scene. Since these paintings depend on the eye for color mixture, the viewing distance is all important. Viewed closely, the dots are visible in the painting; at a distance, they are not, and we see the additive mixture. At just the right distance, called the *fusion point,* they seem to "shimmer" as the eye alternately integrates and separates them. (Museums should display these paintings appropriately with regard for this fusion distance.) The pointillist technique is an obvious attempt to use additive color mixture as an artistic tool.

In most classical representative painting, this tool is also used for artistic effect but without the obvious extensive use of dots based on the strict application of the scientific theory. Most classical paintings, as well as modern paintings done with certain traditional painterly style techniques, are not uniform in color in every area. The artist may have dipped the brush into several colorants before applying his paint to the canvas, resulting in streaks of color. Or the paint may have been scumbled (resulting in a granular color surface achieved by rapid overpainting with a thin layer of opaque or semiopaque color using a dry-brush technique), or small highlights may have been applied. As the eye integrates (additively combines) these mixtures, so will a color-measuring instrument, depending on the size of the area viewed by the instrument. We must not forget this possibility in the act of measurement; it is dealt with later at greater length. For our purposes, the solution to minimizing the effect of additive mixing of areas of different pigmentation on a painting is to make multiple measurements, and this is practical with modern high-speed instruments. For the skilled interpreter, spectral reflectance curves from a number of areas will quickly indicate similarities that will provide a key to the basic palette. This is part of the skill defined in this monograph.

The CIE System

Many of the various descriptors for color, as it is perceived, are based on what is known as the CIE system, from the initials of the Commission Internationale de l'Eclairage, or the International Commission on Illumination, the organization that has administered the system since its beginnings in 1931. (In older publications, ICI—the initials for the English name of the commission—may be encountered.) In the preceding chapter on spectrophotometry, it was pointed out that, from an analysis of spectral curve shapes, the color dimensions of hue, lightness, and saturation could be deduced in a qualitative way. These three terms describe the perceptual (that is, psychological) dimensions of color. In the introductory section to this chapter on colorimetry, it was emphasized that there are only three basic methods for creating an orderly arrangement of colors. The perceptual system, which is based on visual estimates of hue, lightness, and saturation, is one of them. The CIE system is of the second type, that is, a psychophysical system based on additive color mixture and on the visual response to various wavelengths of light reflected or transmitted to a normal human observer.

The colors that we see in a scene depend on the spectral distribution of the light illuminating it and on our spectral response to the light reaching our eyes after it is reflected or transmitted by the elements in the scene. If these two aspects—the nature of the light source and the response characteristics of the observer—can be defined, then the colors reflected or transmitted in the scene can be described mathematically.

In 1931 the original method for the calculation of three-dimensional color descriptors was introduced by the CIE, and it has been accepted widely as an internationally recognized color language. Included in the 1931 method were three standard light sources, indicated by the letters A, B, and C, and the spectral color-matching functions for a standard observer. Later, the spectral power distributions of the light sources were measured, and these data became the official definitions of illuminants A, B, and C. In 1965 the CIE system was augmented by adding the daylight, D, illuminant; the year before, a supplementary standard observer had been added to the system. The 1931 standard observer represents distance viewing based on a 2° subtended angle of viewing for determining the color-matching functions; the 1964 standard observer represents closer viewing, described as the 10° subtended angle response or, roughly, as viewing at arm's length. For detailed information on the CIE methods, the CIE and ASTM publications may be consulted (CIE 1986; ASTM Standard E 308), as well as any of the standard color science texts listed in appendix E. The corresponding terminology is given in the *International Lighting Vocabulary* (CIE 1987) and in ASTM Standard E 284.

The 1931 standard light sources were A, representing the color temperature of an incandescent lamp at 2856 K; B, representing mean noon sunlight obtained by filtering a tungsten lamp (4874 K); and C, representing average daylight (6774 K). The last may be obtained by using special blue filters over the source A incandescent lamp. Because incandescent lamps do not include ultraviolet wavelengths to the extent that sunlight does, all of these originally defined illuminants (sources) were inadequate for measuring color as observed on fluorescent materials, which depend at least partially on absorption of ultraviolet energy. Recognizing this, the CIE in 1964 defined a series of daylight illuminants that closely match the relative spectral power distribution of natural daylight. Of these, the average daylight with 6500 K color temperature (abbreviated D65) is the most important and most widely used. Figure 2.4 illustrates the relative spectral power distribution of the three original CIE illuminants (A, B, C) and of D65. The large difference between D65 and the others in the ultraviolet region 300–400 nm is readily apparent. Unfortunately, there is no real light source that simulates illuminant D65 closely, especially in the ultraviolet. Illuminant B has been declared obsolete by the CIE. Illuminant C is still used, but D65 is becoming increasingly more common and is the recommended illuminant today. For nonfluorescent samples, illuminant C is adequate and, unless otherwise specified, is assumed to be used in this monograph; it was used in many colorimeters and in most of the older literature dealing with nonfluorescent colorants. The other widely used illuminant is A, incandescent light. Used less frequently are fluorescent illuminants described by the CIE (1986).

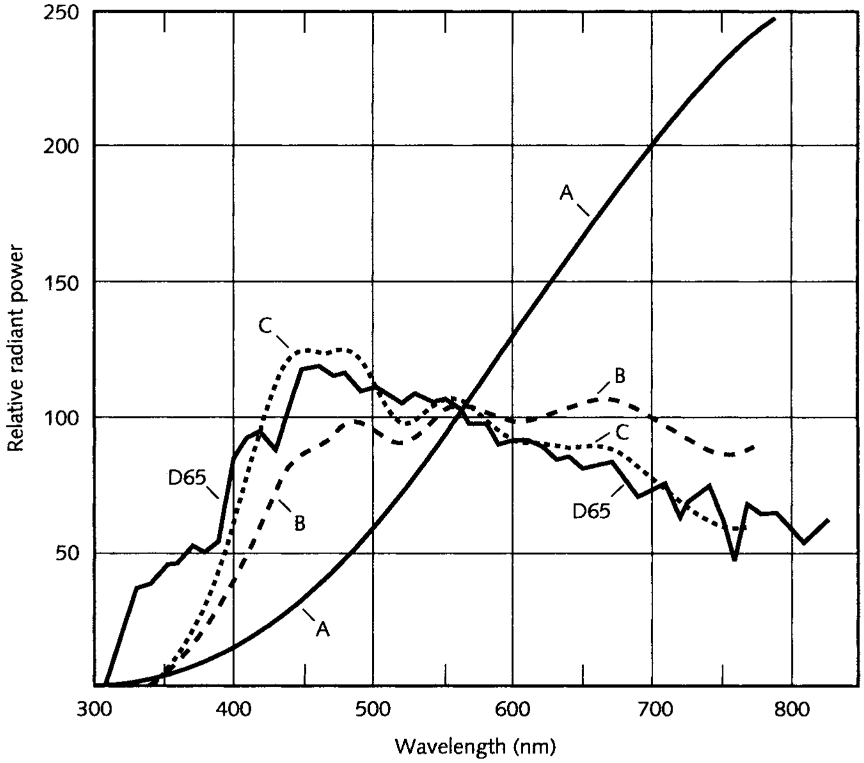

Figure 2.4

Relative spectral radiant power distributions of CIE illuminants A, B, C, and D65. Note that illuminant B has been discontinued as one of the standard illuminants (from Wyszecki and Stiles 1982. Copyright © 1982 John Wiley & Sons, Inc. Reprinted by permission).

In addition to the nature of the light source, the second factor affecting the perception of the color of an object by an observer is the spectral sensitivity of the eye. This visual response can be measured in terms of the amounts of three primary lights required to be *additively* mixed to match the light at each wavelength in the visible region of the spectrum. A schematic diagram of the experimental method is shown in figure 2.5. All humans with normal color vision do not have identical responses. However, the differences are small in comparison to the differ-

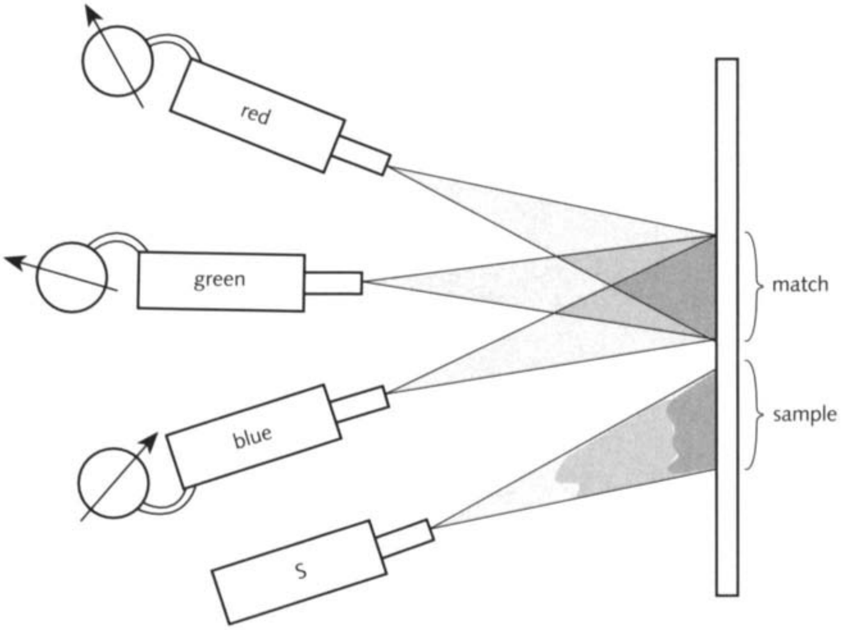

Figure 2.5

Diagram illustrating the method of additive tristimulus matching. The portion of the screen showing the samples is matched by varying the amounts of light from the three-color projector illuminating the other (match) portion of the screen.

ences that occur in persons with abnormal color vision (some degree of color blindness). In 1931 the CIE established a *standard observer* in terms of the average measured response characteristics for a group of normal observers. Three response curves were defined, one for each primary light used in matching many wavelengths across the spectrum. The experiments were carried out using red, green, and blue primary lights. For reasons of mathematical simplicity, the experimental data were transformed to another set of primaries that bear no relation to any real lights. These transformed response values, used ever since, are called the color-matching functions, $\bar{x}$, $\bar{y}$, $\bar{z}$, and are illustrated as spectral curves in figure 2.6. When the mathematical transformations were made, the Y tristimulus value was made to correspond to the lightness response.

The light incident upon the eye is the summation of the product of the radiant power from the illuminant, $S(\lambda)$, and the fraction of this light that is reflected (or transmitted) by the object at each wavelength, $R(\lambda)$. This product summation is generally denoted as $\Sigma S(\lambda)R(\lambda)\Delta\lambda$, where $\Delta\lambda$ describes the wavelength interval used. The wavelength interval, $\Delta\lambda$, is constant across the spectrum and must be sufficiently small that the characteristics of the spectral curves are adequately represented. Often $\Delta\lambda$ is 10 nm, for example.

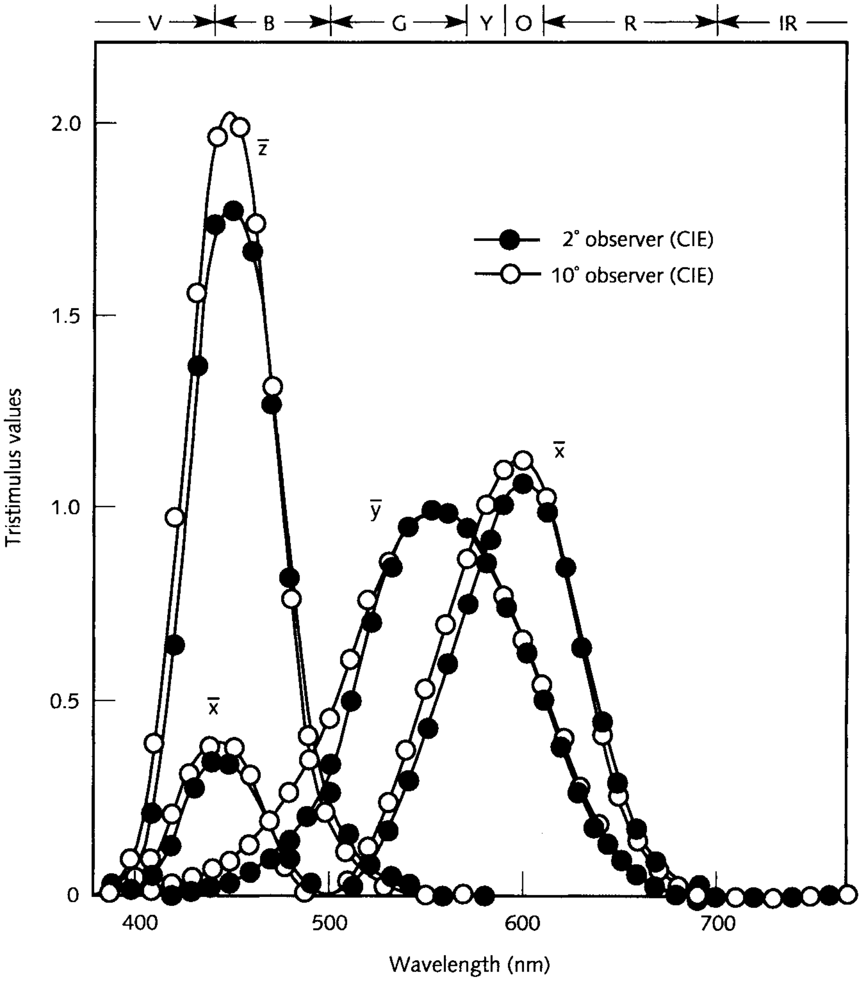

Figure 2.6

Comparison of CIE 2° and 10° standard observer color-matching functions (from Judd and Wyszecki 1963. Copyright © 1963 John Wiley & Sons, Inc. Reprinted by permission).

Knowing the spectral characteristics of the light reaching the eye, a description of the color as seen by the standard observer can be calculated. The product $S(\lambda)R(\lambda)$ for each wavelength is multiplied by each of the three color-matching functions, $\bar{x}$, $\bar{y}$, $\bar{z}$, at the same wavelength. The curves of the spectral color-matching functions for the 2° (1931) and for the 10° (1964) standard observers are illustrated in figure 2.6. The products are then summed (the symbol Σ) for each primary to give a three-dimensional description of the color. The results are called the tristimulus values: X, Y (lightness), and Z:

$$\begin{aligned} X &= \mathrm{k}\Sigma S(\lambda)R(\lambda)\,\bar{x}(\lambda)\Delta\lambda \\ Y &= \mathrm{k}\Sigma S(\lambda)R(\lambda)\,\bar{y}(\lambda)\Delta\lambda \\ Z &= \mathrm{k}\Sigma S(\lambda)R(\lambda)\,\bar{z}(\lambda)\Delta\lambda \end{aligned} \tag{2.1}$$

where k is a normalizing factor to make Y equal to 100 for the white reference standard (the so-called perfect reflecting diffuser), thus describing the lightness. The tristimulus values may vary depending on the number of equally spaced wavelengths used in the summations. If $\Delta\lambda$ is 1 nm or less, the summations become true integrations (the symbol $\int$):

$$\begin{aligned} X &= \mathrm{k}\int S(\lambda)R(\lambda)\,\bar{x}(\lambda)d\lambda \\ Y &= \mathrm{k}\int S(\lambda)R(\lambda)\,\bar{y}(\lambda)d\lambda \\ Z &= \mathrm{k}\int S(\lambda)R(\lambda)\,\bar{z}(\lambda)d\lambda \end{aligned} \tag{2.2}$$

This integrative process may be more clear if shown graphically, as in figure 2.7. The spectral curves for illuminant C and for the reflectance of an object are shown at the top. From our knowledge of spectrophotometry, it can be seen that the reflectance curve represents that of a blue object of moderate lightness and purity (saturation). The product of these curves, $S(\lambda)R(\lambda)$, which is shown immediately below the illuminant and object curves in figure 2.7, describes the spectral light that would be incident on the eye. Below this curve are the spectral response characteristics, $\bar{x}$, $\bar{y}$, $\bar{z}$ (color-matching functions), for the 1931 standard observer. The product of multiplying each of the color-matching functions by $S(\lambda)R(\lambda)$ is shown by the curves at the bottom of figure 2.7. When the relative *areas* under curves $S(\lambda)R(\lambda)\,\bar{x}(\lambda)$, $S(\lambda)R(\lambda)\,\bar{y}(\lambda)$, and $S(\lambda)R(\lambda)\,\bar{z}(\lambda)$ are determined (i.e., the curves are integrated), we find that the tristimulus values for this blue object under illuminant C as seen by the 1931 2° standard observer are $X = 55.55$, $Y = 57.33$, and $Z = 90.25$.

We can now state the results obtained with the CIE system. This system provides methods for computing sets of tristimulus values such that if two specimens have the same tristimulus values, for a stated illuminant and observer, they match in color; if they do not have the same tristimulus values, they do not match. Although, strictly speaking, the 1931 CIE system was not designed to describe the colors or the differences between them if they do not match, these applications and many more described later have been added to the original system since its beginnings.

In the case of the tristimulus values described above, it can be assumed that the color is blue because the Z tristimulus value is so much larger than the X and Y values. However, if we had another blue sample at similar lightness (Y) but with a different reflectance curve, such that $X = 50.34$, $Y = 54.19$, and $Z = 85.69$, it would be difficult to visualize

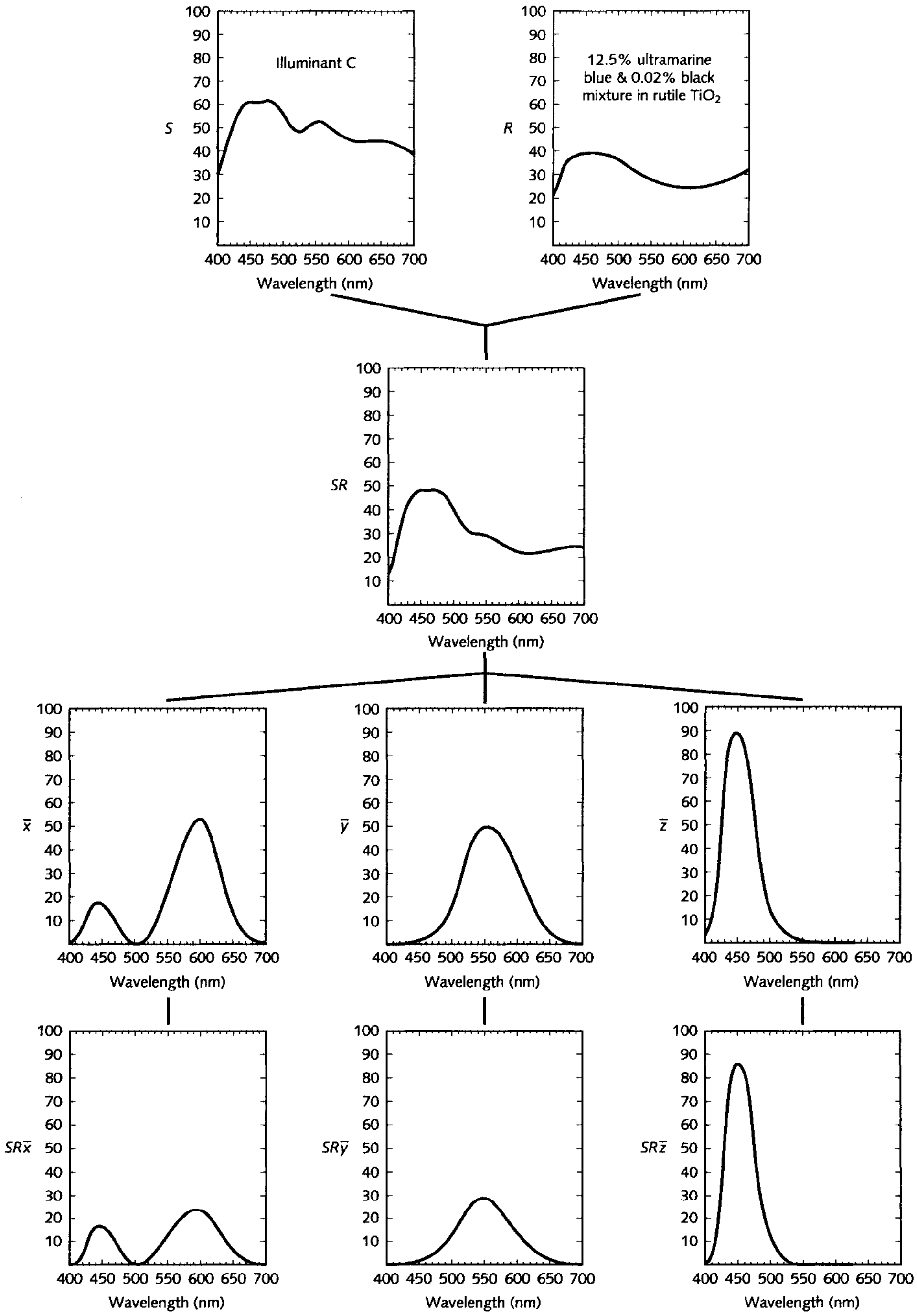

Figure 2.7

Graphical illustration of the calculation of the CIE tristimulus values. The blue sample is a mixture of 12.5% ultramarine blue, 0.02% carbon black, and 87.48% rutile TiO_2 in a glossy paint medium.

the relationship between the two samples on the basis of the tristimulus values, X, Y, and Z, alone. To aid in this visualization, the CIE has defined chromaticity coordinates (symbols x, y, and z) derived from the three tristimulus values:

$$x = \frac{X}{X+Y+Z}$$

$$y = \frac{Y}{X+Y+Z} \tag{2.3}$$

$$z = \frac{Z}{X+Y+Z} = 1-(x+y)$$

To describe the color completely, the lightness (the Y tristimulus value) must be included with two chromaticity coordinates, x and y, to describe the three dimensions adequately. To avoid confusion, the tristimulus values (X, Y, and Z) are generally (except in very old literature) multiplied by 100, such that Y for a perfect reflecting white diffuser equals 100. The x and y chromaticity coordinates are designated as decimal fractions.

We now have two ways to describe a color in the CIE system: (1) in terms of its tristimulus values (X, Y, and Z), and (2) in terms of its chromaticity coordinates, x and y, and Y.

Because the sum of all three chromaticity coordinates is unity, two of them, generally x and y, may be plotted on a two-dimensional graph. When the chromaticity coordinates for each wavelength in the spectrum are plotted, a horseshoe-shaped diagram is obtained, as illustrated by the outline in figure 2.8. This diagram is based on illuminant C and the 1931 2° standard observer. The chromaticity diagram for illuminant D65 is very similar.

The outside of the horseshoe diagram in figure 2.8, formed by plotting the chromaticity coordinates, x and y, for the pure spectrum colors, is called the *spectrum locus* and represents the purest and most saturated colors that can occur. The short-wavelength violet is at bottom left beginning at 380 nm; the long-wavelength red is at bottom right at 780 nm; and the green at 520 nm is at the top of the horseshoe. The point C in the interior of the diagram is located at the chromaticity coordinates for illuminant C and represents zero color. Approximate color names associated with various parts of the diagram are indicated. These are not sanctioned by the CIE, but they have been found to be helpful as a guide in relating colors on the chromaticity diagram. The oval area around the illuminant point, which has no color name, is the more neutral area of the diagram. It includes hues decreasing in saturation as the illuminant point (also known as the achromatic point) is approached. This diagram represents the chromaticity plane. The third dimension, which is the lightness described by the Y tristimulus value, is perpendicular to this plane.

Figure 2.9 shows another use of the chromaticity diagram. One of the features of this diagram is an illustration of the additivity of color mixtures. When any pure spectrum color is mixed with the illuminant color, the resulting chromaticity coordinates fall on a straight line connecting the point on the spectrum locus with the color of the illuminant. The lines radiating from the illuminant point to the spectrum locus are called lines of constant dominant wavelength, λ_d, and describe the hue in terms of the wavelengths in nanometers at the intersections of the lines with the spectrum locus. The chromaticity of any two colored lights mixed additively falls on a straight line connecting chromaticities of the two lights. If the straight line passes through the illuminant point, the two colors are said to be complementary. Thus an orange of 587 nm dominant wavelength and a blue of 485 nm dominant wavelength are complementary because their additive mixture line passes through the illuminant point.

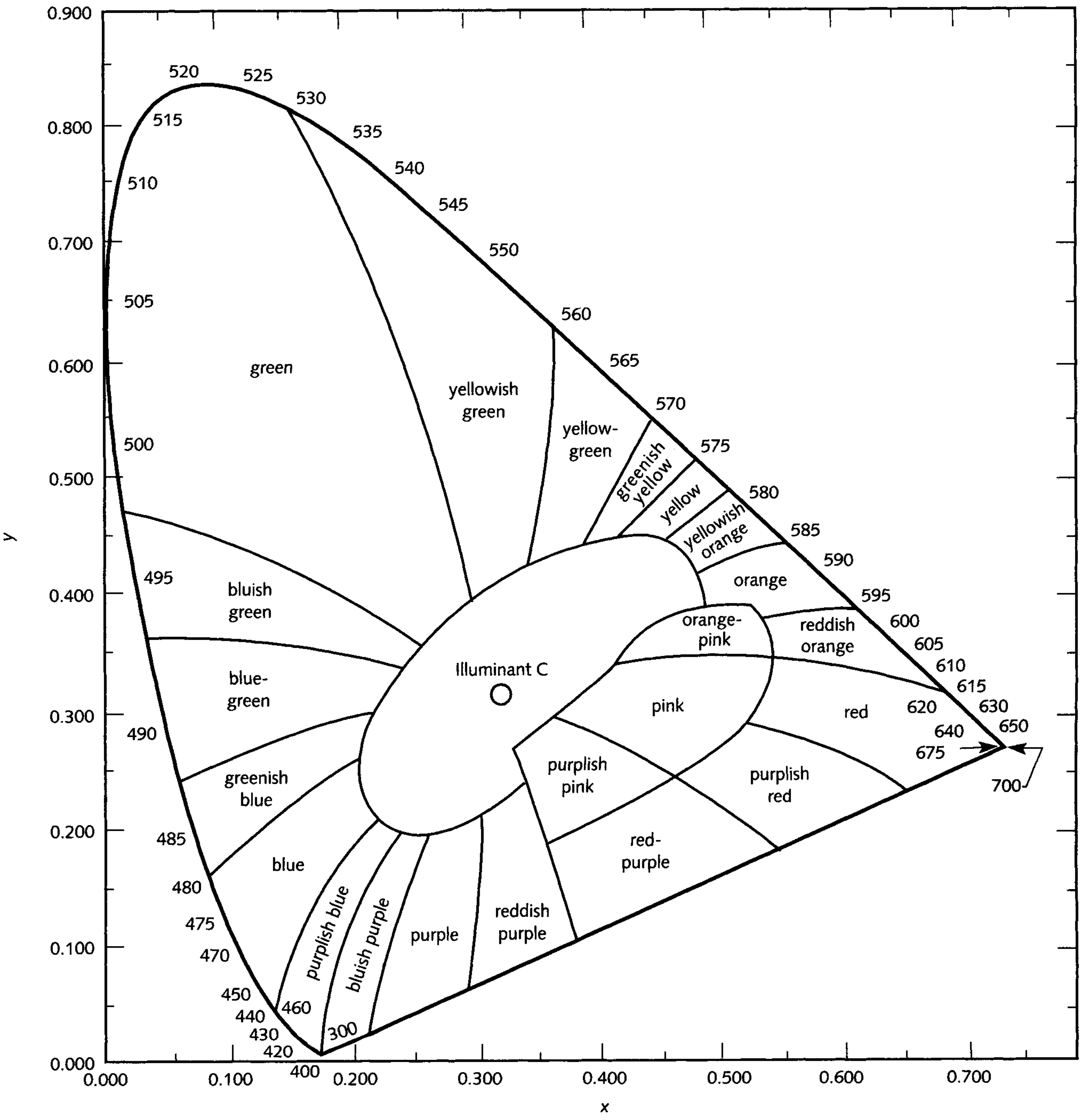

Figure 2.8

Hue names associated with areas of the 1931 CIE chromaticity diagram (after Judd 1950).

This property of additive mixture when plotted on a chromaticity diagram enables us to describe purples, which are not spectrum colors, as being mixtures of red light (long wavelength) and violet light (short wavelength). These nonspectral colors have no dominant wavelength; they are described in terms of the colors to which they are complementary. They are indicated on the diagram with a subscript c following the dominant wavelength of the complementary green color.

The total distance from the illuminant point to the spectrum locus represents 0–100% purity. Divided into percentage distances from the illuminant, the series of concentric horseshoelike lines are a measure of the excitation purity (or simply purity), p_e. The series of smaller

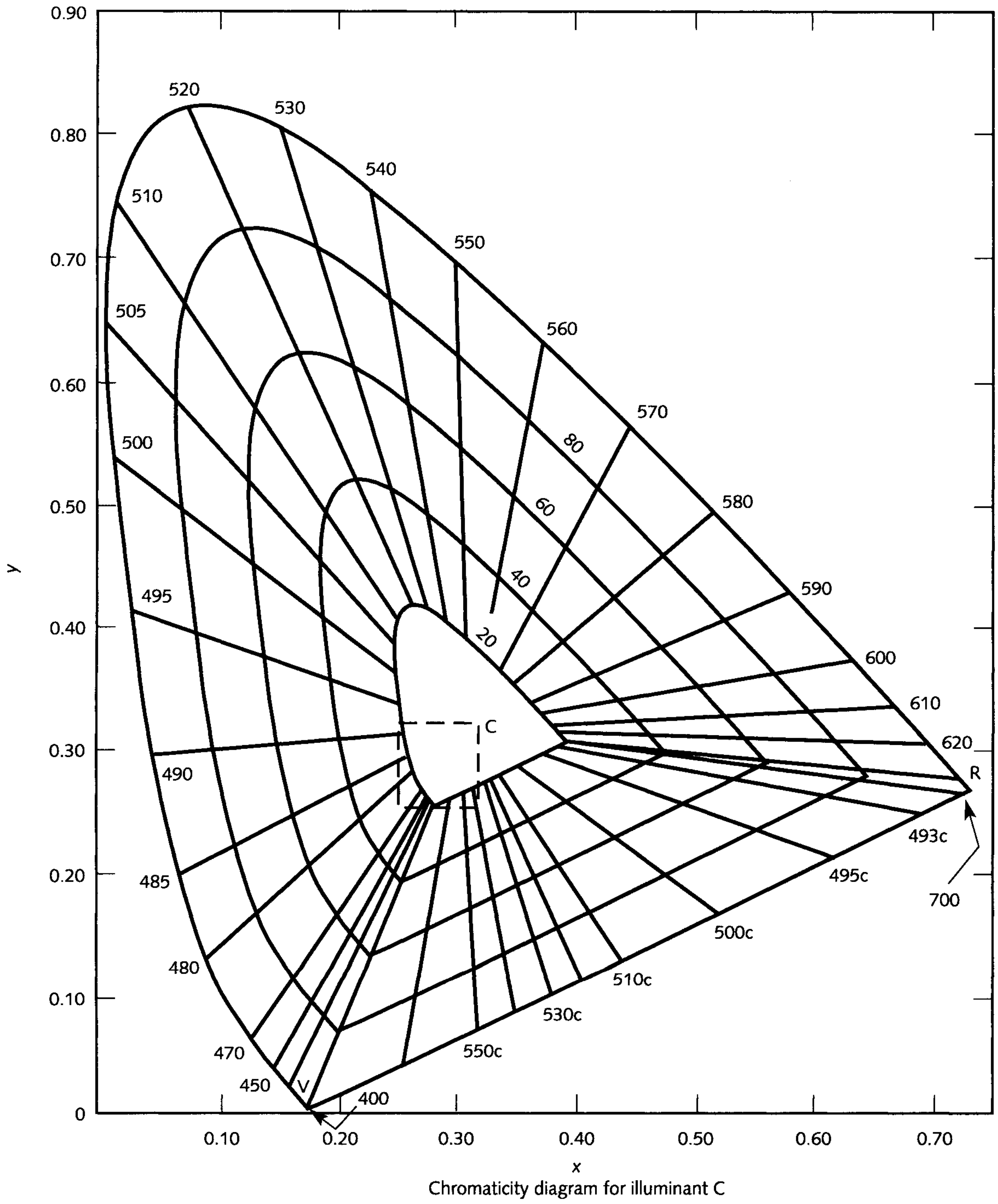

Figure 2.9

Chromaticity diagram for the 1931 standard observer. The section outlined by the dashed square is enlarged in figure 2.11.

horseshoes in figure 2.9 are constant purity loci. For any given sample point on this diagram, the purity can be estimated from precalculated lines (Hardy 1936) or by direct measurement of the distance from the illuminant, divided by the total distance of the illuminant through the sample point to the spectrum locus, and then multiplied by 100 to get a percentage.

Thus, a third set of color descriptors in the CIE system is the dominant wavelength (λ_d), the excitation purity (p_e), and the lightness (Y). Note that Y must always be included.

Table 2.1

Color descriptions in the CIE system: tristimulus values (X, Y, and Z), chromaticity coordinates (x and y), dominant wavelength, and excitation purity.

X	Y	Z	x	y	Dominant wavelength	Excitation purity
31.39	19.77	10.74	0.5071	0.3194	614.0 nm	56.6%
32.84	43.06	9.35	0.3852	0.5051	566.0 nm	69.2%
29.17	19.77	26.23	0.3880	0.2630	499.4c nm	36.0%

A few examples are given in table 2.1. The reader may confirm the chromaticity coordinates and then use figure 2.9 to confirm the dominant wavelength and purity.

The development of the CIE system has been only briefly covered; the reader is referred to the references in appendix E for more complete explanations and for descriptions of the experimental procedures and mathematical methods involved. It suffices to describe here the usefulness of plotting colors on a chromaticity diagram to obtain information on the relationships of measured colors.

Examples

Figure 2.10 illustrates the spectrophotometric curves for three blue paints. Blue 1 is made with ultramarine blue (12.5%), carbon black (0.02%), and rutile TiO_2 (87.48%); the curve shape at 600–700 nm is characteristic of ultramarine blue (see fig. A.8). Blue 2 is made with phthalocyanine blue (0.25%), carbon black (0.10%), and rutile TiO_2 (99.65%); the curve shape at 600–700 nm is characteristic of phthalo blue (see fig. A.10). Blue 3 is a 50:50 mixture of blue 1 and blue 2. Note that the pigment concentrations are expressed as relative dry pigment concentrations based on the fact that the pigment total is 100.00% regardless of the exact weights or volumes used. The chromaticity coordinates (x, y) and the luminous reflectance, or lightness (Y), of the three blues are given in table 2.2. These values are for illuminant C and the 1931 standard observer. The Y tristimulus value indicates that blue 1 is the lightest. But in what way do the three blue paints differ in chromaticity?

By plotting them on an expanded portion of the blue section of the chromaticity diagram, their relationship becomes clear. This is illustrated in figure 2.11, which is the area enclosed by the dashed square shown in figure 2.9. Blue 1, made with ultramarine, is seen to be redder (more violet) and lower in purity than blue 2, which is made with phthalo blue. Blue 3 is midway between the other two, as it should be; it is a 50:50 mixture of the other two blues.

On the expanded portion of the chromaticity diagram (fig. 2.11), the illuminant point as well as reference purity and dominant wavelength lines are shown. Although helpful, they are not necessary for

Table 2.2

Chromaticity coordinates (x and y) and the luminous reflectance, or lightness (Y), of three blues.

Blue	x	y	Y
1	0.2711	0.2800	53.33
2	0.2614	0.2827	50.19
3	0.2655	0.2813	51.48

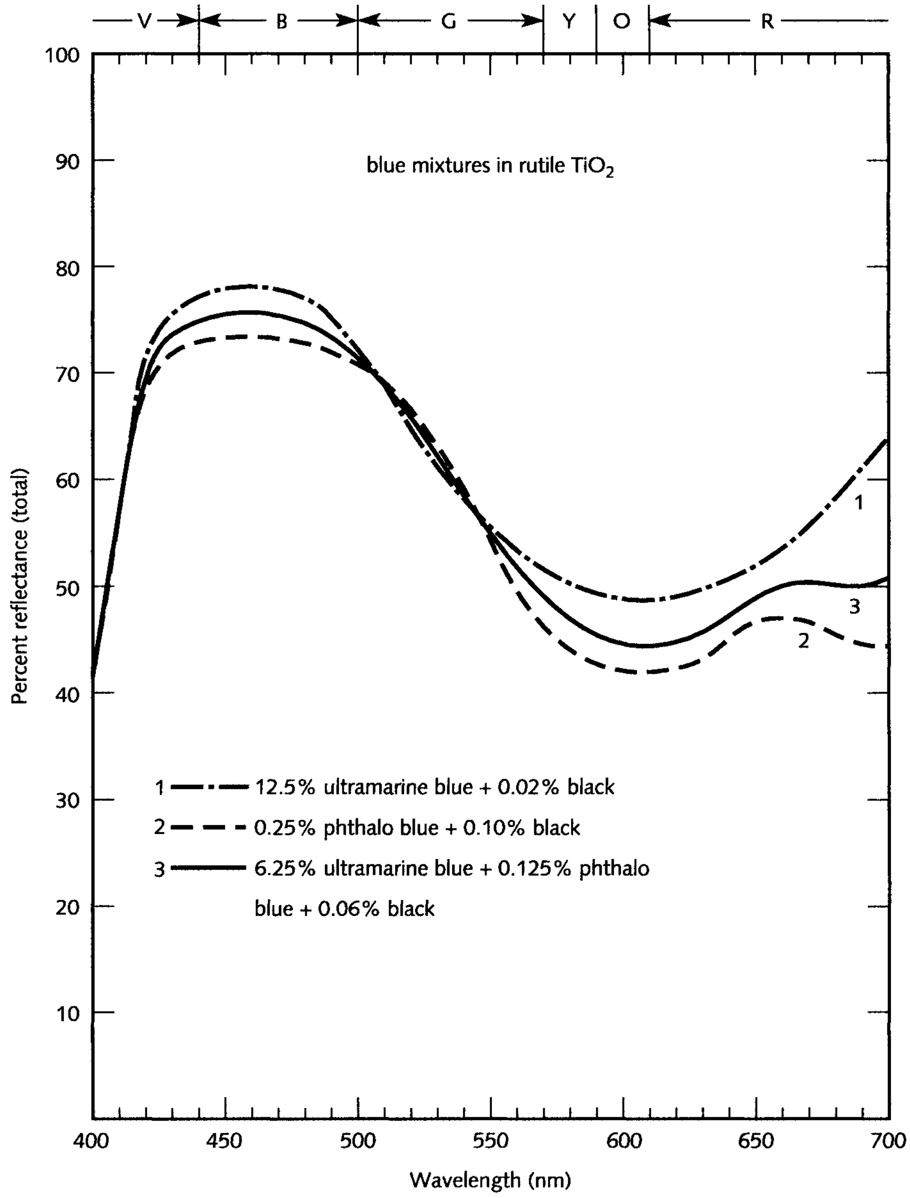

Figure 2.10

Spectrophotometric curves for paints made up of mixtures of ultramarine blue and black (curve 1) and for phthalo blue and black (curve 2), both with rutile TiO_2; curve 3 is their mixture in equal parts by weight.

quick analytical work. With a little practice one learns to relate adjacent chromaticity points qualitatively without the reference values, from the visualization of the relationships of colors in the various areas of the diagram. An atlas of expanded diagrams may be found in the *Handbook of Colorimetry* (Hardy 1936). These diagrams can be used to determine the dominant wavelength and the excitation purity for any set of chromaticity coordinates. Today the dominant wavelength and purity can be calculated with a computer (McCarley, Green, and Horowitz 1965). The computer programs supplied with many color-measuring instruments calculate the chromaticity coordinates and also display them, and may print them on a chromaticity diagram.

From graphing the chromaticity coordinates of the three blues used in the example, we have determined that the first blue is redder and lower in purity than the others, and the values of Y indicate it is lighter than the second blue. This is a qualitative description of what one

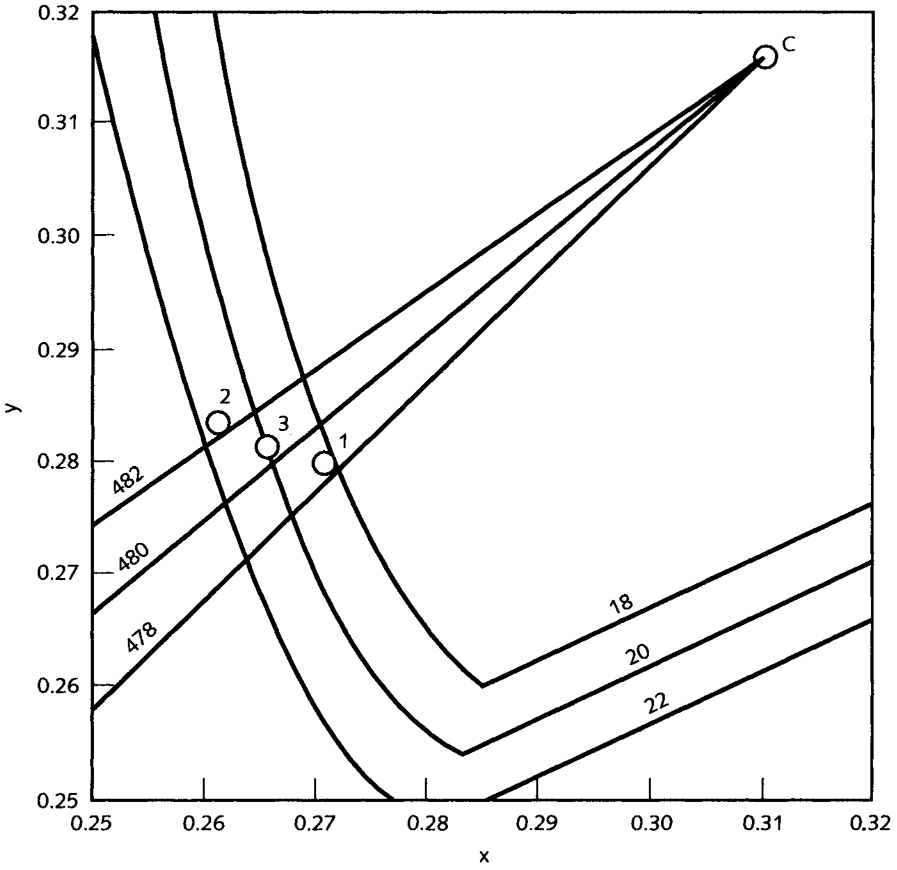

Figure 2.11
Enlarged section of the chromaticity diagram (fig. 2.9) showing the locations of the samples whose spectral curves are illustrated in figure 2.10. Note the near-straight-line relationship of the chromaticities of the three colors.

would see. But the CIE chromaticity diagram is based on additive mixture, and we are primarily interested in pigment mixtures, that is, subtractive mixture. Of what use in subtractive mixture is this diagram, which is based on additive mixture?

Subtractive mixtures do not fall on straight lines on the chromaticity diagram; some lines are relatively close to being straight, and others do loops and turnarounds when the individual pigments are mixed with white pigment. Figure 2.12 illustrates some typical pigment mixtures at various ratios of rutile TiO_2. The reasons why some lines loop around and others approach straight lines are presented in chapters 3 and 4 in the discussions of subtractive mixture and its dependence on the absorption and scattering characteristics of the pigments used in the mixture.

If the area outlined by the dashed square on the chromaticity diagram in figure 2.9 is expanded 100 times, as was done to create figure 2.11, the assumption of a straight-line relationship in subtractive mixtures that are very *similar* in color is not unrealistic. For example, if we make a 50:50 mixture of blue 1 and blue 2—which is represented by blue 3—and plot the chromaticity coordinates on the expanded diagram, it is seen that the chromaticity of the blue 3 mixture in figure 2.11 falls very close to the straight line connecting the chromaticities of blue 1 and blue 2. Thus the assumption of a straight-line relationship between the chromaticity points for similar colors is a practical and meaningful way to interpret relationships of closely related colors made by subtractive mixture. For example, the chromaticity coordinates and luminous

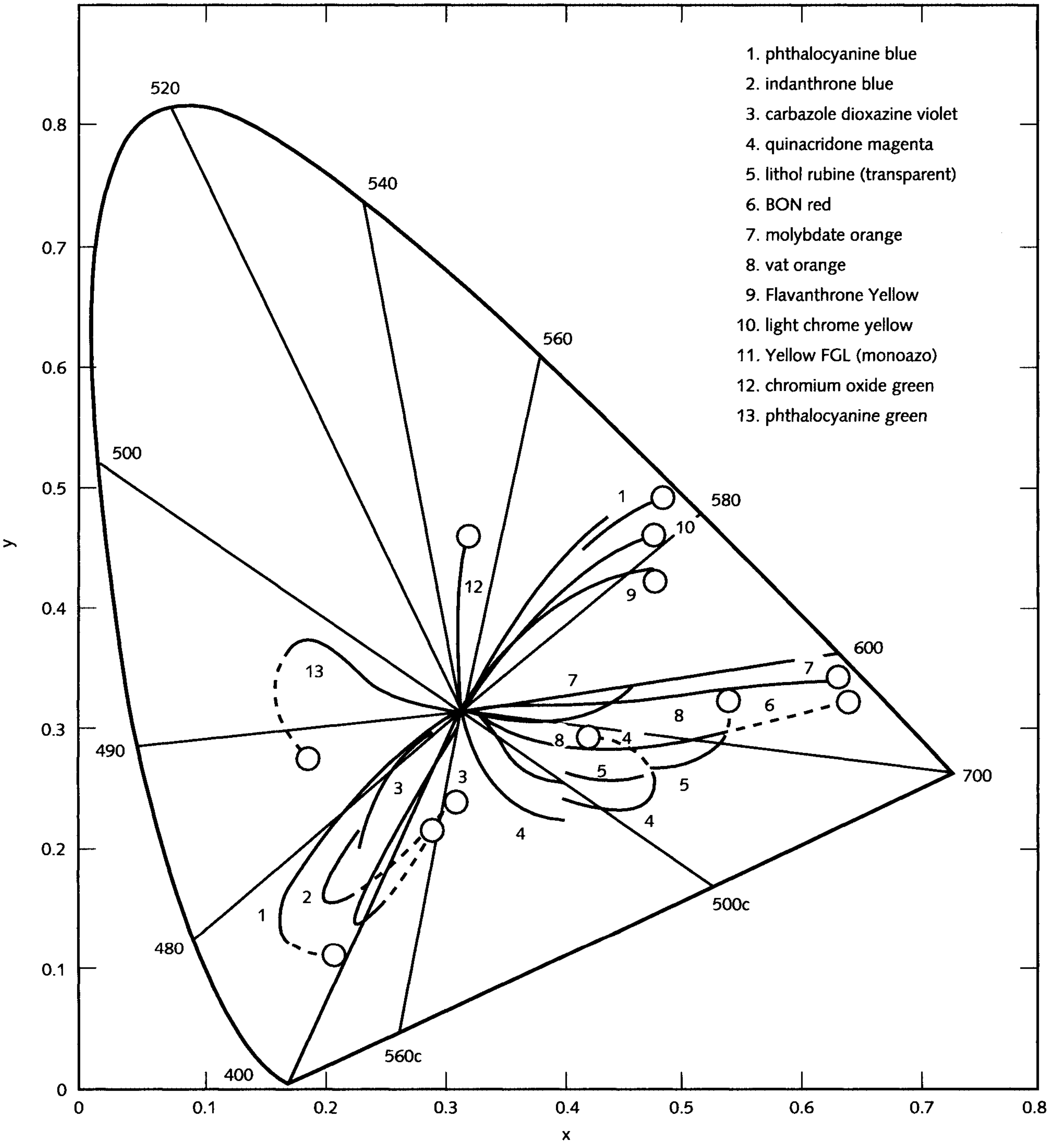

Figure 2.12

Loci of the chromaticity coordinates of common pigments mixed with varying amounts of rutile TiO_2 white in a glossy paint medium. Discontinuities are due to changes in pigment volume concentration (PVC). Dotted sections are interpolated (Johnston 1973).

reflectance, or lightness, Y, for blue 3 are very close to the average for blue 1 and blue 2, as shown in table 2.3.

Although the pigmentations of blue 1 and blue 2 are different, the calculated average chromaticity is still close to that actually measured. If the target or aim color is blue 3, and blues on different sides of the aim point on the chromaticity diagram had been prepared, a very good estimate for a pigment formula that is a close match can be made. No computer color-matching program would be needed to adjust the composition to make a desired color. Even with computer color-matching

Table 2.3
Comparison of chromaticity coordinates (x and y) and the luminous reflectance, or lightness (Y), for blue 3 and the average values for blues 1 and 2.

	x	y	Y
Blue 3	0.2655	0.2813	51.48
Average of blues 1 and 2	0.2662	0.2814	51.76

facilities available, the technique described serves as an excellent evaluation and guide.

The major topic of this monograph is the use of spectrophotometric curves as a guide to pigment identification. However, as was shown, the application of colorimetry is also indispensable in utilizing visible spectral curve measurements to obtain maximum useful information concerning the color composition of objects and materials of interest.

Color-Difference Equations

In the previous section, the CIE system was described as based on additive color mixture. The system was not intended to be visually uniform, such that a fixed distance in color space would represent a constant degree of perceived difference in all regions of color space. Consequently, since the beginning of the CIE in 1931, many attempts have been made to transform mathematically the CIE notation into a system that is visually more uniform. Many equations have been proposed. For a history of this evolution, consult one of the basic reference books on color in appendix E, or see the concise historical summary given by Johnston (1973).

Suffice it to say that any unit of color difference can be helpful in describing the relationship between similar colors, but that the ideal transformation into a truly uniform color space is still elusive and probably does not exist. Nevertheless, whatever transformation equations are used, the resulting information can be helpful for comparing *similar* colors. However, the magnitudes of the visual differences between colors in different regions of color space are not generally comparable: one unit of color difference in the blue region does not represent the same perceived difference as one unit in the red region. To add to the uncertainty in the reliability and usefulness of color-difference measurements in the practical world, surrounding colors in a scene or setting can have a profound effect on a perceived color and hence on perceived color differences.

The reasons for this stem from the complexity of the human perception process, involving the eye and the brain. Psychological effects of contrast, adaptation, scene complexity, memory, association, and so forth, all contribute to our perception. Physical differences in materials—gloss and texture, for example—also introduce confusion. It would be all but impossible to include factors for all of these visual variables in a single color-difference equation, even if they were much better understood.

For some wonderful visual illustrations of these psychological influences on color relationships, the reader is referred to any of the books by Ralph Evans (1948, 1959, 1974). Burnham, Hanes, and Bartleson (1963) present some wonderful illustrations of contrast effects.

To those concerned with complex colored objects—paintings, textiles, etc.—the psychological effects are extremely important. For example, the author had the privilege of measuring the color used in some very old Russian icons that appeared to be brilliantly colored. Measurement revealed, however, that the colors were not brilliant in terms of luminosity or purity; the color contrasts and juxtapositions made them appear so. Likewise, measuring the individual colors used in some oriental rugs also revealed that the colors were not brilliant. Skilled artists and artisans have always learned to utilize the psychological effects inherent in color relationships to create their works of beauty. To the person measuring the colors in these complex scenes, their true physical description can be a bit of a shock. For that very reason, objective measurements are of great help.

In color-difference equations, the total color difference is generally expressed as ΔE, the difference due only to chromaticity differences as ΔC, and the difference in lightness as ΔL. The magnitude of a unit of ΔE calculated for the same pair of colors using different equations is not the same and can vary widely. There is a common misconception that a ΔE of 1.0 represents a just perceptible difference. Instead, for example, the ΔE calculated from equation 2.4, which follows, represents, on the average, about three times a just perceptible difference. This equation, which is one of two recommended by the CIE, is formally referred to as the 1976 CIE L*a*b* equation, but it is also known by its official CIE abbreviation: CIELAB (pronounced "sea-lab"). The CIE did not recommend it because it is the best color-difference equation, but because it could be computed easily with a desk calculator and because a single standard of usage would help to decrease the confusion and misunderstandings that have existed from the use of many different formulas. Its use is recommended for object colors, particularly because it is scaled directly to the ANLAB 40 equation (Adams–Nickerson equation with a scaling constant of 40) widely used by industries dealing primarily with reflecting materials. Color differences calculated with the ANLAB 40 equation may be converted to the CIELAB basis by multiplying by 1.1 (CIE 1986). This is the only instance in which a constant factor can be used to convert color differences calculated using one formula to those obtained using some other equation.

Industries for which additive color mixtures of lights is the major concern prefer to use the 1976 CIE L*U*V* (CIELUV, pronounced "sea-love") equation because of the additivity of its accompanying u, v uniform chromaticity diagram. Note that CIELAB is not similarly additive and does not have chromaticity coordinates or a chromaticity diagram. Texts listed in appendix E and written after about 1978 may be consulted for details about these equations.

In the following CIE L*a*b* formula, ΔE^* represents the total color difference; ΔL^* represents the lightness–darkness difference; Δa^* describes the redness–greenness (+ red–green); and Δb^* describes the yellowness–blueness (+ yellow–blue) (CIE 1986; ASTM Standards D 2244, E 308):

$$\Delta E^*_{ab} = [(\Delta L^*)^2 + (\Delta a^*)^2 = (\Delta b^*)^2]^{1/2} \quad (2.4)$$

where the Δ sign refers to the difference between the sample and the standard in the three dimensions: L (lightness); a (redness–greenness); and b (yellowness–blueness), and

$$L^* = 116(Y/Y_n)^{1/3} - 16 \quad (2.5)$$
$$a^* = 500[(X/X_n)^{1/3} - (Y/Y_n)^{1/3}] \quad (2.6)$$
$$b^* = 200[(Y/Y_n)^{1/3} - (Z/Z_n)^{1/3}] \quad (2.7)$$

The subscript n refers to the tristimulus values for a perfect reflecting diffuser for the illuminant and observer used. For illuminant C and the 2° standard observer, $X_n = 98.074$, $Y_n = 100.000$, and $Z_n = 118.232$.

The above equations are correct when X/X_n, Y/Y_n, and Z/Z_n are all greater than about 0.01, as is usually the case with object colors. The CIE (1986) and most reference texts written after 1978 provide alternative equations for smaller values.

For judging the direction of color differences between two colors, the CIE 1976 hue angle, h_{ab}, and chroma, C^*_{ab}, may be calculated by

$$h_{ab} = \tan^{-1} (b^*/a^*) \quad (2.8)$$
$$C^*_{ab} = [(a^*)^2 + (b^*)^2]^{1/2} \quad (2.9)$$

When describing the difference between two colors using the equation for the total color difference, ΔE^*_{ab}, the lightness difference and the chroma difference are calculated by

$$\Delta L^* = L^* \text{ (sample)} - L^* \text{ (standard)} \quad (2.10)$$

and the chroma difference is described as

$$\Delta C^* = C^* \text{ (sample)} - C^* \text{ (standard)} \quad (2.11)$$

Note that the hue angle, h_{ab}, is expressed in degrees (eq. 2.8) and cannot be used in any equation to describe the total color difference, ΔE. It is useful, however, for visualizing the relationship of colors using graphical techniques, particularly for purposes of hue specifications.

The contribution of the hue difference, as distinct from the chroma and lightness differences, can be computed from the total color difference (eq. 2.4) by

$$\Delta H^*_{ab} = [(\Delta E^*_{ab})^2 - (\Delta L^*_{ab})^2 - (\Delta C^*_{ab})^2]^{1/2} \quad (2.12)$$

Table 2.4 is an example of the calculation for blue 1 and blue 2, whose spectral curves are illustrated in figure 2.10.

Table 2.4

Calculations showing color differences between blue 1 and blue 2.

Blue	X	Y	Z	L^*	a^*	b^*	C^*_{ab}	h_{ab}
1	51.63	53.33	85.52	78.07	−1.64	−17.46	17.54	84.63° + 180° = 264.63°
2	46.42	50.19	80.96	76.19	−7.60	−17.45	19.03	66.46° + 180° = 246.46°

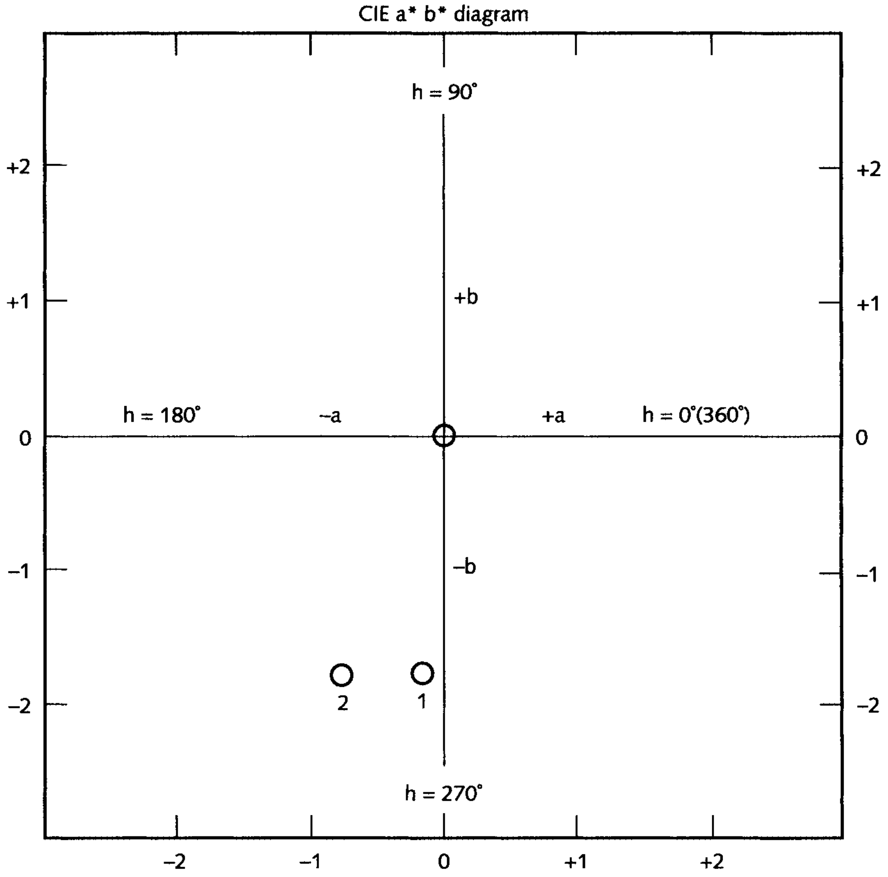

Figure 2.13
Illustration of a method of plotting CIE a*b* coordinates. The small circles labeled 1 and 2 are calculated coordinates for the curves of the two blues illustrated in figure 2.10. It can be seen that they fall in the quadrant bounded by hue angles of 180° and 270°.

A graph of a^* versus b^* is illustrated in figure 2.13. (Because the color is in the third quadrant, 180° have to be added to the calculated hue angle as indicated.) It is apparent that blue 1 is redder than blue 2.

The color differences calculated for blue 2 versus blue 1 as standard are

ΔL^*	Δa^*	Δb^*	ΔC^*_{ab}	ΔH^*_{ab}	ΔE^*_{ab}
–1.88	–5.96	–0.01	1.50	5.08	6.28

From these values it can be seen that the major difference between these two blues is in hue (ΔH): blue 2 is much less red (or is greener) than blue 1 (Δa^* is very negative). Blue 2 is also darker ($\Delta L^* = -1.88$).

Most modern computerized color-measuring instruments use the CIELAB equation, not because it is the best—modifications to it have been made that supposedly better fit visual data—but because, in support of the CIE recommendations for standard practice, the equation is widely recognized and understood. Suffice it to say: *whatever unit of color difference is used in a research report, the equation used must be specified for the benefit of the reader. And for quality control applications, the specific unit to be used must be agreed upon by the correspondents concerned.* The CIELAB color-difference equation (eq. 2.4) will be used throughout this monograph.

It has been common, in specifying total color difference, to refer to the so-called National Bureau of Standards (NBS) color-difference unit. This NBS unit, ΔE, is calculated according to the following equation:

$$\Delta E = f_g \{[221 Y^{1/4}(\Delta\alpha^2 + \Delta\beta^2)^{1/2}]^2 + [k\Delta(Y^{1/2})]^2\}^{1/2}$$

where f_g takes account of the masking influence of a glossy surface on the detection of color differences, k relates the lightness and chromaticity scales, and α and β are defined below. The gloss factor is $f_g = Y/Y + K)$, where K is usually taken as 2.5, and k is usually taken as 10.

$$\alpha = \frac{2.4266x - 1.3631y - 0.3214}{1.0000x + 2.2633y + 1.1054}$$

$$\beta = \frac{0.5710x + 1.2447y - 0.5708}{1.0000x + 2.2633y + 1.1054}$$

Regardless of how it is obtained, the only true NBS unit is that calculated according to the above equation, which is Hunter's modification of Judd's original equation (Judd 1939; Hunter 1942). When this equation was scaled, the assumption was made that a color difference of 1.0 ΔE was a good *commercial* color match, even though it was known to be two to four times the just perceptible difference. The general feeling was that this was a reasonable limit to which commercial color matching could be controlled. Unfortunately, there has long been a misconception that 1 NBS unit or that 1 ΔE^*_{ab}—or another equation scaled to the NBS unit—is a just perceptible difference. This is not correct. This "true" NBS equation was never used widely, probably because it was too complicated for the equipment that was readily available at that time.

Many attempts have been made to transform the CIE color space into more uniform color spaces and better color-difference equations, with better meaning in terms of the ease of calculation and measurement or in terms of better agreement with visual evaluation. Some of these equations were scaled, on average, to agree in magnitude with the NBS unit and were then, unfortunately, called "NBS units." For example, the constant 40 in the ANLAB 40 color-difference equation mentioned above (in the discussion of the CIELAB equation) was added as a scalar constant to adjust the magnitude to be close to the NBS unit, ΔE. As a result, one must always ask which equation was used when one encounters references to an "NBS unit of color difference." In the CIELAB equation presented earlier, ΔE is also scaled to agree generally in magnitude with the NBS unit, but it is not an NBS unit either.

One of the notably different color-difference equations used in the more recent past was based on the research of MacAdam (1942, 1943; Brown and MacAdam 1957). His work resulted in color-difference equations (FMC equations) based on perceptibility ellipses obtained by matching lights (Chickering 1967, 1971; see also ASTM Standard D 2244). These equations were scaled so that 1 unit of difference, Δe, is equivalent to a just perceptible difference. (The unit scaled to the just perceptible difference is designated Δe here to distinguish it from ΔE, which is scaled to the NBS unit.) A difference of 1.0 Δe based on MacAdam's perceptibility thresholds is on the average 0.2 to 0.5 in NBS-scaled units. No fixed conversion factor exists, however, because of the very different mathematical approaches used. The reader is directed to the standard texts on color science in appendix E for further information on the numerous color-difference equations and their supposed merits.

Since the adoption of the 1976 CIE recommendations, a number of new color-difference equations have been developed. Most prominent among them is the CMC equation (McDonald 1980), which is based on the *L*,*C*, *H* form of CIELAB and has significantly improved visual uniformity.

Tristimulus filter colorimeters

Color-difference equations were originally developed for industrial quality control. In the 1940s and the 1950s, photoelectric spectrophotometers were either manually operated and hence very time consuming to use, or automatically recording and consequently very expensive. This situation led to the development of tristimulus filter colorimeters designed to measure how closely a sample matched a standard. Hence they were often called color-difference meters. Their design incorporated sets of three filters that provided measurements approximating the three tristimulus values X, Y, Z. The filters were selected to take into account the spectral characteristics of the light source and of the detector response, in addition to the $\bar{x}$, $\bar{y}$, $\bar{z}$ color-matching functions of the CIE 1931 standard observer and illuminant C. Thus the instruments were an attempt to perform, in essence, an optical integration instead of a mathematical integration at individual wavelengths to obtain the tristimulus values X, Y, and Z. The readings so obtained were called R, G, and B, and were in terms of percentages. To obtain the tristimulus values for the 1931 standard observer and illuminant C, the following equations were used:

$$\begin{aligned} X &= (0.8R + 0.2B)/0.98 \\ Y &= G \\ Z &= 1.18B \end{aligned} \tag{2.13}$$

Later instruments used a fourth filter to measure the blue loop in the X tristimulus value.

A number of tristimulus filter colorimeters were designed. Most of them utilized bidirectional geometry (45°/0° or the reverse). Later, instruments were developed that utilized an integrating sphere.

Widely used color-difference meters incorporated a simple transformation of R, G, and B into a color-difference equation (Hunter 1942, 1958) as follows:

$$L = 10G^{1/2} \tag{2.14a}$$

$$a_{\mathrm{L}} = 17.5(R - G)/G^{1/2} \tag{2.14b}$$

$$b_{\mathrm{L}} = 7.0(G - B)/G^{1/2} \tag{2.14c}$$

$$\Delta E = [(\Delta a_{\mathrm{L}})^2 + (\Delta b_{\mathrm{L}})^2 + (\Delta L)2]^{1/2} \tag{2.15}$$

This simple equation represented an attempt to approximate the NBS color-difference equation. Because the instrument was inexpensive and simple to operate, it was widely used for quality control in paint-related industries and for other applications. The total-color-difference unit, ΔE, was widely called an NBS unit. However, the equation built into the Hunter Color Difference Meter is not the NBS equation, and the ΔE obtained should not be called an NBS unit, although it is scaled to the true NBS unit. Unfortunately, the ΔE determined by use of the above equation was often called an NBS unit of color difference, contributing considerably to the confusion over the equation actually used.

Tristimulus filter colorimeters were not designed to measure tristimulus values accurately. Indeed, the results from early instruments varied significantly from values obtained by spectral integrations; they varied also from instrument to instrument. Later instruments were more carefully controlled as improvements in technology developed. Tristimulus filter colorimeters play a useful role, but only if their limitations as well as their advantages are properly understood. They were designed to compare materials with similar composition, that is, similar spectral curve shapes, and with similar appearances, such as surface reflection and uniformity.

The use of an optical integrating technique (filters) to obtain color differences has a very real advantage over the use of abridged spectrophotometry (measurements at a limited number of wavelengths, such as 20 nm intervals) or abridged calculations of spectral data (such as calculations of tristimulus values at 20 or even 10 nm). This advantage appears when measuring high-chroma (very saturated) yellows, oranges, and reds (also purples). The difference in the curves of two very similar colors of this type is generally manifest in the spectral region where the curves begin their steep rise. The difference may be over a few nanometers (5, for example) in width but would be missed by the use of a limited number of spectral points. And a color match would be indicated, whereas visual examination would indicate no match.

Additional comments

Distinctive color-difference specifications are often written that depend on (1) the area of color space involved—the green, red, or blue area, etc.; (2) the acceptability of variations in specific materials; and (3) preferences. If the color of butter is on the green side of standard, even by a small amount, it is unacceptable. However, butter that is more golden in color, even if different from the standard by the same color difference or more, is perfectly acceptable. Thus, the type or direction of the color difference from the standard is often more important in "acceptability" than is the total color difference, ΔE. Experience has shown that differences in hue are most important; differences in saturation are less important; and differences in lightness are least important. The ratio of difference of tolerance has been estimated to be hue 3, saturation 2, lightness 1. However, all such generalities can fail depending on the color composition in a complex scene and on preferential directions of color differences that may be considered tolerable or acceptable.

The use of color-difference equations to describe color change resulting from exposure to deleterious conditions over a period of time requires special interpretation; this includes, most importantly, analysis of spectral curve changes resulting from changes in colorant concentration (see chap. 4). Simply reporting changes in terms of ΔE is almost useless to the researcher, regardless of the equation used, because quantifying exposure-related changes involves making measurements over extended periods of time. The reliability of such measurements must be ascertained: How carefully is the instrument calibrated and operated? What is the reproducibility with which the instrumental measurements can be made? Are the measured values greater than the uncertainties with which the measurements can be reproduced over the period of time? Consider also the nature of the change: How uniform is it? Has the gloss changed? Has colorant been lost? Have all the colorants in a mixture decreased in concentration in a similar way? Has a paint chalked rather than faded? From a simple ΔE color-difference figure, little of this information can be obtained that will contribute to an understanding of the changes that have taken place. The directional components of color differences, obtained by plotting and comparing colors on a chromaticity or CIELAB a^*b^* diagram, can be more informative. However, when describing changes following exposure in analytical terms, colorant concentration calculations described in chapter 4 and study of the spectral curve changes can be more meaningful in learning the source of, or reasons for, the observed visual change.

Metamerism

Metamerism is a phenomenon that plagues all those who must match colors. Two colors are said to be *metameric* if they appear to be the *same* color (that is, they match) to an observer under one set of illumination and viewing conditions, but appear to be different if any one of these conditions is changed. The conditions include the spectral character of the illuminant under which the pair of colors is observed; the spectral reflectance or transmittance of the objects; the particular response of the observers looking at the color pair; and the directional or geometric conditions of the viewing.

Illuminant differences are illustrated by the spectral distributions of daylight (bluish), incandescent light (orangish), and fluorescent lamps (with various phosphors and strengths of the mercury lines). Observer response differences exist among persons with normal color vision. Most of us are not "standard observers" as represented by the average figures used in the CIE calculations. For a detailed analysis of the uncertainties, the papers by Nimeroff (1957, 1966) may be consulted. Allen (1970) described a calculation for observer metamerism. Older persons whose lenses have yellowed to some degree do not see metameric pairs the same as younger people. Viewers with any degree of abnormal color vision should not be involved in making color-match judgments. It is advisable that all persons involved in making color-match decisions be checked for color vision deficiencies.

When object colors that match—to one person in one light source—no longer appear to be identical if either the illuminant is changed or a different observer looks at them under the same light, the mismatch is the consequence of differences in the spectral distribution, that is, the reflection or transmission curves, of the two object colors. The two object colors are metameric as disclosed by the measurement of their different spectrophotometric curves. One can modify the term metamerism to describe the particular change made in viewing conditions that led to the observation of the phenomenon. Thus *illuminant metamerism* describes the color shift observed when the light source is changed, and *observer metamerism* describes the change that occurs when a different observer views the pair of colors. In either case, the color changes result from differences in the spectral distribution of the pair of samples being observed.

A pair of colors that seem the same when viewed under one angular condition but no longer seem to match when the angle of illumination or viewing is changed have been called geometric metamers, and the phenomenon called *geometric metamerism* (Johnston 1967a; FSCT 1995; Pierce and Marcus 1994). In this case, the change in color relationship observed with a change in angle of illumination or view is generally attributable to differences in the *structure* of the pair of objects or materials being compared, that is, to differences in the *surface* characteristics or in the *internal* particle composition or distribution. Such pairs may also exhibit differences in their spectral distribution curves due to variations in the types of chromatic pigments used so that changes in the spectral character of the illumination and in the response characteristics of the observer will also occur, resulting in two types of metameric differences.

In the paragraphs that follow, illuminant metamerism and observer metamerism will be discussed before geometric metamerism. Use of the term *geometric metamerism* for color changes in color pairs that match under one set of angular viewing conditions but do not match if the angular conditions are changed has been questioned. This issue will be discussed at the end of this section.

An excellent paper on metamerism due to pigment spectral-curve differences, and its importance in the retouching of paintings, is that of Staniforth (1985). One of the interesting facts she points out is that metameric pairs, which seem to match under a particular light source and to most observers, may look different if photographed in color under the same light source. This occurs because the three color-sensitive layers in color film used to produce the colored image are different from the normal sensitivities of the eye, particularly the red-sensitive film layer. The film reacts differently from the eye to differences in spectral distribution. In general, the differences in sensitivity in various color films are much larger than those among normal human observers. One can consider this film sensitivity difference as a special case of observer metamerism, the color film being the observer.

In her article, Staniforth shows the spectral reflectance curves of metameric matches to traditional blue pigments, using a variety of blue pigments available today. In each case only one blue pigment was used in combination with other colored pigments as needed to make the match. Closer, less metameric matches could probably have been made if two or more blue pigments were used in combination. Such complex formulations would be difficult to make by visual means alone, however.

The blues illustrated in figure 2.10 are not metamers because they would not match under any normal light source or to any normal observer. The definition of metamerism bears the stipulation that two colors match under *some* condition of illumination and viewing. The same two blue pigments used to make blues 1 and 2 illustrated in figure 2.10 could be used in a formulation that would match the other under one set of standard conditions. For example, a match to blue 1, made with ultramarine blue, was calculated using blue 2, phthalo blue; a match to blue 2, made with phthalo blue, was calculated using blue 1, ultramarine blue. Table 2.5 shows the formulations obtained and the tristimulus values and chromaticity coordinates for these mixtures. The tristimulus values are based on 5 nm interval reflectances from 400 nm to 700 nm. The data are calculated for illuminant C and the 1931 standard observer, and measurements made with the specular reflection component were excluded.

The tristimulus values and chromaticity coordinates indicate that the metameric matches are not perfect, but nonetheless they are very close. The calculated color differences using the CIELAB equation (eq. 2.4) suggest that the differences are probably imperceptible: $\Delta E^*_{ab} = 0.29$ for the first pair, and $\Delta E^*_{ab} = 0.24$ for the second pair. Figures 2.14 and 2.15 illustrate the spectral reflectance curves for the pairs. Comparing the areas between the curves would lead one to suspect that the blue pair 2–2a would be more metameric than pair 1–1a because there is more space between the curves.

The use of the term "more metameric" implies that there is a degree of metamerism, that is, some pairs are more severely metameric than others. In 1972 the CIE published "Special Metamerism Index: Change of Illuminants" (CIE 1972, 1986). Assuming a pair of colors is a perfect match under a particular illuminant, the color difference—ΔE—calculated for another, defined test illuminant constitutes the Metamerism Index. An example is the calculation of the color difference in illuminant

Table 2.5

Metameric matches to blue 1 and blue 2 in fig. 2.10 (CIE notation for illuminant C, 1931 standard observer).

Blue	Pigmentation	X	Y	Z	x	y
1	12.5% ultramarine blue 0.02% black 87.48% TiO_2	51.63	53.33	85.52	0.2711	0.2800
1a	0.172% phthalo blue 0.181% Quinacridone Red[a] 0.014% black 99.633% TiO_2	51.52	53.31	85.22	0.2711	0.2805
2	0.25% phthalo blue 0.10% black 99.65% TiO_2	46.42	50.19	80.96	0.2614	0.2826
2a	14.435% ultramarine blue 0.158% phthalo green[b] 85.407% TiO_2	46.24	49.93	80.57	0.2616	0.2825

[a] See fig. A.16 in appendix A.

[b] See fig. A.22 in appendix A.

A for a metameric pair that is a perfect match in illuminant C. The index would be the ΔE determined in illuminant A. Color differences under different illuminants are routinely used in computer colorant formulation calculations, but many workers have found this to be of limited value in the real world when the samples are prepared and do not match precisely.

A more general index of metamerism was described by Nimeroff and Yurow (1965). The spectral differences between the curves of a pair of metamers were weighted by the observer color-matching functions and the spectral power distributions for the illuminant in which the pair match. Their suggested index, however, has not been used extensively.

In the real world it is seldom the case that a pair of metamers matches perfectly to the standard observer under the calculated illuminant. However, if the match is very close, as is the case for the blues described above, calculating the color difference for a different illuminant can be helpful. Thus, the first pair of blues (blues 1 and 1a in

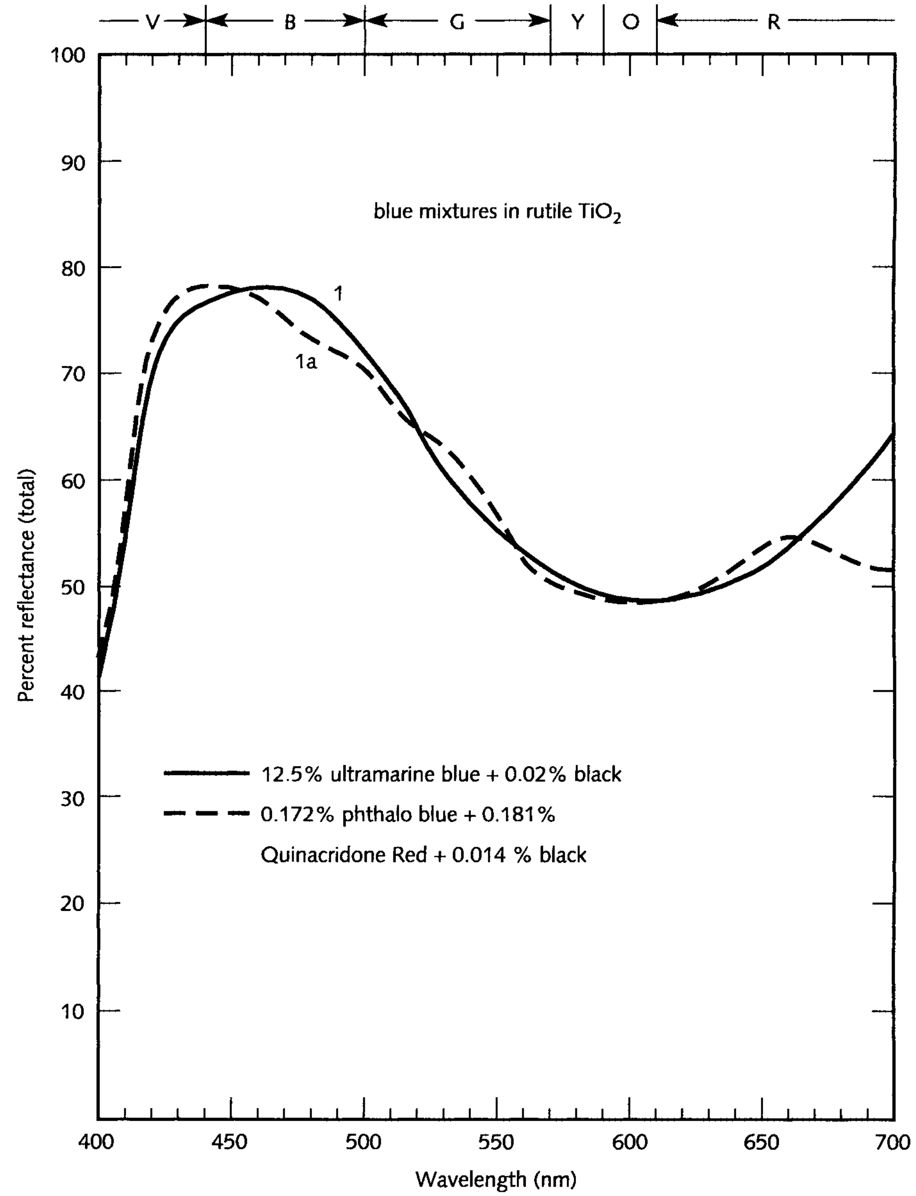

Figure 2.14

Metameric match (curve 1a) to blue 1 made with the same blue pigment, phthalo blue, used in blue 2 (fig. 2.10). Note that Quinacridone Red had to be added to achieve the necessary redness.

fig. 2.14), which had a total color difference ΔE^*_{ab} of 0.29 in illuminant C, has a ΔE^*_{ab} in illuminant A of 0.61. The second pair (blues 2 and 2a in fig. 2.15), which had a ΔE^*_{ab} of 0.24 in illuminant C, has a ΔE^*_{ab} of 0.41 in illuminant A. Thus, we see that the color differences for both are larger in illuminant A. The differences would be readily perceptible in illuminant A but would not be severe.

The CIE recommends that if an exact match cannot be made, a formulation correction should be made. If that is not possible, "an additive or multiplicative correction could be made" (Judd and Wyszecki 1975). While the CIE did not describe the method for doing this correction, Brockes (1969, 1970) has worked out the technique. He found, as have other workers, that the multiplicative method gives the best agreement with visual evaluations. Applying this method to our blue pairs (table 2.5) serves to illustrate the procedure. Let the original samples, 1 and 2, be the standards, and 1a and 2a be the matches.

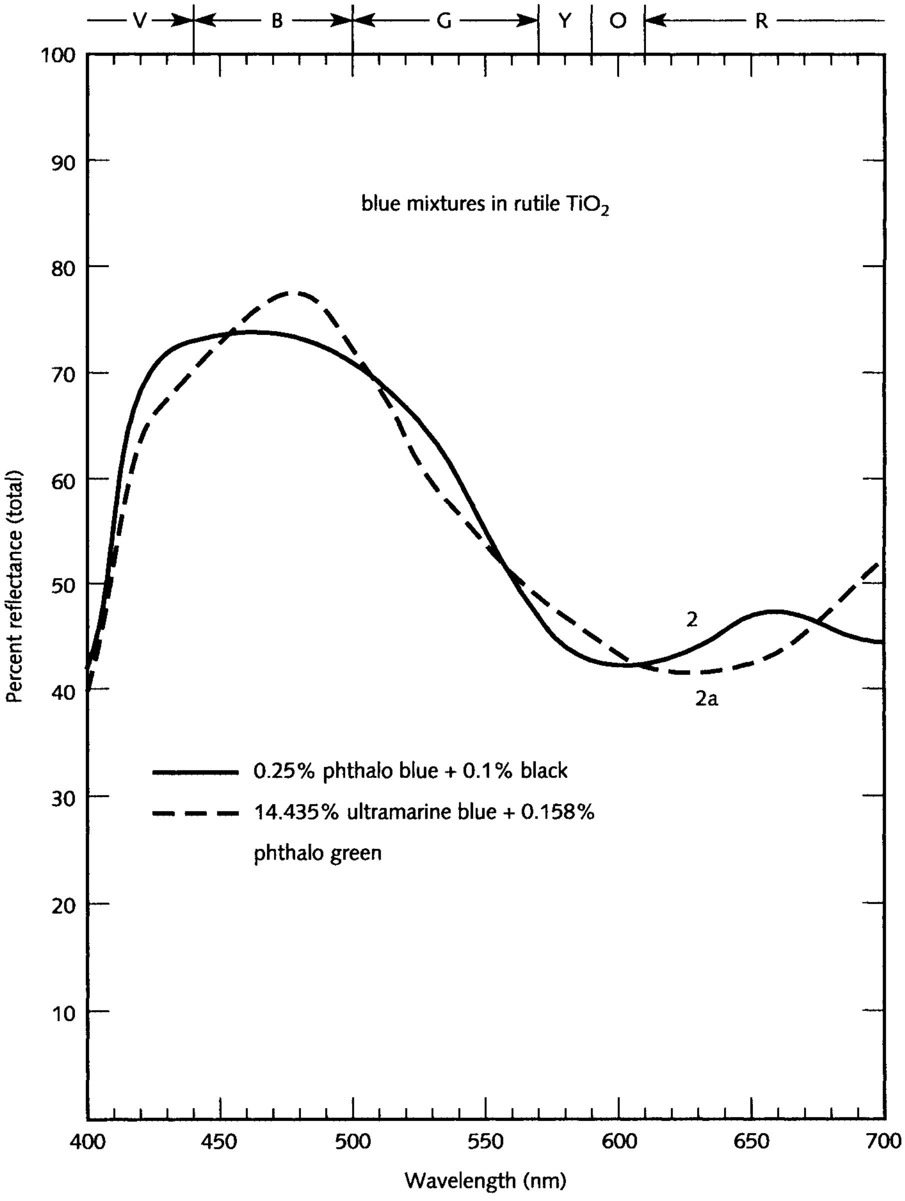

Figure 2.15

Metameric match (curve 2a) to blue 2 made with the same blue pigment, ultramarine blue, used in blue 1 (fig. 2.10). Note that phthalo green had to be added to achieve the necessary greenness.

1. Determine the factors by which X, Y, and Z under the reference illuminant (C in the case of the blues) must be multiplied to give the exact values of X, Y, and Z for the standard:

   For pair 1: $f_X = 51.63/51.52 = 1.002135$
   $f_Y = 53.33/53.31 = 1.0003752$
   $f_Z = 85.52/85.22 = 1.0035203$

Thus, if the tristimulus values of the metameric match (sample 1a in this case) are multiplied by these factors, it will be a perfect match.

2. Multiply the tristimulus values of the metameric match in the test illuminant (A in this instance) by these same factors to adjust them for the mismatch, assuming that the match had been perfect under illuminant C. The tristimulus values under illuminant A for the standard in this case, sample 1, are $X = 53.27$, $Y = 50.90$, $Z = 25.63$. The tristimulus values for sample 1a in illuminant A are $X = 53.05$, $Y = 50.88$, $Z = 25.40$.

   $X_{\text{corr}} = 1.00214\ (53.05) = 53.16$
   $Y_{\text{corr}} = 1.00038\ (50.88) = 50.90$
   $Z_{\text{corr}} = 1.00352\ (25.40) = 25.49$

Calculate the color difference of the adjusted tristimulus values between sample 1a and the standard (sample 1) in illuminant A. This is $\Delta E^*_{ab} = 0.425$, which is smaller than the color difference (0.61) obtained without making the correction. When the tristimulus values for the second pair are similarly corrected, based on the degree of the mismatch in illuminant C, the color difference in illuminant A is 0.788, which is much larger than what the uncorrected data showed and is consistent with the larger areas between the curves for the second pair of blues. In the experience of this author, the index determined in this way is a better index of metamerism for samples in the real world than an index without the correction.

Other factors make it difficult to establish a metamerism index that would serve to describe the degree of metamerism in agreement with visual observation. One, already mentioned, is the fact that most of us are not standard observers. That is, our eyes' color-matching functions (our visual responses) are not the same as the figures used for the CIE standard observers. This fact always presents a problem when one is evaluating the closeness of a metameric match that must satisfy more than one observer. Two colors may appear to match when viewed by the person who made the samples, but not by someone else, perhaps a client, who evaluates the pair under the same illumination and viewing conditions. This is the very practical meaning of observer metamerism.

An important factor that basically affects all CIE measurements, and hence also all equations based on CIE values, is the method of making the measurements, particularly the instrument band pass (resolution) and the wavelength interval used in the measurement and in the integration calculation. The color differences calculated by different laboratories using instruments of different design may be different. For nonmetameric pairs, or those with very similar spectral curve shapes, the use of large wavelength intervals, such as 20 nm (16 wavelengths), will have a minimal effect on the color differences calculated, even though the tristimulus values will not necessarily be the same as those based on, say, 5 nm intervals. However, when the samples are metameric and have notably different curve shapes, the color differences calculated will be very much dependent on the wavelength intervals used; the greater the differences in area between spectral curve shapes of the individuals of the metameric pair, the more serious the discrepancy may be in the calculated tristimulus values and, hence, in the calculated color differences. A band pass and wavelength interval of 5 nm or less has been shown to provide values that are not significantly different from those obtained by continuous integration (CIE 1986; ASTM Standard E 308).

One may well ask: If a continuous integration is desirable, why not use a tristimulus colorimeter to make the measurements, since such instruments simulate a continuous integration by the use of filters? The answer is that most of the tristimulus filter instruments available in the past, and some that are still used today, were essentially color blind: the combination of light source, filters, and detector response characteristics did not match the CIE color-matching functions and illuminant distribution very well. They were, and are, basically unsuitable for measuring the color difference between colors that are metameric. Some tristimulus colorimeters available today approach agreement with the CIE functions for one illuminant and one observer, but they cannot provide the measurements for another illuminant or observer necessary for determining the degree of metamerism.

An additional characteristic of the phenomenon of metamerism, although perhaps obvious, is the fact that the degree of metamerism can be most severe on low-chroma colors, such as near neutrals, which can be made with many different colorants. Bright, high-chroma colors, especially yellows, oranges, and reds, if they can be matched at all, will have to have almost identical spectral curves and will not be noticeably metameric even if made with different colorants. On such colors, which have very steep rises in reflectance, use of a band pass and measurement interval of 5 nm or less is desirable for accurate measurements. Even when using 10 nm intervals, one can miss the important wavelength where the steep rise in the curve takes place. On such high-chroma samples, which are essentially nonmetameric, as mentioned before, a tristimulus filter colorimeter is more satisfactory for measuring small differences in color; it provides more sensitive and more accurate results than those obtained with measurements at 20 nm or even 10 nm intervals. For these high-chroma yellows, oranges, and reds, an index of metamerism is generally not necessary, but accurate measurements of color differences are. The blue metamers described earlier were measured at 5 nm intervals. If the degree of metamerism were determined by measurement at 20 nm intervals, the index would be different.

Formulation of nonmetameric matches for pastel shades and near neutrals can be challenging without some information on the colorants involved. This can be learned either from the spectral reflectance curve shape or from some other analytical technique. Determining the palette of colorants used by measuring the reflectance spectra in various parts of a multicolored or variegated object can often be helpful. However, even though an identification has been achieved, decisions still often must be made on whether or not to use the same colorants in formulating a match, taking into consideration such factors as their lightfastness, availability, cost, and so forth.

A basic feature of the spectral curves of metameric pairs is that they must intersect or cross one another at least three times (Stiles and Wyszecki 1968). Our metameric blues intersected five times. A perfect curve match represents an infinite number of crossovers; a pair of samples with curves that intersect only once or twice are not metamers.

Because metameric color matches cause so much confusion, it is obviously desirable to avoid having to make them. Instead, it would be better to use the same colorants in the match that are used in the standard. This has traditionally been attempted by conservators when inpainting losses in objects of fine art. However, this is not always possible. So if imperfect matches must be settled for, it is best to make them with as little metamerism as possible.

Geometric metamerism—a special case

Pairs of colors that appear to be the same at one angle of illumination and a particular angle of viewing, but do not appear to be the same if either the angle of illumination or the angle of viewing is changed, have been called geometric metamers. The term *geometric metamerism* has not been accepted officially by any standardizing organization (Johnston 1967a; FSCT 1995; Pierce and Marcus 1994). Nevertheless, it remains a useful descriptor for this phenomenon. Such pairs of colors change from a match to a mismatch as the illumination angle is changed while the viewing angle is kept constant, and vice versa. The change in color, lightness, and chromaticity can be observed by holding the sample pair side by side in a viewing booth, observing the color from the front and then rotating the sample pair with the result that the light from the lamps in the inside top of the booth illuminates the samples at different angles. If both colors appear to match at one particular angle of illumination, but then one color appears lighter if rotated in one direction and darker if rotated in the other direction from the match point, or if their hues or chromas appear to change, the pair is exhibiting geometric metamerism.

The causes of the phenomenon are generally associated with structural differences rather than spectral differences. The structural differences may occur inside the materials, or they may occur on the surface, particularly with materials of low gloss.

In order to measure the reflected color change with angle, a goniospectrophotometer is necessary (Judd and Wyszecki 1975). Such an instrument was described in chapter 1. All of the angular measurements described in this monograph, including the ones in chapter 5 and in the description of surface reflection in chapter 6, were made using the Trilac spectrophotometer operated in the gonio mode; the tristimulus values were calculated at 10 nm wavelength intervals.

When *colorimetric metamerism* (metamerism due to differences in spectral curve shape) as well as geometric metamerism both occur in a pair of samples, the problem can be very confusing and difficult to explain without the aid of goniospectrophotometry.

Discussion

There are differences of opinion about the proper definitions for many terms used to describe appearance phenomena such as metamerism. In the author's opinion, the criteria for a good definition are that it be (1) as descriptive of the particular appearance aspect as possible and (2) that it be as simple and as easily understood as possible. The subject of this section is metamerism, an appearance phenomenon, and its definition given in the first paragraph of this section describes it without reference to causes. Various causes of the phenomenon are described in terms of changes in the characteristics of the illumination, observer, or angular viewing conditions. Thus, we have used the terms *illuminant metamerism, observer metamerism,* and *geometric metamerism.* To the author, these terms are simple and understandable, and they will be used throughout this book. If the specific type of metamerism is not indicated, it is assumed that the phenomenon is caused by differences in the spectral reflection or transmission curves of the materials being compared.

Other terms, which haven't gained general acceptance, have been proposed to describe the color change in materials when the angular conditions of illumination or view are changed. For example, a *single* color may appear different at different angles. Such a color has been described as goniochromatic, and the phenomenon is called *goniochromatism* (Hemmendinger and Johnston 1970; FSCT 1995). It follows that a *pair* of colors that appear to match under one angular arrangement of light source and observer, but no longer match when the conditions are changed, are called a goniometachromatic pair, and they are exhibiting *goniometachromatism.* If a pair matches at all angular conditions, they are said to be gonioisochromatic and exhibiting *gonioisochromatism.* These terms are cumbersome and not widely used.

The term *metamerism* also applies to a pair of light sources that appear to be the same to one observer but not to another, and that illuminate one colored object identically but not another object of different spectral reflection or transmission characteristics. This phenomenon is an important consideration in museums and in conservation studios. The color of a light source is generally described by its correlated color temperature, *K*, which does not describe its spectral distribution. Two light sources may have the same correlated color temperatures but different spectral emissions—in essence, exhibiting metamerism. However, the term *metamerism* is not applied to light sources. Instead, the degree of difference of a test light source relative to a reference light source is described by its color rendering index (CIE 1995). Briefly, as the index approaches 100 (identity to the test reference lamp), the more closely the spectral emission of the test lamp matches that of the reference lamp.

Considering the many materials used in producing colors—colorants, photographic film, the phosphors used in a television tube, etc.—one realizes the many opportunities for metamerism to occur. It is a tribute to those individuals who study and work to minimize the magnitude of the differences that many observers are not more aware of the phenomenon.

Other Color Notation Systems

At the beginning of this chapter, it was pointed out that any system for describing color must be three-dimensional. There can be three bases for arranging colors in an orderly array: (1) on the basis of appearance (a perceptual evaluation); (2) on the basis of additive color mixture (psychophysical); or (3) on the basis of subtractive colorant mixture (physical mixing of colorants). Of the many color systems, only a few will be discussed here. For more information the reader is referred to the description of methods for describing color given by Judd and Wyszecki (1975); to the references in appendix E; and to the specific articles cited later. A book by Agoston (1987) presents the usefulness of color theories and systems from an art historical point of view, including the theories of Goethe, Chevreul, and Rood.

The CIE system described earlier in this chapter is based on additive color mixture, and no collection of color samples exists for this system. In order to visualize the colors represented by the CIE values, it is necessary to compare them to real colored materials defined in CIE notation. One of the most extensive and widely used collections of carefully controlled color chips are those representing the Munsell system.

Munsell system

Of the many color-order systems devised, the Munsell system, which is based on appearance, is most widely used (Munsell 1905; Nickerson 1940). Color chips illustrating the system are readily available in the *Munsell Book of Color*. The three dimensions in this system are perceptual, and they correspond in general to hue, saturation, and lightness. *Munsell Hue* describes hue; *Munsell Chroma* corresponds to saturation; and *Munsell Value* corresponds to lightness. Throughout this book, capitalized Hue, Chroma, and Value will be used to identify Munsell dimensions.

The system arranges five basic Hues—red, yellow, green, blue, and purple—in a circle. They are designated by the capital letters R, Y, G, B, and P. Five intermediate Hues are designated YR (yellow-reds or oranges), GY (green-yellows), BG (blue-greens), PB (purple-blues), and RP (red-purples). A numerical prefix is used to further differentiate the Hues, based on ten steps. For example, starting at the center of the reds, which is designated 5R, and moving clockwise around the Hue Circle, we find that 10R equals 0YR; 10YR equals 0Y; 10Y equals 0GY, and so on. (See the Hue Circle at the bottom of fig. 2.16.) If no number is used with the Hue designation letter, the assumption is that it is 5, the center

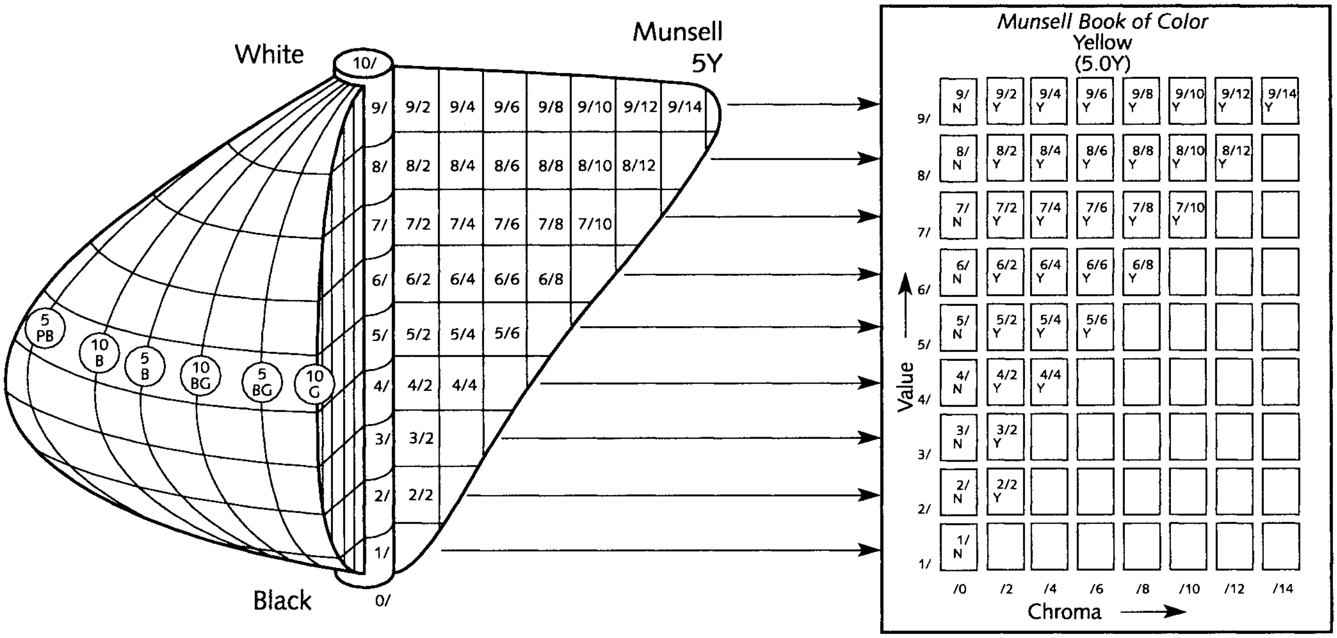

Munsell Book of Color
Yellow
(5.0Y)

Value	/0	/2	/4	/6	/8	/10	/12	/14
9/	9/ N	9/2 Y	9/4 Y	9/6 Y	9/8 Y	9/10 Y	9/12 Y	9/14 Y
8/	8/ N	8/2 Y	8/4 Y	8/6 Y	8/8 Y	8/10 Y	8/12 Y	
7/	7/ N	7/2 Y	7/4 Y	7/6 Y	7/8 Y	7/10 Y		
6/	6/ N	6/2 Y	6/4 Y	6/6 Y	6/8 Y			
5/	5/ N	5/2 Y	5/4 Y	5/6 Y				
4/	4/ N	4/2 Y	4/4 Y					
3/	3/ N	3/2 Y						
2/	2/ N	2/2 Y						
1/	1/ N							

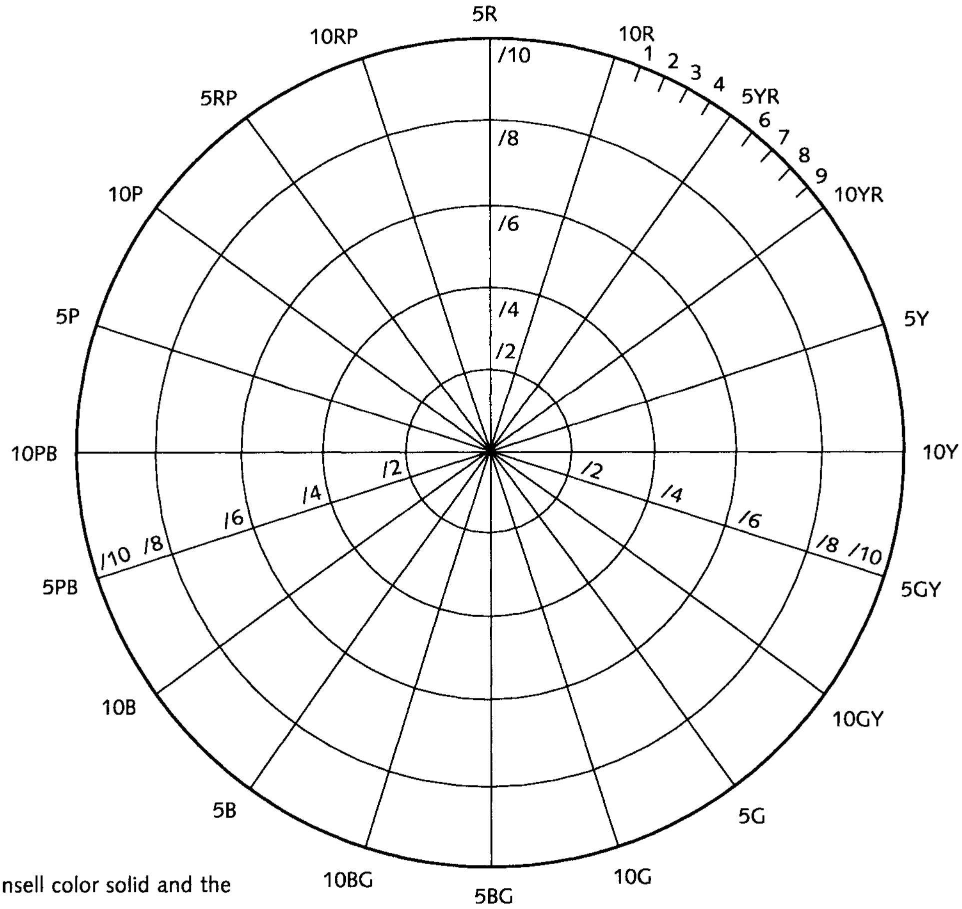

Figure 2.16

Cutaway of the Munsell color solid and the corresponding constant Hue page, 5Y, from the *Munsell Book of Color* (top). The Hue Circle, with Hue letters and numbers and Chroma designations radiating from the center (bottom).

of that Hue category. Decimal fractions may be added to the number prefix to subdivide Hue further, for example, 5.8R.

At the center of the Hue Circle is the gray or neutral point. A perpendicular gray axis through this point, black at the bottom and white at the top, leads to a three-dimensional array. Ten steps of Munsell Value (lightness) start at 0 for black and end at 10 for white, with intermediate steps perceived as having uniform differences in Munsell Value. Again, decimal fractions may be used to define Munsell Value precisely.

The three-dimensional nature of the system is illustrated by the Munsell color solid in the upper portion of figure 2.16. Radiating outward from the neutral axis, the colors increase in Munsell Chroma as the radius increases, so that the purest colors occur at the periphery. The numerical designation of Munsell Chroma starts at 0 for neutral gray and increases outward to the most saturated colors, with a Chroma in the range 14–16 indicating very pure colors. Decimal fractions again define colors precisely. The Chroma scale is open-ended so that it may be expanded to include colors approaching the spectral limits.

Munsell devised the following notation scheme for his color-order system: Hue Value/Chroma, for example, 5.1Y 7.8/10. A cutaway view of the Munsell color solid for Munsell Hue 5.0Y (5.0 yellow) is also shown in figure 2.16 as a page from the *Munsell Book of Color*. The chips in the glossy edition of the book are removable for easy comparison.

The Munsell notations for the three blues discussed earlier and illustrated in figure 2.10 are

blue 1	3.73PB 7.66/4.60
blue 2	0.05PB 7.47/4.79
blue 3	2.18PB 7.55/4.66

Because the Munsell notation describes visual appearance, it is always determined from spectrophotometric measurements made with the specular reflectance excluded. The Munsell notations are included in accompanying tables for all of the spectral curves in appendix A.

There are many reasons for the popularity and usefulness of the Munsell system. It is exemplified by real color chips in the *Munsell Book of Color*, which is a carefully controlled illustration of the system; it is an open-ended system in the Chroma dimension so that the development of new, vivid colorants and new sources of color can be accommodated; and, last, it has been defined in terms of the 1931 CIE system for illuminant C, enabling one to transform between measured CIE values and Munsell notation. The accepted CIE values are for the renotation resulting from the smoothing of the system published by Newhall, Nickerson, and Judd (1943).

It should be emphasized that the *Munsell Book of Color* is a representation of the concept of Munsell spacing; it is a carefully made illustration of the Munsell system. The color, gloss, and spectral curves of the chips in the book are carefully controlled. Even so, small differences in chips bearing the same notation do exist for practical reasons of colorant durability and availability, and the use of new types of more stable colorants. In addition, there can be small, visible differences in color matching from batch to batch. Thus, the chips in the book are not primary standards.

In *Principles of Color Technology,* Billmeyer and Saltzman (1981) present colored illustrations of a page from the *Munsell Book of Color;* a three-dimensional Munsell Color Tree; a diagram of the organization of the Munsell system; and examples of color tolerance charts.

The relationship between Munsell notation and CIE color notation is not a simple one. Traditionally, Munsell notation was established from measured CIE values by using a table of Munsell Value versus the tristimulus value Y, and by referral to a published set of chromaticity charts (such as shown in fig. 2.17) for Munsell Values 1 through 9 at whole-number Value steps, and for near neutrals on an expanded scale for Values 5 through 9. When the Munsell Value of the sample determined from the table of CIE Y tristimulus values versus Munsell Value is not a whole number, as represented in the charts, interpolation between charts of the two adjacent Values must be made. The table of Munsell Value versus Y, along with small (about 5 × 6 inches) conversion charts and the method for using them, are described in ASTM Standard D 1535 and in the book by Wyszecki and Stiles (1982). The chart for the level of Munsell Value 6 in CIE 1931 color space is illustrated as figure 2.17. Enlarged charts, 22 × 26 inches, make the task of converting between systems much easier. They may be purchased from Munsell (see *Munsell Book of Color* in references).

This laborious graphical technique was used for many years to control the Munsell color chips. Today computer programs are available for calculating Munsell notation (Rheinboldt and Menard 1960). The reader is warned, however, that the Munsell notations as read out by

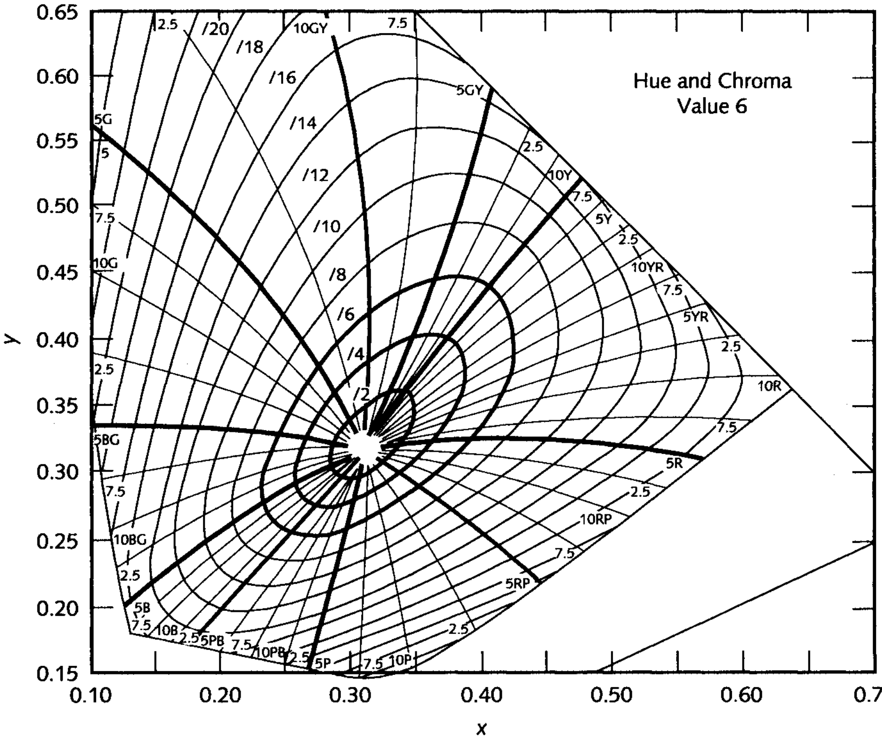

Figure 2.17

CIE 1931 chromaticity diagram showing loci of constant Munsell Chroma and constant Munsell Hue at Value 6 (after ASTM Standard D1535).

some relatively inexpensive measuring instruments may be quite inaccurate. Because of the nature of the CIE–Munsell conversion, one can occasionally get an incorrect notation or no notation at all, even with the best of programs. In the author's experience, this generally occurs with very high chroma colors such as can be made with transparent glazes. If the conversion between CIE notation and Munsell notation needs to be made frequently, it is a good idea to have a set of the charts, particularly the enlarged charts, for reference, as well as the *Munsell Book of Color* for visual comparisons, in case the computer program fails. With the charts, extrapolations can be made over a small range for higher chroma colors. As usual, if no measurement can be made on a particular sample, the chips in the *Munsell Book of Color* can be used for a visual estimate of the color notation by interpolating among the nearest chips in the book.

Special color chips and cards with accurate Munsell notations—for example, soil charts that describe earth colors—are offered by Munsell. The company will also make special chips to match a desired color, as well as tolerance charts representing the desired limits of color variation about a standard.

Universal color names and dictionary

Another publication that describes a language for color description and is very useful in a number of ways is *Color: Universal Language and Dictionary of Names* by Kelly and Judd (1976). The title of the earlier edition indicates the origin of the work: *The ISCC–NBS Method of Designating Colors and a Dictionary of Color Names* (Kelly and Judd 1955). The ISCC is the Inter-Society Color Council, and the NBS was the National Bureau of Standards (now known as the National Institute for Standards and Technology). The original publication was a joint effort of these two organizations. The 1976 book provides a six-level system for describing colors in order of increasing preciseness from a simple color name, such as pink, level 1, up to level 6, with accurately measured descriptions such as the CIE notation or Munsell notation calculated from the CIE values. The level just below the samples in the *Munsell Book of Color* is the ISCC–NBS Universal Color Language, level 3. In this level, one of 267 descriptive names is assigned to a color, based on its Munsell notation, using charts of Munsell Value versus Munsell Chroma for a range of adjacent Munsell Hues. There are thirty-one such color-name charts. A representative one is reproduced in figure 2.18 for the Munsell Hue range 9B–5PB, reproduced from the 1976 edition. Included in this figure are the loci of the three blues discussed earlier in this chapter. In the Universal Color Language they would be called "pale blue" or "very pale blue," being very close to the line dividing these two regions. This description is its color name in the Universal Color Language.

Thus, the Universal Color Name can be determined for any Munsell notation. It may be obtained from comparison with the nearest Munsell chip in the *Munsell Book of Color* (level 4) or from visual interpolation between neighboring chips in the *Munsell Book of Color* (level 5). All of the pigments described in volume one of *Artists' Pigments: A Handbook*

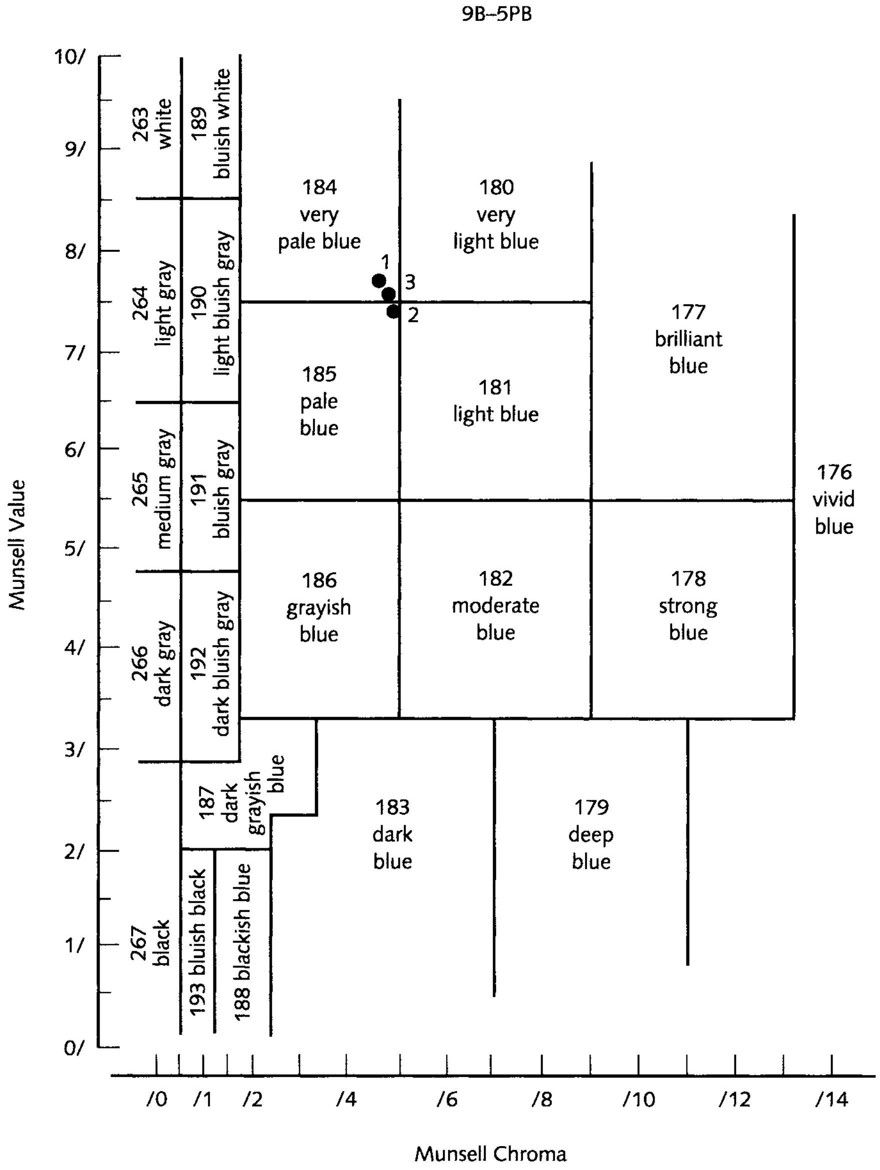

Figure 2.18

Page for Munsell Hues 9B–5PB from *Color: Universal Language and Dictionary of Names* (Kelly and Judd 1976), illustrating the color names assigned for the indicated Munsell Chroma and Munsell Value blocks, and the number reference used in the *Dictionary of Color Names* (Kelly and Judd 1955). The three blue colors illustrated in figure 2.10 are shown as dots in the blocks labeled pale blue.

of Their History and Characteristics (Feller 1986) were described in the Universal Color Language; Munsell notations were also presented.

Figure 2.18 also shows that each block on the Hue Chart was reproduced from the 1976 edition and has a number as well as a name. There are thirty more charts for the other Hue ranges. This number is used in the "Dictionary of Color Names," which makes up the last portion of both books. About seventy-five hundred color names are listed alphabetically with references to the source of the names and to the number of the color-name block in the Munsell Value–Munsell Chroma charts in the 1976 edition. The earlier edition did not have numbers on the color-name block of the color-name charts. The thirty sources cited include the Ridgway (1912) collection of color plates and color names, and the Maerz and Paul collection (1930). Both collections are of considerable historical interest. Beginning in the last part of the nineteenth century, more color was used in fine and applied arts (partially, at least, because more colorants became available), and as a result more color names were created. The trend continues today. Thus, the need for the use of the Universal Color Language to describe colors more clearly is still valid. The dictionary portion of the books contains color names gleaned from past collections of color chips that still exist and were used in the past. Curators and technical people in art conservation could identify a color name from this dictionary by which others could visualize an approximate color. Commercial names could be as exotic as desired so long as their exotic name was also identified with the Universal Color Name.

When a need exists to identify a color referred to in the past, using the color-name dictionary for this purpose may seem difficult at first. An example may be helpful. If one encountered the name "Corinthian Pink" and wished to know what the color might have been that was so described, one could look under the C's in the dictionary for Corinthian Pink. The following information would be found:

Corinthian Pink	M,m.Pk5; l.gy.R18
Corinthian Pink	R,m.Pk5

The first capital letter gives the reference, and the next series of letters and numbers describe the color-block area of the color-name charts similar to figure 2.18. Thus, in the first entry above, M refers to the Maerz and Paul *Dictionary of Color* (1930); in the second entry, R refers to the Ridgway *Color Standards and Color Nomenclature* (1912). (Copies of these books may be found in libraries or in antiquarian bookstores.) The location abbreviation, m.Pk5, refers to moderate pink in area 5 on the color-name charts. Since numbering begins on the first color-name chart, for the Hue range 1R–4R, one looks first on this chart and locates m.Pk5 there. It is important to realize, however, that many of the color names were used over a range of colors, so it is advisable to check adjacent diagrams to see if they are also located there. In this case, m.Pk5 is also found on a second chart, covering 4R–6R. To determine if the color is also located on the diagram preceding the first one in the Hue Circle, the second diagram adjacent to the first one is consulted (the last one, 9RP–1R); this also has an area named m.Pk5. None of the other Hue Charts contain m.Pk5; hence, the range of Hues where this name was used corresponds to 9RP–6R. The Munsell Value range of the area is 6.5–8.0, and the Munsell Chroma range is 3.0–7.0. Thus, the range in the Munsell notation is 9RP–6R 6.5–8/3–7.0. Corinthian Pink is a light, soft pink, not a strong or vivid pink. Reference to the chips in the *Munsell Book of Color* will illustrate the range of colors described. Maerz and Paul also list l.gy.R18 for Corinthian Pink. That is a light grayish red in area 18. This area is located on each of the first four charts, 1R–8R. The Munsell range is expanded to 9RP–8R 5.5–9.0/2–7. Hence the color may also have been slightly darker and grayer than the m.Pk5. The date of the reference to Corinthian Pink would be a helpful guide in the selection of the probable area to be most representative.

The abbreviations used above are explained in the texts of both editions. There is also a series of color wheels at Munsell Value levels of 1–8.75. These show the range of the Munsell Hue names used in the charts. The example of Corinthian Pink was selected deliberately to describe a difficult color, because the m.Pk5 designation occurs on charts at the beginning and at the end of the sequences. Most color names are not as broad and are generally described on a single color-name chart.

A great deal of careful research and hard work by a group of color experts headed by Kelly and Judd went into the preparation of this dictionary and into the Universal Color Language. The original report, issued as National Bureau of Standards Circular 553, was published in a green hardcover in 1955. A later version, with added text by Kelly and some color plates, was published in 1976. As of this writing, however, this 158-page booklet is available only as a photocopy. Nonetheless, the system deserves to be used much more widely.

OSA Uniform Color Scales

Many years of visual evaluations, and the preparation of thousands of color chips made for the evaluations, culminated in the OSA (Optical Society of America) Uniform Color Scales System (MacAdam 1974; Nickerson 1981). Based on equal perceptual differences in all three dimensions, the OSA system represents the most visually uniform arrangement created to date. The color chips have been defined in CIE notation based on the 1964 standard observer and illuminant D65 (MacAdam 1978), and in Munsell renotation (Nickerson 1978). There are 558 samples in the OSA system, each described in terms of lightness (L), redness–greenness (g), and yellowness–blueness (j); they are arranged in a regular rhombohedral-lattice spacing. Each sample, except the edge samples, is surrounded by twelve others equally visually distant from it. The system is described by Wyszecki and Stiles (1982) and in ASTM Standard E 1360. Sets of the chips are currently available from the Optical Society of America, Washington, D.C.

In the brief section on color harmony presented by Judd and Wyszecki (1975), their basic theme is that color harmony results from an orderly plan that is inherently satisfying, a plan that consists of an unambiguous selection of colors in the total scene. In the author's opinion, the OSA system is also an incredibly beautiful work of art. In addition, there is probably no color-order system that has been so thoroughly documented in scientific terms. It has been defined in CIE notation based on the 1964 standard observer and illuminant D65 (MacAdam 1978) and in the Munsell system (Nickerson 1975, 1978). The preparation of the samples has been described by Davidson (1978). The history of this extensive study has been described by Nickerson (1977).

Other systems

Many color-order systems illustrated by physical samples have been created in the past, and several new ones have appeared recently. A few of these are listed here.

The Ostwald color system (Ostwald 1931, 1969) is of historical interest, even though the atlases of color chips—known as *The Color Harmony Manual,* formerly published in several editions by the Container Corporation of America—are no longer available. The colors of the chips were based on additive color mixture obtained by disk colorimetry according to Ostwald's concept that colors can be described in terms of their pure color combined with white and black. Jacobson (1948) presents a discussion of the usefulness of the arrangement, particularly to artists and designers, and provides illustrative color prints. For a recent discussion of the system, the article by Granville (1994) may be consulted.

More recent color-order systems are available and still in use. One of these is the DIN (Deutsche Industrie Norm) system, the official German standard color system developed by Richter (1953, 1955). A description of the system and the CIE notation for the color chips may be found in the book by Wyszecki and Stiles (1982).

The Natural Color System, which is the Swedish national standard color-order system, was developed in the 1960s and 1970s (Hård and Sivik 1981). It is based on the four unique hues—red, green, blue, and yellow—combined with black and white that are seen in each color. In this sense it resembles the Ostwald system, except that the unique hues are imaginary.

The most recent system to appear in the United States is the Colorcurve system (Stanziola 1992). It consists of an atlas of color chips with tristimulus values and reflectance factors at 20 nm intervals. These data and the description of the system are presented in ASTM Standard E 1541. The system was particularly designed to be an aid in computer color matching.

Orderly collections of colors are used in the color printing industry, and they are based on subtractive colorant mixtures of printing inks. One of these collections is produced by Pantone, Incorporated, Carlstadt, New Jersey. The problem with producing any printed collection is that the printing process generates entire pages of colors at once, so there is no chance to adjust each color to the closest approach to its aim point. In addition, the reproducibility between successive printings is difficult to control with high accuracy.

All orderly arrays of color samples and color descriptions are useful for purposes of communication and visualization. Today the CIE notation is fundamental in communication, and the *Munsell Book of Color* is the most widely used collection of color samples.

Chapter 3

Colorant Characteristics

Generally, materials used to impart color to objects are either dyes or pigments. Dyes are distinguished from pigments by their solubility in a solvent or medium; the resulting dye solutions are clear and transparent. When a dye is incorporated into a compatible solid matrix, such as plastic or glass, the result is a material that may be transparent, like a color filter, or opaque, if the concentration of dye is sufficiently high to absorb all of the incident light. When dye solutions are used to color textiles, paper, etc., the opacity is usually attributable to the base material (fabric, fibers, paper, etc.), which may be colorless itself but which scatters most wavelengths of incident light. The dye selectively absorbs some wavelengths of the incident light, thus contributing the color, while the substrate scatters the wavelengths of light transmitted by the dye, thus contributing the opacity. In the case of dyed textiles, the substrate is air, with a refractive index of 1.00, rather than the textile fibers, including synthetics, which have indices of refraction in the range 1.46–1.65. This is because the medium adjacent to the fibers is air, and many dyes are deposited on the surface of the fibers surrounded by air.

In discussing subtractive colorant mixture, we are concerned with these two optical characteristics—absorption and scattering of the incident light. Their relative magnitudes are determined by the chemical and physical structures of the materials. For a detailed discussion on the origin of color, the reader is referred to the literature (Nassau 1983; McLaren 1986; Feynman 1985). The experienced colorist knows that a number of factors come into play in determining the behavior of colorants, but when all others are equal, it is the light absorption and scattering characteristics of a material that are fundamental.

Absorption of light is a relatively straightforward phenomenon. Scattering of light is more complex, and it is encountered with pigments. Unlike dyes, pigments do not dissolve in the system. They exist as a suspension—*dispersion* is the term often applied to pigments—that is, as tiny suspended particles that have the ability to scatter as well as absorb light. The amount of scattering is a function of the difference in the refractive index of the pigment and the suspending medium, and of the particle size relative to the wavelength of the incident light. Reference to low and high refractive index pigments is relative to that of the typical transparent binder to which they may be added; the refractive index, n_D, of the typical binder is about 1.46–1.65. In this chapter, when we speak of scattering, we are assuming that, unless otherwise stated, the scattering is *backscattering* or *multiple scattering*, that is, scattering that returns incident light back toward the light source and to our observing eyes. In actuality, though, scattering may occur in all directions, both forward and backward. In some systems, for example, a small addition of TiO_2 white pigment may result in a perceived darkening of the color, because most of the incident light is scattered in the forward direction. There are probably not many situations encountered in the examination of art objects where this phenomenon is significant. It may, however, be encountered in glazes and in translucent materials (see chap. 4), and in metallic flake pigmented paints (see chap. 5).

We can divide all conventional pigments (excluding interference and metallic flake pigments) into three types: type I pigments scatter much more light than they absorb (for example, white pigments); type II absorb much more light than they scatter (for example, carbon black and many organic pigments of small particle size); and type III both scatter and absorb light significantly (for example, many of the inorganic pigments).

Type I pigments, which primarily scatter light with little absorption, are the white pigments. Those with the highest index of refraction relative to the medium in which they are suspended scatter the most, for example, the titanium dioxides: rutile at $n_D = 2.76$ and anatase at $n_D = 2.55$. In contrast, lead white (basic lead carbonate $[Pb(OH)_2{\cdot}2PbCO_3]$) and zinc oxide (ZnO) have refractive indices of about 2. $BaSO_4$ (barytes or blanc fixe) has a refractive index of about 1.64, which is close to that of the traditional media in which it is usually dispersed. The result is that $BaSO_4$ is not considered a true pigment but rather an extender or inert (see chap. 6).

Type II pigments, which absorb much more light than they scatter, include most of the organic pigments as well as the organic carbon blacks, lamp blacks, etc. (Black iron oxide, however, is a type III pigment with a refractive index of about 2.4.) The organic pigments may be of two types: toners or lakes. Patton (1973) described a toner as "an organic pigment that is free of inorganic pigment or inorganic carrying base. It is an undiluted organic colorant having maximum tinting strength for its specific type." He described a lake as "an organic coloring matter that has been more or less definitely combined with some inorganic substrate or carrier."

Type III pigments, which both absorb and scatter light, include most of the inorganic pigments, such as the iron oxides, and those organic pigments modified to increase their particle sizes.

Today some synthetic textile fibers are pigmented; the pigmenting is done in the spinning process. In this case, the pigments exhibit the same behavior that is encountered in paints or plastics, that is, they absorb *and* scatter light. However, there is also significant surface reflection from the fiber filaments, which adds to the scattering appearance. (See the discussion on surface reflection in chap. 4.)

Many patterned textiles today are printed with coatings that are pigmented. As with pigmented printing inks, the colors obtained are dependent on both the absorption and the scattering characteristics of the pigments used in the printing formulation. Hiding may not be complete in these applications—a situation similar to that encountered with glazes used by painters working with both oil and watercolor. (See the discussion on glazes in chap. 4.)

The degree of both light scattering and absorption is dependent on the particle size of the pigment, as well as its refractive index. Descriptions of particle size in a given pigment preparation are often presented graphically in terms of the cumulative percentage of the total quantity of pigment that exists below each designated particle size. Size is customarily plotted as the ordinate on a logarithmic scale, and the cumulative percentage as the abscissa on a linear scale. Such a distribution is called log-normal. This method of describing particle size is commonly used by modern pigment manufacturers and is found throughout the *Pigment Handbook* (Patton 1973). A representative graph for TiO_2 pigments (rutile and anatase) is shown in figure 3.1. The single number most convenient for describing such a distribution is the median particle size, that is, the size at the 50% cumulative distribution. In the past, particle sizes were traditionally determined by their passage through fine mesh screens of designated particle sizes. Thus, it was the maximum particle dimension that determined the particle size designation; all smaller particles passed through the screen.

An accurate method used today for size determination is counting particle sizes from electron micrographs. Automatic optical counters have been developed for this use. Electron microscopy also enables the user to determine the degree of particle dispersion in a polymer matrix. Centrifugal sedimentation is particularly useful for determining the particle size distribution of very finely divided pigments, such as many of the organic pigments (Fraser 1973). This technique replaces the older gravity sedimentation methods described by Orr (1973).

For modern pigments, the 50% cumulative distribution size varies from 0.017 μm to 0.5 μm for carbon blacks; it is a little larger for bone blacks (Garrett 1973). Most synthetic organic pigments are generally less than 1.0 μm in diameter (Carr 1973). The median diameter for TiO_2 varies from about 0.2 μm to 0.25 μm (Kampfer 1973). Basic lead carbonate is about 2.6 μm in diameter (in modern production), and basic lead sulfate is about 1 μm (Dunn 1973). The natural iron oxides vary from 2 μm to 5 μm (Love 1973) in modern materials, and the synthetic iron oxides—yellow and red—vary from 0.2 μm to 1.0 μm (Fuller 1973).

The resolution limit for an optical microscope is about 1 μm; below this value particles can be detected only by electron microscopy (McCrone 1973a). McCrone (1973b) has outlined a scheme for pigment identification by microscopic techniques.

Modern pigments are manufactured to have particle sizes providing the desired optical properties according to their refractive indices. Because the refractive indices of most organic pigments are so low relative to those of the matrices in which they are suspended, the particle size of these pigments would have to be increased considerably to obtain significant scattering, resulting in a high absorption loss. Only

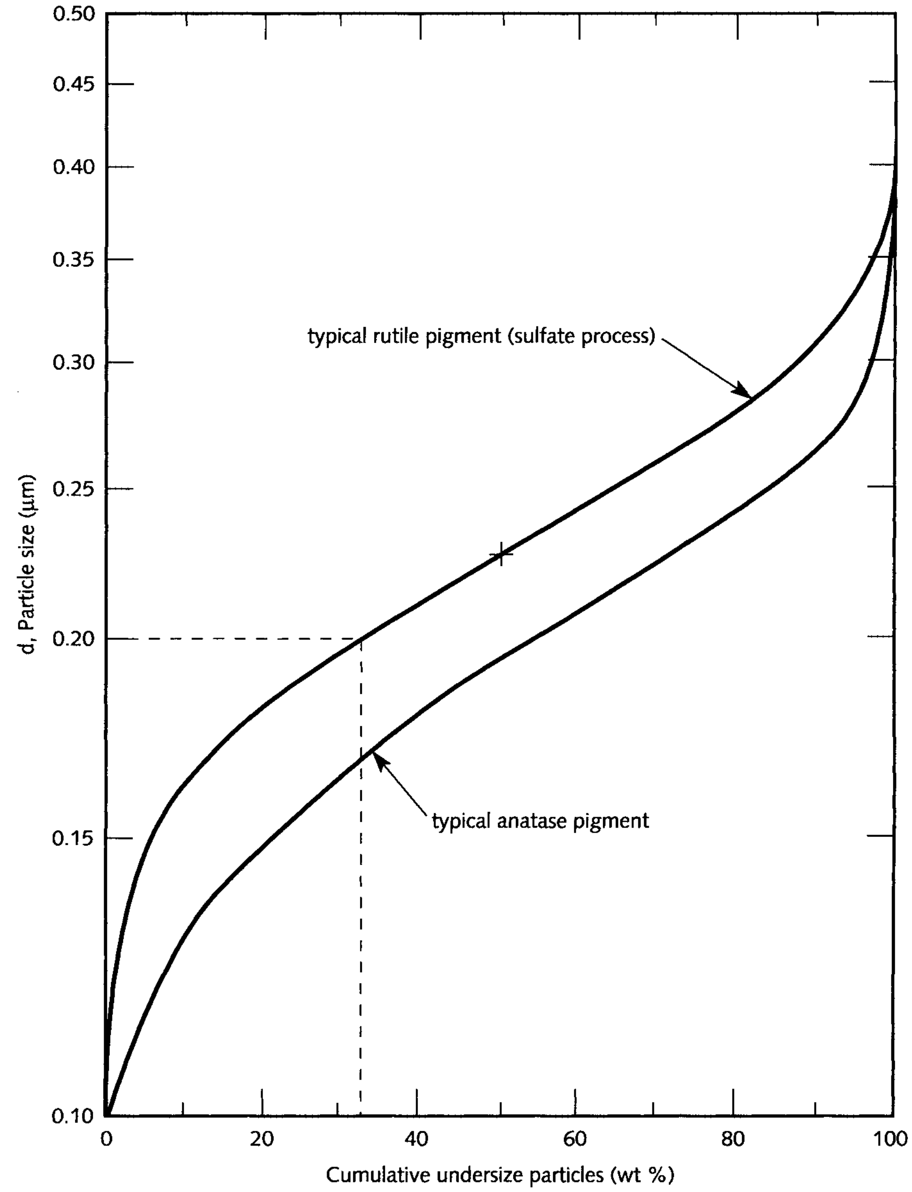

Figure 3.1

Cumulative particle size distribution curves for typical anatase and rutile TiO_2 pigments. The graph illustrates the standard graphing nomenclature used by pigment manufacturers to describe the particle size distribution of their product. The abscissa, a log scale, is the pigment particle diameter, d. The ordinate is the weight percentage of all particles below the size indicated on the abscissa. Thus, the dotted lines on the graph illustrate that about 26.5% of the particles of rutile TiO_2 are *smaller* than 0.2 µm or, conversely, that about 73.5% of the particles are larger than 0.2 µm. The size at the 50% cumulative distribution point is about 0.225 µm, as indicated by the cross (from Kampfer 1973. Copyright © 1973 John Wiley & Sons, Inc. Reprinted by permission).

pigments with refractive indices considerably higher than that of the suspending matrix can scatter light significantly. In the section dealing with opacity in chapter 4, the theories relating particle size and refractive index to light absorption and scattering are presented.

There are special types of colorants that may be used to create particular optical effects in materials. Examples are pearlescent and iridescent pigments, and metallic flake or powder pigments, all of which are discussed in chapter 5, as well as fluorescent pigments or dyes, which are discussed in chapter 6. However, most colored materials encountered owe their color characteristics to the absorption and/or scattering of light rather than to these special effects. Chapter 4 deals with the materials and objects whose color depends on the absorption and scattering of light.

Chapter 4

Colorant Mixture

Transparent Materials: The Beer–Bouguer Equation

The Beer–Bouguer equation relates the transmittance of radiant energy through a transparent material (liquid or solid) to both the material's thickness and its absorption. It applies to one wavelength at a time. Sometimes in the literature it is referred to as the Beer–Lambert equation or simply as Beer's law. The Beer–Bouguer equation is a combination of two earlier ones, which are described below.

Bouguer's (Lambert's) law

An equation relating thickness to transmittance was first formulated by Bouguer (1729). In 1760 it was "rediscovered" by Lambert (1760). Although the equation is variously called Bouguer's law or Lambert's law, the former name has been chosen here because of the earlier exposition. The law states that the intensity of light passing through an absorbing, nonscattering material is decreased in proportion to the thickness, X, of the absorbing material with absorption coefficient, A:

$$\log(I/I_0) = -AX \tag{4.1a}$$

where I_0 is the intensity of the incident light, and I is the intensity of the transmitted light. The ratio I/I_0 is the transmittance, T. Therefore,

$$\text{at each } \lambda\text{: } -\log T = AX \tag{4.1b}$$

It is assumed that A is a constant so that $-\log T$ —or $\log(I_0/I)$—is proportional to the thickness, X.

A superposing of several layers of materials with different absorptions and thicknessess is described by the following form of the Bouguer equation:

$$\text{at each } \lambda\text{: } -\log T = \log(I_0/I) = A_1X_1 + A_2X_2 \ldots \tag{4.2}$$

where the A's represent the fixed absorptions of the components identified with the numbered subscripts, and the X's represent the thicknesses of the corresponding components. The Bouguer equation is frequently written in this form. The assumption is made that the multiple layers are in optical contact, that is, there is no difference in refractive index between layers. The Bouguer equation relating to thickness is customarily called a law because, as far as it is known, there are no exceptions to it.

This is the law used in making complex filters to simulate the tristimulus functions in tristimulus colorimeters, where the spectral characteristics of the source used and the spectral sensitivity of the receiver must also be taken into account. If light illuminates the sample before passing through the filters, the spectral characteristics of the light source must be filtered to simulate the desired illuminant. The tristimulus filters must then be made to correspond to each of the color-matching functions of a CIE standard observer in combination with the spectral sensitivity of the photodetector, to match as closely as possible the desired tristimulus spectral responses. Multiple filters are usually cemented together to achieve this approximation; an adhesive or a cement with the same refractive index as the filters is used to eliminate any specular reflection between layers. If the light is filtered to simulate the tristimulus responses before falling on the sample, a combination simulating the spectral characteristics of the light source, the color-matching functions, and the detector responsivity may be assembled into one so-called filter pack.

There are times when a single layer must be measured in order to compute its transmittance at a different thickness. In this case, surface specular reflection must be taken into account because light is reflected specularly at the surface–air interface where there are differences in refractive index. The importance of surface reflection in computing colorant formulations is discussed later in this chapter, and the general role that surface reflection plays in object appearance is discussed more completely in chapter 6.

When the incident light is *perpendicular* to the surface, the light reflected at an interface between two layers having different refractive indices is calculated by Fresnel's law:

$$k_1 = \frac{\left(n_2/n_1 - 1\right)^2}{\left(n_2/n_1 + 1\right)^2} = \left(\frac{n_2 - n_1}{n_2 + n_1}\right)^2 \tag{4.3}$$

where n_1 is the lower refractive index, n_2 is the higher refractive index, and k_1 is the decimal fraction of the incident light that is reflected back at the first interface. (The Greek letter ρ or simply R may be found in the literature in place of k to describe the specular or Fresnel reflection at interfaces.) Unless specified otherwise, the refractive index is measured at the sodium D lines, about 589–590 nm. If the lower refractive index medium is air, n_1 is set equal to 1.000. The resulting reflection is called the specular (mirrorlike) reflection, where the angle of reflection is equal and opposite to the incident angle. It is also called the Fresnel reflection because it is based on Fresnel's law (eq. 4.3). Thus if light is incident perpendicularly on a piece of opaque polished glass or plastic of refractive index 1.5, the first surface specular reflectance will be $(0.5)^2/(2.5)^2 = 0.25/6.25 = 0.04$, or 4% of the incident light.

In the case of transparent materials, such as plastic sheets or filters, light must also exit when it encounters another air interface. This results in internal specular or Fresnel reflection—a second reflection due to an interface. Therefore, the resulting transmittance is decreased further as shown in the following:

$$T_m = (1 - \rho)^2 T_i \tag{4.4}$$

where ρ (here used in place of k) describes the interface specular reflection, T_m is the fractional transmittance measured, and T_i is the internal transmittance predicted by the Bouguer equation (eq. 4.1b). In the above example of a perfectly transparent plastic or glass sheet of refractive index 1.5, with incident light normal to the surface, and *no* absorption, the measured transmittance is $(0.96)^2$ or 0.9216 or 92.16%.

All of the above equations describing surface reflectance calculations are special cases for incident light that is perpendicular to the surface as described by Fresnel's law. When the angle of incidence becomes greater than about 10° off the perpendicular, the simple equation for calculating the specular, or Fresnel, reflection is no longer correct. The relationship becomes more complex (see eq. 6.2). In this case, the angle of incidence has to be taken into account as well as the polarization state of the incident light. The Fresnel equations for both horizontally polarized and vertically polarized light are presented by Judd and Wyszecki (1975). The authors include graphs for the value of the Fresnel reflection, ρ, as a function of the angle of incidence for both the plane polarized light and the perpendicularly polarized light when the refractive index is 1.5. They point out that for unpolarized light, the specular (Fresnel) reflection is the average of the two, and they include this on their graph as well. In a second graph, the authors present the Fresnel reflection, ρ, for unpolarized light as a function of the angle of incidence for materials having refractive indices from 1.1 to 1.9, at intervals of 0.1.

Beer's equation (the Beer–Bouguer equation)

When thickness, X, is constant, the equation relating the transmission through a transparent material with absorption coefficient, A, as a function of the concentration, C, is that of Beer (1852):

$$\log(I/I_0) = -XCA \tag{4.5a}$$

or

$$\log(I_0/I) = XCA \tag{4.5b}$$

For a mixture of absorbing components, Beer's equation becomes

$$\log(1/T_i) = X(C_1A_1 + C_2A_2 + C_3A_3 + \dots) \tag{4.5c}$$

where X refers to the thickness, the C's refer to the concentration of absorbing components, and the A's to the specific absorption coefficients of the components designated numerically. Obviously Beer's equation is always used with a designated thickness, X, as described by Bouguer; consequently, it is also called the Beer–Bouguer equation. In practice, though, the equation is often referred to by the familiar term "Beer's law," even though it is not, strictly speaking, a law, as will be explained later.

For a mixture of materials such as films in optical contact, where both the thickness and the concentration of each absorber are variable, the Beer–Bouguer equation becomes

$$\log(1/T_i) = \log(I_0/I) = X_1C_1A_1 + X_2C_2A_2 + \ldots \tag{4.6}$$

It can be seen that changing the concentration has the same effect on the transmittance as changing the thickness by the same factor. Log(I_0/I)—or log($1/T$)—is the absorbance or the *optical density.* Many of the spectrophotometers designed for transmission measurements may also record or read out in terms of this quantity.

The absorption coefficient, A, is the optical density—log($1/T$) or log(I_0/I)—per unit concentration and thickness. The coefficient may be expressed as grams per liter for a 1 cm thickness, sometimes with the symbol alpha (α); it may also be expressed as the molar extinction coefficient in moles per liter for a 1 cm thickness, with the symbol epsilon (ε). These are the most commonly used absorption coefficients in analytical spectrophotometry. The choice of which to use depends on the nature of the application. The transparent solvent used in obtaining the unit absorption coefficient of a compound in solution must be specified because the absorption spectra may be different in another solvent. Likewise, the diluent used for solid mixtures must be specified because the spectral curve may be different with a different diluent (DiBernardo and Resnick 1959). The concentration units (the C's) as well as the thicknesses (the X's) in equations 4.5a–c and 4.6 must be expressed in the same units as the specific absorption coefficient.

When there is no significant degree of scattering in the materials, the Beer–Bouguer equation is used in spectrophotometry regardless of the wavelength of the radiant energy, whether in the visible, the ultraviolet, or the infrared. When measuring solutions in a solvent placed in a cell or container of known thickness, it is customary to put a matched cell containing only solvent in the reference beam of the measuring instrument (spectrophotometer or colorimeter). When this is done, the specular reflections from the cell faces cancel out, and no corrections need be made for interfacial reflections. When measuring solid sheets of plastic or glass, an undyed or unpigmented sheet of the same thickness may also be used in the reference beam to cancel out the surface reflection effects.

Beer's law—the common name often used for the Beer–Bouguer equation—probably should not be called a "law" because there are exceptions to its validity; in such cases Beer's law is said to fail. The equation has been found generally to be valid at low and moderate concentrations. At higher concentrations, however, many solutions do not obey Beer's law; the deviations are associated with the formation or breakup of molecular aggregates and other modifications of the absorbing molecules and the solvent (Wyszecki and Stiles 1982). Stearns (1969) presents an extensive summary of the factors affecting the results in solution spectrophotometry; these factors include solvent, pH, concentration, temperature, interfering ions, oxygen content, and so on. To account for these factors, it is customary to prepare reference mixtures at a variety of concentrations to determine the range of concentrations—that is, a calibration curve—over which Beer's law is valid. Often such calibrations reveal that Beer's law fails if the concentration becomes too high.

Such an observed failure may or may not be due to chemical interactions. Instead, it may simply be caused by the lack of sensitivity of the measuring instrument. Remember that the range of transmission measurements is 0–100%. Even if the instrument records optical densities up to 4, the optical density unit—$\log(I_0/I)$—is based on the measurement of the transmittance, I/I_0. For $\log(I_0/I) = 4$, the transmittance as measured is 0.01%. Few instruments are capable of making precise measurements at such levels. For accurate measurements, then, the concentration must be decreased by dilution, or the thickness of the material must be decreased.

At the other end of the scale, as transmittance approaches 100%, sensitivity is also limited. Just because the transmittance measurement made on a material is very close to 100%, $\log(I_0/I) = 0$ does not necessarily mean that there is no absorption at all. It merely indicates that the amount of absorption is below the amount that can be detected by the technique used. If the thickness were increased 100-fold or 1,000-fold, the same technique might reveal the presence of an absorber.

In the ultraviolet, visible, and near-infrared spectral regions, many compounds absorb because of their electronic structure; often in the case of organic compounds this is due to conjugated unsaturation (double bonds). Spectra of organic materials exhibit extremely high absorption coefficients: molar extinction coefficients of 10,000 or more, that is, $\log(I_0/I) = 10{,}000$ for a 1 cm thick solution of 1 M (mole per liter) concentration. Thus, in order to measure the transmittance of such a material, it would have to be diluted to a concentration of 0.0001 M, giving $\log(I_0/I) = 1.000$, or a transmittance of 10%; this is barely satisfactory for precision on a good instrument. The range of optical densities—$\log(I_0/I)$—for both visual or instrumental optimum sensitivity is 0.25 to 0.8, corresponding to transmittances from 56% down to 16%. In the example of an absorber with a molar extinction coefficient of 10,000, a concentration of 0.0001 M for an absorber with a molecular weight of 250 would correspond to a weight concentration of 0.025 g 1^{-1}. Thus, if one were to have a sample containing this material dissolved in 10 ml of solvent, the presence of 0.00025 g of the material could be detected at $\log(I_0/I) = 1.000$; similarly, 0.00010 g of material could be detected if $\log(I_0/I) = 0.4$ instead of 1, a very good range of concentration.

It is not unusual for molar extinction coefficients of dyes and pigments in solution to be many times higher, even ten times or more, than the example above. Thus very small amounts of colorants may be detected, and they may have a significant effect on perceived color (see "Comments on Colorant Calculations and Identifications" later in this chapter). This great sensitivity is one of the chief advantages of the solution spectrophotometric technique for determining very small amounts of colorants, dyes, or pigments. Today Saltzman is the most knowledgeable proponent and exponent of this technique (Saltzman and Keay 1967; Saltzman 1986). Kumar (1981) describes in helpful detail a series of analytical schemes for identifying organic pigments this way. Kumar's research, partially funded by a grant from the National Museum Act, included curves of more than 150 different colorants and illustrated the application of the technique to paints, plastics, printing inks, and many artists' materials. (Reference curves are available from Billmeyer. See references section for address.) Although the solution spectrophotometric technique requires taking a very small sample of the object, it is useful where necessary.

Another microtechnique useful in analyzing very small samples is thin-layer chromatography coupled with microspectrophotometry. Fuller (1985) describes this technique and presents several examples of its application in forensic science.

Another useful technique, described more completely in chapter 7, is that of dispersing a small sample of a dark or high-chroma color in a white-pigmented base using a micro ball mill, painting an area, measuring it when dry, and examining the reflectance curve.

It should be kept in mind, however, that reflectance spectrophotometry is a useful first step in analyzing materials because it is nondestructive.

The discussion in this section applies primarily to organic materials, including dyes and dissolved pigments. Generally speaking, inorganic materials in solution do not absorb as highly or as specifically as organic materials. Libraries of curves of the electronic absorption spectra of compounds in solution as measured in the ultraviolet or the visible regions are listed by Stearns (1969).

Absorbing and Scattering Materials: The Kubelka–Munk Equation

The most widely used equation relating the reflectance to the concentration of pigments is that of Kubelka and Munk (1931) and of Kubelka (1948, 1954). The pigments are characterized in terms of their absorption, K, and scattering, S. When hiding is complete (no substrate color is visible), the Kubelka–Munk equation states that at each wavelength (λ),

$$[1 - R(\lambda)]^2/2R(\lambda) = K(\lambda)/S(\lambda)$$

$$\text{or simply } \frac{(1-R)^2}{2R} = \frac{K}{S} \text{ (at each wavelength, } \lambda) \qquad (4.7)$$

where R is the decimal fractional reflectance at wavelength λ; $K(\lambda)$ is the total absorption in the material at the same wavelength; and $S(\lambda)$ is the total scattering in the material at this wavelength. (Generally, the designation (λ) is omitted for simplicity.) The Kubelka–Munk absorption coefficient K is not the same as the absorption coefficient A used in the Beer–Bouguer equation for transmittance (eq. 4.6). The K in the Kubelka–Munk equation (eq. 4.7) is twice the A in equation 4.6 when S approaches zero (Judd and Wyszecki 1975). In addition to the limitation that it applies to one wavelength at a time, the simple Kubelka–Munk relationship (eq. 4.7) applies only to materials that are *completely* *opaque,* that is, for those materials that transmit no light through to the background. (When a pigmented material is not completely opaque, other forms of the equation must be used that take into account the color of the background or the substrate. See the sections on glazes and opacity later in this chapter.) Note that the ratio K/S is dimensionless; K and S must be expressed in the same units based on weight or volume.

This simple relationship tells us that if we increase the total absorption in the material without changing the total scattering, the reflectance will decrease. Conversely, if we increase the total scattering without changing the total absorption, the reflectance will increase. Figure 4.1 shows a graph of the relationship between K/S and the reflectance, R, as defined in equation 4.7.

The Kubelka–Munk equation states mathematically the well-known fact that if we add black (which has a high K and absorbs strongly), we lower R and darken the color; if we add white (which scatters strongly), we increase R and lighten the color. A half century ago, Saunderson (1942) showed how the equation could be used in calculating colorant concentration in some plastics.

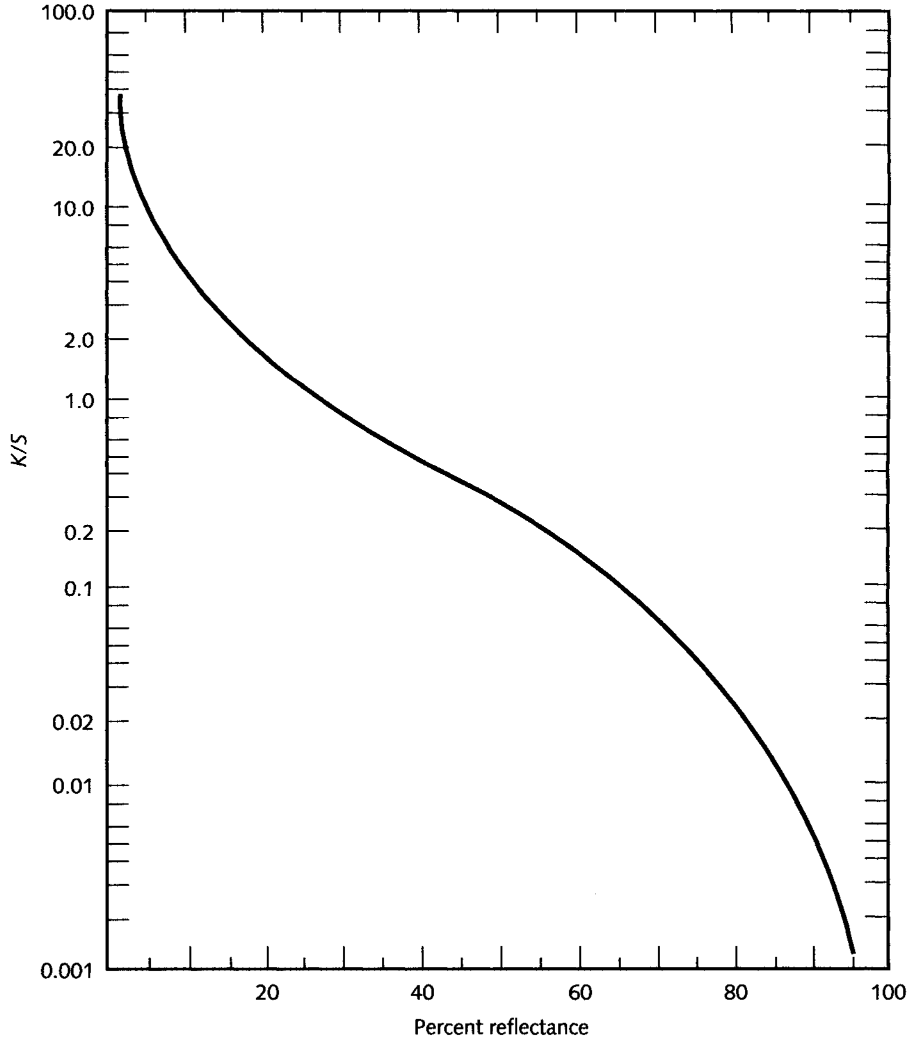

Figure 4.1
The relationship between the percent reflectance and the ratio K/S calculated from $(1-R)^2/2R = K/S$ (eq. 4.7), in which R is expressed as a decimal fraction.

Duncan (1962), working with paints, showed that the total *absorption* of a system made with a mixture of pigments is the sum of the fractional amounts of absorption from each pigment based on the relative concentration, and that the total *scattering* is also the sum of the fractional amounts of scattering from each pigment present. The basic Kubelka–Munk equation then becomes

$$\frac{(1-R^2)}{2R}=\left(\frac{K}{S}\right)_M=\frac{C_1K_1+C_2K_2+C_3K_3+\ldots}{C_1S_1+C_2S_2+C_3S_3+\ldots} \qquad (4.8)$$

Note that the designation (λ), meaning "at each wavelength," has been omitted for simplicity, as described earlier. Here the subscript M indicates the mixture, and the subscript numerals identify the pigments in the mixture. The *C*'s are the *relative* fractional concentrations of the individual components in the mixture, such that the total of the concentrations is unity. Again, the assumption is made that hiding is complete—the layer is opaque. The *K*'s and the *S*'s must be in the same units of concentration. It is this form of the equation that we consider first, the form that is widely used for color matching with the aid of a computer. Generally, this equation is solved simultaneously at a minimum of 16 wavelengths. In chapters 4 and 5 of *Computer Colorant Formulation,* Kuehni (1975) presents a summary of the techniques used in writing a computer program for colorant matching using equation 4.8.

One of the factors that the above relationship (eq. 4.8) tells us, and which needs to be emphasized, is that when the colored material is completely opaque, the *relative* concentrations of pigments in the mixture determine the reflectance; the color is, therefore, not dependent on the *absolute* concentrations of pigments present. This is not strictly true, as the trained colorist knows, but the color differences encountered when changing the absolute pigment concentrations are small unless the critical pigment volume concentration (CPVC) is exceeded (see chap. 6), resulting in changes in gloss and pigment efficiency.

When used alone with no other pigments present, that is, as a masstone, type II pigments described in chapter 3 (pigments that absorb strongly relative to their scattering) look almost black and cannot be identified from their spectral reflectance curves. Examples are carbon black, phthalocyanine blue, carbazole dioxazine violet, phthalocyanine green, and some quinacridone reds and violets—all are transparent organic pigments. This fact explains why some mixtures of white and a chromatic pigment "loop around" on the chromaticity diagram as their relative concentration in mixture with white is increased. Since they approach neutral in very high concentrations, there is a critical concentration in admixtures with a specified white where maximum purity or saturation occurs, as illustrated in figure 2.12 (Johnston 1973). Examination of the loci shows that the pigments that do not exhibit near-straight-line progressions on the chromaticity diagram are all type II organic pigments, those that absorb strongly relative to their scattering.

Because their masstone color is nearly black, they are not used singly but are either mixed with a scattering pigment, such as white, or applied at incomplete hiding over a reflecting substrate (see sections on glazes and opacity later in this chapter). In both types of application, the reflectance spectrum in the absorption region shows the individual absorption bands that are useful for identification.

Those pigments that exhibit significant reflectance when used in a masstone are either type I nonabsorbing white pigments or type III absorbing and scattering pigments. When mixed with decreasing amounts of white, type III pigments continue to move in a relatively straight line on the chromaticity diagram all the way to the masstone color, as illustrated by molybdate orange and light chrome yellow in figure 2.12. Both are inorganic, absorbing and scattering pigments. As the scattering from the lessening amount of white decreases, the loss is compensated by the increased scattering due to the increasing concentration of the chromatic pigment.

The organic yellow FGL shown in the figure illustrates that not all organic colorants exhibit low scattering. Factors that affect the absorption and scattering strengths of pigments are discussed later in this chapter.

Qualitative Application of the Kubelka–Munk Relationship

The reflectance curves in appendix A will be referenced for the initial discussion of the techniques for qualitative identification of colorants by spectral reflectance curve analysis. These curves comprise four white pigments, carbon black, and eleven chromatic colorants. Appendix A also includes tables of the CIE and Munsell notations based on nonspecular curves (total percent reflectance minus 4%).

The achromatic colorants—the whites and the blacks—have few characteristic clues for identification by reflectance spectrophotometry because they either absorb all the way across the spectrum, as does carbon black (fig. A.3), or essentially scatter throughout, as do the whites. The one white pigment exception is rutile TiO_2. Figure A.3 shows the reflectance curves of carbon black in mixture with rutile TiO_2 at several concentrations. At all concentrations shown—from 0.1% black and 99.9% TiO_2, to 8% black and 92% TiO_2—the reflectance decreases as the wavelength decreases below 420 nm. At 0% black (100% TiO_2), the same increase in absorption (decrease in reflectance) occurs. This absorption is characteristic of rutile TiO_2. Because absorbances in mixtures are additive, this characteristic frequently appears; when seen in curves of mixtures with white, it indicates rutile TiO_2. The carbon black has no absorption maximum. The maximum reflectance occurring at 420 nm in figure A.3 is caused by the scattering maximum of the rutile TiO_2 in this region. Anatase TiO_2 white begins to absorb only below about 405 nm.

If this same carbon black is mixed with different white pigments, such as anatase TiO_2, zinc oxide (ZnO), or lead white (basic lead carbonate [$Pb(OH)_2 \cdot 2PbCO_3$]), the spectral curves are different because the coefficients of absorption and scattering of the white in the mixtures are different. Figure A.4 shows the spectral curves of four mixtures of carbon black with these white pigments. Note that the concentration of black is different for each of the mixtures, taking into account differences in *tinting strength* of the whites. (The tinting strength of white pigments depends on their scattering strength; this is discussed later in this chapter.) The differences in concentration were chosen to give spectral curves of similar luminous reflectance (tristimulus value Y), so that comparisons of the spectral reflectance curves and the resultant color of the mixtures could easily be made.

Table 4.1 gives the tristimulus values and chromaticity coordinates for the four mixtures based on diffuse reflectance measurements.

Figure A.2 shows the data in table 4.1 plotted on a chromaticity diagram. Although all of the mixtures are bluish, the lead white mixture is most nearly neutral (closest to the illuminant), corresponding to the greater flatness of the spectral curve. These mixtures of black and white pigments demonstrate the scattering characteristics of the whites. To picture the absorption characteristics of the whites, a curve of each white pigment by itself (masstone), based on a complete hiding film, can be examined in figure A.5. From the curves it can be seen that rutile TiO_2 absorbs most strongly in the violet, and that the other white pigments absorb much less. The corresponding Munsell notations are given in table A.1.

It must be emphasized that these data are based on specific samples of the pigments, but some general statements can be made: (1) Rutile TiO_2 always absorbs in the violet, giving it a yellowish hue in masstone. During manufacturing, the particle size of many rutile TiO_2 pigments is adjusted to have a scattering maximum in the violet region in order to offset, to some extent, the yellowness due to its violet absorption. (2) It is difficult to distinguish, on the basis of the spectrophotometric curves alone, among anatase TiO_2, ZnO, and lead white when mixed with chromatic pigments.

White pigments, being of mineral nature, can be identified by X-ray fluorescence or, if a tiny sample can be taken, by X-ray diffraction. Levison (1976) points out that TiO_2 (anatase in oils, primarily, and rutile in water-based paints) is often diluted with blanc fixe ($BaSO_4$) or with ZnO for better working properties in artists' paints (see chap. 6). He also reports that the addition of a small amount of ZnO to the TiO_2 retards the yellowing of linseed oil or safflower oil vehicles.

Though not a neutral in the sense of not exhibiting any significant wavelength selectivity, burnt umber is a favorite near neutral to replace black on artists' palettes, even though it is yellowish. When industrial tinting (or shading) was done by visual means alone, burnt umber was also a favorite of tinters (or "shaders") because it is easier to

Table 4.1

Tristimulus values and chromaticity coordinates for the white plus trace of black mixtures in fig. A.4 (see appendix A) (CIE illuminant C, 1931 standard observer).

Mixture	X	Y	Z	x	y
1% black + R. TiO_2	37.59	38.65	51.32	0.2947	0.3030
0.95% black + A. TiO_2	36.08	36.98	52.18	0.2881	0.2953
0.1927% black + ZnO	38.90	39.57	57.87	0.2853	0.2902
0.2275% black + Pb white	40.45	41.34	52.34	0.3016	0.3082

control its effect on mixtures than it is to control the effect of the more strongly absorbing carbon blacks. Since burnt umber is a natural iron oxide pigment, its permanence is very good.

Figure A.6 shows the spectrophotometric curves of several concentrations of burnt umber in mixture with rutile TiO_2. It can be seen that the resultant colors are yellowish compared with the more neutral carbon blacks; burnt umber has selective absorption in the violet and blue regions up to about 530 nm. Even in masstone, it exhibits a dark yellowish color. The reason for this persistent yellowness is simply that it also scatters significantly in the yellow-orange and red regions. We shall see later how important this characteristic is.

Because of the wide use of burnt umber, all of the chromatic pigments in the abbreviated library in appendix A were compared in mixture with rutile TiO_2 and with burnt umber, as well as with black. Table A.1 gives the CIE and Munsell notations for both the black–TiO_2 mixtures and for the burnt umber–TiO_2 mixtures. The reflectance curves for one mixture of each colorant in rutile TiO_2, alone and with black and with burnt umber, are illustrated after the corresponding series of mixtures made with rutile TiO_2.

The primary chromatic pigments are blue, red, and yellow; they will be discussed next.

The reflectance curves for ultramarine blue (fig. A.8) and for phthalocyanine (phthalo) blue (fig. A.10) show that the maximum absorption (minimum reflectance) occurs in the complementary wavelength (orange) region at about 600 nm. The shape of the absorption tail on the phthalo blue at 600–700 nm is highly characteristic and provides a clue to the pigment's presence. The ultramarine blue is less distinctive, having a broad region of absorption that decreases in the red region with a characteristic red reflection tail in its spectrum. This gives it a more reddish hue than that of phthalo blue, as can be seen from the Munsell notations in table A.2.

Figure A.11 shows the effect on the curve shape of adding a small amount of black to the phthalo blue–rutile TiO_2 mixture illustrated in figure A.10. It is apparent that the addition lowers the reflectance in the blue (maximum reflectance) region significantly but does not change the reflectance in the red (minimum reflectance, maximum absorption) region nearly as much. Because the absorption, K, is very low in the blue region (high reflectance, so that it looks blue), the addition of the strongly absorbing black makes a significant change in the K/S ratio in the blue region; this lowers the reflectance, R, drastically. In the orange region, however, the addition of black has far less effect on the reflectance because the absorption, K, of the phthalo blue is already very high in this region.

With the addition of burnt umber, the absorption of the umber in the violet becomes apparent in the curve, leading to yellowness by shifting the reflectance maximum significantly into the green region. Note, however, that because of the long-wavelength scattering of the burnt umber in the orange and red regions, the added absorption in this range is partially offset by the moderately high scattering of the umber.

The CIE and Munsell notations for the blue curves are presented in table A.2. Figure A.7 shows a chromaticity plot of the colorants mixed with white, and with black or umber added. The yellowing effect of the burnt umber is apparent.

The mixtures of ultramarine blue with rutile TiO_2 (fig. A.8), and also those mixtures with small amounts of black or umber added (fig. A.9), further illustrate the principle of how the sum of absorption and scattering in a mixture affects the reflectance. Figure A.9 illustrates how the addition of two concentrations of black affect the curve shape. The reflectance maxima for both of the mixtures with black are in a bluer region and are higher than the maximum for the mixture made with burnt umber, even though the curves in the absorption region for two of them—0.02% black and 0.5% burnt umber—are similar. The short-wavelength violet absorption of the burnt umber dominates the resultant hue, making it more greenish. Notice, however, that the long-wavelength scattering of the umber raises up the reflectance to nearly that of the lowest amount of black, 0.02%.

Thus, it can be seen that, on a qualitative basis of interpretation, the relationship of the resultant reflectance to the ratio of the total absorption and scattering makes it possible to understand much about pigment mixtures: the characteristic absorptions are not obscured in mixtures. When pigments scatter, that effect must also be taken into account, as in the case of the umber. It should be pointed out, however, that pigment scattering is generally not highly spectrally selective but exhibits relatively gradual changes with wavelength. Note also that the absorption bands of pigments in mixtures, when the bands occur in the scattering region of another pigment, are not obscured even in the region of significant scattering from the other pigment in the mixture.

Figure A.12 shows the spectral reflectance curves of red iron oxide in mixture with rutile TiO_2. This particular sample of red oxide is borderline to an orange. However, all red iron oxides have similar curves absorbing in the violet, blue, and green regions and reflecting the long wavelengths. The wavelength at which the reflectance rises determines the hue; the longer the wavelength at which the rise occurs, the redder, or less orange, is the pigment. This particular sample is of synthetic origin, but the natural red oxides exhibit similar absorptions, although they are generally lower in chroma, reflecting less in the red region. There are no distinguishing features in the absorption region other than the flatness. However, this pigment exhibits a characteristic reflectance in the red region, rising continuously after 620 nm in a characteristic upward pattern. Both natural and synthetic red iron oxides exhibit this feature.

Bright reds with little or no white (masstones or near masstones) exhibit flat, low-reflectance curves in the region below about 600 nm. (See fig. A.14 for masstone BON red, 100.0%; this is an organic red.) Therefore, as mentioned earlier, the spectral reflectances of masstones aid little in identification. However, when a bright red is mixed with a scattering white pigment, one may often observe characteristic absorption bands. Some, like the BON red illustrated, exhibit a single strong absorption maximum in the white mixture. Others, such as Quinacridone Red (fig. A.16), have two or more distinctive absorption bands. Their curve shape is specific to Quinacridone Red; no other red pigment has this unique fingerprint. Even when the red is mixed with other pigments, the pattern remains intact. Figures A.15 and A.17 illustrate the effect of adding black or burnt umber to the BON red and to the Quinacridone Red, respectively. For both red pigments, the addition of black lowers the reflectance significantly in the long-wavelength, high-reflectance region. The burnt umber also affects the short-wavelength region, shifting the hue a little toward orange. All of the visual, perceived changes are reflected in the CIE and Munsell notations in table A.3. Figure A.7 shows the hues and dominant wavelengths on the chromaticity diagram.

The remaining primary subtractive color to be considered is yellow. Yellow pigments absorb in the short-wavelength, blue-violet region of the spectrum—up to 480 nm, for example. Most yellows exhibit only one absorption band in the visible region of the spectrum. Figure A.18 for yellow iron oxide and figure A.20 for Permanent Yellow FGL are illustrative of yellows in mixture with rutile TiO_2. There are subtle differences we can sometimes use as a possible clue to identify each yellow, but it is difficult to be absolutely certain solely on the basis of the reflectance in the visible region.

The mixtures of the yellows with black and umber illustrate a well-known problem in graying colors with black. Figures A.19 and A.21 illustrate the reflectance curves of such mixtures. Mixing carbon-black pigments, which absorb and do not scatter light, with yellow pigments, such as the yellow oxide and the FGL, that do scatter, results in a green color because yellows exhibit their maximum scattering in the green region. Indeed, olive greens are frequently made this way—by the admixture of yellow and black; they contain no green pigment at all. Graying with burnt umber instead of black alleviates this tendency to shift toward green. In table A.4, the Munsell notations reflect this difference. Refer to the Munsell Hue Circle in figure 2.16. With just white and 10% yellow oxide, the Munsell Hue is 1.51Y. With black added, the hue moves toward the green, to 9.09Y. With umber added, the hue shifts toward the red, to 9.83YR. The Permanent Yellow FGL at 1.00% in TiO_2 has hue of 9.71Y. With black added, it shifts to greenish yellow, 4.24GY; with umber, it shifts back to more reddish yellow, 4.79Y. These changes are very apparent on the chromaticity diagram (fig. A.7).

The secondary colorants are the greens, the purples (often called violets), and the oranges. They are called secondary because the hue can be made by the admixture of two of the primary pigments: green by mixing blue and yellow pigments; purple by mixing red and blue pigments; and orange by mixing red and yellow pigments. Secondary colors, however, can also be distinctive pigments and not mixtures. When observing a colored material visually, therefore, we cannot be certain whether a secondary color is based on a single pigment in mixture with white, or if it is an admixture of two primary colors.

The only green pigment illustrated in the limited library given in appendix A is phthalocyanine green (phthalo green) (see fig. A.22). Note the characteristically shaped tail in the red region, 620–700 nm.

This shape uniquely identifies phthalo green. Note that its absorption maximum is in the red at about 650 nm.

Reflectance curves of mixtures of phthalo green in TiO_2 white with black or burnt umber are illustrated in figure A.23. The addition of both of these pigments decreases the reflectance in the green, but the burnt umber moves the reflectance maximum to longer wavelengths so that it appears more yellow. CIE and Munsell notations are given in table A.5.

When examining unknown green pigments, the reflectance region is *not* the characteristic region. It is the minimum reflectance (maximum absorption) region that is characteristic. When using spectral reflectance curves for identification, the sleuth should begin examining the curve at the *long-wavelength red region* where greens and blues absorb. The reason for this is that reds, oranges, and yellows do not absorb significantly in this long-wavelength red region, and neither do the purples, but most green and blue pigments do.

Compare the shape of the green made with a single pigment, phthalo green (see fig. A.22), with those of the greens made by admixture of blues and yellows illustrated in figure A.24. Curves 1 and 2 in figure A.24 have obviously been made with a phthalo blue: the fingerprint long-wavelength tail uniquely identifies phthalo blue. The differences between the two curves are due to the use of the two different yellows. Curve 1 is highest in chroma; it is made with the higher-chroma yellow among our reference pigments—Permanent Yellow FGL (fig. A.20). The reflectance in the blue region rises at a shorter wavelength than does the reflectance of the yellow oxide in our limited library. See figure A.18. Given a choice between these two yellows, the selection of the yellow that was used is easy. However, in an unknown palette, the identification is far from certain. The presence of the phthalo blue, though, is rather certain. This example points out a very important aspect of the reflectance curves of yellow pigments: the wavelength at which the reflectance rises at the short wavelength limits the selection of possible yellows used.

The other two greens in figure A.24 are obviously made with the other blue, ultramarine blue, in the limited library of examples (fig. A.8). Again, choosing between the two yellows in our library, it is easy to see that the mixture of curve 3 is made with the higher-chroma Permanent Yellow FGL, and that of curve 4 is made with the lower-chroma, redder, yellow iron oxide. CIE and Munsell notations are given in table A.5.

Purples reflect in both the red and the violet regions, being complementary to green or yellow-green, the spectral region in which the purples have their absorption maxima. In our collection of pigments in appendix A, there is only one purple: carbazole dioxazine violet, which will be referred to as simply carbazole violet. It is illustrated in figure A.25. Note that this purple exhibits three characteristic absorption bands, giving a very distinctive curve shape in the absorption region. In mixtures with black and umber (fig. A.26), this shape is still apparent.

Contrast this shape with that for the violets in figure A.27 made by the mixture of blues and reds. Beginning in the long-wavelength region, we immediately identify phthalo blue in curve 3. The red used with it is also unmistakable: the three absorption bands uniquely identify Quinacridone Red. Examining curves 1 and 2 in the long-wavelength region, we see that they are made with ultramarine blue, the other blue in our limited library in appendix A. If we had many more blue pigments to contend with, our identification would not be quite as certain, but we could say with certainty that phthalo blue was *not* used in a major amount if its characteristic absorption is not present. In these two curves we cannot identify the reds with certainty, except within the limitation of our library. Curve 1 is higher in chroma than curve 2, indicating it may have been made with a red higher in chroma. Our only other organic, high-chroma red is the BON red (fig. A.14). The absorption shape, with a maximum at 560 nm, suggests that this could be the red used. The mixture of curve 2 could have been made with red oxide because of its relative flatness in the violet and blue regions. We can say with certainty, however, that Quinacridone Red was *not* used to obtain curves 1 and 2; its characteristic three-band absorption shape is not present. CIE and Munsell notations are presented in table A.6, and chromaticity graphs are shown in figures A.1 and A.7.

Our final secondary color is orange. Oranges are complementary to blue. In our limited library there is only one orange—molybdate orange (fig. A.28). This particular inorganic orange absorbs in the violet, blue, and green regions, making a very flat reflection curve in this region, with no distinguishing bands. In mixture with black and umber, this orange (fig. A.29) produces curves similar to those in figure A.13 for red iron oxide. However, note that the upward tail of the red oxide is a clue to red oxide—although a subtle one—to distinguish it from the molybdate orange.

Oranges can be made by mixture of red and yellow. Some mixtures made with the pigments in our library are shown in figure A.30. Beginning our examination at the long wavelength, the reflectance tail on curve 3 suggests that red oxide (fig. A.12) is present. Neither curve 2 nor curve 1 has any character in this region. Working down to the middle of the spectrum, curve 2 should catch our eye. The shape is reminiscent of Quinacridone Red, except that the absorption band of the shortest wavelength of the three characteristic bands is not readily visible; it has been obscured by the strong absorption of a yellow pigment. Because of the high chroma we chose Permanent Yellow FGL as the strong absorber in this mixture. Curve 1 is also a high-chroma orange. The absorption maximum at 560 nm suggests that BON red is present. Given an extensive choice of reds, however, no such identification could be made because many high-chroma reds have only a single absorption band (see appendix D). The shape of the short-wavelength absorption, which begins to decrease at 470 nm, suggests a high-chroma yellow pigment. From our library we select Permanent Yellow FGL. We could not identify the yellow on the basis of spectral curve shape alone, however. We could say it is *not* yellow oxide because that pigment does not begin to decrease in absorption until about 500–510 nm. For comparison, the curve for molybdate orange (curve 4) is included in figure A.30. Munsell and CIE notations are presented in table A.7, and chromaticity diagrams are illustrated in figures A.1 and A.7.

Probably the most difficult colors to match precisely, with no significant degree of metamerism, are the near neutrals. Grays and tans can be made using a wide variety of mixtures. Two examples of such chromatic pigment mixtures are illustrated in figure A.31. Included for comparison are the flat curves for 0.5% and 2.0% black. In examining the three chromatic mixtures, we again begin in the long-wavelength regions. The fingerprint for curve 1 reads phthalo blue and for curve 2, phthalo green; refer again to figures A.10 (phthalo blue) and A.22 (phthalo green). The next lower-wavelength absorption maximum on curve 2 is at 560 nm. Checking our reference curves in appendix A we find that BON red (fig. A.14) has a maximum absorption at this wavelength. Curve 3 is much less characteristic, but we would expect from its flatness that there could be an orange or orange-red to absorb in the violet, blue, and green regions. In this case red oxide was used. Curve 3 is not very characteristic, but it has an indication of an absorption band at 600 nm, in the orange region, so it must contain a blue. It is obviously not phthalo blue as used in curve 1, but it certainly could be ultramarine blue because of the red upward tail (see fig. A.8). The next slight indication of an absorption band is at about 550 nm. This could be caused by an orange such as molybdate orange (fig. A.28) or an iron oxide orange made with red oxide (fig. A.12) and yellow oxide (fig. A.18), for example. As indicated in figure A.31, the latter is the way it was actually made.

In this section we have illustrated the basic principles used in the qualitative analysis of spectrophotometric reflectance curves, utilizing a very limited library of reference pigments. In essence, the approach to analyzing the shape of the reflectance curve is to start the examination for characteristic absorption (low-reflection) bands in the long-wavelength region, and to proceed in the examination progressively toward the short-wavelength region. We have also tried to show how the reflectance curves relate to our visual observations, and how they relate to the derived colorimetric descriptions, to the CIE coordinates, and to the Munsell notations. The usefulness of plotting the colorimetric coordinates has been emphasized. In short, the major point of this section is that we should use every tool derived from the measured spectrophotometric curve in our analysis—colorimetry as well as spectrophotometric curve shape.

The limited number of pigments used for illustration represents only a small fraction of the pigment types that might be utilized by an artist. Later in this monograph we describe and discuss other pigments and their characteristic reflectance curves, many of which are illustrated in chapter 7. It is hoped that a library of reflection curves can be accumulated for future reference, similar to the atlas of infrared curves published by the Federation of Societies for Coatings Technology (1991) and to the solution spectra sources summarized by Stearns (1969). An example of how such a library could be organized is presented in appendix D.

This limited number of pigments—chromatic colorants plus black, white, and umber—is probably about the maximum number of different pigments an artist might use in any single painting. By measuring many areas of color on a painting, one can get an idea of the palette the artist may have used or at least narrow down the possibilities. Chapter 8 describes a protocol for organizing many multiple measurements and evaluations. If all we can say for certain about many areas is that they were *not* made with certain pigments, we have, at least, eliminated some of the possibilities. We may confirm the presence of the inorganic pigments by X-ray fluorescence. A consideration of the information obtained by these nondestructive techniques allows the examiner to limit the number of samples that need to be taken from a valuable museum object.

Quantitative Application of the Kubelka–Munk Equation

The Kubelka–Munk equation described earlier in this chapter (eq. 4.8) describes the separate additivity of the *K*'s (absorption) and *S*'s (scattering) for the pigments in a mixture. Each of the *K*'s and *S*'s is multiplied by the relative concentration of the pigment it represents. Since the *K*'s and *S*'s refer to the absorption and scattering of unit concentrations of the pigments, they are called unit *K*'s and *S*'s. They may be determined from reflectances measured on samples of known concentration for selected pigment mixtures and on masstones.

Simple estimation

In the previous section, the qualitative application of equation 4.8 was based on measurements of opaque mixtures of individual pigments with white. In this instance, most of the scattering comes from the white pigment. What is observed in the characterization of each chromatic pigment in this manner is its characteristic absorption, *K*, as a function of wavelength, relative to the major scattering from the white pigment, S_W. From this point of view, equation 4.8 can be rewritten in the following form:

$$\left[(1-R)^2/2R\right]_M = K_M/S_W = C_1\left(K_1/S_W\right)+C_2\left(K_2/S_W\right)+\ldots+C_W\left(K_W/S_W\right) \qquad (4.9)$$

where the subscript numbers refer to the individual pigments in the mixture, M. This equation applies at each wavelength, but for simplicity we have omitted the designation (λ) that should always follow *R*, *K*, and *S* to indicate their wavelength dependency.

Since the scattering of the white pigment, S_W, is constant in the equation, and it is only the ratio of *K* to *S* that matters for opaque samples, S_W can be set equal to 1.0000 at all wavelengths. Now the unit K_P/S_W for each pigment can be calculated from a mixture of each chromatic pigment, subscript P, with the white pigment, subscript W, by arranging equation 4.9 for one pigment, P, in mixture with white. Note that S_W must be that of the same white pigment in the same vehicle for all of the unit (K_P/S_W) values used.

This equation works well for mixtures where most of the scattering is due to one white pigment. It is also used for dyes on fabrics that supply the scattering.

Since only the ratio *K/S* is used, these calculations are known as single-constant Kubelka–Munk calculations. From the measured reflectance, the *K/S* ratio can easily be obtained using a small desk calculator. However, there are published tables of the value of *K/S* for any reflectance greater than 0.1%, up to 100.0% at 0.1% intervals; one such table is reproduced in appendix B. Recall that the relationship between *K/S* and *R* is illustrated graphically in figure 4.1.

There is one further calculation that must be considered in the quantitative application of the Kubelka–Munk equation. This involves the reflection at the air–object interface. Whenever a beam of light strikes a surface of different refractive index, some of the incident light is reflected from this interface. The reflectances shown for the pigments in appendix A (all glossy samples) are *total* reflectances designated as $\%R_T$; the surface reflection is included. When the light incident on a glossy surface is perpendicular (normal to the surface) or near perpendicular, the amount of light reflected at the interface, k, is related to the refractive index of the material at the interface by the Fresnel equation (eq. 4.3), which was introduced earlier:

$$k_1 = \frac{\left(n_2/n_1 - 1\right)^2}{\left(n_2/n_1 + 1\right)^2} = \left(\frac{n_2 - n_1}{n_2 + n_1}\right)^2$$

where n_1 is the lower refractive index, often air, and n_2 is the higher refractive index of the material at the interface.

This is the same equation described at the beginning of this chapter for transparent materials when the angle of incidence is near to the perpendicular. The k_1 is the amount of light reflected at an angle equal and opposite to the incident angle. For air, n_1 is 1.000. If the refractive index at the interface material is 1.500, which is an average for organic vehicles, then k_1 (the first-surface reflection) on glossy samples is 0.04, or 4% of the incident light. This is called the specular (or mirror-like) reflection. If the incident light were totally diffuse, instead of being perpendicular to the surface, k_1 would be equal to 9.2% (Judd 1942). If the surface were perfectly diffuse, k_1 would also be 9.2%. However, we seldom see such perfectly diffuse surfaces. Due to their multiple surfaces, pigmented filament fibers may be glossy and exhibit a high degree of surface reflection when woven, resulting in specular reflection at many angles that approaches diffuse reflection. Pressed-powder white standards used with color-measuring instruments may be nearly ideally diffuse. Their surface characteristics depend on the skill of the preparer and on the equipment used. Near-white matte paints made with rutile TiO_2 can be highly diffuse reflectors because the amount of white is above its critical pigment volume concentration. In this situation, the interface surface contains almost no binder. The high refractive index of the TiO_2 provides highly diffuse reflection. Examples of the effects of surface reflection characteristics on color and appearance are presented in chapter 6.

The importance of the surface correction for light exiting a paint or plastic interface as well as entering this material is discussed later in this section. As a simple approximation, 4% may be subtracted from the total reflectance measured at each wavelength for the curves shown in appendix A. The resulting value can be designated with the subscript NS, meaning nonspecular reflectance or simply diffuse reflectance. It is this lower value of reflectance that is used to calculate the *K/S* values that are used in this single-constant approximation. It is also the value that would be obtained if these glossy samples were measured with the specular reflection excluded. Kubelka–Munk theory does not take into account the surface reflection. It is based on the assumption that there is no interface; hence, this correction must be made if the total reflectance has been measured.

The first step in the quantitative application of single-constant Kubelka–Munk calculations is the quantitative determination of the unit *K/S* values of the pigments of interest. In order to do this, dry pigments must first be dispersed, that is, ground into the vehicle used. Artists' tube colorants are predispersed, so this step is not necessary. Generally, predispersed pigments exist in the vehicle as more finely divided particles than the pigment particles in dispersions made by hand, for example, with a muller.

Since the individual pigments are to be calibrated relative to one particular white, the absorption for the white is simply obtained by measuring the reflectance of the white film at complete hiding: $K_W = (1 - R)^2/2R$, where R is the decimal fraction of the diffuse (nonspecular) reflectance. When K_W is known, the unit $(K/S)_P$ for each absorbing pigment can be calculated from the reflectance of a film (at complete hiding) for each pigment when mixed with the white pigment by the following:

$$(K/S)_P = \frac{(K/S)_M - C_W(K/S)_W}{C_P} \qquad (4.10)$$

where the subscript M refers to the pigment–white mixture, the subscript W to the white, and the subscript P to each absorbing pigment. C is the decimal fractional relative concentration, such that C_W is equal to 1.000 minus the total concentration, C_P, for the absorbing pigments.

To even partially define the spectral curve, the reflectance must be determined for at least 16 wavelengths, for example, every 20 nm from 400 to 700 nm. The unit $(K/S)_P$ values at each wavelength are specific for the particular vehicle system and white pigment used. These unit values for the pigments of interest constitute the pigment calibration library for future use. Once created, given good quantitative preparation of the samples and good measurement repeatability, the experiments leading to this library need not be repeated. For maximum accuracy, the measured reflectance for the pigment–white mixtures at the wavelength of maximum absorption should be about 40%, the value for the most precise measurement on a spectrophotometer (Stearns 1969) and for the greatest sensitivity to change in reflectance with concentration (Johnston-Feller and Bailie 1982b).

Using a single wavelength only, an example will serve to illustrate the pigment calibration just described. In appendix A, the curve for the phthalo blue–white mixture in figure A.10 can be used, along with the curve for the masstone rutile TiO_2 from figure A.5. At the absorption maximum of the mixture, 610 nm, the nonspecular reflectance (R_T – 4%) nearest 40% is that for 0.25% blue and 99.75% white, that is, R_P = 39.8%. At the same wavelength, the nonspecular reflectance for the white is 91.0%. From the tables of K/S versus R values in appendix B, the K/S values for these reflectances are $(K/S)_W = 0.00444$ and $(K/S)_M = 0.455$. Substituting these values into equation 4.10, the unit K/S value (for 100%) at 610 nm for the blue is

$$\left(K/S\right)_P = \frac{0.455 - 0.9975\left(.0044\right)}{.0025} = 180.4$$

From other similar pigment–white mixtures of known concentration, a library may be established. With the library of unit K/S values established, the determination of the concentration of an unknown is routine. Equation 4.10 rearranged to solve for an unknown pigment concentration in a white mixture becomes

$$C_P = \frac{\left(K/S\right)_M - C_W\left(K/S\right)_W}{\left(K/S\right)_P} \tag{4.11a}$$

where the subscript M refers to the measured mixture. The concentration of the white is unknown, but as can be seen in the example of the phthalo blue above, the actual value of C_W is only insignificantly different from, and can generally be set equal to, unity. Because the absorption is so low, the quantity $(K/S)_W$ can be subtracted for a first approximation without introducing appreciable error. (In the case of rutile TiO_2, wavelengths below 430 nm, where this pigment begins to absorb significantly, are generally avoided in simple approximations of pigment concentration.)

A more accurate estimate of concentration, even using single-constant Kubelka–Munk theory where S_W is set equal to 1.000, requires the use of all 16 or more wavelengths, a formidable task without a computer program. However, much can be learned without the use of such a program, if a knowledge of absorption mixtures is considered. As in the example above of a single pigment mixed with white, only the wavelength of maximum absorption need be considered. Thus, some simple estimations of concentrations can be made using only a few judiciously selected wavelengths; this is a valuable and rapid procedure.

When the examination of a measured reflectance curve suggests that two or more chromatic colorants in mixture with white, having absorption maxima in different wavelength regions, have been used to make the color, the estimate of the concentration of each pigment requires the use of reflectance values at the maximum absorption region of each. Thus, if a blue is mixed with a yellow to make a green, the wavelength of the long-wavelength absorption maximum for the blue and the short-wavelength absorption maximum for the yellow would be used. The amount of white is obtained by difference. Since it absorbs only slightly, its concentration, C_W, can be set equal to unity unless the color of the mixture is very dark or very high in chroma. (Indeed, the low absorption of the white is often ignored completely for a first estimation.) If the assumption is made that the white absorption is unity, the concentrations of two colorants in a mixture can be calculated from the following two equations:

$$\text{at } \lambda_l\text{: } (K/S)_{Ml} = C_1(K/S)_{1l} + C_2(K/S)_{2l} + C_W(K/S)_{Wl} \tag{4.11b}$$

$$\text{at } \lambda_s\text{: } (K/S)_{Ms} = C_1(K/S)_{1s} + C_2(K/S)_{2s} + C_W(K/S)_{Ws} \tag{4.11c}$$

where the subscripts l and s refer to the long and short wavelengths; M refers to the mixture; and the numbers refer to the individual pigments. The *K/S* values can be determined from the reflectance values by use of equation 4.7 or from the table in appendix B.

An example of the calculation of two chromatic colorants mixed with white will illustrate the use of this technique. Consider the orange represented by the solid line in figure A.30. If the identifications and quantities of pigments were not known, the examination would be carried out in the same way as for any unknown: look for absorption maxima (reflectance minima) beginning in the long-wavelength region and moving toward shorter wavelengths for other clues. The first absorption maximum (reflectance minimum) is found at 560 nm. This is the green wavelength region where red pigments absorb. So the curves of red pigments in our limited library can be consulted. BON red is quickly identified as having a single absorption maximum in this region (fig. A.14). Moving to shorter wavelengths, a maximum can be found at 450 nm in the violet, where yellow colorants absorb. There is little clue to identify the yellow except the wavelength region where the absorption decreases; this is just beyond 450 nm. From our limited library this can only be Permanent Yellow FGL (fig. A.20). The very short wavelength absorption is due to rutile TiO_2 (fig. A.5).

In order to estimate the quantities of the red and the yellow, the absorptions at the two wavelength maxima identified for both—560 nm for the red and 450 nm for the yellow—can be used. But before any calculations can be made on the unknown, it is necessary to determine unit absorption coefficients for each of the identified pigments (the BON red and the Permanent Yellow FGL) as well as the rutile TiO_2 white at these two wavelengths. Referring to figure A.14, the reflectances for 1% BON red–99% rutile TiO_2 can be read from the curve at these two wavelengths; similarly, using figure A.20, reflectances for 2.5% Permanent Yellow FGL at the same wavelengths can be read. The rutile TiO_2 is starting to absorb more at 450 nm, so a correction for the small amount of white can be made. Table 4.2 summarizes the total reflectances, R_T, read from the curves; the reflectances corrected by subtracting 4% for the surface reflectance, designated R_{NS}; the corresponding *K/S* values read from the table in appendix B; and the unit absorption coefficients calculated using equation 4.10. The pigment concentrations used in the calculations are decimal fractions so the unit *K/S* values are for unity (100%).

Table 4.2
Total reflectance (R_T), read from the spectral curves; reflectances created by subtracting 4% from the surface reflectance (R_{NS}); the corresponding K/S values (from appendix B); and the unit absorption coefficients (calculated with eq. 4.10).

Pigment	λ	R_T	R_{NS}	K/S	$(K/S)_{corr}$	Conc. (%)	$(K/S)_{100}$
TiO_2	560	95.0	91.0	0.0044		100	0.0044
TiO_2	450	93.0	89.0			100	0.00608
BON	560	46.0	42.0	0.401	0.397	1	39.7
BON	450	57.5	53.5	0.202	0.196	1	19.6
FGL	560	95.0	91.0	0.0044	0	2.5	0
FGL	450	38.0	34.0	0.641	0.635	2.5	25.4

The calculation for the unit concentration of the FGL is illustrated by:

$$(K/S)_{100\%} = \left[\frac{0.641-0.006}{0.025}\right] = 25.4$$

The reflectances for the orange may now be read from the curve in figure A.30 at the two wavelengths: at 560 nm, $R_T = 39.0$ ($R_{NS} = 35.0$); and at 450 nm, $R_T = 33.5$ ($R_{NS} = 29.5$). The absorptions at each wavelength are the sum of the K/S values contributed by the fraction of each pigment present. When the color obviously contains a large amount of white, the exact concentration of the white is not needed to get an estimate of the amounts of the absorbing pigments present because its absorption is so low. In the case of the orange example, then, just two equations—one for each wavelength—are required to estimate the concentrations of the two absorbing pigments. The equations are of the following type:

$$\text{at } \lambda_1 \text{ and } \lambda_2\text{: } (K/S)_O = C_R(K/S)_R + C_Y(K/S)_Y + (K/S)_W \tag{4.11d}$$

where $(K/S)_O$ is the absorption of the orange mixture based on the reflectance corrected for the 4% surface reflection, and subscript R refers to the red pigment; subscript Y refers to the yellow pigment; and subscript W refers to the white pigment.

Substituting the K/S values of the above reflectances into the equations for each wavelength gives the following:

$$\text{at 560 nm: } 0.604 = C_R(39.7) + C_Y(0.00) + (0.004)$$
$$\text{at 450 nm: } 0.842 = C_R(19.5) + C_Y(25.5) + (0.006)$$

The two equations are easily solved because the absorption of the yellow at 560 nm is zero:

$$0.604 = C_R(39.7) + (0.004)$$
$$C_R = 0.0151, \text{ or } 1.5\%$$

Now that C_R is known, the concentration of the yellow is calculated from the equation for 450 nm:

$$C_Y = [.842 - 0.006 - .0151(19.5)]/25.5$$
$$C_Y = 0.0213, \text{ or } 2.13\%$$

Thus, our estimate using two equations is not quite in agreement with the concentrations, but it is close for a first trial. The reasons that it does not agree perfectly are several; the variance is primarily due to their concentrations having been calculated originally using the two-constant Kubelka–Munk equation (eq. 4.8), and to corrections for internal surface reflection, k_2, as well as the correction for external surface reflection, k_1 (eq. 4.12b). The use of these equations is discussed in the next section.

The important point of this illustration is not that the results are not identical but that they are close enough for a trial that, if the concentrations and preparations of colorants are reasonably constant, would yield a preparation that is close in hue and strength and could easily be corrected to produce the desired color. Additionally, the results did not require the use of any elaborate computer program. Even if one has access to such a program, it is important to understand what is happening in the program and to have the ability to interpret quickly whether the computer results are reasonable.

Up to this point no mention has been made of the metric used to specify the concentrations. The unit used to describe concentrations of the pigments in our illustration is relative weight of dry pigment in wet paint. It could just as well be volume of pigment instead of weight. Weight or volume, wet or dry, any unit may be used provided it is used consistently. It is not necessary to know the dry colorant concentration if a colorant is made using only one colorant that primarily absorbs, or one pigment that primarily scatters. In the case of artists' tube colorants, the concentration of the dry pigment is not known. If there are no other absorbing or scattering materials in the mixture of pigment and vehicle, the concentration of the undiluted wet mixture is set equal to unity, and fractions are calculated on this basis. The pigments present should be identified on the tube. If more than one pigment is present, the technique of setting the unknown concentrations to unity is not valid. A single pigment calibration would not suffice; instead, a series of preparations at different concentrations in white would have to be prepared. An attempt could then be made to identify the absorption regions of each individual colorant in the mixture.

This same basic technique can be extended to mixtures of three or more absorbing pigments; wavelengths representing individual pigment absorption maxima should be selected judiciously, and the equations should be solved simultaneously.

An alternative technique for calculating mixtures of two or more absorbing pigments with white is an iterative method using the following equations, which make the assumption at first that at the wavelength of maximum absorption, the other component does not contribute significantly. Thus,

$$\text{at } \lambda_1\text{: } C_1 = \frac{(K/S)_{\mathrm{M}}}{(K/S)_1} \tag{4.11e}$$

where λ_1 is the wavelength of absorption of the major component (designated by subscript 1). After estimating C_1 from this equation, the value for C_1 is substituted in the following equation to calculate the concentration, C_2, of the second component at λ_2:

$$\text{at } \lambda_2\text{: } C_2 = \frac{\left[(K/S)_M - C_1(K/S)_1\right]}{(K/S)_2} \tag{4.11f}$$

Once the concentration of the second component, C_2, is determined, this value is substituted in the recalculation of the concentration of the major component, C_1, at λ_1:

$$\text{at } \lambda 1\text{: } C_1 = \frac{\left[(K/S)_M - C_2(K/S)_2\right]}{(K/S)_1} \tag{4.11g}$$

This series of calculations—the iteration—is repeated, using equations 4.11f and 4.11g until equation 4.9 is satisfied. (The concentration of the white may or may not be added into equation 4.9, depending on the precision desired. It is often of little significance compared with the accuracy with which the pigment mixtures can be made.)

The techniques described above for calculating opaque colorant mixtures using single-constant Kubelka–Munk equations for pigment mixtures and for dyes on fabrics, or for calculating transparent colorant mixtures using the Beer–Bouguer equation, are the simple techniques used in analytical spectrophotometry. They are as valid today as they were fifty years ago.

Using a few selected wavelengths for analyzing the spectral curves of mixtures is a shorthand method of carrying out a complete spectral curve analysis, sometimes called a differential spectral curve analysis. In a complete analysis, the curve of the mixture is broken down into the absorption curves of the individual components that additively combine to make the absorption total. In the field of color science, the pioneering computer for carrying out a curve analysis was the analog Colorant Mixture Computer, COMIC, designed and manufactured by Davidson and Hemmendinger (Davidson, Hemmendinger, and Landry 1963). The introduction of this simple tool began the use of visible spectral curve measurement and analysis for industrial color control in manufacturing processes. The operator of the computer observed 16 dots on an oscilloscope screen; these dots represented the *K*/*S* values for 16 equally spaced wavelengths. By adjusting the amounts of *K*/*S* from one to five components, the curve dots could be zeroed to balance the *K*/*S* of the sample in question. On occasion, the author has used it for some samples measured by transmission in the infrared region as well. Differential spectral curve analysis can be useful in any region of the spectrum, and it is the basis for all analytical interpretation of spectral curves.

Use of the Kubelka–Munk single-constant theory (using *K*/*S* instead of separate *K*'s and *S*'s) is presented by Billmeyer and Saltzman (1981). These authors follow this illustration with a picture of COMIC (the analog computer) and a flowchart illustrating the iterative procedure used in computer colorant matching. Kuehni (1975) illustrates a digital computer colorant-matching program.

Basing the reference library on a single colorant–white mixture was, and is, not generally sufficient for accurate analytical work. Instead, a range of concentration mixtures was made, that is, a calibration curve of *K*/*S* versus concentration was prepared for each absorbing material, and the calibration closest to that estimated to be present was used in the final calculation. Today, with computers, this may also be done, and a range of unit concentration values may be stored. However, as in the case of mixtures, if the scattering may come from more than the white in a pigment mixture, the more complete two-constant Kubelka–Munk equation is generally used. The examples presented in this monograph were calculated using two-constant theory, where separate values for *K* and *S* for all pigments are used in the calculation. In addition, surface corrections for internal reflections are also used.

More complex estimation

In the estimation procedure described earlier in this chapter, two significant simplifications are made. The first is that the only surface reflection correction necessary is the subtraction of the first-surface reflectance from the total measured reflectance. However, before light that has entered the paint film can exit the film, it encounters another interface—the paint-to-air interface—where part of the exiting light is reflected back into the film. The same reflections occur with all dielectric materials—plastic, glass, paper, etc. The second simplification is that all the scattering comes from the white pigment or from some other low-absorbing, scattering component. In many situations, particularly with dark or high-chroma colors, this additional assumption is not adequate. Several such cases are pointed out earlier in this chapter (see the section on "Absorbing and Scattering Materials").

The total reflectance measured is described by the following equation for dielectric materials (nonconductors of electromagnetic energy, that is, nonmetals):

$$R_{\mathrm{T}} = k_1 + \frac{(1-k_1)(1-k_2)R_{\mathrm{i}}}{1-k_2R_{\mathrm{i}}} \tag{4.12a}$$

where R_{T} is the total decimal reflectance; R_{i} is the internal decimal reflectance (see eq. 4.12b); k_1 is the decimal amount of the first-surface reflection coefficient (air-to-paint interface); and k_2 is the decimal amount of the internal surface reflection (paint-to-air interface).

R_{i} is used in the Kubelka–Munk equation and is obtained by rearranging equation 4.12a so that

$$R_{\mathrm{i}} = \frac{R_{\mathrm{T}} - k_{\mathrm{i}}}{(1-k_1-k_2)+R_{\mathrm{T}}k_2} \tag{4.12b}$$

The assumption is made in both equations that the light is totally diffuse internally, striking the interface in equal amounts at all angles. Equation 4.12a was first described by Walsh (1926), but it is now generally called the Saunderson correction because Saunderson first pointed out its importance when using the Kubelka–Munk equation (Saunderson 1942).

If the refractive index of the paint at the interface is 1.5, then k_1 is 0.04 (4%), and k_2 is 0.60 (60%). Saunderson found that using k_2 equal to 0.4 (40%) gave the best results on his polystyrene samples. Experience has shown that it really does not make much difference, within experimental error, whether 40% or 60% is used, provided that for any pigmented system, one is consistent and uses the same value for all pigmented samples, including those used in preparing the pigment calibration library (Giovanelli 1956; Brockes 1960). For paints, the author has used the higher, theoretical figure for k_2—0.6 (60%). More complete discussions of the best value of k_2 may be found in papers by Mudgett and Richards (1973) and by Phillips and Billmeyer (1976).

The relationship between refractive index and the surface reflection is described by Judd (1942; Judd and Wyszecki 1963). Judd's curve is reproduced here as figure 4.2. A table of exact values of k_1 and k_2 was computed and published by Billmeyer and Alman (1973).

Another diagram in Judd and Wyszecki's books (1963, 1975), reproduced here as figure 4.3, illustrates why k_2 (the internal exiting reflection loss) is so high. It shows how light rays are refracted when entering a medium of different refractive index. When entering a medium of higher refractive index, the rays are bent toward the perpendicular to the surface; when exiting from a medium of higher refractive

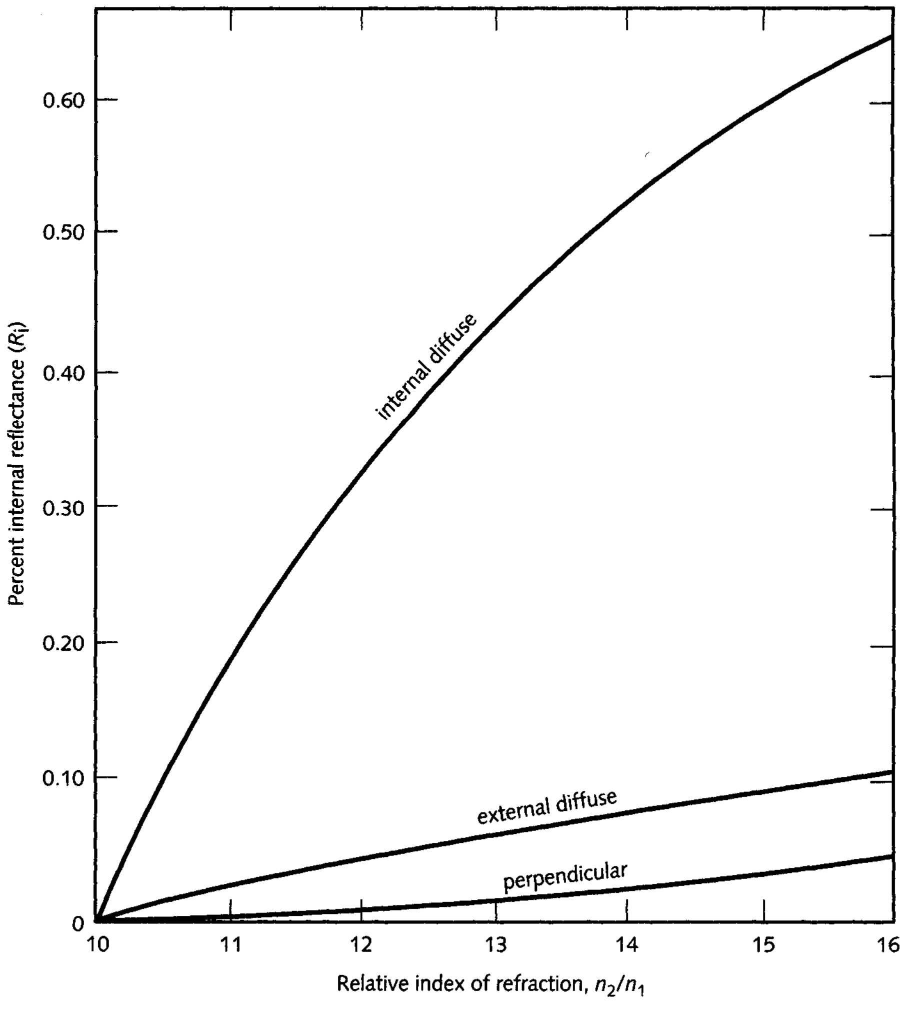

Figure 4.2

Interfacial reflectances as a function of the refractive index ratio, n_2/n_1, where n_2 is the denser medium (from Judd and Wyszecki 1963. Copyright © 1963 John Wiley & Sons, Inc. Reprinted by permission).

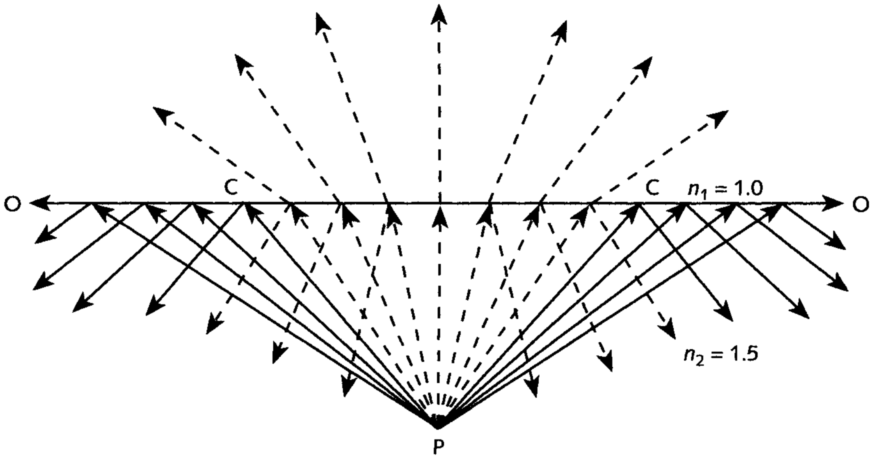

Figure 4.3
Illustration shows how light rays emanating from point P inside a material of refractive index 1.5 (n_2) are bent when entering a less-dense medium, such as air (n_1). Because the exiting rays are bent away from the perpendicular, about 60% of the light is reflected back into the material. The light striking the surface at point C (42°) travels to point O, and at angles greater than 42°, the light is totally reflected back into the dense medium. The 42° angle is the critical angle when the refractive index of the denser material is 1.5 (from Judd and Wyszecki 1963. Copyright © 1963 John Wiley & Sons, Inc. Reprinted by permission).

index to a lower one, such as air, the rays are bent away from the perpendicular so much that many of them are totally reflected back and cannot escape. The angle at which light striking the interface from inside begins to be totally reflected is called the *critical angle,* and it depends on the refractive index. For a refractive index of 1.5, this angle is about 42° from the perpendicular.

Figure 4.2 shows that the higher the refractive index of the vehicle, the larger will be the reflection at the interface for light both entering and exiting the film. The relationship between $\%R_T$ and $\%R_i$ for a refractive index of 1.5, based on equation 4.12a, is shown graphically in figure 4.4. Applying these surface corrections is extremely important for very dark colors and for colors of very high chroma, where in some regions of the spectrum the reflectance is very low.

The second simplification made earlier in this chapter is that all of the scattering comes from the white pigment.

In the case of the yellow–black mixtures, which make an olive green, it was pointed out that this color results because the yellows have their maximum scattering in the green region. And even though a mixture may contain significant amounts of rutile TiO_2, the scattering of the yellows plays an important role (see figs. A.19 and A.21). If we were to use the full two-constant Kubelka–Munk equation (eq. 4.8), this behavior would be predicted.

The full two-constant equation relates the *K/S* of the total mixture to the sum of the fractional concentrations of each pigment, C_P, times each corresponding unit absorption coefficient, K_P, divided by the sum of the fractional concentration of each pigment, the C_P's, multiplied by its corresponding unit scattering coefficient, S_P, as follows:

$$\left(\frac{K}{S}\right)_M = \frac{C_1K_1 + C_2K_2 + C_3K_3 + \ldots}{C_1S_1 + C_2S_2 + C_3S_3 + \ldots}$$

where the subscript numerals identify the individual pigments, and the C's are relative concentrations such that their sum is unity (100%). The $(K/S)_M$ is determined from the calculation of the internal reflectance, R_i, from the measured total reflectance from equation 4.12b. If diffuse

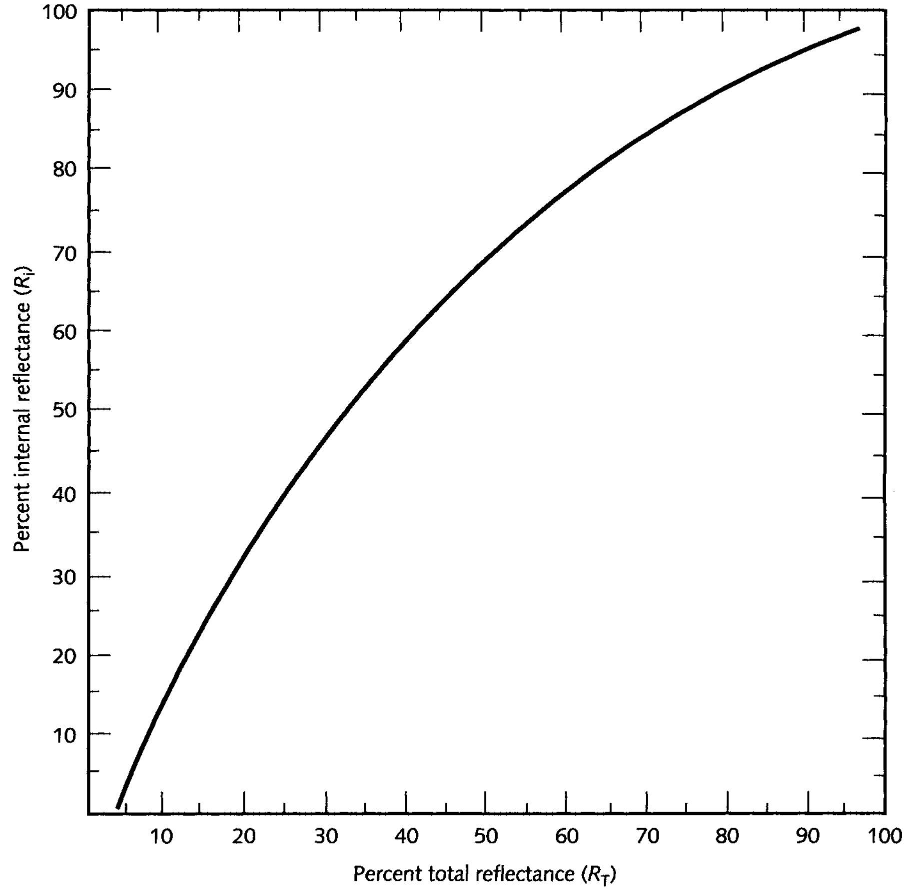

Figure 4.4
Relationship between total reflectance and internal reflectance calculated from eq. 4.12 for perpendicular incidence and a refractive index of 1.5.

reflectance is measured instead of total reflectance, the numerator on the right side of the equation becomes simply R_T. The assumption is made that the paint film is opaque, completely hiding the substrate at all wavelengths. Solving this equation for unknown concentrations using 16 wavelengths and 4 appropriate pigments becomes a formidable task without the use of a computer.

It is not the purpose of these discussions to dwell on the complex computer color-matching technique using the two-constant Kubelka–Munk equation, nor to present actual examples. However, a reader interested in making color matches may wonder how the utilization of equation 4.8 is carried out. The first step involves the determination of the individual pigment characteristics—the *K*'s and *S*'s.

Since there are two unknowns, K_P and S_P, two equations are required to determine the unit values of K_P and S_P at each wavelength. In order to calibrate each pigment, that is, to describe its unit *K* and *S* for each wavelength, two mixture relationships, or two equations for known mixture concentrations, are necessary. For example, the reflectance measurements of a known mixture with a standard white and a second known mixture with a standard black give the two equations needed for simultaneous solution. The procedure requires a standard white and a standard black. A further quantity that can be of value in pigment calibration is the reflectance of the masstone of a single pigment that contains no black and no white. Thus, there is a choice among the following three equations for obtaining the unit K_P and S_P values.

$$\text{For white mixtures: } \left(\frac{K}{S}\right)_M = \frac{C_P K_P + C_W K_W}{C_P S_P + C_W K_W} \tag{4.13}$$

For a masstone (eq. 4.7): $(1 - R_i)^2/2R_i = K_P/S_P$

$$\text{For black mixtures: } \left(\frac{K}{S}\right)_M = \frac{C_P K_P + C_B K_B}{C_P S_P + C_B K_B} \tag{4.14}$$

Note that all reflectances used in the Kubelka–Munk equation are internal reflectances obtained by use of equation 4.12a rearranged as equation 4.12b.

From the two pairs of equations—equation 4.13 with equation 4.7; or equation 4.14 with equation 4.7—two sets of K's and S's can be computed. The K's and S's of the pigment in the *absorption* region of the spectrum are selected using results obtained from equation 4.13 for the white mixture and equation 4.7 for the masstone. The K's and S's of the pigment in its *scattering* region are selected from the wavelengths of its *maximum* reflectance using results obtained from equation 4.14 for the black mixture and equation 4.7 for the masstone. The values of the K's and S's in the crossover region between the two sets of data are selected on the steepest part of the reflectance curve between minimum and maximum by smoothing the values; generally there is a wavelength where the two sets of values are very close. In the case of transparent pigments, when mixtures with black are near black, all of the values used are from the white and the masstone, equations 4.13 and 4.7. This procedure for determining the K's and S's used for computing colorant formulations was first described by Davidson and Hemmendinger (1966). If a masstone cannot be prepared at complete hiding, its reflectance may be calculated from films measured over white and over black using the equations for incomplete hiding described below under the heading "Opacity, Translucency, and Hiding Power."

It must be remembered that all of the unit K's and S's are *relative* to the particular white used in the calibration procedure. If a different white is desired or necessary, its K's and S's must be calculated relative to those of the original white. For example, if rutile TiO_2 had been used for the calculation of the unit K's and S's of the pigments, but a calibration for ZnO white is desired, the K's and S's for the ZnO must be determined relative to the K's and S's for the rutile TiO_2. This is most readily done from a mixture of the ZnO with the standard black and a ZnO masstone with equations 4.14 and 4.7.

A method for obtaining the K's and S's for the standard white and the standard black pigments remains to be described. There are two methods for determining the K and S for the white. The first of these is a relative method and the second, an absolute method. The relative method for determining the K and S of the white involves only the preparation of a masstone white that is completely opaque. The scattering coefficients, the S's, are set equal to 1.000 at all wavelengths, and the absorption coefficients, the K's, are calculated with equation 4.7 (the equation for the masstone). The K's and S's for the standard black are then calculated relative to these values for white by use of equations 4.13 and 4.7, that is, from a white–black mixture and the masstone black. This relative method works well as long as the samples are at complete hiding.

When hiding is incomplete, a different version of the Kubelka–Munk equation must be used (Kubelka 1948; Ross 1967):

$$R_\mathrm{i} = \frac{1 - R_\mathrm{g}(a - b\,\mathrm{ctgh}\,bSX)}{a - R_\mathrm{g} + b\ \mathrm{ctgh}\,bSX} \tag{4.15}$$

where R_i is the decimal internal reflectance of the film over the substrate of internal reflectance, R_g.

$$a = \left(S + K\right)\Big/ S = \frac{1}{2}\left[R + \frac{R_0 - R + R_\mathrm{g}}{1 - R_0 R_\mathrm{g}}\right] = \frac{1}{2}\left[\left(\frac{1}{R_\infty}\right) + R_\infty\right] \tag{4.16}$$

$$b = \left(a^2 - 1\right)^{1/2} \tag{4.17}$$

R_0 = reflectance over a black of 0% internal reflectance
R_∞ = internal reflectance at complete hiding
X = thickness (actually CX, since altering the concentration, C, has the same effect as altering the thickness, X, by the same multiple)
ctgh = the hyperbolic cotangent

Tables of hyperbolic cotangents are available, for example, in Judd and Wyszecki (1975), which also gives equations for calculating hyperbolic functions.

An equation useful for determining the scattering coefficient S is

$$SX = \frac{1}{b}\left[\mathrm{ctgh}^{-1}\left(\frac{1 - aR_0}{bR_0}\right)\right] \tag{4.18}$$

where ctgh^{-1} is the inverse hyperbolic cotangent. From these equations it can be seen that S can be determined from the values of a calculated from reflectances, R_i, measured over a light substrate of reflectance, R_g and R_0, or calculated from R_0 and R_∞ by use of the appropriate equation from those in equation 4.16. In either case the thickness, X, and concentration, C, must be known. The value for K is calculated from the relationship $a = (S + K)/S$. The absorption and scattering coefficients thus calculated are dimensioned, being in terms of the thickness, X, and the absolute concentration, C. (The absolute concentration is the volume or weight percentage in the dried paint film or in the solid plastic piece, for example.)

The K's and S's of the black and of the individual colorants are subsequently determined as before; now the absolute values of the white are substituted for the relative values used when all S's were set equal to unity in the complete hiding calculation. These pigment calibrations made relative to the absolute values of the standard white may now be used to calculate hiding power or to predict R_∞ from samples at incomplete hiding. If one wishes to calculate the colorant composition for a glaze to be applied over another color, these absolute values are needed (see "Glazes" below). If one wishes to determine the absolute amount of pigment necessary to achieve a desired degree of opacity (Osmer 1978), these values are also needed (see "Opacity, Translucency, and Hiding Power" below). Not all of the colorant-formulation computer programs available include this type of calculation, which is so very useful in many situations involving incomplete hiding layers.

After determining the unit *K*'s and *S*'s at 20 nm intervals or, preferably, at 10 or 5 nm intervals, the colorant formulation can be calculated to match the color desired. This is described in terms of the reflectances at the same wavelengths as those used for the pigment calibrations. The amounts of individual pigments are determined by means of simultaneous equations. How the match is achieved may vary with the particular computer program, but, in general, an iterative calculation is carried out by use of a variety of pigments designated by the operator. The initial goodness of match may be estimated by a least-squares calculation of the reflectances; a visually weighted least-squares calculation of the reflectances; or the calculation of tristimulus values and color differences.

After calculating each possible match, most computer color-matching programs select those matches that are least metameric by calculating the tristimulus values for other selected illuminants and then calculating the color differences for each from the desired color. Thus, if a match has been made for illuminant C, such that ΔE is zero, the color differences for several other illuminants, such as illuminant A (incandescent light source) and a fluorescent lamp (often abbreviated F) are then calculated. These differences are an approximate measure of the degree of metamerism (see the section on "Metamerism" in chap. 2).

Use of the computer color-matching program is not limited to applications involving color. Computer programs for two-constant color matching may not be as versatile as those for single-constant, but they can be useful in other regions of the spectrum. Osmer (1982) illustrated their usefulness in computing pigment formulations in the near-infrared region as well as in the visible region for paints to be used for camouflage applications. (Incidentally, with the matches for the very dark green, he illustrates that computer matches can be calculated that contain no white pigment but depend on chromatic colorants for pigment scattering.)

Although digital computer color-matching programs have many applications, they are not a substitute for intelligence nor a panacea for sloppy control and handling of the components. If the operator offers the computer twelve pigments to use four at a time, he will often get a very large number of matches. However, a knowledge of the spectral curve shapes of pigments enables the intelligent operator to narrow down considerably to the most likely or the most suitable pigment choices at the beginning, saving much time and paper.

Applications of Kubelka–Munk Formulas

Study of colorant changes

One important application of the Kubelka–Munk equations, which is of particular interest in the museum world, is in the study of colorant fading or darkening. Knowledge of the rate of these changes of the colorants used in materials enables the museum personnel to develop the best conditions for the preservation of the objects in their care while still allowing them to be displayed.

Basically, establishing the rate of fading, or darkening, is an analytical problem involving measurement of the change in concentration of the colorants. Thus, use of the Kubelka–Munk equation for the determination of concentration changes can provide the analytical data necessary for studying the types and rates of change that occur during aging or following exposure to deleterious conditions.

In the introduction to this monograph, it was pointed out that our eyes are not analytical but are integrative, in terms of the stimulus that forms the basis of our perception of what we see. The CIE method of describing color, and any derived color-difference equations, represents an attempt to provide a numerical description of what we see. Thus, the use of such calculated data is inappropriate for *analytically* describing the changes in the *concentrations* of the coloring agents.

Color plate 1 illustrates a series of seven different mixtures of alizarin with rutile TiO_2. Compare the series on the left with that on the right. Can one tell by visual evaluation the fraction of the original alizarin concentration in the left column of color chips that remains in the corresponding color chips on the right? Not at all. The fact is that the color chips in the right column illustrated in color plate 1 all have lost 30% of the original alizarin concentration present in the corresponding chips shown in the left column.

In applying Kubelka–Munk calculations to determine the rate of colorant change, the simplest situation will be described first: evaluating the concentration change of a specific single pigment mixed with white in a particular vehicle, exposed in a specified manner. (In the case of the evaluation of dye fading, the analogous simple situation is evaluating the concentration of a single dye applied to a colorless substrate in a specified manner.)

Many pigments, with the exception of some of the highly inert inorganic pigments, vary in stability when exposed to light, heat, high humidity, or extreme values of pH, depending on the surrounding medium (the vehicle). Therefore, it is important that the stability be described in relation to the particular pigment–medium (vehicle) system. The application to be described involves a known single pigment, or single pigment–white mixture, exposed to whatever deleterious factors are considered important. Accelerated-aging exposures may also be used, if one remembers that these conditions do not necessarily represent the real world exactly.

In the limited application to be discussed, the test samples prepared for evaluation are simple mixtures with white, in the case of pigments, or single dyeings in the case of dyes, prepared for the specific purpose of the study. For this simple application, one does not even have to know the exact concentration. One simply makes the assumption that the white pigment does not absorb significantly in the region of the absorption maximum. The reflectance at this wavelength is measured, and the nonspecular reflectance converted to *K/S*. The quantity $(K/S)_o$ for the unexposed sample is the reference to which the subsequent $(K/S)_e$ values for the exposed samples are compared as follows:

$$100\left[(K/S)_e \Big/ (K/S)_o\right] = \% \text{ colorant remaining} \tag{4.19}$$

The subscript e refers to the exposed sample and the subscript o to the unexposed reference. The *K/S* values are based on the diffuse reflectance. If the original concentration is known, it may be multiplied by the fraction remaining to obtain the actual concentration remaining. This example is an illustration of the simple estimation of colorant concentration described above in the section "Quantitative Application of the Kubelka–Munk Equation." The rate of change can then be interpreted by application of the principles used in the study of the kinetics of chemical reactions.

In this initial discussion the assumption is made that the pigment fades to a form that does not absorb in the region of the original absorption maximum. Many pigments do this. Some organic reds, such as synthetic alizarin lake, fade through a yellow form in the progress of becoming completely colorless. However, the yellows formed do not absorb in the region of the absorption maximum of the red form, so they do not interfere with this estimate of concentration remaining (Johnston-Feller 1986). Figure 4.5 illustrates the fading of alizarin following exposure in the Atlas xenon arc Fade-Ometer.

A few pigments darken instead of fading to a colorless form. Vermilion (the red form of mercuric sulfide) is one of these. Other inorganic pigments that darken include some that contain lead, such as chrome yellow and molybdate orange; Emerald Green (copper acetate–copper arsenate) also may darken. Feller (1967) published spectrophotometric curves showing the darkening of vermilion in oil without added white pigment. Some of those curves are shown in figure 4.6. Studying the curves, one can see that two changes are occurring: (1) at the long-wavelength region of maximum reflectance, the reflectance is decreasing due to the darkening; and (2) at the short-wavelength (absorption) region, the reflectance is increasing as the concentration of the red vermilion decreases. Feller discusses the rate of darkening as measured by the change in *K/S* in the long-wavelength region.

Studies of pigment change can be profitably analyzed by use of a color-matching program, utilizing the multiple wavelengths described above (in the "Quantitative Application of the Kubelka–Munk Equation" section) and the full two-constant equation, equation 4.8. When computer color-matching programs are applied to the study of color changes following exposure of a single colorant–white mixture, it is necessary to use calibrations for four pigments (including white) in order

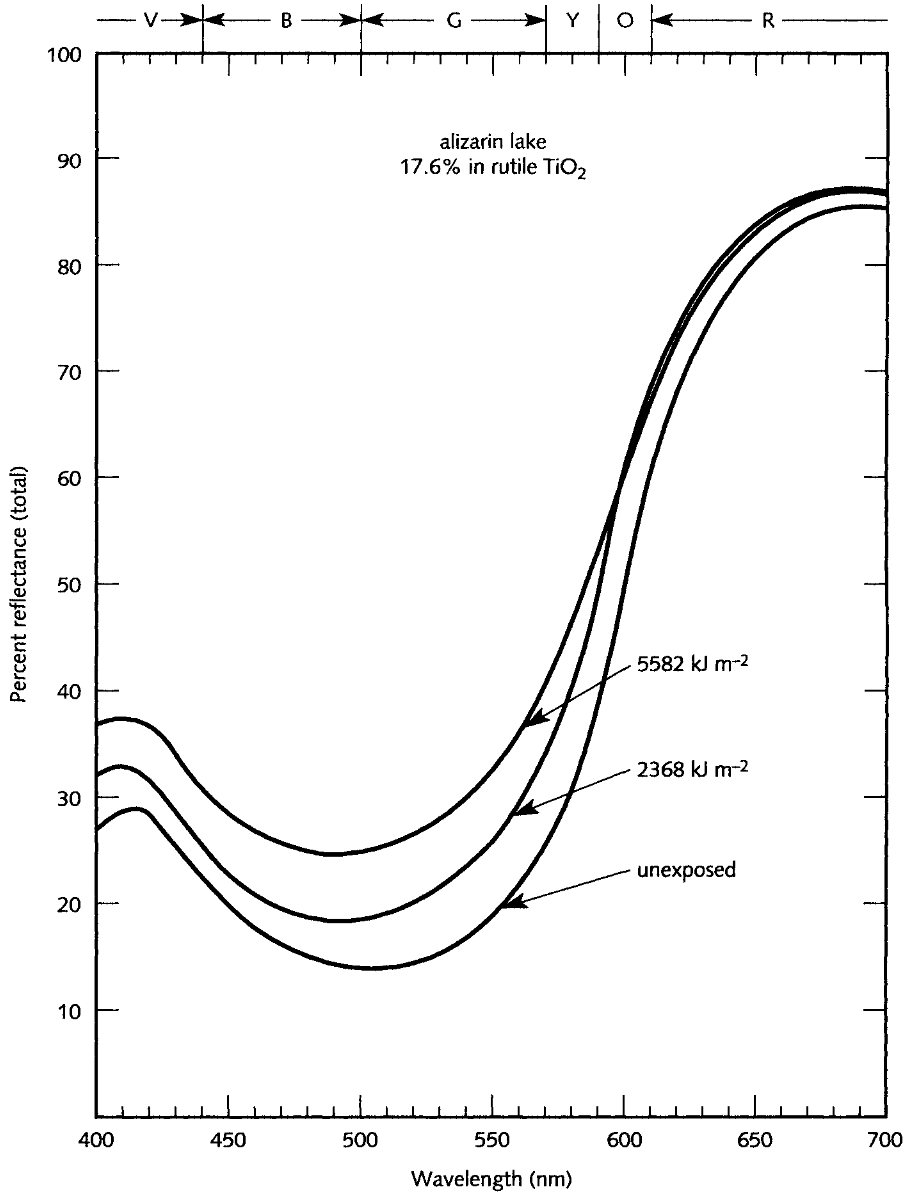

Figure 4.5

Reflectance curves of alizarin in mixture with rutile TiO_2, initially and following exposure in the Atlas xenon arc Fade-Ometer. The exposure is expressed in terms of kilojoules per square meter as measured at 420 nm (after Johnston-Feller 1986).

to have the necessary three degrees of freedom in color space. Thus, in the case of a single pigment in mixture with white, two other pigment calibrations must be included in the calculation. The three must be selected so that one controls the redness–greenness, one controls yellowness–blueness, and one controls lightness–darkness. In the case of the calculations for the alizarin–TiO_2 illustrated in figure 4.5, calibrations for a yellow pigment and for a black pigment were used in addition to those for the alizarin and the rutile TiO_2. In this way, fading, yellowing, and darkening could be determined (Johnston-Feller et al. 1984). By use of this technique, it was shown that synthetic alizarin pigment in mixture with white faded through a yellow intermediate before fading to a colorless form, and the amount of the yellow intermediate was quantified.

A further reminder concerning such studies must be emphasized. The samples prepared for study must be at complete hiding and at such thickness and pigment volume concentration that hiding remains

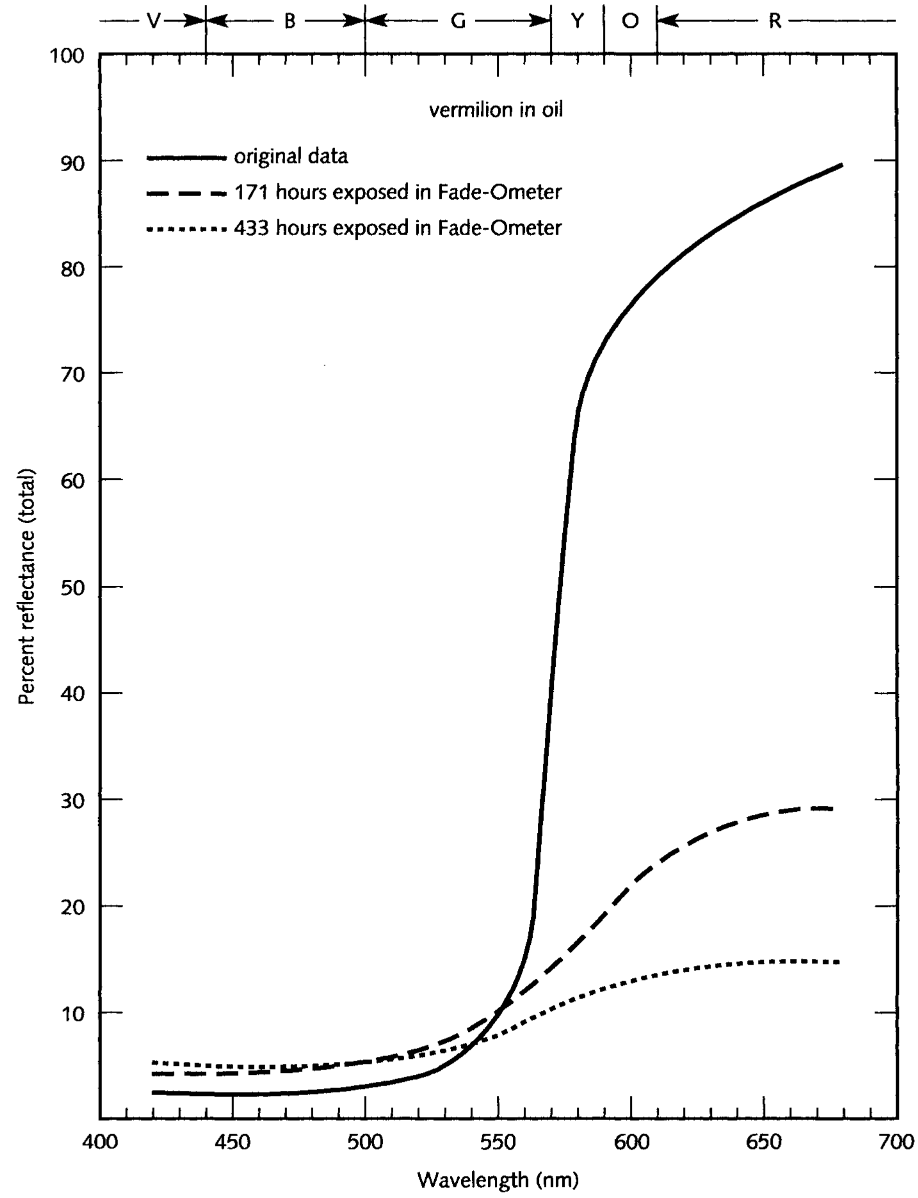

Figure 4.6

Reflectance of vermilion (cinnabar) before and after exposure in the Fade-Ometer. It can be seen that the color is approaching the very dark gray characteristic of metacinnabar.

complete over the time of the study. Pigment deterioration increases as light penetrates more deeply into the film and fading continues. For this reason, measurements on the samples should be made over white and over black. When hiding becomes incomplete so that the black backing can be seen, the simplified Kubelka–Munk equation (eq. 4.7) is no longer valid. The dependence of the depth of fading on the pigment volume concentration of the TiO_2 and on the relative alizarin concentration in the alizarin–TiO_2 samples made at constant thickness is illustrated in color plate 2. The height of the dowels corresponds to the depth of fading. The dowels were painted with the actual material used in the samples (see figs. 9 and 10 in Johnston-Feller 1986).

Changes in color perceived as fading or darkening can result from reasons other than deterioration of the pigment. For example, if the surface reflection characteristic of a paint changes over time, the appearance may seem to indicate a change in colorant concentration. The gloss of high-gloss samples may decrease, resulting in an increase in the surface scattering and thereby giving the appearance of fading. In the case of low-gloss (matte) materials, the gloss may increase because of burnishing, fingerprints, washing, addition of varnish, and so on, resulting in a perceived darkening of the color. Whether the exposed sample is lighter or darker, the changes in the spectral reflectance curve due to changes in the surface reflection are different from the changes due to pigment deterioration: reflectance changes due to surface changes tend to occur uniformly at *all wavelengths,* resulting in a nearly constant increase or decrease in reflectance across the spectrum (see remarks on chalking of paint, Johnston and Feller 1967).

Spectrally uniform changes in reflectance also result from increases or decreases in light scattering that occur *inside* the coating, such as at the pigment–vehicle interface. If the suspending vehicle (medium) matrix shrinks over time, for example, the result may be the formation of microscopic voids surrounding the pigment particles. Such voids scatter light very effectively, creating the effect of added white pigment and lightening the perceived color (see "Microvoids and Vesiculated Beads" in chap. 6). Thus, though the appearance may be that of fading (loss of colorant), the actual cause can be quite different.

Figure 4.7 shows a transmission electron micrograph of an exposed fluorocarbon plastic pigmented with TiO_2 and carbon black. Carbon black and TiO_2 incorporated in a stable plastic matrix (vehicle or medium) normally do not exhibit fading. Yet this sample appeared to have faded. Careful study by electron microscopy of the cross section of the exposed material revealed that voids exist around pigment clumps in many regions (disregard the streaks in this picture—they are caused by the microtome slicing). The voids contain no vehicle and no pigment; they are virtually empty cavities, possibly filled with air if it has diffused into them. The voids have a much lower refractive index than the surrounding material. Hence they scatter light, increasing the perceived reflectance. Such a change inside the film cannot be detected by spectral analysis as being different from fading (loss of colorant).

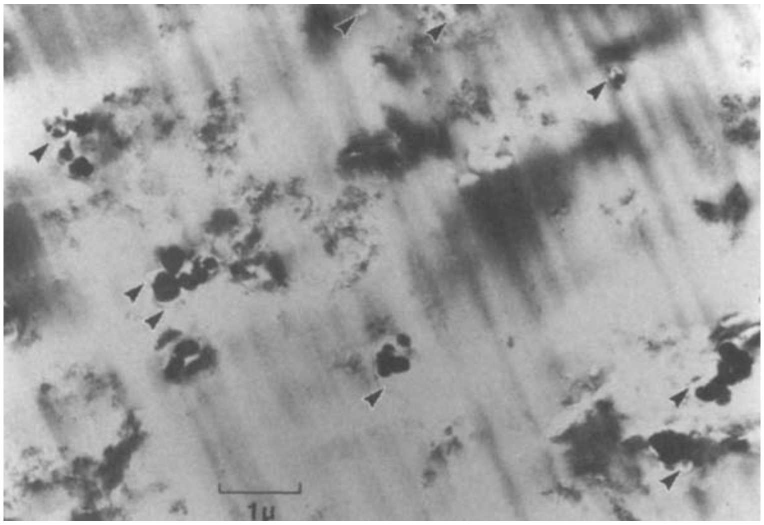

Figure 4.7

Transmission electron micrograph of a cross section of a fluorocarbon plastic pigmented with TiO_2 (large black particles) and with carbon black (clouds of fine black dots). The arrows point to voids that surround the pigment clusters.

Note also in this electron photomicrograph that the concentration of the TiO_2 particles (large black particles) and of the tiny, black, dot-size carbon black particles is not uniform throughout the plastic matrix. As is apparent, the pigment volume concentration (PVC) is low, which is typical in thick plastics; the pigments tend to clump together and are not uniformly distributed throughout the material. This occurs in many paint films made at low PVC. For example, Buttignol (1968) shows electron micrographs of paint samples made at PVCs of 0.3 to 1.3 (generally low for paints). The uneven distribution of pigment can be observed in his figure 5 for transparent synthetic yellow oxide and in his figure 9 for transparent red oxide, even though the dry pigments were fairly uniform in particle size. The causes of this nonuniformity could include lack of wetting of the pigment particles by the vehicle, so that van der Waals forces hold the pigment particles together; the presence of moisture surrounding the pigment particles; or the interaction of the pigments with the vehicle (some pigments tend to inhibit the curing of the vehicle).

The lack of wetting can be serious in other cases. For example, if paint used to retouch areas of a painting does not adhere well to the original, the added paint layer may separate from the original over a period of time. The air present between the layers causes light scattering and an increase in reflectance across the spectrum.

If the pigment particles are not thoroughly wetted in the initial pigment dispersion, darkening may also result during exposure. Perhaps the fluid decomposition components in the vehicle are able to wet the pigment more than the "fresh" vehicle in the original dispersion. This would result in a significant change in transparency as well, because of the lower degree of scattering. Feller (1968) contrasts the absorption *K/S* curves of two greens, both of which darkened on exposure: Emerald Green (copper acetate–copper arsenate), which darkened because of pigment change in the oil vehicle; and Green Earth in oil, which presumably darkened because of an increase in wetting of pigment–vehicle interfaces or interstices. Figure 4.8 (from Feller's fig. 6) illustrates the reflectance change of Emerald Green following exposure in a Fade-Ometer. From the reflectance curve shape it is not readily apparent what is happening. But when the absorption *K/S* curves are plotted on a logarithmic scale, an interpretation of the change can be made. Figure 4.9 (from Feller's fig. 7) illustrates the changes in absorption *K/S* of the Emerald Green and the Green Earth before and after exposure.

There are two important points to be emphasized in these curves. The first is the value of studying *log* absorption *K/S* curves graphically—*K/S* on semilog paper versus wavelength—that is, learning to visualize spectral curves in absorption terms rather than simply in reflectance terms. Log absorption curves retain a constant shape regardless of the concentration of the absorber (Derby 1952). Thus, if a pigment appears to decrease in concentration, the change in the spectral log *absorption* curve will be the same at all wavelengths, *decreasing uniformly;* conversely, if the pigment appears to increase in concentration, the scattering may have decreased, or the absorption may have increased uniformly at all wavelengths (see discussion in the next section).

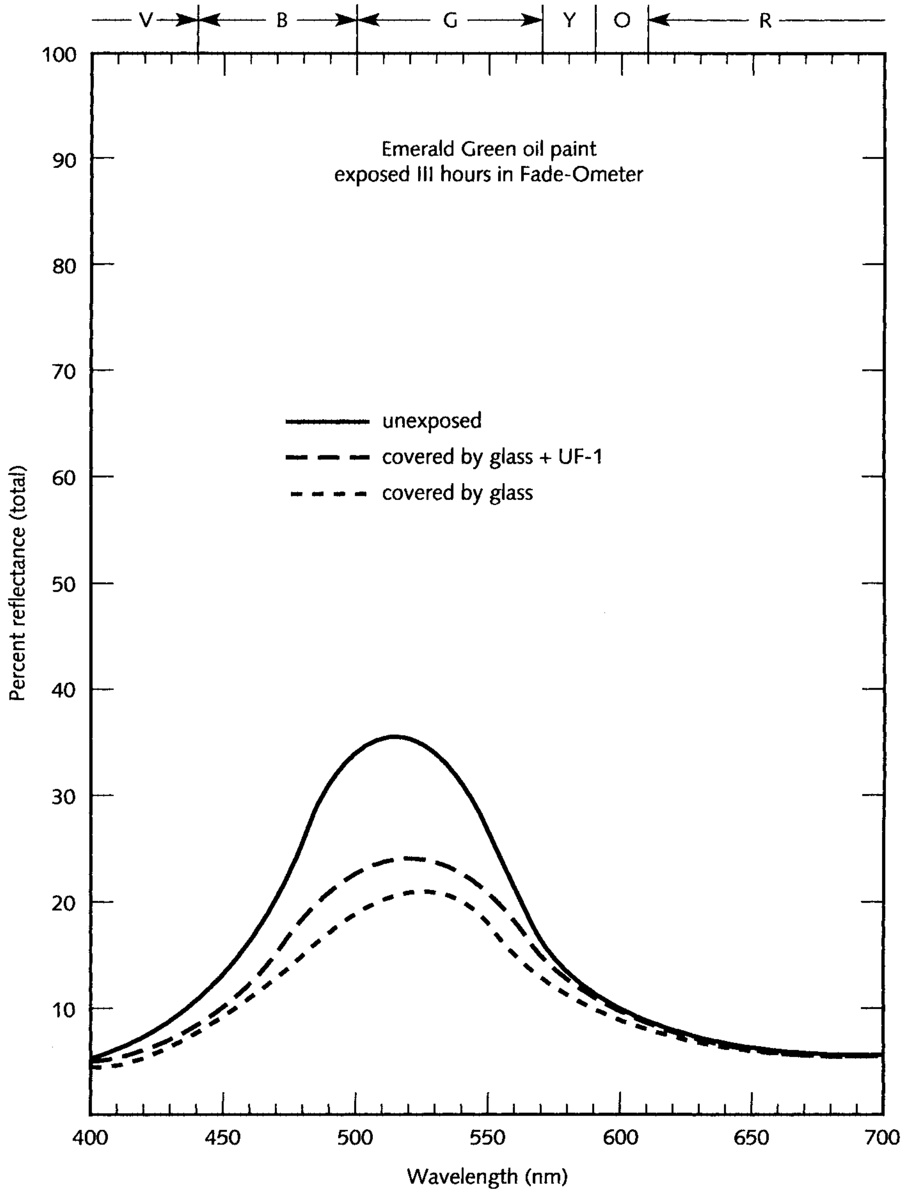

Figure 4.8

Reflectance of Emerald Green (copper acetate–copper arsenate) before exposure in the Fade-Ometer and after exposure under glass, with and without an ultraviolet filter (Plexiglas UF-1). Note that the darkening is less for the exposure under the UF-1 filter than for the exposure under glass (after Feller 1968).

The second point is that when the *difference* between exposed and unexposed log *K*/*S* curves is not uniform, there must have been a change in the colorant system, not just a change in colorant concentration.

The curves in figure 4.9 illustrate these points. The log absorption curves for the exposed and unexposed Emerald Green differ by unequal amounts at different wavelengths, evidence that a change in colorant has occurred. Since the maximum change has occurred at the absorption minimum (reflectance maximum), darkening has taken place (which can be judged visually as well), as exhibited also by some degree of increase in absorption at all wavelengths. In contrast, the two curves for the exposed and unexposed Green Earth are more nearly uniformly separated, indicating that the primary change is simply an increase in absorption or, more likely, a decrease in scattering owing to a change in the pigment dispersion or pigment–vehicle wetting. One can postulate that this apparent increase in absorption may have occurred because of

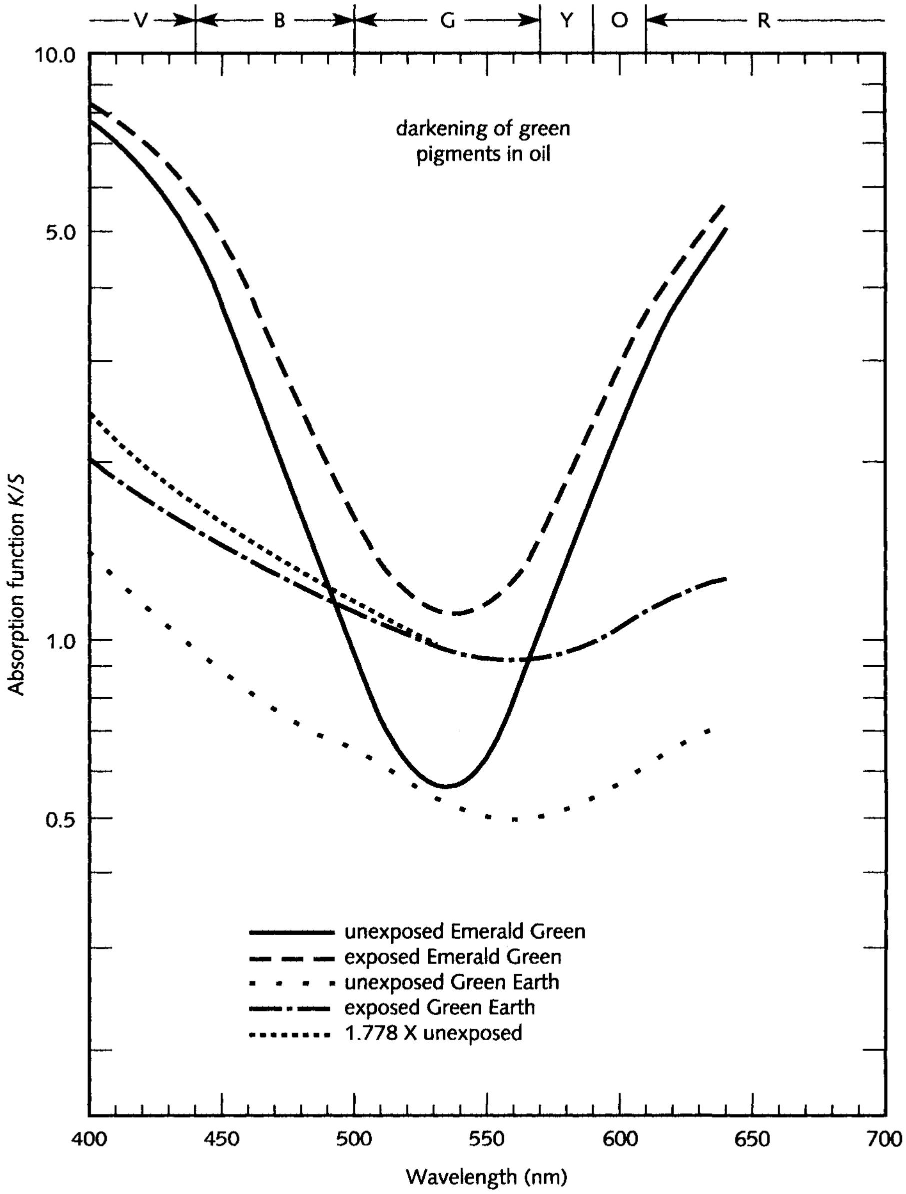

Figure 4.9

Comparison of two types of darkening for two different green pigments in oil. The increased absorption of the Emerald Green when exposed (decreased reflectance under the ultraviolet filter illustrated in fig. 4.8) is greatest at the absorption maximum at 530 nm and decreases at other wavelengths, indicating a change in the chemical structure to a darker form. The Green Earth, in contrast, darkened uniformly at all wavelengths, suggesting an increase in the wetting of this pigment. Bleaching of the vehicle accounts for the lack of parallelism between the *K/S* values for the exposed and unexposed Green Earth oil paint.

increased refractive index of the linoxyn (oxidized linseed-oil vehicle); or because of increased wetting of the pigment, possibly by low-molecular-weight degradation products in the vehicle, with a subsequent decrease in scattering due to air initially entrapped in and around the pigment particles. Feller suggests that "this is a type of alteration [decreased scattering] that may lead to pentimenti [a perceived increase in transparency]." The smaller change observed at the short-wavelength region, indicating less absorption, strongly suggests that the oil vehicle has also bleached, a not-uncommon change when linseed oil is exposed to ultraviolet light.

Instruments can be helpful in diagnosing the nature of perceived changes. Surface change can be measured with a spectrophotometer if the instrument is designed for the inclusion and exclusion of the specular reflectance. Generally, such an instrument uses an integrating sphere for collecting the reflected light. The incident light beam is off the sample perpendicular by about 8°–10°. At the angle equal and opposite to the incident angle, that is, –8° to –10°, there is a removable port in the sphere wall. With a black port or a light trap in place, the specular reflectance is absorbed and only the diffuse light reflected by the color is measured. If a white port is inserted instead (one that matches the sphere wall), all of the light—that is, the total reflectance—is measured. The difference between these two (total reflectance minus diffuse) is a measure of the specular reflectance. When measuring exposed colors, both types of measurement should be made whenever possible. This procedure will demonstrate whether a change in the surface reflectance (gloss) has occurred.

A procedure for quantifying the changes occurring following exposure was outlined by Johnston-Feller and Osmer (1977). Their technique was based on measurements made on a sphere-type spectrophotometer with the specular reflectance both included and excluded. A further step suggested was a gentle washing of the surface to remove the chalking and any dirt accumulation. With the aid of a computer program, the quantification of the different types of changes, calculated in visual terms, could be made. Analytical data concerning the concentrations of the pigments could also be calculated.

Changes in the surface reflection can also be measured using a glossmeter, but quantification in visual terms (ΔE) cannot be calculated by this means.

If no computer program is available, the analysis described for hand calculation earlier in this chapter can be adapted for measurements made with the specular reflectance included and excluded, and by use of the same techniques described by Johnston-Feller and Osmer. If there is no area of the object where the color was protected, such as under the rabbet of a framed painting, there is no way to know what may have changed or by how much. It is only when there is a reference point at some time during the exposure that any of the changes discussed above—fading, darkening, changes in the dispersion, or changes in gloss—can be quantified.

The logical conclusion is that all objects of great value, particularly those subjected to long exposure to light and to changes in environment, should be measured periodically. However, not only could this be a Herculean task, but many materials, when exposed in a museum environment, change very slowly, so that the small changes would scarcely be evident in a single generation, say twenty-five years. Moreover, in this day of rapidly changing technology, commercial instrument obsolescence takes place in only five to ten years, making the spectrophotometric measurements of reflectance difficult to reproduce exactly over very long periods of time. An elaborate program for instrument calibration and a supply of very stable reference standards would be necessary before a program of detecting small changes in color over long periods of time could be embarked upon.

The problem of making reflectance measurements reproducible with a view to detecting small changes will be discussed again in the instrumentation overview provided in chapter 9. In the case of objects made with fugitive colorants, such as Japanese prints, changes are sufficiently rapid that the use of readily available methods of reflectance spectrophotometry can be very helpful (Feller, Curran, and Bailie 1984).

In recent years the National Gallery, London, has undertaken an extensive program to develop the instrumentation and technology to monitor color change in paintings using modern image processing and computational capabilities (Saunders 1988; Saunders and Cupitt 1993).

Vehicle (medium) or substrate change

Another important factor in studying works of art—paintings in any medium and on any substrate, or textiles—is to determine whether the observed changes in color are due to vehicle changes, to substrate changes (fabric or paper, for example), or primarily to a change in the pigment. In general, following exposure, painting media (vehicle) changes, white paper discoloration, and textile substrate deterioration are characterized by yellowing and, occasionally, by slight darkening. With some materials, such as old linseed-oil films, bleaching may occur. Since changes in absorption involving yellowing are most apparent in the blue region of the spectrum, they are most significant on the violets, blues, and purples, which exhibit their major reflection in this short-wavelength region. On the other hand, the color of yellows, oranges, and even reds are less visually affected by this increased absorption in the short-wavelength blue and violet region, where they already absorb significantly. Thus, vehicle or other substrate yellowing can lead to a considerable distortion in the overall color balance originally present in a museum object. These basic principles were pointed out by Laurie (1926) in his groundbreaking book *The Painter's Methods and Materials.*

An example from Johnston (1967b) may make this effect more clear. Two unsaturated polyester plastic panels containing white and a single chromatic pigment were exposed outdoors in Florida. After six months of exposure, both panels had changed slightly with a ΔE of 1.5 CIELAB units, several times more than a minimum perceptible amount. One panel was pigmented with 5% of a green-shade cobalt blue with 95% rutile TiO_2, the other with 20% cadmium orange with 80% rutile TiO_2. The curves are reproduced here as figure 4.10 for the cobalt blue panel and figure 4.11 for the cadmium orange panel. Examination of the curves for the cobalt blue indicates that the concentration of the blue pigment, as indicated by the absorption maximum at 640 nm, had not changed at all. All of the change occurred in the short-wavelength blue region because of increased absorption due to vehicle yellowing. The changes in the curves for the cadmium orange (fig. 4.11) are also limited to this short-wavelength region. Differential spectral curve analysis of both panels showed that, while all of the change in the blue panel was caused by vehicle yellowing, the differences in the cadmium orange panel were attributable to the combination of fading of the cadmium orange and yellowing of the vehicle. The latter partially offset the loss of about 16% of the orange pigment originally present. The amount of yellowing due to the vehicle was about the same in both panels. The analysis of the cadmium orange panel following exposure was difficult because both the pigment and the dirty yellowing of the plastic absorb in the same wave-

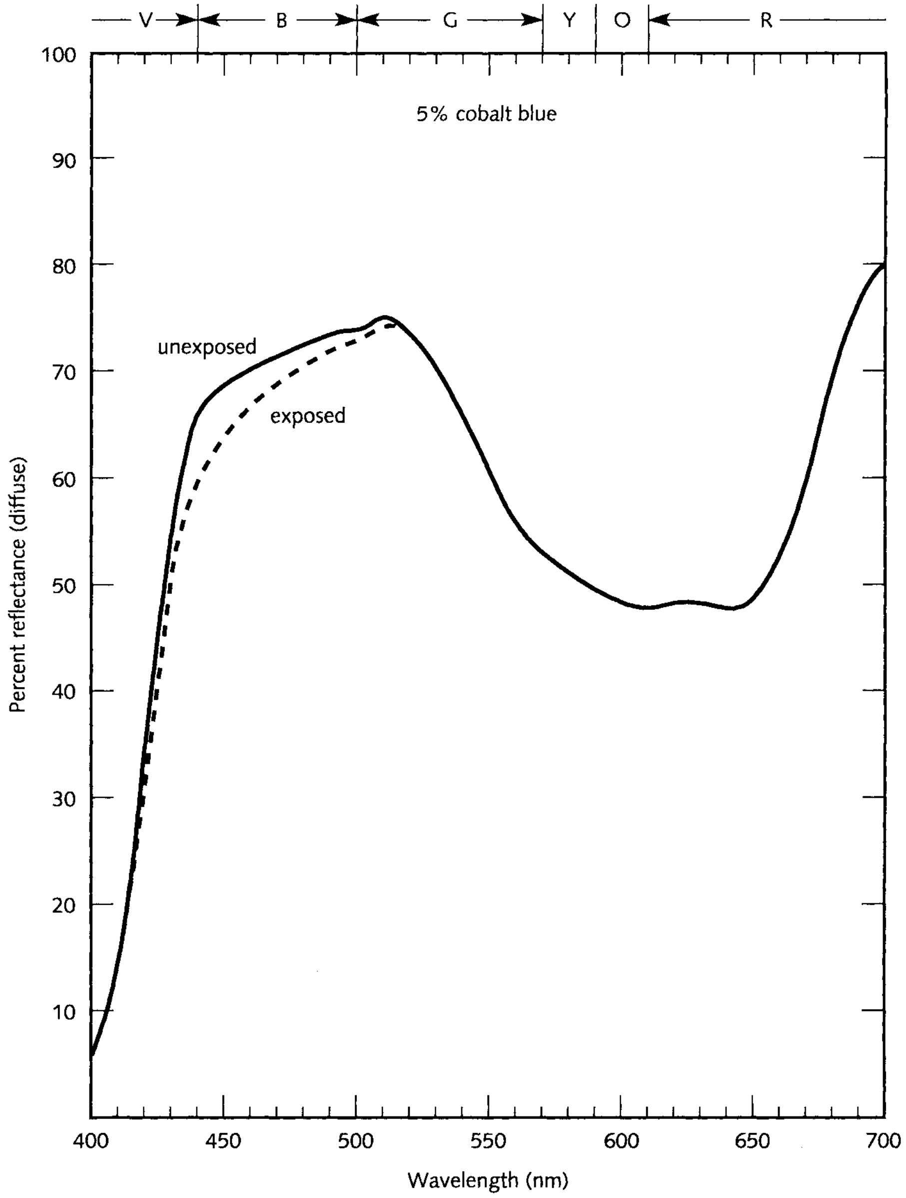

Figure 4.10
Curves of a colored plastic made with cobalt blue pigment and rutile TiO_2 before and after exposure outdoors in Florida for six months. No change in the concentration of cobalt blue has occurred, as can be seen at the absorption maximum at 610–640 nm. All of the color change is caused by yellowing of the plastic vehicle; this is shown by the decrease in the reflectance in the violet-blue region of the spectrum.

length region. The two exhibit differently shaped spectral curves, however. Use of differential spectral curve analysis techniques with COMIC provided an approximation of the amounts of each factor present, the concentration of orange remaining, and the absorption curve of the yellow component that was formed (the yellow could be quantified arbitrarily as a real yellow pigment with a similar curve).

Figure 4.12 shows the reflectance curve of a yellowed varnish on white gesso, measured with the specular reflectance excluded. The corresponding values of *K*/*S* are shown on the right ordinate of the graph. This illustration of a transparent but absorbing layer applied over a reflecting substrate can be considered that of a glaze, although it is not often thought of as such. Glazes are discussed more fully in the next section.

The important point in illustrating increased yellowing upon exposure, which is so characteristic of deterioration, is that, in general, changes in the substrate, such as paper or a textile, look very similar in

Figure 4.11

Curves of a colored plastic made with cadmium orange pigment in TiO_2 before and after exposure outdoors for six months in Florida—the same exposure period as that of the cobalt blue illustrated in figure 4.10. The amount of yellowing of the vehicle was the same as for the cobalt blue sample, but because the cadmium orange faded, the visual color change was little noticeable. Differential curve analysis showed that 16% of the cadmium orange had faded, but the resulting loss of absorption of the cadmium orange was counterbalanced by vehicle yellowing, which increased the absorption in the short-wavelength region.

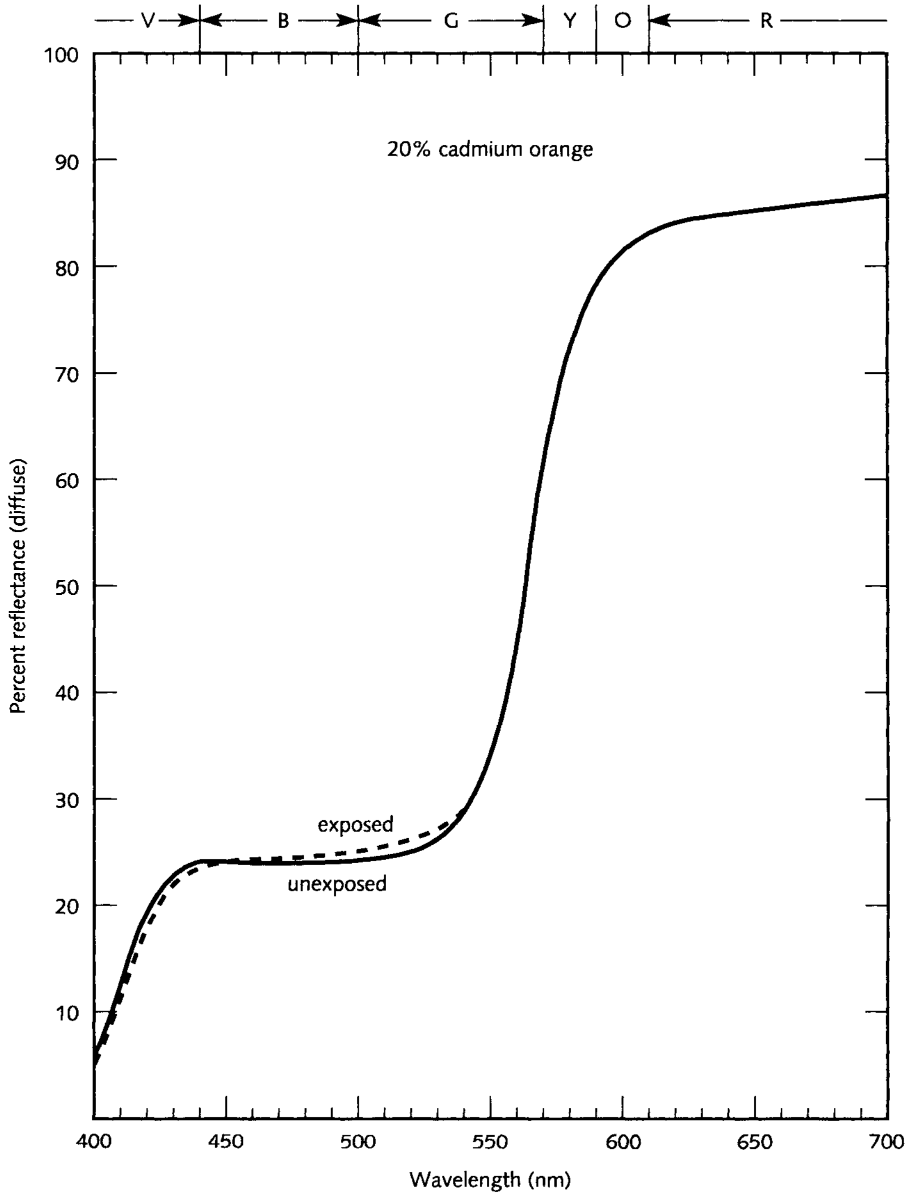

change of curve shape to that for the yellowing of a traditional natural-resin varnish such as damar. Figure 4.13, for example, illustrates the effect of adding lignin to paper. The curve shape changes are not identical to those of the yellowing curve in figure 4.12 for damar varnish, but the general shape is that of yellowness and slight darkening, which is characteristic of deterioration of colorless or white organic compounds such as vehicles (media) or substrates (paper or textiles). Learning to read these characteristic changes in terms of the spectral curves can be extremely helpful in diagnosing the type of change that may have occurred following exposure.

If a computer color-matching program is available, it can be used to great advantage when the changes following exposure are studied. By this technique it was found that in white mixtures at complete hiding, alizarin faded to a yellow form before becoming colorless; a yel-

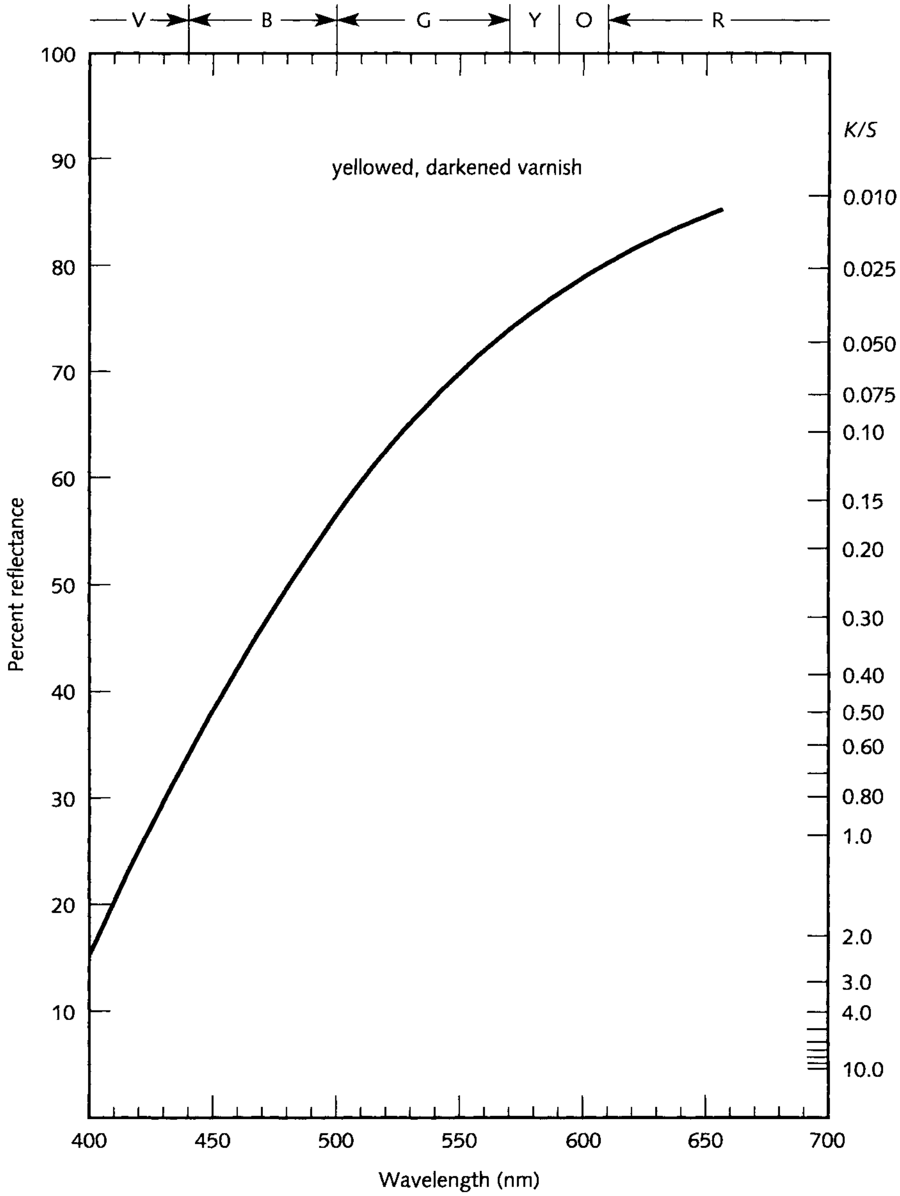

Figure 4.12
Reflectance curve of a yellowed varnish (damar). The absorption in terms of *K/S* is indicated on the right.

low component had to be added to match the exposed samples (Johnston-Feller and Bailie 1982a). Computation to match the exposed Emerald Green (figs. 4.8 and 4.9) indicated that black had to be added to create the match. However, computation to match the exposed Green Earth (illustrated in fig. 4.9) indicated that Green Earth had to be added and that yellowed vehicle had to be subtracted. Such computer color-matching techniques are simply another method of differential spectral curve analysis.

An interesting and useful diagnostic tool for museum conservators concerned with color-balance distortion due to deterioration yellowing was described by LaFontaine (1986). He proposed that one look at the object illuminated by an auxiliary light source filtered to provide extra blue light and less yellow light, in order to restore the reflected light distribution as it would have been if the yellowing of the varnish or

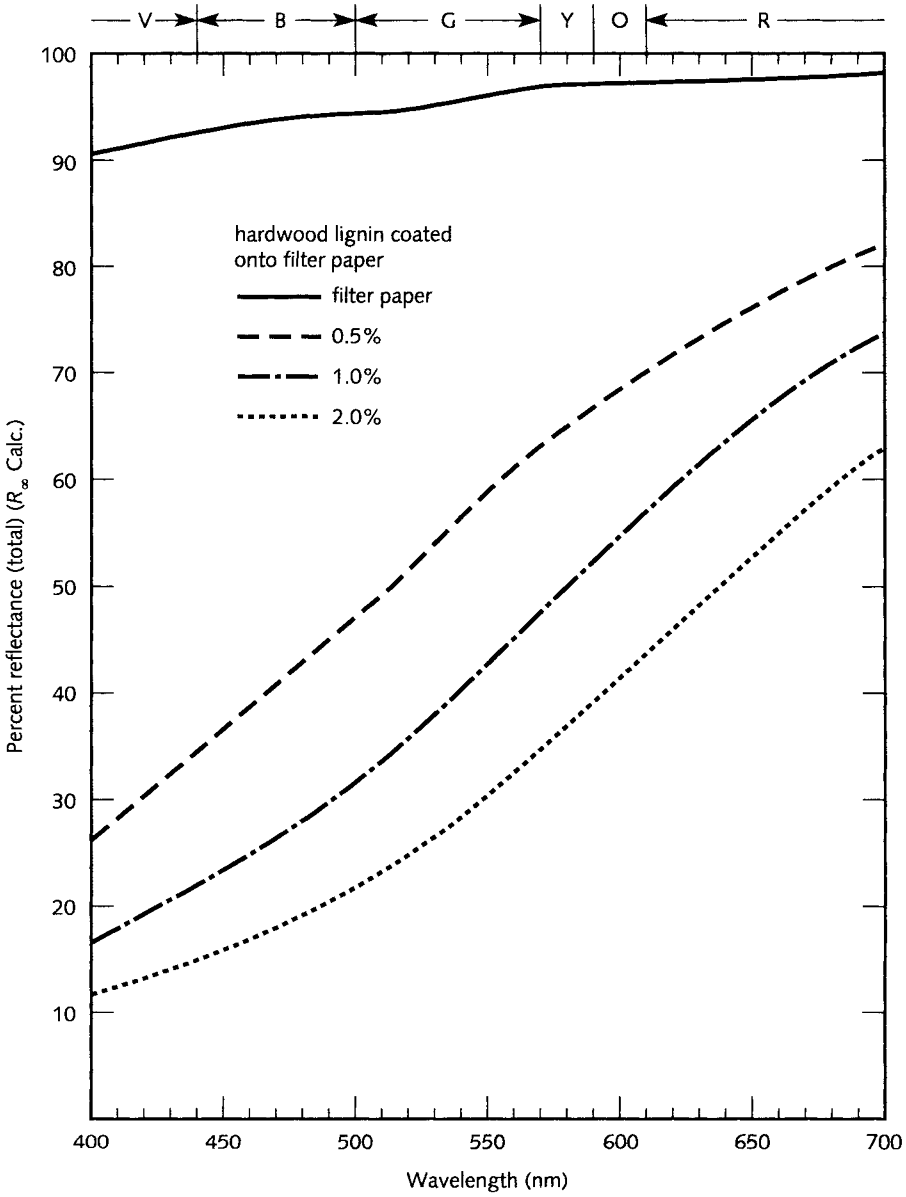

Figure 4.13

The effect of increased amounts of lignin coated onto a white filter paper. Although not identical in curve shape to the yellowed damar of figure 4.12, the nonselective spectral absorption decrease with increasing wavelength is roughly similar—both are dirty yellowing curves (after Johnston and Feller 1967).

vehicle had not occurred. When examining paintings using this technique, the amount of yellowness compensated for can be adjusted by use of a dimmer on the filtered auxiliary light source. This method of viewing deserves to be used widely by conservators and curators when examining objects where yellowing from deterioration is suspected—on paintings, drawings, decorative painting, printing on paper, and textile samples.

Glazes

The applications of the Kubelka-Munk equations discussed so far have been based on the assumption that the samples are opaque, that is, the substrate is completely obscured and does not contribute to the observed color (the condition of complete hiding). As mentioned, however, the problems of yellowed varnish, vehicle, or substrate are not limited to samples at complete hiding. Multiple layers of pigments applied over one another at incomplete hiding may be encountered in the study of many museum objects and materials. The term *glazes,* as used here, refers to the situation in which one or more chromatic layers do not completely obscure the substrate—that is, the circumstances do not correspond to complete hiding. According to this definition, most watercolors, some printing inks, and some textiles fit into this category, in addition to paint layers at incomplete hiding—the traditional glazes.

Kubelka (1948) described the hyperbolic mathematical solutions (eqs. 4.15–4.17) to the equations for the original Kubelka-Munk model (Kubelka and Munk 1931) described earlier in this chapter. To review, equations 4.15–4.17 are

$$R_i = \frac{1 - R_g(a - b \text{ ctgh } bSCX)}{a - R_g + b \text{ ctgh } bSCX} \tag{4.15}$$

where R_i = reflectance (internal) over substrate R_g

R_g = reflectance (internal) of the substrate

$$a = 1 + K/S \tag{4.16}$$

$$b = \left(a^2 - 1\right)^{1/2} \tag{4.17}$$

CX = absolute concentration times thickness

ctgh = hyperbolic cotangent

For a mixture in the incomplete hiding layer of thickness X,

$$a = 1 + X\left(\frac{C_1K_1 + C_2K_2 + C_3K_3 + \cdots}{C_1S_1 + C_2S_2 + C_3S_3 + \cdots}\right) \tag{4.20}$$

Additional equations are described in the appendix of an article on glazes by Johnston-Feller and Bailie (1982a) and in the next section of this chapter. These more complex equations point out that the perceived color and the spectral reflectance curve are different for (1) the case of two colorants applied at incomplete hiding over each other, compared with (2) the case of the same two colorants physically mixed together and applied at complete hiding.

Johnston and Feller (1967) published the reflectance curves for four pigments—two yellows and two reds—that differed in scattering; they were made up as glazes over rutile TiO_2 and in mixture with the same TiO_2. Also included in their examples were the curves for the masstones and for the glazes applied over black made at the same thickness and concentration as the glazes over white. The curves are reproduced here as figures 4.14–4.17.

Figure 4.14 shows chrome yellow light as an example of a highly scattering, largely opaque pigment. Figure 4.15 for Flavanthrone Yellow is an example of a low-scattering, transparent yellow. The difference in scattering is apparent from the curves for the masstones and for the glazes applied over black. The masstone chrome yellow reflects highly and is a bright yellow; the masstone Flavanthrone Yellow reflects much less and is a dirty, low-chroma yellow. The glazes applied over black exhibit the scattering characteristics strikingly. Note that the reflectance

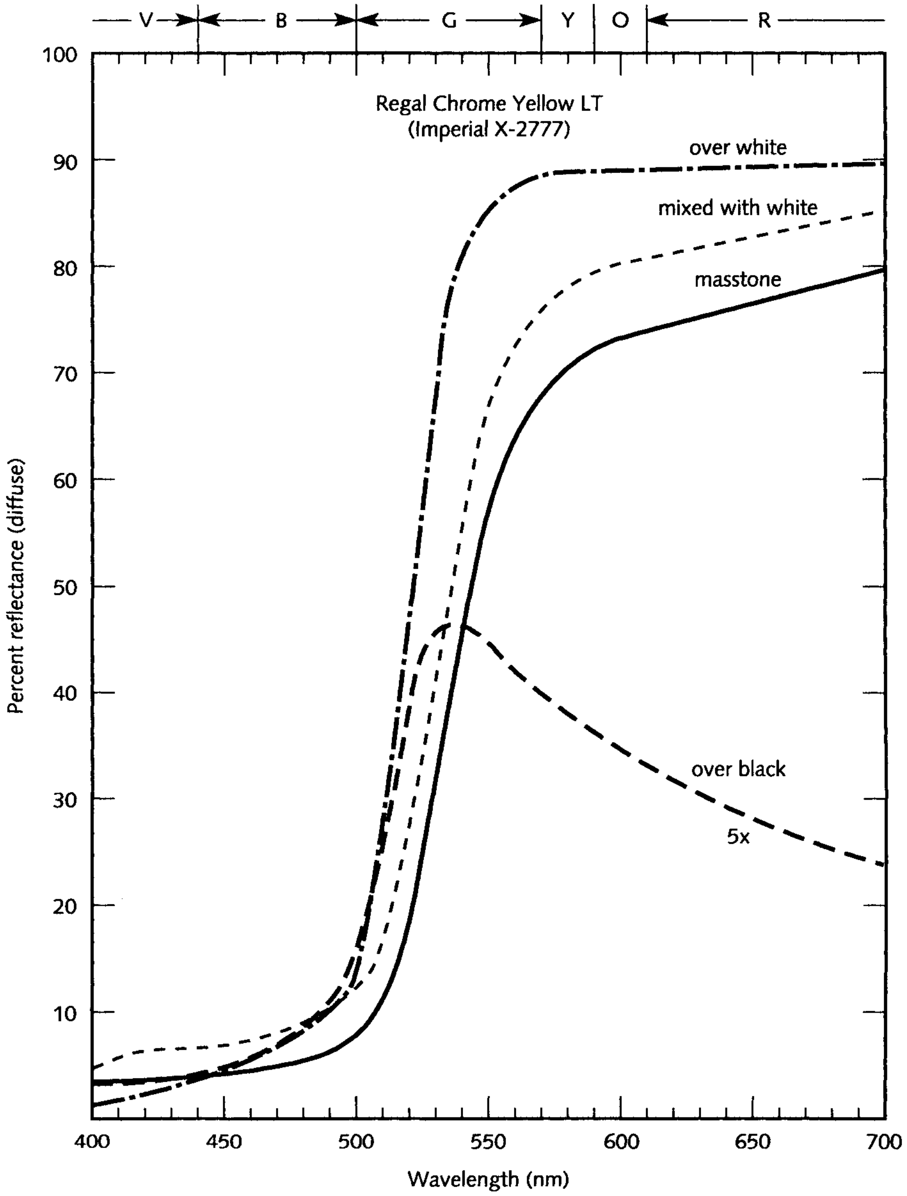

Figure 4.14
Reflectance curves of an opaque chrome yellow pigment mixed with rutile TiO_2 applied at complete hiding; a masstone applied at complete hiding; a masstone applied at incomplete hiding over rutile TiO_2; and the same thickness applied at incomplete hiding over black. Note that the reflectance over black is plotted at 5 times the measured reflectance.

curves for the latter are multiplied by 5 in the plot. Chrome yellow scatters much more light than the Flavanthrone Yellow. Note that the resultant color in each case is a green, because of the greater scattering in the green wavelengths relative to the scattering in the yellow, orange, and red longer-wavelength region.

Figure 4.16 illustrates the reflectances of comparable paint samples prepared from cadmium red medium, a moderately scattering pigment. Figure 4.17 illustrates the reflectances of samples prepared from Quinacridone Red, a relatively low scattering, transparent, red pigment. The masstone colors depend on the relative scattering: cadmium red is a moderately bright red, while the quinacridone pigment, also a red, is relatively dark. (Many coats of paint were required to prepare the Quinacridone Red masstone at complete hiding.)

Comparison of those mixtures *with* white to the glazes *over* white, for all four pigments, illustrates a basic principle: *glazes over*

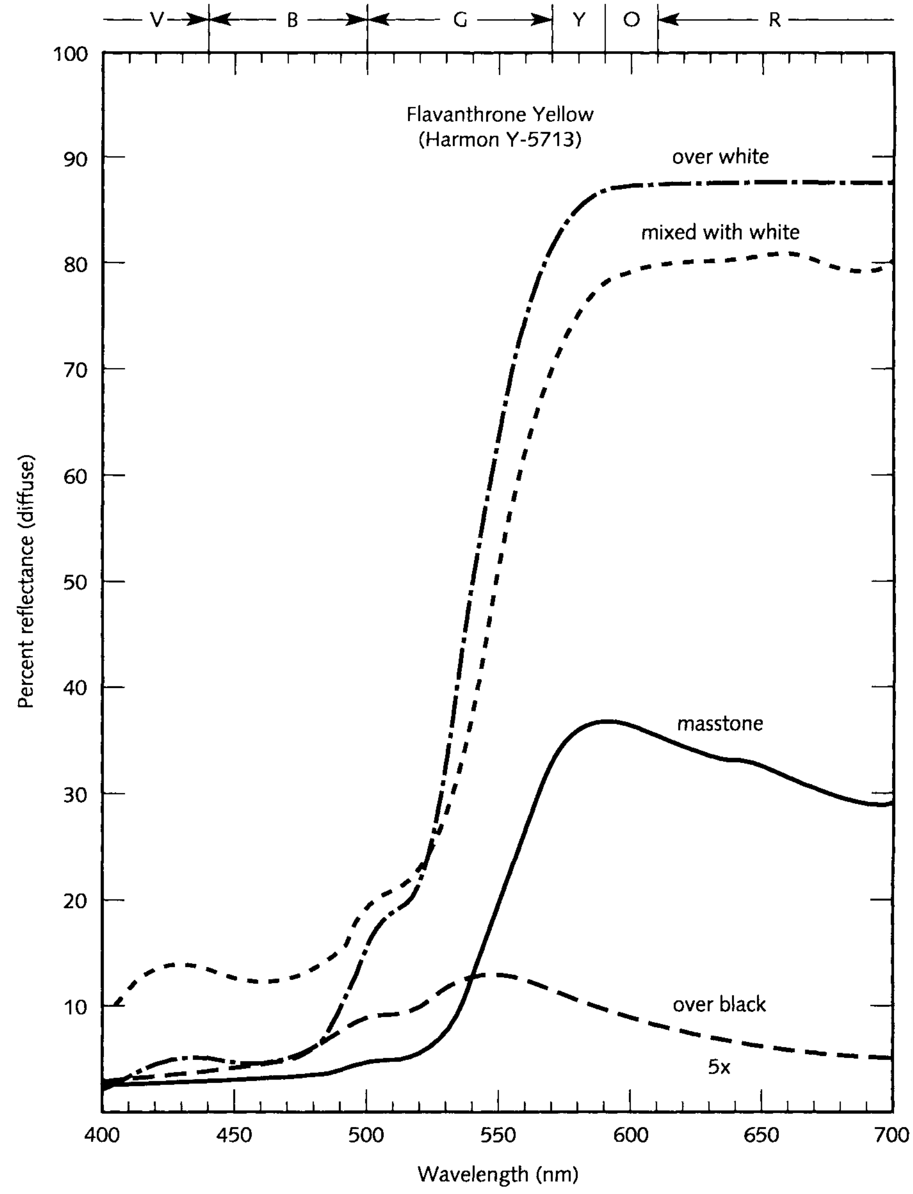

Figure 4.15

Reflectance curves of a transparent organic yellow pigment mixed with rutile TiO_2 applied at complete hiding; a masstone applied at complete hiding; a masstone applied at incomplete hiding over rutile TiO_2; and the same thickness applied at incomplete hiding over black. Note that the reflectance over black is plotted at 5 times the measured values. The slight dip at long wavelengths in the TiO_2 mixture is due to a minor contamination by phthalocyanine blue (see chap. 7 and fig. 7.7).

white result in higher chroma than can be achieved by mixture with white in all cases, whether the pigment is a high or a low scatterer.

Artists have used glazes for their unique optical effects for many years. When the substrate is not white but chromatic, many different color effects can be achieved. In appendix A, the greenish color achieved when black is mixed with yellow (figs. A.19 and A.21) is illustrated. However, when a scattering yellow, such as the chrome yellow light of figure 4.14, is applied as an incomplete hiding film, or glaze, *over* black (or some other dark substrate), the optical effect is unique—eerie and tenuous in substance. What fun an artist can have!

An important conclusion from a comparison of the mixtures over white (the glazes) with the mixtures with white (discussed in an earlier section) is that the characteristic absorption patterns are present in both. The two transparent organic pigments, Flavanthrone Yellow (fig. 4.15) and Quinacridone Red (fig. 4.17) clearly illustrate this constancy in

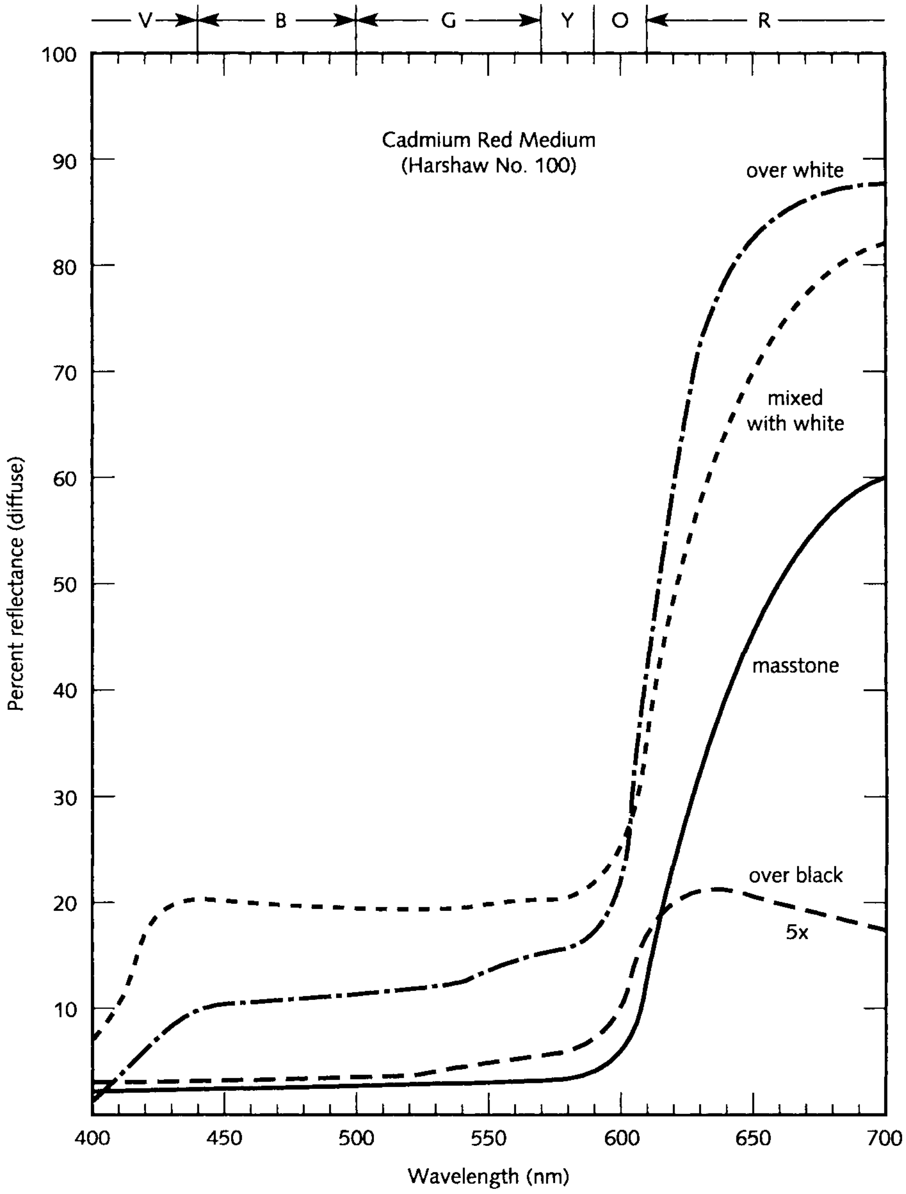

Figure 4.16

Reflectance curves of an opaque cadmium red pigment mixed with rutile TiO_2 applied at complete hiding; a masstone applied at complete hiding; a masstone applied at incomplete hiding over rutile TiO_2; and the same thickness applied at incomplete hiding over black. Note that the reflectance over black is plotted at 5 times the measured reflectance.

the characteristic absorption bands. Note the two bands of the flavanthrone (a distinctive pattern when encountered in a yellow colorant) and the three bands for the Quinacridone Red, also unique. *Whether the pigment is used as a glaze or as a mixture with white, the characteristic absorptions remain.*

A yellowed varnish is, in effect, a yellow glaze over the entire painting. Removing this glaze results in a considerable change in the observed color balance. Frequently controversy may arise as to whether something else—an intentional colored glaze, for example—might have been removed as well as the yellowed varnish. Analyzing the differences in the spectral curve shapes before and after varnish removal can sometimes be helpful. Johnston and Feller (1963) published an illustration of such a spectral curve analysis for an exposed red-orange, glossy paint panel. The reflectance curves of the panel before and after varnish removal are reproduced as figure 4.18. Inspection of the reflectance

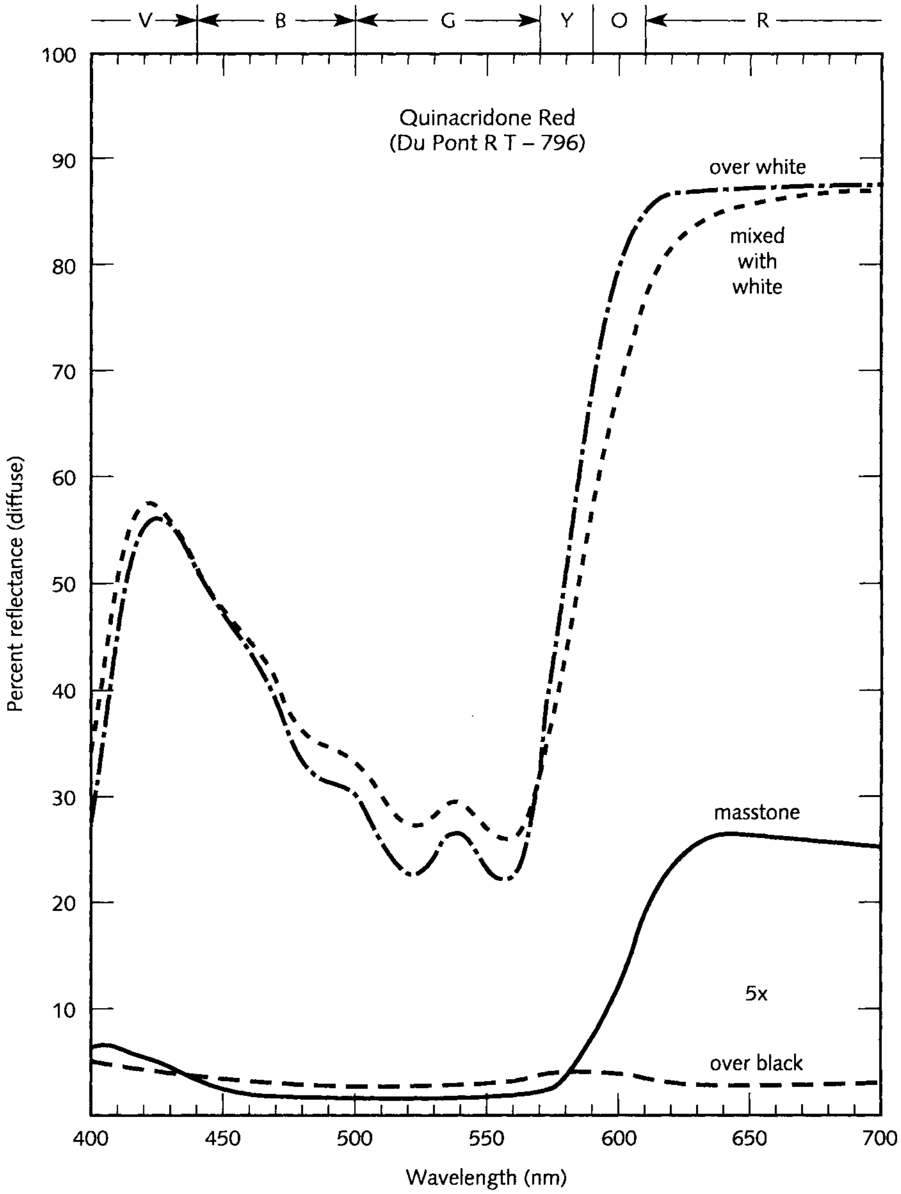

Figure 4.17

Reflectance curves of a transparent organic red pigment mixed with rutile TiO_2 applied at complete hiding; a masstone applied at complete hiding; a masstone applied at incomplete hiding over rutile TiO_2; and the same thickness applied at incomplete hiding over black. Note that the reflectance over black is plotted at 5 times the measured reflectance.

curves reveals that after varnish removal the curve is lighter and bluer. Beginning the inspection at the long wavelengths, the increased reflectance in the red region indicates that some absorber has been removed, possibly dirt. The increased reflectance in the green region, around 540 nm, indicates that some absorption has been removed here, where a red might absorb, in addition to absorption loss observed at the long-wavelength region. The large increase in reflectance in the violet region, around 440 nm, indicates that a yellow has been removed. This analysis raises questions: (1) Was the increased reflectance in the green region due to a loss of red from the original painting? (2) Was this apparent loss of red due to a red-tinted glaze that was removed? (3) Was a yellow glaze removed? Observation of the swabs used to remove the varnish indicated that a red had been removed, but with just this evidence, its identification could be made only by solution pigment identification techniques (Johnston and Feller 1963).

If the reflectance curves in figure 4.18 are converted to the absorption function, *K/S*, the absorption curve of the material removed can then be obtained by subtraction (differential spectral curve analysis). Figure 4.19 illustrates the results (Johnston and Feller's original fig. 5). Note that the *K/S* absorption values are plotted on a log scale so the shape of the curves is independent of the concentration. The difference curve (curve 1) shows two absorption bands at about 560 nm and 520 nm, present in both the before and after curves. Absorption at these wavelengths is characteristic of carmine. Subsequent removal of another layer, also red, resulted in a color with a different red curve, one with a single absorption band, which could be attributed to alizarin. One suspects, therefore, that a carmine glaze had been applied over the alizarin (a red over a red). For reference, the absorption curves of the yellowed varnish (fig. 4.12) and of alizarin and carmine are also included. Differential curve analysis is thus a useful tool to aid in pigment

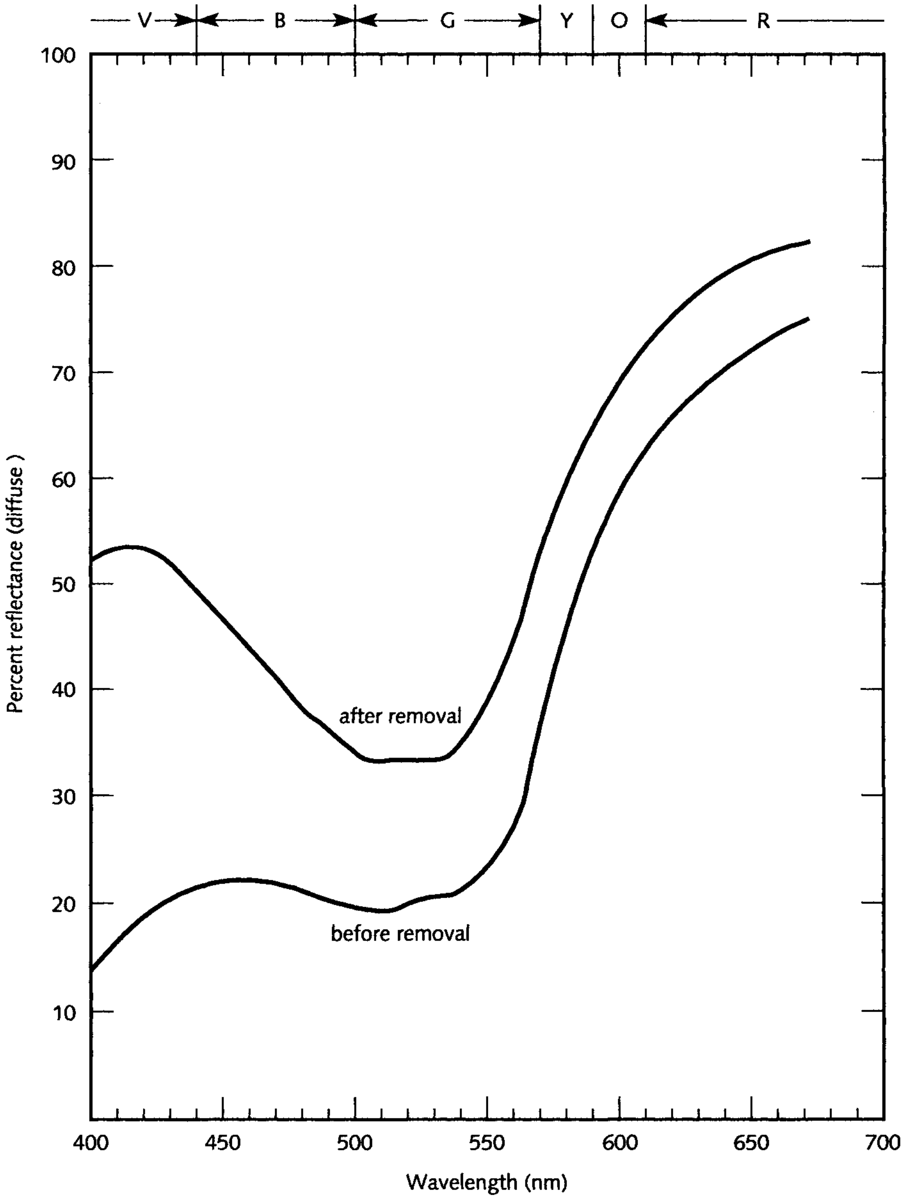

Figure 4.18

Reflectance curves of a red area of paint before and after removal of a yellowed varnish.

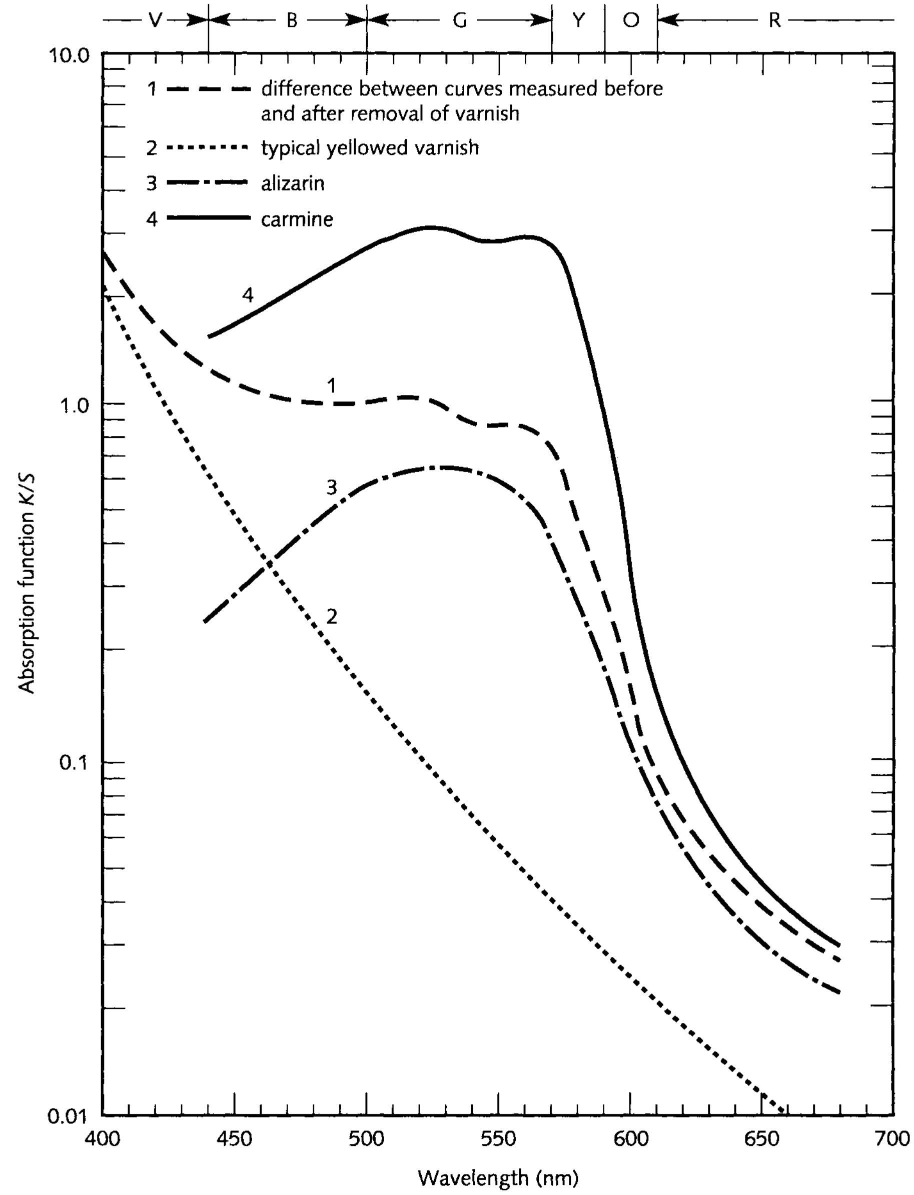

Figure 4.19

Spectral absorption curve 1 shows the difference between the reflectance curves in figure 4.18. Alizarin (curve 3), carmine (curve 4), and a typical yellowed varnish (curve 2) are also illustrated.

identification and quantification, and in other analytical applications of interest to the conservation of museum objects.

Earlier in this chapter it was pointed out that type II chromatic pigments, those that absorb much more than they scatter, when mixed with white, exhibit a critical concentration at which maximum chroma occurs. This behavior is illustrated on the chromaticity diagram in figure 2.12. All of the samples illustrated in the figure were paints applied at complete hiding.

In the case of glazes, there is a critical concentration where maximum chroma is reached for an incomplete hiding film applied over a reflecting substrate for all chromatic colorants, types II and III. In this case the concentration is actually the product of the concentration times the thickness, or CX. Thus, for glazes, such a critical concentration exists for type III colorants, those that both scatter and absorb significantly, as well as for type II pigments.

The effect of this phenomenon is illustrated by a series of five concentrations of alizarin glazes applied at incomplete hiding. The glazes were used to paint the sleeves of a blouse in a portrait done on a Mylar sheet that was then exposed over a white background for increasing periods of time in a xenon arc Fade-Ometer (Johnston-Feller 1986). At intervals during the exposure, the portrait was removed, the glazes were measured over white, and photographs were taken under carefully controlled conditions. The bodice of the blouse was made with a stable blue pigment that did not fade. The photographs are reproduced in color plate 3. The black-and-white graph of the Munsell Chroma versus the Munsell Value illustrates that the more-concentrated glazes (those of lowest Munsell Value) increased in Munsell Chroma as the concentration of alizarin decreased from fading: samples 1, 2, and 3. In the course of fading, sample 3 (the middle concentration studied) reached maximum Chroma, exhibiting the critical concentration for alizarin glazes over this white substrate. Visual inspection of the photographs illustrates the effect of the phenomenon—a severe loss in the modeling of the drapery of the sleeves.

In summary, one cannot tell with certainty from the spectral reflectance whether a pigment has been mixed with another pigment or applied as an incomplete hiding film, or glaze, over the other. Both are examples of subtractive colorant mixtures, revealing the characteristic absorption bands of each pigment. If the film is applied at incomplete hiding over a white, the contrast in the absorption bands is enhanced. Undoubtedly there are also many instances when incomplete hiding layers are applied over opaque chromatic substrates. Even if the mode of mixing is not known, whether by mixture with white or other chromatic colorants or by means of incomplete hiding films or glazes, the characteristic absorption bands are still visible to aid in the identification of the pigments used.

Opacity, translucency, and hiding power

Up to the discussion of glazes in the previous section, all of the applications of the Kubelka–Munk equation described were based on opaque materials, that is, substances that completely hide the background or substrate. Many materials do not fit this restricted category, however. While glazes represent a special type of translucent (incomplete hiding) colorant layer, a wide range of other materials present problems where their degree of opacity or translucency has an effect on their appearance. In this section, other applications of the Kubelka–Munk incomplete hiding equation (eq. 4.15) will be discussed.

Definitions

The terms used to tell whether or not a substrate is hidden must be defined and used carefully. Definitions in common language dictionaries are often not precise enough. One must distinguish between absolute (or quantitative) and relative (or qualitative) terms, and among processes, measured quantities, and properties. The following descriptions are based on ASTM Standard E 284, "Standard Terminology of Appearance."

The property of *opacity*, which is the ability of a sample to prevent all transmission of light, is described by the adjective *opaque,* meaning transmitting no light. Both of these are absolute terms: either a sample is opaque or it is not; there is no intermediate state. It is incorrect to describe a sample as "more (or less) opaque" than another.

The noun *transmission* and the verb *transmit* describe the process whereby light passes through a sample. These terms are relative: a sample may transmit more or less light than another. The quantity of light transmitted is measured by the *transmittance,* which is the ratio of the transmitted light to the incident light. Thus transmittance is also a relative term. The transmittance of samples that do not scatter light is a measure of the amount of light they absorb.

If a sample transmits light without scattering or diffusion, it is said to be *transparent,* which is an absolute term. However, the related term *transparency* has a special meaning in appearance measurement; it is described in the discussion of plastics near the end of this section.

Samples that *do* scatter or diffuse light, unless they are opaque, are said to be *translucent.* This is a relative term, since some samples scatter more light than others. Translucency implies that, because of a sample's scattering or diffusion of light, objects located beyond it cannot be seen clearly through it. Of course, translucent samples may absorb as well as scatter light.

Like transmission, *reflection* and *absorption* refer to processes. Like transmittance, *reflectance* and *absorbance* refer to measured quantities. All of these are relative terms. But recall that, while reflectance is defined like transmittance as a ratio (reflected light to incident light), what is always measured is the *reflectance factor,* that is, the ratio of the light reflected from the sample to the light reflected from the white standard. However, for simplicity, we use the term *reflectance* in place of *reflectance factor* in this monograph.

The third term used in the title of this section is *hiding power,* which is the relative degree of hiding of the substrate. This relative term as normally interpreted refers to the reflectance measured over a black substrate (designated R_0) divided by the reflectance over a white substrate (designated R_w)—that is, R_0/R_w. This relationship is called the *contrast ratio.* Discussed at greater length later in this section, this ratio describes materials that are not at complete hiding.

Even when materials appear to be opaque—that is, the materials appear to be the same color when observed over a black and over a white substrate—there may be a perceptible *appearance* difference between them in the characteristic we call translucency. In this situation, the materials exhibit more or less depth of the light penetration into the material, a subtle, but important, visual appearance characteristic. Some materials are perceived to have a greater depth of light penetration than others. Unless we can section such materials horizontally, in order to decrease the thickness so that we can measure differences over white and black substrates at various levels within the material, it is difficult to characterize this aspect of translucency numerically.

Opacity calculations

In the simple Kubelka–Munk equation (eq. 4.7) for samples at complete hiding

$$(1-R)^2/2R = K/S$$

the ratio *K/S* is dimensionless because the absorption coefficient, *K*, and the scattering coefficient, *S*, have the same units. However, when hiding is incomplete, the *K* and *S* do not appear as a ratio, and their dimensions must be defined. The following equations and procedures are used to determine dimensioned scattering and absorption coefficients.

$$SCX = \frac{1}{2b} \ln\left[\frac{R_\infty(1-R_0R_\infty)}{R_\infty - R_0}\right] \tag{4.21}$$

where S is the scattering coefficient, C is the absolute concentration of the pigment, X is the measured thickness of the film, R_0 is the internal reflectance measured over black, and R_∞ is the internal reflectance of a completely hiding, opaque layer of the same material.

$$R_\infty = a - b \tag{4.22}$$

where a and b are factors based on reflectance measurements and calculated using the equations seen here.

The calculations also require equation 4.16

$$a = \frac{1}{2}\left(R + \frac{R_0 - R + R_g}{1 - R_0R_g}\right)$$

and equation 4.17

$$b = (a^2 - 1)^{1/2}$$

To determine S, a is first determined based on measurements made over a black substrate, R_0, over a white or near-white substrate, R, and on the near-white substrate itself, R_g, using equation 4.16. The thickness and concentration of the samples over the near-white or white substrate and the black substrate should be identical. From the value for a thus obtained, b is calculated from equation 4.17. Once a and b are known, R_∞ is calculated from equation 4.22. The value for SCX can then be calculated from equation 4.21. The unit value for S is then determined by dividing SCX by the known absolute values for C (the concentration of the colorant) and X (the thickness of the sample). The scattering coefficient, S, is thus dimensioned in terms of the units used for C and X. To determine K, the following equation can be used:

$$K = S(a - 1) \tag{4.23}$$

K then has the same dimensions as S.

If the thickness is expressed in mils (0.001 in.), the coefficients K and S are for a 1 mil thickness. The concentration may be expressed in terms of volume, such as cubic centimeters of scattering material per cubic centimeter of solid material (for example, the pigment volume concentration, PVC); or in terms of weight: grams of pigment per gram of pigment plus cured vehicle (pigment weight concentration, PWC).

From these absolute absorption and scattering coefficients so determined, the reflectance can be calculated at any desired concentration and thickness. The incomplete hiding reflectance over any substrate, chromatic or achromatic, can be calculated from equation 4.15:

$$R_i = \frac{1 - R_g(a - b \text{ ctgh } bSCX)}{a - R_g + b \text{ ctgh } bSCX}$$

where ctgh is the hyperbolic cotangent. Tables of the values of ctgh are given by Judd and Wyszecki (1975).

It must be remembered that most of the reflectance values used in the Kubelka–Munk equations are internal reflectances. Proper corrections for the surface reflection should be made using the Saunderson correction.

When pigment mixtures are used, it is not necessary to determine dimensioned K's and S's for all of the pigments in the library. (In fact, it is difficult to do so in the case of very transparent pigments applied over black.) One simply uses the absolute K's and S's for the white pigment as described above, rather than setting all the S's equal to 1.0. The procedure for determining the K's and S's of the other pigments in the library is identical to that described for the complete-hiding samples in the previous section. The absorption and scattering coefficients of the colored pigments are then in the same units as those of the white pigment.

After determining the K's and S's for all of the pigments in the library, the reflectance of mixtures at incomplete hiding over any substrate can be calculated by use of equation 4.20 followed by equations for b (eq. 4.17), for R (eq. 4.15), or for R_∞ (eq. 4.22).

Many of the variables encountered when working with colored materials may be studied by use of a suitable version of these equations. For example, when making calibrations on transparent pigments as described in the previous section, preparing a film that is at complete hiding (R_∞) is often difficult; many layers have to be applied to build up the necessary thickness. By using the above technique (measurements over white and over black), R_∞ can be calculated for use in the equations. It has been found that a contrast ratio (R_0/R_w) of at least 0.75 at the reflectance maximum should be used for calculating R_∞ reliably using equations 4.16, 4.17, and 4.22 (Osmer 1978).

One of the difficulties encountered when applying these equations to highly reflecting white pigments is that a may be less than 1.0. It is therefore impossible to calculate b using equation 4.17 because one cannot take the square root of a negative number. Equations described by Ross (1967) circumvent this problem.

The color or reflectance observed at any given thickness is that of a cross-sectional area through the thickness of the film; it is dependent on the volume of pigment particles that the incident light encountered as it passed through the defined depth of material. Expressing concentration in terms of volume units is, therefore, most appropriate.

As was pointed out in the beginning of this chapter, when describing changes that occur during aging, pigment particles may exist as agglomerates, not as simple particles, making their volume difficult to ascertain when they are incorporated into a polymer matrix. In practice, pigment mixtures are more reliably measured on a weight basis, which is then converted to a volume basis using the pigment density (weight per unit volume). Also, as mentioned, in the case of incomplete hiding, the concentrations must be expressed in absolute terms based on the pigment volume per unit volume of the total cured material. This is not the same as the relative concentration unit used in equation 4.8 describing the complete hiding (opaque) materials, where the total pigment concentration was considered to be unity.

Scattering, simple and multiple

In chapter 3, in the description of colorant characteristics, it was pointed out that for pigments, the two optical characteristics of importance are the absorption and the scattering of light. It was stated there that absorption is a relatively simple interaction with light, but that scattering is more complex. The amount and the angular distribution of scattered light depend in complicated ways on the particle size, refractive index, and concentration of the pigment. The brief discussion on light scattering presented here is limited to pigments with the right size to scatter light strongly—a particle diameter of about half the wavelength of the light (too small for the individual pigment particles to be visible in a light microscope)—and a refractive index quite different from that of the binder or medium.

When the concentration of pigment particles is quite low, there is a good chance that the light scattered by a particle will find its way out of the sample without encountering another scattering particle. This type of scattering is called *single scattering* and is described by the Mie (1908) theory. Experiments confirm the theory and show that in single scattering most of the scattered light travels in the forward direction—that is, away from the light source. (An example is given in the next chapter, in the section describing metallic flakes.) In contrast, when the concentration of pigment particles is high, the light scattered by one particle strikes another particle and is rescattered. This occurs many times before the light reaches the front or back surface of the sample; this is called *multiple scattering*. When multiple scattering takes place, the result is that the light is distributed isotropically, that is, equal amounts travel in all possible directions, in the backward as well as the forward hemisphere around the particle. One of the key assumptions of the Kubelka–Munk theory is that the scattering is isotropic.

In beautiful pieces of experimental work, Craker and Robinson (1967) measured the effect of PVC and thickness of rutile TiO_2 in paint films on the relative amounts of forward and isotropic scattering. They first measured the regular (undeviated) transmittance—that is, the unscattered transmitted energy—using a conventional commercial spectrophotometer. Figure 4.20 presents their data graphically as measured on a Unicam SP500 spectrophotometer. Note that the ordinate (the transmittance) is a log scale. The abscissa is the product of the PVC—symbol V—times the thickness, X, in mils. It can be seen that in zone 1, at low concentrations of scattering (nonabsorbing) white particles, the log of the transmittance decreases linearly with increases in concentration. This behavior, which appears to resemble the Beer–Bouguer equation (Beer's law) (eq. 4.5c), is described by $-\log t = VXk$, where t is the transmittance, V is the PVC, X is the thickness, and k is a constant characteristic of the material. Thus, VX is the volume of the particles. In zone 2, a transition from forward scattering to isotropic scattering is occurring. In this area, slight changes in thickness can effect a significant change in the ratio of the two types of scattering, particularly for VX in the range of 1.3 to 1.8. In concentration zone 3, there is no unscattered (regularly transmitted) light coming directly through the film; the scattering is isotropic, as assumed in the Kubelka–Munk equation.

Craker and Robinson also measured the angular distribution of energy scattered around a paint film using an experimental goniospectrometer. Figure 4.21 is redrawn from their figure 2; it shows typical angular results plotted on a polar diagram for a thin film, area A, and for a thicker film, area B. In the illustration, the incident light is designated I_0, the regularly transmitted light is T, the forward scattered energy is E_F, and the backward scattered energy is E_B. In area A (the thin film), the sharp spike opposite the incident light is the regularly transmitted light. The diffusely scattered light is greater in the forward direction than in the backward direction. In area B, measurements were made on a thicker film, and there is no regularly transmitted energy, that is, no spike. Most of the scattering is isotropic.

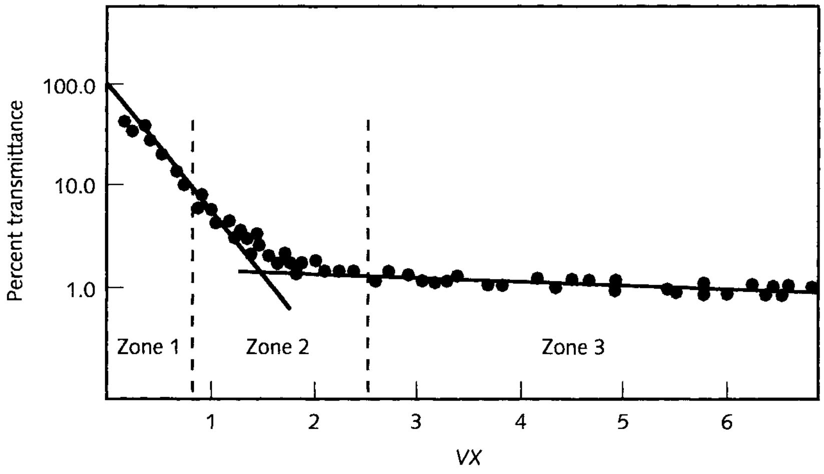

Figure 4.20

Percent transmittance of films pigmented with rutile TiO_2 plotted as a function of the pigment volume concentration, V, multiplied by the thickness, X. In zone 1 the scattering is in the forward direction, which decreases the transmittance, as though the pigment in the film were an absorber. In zone 2 a transition is taking place, and the forward scattering is increasingly replaced by isotropic scattering. In zone 3 the transmittance does not change, because all of the scattering is isotropic: the film is opaque. Zone 1 is often referred to as the Mie range; zone 3 as the Kubelka–Munk range (after Craker and Robinson 1967).

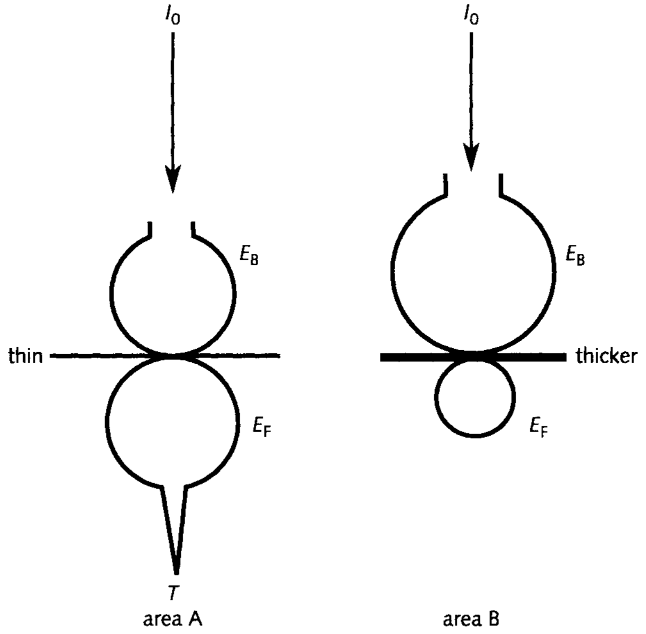

Figure 4.21
Angular distributions of light reflected by rutile TiO_2 pigmented films. With thin films, area A appears to be near the transition area between zones 1 and 2 of figure 4.20. In the thick film (area B), where no direct transmittance is apparent, the reflectances are closer to zone 3, the isotropic scattering zone, in figure 4.20 (after Craker and Robinson 1967).

These angular distributions for the thin and thick films can be associated with the transmittance curve of figure 4.20. The thin-film reflectances, described as area A in figure 4.21, appear to be near the onset of the transition area between zones 1 and 2; in the thick film, area B, where no regular transmittance is apparent, the behavior appears to be closer to that in zone 3, the isotropic zone.

The phenomenon of the relative amounts of forward (single particle) scattering to isotropic (multiple particle) scattering is important when the problem of translucency is considered. It also explains some examples of seemingly anomalous behavior encountered in the everyday world. For example, a printer once showed the author a pair of samples where thin films of white (probably TiO_2) were printed on aluminum foil. The first sample had one coat of the white ink, and the second sample had two coats. The second sample was darker than the first one. He was asked what would happen if he put a third coat on the second sample, and he stated that it would be lighter than when the sample had two coats. The probable explanation is that the CX of the double coat of white ink was in the zone 1 region where the scattering is in the forward direction, but that the addition of the third coat moved the material into zone 2, where isotropic scattering began to occur. The low diffuse reflectance of aluminum foil (on the order of 20%) contributed absorption of the forward-scattered light from the first coats.

It is important to remember that the phenomenon of forward or isotropic scattering with change in pigment concentration is not limited to white pigments but may occur with any pigment that scatters significantly (type III pigments as described in chap. 3).

For a theoretical discussion of single and multiple scattering, the reader is referred particularly to chapter 3 in the book by Kortüm (1969).

The degree of translucency or the relative opacity of materials is not an easy characteristic to measure. Obviously, because translucency is dependent on the scattering characteristics, an instrument with an integrating sphere is necessary. If a material to be measured is not at complete hiding, a number of measurements can be helpful in characterizing the degree of translucency. Figure 4.22 presents a diagram of the integrating sphere of a typical commercial double-beam spectrophotometer used for color measurement. There are six openings in the sphere wall (excluding the receptor opening). The first two openings are for the entrance of the incident light, one for the sample light beam and one for the reference standard beam. Nearly perpendicular (8°–10° off normal) to the incident beams, on the opposite side of the sphere, are two more ports for the measurement of the reflectance of a sample relative to a standard (usually the white reference), which is in the second port. The third set of openings is located on the wall opposite these reflection ports at the angle equal and opposite to the incident light angle, providing for the inclusion or exclusion of the specular reflection from the sample and reference standard.

For rigid translucent materials, such as pieces of plastic, ceramic, and so on, the total transmittance through the sample in the forward direction may be measured by mounting the sample at the entrance port. For the corresponding reference beam, either no sample may be inserted, in which case the reference is air, or a piece of unpigmented material may be used. The latter arrangement makes an optical compensation for the first-surface (interfacial) reflection. However, the surface correction at the opposite side, where the light is exiting from the materials, is not correct, because more surface reflection occurs on the scattering sample than on the reference clear material. To simplify the measurement, air is generally used as the reference.

If the reflection ports and the specular inclusion ports are made white to match the sphere wall, all of the light transmitted in the

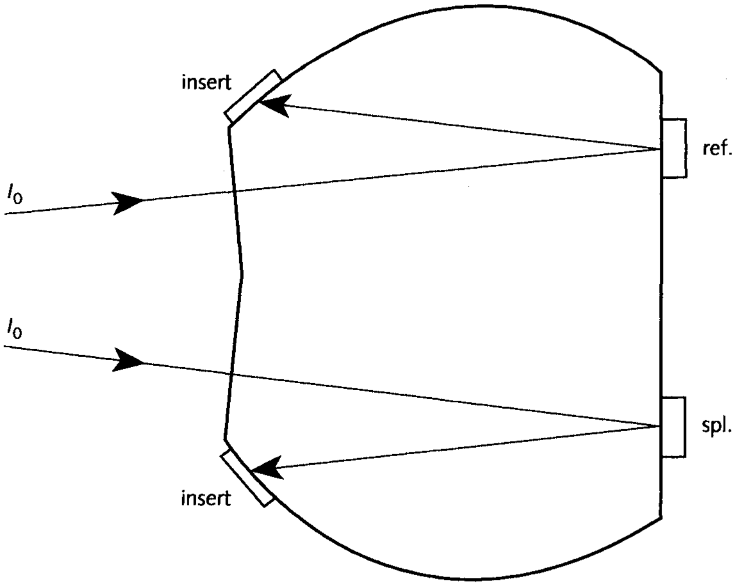

Figure 4.22
Schematic diagram of the integrating sphere of spectrophotometers and colorimeters with near-normal incident light, I_0, striking the sample and reference at an angle about 8° off the normal (perpendicular). If the inserts in the sphere wall are black, or a light trap, the specular reflectance, at –8°, is absorbed, and only the diffusely reflected light is measured by a photodetector perpendicular to the plane illustrated. If the inserts are white, matching the sphere wall, all of the light reflected by the sample is included in the measurement.

forward direction is measured. If the sample reflection port is black, however, the regular transmission—that is, the unscattered light—is absorbed by the black, and only the light scattered diffusely in the forward direction is measured. The difference between these two measurements is a measure of the regular transmittance. Note that when the sample is mounted in the entrance port in this type of measurement, all of the light scattered in the backward direction is excluded from the measurement and is reflected back into the instrument.

If one wishes to determine the amount of light scattered in the reverse direction—that is, reflected rather than transmitted—the sample must be mounted in the reflection port on the opposite side of the sphere, along with a reference standard in the other port, as is normally done for reflectance measurements. When samples of interest are not opaque, they must be mounted on an opaque substrate for measurement. To avoid problems of surface reflection at a rear–air interface, the backing should be optically sealed to the sample. (This is achieved by use of a viscous sealing material of refractive index similar to that of the sample; this eliminates air between the two materials when the "sandwich" is made.) If the backing is white, all of the light transmitted or scattered in the forward direction, as well as the reflected light, is measured. If the backing is black, only the light reflected backward into the sphere is measured. The specular ports in the sphere are used for exclusion or inclusion of the first surface specular reflection: black for exclusion and white for inclusion.

Designations for these measurements are usually R_0 for the measurement over black and R_w for the measurement over white. If the white backing is not perfectly white, that is, $R < 100\%$, and if the black backing is not a perfect black, that is, $R > 0\%$, corrections can be made for the actual values so that R_w and R_0 are properly corrected (see Ross 1967). When the substrates are in optical contact with the films, R_w and R_g are the total reflectances. The total light transmitted and reflected in the forward direction, that is, T_T, can be calculated from these two measurements by

$$T_T = \left[\left(R_w - R_0\right)\left(1 - R_0\right)\right]^{1/2} \tag{4.24a}$$

If the reflectance of the black backing is less than 1%, but the white backing (substrate) does not reflect 100%, the following equation can be used:

$$T_T = \left[\left(R_w - R_0\right)\left(1/R_g - R_0\right)\right]^{1/2} \tag{4.24b}$$

where R_g is the reflectance of the near-white substrate. The T_T determined by this reflectance technique should be the same as that obtained by measuring the total transmittance in the forward direction when the sample is mounted at the entrance port, as explained earlier.

The techniques just described for measuring the reflectance and transmittance of translucent materials apply only to materials that are not completely opaque. But, as mentioned near the beginning of this section, opaque materials may vary in appearance in a subtle way as a result of the perception of depth of light penetration into the materials—that is, their degree of translucency. For example, a problem presented to the author was to help in designing plastic piano keys to replace the natural ivory traditionally used. Not only did the gloss, color, and grain of the ivory have to be simulated, but the degree of translucency had to be approximated as well. In fact, wider differences in color were found to be acceptable than differences in translucency. Natural ivory keys were first measured for color and translucency, using the techniques over black and white substrates as just described. Subsequently, synthetic plastic approximations were measured in the same way for comparison. Plastic simulations were produced that adequately reproduced the real thing. Results of the measurement work on this project are described in U.S. Patent 4,346,639 issued to Vagias (1982).

Unless an opaque translucent material is expendable so that it can be sectioned horizontally, or the thickness can be decreased by abrasion or dissolution, measurements over black and white cannot be exploited, and the character of the translucency cannot be calculated using the Kubelka–Munk equations described.

The depth of penetration of incident light is also a major appearance attribute of glazes (described in the previous section). It is not possible to match the appearance, even though the instrumentally measured color can be matched, unless the substrate and glaze colorants are applied in a manner similar to that used in the original. *One must not forget that color is only one aspect of appearance.*

Among industrial products, white light diffusers, particularly those used with fluorescent fixtures, represent a practical application of the principles of translucency described above. In this case, the scattering of the white particles has to be in the forward direction for greatest efficiency. Thus the pigment concentration and particle size must be carefully controlled.

Should the reader assume that the techniques for measuring translucency of relatively thick materials are easy to carry out with accuracy, a word of caution must be mentioned. The measurements are subject to many variables due to instrument design, even though an integrating sphere instrument is used. In addition, sample size and thickness, surface reflection, and the substrate backings also affect the measurements. One of the troublesome effects of sample size and thickness is loss of light scattered out of the edges of translucent sheets. Atkins and Billmeyer (1966) tested a number of commercially available instruments and concluded that none of them could "measure the transmittance and reflectance of relatively thick translucent specimens with high absolute accuracy." Nevertheless, if measurements are made on one particular instrument type in the same manner each time, valuable comparative results can be obtained.

In the case of thin, translucent films in good optical contact with the substrates, the reproducibility can be very good. The paint industry, for example, relies heavily on the measurement of substrate hiding in terms of the contrast ratio, which is a measurement of reflectance of a film applied over black divided by the reflectance of a film of the same thickness and pigment concentration applied over white. Hiding power is discussed at greater length below.

The plastics industry extensively uses the determination of the opacity of sheets and of thin films. It applies a special term to describe the scattering in translucent and near-transparent sheets when the scattering is in the forward direction. The term used is *haze,* defined in ASTM Standard D 1003 as the light flux deviating from the incident transmitted beam direction by more than 2.5°. Hazemeters were developed and are commercially available for making the measurement of haze and luminous transmittance. A conventional spectrophotometer with an integrating sphere of the type illustrated in figure 4.22 may also be used. The use of the term *haze* in this sense seems to be unique to the plastics industry. In the paint industry, haze generally refers to the slight scattering from a glossy surface that decreases distinctness-of-image gloss (FSCT 1995). Other methods used in the plastics industry to measure transparency and translucency are ASTM Standards D 1494 and D 1746. The techniques for measuring and adjusting the opacity of poly(vinyl chloride) sheets were discussed by Osmer (1978).

Charts for determining opacity

The paper industry was one of the first to utilize the Kubelka–Munk equation for determining opacity. The original Kubelka–Munk equation for incomplete hiding had been used since the late 1930s for determining opacity in terms of the contrast ratio R_0/R_w, based on precalculated charts for a substrate $R_w = 0.89$. In its original 1931 form, the Kubelka–Munk equation, shown as equation 4.25 below, could not be used to determine the scattering coefficient directly.

$$R = \frac{\left(R_g - R_\infty\right)/R_\infty - R_\infty\left(R_g - 1/R_\infty\right)e^{SX(1/R_\infty - R_\infty)}}{R_g - R_\infty - \left(R_g - 1/R_\infty\right)e^{SX(1/R_\infty - R_\infty)}} \tag{4.25}$$

K is not in the equation but is implicit in the relationship: $K/S = (1 - R_\infty)^2/2R_\infty$. Tables of the exponential function, e^x, were used to compute some theoretical information that could then be plotted for use in making graphical solutions for specific situations (Judd 1937). Specifically, graphs were developed for the case where the reflectance of the white substrate was 0.89, as used by the paper industry; or 0.80, as used by the paint industry; or 0.70, as used by the dental industry. The ordinate of these graphs was the reflectance over black, R_0; the abscissa was the hiding power in terms of the contrast ratio, R_0/R_w. Plotted on the graph were the R_∞ and *SX* (to be interpreted as *SCX* to account for the concentration as well as the thickness). Thus, if one knew any two of these values, the others could be determined from one of the graphs for one of the specific white substrates, R_w.

Use of such charts has now been largely replaced by computing techniques, easily carried out with a computer or programmable calculator. The computing task was made straightforward when Kubelka (1948) published the hyperbolic solutions of the original Kubelka–Munk equation (eq. 4.25) described above.

Why mention the old charts? Because a ready estimate of R_∞ and SX (that is, SCX) can be obtained with a very simple tristimulus colorimeter, without any calculations at all, by making the Y, or G, filter measurements of a sample over white and over black, as well as measurement of the white substrate. Such a substitution of Y or G for R should be used only for white or neutral materials. The chart is a quick guide. Information for determining thickness or concentration corrections to attain desired properties can be estimated from the charts without extensive calculations. The chart for the white substrate of 89% (as used in the paper industry) is reproduced here, as figure 4.23. The 89% reflectance substrate is a good average for white pigments. (See the test methods published by the Technical Association of the Pulp and Paper Industry [TAPPI 1992b, 1992d].)

Hiding power

Examination of the charts shows that when the contrast ratio—Y_0/Y_w or R_0/R_w—approaches 1.000 (100%), it becomes increasingly difficult to read the graphs accurately. As a consequence, when these graphs were

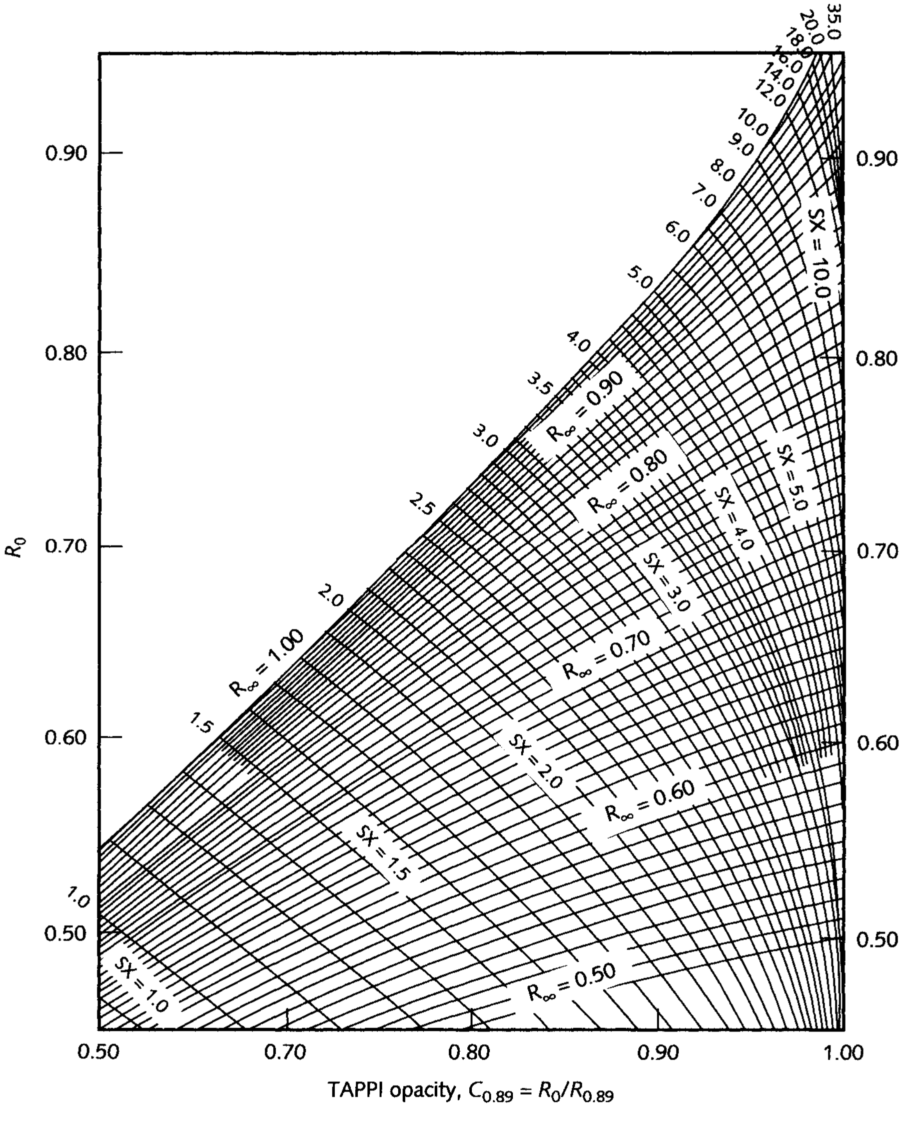

Figure 4.23

Diagram showing the interrelation of reflectance at incomplete hiding over black, R_0; reflectance at complete hiding, R_∞; TAPPI opacity, $C_{0.89} = R_0/R_{0.89}$; and SX, the scattering power times the thickness. It must be remembered that a change in concentration has the same effect on the color, when hiding is incomplete, as a change in thickness, so SX is, in reality, SCX; increasing the pigment volume concentration has the same effect as increasing the thickness by the same multiple (after Judd 1937).

first used early in the history of determinations of hiding power, many industries established a contrast ratio (Y_0/Y_w) of 0.98 as equivalent to complete visual hiding. This is seldom strictly true, but that ratio is still widely used as a standard. See ASTM Standard D 2805 for its use in the paint industry.

The contrast ratio of 0.98 as complete hiding is strictly valid only for perfect whites. Therefore, a contrast ratio of 0.98 does not always correspond to complete visual hiding. Nonetheless, for many applications, determination of satisfactory hiding power in terms of a contrast ratio of 0.98, which is generally very close to complete visual hiding, is acceptable. If an effort is made to increase the hiding, even to a contrast ratio of 0.985, reference to the charts shows that the concentration of scattering pigment must be increased by at least 10–20%, adding significantly to the cost and possibly altering physical properties of the pigmented material as well. In many commercial applications such an effort is deemed not worth the increased cost and formulation problems. Incidentally, the small addition of an absorbing pigment such as black will also improve the hiding, but, of course, this will lower the reflectance, R_∞.

In many applications, with many materials, the degree of visual hiding is not the most important consideration. Whenever the stability of a material that might be exposed to light is paramount, the *spectrophotometric hiding* must be considered. Perfect spectrophotometric hiding is defined as a contrast ratio of unity (1.000) at every wavelength, as calculated from reflectance measurements made over a perfect white (R = 100%) and a perfect black (R = 0%) in the near-infrared and near-ultraviolet spectral regions as well as in the visible. Incomplete spectrophotometric hiding is the contrast ratio calculated from reflectance measured at the wavelength (or selected wavelengths) at the reflectance maximum over a white of defined reflectance and a black of near-zero (< 1%) reflectance. In the discussion that follows, the contrast ratio based on the Y tristimulus value is abbreviated $(CR)_Y$, and the contrast ratio based on reflectance measurements at specific wavelengths is abbreviated $(CR)_R$. In figure 4.24 the two types of contrast ratios are illustrated (Johnston-Feller 1986) for two samples of alizarin–TiO_2 mixtures. Sample B appears to be very close to complete visual hiding, $(CR)_Y$, that is, $Y_0/Y_w = 0.976$ when $R_w = 1.00$. However, in the red region, the $(CR)_R$ average is only 0.877. This is clearly evident from an examination of the spectral curves illustrated; the reflectance in the red region for the sample measured over black is much lower than the reflectance measured over white. Sample A, on the other hand, is at incomplete hiding both in terms of the $(CR)_Y = 0.923$, and in terms of the reflectance in the red region, $(CR)_R = 0.727$. The point is made in the cited 1986 article that the *rate of fading* of sample B is 30% higher when exposed over white and 50% higher when exposed over black, when spectrophotometric hiding is incomplete in the red region, than when hiding is complete at *all* wavelengths. The increased rate of fading over black is probably a heat effect; the painted panel, which transmits in the red region, gets hotter due to the black background's absorption of the infrared wavelengths.

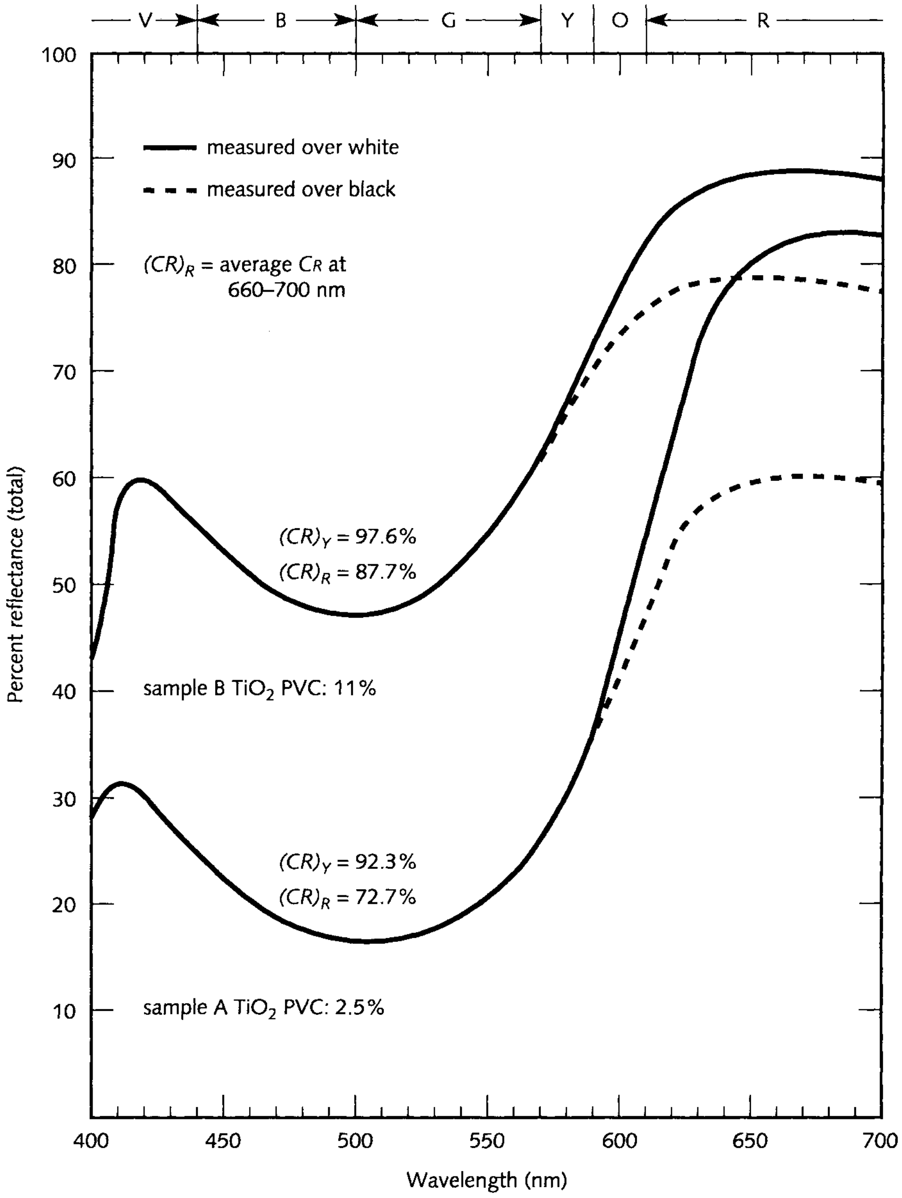

Figure 4.24

Two formulations of alizarin lake mixed with rutile TiO_2 in poly(vinyl acetate) (Vinac B-7) applied at incomplete hiding over a white of 100% reflectance and a black of 0% reflectance. The contrast ratio based on the luminous reflectance, *Y*, is designated as $(CR)_Y$. The contrast ratio for the average reflectance in the red region of 660–700 nm is $(CR)_R$. Note that $(CR)_Y$ for sample B is very close to the 98% contrast ratio widely considered to be equivalent to complete hiding, but in the red region of the spectrum, hiding is far from complete. Sample A is lower in hiding, as indicated by the lower contrast ratios.

When hiding is incomplete at all wavelengths, the rate of fading is more than twice that for samples at complete spectrophotometric hiding at all wavelengths.

The contrast ratios illustrated in figure 4.24 were calculated for a white substrate reflecting 100%. If the white substrate reflectance were significantly lower than this value—for example, 80% (the average reflectance of the white portion of the black-and-white contrast paper widely used in the paint industry)—the measured contrast ratios would be higher; from an analytical point of view, this would be misleading. For sample B in figure 4.24, the $(CR)_Y$ would be above 0.99, compared with 0.976 over the 100% reflecting white; the $(CR)_R$ would be 0.99, compared with 0.877. The result would imply that the sample is very close to complete hiding, possibly within experimental error, as it would visually appear to be over a substrate of 80% reflectance. For sample A, the spectrophotometric $(CR)_R$ in the red region would rise from about

0.73 for a substrate reflectance of 100% to 0.95 for a substrate of 80% reflectance! Thus, when spectrophotometric, rather than visual, hiding may be of prime importance in determining the effect of light exposure on the performance of a specific thickness of a material or of a particular colorant formulation, the reflectance contrast ratios at wavelengths of maximum reflectance (minimum absorption) should be calculated for the substrates of ideal reflectances: a white of 100% reflectance and a black of 0% reflectance. Alternatively, the reflectance, R_w , of the intended substrate—if known—can be used in the measurements and calculations. With computers, the calculation to $R_w = 100\%$ is relatively straightforward. However, the concept is not always appreciated, and the calculation is not often done.

The reader may well question when a substrate of 100% reflectance is ever encountered. The answer is that when the substrate is a metal (a nondielectric), the specular reflection may be extremely high at the specular angles, approaching mirror reflection. It is important also to realize that the concepts described apply equally to the nonvisible portions of the solar spectrum: the actinic ultraviolet regions as well as the thermal infrared regions.

The list of materials requiring knowledge of translucency and opacity is almost limitless. It includes paints, plastics, ceramics, and textiles, as well as liquids, both natural and manufactured. Even the scattering in gases—such as in clouds, which contain finely dispersed particulates (water droplets, ice crystals, dust, etc.)—has been studied extensively by use of radiation transfer theories such as those of Mie and Kubelka–Munk.

Tinting strength: absorption and scattering

Of major importance to the user of colorants is their strength, that is, their ability to alter the color in a particular manner when mixed with one or more other dyes or pigments in a particular application. The term *tinting strength* is generally applied to this characteristic. As most commonly used, it is not an absolute measurement but a relative one; that is, it is used in a comparative sense: one particular colorant may be found to have a higher tinting strength than another when different colorant types or different samples of the same type are compared. Tinting strength is an important characteristic when determining relative costs of different colorants, when formulating or reformulating to achieve optimum characteristics, or when ensuring quality control in purchasing and manufacturing.

As an example, an artist, when purchasing a tube of a particular colorant, may wish to know which brands are the best value. Price alone may not be the best indicator. If a more expensive tube contains more pigment per unit volume and thus has a higher tinting strength, it may be the cheaper in terms of effect.

In the case of dyes, which do not scatter light, the absorption values determine the tinting strength. Their strength is best determined from a measurement of the absorption at the wavelength of the absorption maximum. This may be done by measuring the transmittance of a solution of the dye and using the Beer–Bouguer equation; or by making a dyeing using a standard procedure, measuring the reflectance, and applying the single-constant Kubelka–Munk equation described earlier in this chapter. The Beer–Bouguer equation for the absorption determined for a transparent solution was originally introduced as equation 4.5c. It can be restated as

$$\log\left(\frac{1}{T}\right)=CXA \qquad \text{or} \qquad A=\log\left(\frac{1}{T}\right)\Big/CX \tag{4.26}$$

where T is the decimal fractional transmittance, C is the concentration, X is the cell thickness, and A is the unit absorption coefficient.

The relative tinting strength (TS) is calculated at the absorption-maximum region of the sample (Spl) in question relative to the same measured absorption of the standard (Std) (Kuehni 1983) by the following:

$$\%TS=100\left(\frac{A_{\mathrm{Spl}}}{A_{\mathrm{Std}}}\right) \tag{4.27}$$

When standard dyeings are being compared, the single-constant Kubelka–Munk equation used on opaque materials relates the reflectance to the absorption as

$$\frac{(1-R)^2}{2R}=C\left(\frac{K}{S}\right) \qquad \text{or} \qquad \left(\frac{K}{S}\right)=\frac{(1-R)^2}{2R}\Big/C \tag{4.28}$$

where R is the decimal fractional reflectance, C is the decimal fractional concentration of the dyestuff, S is the substrate scattering, and K is the unit absorption coefficient. The dyeing is made on identical standard substrates for the sample and the standard; S is set equal to unity (1.000) for the standard substrate. The relative tinting strength (TS) is then calculated in the same way (Garland 1983) with the following:

$$\%(TS)_K=100\left[\frac{(K/S)_{\mathrm{Spl}}}{(K/S)_{\mathrm{Std}}}\right] \tag{4.29}$$

where $(TS)_K$ refers to absorption tinting strength. Recall that the Beer–Bouguer absorption coefficient A is not the same as the Kubelka–Munk absorption coefficient K. The Kubelka–Munk unit K is twice the value of the Beer–Bouguer unit A (Judd and Wyszecki 1975).

The relative tinting strength of a dye determined by the two methods—by measurement in solution and the use of equations 4.26 and 4.27, or by measurement on dyed fabric and the use of equations 4.28 and 4.29—may not be in agreement. The difference may be attributable to variations in dyeability caused by the effects of processing and by possible interactions with other constituents used in the application.

In the case of pigments, the measurement of tinting strength is generally based on the preparation of opaque samples—for example, paint films at complete hiding or plastic samples of sufficient thickness to be opaque.

In chapter 3 it was pointed out that pigments may be placed into one of three categories. Type I pigments scatter much more light than they absorb; an example is white pigments. Type II pigments absorb much more light than they scatter; these include most blacks and many transparent, primarily organic, pigments of small particle size. Type III pigments both absorb and scatter light significantly; examples are many inorganic pigments of higher refractive index and organic pigments, both of larger particle size.

The tinting strength of type I pigments, such as whites, depends primarily on their scattering coefficient, S. This is generally determined by preparing a sample of the material mixed with a prescribed amount of a standard reference absorbing pigment, such as a black. For type I scattering pigments, the scattering strength is determined as follows:

$$\%(TS)_S = 100\left[\frac{(K/S)_{\mathrm{Std}}}{(K/S)_{\mathrm{Spl}}}\right] \tag{4.30}$$

where $(TS)_S$ refers to the scattering tinting strength. Note that in determining the relative scattering strength, the K/S ratios are inverted from what they are in equation 4.29 for determining absorption tinting strength. This is because S is in the denominator of the K/S ratio.

The calculation of the absorption tinting strength for absorbing, low-scattering, type II pigments is described by equations 4.28 and 4.29, except that S is based on a standard white pigment used in admixture. The strength of type II pigments depends on their absorption coefficient, K, and is generally determined by preparing a sample of a prescribed amount of pigment in a mixture with a prescribed amount of the standard reference white pigment. In this case, the form of the single-constant Kubelka–Munk equation shown in equation 4.7 is generally used, and K/S is determined at the wavelength of the absorption maximum. The relative absorption tinting is then calculated by use of equation 4.29.

Determining the tinting strengths of pigments that both absorb and scatter significantly—that is, type III pigments—presents a more complex problem. The strength of these pigments depends on the way they are to be used. If they are used to make a light color, for example, a color equal to or above a Munsell Value of about 5 (20% luminous reflectance), the white contributes almost all of the scattering, and the type III pigment contributes the significant absorption. Such a pigment's tinting strength is then attributable to its absorption characteristics and may be calculated from equation 4.29, the same as for type II pigments and for textile dyeings. In this case, the pigment's scattering characteristics are not of great significance.

If a type III pigment is used in a mixture containing a small amount, or none at all, of scattering pigment, the problem of its strength becomes less clear. Is the strength dependent on its absorption or on its scattering, or on both characteristics? An example of such a mixture is the dark olive drab green that was once used to paint some telephone company trucks. Until industry was required to use lead-free pigments, this color was often made by mixing a yellow lead chromate pigment and a black pigment; the black supplied the absorption, and the yellow supplied the scattering. A green color resulted because the chrome yellow exhibited its maximum scattering in the green region. The absorption of the chrome yellow did not matter; the black supplied the absorption. The tinting strength of the yellow pigment in this application was due to its scattering characteristics. Its tinting strength could be calculated from measurement of a mixture with a standard black pigment according to equation 4.30, as is used for type I white pigments. In this case of wavelength-selective scattering, the scattering tinting strength would be measured at the wavelength of the scattering maximum.

When a type III colorant, which both absorbs and scatters significantly, is applied at incomplete hiding, as a glaze, over a reflecting substrate such as white, its absorption primarily determines its color because the transmitted light is subsequently reflected. The white substrate provides the scattering. If the same colorant is applied at the same concentration and thickness over an absorbing substrate such as black, however, its scattering characteristics determine the color. The transmitted light is absorbed by the black substrate. Thus, the yellow lead chromate pigment described above, which was used to make olive drab colors in mixture with black, also makes a low-chroma olive green when applied at incomplete hiding over black.

Figure 4.14 presented earlier shows the reflectance curves of a yellow lead chromate applied at incomplete hiding over a white substrate and over a black substrate (Johnston and Feller 1967; Johnston 1973). The maximum reflectance of the sample over black occurs at about 520 nm, in the green region. By contrast, a type II yellow—flavanthrone, which absorbs far more light than it scatters—applied over black makes a very small change in the black substrate color, but that small change is to a slight green tinge, as illustrated in figure 4.15. Applied over a white substrate, Flavanthrone Yellow results in a high-chroma yellow because of its high yellow transmittance. Note that the glazes applied over black are plotted at 5 times their actual values; the reflectance of the more transparent Flavanthrone Yellow applied over black is less than 3% at the scattering maximum (535 nm), whereas that of the chrome yellow applied over black is close to 10%. These values are relative only.

In figures 4.16 and 4.17, two red pigments are illustrated as applied over white and over black: cadmium red, a type III colorant that scatters and absorbs significantly, and a more transparent type II pigment, Quinacridone Red, which absorbs strongly but scatters little (Johnston and Feller 1967; Johnston 1973). The reflectance of the Quinacridone Red glaze over black is less than 1%.

Some mixtures of type II and type III pigments result in seemingly surprising colors. For example, years ago many commercial high-chroma red paints and plastics were made by mixing a transparent type II absorbing organic violet, or bluish red, in mixture with molybdate orange, a type III pigment. That a very dark violet in mixture with a bright orange would result in a bright red may, at first, seem surprising. But the explanation is straightforward in terms of their absorption and scattering characteristics. The molybdate orange absorbs most of the light from 400 to 550 nm, thus absorbing the violet reflectance. The violet, on the other hand, has its maximum absorption in the yellow and yellow-orange region, 560 to 620 nm, thus removing these wavelengths from the molybdate reflectance. The molybdate reflects highly in the red region because of its high scattering, and the absorption of the violet decreases in this long-wavelength region. The nonabsorbed reflectances remaining are in the red region, so the color of the mixture is bright red.

In the case of a bluish transparent red mixed with molybdate orange, the resulting red is of higher chroma than the mixture with a violet. Figure 4.25 illustrates the curves of the masstone of molybdate orange, type III, and of Quinacridone Red, a type II organic bluish red pigment, as well as the curve of a mixture of 75% molybdate orange and 25% Quinacridone Red. In order to see the typical absorption bands of the Quinacridone Red, obscured in the very dark masstone curve, the curve of a mixture of 10% Quinacridone Red in TiO_2 is included in the figure. As can be seen by the curve of the mixture of Quinacridone Red and molybdate orange, the color is a bright red.

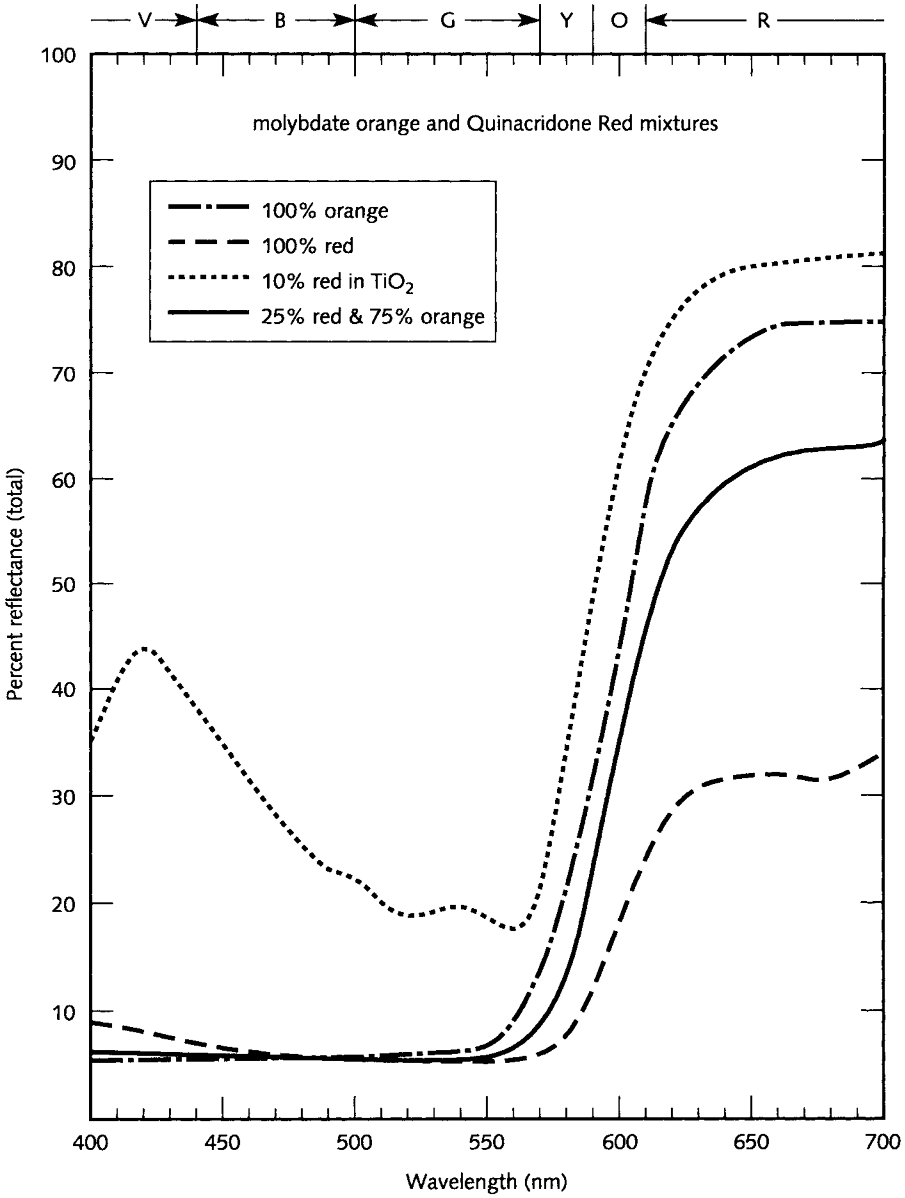

Figure 4.25

Reflectance curves of molybdate orange masstone, Quinacridone Red masstone, and a mixture of 25% Quinacridone Red with 75% molybdate orange. The mixture (solid line) is a high-chroma red. In this case the greater absorption of the Quinacridone Red in the middle of the spectrum shifts the curve so that the reflectances in the yellow and orange wavelengths are decreased, leaving only the red wavelengths to be reflected. The molybdate orange absorbs all of the short wavelengths, where the bluish Quinacridone Red has significant reflectance in mixture with a white pigment (dotted curve).

Thus, we see that when a type III pigment, which both absorbs and scatters significantly, is used in mixture with or applied over a type I pigment such as white, which scatters far more than it absorbs, the tinting strength of the type III pigment is dependent on its absorption characteristic as calculated from its Kubelka–Munk *K*/*S* value. However, if a type III pigment is used in mixture with or applied over a type II pigment such as black, which absorbs far more significantly than it scatters, it is the scattering characteristic of the type III pigment—as calculated from its Kubelka–Munk *S* coefficient—that determines its tinting strength. Nonetheless, in some two-pigment mixtures of types II and III, both the absorption and the scattering characteristics of the type III pigment are important, as exemplified by the molybdate orange in the Quinacridone Red–molybdate orange mixture discussed above.

When both absorption and scattering properties are important, each may be checked. Make a mixture with white and use equations 4.28 and 4.29 to calculate *K*'s; then make a mixture with black to calculate the *S*'s using equations 4.28 and 4.30. A quick visual comparison between two pigments can be made by applying each at incomplete hiding over black and white substrates. If they are made at the same concentration and thickness, their relative absorption strength can be seen from the area coated over white, and their relative scattering strength from the area over black.

In the case of mixtures of two or more type III pigments, which both absorb and scatter light significantly, it is difficult to predict which optical characteristic of each is of primary importance in determining the color of the mixture. Generally speaking, the only way to determine this is by trying various amounts of each pigment in the mixture. If a computer color-matching program is available, this can be done without making up samples; if not, trials can be made by varying the concentration of each pigment and observing what happens.

One of the reasons it is so difficult to predict which pigment is primarily responsible for either the scattering or the absorption of a type III pigment mixture is that typical type III pigments are inorganics with refractive indices of 2.0 or above. The most frequent variation encountered in these pigments is in their particle size. And the particle size is dependent not only on how the pigment is manufactured but also on how it is dispersed.

(Anyone who examines the works of old masters and compares them with the works of modern artists knows that in the days long before commercial dispersions were developed, artists used whatever pigments were available from natural sources or from crude manufacturing operations. They ground the pigments by hand, using a muller or just a spatula; the result was paints containing pigments that were coarsely ground in comparison with modern pigments produced commercially.)

Fortunately, changes in the particle size of type III inorganic pigments with refractive indices of 2.0 or more affect the absorption and scattering coefficients in a similar manner—that is, if the particle size is either increased or decreased from the size required for maximum absorption and scattering power, both absorption and scattering will decrease. The rates of change in absorption and scattering efficiency are not the same, but they are also not so different that, qualitatively, the concept fails to be a helpful guide.

Figure 4.26 is an illustration of the relationship of the absorption and scattering coefficients to the particle size of iron oxide pigments, as calculated from Mie theory (Brockes 1964; Buttignol 1968). In the previous section it was stated that Mie theory applied to single scattering only. However, Mie theory also provides an excellent guide to relative absorption and scattering ratios in multiple-scattering situations. In the article by Buttignol, the qualitative agreement between the absorption and scattering coefficients for iron oxide pigments was demonstrated, as determined both from Mie theory and from Kubelka–Munk theory. From the graph shown in figure 4.26, it can be seen that the optimum particle size for maximum scattering is virtually the same as that for maximum absorption, and that either decreasing or increasing the particle size from this maximum results in a decrease in both the absorption and scattering efficiency.

Although the curves in figure 4.26 were calculated for iron oxide pigments, they are qualitatively applicable to other type III inorganic pigments of refractive index greater than 2.0. For example, molyb-

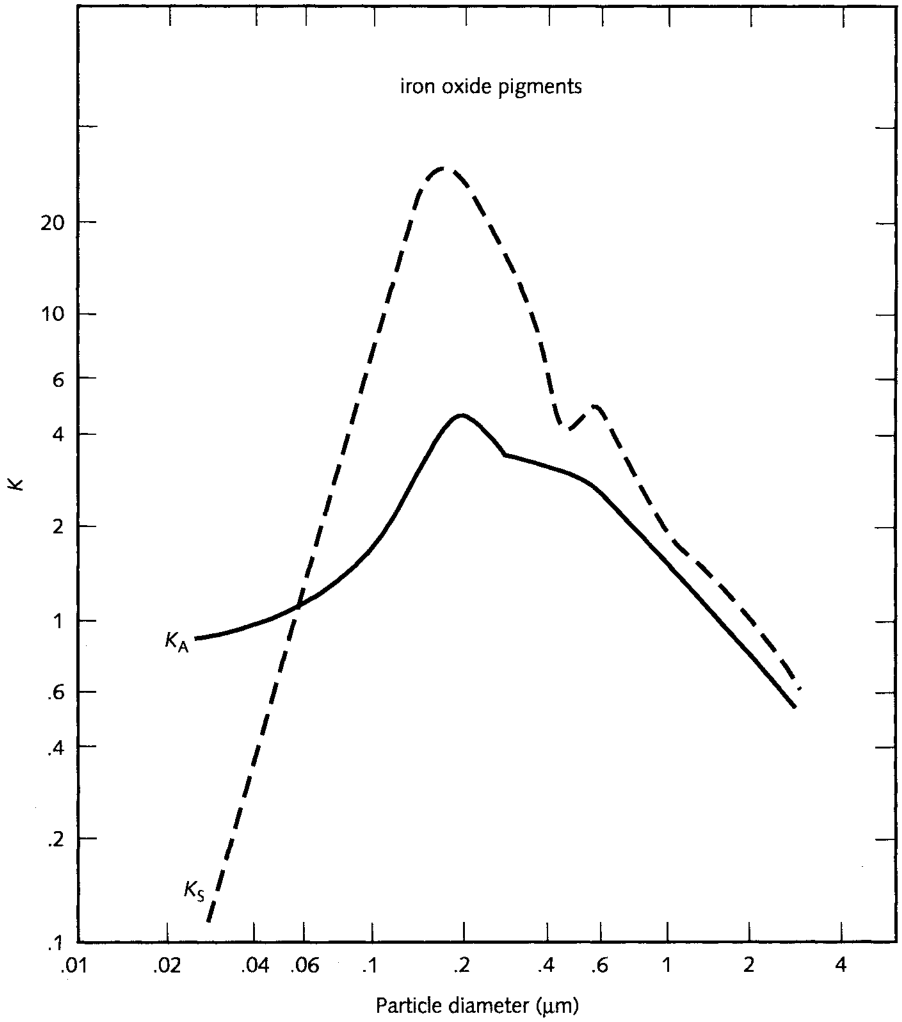

Figure 4.26

The change in the absorption coefficient, K_A, and the scattering coefficient, K_S, as the particle diameter of iron oxide pigments is changed (calculated from Mie theory [after Brockes 1964; Buttignol 1968]).

date orange (fig. A.28) can be easily overground, that is, ground smaller than the optimum particle size in the dispersion process. When this happens, both the absorption and scattering coefficients are decreased, as would be predicted from the curves in figure 4.26. The masstone color becomes dirty because of the decrease in the orange and red scattering, and a mixture with white pigment, such as TiO_2, shows the overground pigment to be paler as well, due to the reduction of the absorption.

It is not possible to categorize absorbing pigments as either type II or type III solely on the basis of refractive index, because organic pigments of refractive index of 2.0 or less can both absorb and scatter significantly if the particle size is in the proper range to achieve scattering.

In figure 4.27, Brockes's curve for organic pigments, calculated from Mie theory, is shown (Brockes 1964). It can be seen that the shapes of the absorption and scattering curves are dependent on the particle sizes as well as on refractive indices. They are very different from the curves for the iron oxide pigments and other pigments of refractive index greater than 2.0 illustrated in figure 4.26. Also apparent from this graph is that the greatest absorption is reached (absorption tinting strength) at the smallest particle sizes. (The calculations were stopped before the absorption increased as particle size decreased further.) Organic pigments (toners) do not lose absorption strength as the particle size is decreased as do the type III pigments. In the past—in general, prior to the 1970s—organic pigments were almost always manufactured so that the scattering was low and the absorption high—typical type II pigments. Such organic pigments, as manufactured to achieve maximum absorption tinting strength, have little hiding power because their scattering is so low.

Prior to the 1970s, many of the bright yellows, oranges, and reds in paints and plastics were pigmented with colorants containing heavy metals, such as lead, which is dangerously toxic to animals and humans if ingested, because the metallic elements accumulate in the body. Other heavy metals, such as cadmium, used in plastics were less commonly encountered but were also unhealthy if ingested. Soon thereafter, a great movement in pigmentation changes occurred to replace the materials made with pigments containing heavy metals, particularly lead, which had been used for so many years in the form of lead white and also as lead chromates for making bright yellows and oranges. Many of the organic pigments introduced as replacements are completely metabolized by the human body and represent no problem if ingested.

Examination of the Mie curve (fig. 4.27) shows that if one is willing to sacrifice absorption strength, one can make an organic pigment that scatters significantly by increasing the particle size. As a result of the mandate to eliminate lead from commercial paints and plastics, changes have come about in industrial pigment production so that organic colorants with larger particle size and lower absorption tinting strength but higher scattering strength may be encountered.

Schäfer and Wallisch (1981) described this trade-off in optical properties for Pigment Yellow 74 (Dalamar Yellow), a Hansa-type organic pigment. They illustrated the curves of pigment particle size

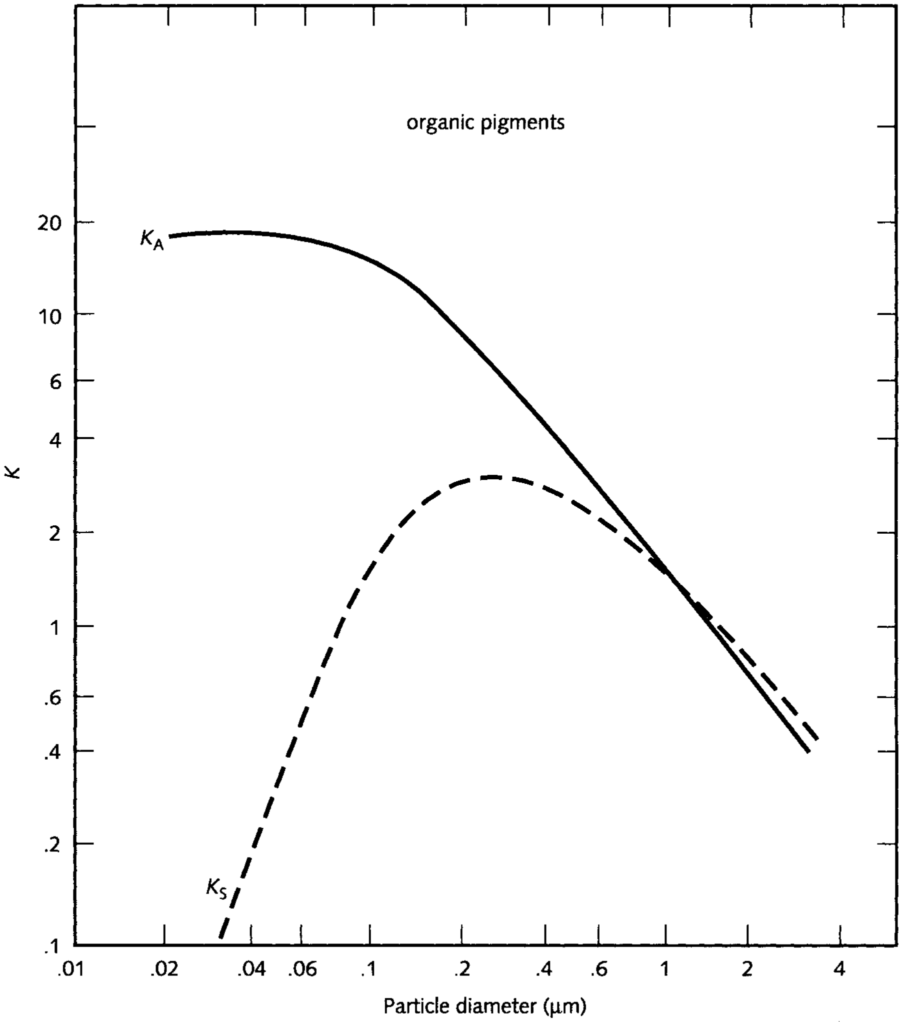

Figure 4.27

The change in the absorption coefficient, K_A, and the scattering coefficient, K_S, as the particle size of organic pigments of refractive index less than 2.0 is changed (calculated from Mie theory [after Brockes 1964]).

distribution and also provided electron micrographs for three different versions of PY 74: one with high (absorption) strength; a standard; and another with high opacity (high scattering). The median particle sizes were 0.15 μm for the high-absorption-strength type; 0.22 μm for the standard; and 0.33 μm for the high-opacity version. The relative effects on the absorption tinting strengths and the opacities (indicative of the relative scattering tinting strengths) for these pigments, as used in a long-oil alkyd paint, are summarized in table 4.3. The trade-off between absorption tinting strength and scattering strength (described as relative opacity) illustrated in this table is in qualitative agreement with the Mie curve for organic pigments illustrated in figure 4.27. An excellent overview containing illustrations of γ-quinacridone pigments of different particle sizes, presented in electron micrographs as well as in color plates, is that by Gerstner (1966).

Table 4.3

Relative absorption tinting strength and opacity of samples of Pigment Yellow 74 (PY 74) compared to their average particle size (Schäfer and Wallisch 1981).

Type	Median particle size (μm)	Relative tinting strength	Relative opacity
High-strength PY 74	0.15	120	42
Standard PY 74	0.22	100	100
High-opacity PY 74	0.33	58	175

The type II pigments illustrated by the Mie curve of figure 4.27 may also be types that contain inorganic constituents. Some are lakes, which are dyes precipitated on inorganic bases or substrates. An example is the calcium-alumina lake of alizarin. The organic chemical, in pure form, is a yellow, but when precipitated on inorganic aluminum hydrate, it forms a brilliant, unique red. The spectrophotometric reflectance curve for the pure alizarin (1,2-dihydroxyanthraquinone) dispersed in a rutile TiO_2 paint system is shown in figure 4.28. The spectral curve is obviously that of a yellow of moderate chroma. Also included in this figure is the spectral curve of the calcium-alumina lake of the chemical dispersed in the same rutile TiO_2 paint system. It is readily apparent that the lake is the result of a reaction between the 1,2-dihydroxyanthraquinone and the calcium-alumina carrier. Not all transparent organic chemicals, when made into a lake on inorganic particles, change hue so radically. Many of the modern transparent organic pigments are offered for sale either as the lake or as the pure material, called a toner.

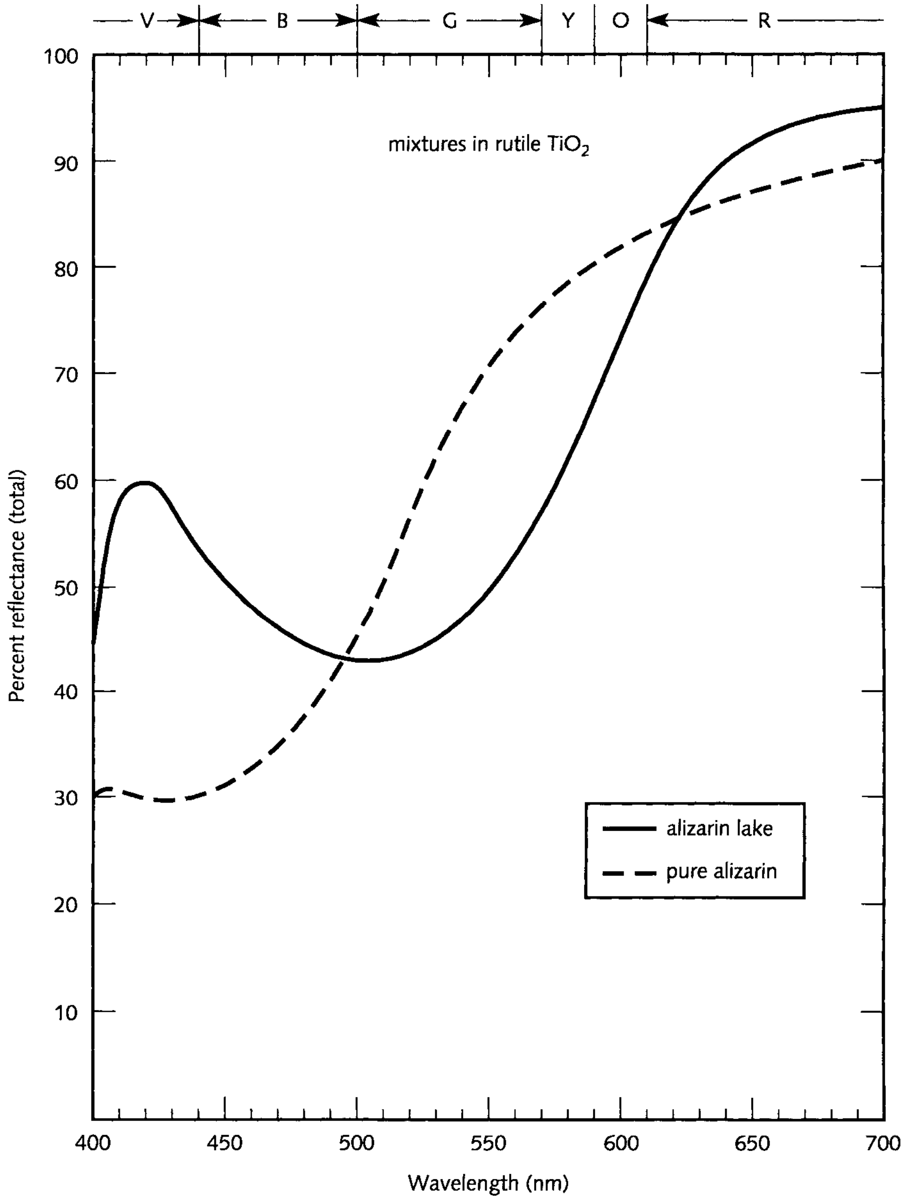

Figure 4.28

Spectral reflectance curves of alizarin (1,2-dihydroxyanthraquinone) mixed with TiO_2 The pure alizarin is yellow; the calcium-alumina lake is the familiar bluish red.

One of the type II pigments of important historical interest is iron blue, also called Prussian blue. Because the word "iron" is in its name, it may be confused with an inorganic pigment, but this is a transparent, complex organic (carbon-containing) pigment—ferric ferrocyanide—which has a low refractive index (n = 1.56 at 560 nm) and a high tinctorial (absorption) strength.

In the case of TiO_2, a type I pigment that does not absorb appreciably, the Mie scattering can be predicted from a simple graph. It has been called the universal scattering curve and was first published by LaMer (LaMer et al. 1945) and later by DeVore and Pfund (1947). It is reproduced here as figure 4.29. The abscissa contains the values for n_v, the refractive index of the vehicle; n_p, the refractive index of the pigment; D, the diameter of the white pigment particles expressed in micrometers (μm); λ, the wavelength (μm); and m, the ratio n_p/n_v. Mitton (1973) shows that the opacity and tinting strength of white pigments is linearly proportional to the value of M^2, when $M = (n_p/n_o)^2 - 1/(n_p/n_o)^2 + 2$, where n_o is the refractive index of the vehicle and n_p is the index of the pigment. An approximate expression for M is $M \approx 0.4(n_p - n_o)$. In Mitton's figure 2, he relates the square of M for rutile and anatase TiO_2, lead white, ZnO, calcium carbonate, and $BaSO_4$ to their relative hiding power (or scattering tinting strength).

Gerstner (1966) presents electron micrographs and color plates of two TiO_2 pigments of different particle size. The color plates show the two whites tinted with blue to illustrate the differences in the tinting strengths of the two white pigments. The TiO_2, which is ~0.25 μm

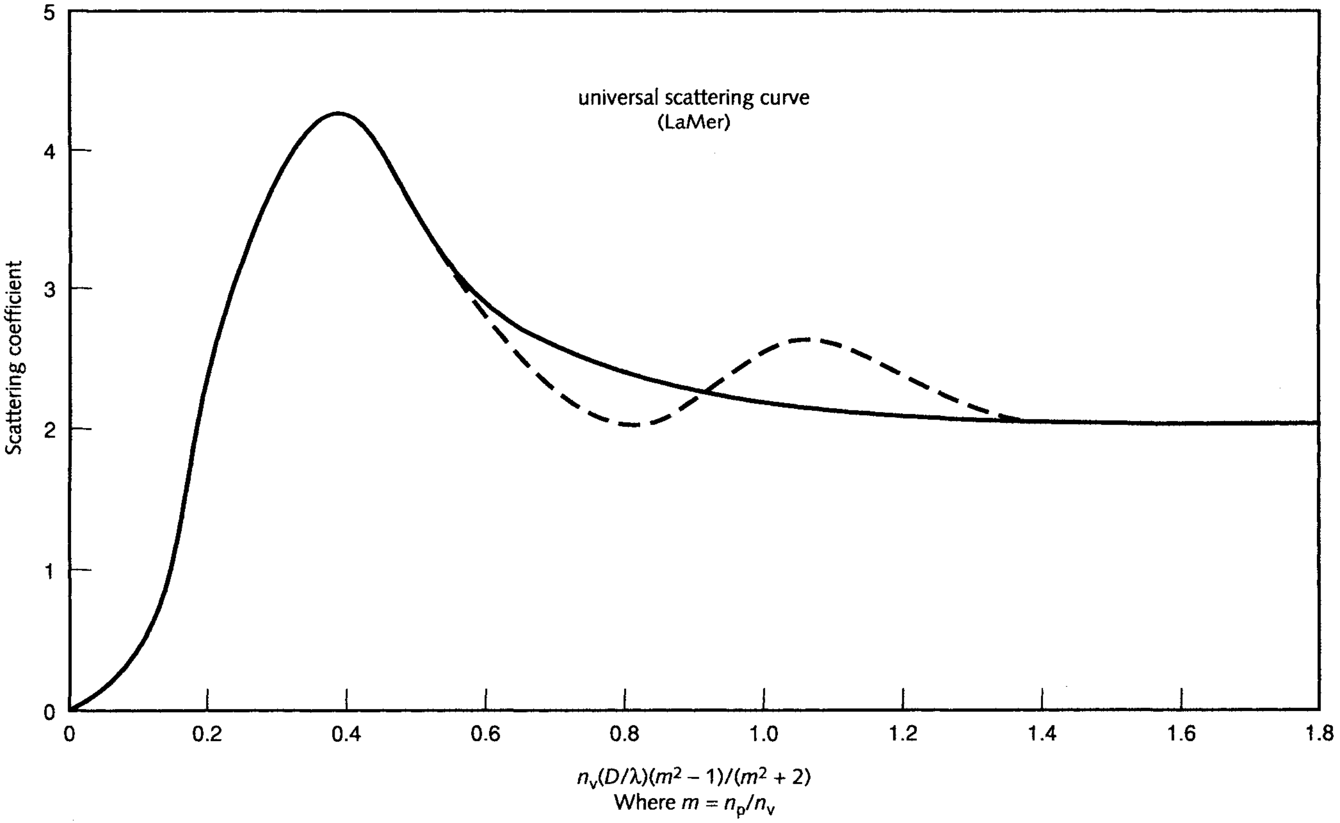

Figure 4.29

Universal scattering curve for nonabsorbing pigments as a function of particle diameter, D (in μm); wavelength, λ (in μm); and the ratio, m, of the refractive indices of the pigment, n_p, and the vehicle, n_v (after LaMer et al. 1945).

in diameter, has more lightening effect—that is, scattering power—than the TiO_2 at ~0.38 µm.

Throughout these remarks concerning the tinting strength of colorants, details of measurement techniques have thus far not been presented. If color-measuring equipment is not available, two samples may be tested visually. Paints of both are prepared identically and then compared visually. To obtain a quantitative measure, a second preparation of the sample in question can be made at a concentration estimated to make the two match. If the first adjustment is not correct so that the color of the second preparation concentration does not visually match the reference standard, the procedure is repeated. To obtain an exact estimate by this trial-and-error procedure is time consuming, but it can be done. Often an absolutely exact, quantitative measure is not necessary; an approximation will suffice.

If color-measuring instruments are available, relative tinting strengths can be calculated with the appropriate equations (eqs. 4.26–4.30). It was stated earlier that the colorant absorption strength is measured at the *absorption maximum.* Using a spectrophotometer, the wavelength of the absorption maximum can readily be determined. To determine the tinting strength, the measured reflectance is converted to K/S and the relative strength calculated with equation 4.29 or 4.30.

But tinting strength can also be measured with a tristimulus colorimeter, provided that the following procedures are followed: (1) If the colorimeter reads directly in terms of R, G, and B (red, green, and blue) filter measurements, the values are used directly as reflectances in the appropriate calculations; no corrections are necessary. (2) If, however, the tristimulus colorimeter measures in terms of CIE tristimulus values, each tristimulus value must be normalized to unity, that is, to R, G, and B reflectance. The tristimulus values obtained with a tristimulus filter colorimeter are generally in terms of illuminant C and the 1931 2° standard observer. Thus, for the reference white, $X = 98.0\%$, $Y = 100.0\%$, and $Z = 118.0\%$. Because the X value contains a portion (20%) of the blue reflectance, it must be corrected to obtain the red reflectance, R, which would be obtained if a filter with only red transmission had been used. The following equation group describes the conversion of the tristimulus values, X, Y, and Z, to a reflectance basis, that is, in terms of R, G, and B filter reflectances to be used in calculating the tinting strength:

$$B = \frac{Z}{1.18} \qquad G = Y \qquad R = \frac{(X/0.98 - 0.2B)}{0.8} \tag{4.31}$$

The values are all expressed as decimal fractions. The R, G, or B value is converted to K/S, and the appropriate equation for tinting strength is used: equation 4.29 for absorption strength and equation 4.30 for scattering strength. To measure the scattering strength of a white pigment from a mixture with black, the G reflectance is used.

In recent years colorimeters have become available that use a dispersive element (such as a prism, grating, or interference wedge) instead of filters. Known as *spectrocolorimeters,* they provide only colorimetric data, such as tristimulus values, and not the spectral data from which the colorimetric data are derived by computation. From such spectrocolorimeters, tristimulus values for other illuminants (such as D65) and for other observers (such as the 1964 10° standard observer) may be obtained. In this case, other equations must be used to normalize the tristimulus values. For example, the following group of equations may be used to calculate the reflectances used in tinting strength calculations for illuminant D65 and the 10° standard observer:

$$B = \frac{Z_{10}}{1.073} \qquad G = Y_{10} \qquad R = \frac{\left(X_{10}/0.9481 - 0.199B\right)}{0.8} \tag{4.32}$$

For calculating relative tinting strengths, the filter (X, Y, or Z; or R, G, or B) to be used for the measurement is selected on the basis of the hue of the colorant being tested. The filter reading is treated as if it were a reflectance value and is converted to an absorption value such as K/S, according to equation 4.28. This technique of using tristimulus filter measurements can be thought of as akin to using an instrument with broadband filters. For blue and green colorants, use the red, R, filter measurement to calculate the relative tinting strength (their absorption maxima are in the red reflectance region); for purple and red colorants, use the green, G, filter measurement (their absorption maxima are in the green region); and for yellow and orange colorants use the blue, B, filter measurement (their absorption maxima are in the violet and blue region). Details of this procedure for calculating relative tinting strengths with tristimulus colorimeters are presented in ASTM Standard D 4838. The method is based on the work of Johnston-Feller and Bailie (1982b). In these publications it is pointed out that the best accuracy and reproducibility are obtained if the samples are made up to have a reflectance of 35% to 45% at the absorption maximum. As the reflectances deviate from this range, either up or down, both visual and instrumental sensitivity decreases.

Also emphasized in these articles is the advantage of using such broadband filter measurements in certain instances, as opposed to using higher-resolution spectrophotometric measurements at a single wavelength. Basically, there are two advantages. The first is the case in which the chroma of one colorant is higher than the chroma of another; corrections can be made by use of the filter measurements made at the region of maximum reflectance, or minimum absorption. If only the region of maximum absorption is used, the presence of a contaminant, such as dirt, cannot be easily detected, and the tinting strength would be too high because of the extraneous absorption of the contaminant. Likewise, when comparing relative tinting strengths of different pigments, the chroma can be as important as the tinting strength. Hence, the correction can be made by subtracting the absorptions at the region of maximum reflectance. The technique for making such corrections is described in the two previously cited publications.

The second advantage is in comparing colorants that have slightly different specific absorption maxima—that is, different spectrophotometric curves; the integrated reflectances over a broad range of wavelengths in the region of absorption are often more suitable than the reflectance measured at a single wavelength. The latter situation occurs when colorants of similar hue but different chemical composition (and, as a result, slightly different spectral curves) are compared. Relative tinting strength is generally considered when colorants of similar chemical composition are compared. However, there may be times when the relative value of two different chemical types—widely different in price and strength—may be of interest. An example is the comparison of the relative values of red-shade indanthrone blue (PB 64) and ultramarine blue (PB 29), both reddish blues. (PB 29 and PB 64 are Colour Index names; see appendix C.)

Indanthrone blue has much higher tinting strength than ultramarine blue, but it is also more expensive. The spectral reflectances for two concentrations of each blue mixed with rutile TiO_2 are illustrated in figure 4.30. It can be noted that indanthrone blue has about ten times as

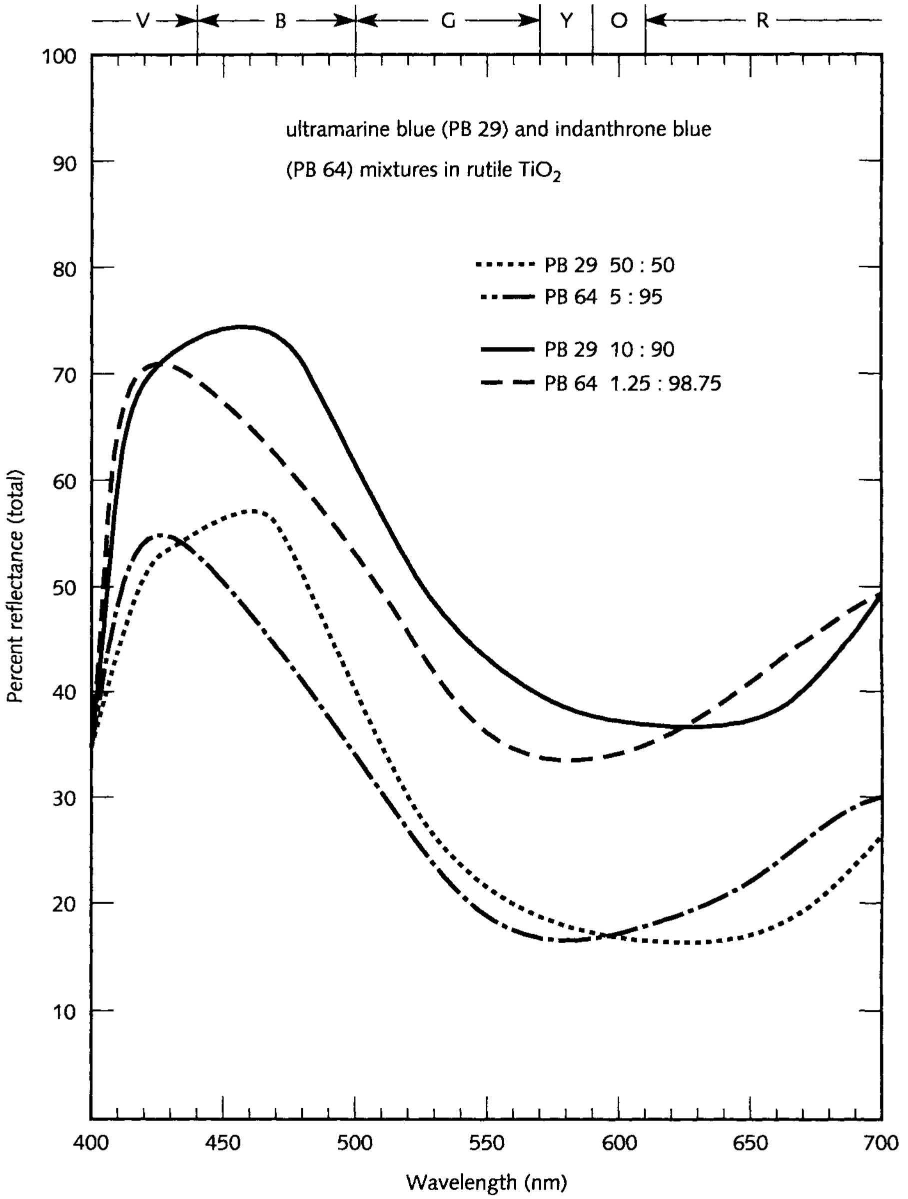

Figure 4.30

Spectral reflectance curves of indanthrone blue (PB 64) and ultramarine blue (PB 29) in mixture with rutile TiO_2. Comparison of the concentrations indicates that the tinting strength of PB 64 is almost ten times that of PB 29.

much tinting strength as ultramarine blue. Careful inspection of the contrast in the curves between the reflectance maximum and the reflectance minimum would lead one to expect that the ultramarine blue is higher in chroma (purity)—not important if high-chroma blues are not required. The spectral curve shapes, however, are quite different, so it is difficult to compare the relative tinting strengths of the two blues. In table 4.4 the CIE descriptions of the two blues are summarized for the 1931 standard observer and illuminant C.

The spectrophotometric data and the tristimulus data allow us to compare the two methods for calculating tinting strength: (1) use of spectral reflectance at the absorption maximum (reflectance minimum), and (2) the tristimulus values from the red broadband filter, calculated in this case from the X tristimulus value (or as measured directly on a tristimulus colorimeter measuring R, G, B values). Using spectrophotometric reflectance data, the analyst would select the wavelength of maximum absorption for each of the blues: 630 nm for the ultramarine and 580 nm for the indanthrone blue. He would compare the two for each of the pairs closest in reflectance, using equation 4.28 for spectral reflectance data to calculate unit K/S; equation 4.31 for calculating R from X; and equation 4.28 again, assuming the R filter value is reflectance. The *relative* tinting strengths are then calculated with equation 4.29. Table 4.5 summarizes the results of these calculations. Ultramarine blue (PB 29) is used as the standard for these calculations. The overall average tinting strength is 9.45 ± 0.5% for the two methods and two concentrations. As can be seen from these data, the agreement between the two methods of determining tinting strength is excellent, particularly considering the significant differences in the spectral reflectance curve shapes of the two blues.

Returning now to the original question—which blue represents the better value? From a recent price list (Kremer Pigments, Inc.

Table 4.4

CIE notation for two blues: PB 29, ultramarine blue, and PB 64, indanthrone blue (illuminant C, 1931 standard observer).

Sample	Conc. %	X	Y	Z	x	y	Dom. λ	%P
PB 29 Ultramarine blue	50	25.26	24.16	63.82	0.2231	0.2134	474.5	44
PB 64 Indanthrone blue	5	24.37	21.93	56.65	0.2367	0.2130	470.0	40
PB 29 Ultramarine blue	10	44.98	45.25	85.38	0.2561	0.2577	476.0	26.5
PB 64 Indanthrone blue	1.25	41.58	39.88	77.22	0.2620	0.2513	471.0	25.6

Table 4.5

Examples of spectrophotometric and tristimulus methods for calculating relative absorption tinting strength (TS) by comparing PB 29, ultramarine blue, and PB 64, indanthrone blue.

Concentration of PB 29 (%) Standard	Concentration of PB 64 (%)	Calculation method PB 29	PB 64	TS PB 64/PB 29	Average TS
50	5	630 nm	580 nm	9.6	—
10	1.25	630 nm	580 nm	9.2	9.4
50	5	X to R filter		9.7	—
10	1.25	X to R filter		9.3	9.5

Plate 1

Can you tell by looking at the exposed samples in the lighter column (right) how much alizarin red pigment was lost from the corresponding samples in the darker column (left)? We humans cannot tell by visual examination the amount of pigment lost by fading when comparing the faded samples to the original unexposed samples. However, the relative amount lost can be calculated based on measurements of the reflectances of the samples. The answer to the question above is that the samples in the faded column on the right have all lost 30% of the alizarin initially present, even though the lightest and the darkest samples in the faded column appear to show less difference with their corresponding samples in the unexposed column than do the other sample pairs (from Johnston-Feller 1986, with permission).

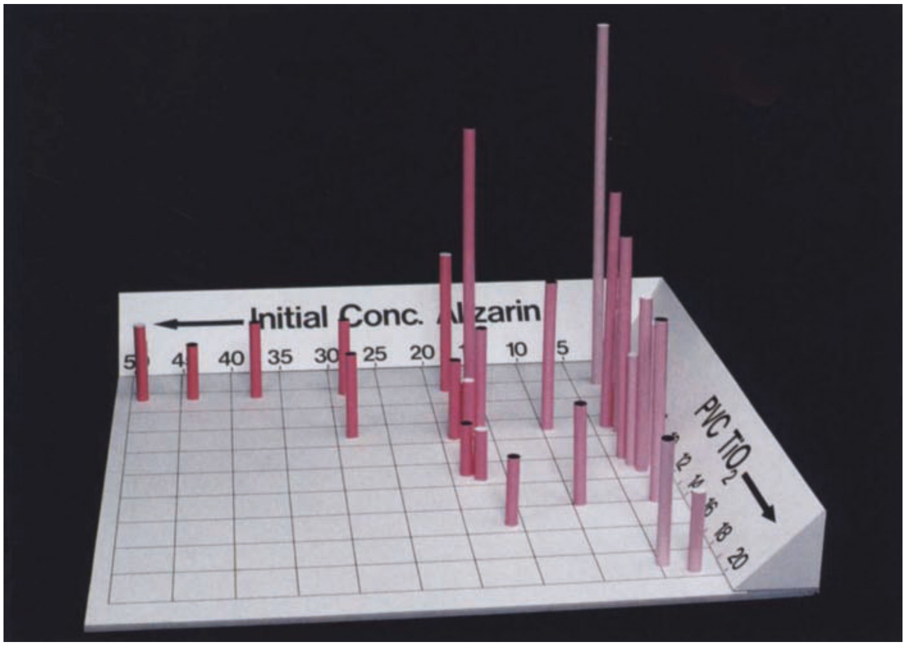

Plate 2

This photograph shows a three-dimensional graph constructed to illustrate the depth of fading in a series of paint films pigmented with rutile TiO_2 and alizarin and exposed in a Fade-Ometer. The two variables illustrated are the concentration of the alizarin relative to the total pigment concentration (the scale on the *x* axis, increasing to the left from the origin) and the pigment volume concentration (PVC) of the TiO_2 (the scale on the *y* axis, increasing toward the right and front). The dowels are located according to their initial pigment concentration. The height of the dowels corresponds to the depth of fading that was measured; the color of the dowels reflects the color of the unexposed samples; and the color on the top of the dowels (white or black) corresponds to the color of the substrate. The precision was poor, but the general tendencies are readily apparent: increasing the concentrations of either pigment decreases the depth of the fading. This is what is expected. The depths of fading were measured microscopically by several observers who examined cross sections of exposed samples imbedded in beeswax, using a calibrated grid in the eyepiece of the microscope. The observers repeated the task several times. The average is illustrated.

(3a) Unexposed

(3b) 106 hours

(3d) 286 hours

(3e) 393 hours

(3c) 219 hours

(3f) 530 hours

Plates 3a–f

This sequence of images shows a portrait painted on a Mylar sheet; five concentrations of alizarin in glazes were used to model the sleeves. The painting was backed with white and mounted around the drum of a Fade-Ometer in which it was exposed to the light from a xenon lamp for a series of exposure times. The squares to the left of each image illustrate the five different concentrations of glaze used. After the painting had been in the Fade-Ometer for a specified time, it was removed for measurement of the reflectance and for calculation of the concentration of the alizarin remaining in each of the five glazes. At that time, the portrait was also photographed. The resulting photographs are reproduced here with their total exposure time in the Fade-Ometer noted: (a) unexposed painting; (b) 106 h; (c) 219 h; (d) 286 h; (e) 393 h; and (f) 530 h, which is roughly equivalent to a hundred years on a museum wall well illuminated by diffuse daylight.

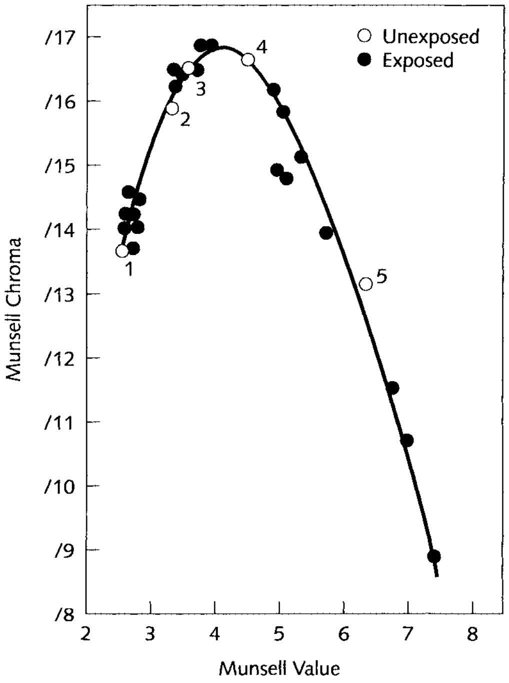

Plate 3g

This graph shows the changes in Munsell Chroma and Munsell Value of the alizarin pigment in the painting's sleeves due to fading. The Value increased on all samples as the alizarin faded. The initially darker (low Munsell Value) glazes, numbered 1, 2, and 3 on the graph, increased in Chroma as fading proceeded; the maximum Chroma was reached by the middle concentration, glaze 3. Glazes 4 and 5, the lightest glazes, decreased in Chroma as the color faded. It is this last type of color change that we customarily recognize as fading. That darker colors actually increase in Chroma, or saturation, thus appearing to get brighter as they get lighter, is often not understood to be the result of fading. All chromatic colorants do this when applied in high concentration at incomplete hiding over a reflecting substrate.

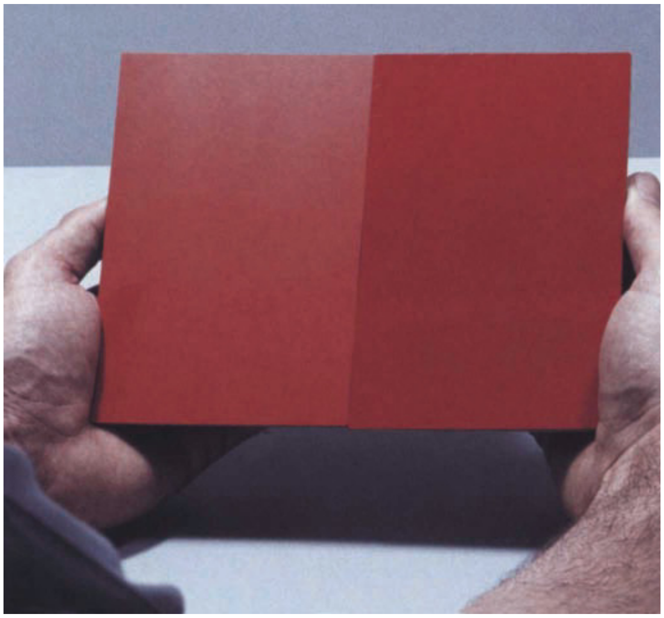

Plate 4

Shown are two glass-fiber gel coats of identical pigment composition but with different surface structures. The panel on the right has a high-gloss surface; the one on the left a matte surface. The surface reflection from the glossy panel is sharply reflected at an angle away from the camera's view. The reflection from the matte surface travels at all angles and is therefore included in the camera's view, lightening the red color as though white pigment had been added to the red pigment. When the two panels are measured in such a manner that the surface reflection is included, the measurements are nearly identical. The spectral curves of these two panels made with surface reflection excluded are shown in figure 6.5. The glossy sample reflects about 1% of the light over half of the visible spectrum, while the matte panel reflects about 5%. This reflected light—violet, blue, green, and yellow—is mixed with the red light reflected by the red pigment particles, and it lightens the red color. That both panels really are painted with the same pigment composition is illustrated when the total reflectance is measured—that is, the surface reflection plus the red pigment reflection—as shown in figure 6.7.

Plates 5a, b

Photographs of the Aach print made with a fluorescent orange pigment, as described in chapter 6. The photo on the left (a) was taken in daylight; the one on the right (b) under BLB black light. When the photographs were taken, the print, framed under glass, had been hanging on the wall of the author's office for seventeen years, during which time it was illuminated by diffuse daylight and by ceiling fluorescent luminaires. The fluorescence in the print has remained strong, evidence that the artist's special formulation of the fluorescent pigment apparently did prolong its effectiveness. Normally the pigment's light stability is found to be poor, and its use by artists has been questioned by scientists for this reason.

(5a)

(5b)

1992), red-shade indanthrone blue is about 8.2 times as expensive as ultramarine blue ($25.35 per kilogram for the ultramarine and $206.80 for the indanthrone blue). However, indanthrone blue is 9.4 times higher in tinting strength, as shown in table 4.5. So the expensive organic pigment is actually a little less expensive in terms of tinting strength. Other characteristics may, however, dictate the choice between the two. The ultramarine blue is higher in chroma (purity), that is, it is cleaner in mixture with white (see table 4.4). However, ultramarine blue has poorer hiding power, particularly in dark shades, than the indanthrone blue when mixed with white to make similar dark blues.

These comments are not meant to promote one pigment over the other but are given to illustrate the concepts and calculations presented. In this particular example, there is no clear decision between the two on the basis of price alone.

Confusion concerning the identification of colorants used in objects made in the past can result from the practice by some manufacturers of toning their colorants with other colorants of different chemical type to adjust them to a standard. For example, a chrome yellow might be toned at one time with a little Hansa yellow and at another with a bit of benzidine yellow, to adjust the hue and absorption strength. Fortunately, this practice is much less common today. One must remember why this practice came about. It is virtually impossible to manufacture pigments each time with identical optical, solubility, and dispersibility characteristics. Prior to the 1960s, the practice of toning with other colorants was not uncommon. Today, however, most modern manufacturers can precisely select and blend different batches to meet a standard. Computer techniques make this practical.

With the sensitive analytical technique of solution spectrophotometry (Saltzman and Keay 1967), even very small amounts of organic colorants may be identified. The compositions of watercolors labeled "indigo," reported by Johnston and Feller (1963), were checked not only by reflectance curve shape but also by solution spectrophotometry. Reflectance curve shape alone could not have identified the complex mixture found in the sample that produced curve 3 of figure 4.31, which is taken from the Johnston and Feller article. When solution techniques were used, phthalo blue, phthalo green, and pyrazolone red were found in sample 3, in addition to ultramarine blue and black, which were obvious from the reflectance curve. The three organic pigments found by solution spectrophotometry were present in small amounts as determined by the subsequent use of differential spectral curve analysis. Who added these? Did the pigment manufacturer tone the ultramarine blue with a little pyrazolone red? Or were all of these mixed together by the artists' tube watercolor manufacturer? If one found such a mixture on a work of art, how could one know where all these pigments came from? Perhaps the artist mixed all of them? (If the brushes were not cleaned well, he might have.) One must systematically look for clues in many other areas of each different color on the object. One could spot phthalo blue and phthalo green, as well as ultramarine blue, in various areas of a painting by their reflectance curves; pyrazolone red also has characteristic double

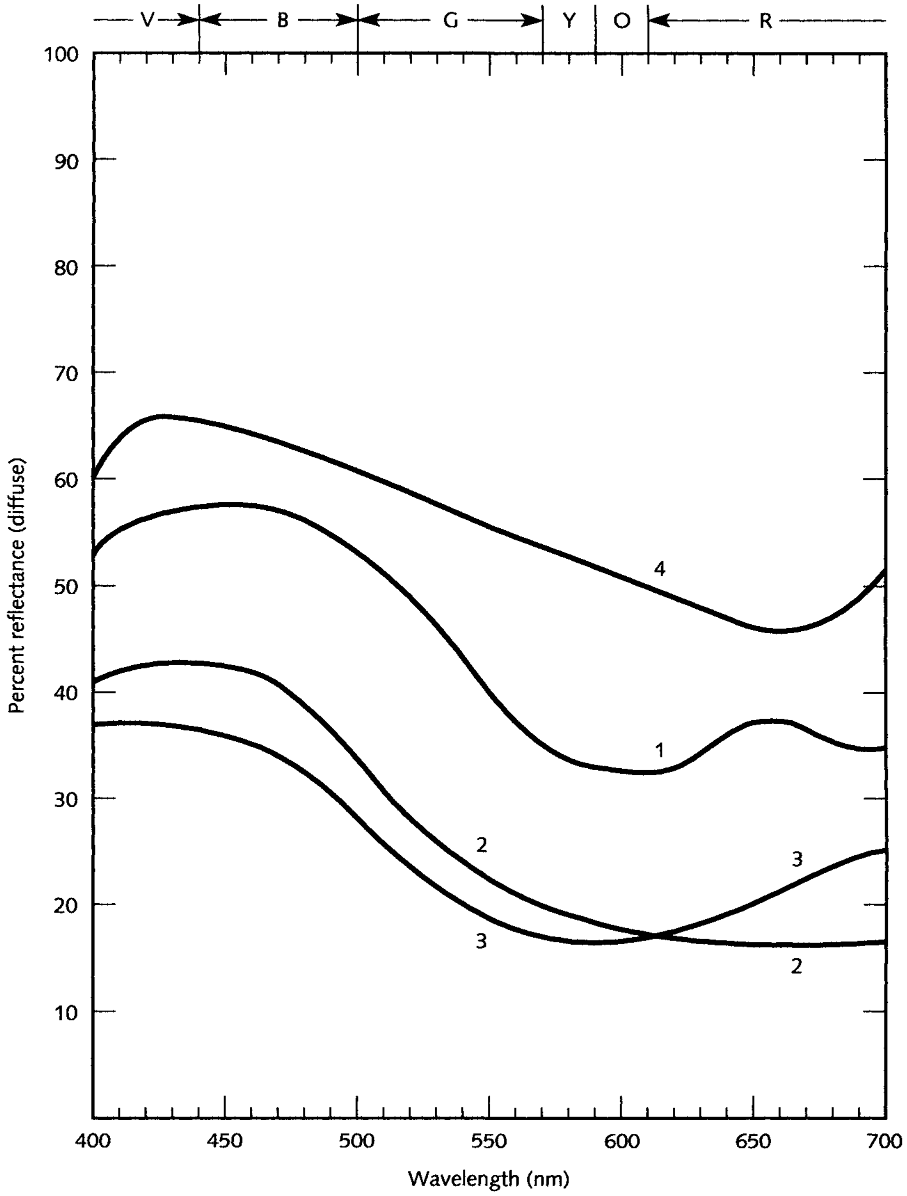

Figure 4.31

Spectral reflectance curves of four tubes of watercolors, all labeled "indigo." Only curve 4 is the real indigo. Curve 1 is a mixture of phthalocyanine blue and black; curve 2 is iron blue, ultramarine blue, and black; and curve 3 is ultramarine blue, phthalocyanine blue, phthalocyanine green, pyrazolone red, and black (after Johnston and Feller 1963).

absorption maxima. (See chap. 8 for a description of a systematic procedure for approaching this problem.)

One last word about tinting strength. If one were comparing two artists' colors labeled "indigo" for relative tinting strength, and if one of them were made with phthalo blue and black and the other with real indigo, the phthalo blue would, if not diluted to the same strength as indigo, be the stronger. But if one indeed wanted to use genuine indigo, analysis is advisable. Many of the major art materials manufacturers are honest today in their labeling, but the practice is not universal, and it certainly was not in the past. Even if an artist has left a record of the names and brands of colorants used in a particular work of art, the specific pigments involved may prove on identification to be quite different.

In summary, the relative tinting strengths of colorants of similar hue may be determined by the techniques outlined above. Nonetheless, tinting strength may not be the only characteristic desired.

Comments on Colorant Calculations and Identifications

Included in this section are discussions of the following: (1) some aspects of the use of the Kubelka–Munk theory for colorant concentration calculations and colorant identification; (2) the use of *reflection density*, which is a measure of reflectance used primarily in the printing industry; and (3) special single-number color scales related to both reflecting and transmitting materials.

Quantitative limitations in the use of the Kubelka–Munk equation

Many factors affect the precision achieved by use of the Kubelka–Munk equation for calculating colorant concentrations. In general these factors can be placed into one of two categories: limitations of the equation itself, and imprecision in the preparation of the colored materials.

Three constrictions inherent in the equation have been alluded to in the previous discussions: (1) The relationship of the absorption coefficient, K, and the scattering coefficient, S, to the reflectance, R, applies only to a single wavelength. (2) No account is taken of the reflectance at the interface between materials, such as air and the surface. (3) The assumption is made that the scattering is isotropic. Not specifically mentioned were the assumptions that the incident light as well as the reflected light are both diffuse; that the pigment particles are randomly oriented; and that they are uniformly dispersed within the medium. In the real world, such idealizations are difficult to realize. Attempts have been made to devise more complex equations that more nearly describe the real-world situation. See, for example, papers by Orchard (1968), Atkins and Billmeyer (1968), and Richards (1970).

The simple relationship described by the Kubelka–Munk equation is extremely useful as a guide for measuring the variations in color encountered in the preparation of colored products. It is extremely difficult to prepare colored products so that each preparation of a certain formulation is identical, exhibiting no visual color difference from the standard. For example, small errors in weighing the colorants in a formulation mixture can result in detectable color differences (see Billmeyer and Phillips [1974] and Stanziola [1980]). Thus, balances used for weighing each colorant must be appropriately accurate for the amount specified. Otherwise, the prepared mixture may not correctly represent the desired formulation.

Johnston (1969) listed twelve areas in paint mixture preparation where problems of poor practice may result in inadequate color control. In addition to weighing errors, some of the sources of variation listed include (a) variations in colorants from batch to batch; (b) variations in behavior of colorants when used in different media and on various substrates; (c) variations in measurements; (d) variations in sample preparation; and (e) use of nonrepresentative samples. One of the least recognized sources of poor color control involves the surface characteristics of the samples. Even slight differences in surface reflection, whether from a glossy surface or a matte (scattering) surface, can affect the perceived color and can be difficult to identify.

In chapter 6 the importance of surface reflection characteristics is discussed at greater length.

In an experimental study of the reproducibility of making a very high quality paint, Johnston (1963) pointed out the care with which measurements and visual evaluations must be made so that the closeness of the sample color match to the standard could be ascertained with a high level of confidence.

In view of these difficulties, the fact that use of the Kubelka–Munk equation for calculating colorant concentrations seldom gives perfect results is not particularly critical in the practical world.

In the case of paints, this technique also allows for small differences in the behavior of colorants in different vehicle types to be taken into account: a paint company may sell fifty different paints, but only a few basic calibrations for the major types need to be made. Adjustments for paints formulated in similar types of vehicles can be calculated from a single set of calibrations by use of predetermined behavior characteristics based on carefully selected mixtures for two reasons: (1) A deviation of the preparation from the calculated amounts, *if calculated consistently,* becomes less significant on the second preparation; for example, a 10% error on the first preparation becomes an error of 10% of 10%—or 1%—on the second. (2) A difference in tinting strength ascertained on the first preparation can be allowed for on the second. For precise work, however, colorant calibrations prepared over a range of concentrations are desirable.

Another admonition given by Johnston (1969) is that, when possible, flexibility should be provided when a calculation is made to match a desired color—that is, there should be three degrees of freedom, one for each direction in color space: lightness–darkness, redness–greenness, and yellowness–blueness. In the case of pigments, this requires the incorporation of four pigments. Significant metamerism may be avoided by the judicious incorporation of small amounts of minor tinting colorants to allow for small directional differences (Johnston 1973). In the case of pigmented systems, it is wise to include a little black to allow for dirtiness, and a little yellow to allow for variations in the yellowness of the vehicles. Likewise, in the case of dyes, a little yellow in the formulation—which can be withheld initially and added only if needed—allows for yellowness in the substrates when applied to textiles or paper.

The various curves for different concentrations of colorants shown in appendix A were computed from a single set of absorption and scattering values using two-constant Kubelka–Munk theory, incorporating surface corrections according to equation 4.12b. These calculations were made for the purpose of preparing the illustrations. If one should attempt to calculate the concentrations shown using simple single-constant Kubelka–Munk theory, the results would not exactly reproduce these curves because of the difference in the equations used, but they would be good rough approximations.

Qualitative applications of the Kubelka–Munk relationship

One of the major points of emphasis throughout this monograph has been the identification of individual colorants from their spectrophotometric reflectance curve shapes. With practice one can become very skilled. However, the exact shape of the reflectance curve depends on the concentration at which a colorant is used. The advantage in plotting *K/S* on a log scale for purposes of identification was pointed out in the previous section in the discussion of pigment fading or darkening. When absorption curves are plotted on a logarithmic scale, the shape becomes independent of the colorant concentration. However, plotting absorption requires learning to read curves "upside down" from what they appear to be in the commonly measured reflectance form. This mental inversion may prove a bit difficult. The problem can be alleviated by plotting 1/(*K/S*) on a log scale—for example, plotting 1/(*K/S*) versus wavelength on semilog paper—or by plotting *K/S* on an "inverted" log scale—that is, with negative values increasing up the ordinate and positive numbers increasing downward.

To illustrate what curves look like when plotted in the various ways, curves for samples with five different concentrations of carbazole dioxazine violet in mixture with white (see fig. A.25) were plotted as follows: diffuse reflectance (total reflectances of fig. A.25 minus 4% first-surface reflectance); *K/S;* 1/(*K/S*); log[1/(*K/S*)]; and log(*K/S*) against wavelength. These are illustrated in figures 4.32–4.36, respectively. Curves of the diffuse reflectance (fig. 4.32), of *K/S* (fig. 4.33), and of 1/(*K/S*) (fig. 4.34) all vary in resolution and shape with the concentration of the colorant. Note that the maximum on the *K/S* curve (fig. 4.33) corresponds to the minimum on the reflectance curve but that the maximum on the 1/(*K/S*) curve (fig. 4.34) corresponds to the maximum on the reflectance curve.

The use of a logarithmic scale, as in figure 4.35, illustrates the parallelism between the curves in the key absorption region between 540 nm and about 640 nm. Because log[1/(*K/S*)] was plotted, the maximum corresponds to the maximum of the reflectance curve. On the right side of figure 4.35 are listed values of the inverse function, log(*K/S*), with negative numbers increasing up the ordinate from zero and positive values increasing downward. Figure 4.36 is similar except that values of log(*K/S*) are on the left ordinate, and those of log[1/(*K/S*)] are on the right. Log(*K/S*), with the negative logarithms increasing up the ordinate from zero and positive log(*K/S*) values increasing downward, as illustrated in figure 4.36, is the scale that was plotted using the R-Cam on the General Electric Recording Spectrophotometer (Derby 1952). This was a very useful aid in identifying colorants and their approximate concentrations before the advent of computers.

The curve shapes illustrated in figures 4.35 and 4.36 in the regions below 540 nm are not parallel because of the significant absorption of the rutile TiO_2 in this region, where the carbazole violet has its minimum absorption. Even on the reflectance curve, there is an indication of the carbazole violet absorption when the concentration is very

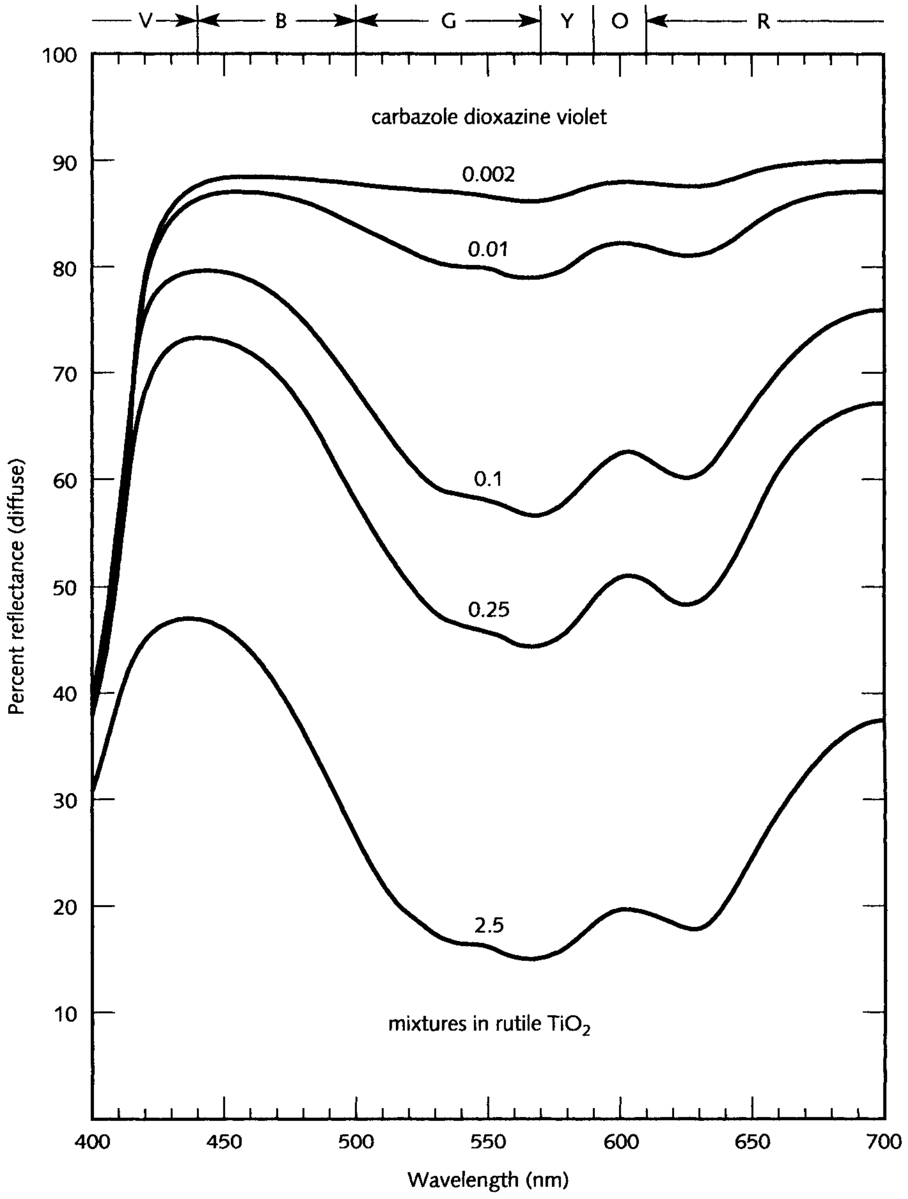

Figure 4.32

Reflectance curves of five concentrations of carbazole dioxazine violet mixed with TiO_2.

low. However, the log(K/S)—or log[1/(K/S)]—curves show greater similarities at most concentrations.

With computers, the transformations among functions of the measured reflectance are relatively simple, and they are particularly useful when combined with curve-plotting capabilities. When curves are generated from digital input, the resolution or visible detail depends not only on the optical design of the instrument (primarily the resolution) but also on the number of data points recorded and plotted. With some modern instruments with excellent resolution, the number of data points is so large—every 2 nm, for example—that a continuous curve is closely approached. The advantage of a continuous curve, that is, of an analog recording, is that it yields a maximum amount of information concerning minute details of curve shape available from the instrument that might be important for identification. For most colored materials measured in the visible region, a 5 nm band-pass and plotting interval are the largest that

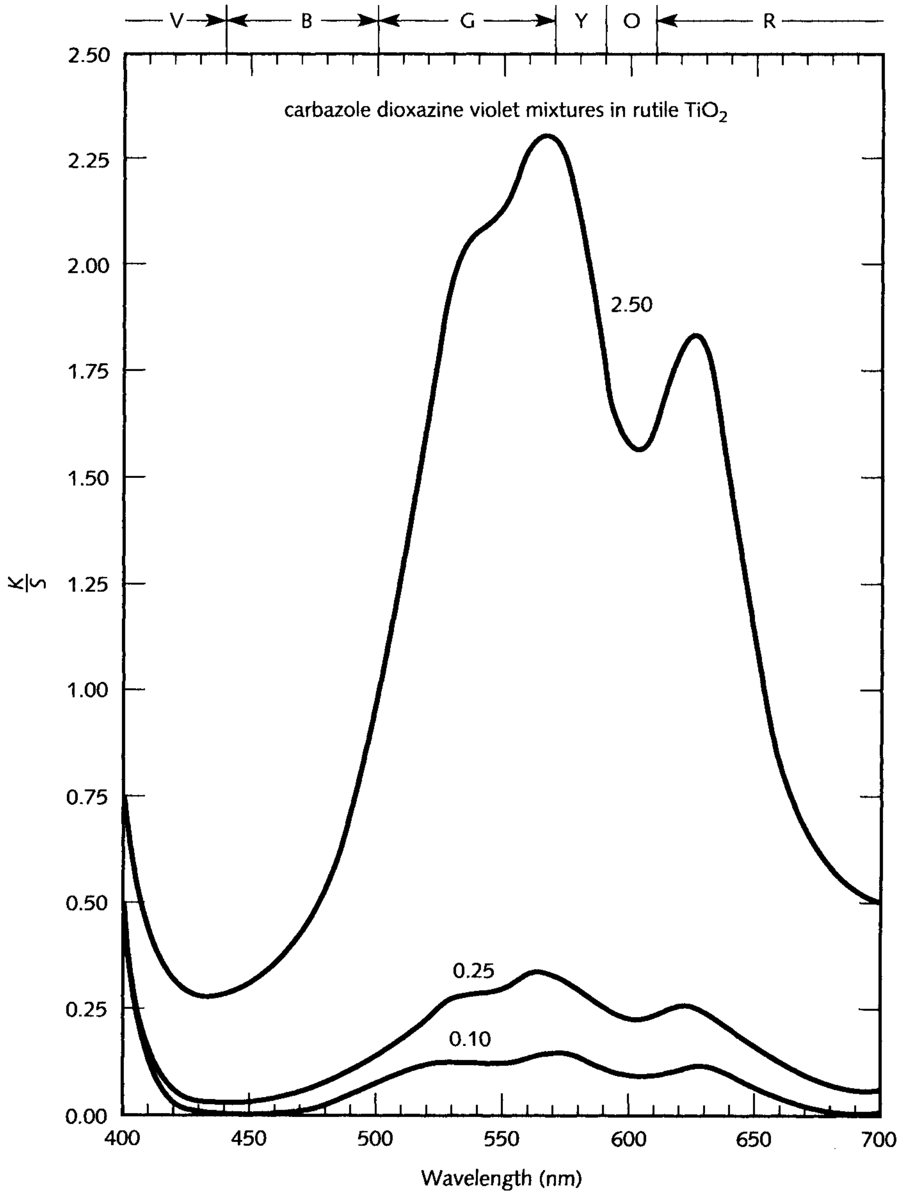

Figure 4.33

Curves of figure 4.32 plotted in terms of *K/S*. Note that the *K/S* maximum corresponds to the reflectance minimum.

would be safe to plot in order to yield reflectance curves that would be unambiguous in their identification. (Transmittance measurements of some transparent materials require higher resolution.)

In summary, transforming the reflectance to log(*K/S*) or log[1/(*K/S*)] can be very helpful in identifying colorants based on measurements and comparisons of their spectral reflectance curve shapes.

Reflection density

Many spectrophotometers designed primarily for measuring the transmittance of nonscattering transparent materials record spectral curves in terms of the optical density as well as in terms of percent transmittance. Optical density, or *absorbance*, is defined as log(1/T) or log(I_0/I), where T is transmittance, I_0 is the intensity of the incident beam, and I is the intensity of the transmitted beam. In transparent samples, the log of this

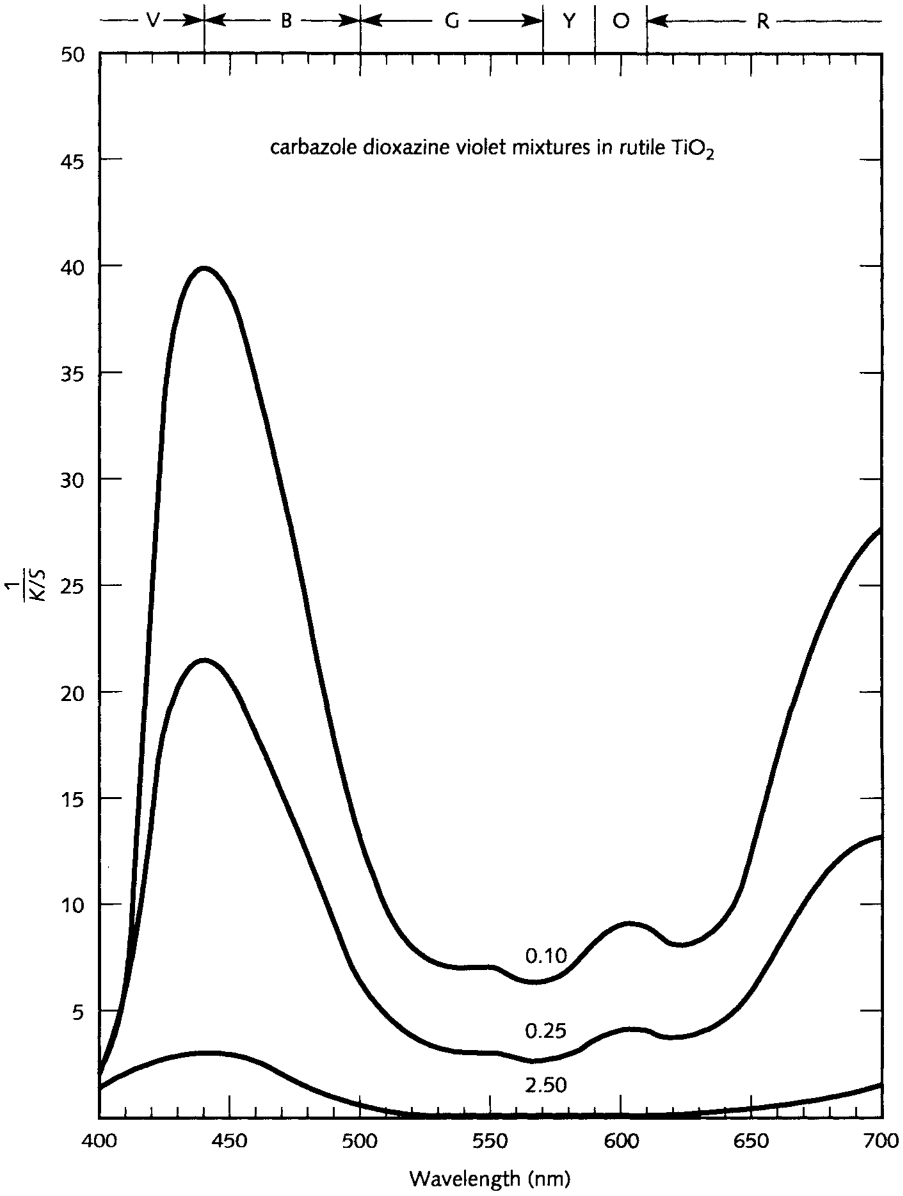

Figure 4.34
Curves of figure 4.32 plotted in terms of $1/(K/S)$. Note that the $1/(K/S)$ maximum corresponds to the reflectance maximum, so that the shapes more closely resemble the shapes of the reflectance curves.

ratio is theoretically proportional to concentration and thickness: $\log(I_0/I) = CXA$. As described in the first section of this chapter, C is the concentration, X is the thickness, and A is the unit absorption coefficient. This relationship is described by the Beer–Bouguer equation. As is pointed out in the next section, when S approaches zero, the absorption coefficient A differs from the Kubelka–Munk absorption coefficient K by a factor of 2—that is, A is half of K.

Many transmission spectrophotometers were also equipped with an attachment for measuring reflectance. If reflectance is plotted versus wavelength, this is fine. However, many workers recorded optical density—in this case, $\log(1/R)$ for reflected light—instead of reflectance itself, mistakenly assuming that optical density was proportional to the concentration of an absorbing material. In certain instances this is true, but it is not generally so for materials with significant scattering.

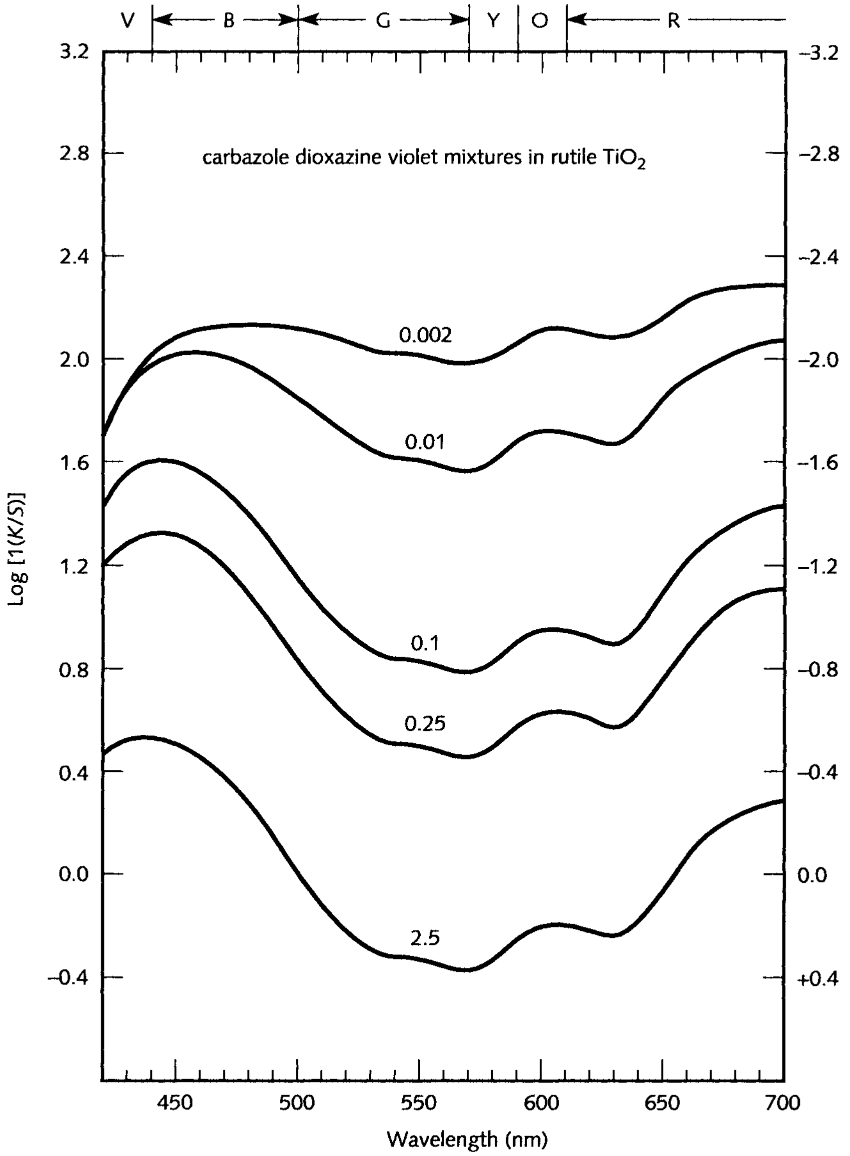

Figure 4.35

Curves of figure 4.34 plotted as log[1/(*K*/*S*)]. On this basis the curves are in general parallel in the characteristic absorption region 530–650 nm. (The short-wavelength differences, as well as the differences at 660–700 nm, are due to the absorption of the rutile TiO$_2$ in the mixture.)

An instrument developed by and widely used in the printing industry for monitoring the color and intensity of the printing inks applied to paper is the densitometer. This instrument measures the optical density of the reflected light—that is, log(1/*R*). In the case of layers of transparent (nonscattering) inks applied over a reflecting substrate, this reflection density is sometimes proportional to the product of the concentration times the thickness, as was pointed out earlier in this chapter in the section on glazes. Thus, the use of log(1/*R*) is valid when all of the scattering comes from the substrate and the ink does not penetrate the substrate—the paper, in the case of the normal printing process. Where the ink penetrates the paper, two layers that both scatter are formed—paper and ink, and paper alone—and the complex Kubelka–Munk equation (eq. 4.15), a hyperbolic equation, must be used.

For opaque materials that scatter as well as absorb, the use of optical density is no longer valid—that is, the value of log(1/*R*) is not proportional to the concentration of the absorbing substance. The

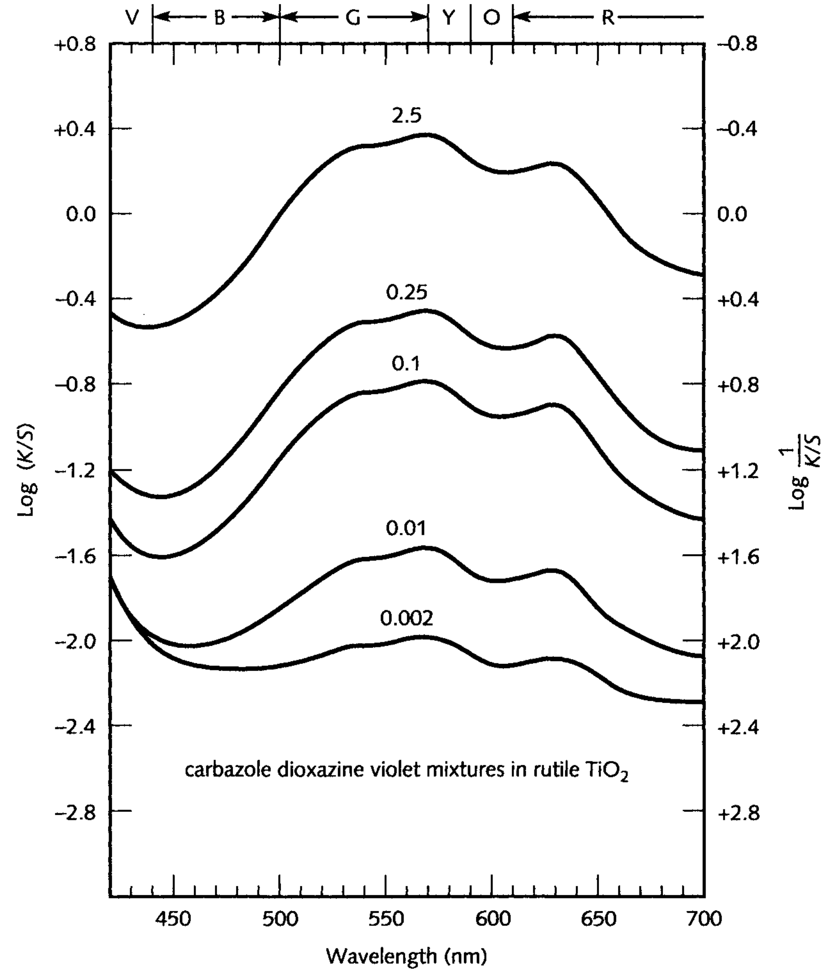

Figure 4.36

Curves of figure 4.33 plotted as log(*K*/*S*), the "upside down" version of figure 4.35.

Kubelka–Munk relationship introduced earlier, $(1 - R)^2/2R = K/S$, should be used. The value of K/S is proportional to the concentration of the absorbing material when scattering is constant, suitably weighted for the individual absorptions and scatterings of each component in the system. Throughout the paper industry, the Kubelka–Munk equations are widely used. For example, Van den Akker (1949) in the United States and Stenius (1951, 1953) in Sweden were two of the early pioneers in studying and developing the Kubelka–Munk equation applications in the paper industry, showing that two constants, one for absorption and one for scattering, had to be used to describe the optical characteristics of paper. If the scattering is a constant for a given type of paper, the scattering coefficient can be set equal to 1 at all wavelengths, and single-constant theory based on K/S can be used as described earlier in this chapter.

To show the relationship between K/S and $\log(1/R)$, the values of each were calculated for a range of reflectances. Figure 4.37 illustrates the relationship between reflectance and K/S, and between reflectance and $\log(1/R)$. Since the curve of $\log(1/R)$ is much flatter than that of K/S, the $\log(1/R)$ relationship, even if it were valid, would be a far less sensitive measure in terms of curve shape than the one based on K/S. This is illustrated in figure 4.38 for 2.5% carbazole dioxazine violet.

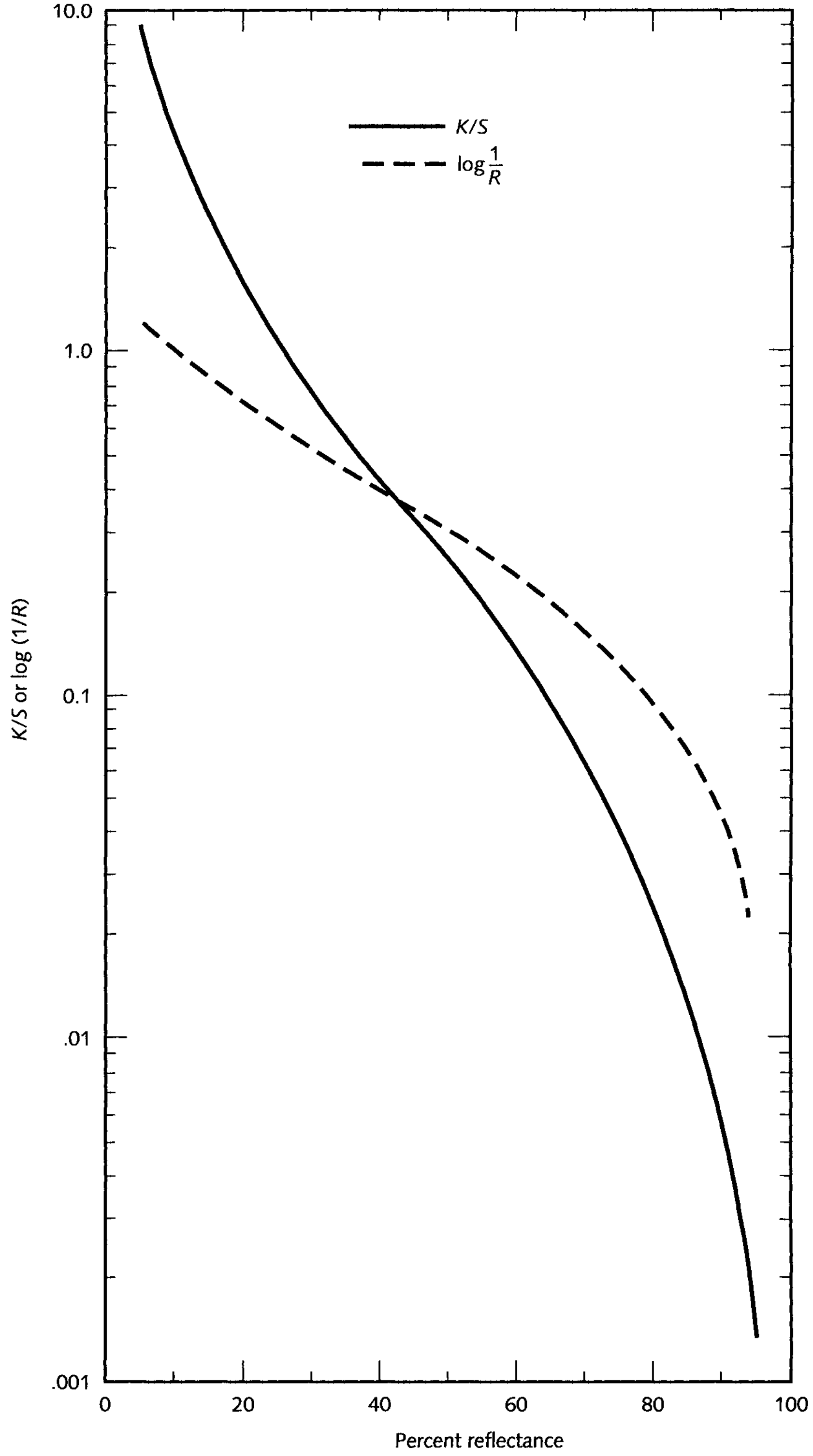

Figure 4.37

Comparison of the reflectance as a function of K/S, which is $(1 - R)^2/2R$, and the reflectance as a function of $\log(1/R)$ [calculated as $\log(I_0/I)$], which is often taken to represent the concentration of scattering materials.

The lack of resolution in the absorption region 520–650 nm limits the amount of information on curve shape in that region.

Talsky and Ristié-Šolajié (1989) describe a technique for using the fourth derivative of the log of $1/R$—$d^4(\log R^{-1})/dl^4$—for distinguishing among the yellow pigments PY 1, PY 3, and PY 97 (see fig. A.20) and the orange PO 1 in artists' paints. They all are Hansa types (acetoacetanilides).

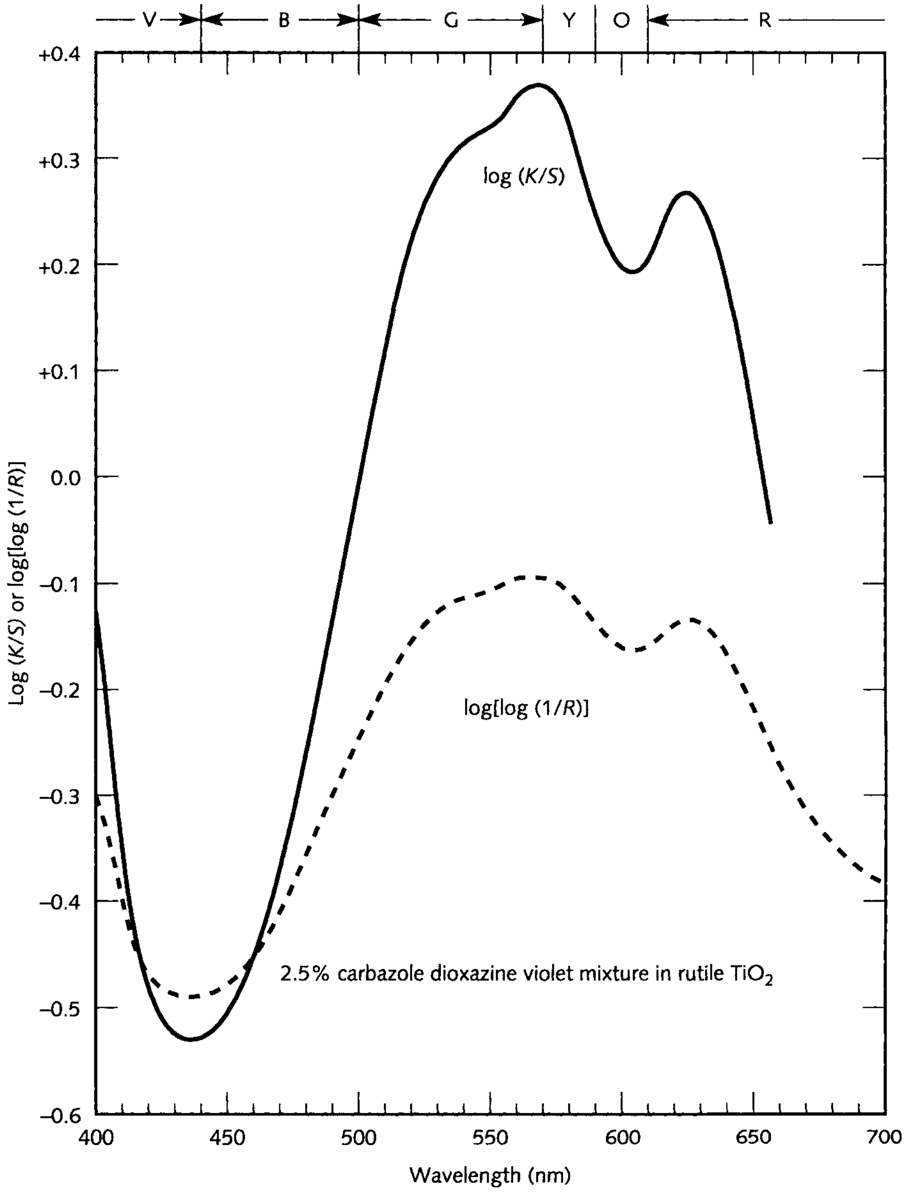

Figure 4.38

Comparison of the data for the sample with 2.5% carbazole dioxazine violet seen in figure 4.32, plotted as log(*K*/*S*) and as log[log(1/*R*)].

As has been stated, in most of the paper industry worldwide, as well as in the paint, plastics, and textile industries, the Kubelka–Munk relationship is used.

Special scales and methods used in industry

Many manufacturing industries—those representing textiles, paints, plastics, and paper, to name a few—have developed special methods for describing the color and appearance of their products and raw materials. Some trade organizations representing these various industries have scientific committees that establish their own standard methods to be used in their industry. Examples of such trade organizations representing raw material manufactures are the American Association of Textile Chemists and Colorists (AATCC) (Celikiz and Kuehni 1983) and the Technical Association of the Pulp and Paper Industries (TAPPI). Other industries establish standard methods in conjunction with the American Society for

Testing and Materials (ASTM), whose extensive methods encompass numerous raw materials and finished products. The society's efforts are overseen by specialized committees. For example, raw materials and products for paint are represented by ASTM Committee D01, for plastics by ASTM Committee D20. Standards for artists' materials are a part of Committee D01 and are under the jurisdiction of Subcommittee D01.57. Other manufacturing organizations utilizing many different products also have their own methods. An example is the Society of Automotive Engineers (SAE). Of the many industry methods, those of the paper industry are of particular interest to conservators of art materials on paper and of library materials.

Applications in the paper industry

Many of the studies made on paper involve the description of the brightness of paper, which is an appearance term, and of the yellowness of paper, either in terms of its yellowness as a visual attribute or as a measure of the concentration of the chromophoric groups causing the yellowness. In the United States, TAPPI brightness is often employed as a specification, as described in TAPPI Method T452 om-92 (1992c) and in ASTM Standard D 985. In this method, brightness is equated with a lack of yellowness; it is measured on a colorimeter in terms of reflectance as measured through a special filter that has its maximum transmittance in the blue spectral region at 457 nm.

It is logical to ask, "Why a special filter? Why not use the *Z* tristimulus filter on a tristimulus colorimeter?" The answer is interesting. Highly reflective whites, particularly those containing TiO_2 pigments, which absorb in the short-wavelength violet region of the spectrum, represent one case in which the CIE 1931 standard observer color-matching functions do not correctly represent visual evaluations of whiteness (Judd and Wyszecki 1975). Jacobsen (1948) had earlier pointed this out. The $\bar{z}$ color-matching function peaks at 445–446 nm. On near-white samples that absorb in the violet, too much of the blue-violet reflectance is eliminated by the *Z* filter of the colorimeter. By measuring with a filter with its maximum transmittance at a slightly longer wavelength, 457 nm, more of the blue-violet light was included in the measurement, which, the paper industry found, agreed better with visual evaluations. Hence the development of the particular filter used to measure TAPPI brightness came about. Judd and Wyszecki (1975) give an interesting history of this problem, which ultimately helped to bring about the establishment in 1964 of the 10° field standard observer functions by the CIE. (The original 2° field of the 1931 color-matching functions for the standard observer are equivalent to observing distant colors; those of the 10° field of the 1964 standard observer represent viewing a material at arm's length.) The 10° standard observer color-matching function for the *Z* primary still peaks at 445 nm. It does give better estimates of yellowness than the 2° standard observer, but it is not as good as the TAPPI 457 nm filter. Moreover, by 1964 the filter characteristics used in the TAPPI brightness instrument were so well established that any change, even if it were for the better, would be disruptive to the industry. Also, making a filter-detector-light-source combination that fits to a specific curve shape for filter colorimeters is not an easy task. So TAPPI brightness remains an industry standard. Although this standard is still widely used, recent work has indicated that TAPPI brightness may not be the best indicator of whiteness of paper (Jordan and O'Neill 1991). This is discussed at greater length in the next section, on single-number color scales for whiteness.

Today many workers with spectrophotometers use the reflectance measured at 460 nm (or 457 nm) in place of the TAPPI filter to produce values that correspond closely to TAPPI brightness. But note that the definition of TAPPI brightness also requires a special illuminating and viewing geometry of 45°/0°, different from the sphere geometry used in many spectrophotometers. In the author's limited experience, the diffuse measurement using sphere geometry (specular excluded) and monochromatic light with a spectrophotometer agreed moderately well with the TAPPI brightness meter. On a difference basis, which is often all that one is interested in, agreement was good.

Although the number is called "brightness," it is actually a measure of yellowness. As a result, TAPPI brightness came to be used to indicate the relative concentrations of chromophoric groups causing yellowness; this is done by converting the reflectance to *K/S,* particularly to indicate the change in yellowness due to exposure to various conditions. In this form, it has been called the Post Color Number, or simply the P.C. No. It is calculated from the TAPPI brightness expressed as a decimal fraction and converted to *K/S* according to TAPPI Method T260 om-91 (1992a), as described in the following equation:

$$P.C.\ No. = 100\left[(K/S)_{\mathrm{t}} - (K/S)_{\mathrm{t_0}}\right] \tag{4.33}$$

where subscript t denotes the reflectance measurement of the exposed sample, and subscript t_0 denotes the reflectance measurement on the unexposed original material. *K/S* is based on the TAPPI brightness or on a spectral reflectance measurement at 457 nm (or 460 nm), both expressed as a decimal fraction. The change in yellowness is sometimes expressed as $100\Delta(K/S)$. If positive, yellowing has occurred; if negative, bleaching of the yellowness has occurred.

Note that the TAPPI brightness is a single-number color scale. As will be discussed in the next section, single-number color scales should be used only when the dominant wavelengths of the materials being compared are similar and there is no metamerism between materials. Note also that the P.C. No. application of the Kubelka–Munk relationship is based on single-constant, simple, colorant-mixture theory as described earlier in this chapter. Therefore, the assumption is made that the scattering coefficient, *S,* is constant. This is generally true when a particular paper is being considered without the addition of any material or treatment that alters the scattering of the paper. Many of the treatments that may alter the scattering of the paper involve physically reinforcing the structure of old paper. Some methods of acid neutralization involve the addition of neutralizing chemicals that result in the formation of metallic oxides, such as ZnO or magnesium oxide, or of calcium carbonate. These will scatter light and lighten the color of both the paper and the absorbing materials in or on the paper. Single-constant theory is, therefore, in this instance inappropriate to describe any changes in the concentration of chromophoric groups, described by the absorption coefficient, K. Thus, the single-constant, simple application of the Kubelka–Munk coefficient, K/S, should not be used in such situations. Berndt (1989) discusses the limitation of single-constant Kubelka–Munk calculations at greater length and provides an overview of the use of the Kubelka–Munk equation in describing the optical characteristics of paper.

Other single-number color scales

Other widely used single-number color scales apply only to near-white reflecting materials or to near-neutral transparent materials. On the subject of near-white reflectance description, two types of scales, in various forms, may be encountered: (1) whiteness indices, and (2) yellowness indices. Either may also be applied to paper products.

Perhaps a whiteness index varies most because of the question of whether whiteness primarily favors blue whiteness or neutral whiteness. In ASTM Standard E 313, a whiteness index was until recently calculated as

$$WI = 4B - 3G \tag{4.34}$$

where B and G are the tristimulus colorimeter filter measurements (B for blue and G for green) or, based on CIE (1931), the tristimulus values ($B = 0.847Z$ and $G = Y$). This index favors blue whites. In this same method, a yellowness index was calculated as

$$YI = 100\ (1 - B/G) \tag{4.35}$$

The plastics industry introduced the following yellowness index, which is different from equation 4.35 (ASTM Standard E 313). This yellowness index was intended to be used for both reflecting samples and for transparent materials.

$$YI = [100(1.28X - 1.06Z)]/Y \tag{4.36}$$

where X, Y, and Z are tristimulus values for the 1931 standard observer and illuminant C. Coefficients for other illuminants and the 10° standard observer are given in ASTM Standard E 313.

In 1986 the CIE completed field tests on an equation for an index of whiteness, W, and an accompanying equation for the tint, T_W (greenish or reddish), of near-white colors. The CIE equations, published the same year, are

$$W = Y + 800(x_0 - x) + 1700(y_0 - y) \tag{4.37}$$

$$T_W = 1000(x_0 - x) - 650(y_0 - y) \tag{4.38}$$

where Y is the Y tristimulus value of the sample, x and y are the chromaticity coordinates of the sample, and x_0 and y_0 are the chromaticity coordinates of the perfect white diffuser, all for illuminant D65 and the 1931 2° standard observer ($x_0 = 0.3127$, $y_0 = 0.3290$). For the 1964 10° standard observer, the equations are unchanged except that the first coefficient in the tint equation is reduced from 1000 to 900 ($x_0 = 0.3138$, $y_0 = 0.3310$). ASTM Standard E 313 recommends the CIE equations shown in equations 4.37 and 4.38.

Note that whiteness is measured as a difference from the coordinates for the perfect white diffuser, for which $W = 100$ (the Y tristimulus value). The higher the value of W, the greater the indicated whiteness. The tint is equal to zero for a yellowish tint. The more positive the value of T_W, the more greenish is the tint; the more negative, the more reddish. The equations are to be used for W greater than 40, and for T_W between +3 and −3.

Since 1986 a number of papers on the CIE indices have appeared, and they have been accepted as standard by many users. A recent publication by Jordan and O'Neill (1991) concerning the visual evaluation of the whiteness of paper indicates that the CIE whiteness index, W, correlates best with the visual evaluation of whiteness. One of the major aspects of their report is that their series of test papers used for visual evaluation included many containing blue fluorescent whitening agents (FWAs).

For a concise summary of a number of whiteness indices that have been proposed, Wyszecki and Stiles (1982) may be consulted.

For transparent liquids, many single-number color scales exist primarily for materials that are near-white or yellowish in color. A review of these many scales was given in Johnston's summary of the work of the Inter-Society Color Council (ISCC) Subcommittee 14 on the use of single-number transparent standards for yellowness (Johnston 1971a). Many liquid comparison standards have been used for products as diverse as water, oils (vegetable and mineral), liquid chemicals, and so on. Most of these are meant to be visual comparison standards, but many of the scales have been converted into color-measurement terms, as described in the report. Such single-number color scales are difficult to use visually; the comparisons involve making matches that may be severely metameric and that involve small differences in hue or dominant wavelength. Nevertheless, they have served as a convenient, inexpensive, and quick means for determining significant characterizations of relative depths of color. That they are still in use is attested to by a recent publication on the use of the Gardner color scale for describing the yellowness of resins and adhesives in the paper industry (Huebner and Monck 1992). (See also ASTM Standards D 156, D 1209, D 1500, and D 1544.)

The results obtained with such reference scales are subject to a significant degree of uncertainty, but the scales do serve a useful role in commerce by at least separating the "best" product color from the "worst."

Chapter 5

Color in Specular (Mirror-Type) Reflection

Color of Metals (Nondielectrics)

In the section on transparent materials in chapter 4, equation 4.3 described the method for calculating the surface or interfacial reflectance—that is, the specular reflection—for dielectric materials on the basis of their refractive indices when the incident light is near normal (perpendicular to the surface). The corresponding equation for nondielectric materials (such as metals) is more complex as shown by the following:

$$\rho = \left[\frac{n(1-jk)-1}{n(1-jk)+1} \right]^2 \qquad \text{at each wavelength}$$

where the quantity $n(1 - jk)$ is the complex refractive index, j is the imaginary constant $\sqrt{-1}$, k is the absorption index, n is the real refractive index, and 1 is the refractive index of a vacuum or, as generally used, of air (Andrews 1960). Again this equation is valid only when the incident light is near normal. When the absorption index, k, is nearly identical at all visible wavelengths, the reflectance does not change significantly with wavelength. But when k changes with wavelength in the visible region, the reflectance also changes with wavelength, and the metal is seen as colored. For metals such as copper, bronze, gold, and so on, k is not constant at all wavelengths in the visible region, so the specular reflection (gloss) is colored.

It is important to remember that the color of metals is due to selective reflection at the air–metal interface. Thus, if a piece of highly polished gold is measured with an instrument that measures only the diffuse reflectance—that is, an instrument that excludes the gloss—the measured reflectance is near zero. Many color-measuring instruments are designed to measure color only on dielectric materials and are inappropriate for use in measuring the color of metals. A detailed discussion of the various types of color-measuring instruments is presented in chapter 9. In summary, instruments using 0°/45° (illumination/viewing angle) geometry, or the reverse, 45°/0° geometry, are inappropriate for measuring the color of metals, as are integrating sphere instruments that have no provision for including the specular reflection. Ideally, for studying the color of metals, an instrument that incorporates the option for excluding or including the specular reflection—that is, for measuring the diffuse reflectance only or the total reflectance—is desirable. This flexibility is particularly helpful in studying the smoothness of the surface or the degree of polish.

If the metal to be measured is not perfectly polished—and few metals are perfect mirrors—some of the light is reflected at the surface at angles other than the specular angle. If the specular reflectance is colored, regardless of the angles, however, this scattered surface reflectance is probably also colored, though lower in chroma. A measure of the total reflectance is required to describe the color. However, a measurement of the nonspecular reflectance provides an indication of the perfection of the surface polish. The ratio of the nonspecular (diffuse) reflectance to the specular reflectance provides an index for the degree of smoothness or polish. The specular reflectance, designated here by S, is calculated from the two types of reflectance measurements: diffuse and total reflectances, abbreviated SCE (specular component of the reflectance excluded) for the diffuse reflectance, and SCI (specular component included) for the total reflectance. (Some color-measurement workers jokingly refer to the two measures as SEX and SIN, respectively.) Thus, the specular reflectance, S, is determined by subtracting the SCE reflectance measurement from the SCI measurement at each wavelength across the visible spectrum. For a perfect mirror, the ratio of the diffuse reflectance, SCE, to the specular reflectance, S, is zero at all wavelengths. The ratio SCE/S is an obvious way to refer to the degree of diffuse reflectance of a metal surface, which is an important aspect of the metal's appearance. The ratio is also a sensitive indicator of change following exposure. One of the first changes that occurs on metals when they are exposed to the elements is an increase in the diffuse reflectance—that is, an increase in the ratio SCE/S. It has been found that this ratio is a more sensitive measure of change than visual evaluations alone.

The color of metal alloys is influenced by the amounts of the various metals present. Some metals affect the hue of the alloy; others affect only the chroma, or color vividness, by introducing a neutral, dilution effect.

Measurements made on a series of bronze samples prepared by W. Thomas Chase (1982) at the Freer Gallery of Art in Washington, D.C., provide an intriguing start toward a study of a possible characterization of the composition of bronzes on the basis of their color. Samples were prepared that contained varying amounts of copper, tin, and lead. Before spectrophotometric measurements were made, the samples were freshly polished. A Color-Eye Model 1500 was used for the reflectance measurements at 20 nm intervals. The instrument is equipped with an integrating sphere for measuring total reflectance (SCI) or diffuse reflectance (SCE). The specular angle is about 8° from the normal. Both types of measurement were made on ten bronze samples and on the one copper sample. Each measurement requires only a few seconds, which is an important feature of the instrument because freshly polished copper begins to change color almost instantly if not protected immediately from the air (by a lacquer, for example). Bronzes also change color quickly.

Table 5.1 presents a summary of the composition (Cu/Sn/Pb proportions) for the ten bronze samples and one copper sample; the CIE tristimulus values and chromaticity coordinates calculated for illuminant C and the 1931 standard observer from the total reflectance measurements; the Munsell notation calculated from the CIE coordinates; and the ratio of the *Y* tristimulus value measured with the specular reflectance excluded (SCE) to the *Y* value for the specular reflectance (S) alone.

The spectral curves of the total reflectances are presented in figures 5.1 and 5.2. Figure 5.3 shows the CIE chromaticity diagram for the total reflectance data from table 5.1; lines of constant dominant wavelength (corresponding approximately to constant Munsell Hue) and

		Total reflectance					Munsell notation		
Sample	**Cu/Sn/Pb**	***X***	***Y***	***Z***	***x***	***y***	**Hue**	**Value/Chroma**	Y_{SCE}/Y_S[a]
A	100/0/0	56.96	51.57	36.85	0.3918	0.3547	3.01YR	7.55/5.44	0.277
B	90/7/3	69.34	67.73	54.31	0.3623	0.3539	7.73YR	8.47/3.56	0.052
C_1	80/10/10	69.85	69.23	57.18	0.3559	0.3527	8.49YR	8.54/3.15	0.064
C_2	old	65.33	64.49	51.89	0.3595	0.3549	8.47YR	8.30/3.35	0.125
D	77.5/22.5/0	63.15	63.58	55.86	0.3458	0.3482	0.19Y	8.25/2.38	0.028
E	76.5/12.6/10.9	63.19	63.63	56.48	0.3447	0.3471	0.09Y	8.25/2.31	0.094
F	75/15/10	63.35	62.89	51.22	0.3570	0.3544	8.79YR	8.21/3.17	0.077
G	70/27.5/2.5	61.21	62.19	62.86	0.3286	0.3339	0.91Y	8.17/1.22	0.038
H	65/2.5/32.5	66.44	63.52	53.44	0.3623	0.3463	4.59YR	8.24/3.64	0.126
I	(not provided)	63.18	63.99	63.12	0.3320	0.3363	0.28Y	8.27/1.45	0.102
J	90/10/0	65.33	63.88	50.58	0.3633	0.3552	7.82YR	8.20/3.63	0.020

[a] The ratio of the *Y* tristimulus value measured with the specular component of the reflectance excluded (SCE, diffuse reflectance) relative to the *Y* value for the specular component of the reflectance, S (S = SCI–SCE). The ratio indicates how near to a perfect mirror the sample appears to be; if perfectly mirrorlike, the ratio would be zero.

Table 5.1

Composition and colorimetric properties of various bronze alloys (alloys provided by T. Chase).

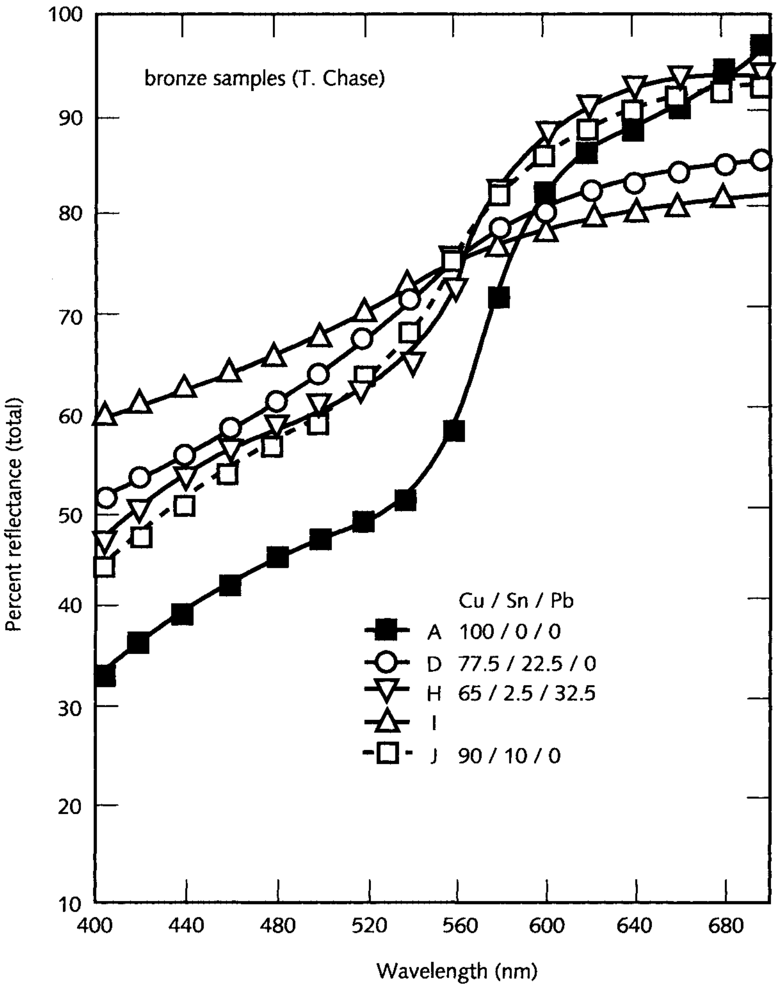

Figure 5.1

Total reflectance curves of bronze samples (data for which are presented in table 5.1) of various compositions as indicated. Note that the curve for pure copper is very different from those for the bronzes. (The composition of sample I was not provided.)

lines of constant excitation purity (corresponding approximately to constant Munsell Chroma) are included for reference.

A brief study of the data indicates that the Munsell Hue is largely dependent on the tin/copper ratio (Sn/Cu) and that the addition of lead (Pb) primarily lowers the Chroma. Figure 5.4 shows a comparison of the calculated Munsell Hue to the tin/copper ratio. No such simple generalization can be made concerning the relationship of the observed Chroma and the lead content, however. The Munsell Value seems to be unaffected by composition for all the bronzes; only pure copper is significantly different, being darker than the bronzes.

As mentioned, the ratio of the diffuse reflectance measurement (SCE) to the specular reflectance measurement (S) is an indicator of the relative amount of smoothness or polish—that is, of surface scattering. From the calculated data presented in the last column of table 5.1, it can be seen that the copper had the highest ratio, indicating that it was least mirrorlike. Indeed, when copper is polished, it immediately begins to change, so that to keep its polish, copper needs to be protected from the atmosphere.

In a program of study concerning the efficacy of clear coatings in protecting copper from loss in gloss and from darkening, it was found that an index of change based on the specular reflectance change

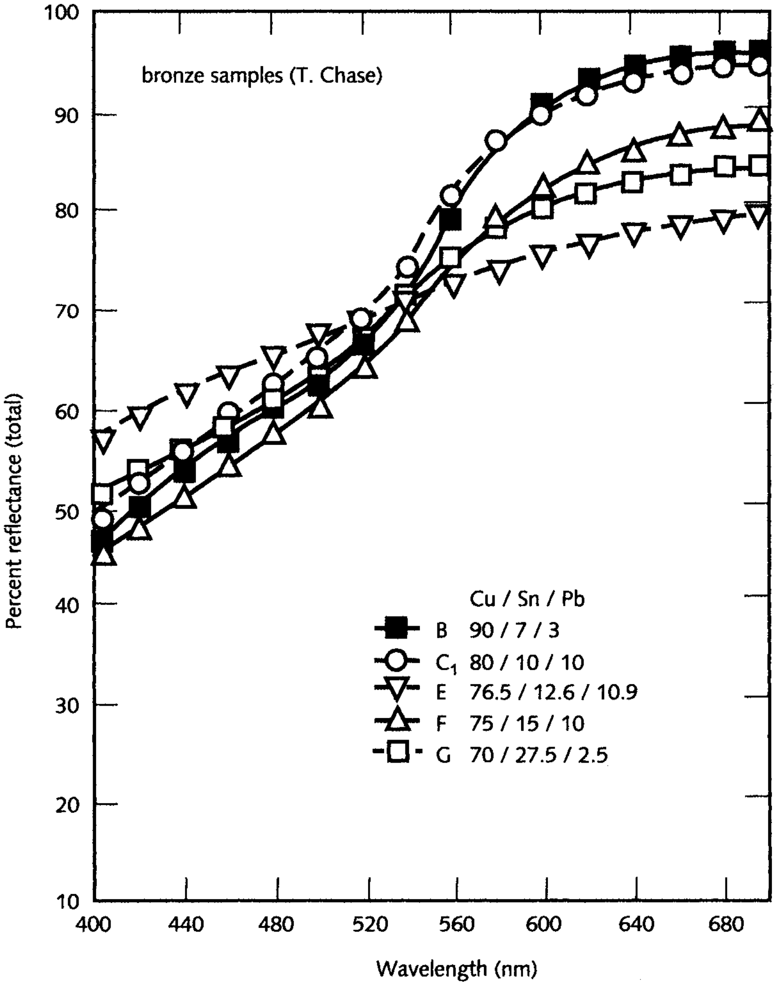

Figure 5.2

Total reflectance curves of bronze samples of various compositions (see fig. 5.1 and table 5.1), as indicated.

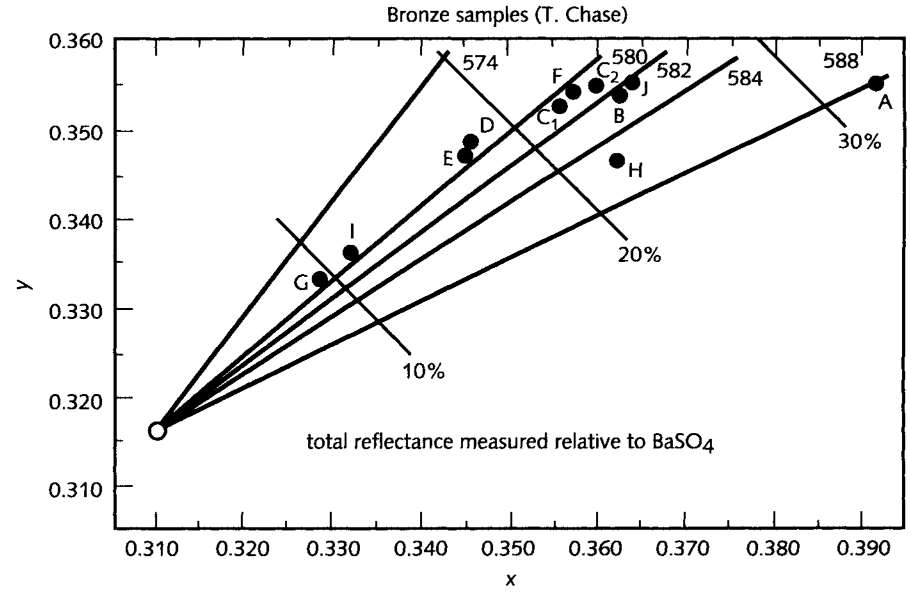

Figure 5.3

Portion of the CIE 1931 chromaticity diagram showing the location of the copper, A, and bronze samples whose curves are shown in figures 5.1 and 5.2. (data taken from table 5.1). The open circle is the illuminant point for illuminant C. Lines radiating out from the illuminant point are lines of constant dominant wavelength for 574, 580, 582, 584, and 588 nm. Lines perpendicular to the dominant wavelength lines are lines of constant 10%, 20%, and 30% purity.

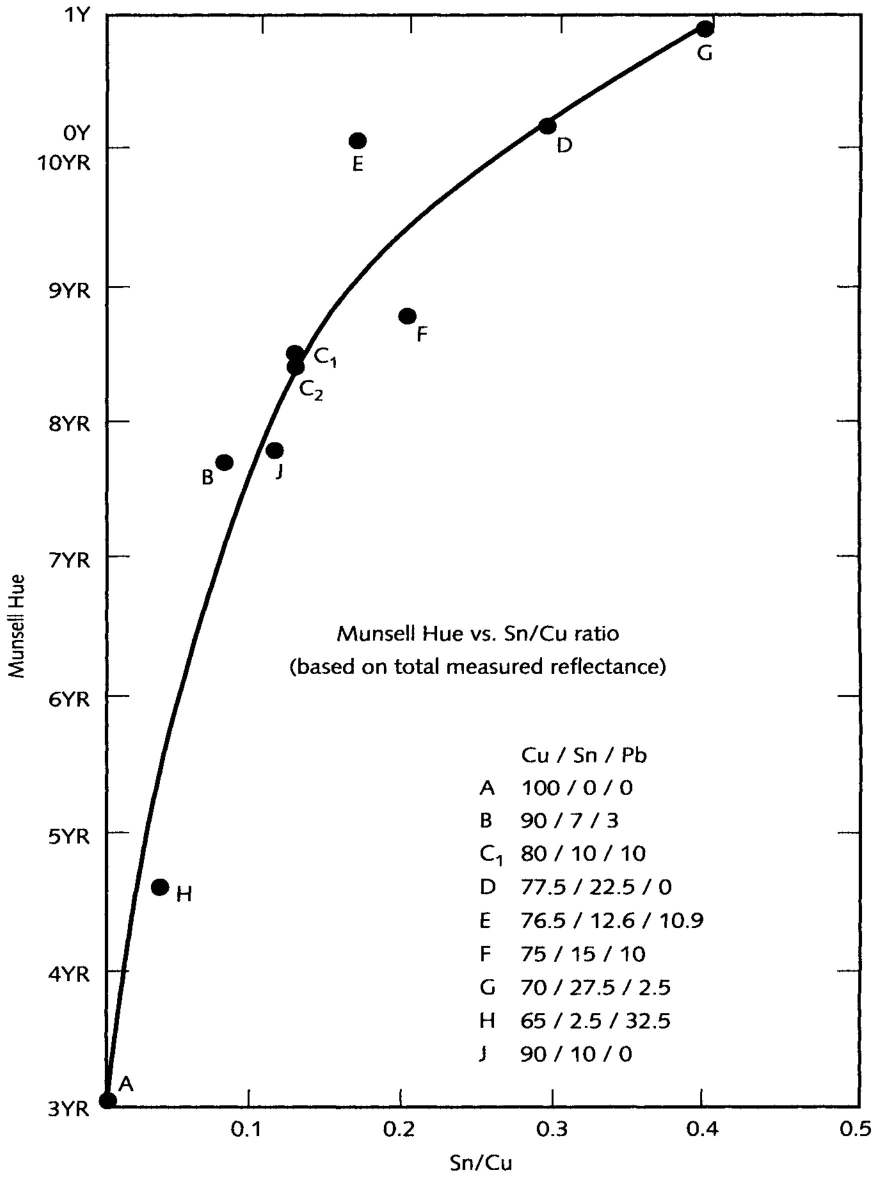

Figure 5.4

Munsell Hue plotted against the tin/copper ratio. With a few exceptions, there appears to be a reasonable correlation between the two.

and on the diffuse reflectance change following exposure provided the most sensitive early prediction of failure of the coating to protect the copper (Spindel 1973).

As with bronze, the color of other metal alloys also changes with composition. The hue of gold, for instance, depends on the relative amounts of other metals, such as copper or silver, in its composition. Even alloys generally considered to be colorless, such as stainless steel and aluminum, may exhibit some color. For a review of methods for appearance evaluation of metals, see ASTM Special Technical Publication 478.

Bronzing

The visual appearance of dielectric (organic) materials can occasionally be metal-like, particularly following exposure. Such materials may exhibit distinct color in the specular reflection, just as metals do. The phenomenon is generally termed "bronzing." Buc and coworkers (1947) characterized two types of bronzing: one being metallic reflection from the air–object interface, which they term "interface bronze," and the other arising from light entering the surface and being reflected specularly from closely adjacent layers, ridges, or particle layers just under the surface; they term this type of specular reflection "interference bronze" (see the next section for a further discussion of interference color). The interference reflection causes the appearance generally called iridescence. Either type of bronzing—though the two have different underlying causes—owes its color appearance to the light reflected at the specular angle. Distinguishing the difference between the two types, whether by visual evaluation or by instrument measurement, involves changing the angles of illumination and viewing: "interface" bronze (as from metals) is the same hue regardless of the incident angle; "interference" bronze (iridescence) changes in hue with a change in the angle of incidence. For complete characterization of interference color, an instrument that measures spectral character using various angles of illuminant incidence and viewing is desirable. Such an instrument is called a goniospectrophotometer, which has only recently become readily available among commercial instruments.

Whatever the origin of the color in the specular reflection, the use of an instrument that measures the color of the specular reflectance is necessary. In a paper by Johnston-Feller and Osmer (1979), two types of instruments were used to characterize the color of bronzed paint films: a goniospectrophotometer and an integrating sphere spectrophotometer capable of measuring both total and diffuse reflectance, from which the color of the specular component could be calculated.

As a demonstration, masstone paint films were pigmented with an azo red, PR 144, at 40% pigment (weight percent in the dry film); a β-phthalocyanine blue, PB 15:3, at 50%; a halogenated copper phthalocyanine green, PG 7, at 45%; and a carbon black, PBk 7, at 38%. At these concentrations all appeared "bronzy." Visual evaluations of the bronzed films resulted in the descriptions given in table 5.2. (The cover of the

March 1979 issue of the *Journal of Coatings Technology* shows Robert Feller's photographs of these bronzed samples.) Covering the bronzed films with a clear, transparent coating decreased the bronzed appearance and, when two such layers were applied, eliminated it completely.

The four samples were measured with the Trilac goniospectrophotometer at two specular angles, 15° and 30° (the geometries are described as –15°/15° and –30°/30°). One of the four, the sample made with β-phthalocyanine blue is illustrated in figure 5.5. The specular reflectance measured on the bronzed sample is purple—reflecting red, blue, and violet wavelengths. The specular reflectance of the same sample, when covered with two coats of clear vehicle, shows primarily the surface reflectance of the colorless vehicle's gloss, reflecting the light source at all wavelengths.

The specular reflectance was also determined from measurements made using the same Trilac spectrophotometer operated in the

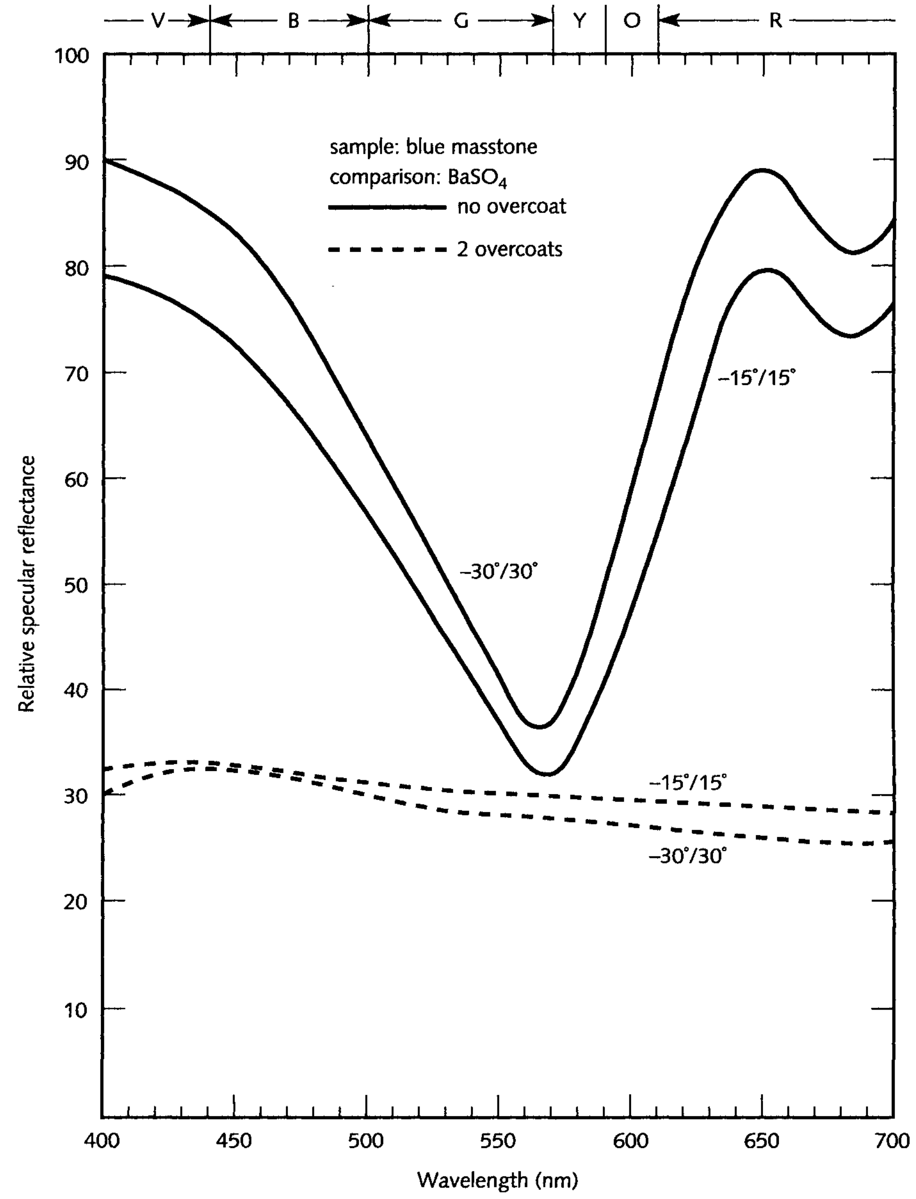

Figure 5.5

Goniospectrophotometric curves of β-phthalocyanine blue masstone paint panels. The upper two curves show the bronzed color (a reddish purple) observed at the specular angles of 15° and 30°. The lower, flat curves were obtained from a panel coated with two layers of clear vehicle, which eliminated the bronzed color on the panel.

sphere mode. The differences in the specular reflectances of the bronzed samples (subscript B) and the coated panels (subscript C) were calculated: $(\mathrm{SCI} - \mathrm{SCE})_B - (\mathrm{SCI} - \mathrm{SCE})_C$. The differences determined at each wavelength are illustrated in figure 5.6. Although the shape of the curve defined by the dots in figure 5.6 and the curve shapes in figure 5.5 are not identical, they are similar in shape, both showing red and blue wavelengths in the specular reflection of the bronzed sample. It can be seen from figure 5.6 that in the green region, complementary to the purple bronzing reflection, the difference of the bronzed sample and the coated sample is negative—that is, the specular reflectance is less on the bronzed sample than on the coated sample. This is frequently encountered when bronzed samples are measured with sphere geometry and the specular reflectance is calculated by difference.

The CIE chromaticity coordinates for the four bronzed samples are plotted in figure 5.7. The open symbols refer to the measurements made with the goniospectrophotometer at the two specular angles illustrated in figure 5.5; the solid black symbols are calculated by the difference method by use of sphere geometry.

Agreement is apparent between the visual evaluation of the bronzed samples (table 5.2) and the estimates of hue (described in fig. 5.7 by the dominant wavelength) and chroma (described in fig. 5.7 by the distance from the illuminant point). The bronze color of phthalo blue is purple and strong; that of azo red is greenish yellow and strong; that of

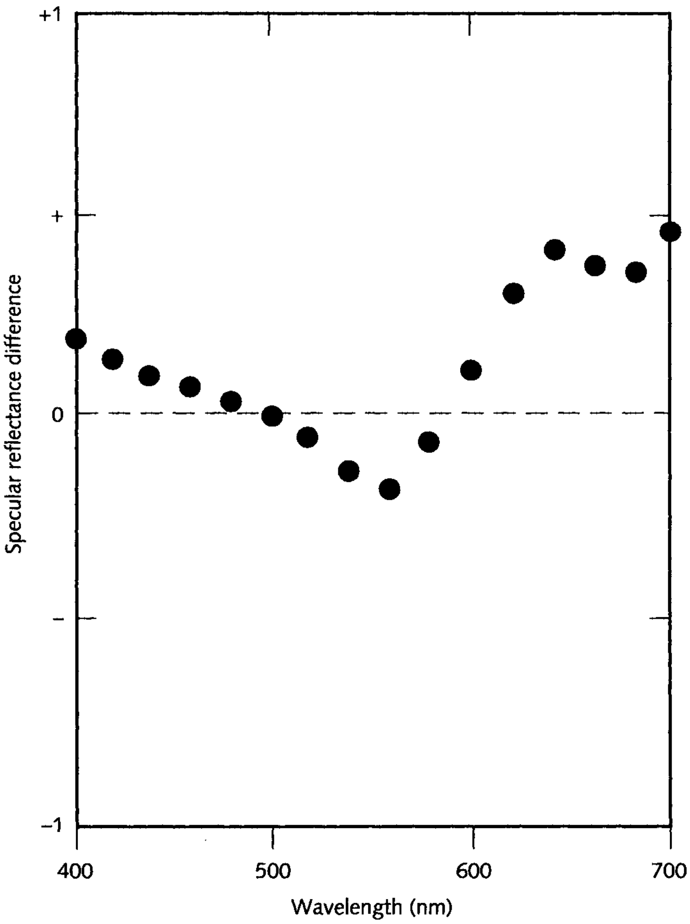

Figure 5.6

Specular reflectance plotted as the difference between the specular reflectances of the bronzed sample of phthalo blue measured with sphere geometry and measurements of the same panel when overcoated with a clear vehicle. The bronze color is reddish purple.

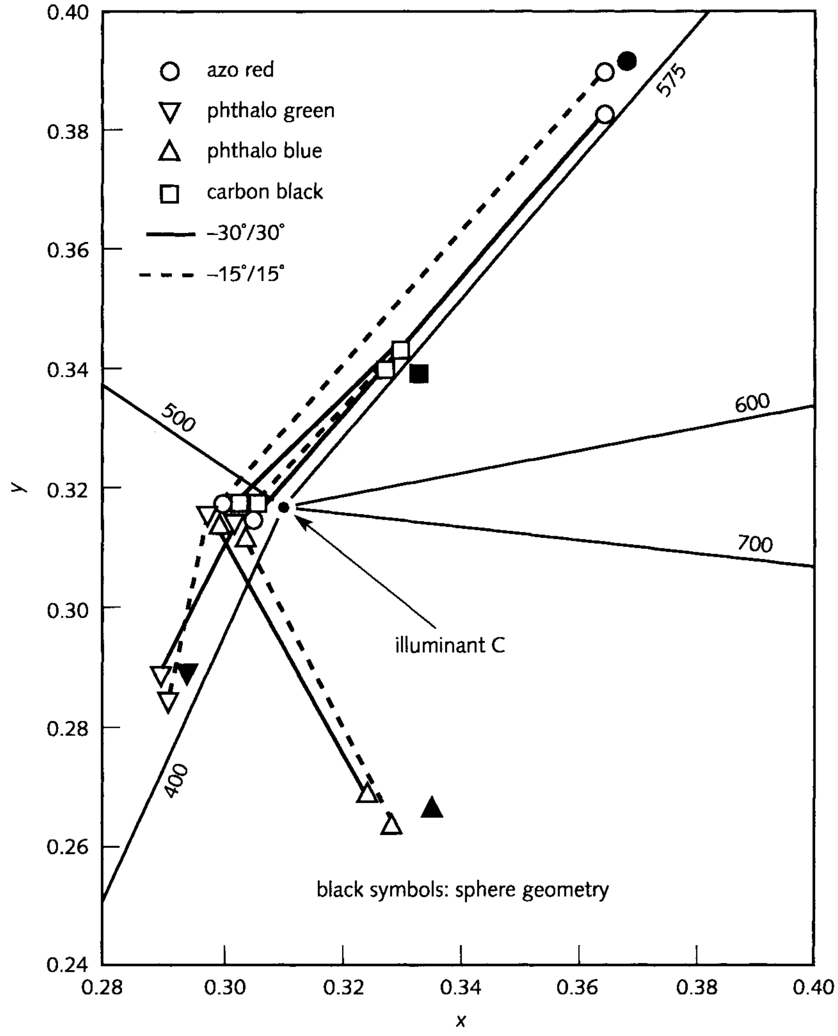

Figure 5.7
Portion of the CIE 1931 chromaticity diagram for illuminant C, showing the loci of the samples measured by the goniospectrophotometric method at two specular angles, 15° and 30° (open symbols). These are connected by lines toward the illuminant point for the samples overcoated with clear vehicle. Solid black symbols are the loci of the points calculated by the difference method from the measurements made with sphere geometry.

Table 5.2
Visual description of bronzed paint samples.

Masstone sample	Visual description of bronzing
Phthalocyanine green	blue, weak
Azo red	yellow, strong
Phthalocyanine blue	purple-red, very strong
Carbon black	yellow, weak

phthalo green is blue-violet and weak; and that of the carbon black is yellow and weak. These properties are consistent between the two types of measurements: goniospectrophotometric measurements and the "sphere difference" calculation of the specular reflectance.

The points plotted near the illuminant point are the variable angle measurements made on the samples with two coats of clear vehicle added. (If the reader is disturbed by the location of these points away from the illuminant point, the explanation is as follows: the variable angle values were measured with a 20% neutral-density filter, with the result that any slight errors have been multiplied by 5; in contrast, in the case of the sphere measurements, the amount of specular light determined was notably small, generally less than 10%.)

It is remarkable that the chromaticity agreement shown in figure 5.7 is so good in both dominant wavelength (hue) and purity (chroma), despite the extreme differences in the magnitude of the measurements. The results serve as an illustration of the sensitivity that can be achieved in measurements of the specular component by taking the difference between the total reflectance and the diffuse reflectance using an integrating-sphere instrument. That the bronze colors measured with –15°/15° and –30°/30° geometries were similar does not necessarily mean that the type of bronzing was not due to interference effects. In fact, the differences may be significant. Buc and coworkers (1947) point out that interference bronzing changes most radically at lower angles of incidence (60° or greater). They add that the color of the observed bronzing may also change following continued exposure.

The reader may well wonder why this phenomenon is discussed in these pages dealing with the color of museum objects and materials. How many times has bronzing occurred and been described? It is difficult to know the answer. However, there are two primary reasons for pointing out the occurrence of this phenomenon: (1) Unless the observer is attuned to looking for bronzing, it may go undetected, particularly when the effect is very small. (2) Many of the newer pigments introduced since 1930 have a greater tendency toward exhibiting this behavior than do most classical pigments. Hence, bronzing may occur more frequently in modern paintings and particularly in modern inks (Smith 1963). One of the traditional pigments subject to bronzing is iron blue (ferric ferrocyanide, or Prussian blue), used by artists for over a century. It exhibits interference bronze; with angular variation, it changes in color from red to green to blue.

Perhaps the most widely used modern pigment subject to a subtle specular reflectance change, particularly following exposure, is rutile TiO_2. Until it is pointed out, the selective color of the specular reflection is often not noted visually. Even though the surface gloss may appear to be unchanged (that is, the reflection is not more diffuse), the spectral distribution of the specular reflection may run the gamut of spectral colors (violet, blue, green, yellow, red, purple)—albeit of low chroma—subtly affecting the visual color. Armstrong and Ross (1966) attribute this phenomenon to interference effects resulting from the microstructure in the rutile paint films. Whether this phenomenon has been observed in modern paintings or on painted objects or buildings is not known, but the reader is forewarned to make careful visual examinations of the *color* of the gloss (the specular reflection).

In the article by Johnston-Feller and Osmer (1979), a number of pertinent references to the subject of bronzing are given. The possibility of the occurrence of this phenomenon is a further reason for measuring colors with the specular component of the reflectance included (total reflectance, SCI) as well as excluded (diffuse reflectance, SCE). The character of the chromaticity of the specular reflection alone can then be analyzed.

Pearlescence and Iridescence

Both pearlescence and iridescence result from the structure of materials, which is often flakes or thin layers with a refractive index higher than that of the surrounding medium. The distinction between pearlescence and iridescence is the nature of the specular light reflected. If at any specular angle the observed reflectance is white, the effect is called *pearlescence* or luster; if the specular reflectance is colored (chromatic) and changes hue when the illuminating and viewing angles are changed, it is called *iridescence* or interference color. In either case, the specular reflection occurs within the object or film and is due to the structure of the object and not to absorbing colorants—dyes or pigments—incorporated into the object.

Numerous examples of interference colors occur in nature: the iridescence of feathers on certain birds, butterfly wings, certain beetles, and some tropical fish; the iridescence arises from structural color and not from pigmentation. The myriad colors of soap bubbles and oil slicks are also familiar examples. As described in the previous section on bronzing of pigmented dielectric films, one type of bronzing (metallic appearance) is attributable to interference and is characterized by changes in color as the angles of illumination and viewing change.

The interference colors so characteristic of many Tiffany glass objects are also illustrative of the phenomenon. Many ancient glasses, buried in the earth for centuries, exhibit beautiful interference colors in the surface that developed during their long burial.

Interference color results when incident light is reflected from a regularly organized structure within an object that can reflect light of certain wavelengths in a particular way: When the reflected light is *in phase* with one particular wavelength of the incident light, it reinforces that wavelength and eliminates other wavelengths that are *out of phase.* Figure 5.8 illustrates this phenomenon. Each line in the figure represents waves of the same wavelength, and each pair illustrates different ways in which two waves may interact. Wavelength is the distance from one crest to the next or from one trough to the next. In the upper pair, one wave has its crest where the other has its trough—the two waves are completely out of phase. The result is complete cancellation of light, that is, darkness. In the middle pair, the two waves partially cancel—that is, they are partially out of phase, with the result that the reflected intensity is very much weakened. In the lower pair, the waves are completely in phase and reinforce one another; the result is a pure, strong color associated with that particular wavelength. The resultant color is pure spectral color of a single wavelength.

The flash of specular color observed at certain angles in many objects exhibiting interference color is most frequently due to laminar structures, that is, layers of different refractive indices of such thickness that interference of light can occur. Examples are mother-of-pearl, butterfly wings, and hummingbird feathers. Modern interference pigments

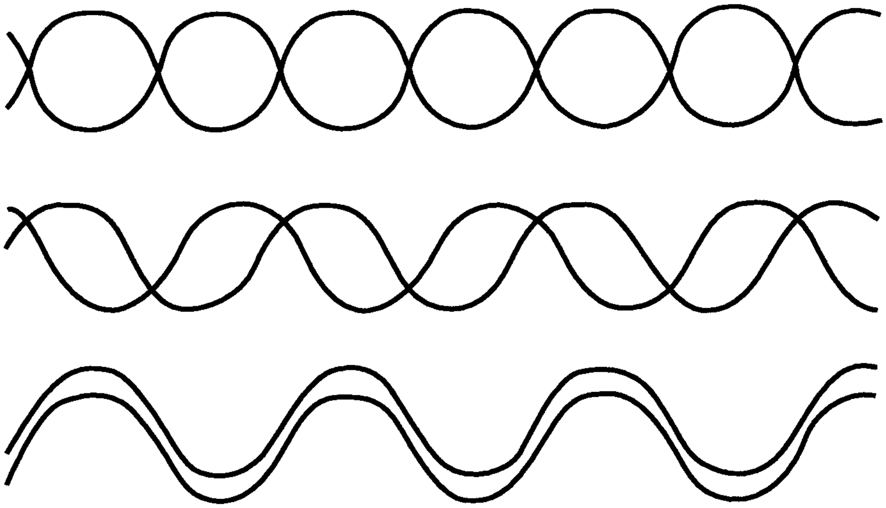

Figure 5.8

Comparison of the behavior of two light rays of the same wavelength (distance from crest to next crest, or from trough to next trough). The upper pair are completely out of phase, so that one wave cancels the other, resulting in darkness. The middle pair are partially out of phase, resulting in weakened light. The bottom pair are completely in phase, and the resulting color is pure and strong.

are likewise laminar structures (platelets or thin flakes). The iridescence depends on two factors: the difference in refractive index between the layers, and the thickness of the layers. Transparent materials in layers reflect at the two interfaces where the refractive index changes: the top and bottom of the layer or film, as described in the section on transparent materials in chapter 4. The amount of light reflected at the interfaces depends on the refractive index difference and on the angle of incidence. Figure 5.9 illustrates how two beams that are incident on a film, one reflected at the top surface of the film and the second from the bottom surface, reinforce each other if the wave trains of the two beams are in phase. In figure 5.10, the optical thickness has been changed, and the reinforced color has a different wavelength from the specularly reflected light of the thicker film illustrated in figure 5.9. The optical thickness can also be changed by increasing the angles of illumination and view, as illustrated in figure 5.11. Here the thickness is the same as in figure 5.9, but the angle of incidence and view is higher, so that the optical path is increased, and the reinforced spectral color is different. (These illustra-

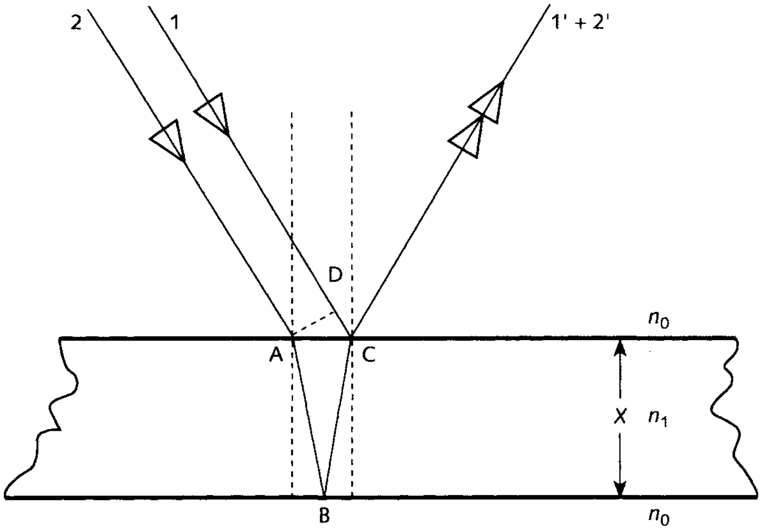

Figure 5.9

Light ray 2 enters the film at point A; is bent toward the perpendicular (dotted lines) when it enters the denser medium; is specularly reflected at the second interface; and, upon exiting, is bent away from the perpendicular (ray 2'). Light ray 1 is specularly reflected as ray 1' at the top surface and is in phase with ray 2', reinforcing the color (n_0 is the lower refractive index; n_1 is the higher refractive index of the denser medium; and X is the thickness) (after Simon 1971).

Figure 5.10

The same phenomenon is occurring here as in figure 5.9, but because the thickness of the film is different, the wavelength of light that is reinforced is different (after Simon 1971).

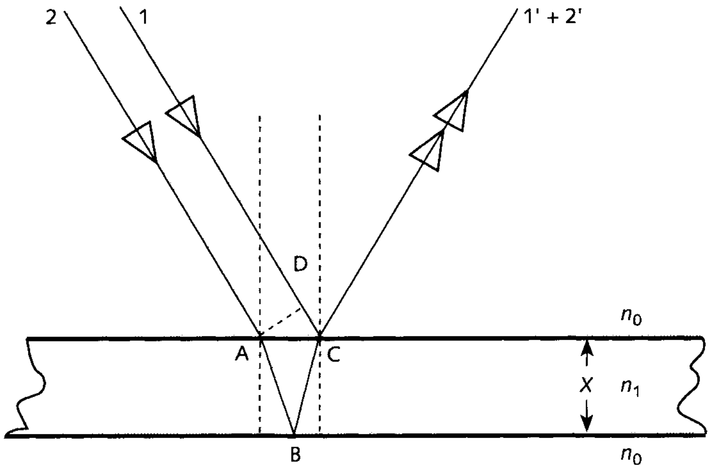

tions are adapted from Simon [1971].) Thus, the colors change constantly as the illuminating and viewing angles are changed, producing a beautiful display of very pure spectral colors in the reflection.

Other structures may also be responsible for selective specular reflection, as Simon (1971) points out and illustrates. An appropriate arrangement of ridges or slits, such as in diffraction gratings, or an appropriate spacing of minute particles in equidistant layers (a space lattice) will also produce interference of light.

One may ask what happens to the wavelengths that are not the same as the one that is specularly reflected? Because the layers that produce the interference are transparent and nonabsorbing, the wavelengths of light other than the one specularly reflected are transmitted. The result is that interference platelets have two characteristic colors, the one that is specularly reflected and the other that is transmitted. The transmitted radiant flux is always lower in purity than the specularly reflected color. In most situations some of the light of both types may be scattered—from the edges of platelets, for example, or from other materials present. To retain the maximum specular reflection, the scattering must be kept as low as possible.

Figure 5.11

The optical path length or thickness is different, because the angle at which the rays strike the surface is greater than in figures 5.9 and 5.10, and the color is again different (after Simon 1971).

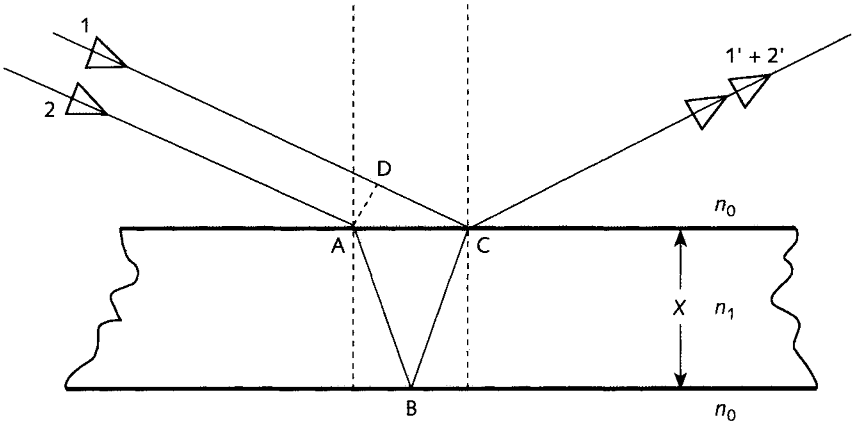

History of pearlescent and iridescent pigments

In the first of his chapters in the *Pigment Handbook*, Greenstein (1973a) traces the commercial development of interference (iridescent) pigments and pearlescent (also called lustrous or nacreous) pigments for use in coloring man-made articles. He attributes the beginnings of this specialized pigment industry to the introduction of plastics, notably the introduction of nitrocellulose, developed about the time of World War I.

All of the pearlescent and interference pigments developed for incorporation into synthetic polymers owe their specular reflectance to thin platelets or flakes.

According to Greenstein, the first pearlescent pigments were made from fish scales, primarily those of herring. The reflective platelets consist of guanine (2-amino-6-hydroxypurine), with lesser amounts of hypoxanthine (6-hydroxypurine). Because the amount of nacreous pigment obtained is less than 0.1% of the weight of the fish, it took a lot of fish to make a pound of pigment. The price reflected this: in 1972 a pound cost $90.91 to $145.45, depending on quality. Fish-scale nacreous material has been used widely for many years in simulated pearls and in cosmetics such as nail enamels. The platelets are sold as suspensions, usually at 11% or 22% concentration.

From the beginning of interest in pearlescent pigments for use in plastics and coatings, attempts were made to create lustrous pigments synthetically. The 1920s saw the development of mercurous chloride. However, the use of this poisonous compound was short lived. In the 1930s there was the development of lead hydrogen phosphate ($PbHPO_4$), but the luster was not very high compared with that of the natural pearlescent pigments. $PbHPO_4$ had its maximum usage in the 1940s and early 1950s.

During the 1940s and 1950s nacreous lead carbonate was developed; it proved to be as lustrous as the natural pearlescents. By varying the thickness of the crystals, interference pigments could be created. Although nacreous lead carbonate was significant in the development of synthetic pearlescent and interference pigments, its place has now largely been taken by newer nonlead pigments with similar optical properties. Although no known case of lead poisoning from pearlescent buttons or pearls has been reported—the pigments are embedded in very stable polymer matrices—the possibility that their use would be frowned upon because of their lead content, even if uningestible, caused most manufacturers to discontinue their production (Greenstein, personal communication, 1993).

Other lustrous, pearlescent pigments developed from the 1940s to the 1960s were lead hydrogen arsenate (not very important commercially because of its toxicity) and bismuth oxychloride ($BiOCl$). The latter is nontoxic. However, since $BiOCl$ darkens on exposure to sunlight, its use in applications other than cosmetics requires protection by ultraviolet absorbers. It is lustrous but not appropriate for making interference pigments.

Probably the most significant event was the development of TiO_2-coated mica flakes in the 1960s. Controlling the size and thickness distribution of the mica platelets and the thickness of the high-refractive-index TiO_2 coating makes it possible to create interference pigments covering a broad spectrum, as well as pearlescent flakes. Because these pigments and flakes are nontoxic and durable, their use has been expanding.

The optical thickness of the coating on the surface of the interference-pigment platelets determines their color. For highest luster, the platelets range in size from about 10 to 40 μm in their longest dimension; their thickness is considerably less, 0.06 to 0.8 μm, depending on the type. The critical dimension is the thickness of the interference layer. For example, an optical thickness of less than 140 nm results in white luster or pearlescence; above 200 nm optical thickness, the interference light is colored. With increasing thicknesses, it varies from yellow to red-gold to magenta to purple to blue to green at 370 nm optical thickness (Greenstein 1988). Further increases in the optical thickness result in a repetition of this order. Increasing the optical thickness in increments of 50% results in waves in phase (because the light travels in two directions, entering and exiting in the layer).

Figure 5.12, reproduced from Greenstein's second article (1973b) in the *Pigment Handbook,* illustrates the change in the specular reflectance with angle of illumination and viewing for a basic lead carbonate, green interference pigment as measured on the Trilac goniospectrophotometer. This instrument is described in chapter 1. As noted there, the incident angle is designated as negative and the viewing angle as positive, because they are on opposite sides of the perpendicular. It can be seen from figure 5.12 that increasing the angles from 15° to 45° results in a change in the hue from green to blue. The explanation and equations that predict this change are presented by Greenstein (1973b).

As described above, one of the characteristics of all pearlescent and interference pigments is their transparency—that is, their lack of absorption. In the case of interference pigments, the transmitted light is complementary in color to that reflected. Figures 5.13 and 5.14, redrawn from Greenstein's article (1973b), illustrate, respectively, the reflectance and transmittance of a blue and a green basic lead carbonate interference pigment. If one examines such pigments under the usual optical microscope, the *transmitted* color is observed. This is the complementary color of the specularly reflected color, as shown in figures 5.13 and 5.14. Note in these illustrations that the transmitted color is much lower in chroma than the specularly reflected color. If the microscope is arranged so that there is vertical illumination in a dark field, the reflected interference color can be observed.

In order for the reflected interference color to be seen alone, the transmitted light must be absorbed. In polymer films, this can be achieved by applying the film over an absorbing substrate, such as a black or dark brown. Mother Nature utilizes this phenomenon in many cases of iridescent color. For example, the underside of the brilliant blue Morpho butterfly wing, a beautiful example of interference color, shows dark brown pigmentation. The hummingbird exhibits its flashes of iridescence only at the specular angle. At all other angles the little bird's feathers are a dull brown, well camouflaged among the branches of a tree, because of

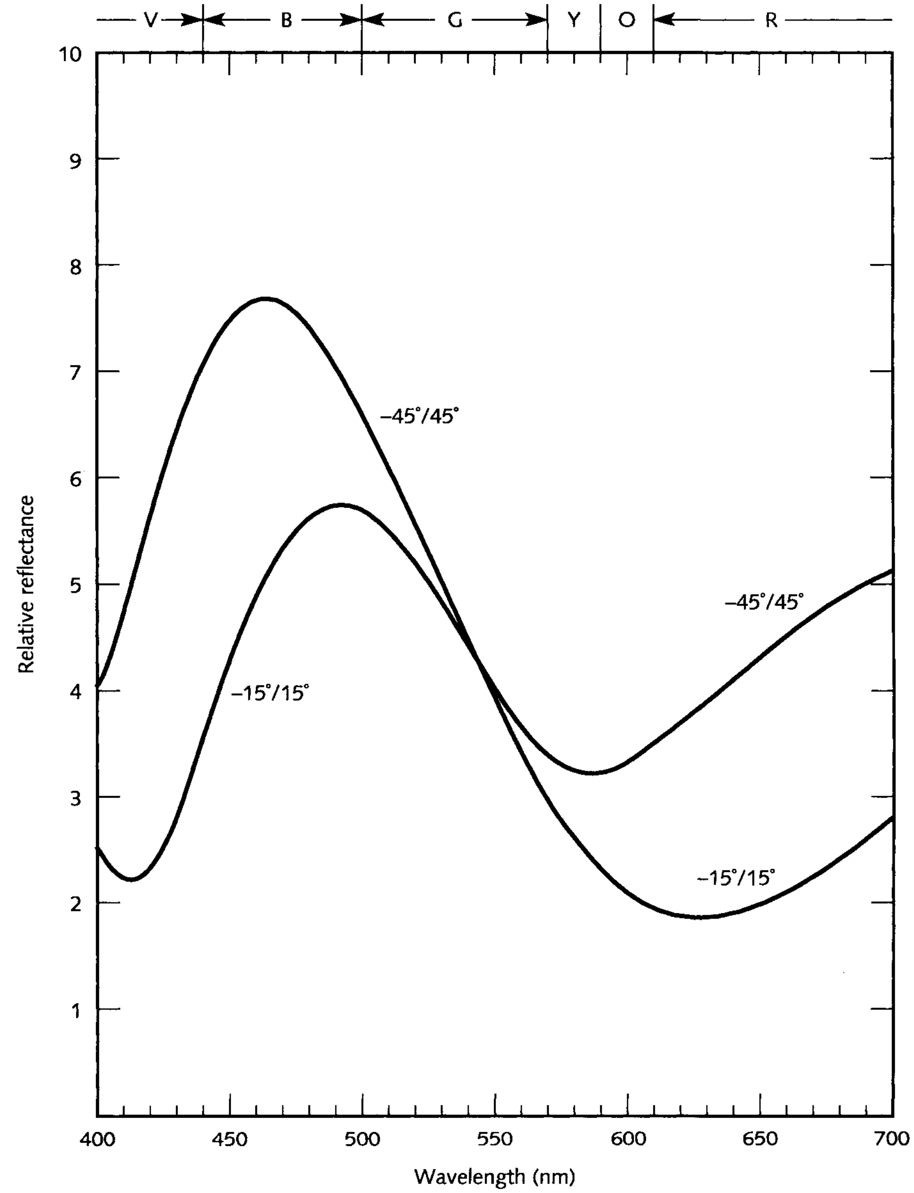

Figure 5.12
Shown here is the change in color in the specular reflectance of a basic lead carbonate green interference pigment as the angle of incidence is changed. At the higher angle of incidence, −45°, the color is a blue instead of the blue-green observed at −15° incidence (from Greenstein 1973b. Copyright © 1973 John Wiley & Sons, Inc. Reprinted by permission).

their absorption color. Thus, at angles other than the specular angle, one observes the substrate color; the transmitted color has been absorbed.

If a thin film of a polymer containing an interference pigment is applied over a highly reflective substrate, such as a white, the interference color is still observed at the specular angle, but the chroma (purity) of the observed color is decreased because of the inclusion of some of the reflection from the substrate—diffuse light that is the color of the transmitted light. Thus, over white, at angles other than the specular angle, the color observed is the transmitted color diffusely reflected by the substrate.

The pigment industry soon realized that the perceived color of pearlescent or interference pigments can be modified by the inclusion into the polymer film of a *transparent* (low-scattering) absorbing pigment, such as a black or a transparent chromatic colorant. Care must be taken in selecting the transparent chromatic colorant to use in combination with an interference pigment. If a transparent pigment that absorbs

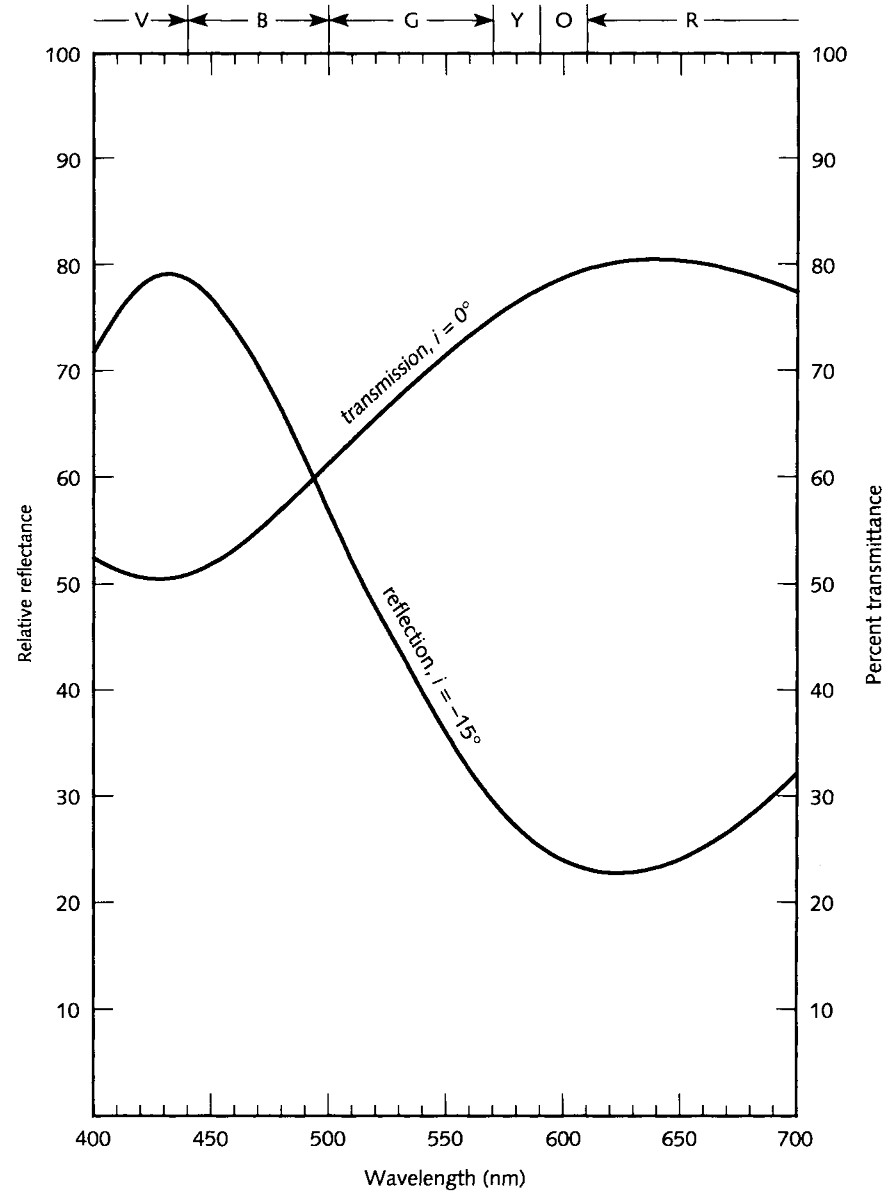

Figure 5.13

Specular reflection of a blue-reflecting basic lead carbonate interference pigment at an incident angle of –15°. The second curve illustrates the transmission color, a low-chroma yellow-orange, the complement of the blue reflection (from Greenstein 1973b. Copyright © 1973 John Wiley & Sons, Inc. Reprinted by permission).

all colors except red is used in combination with a red-reflecting interference pigment, the film of the mixture will appear red at all angles of illumination and viewing, although the red specular reflection will be enhanced by the inclusion of the absorbing pigment. Today some interference pigments of the TiO_2-coated-mica type are manufactured with a layer of transparent absorbing pigment as well as the TiO_2 layer; others may be made by incorporating an absorbing pigment into the TiO_2 layer. When the absorbing pigment has the same hue as the interference color, the highlight color observed at the specular angle is enhanced, and the diffuse color seen at other angles is the same hue if the layer is applied over a reflecting neutral substrate. In contrast, when the absorbing color in the TiO_2 layer is different from the interference color, a two-tone effect can be created, as long as the two colors do not cancel each other. An example of such a modified interference pigment would be a blue interference pigment with a transparent red layer over the TiO_2 layer.

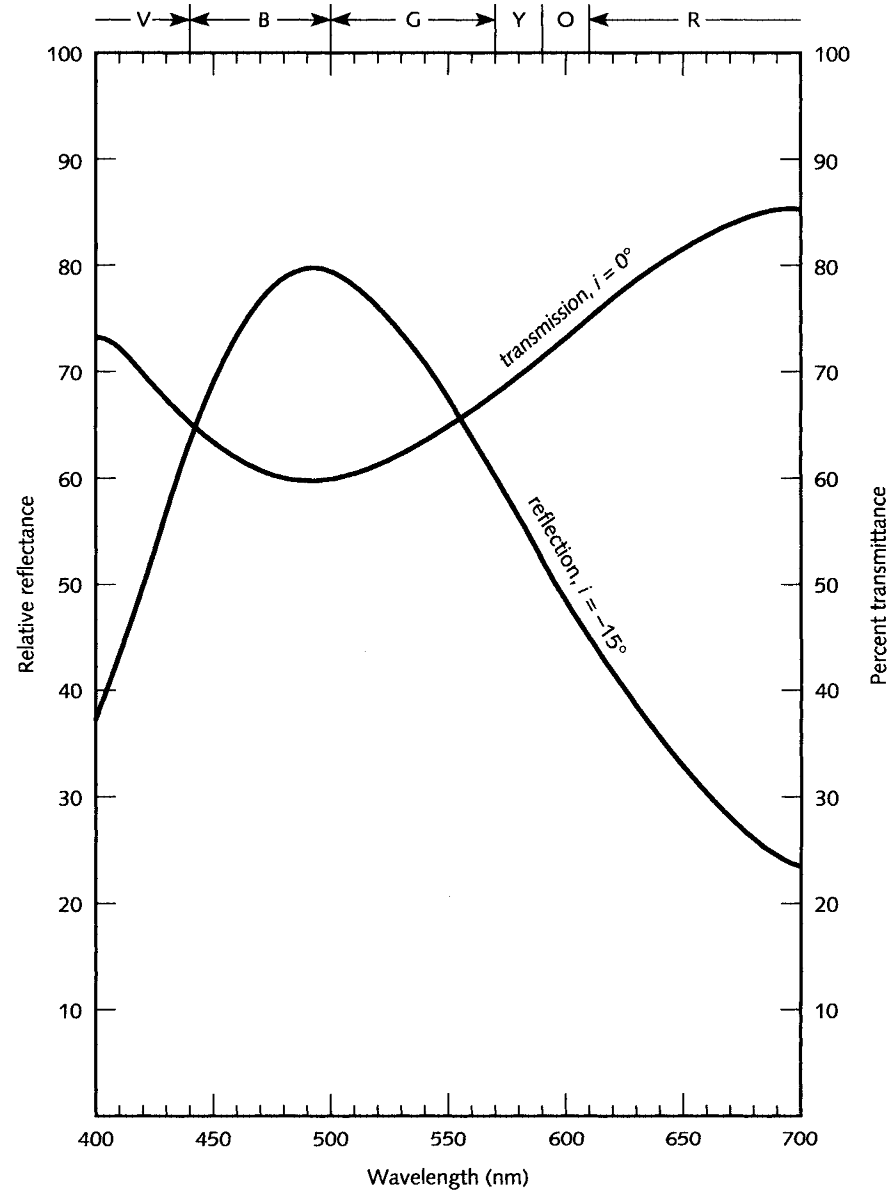

Figure 5.14

Specular reflection of a green-reflecting basic lead carbonate interference pigment at −15° incidence. The transmission color is the complementary hue, a magenta of very low chroma (from Greenstein 1973b. Copyright © 1973 John Wiley & Sons, Inc. Reprinted by permission).

Figure 5.15 illustrates goniospectrophotometric measurements of such a modified interference pigment applied over a white substrate (Greenstein 1988). The transparent red in the anatase TiO_2 layer is carmine, evident by the two absorption bands at 520 and 560 nm (see fig. 4.19).

Because there are so few goniospectrophotometers available, it is worthwhile to illustrate the characteristics of the same type of pigment as measured by use of sphere geometry with the specular reflectance *included.* Figure 5.16 illustrates the spectral curves of the same type of pigment measured over a white substrate and over a black substrate. (The same type of spectrophotometer used in fig. 5.15 was used in the sphere mode to obtain the curves in fig. 5.16.) The curve measured over black, which absorbs the transmission of the blue interference pigment and that of the red absorption pigment, shows only the blue interference color. The curve of the pigment applied over white shows the combination of the blue interference color with the red

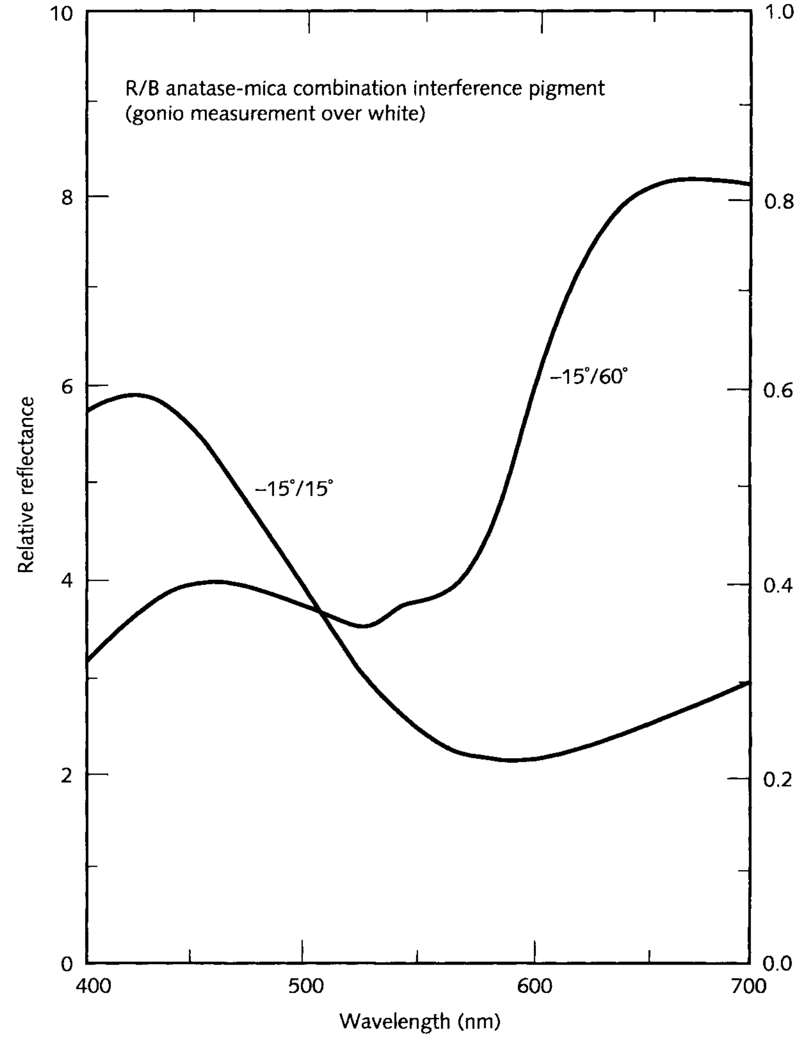

Figure 5.15
A blue interference pigment modified with a red (carmine) transparent pigment layer over the anatase TiO_2 layer; the lacquer film is applied over white. At incident and viewing angles of −15°/15°, the blue specular reflectance color is observed. At a viewing angle of 60° with the same −15° incident angle, the weak red transmission color is combined with the reflection of the carmine red pigment over white: the color observed is a bright red (after Greenstein 1988).

absorption color; the result is a purple. The dominant wavelength of the measurement over black is 473 nm, a blue; over white, it is 500c nm, a purple. These curves and measurements are included to illustrate that considerable information concerning interference pigments can be obtained with an integrating sphere instrument when their optical behavior and appearance are recognized.

The possible optical effects available to the artist or designer are almost limitless and fascinating to imagine: pearlescent pigments, used alone or in combination with transparent absorbing pigments; iridescent (interference) pigments of specific hues, used alone or in combination with transparent chromatic colorants. Changing the substrate color with any of them is an additional variable that can be added to the picture.

Although pearlescent and interference pigments may have achieved up to now only limited usage in the works of artists and artisans, one finds that pearlescent pigments have been included in tubes of artists' colors for many years, with the original use as a pigment to simulate metals. For example, a pearlescent plus a little black makes a beautiful silver and has been sold as "silver." With a little transparent red

Figure 5.16

The total reflectances of the same type of red–blue (R–B) combination inference pigmented lacquer as in figure 5.15 are illustrated here. The curves were measured with an integrating sphere instrument with -8° incidence angle and the specular reflectance included (total reflectance). When the pigment is applied over black, only the interference blue color of 473 nm dominant wavelength is apparent; all of the transmitted light has been absorbed. When it is applied over white, however, the total reflectance includes not only the transmitted color due to the carmine in the TiO_2 layer and the transmittance of the interference pigment, but also the blue interference specular color produced at +8°. The result is a magenta of 500c nm dominant wavelength, which more closely describes the color observed in semidiffuse directional illumination, as would be seen in commonly encountered illumination and viewing conditions. The interplay of the various types of reflections creates a myriad of illusory colors.

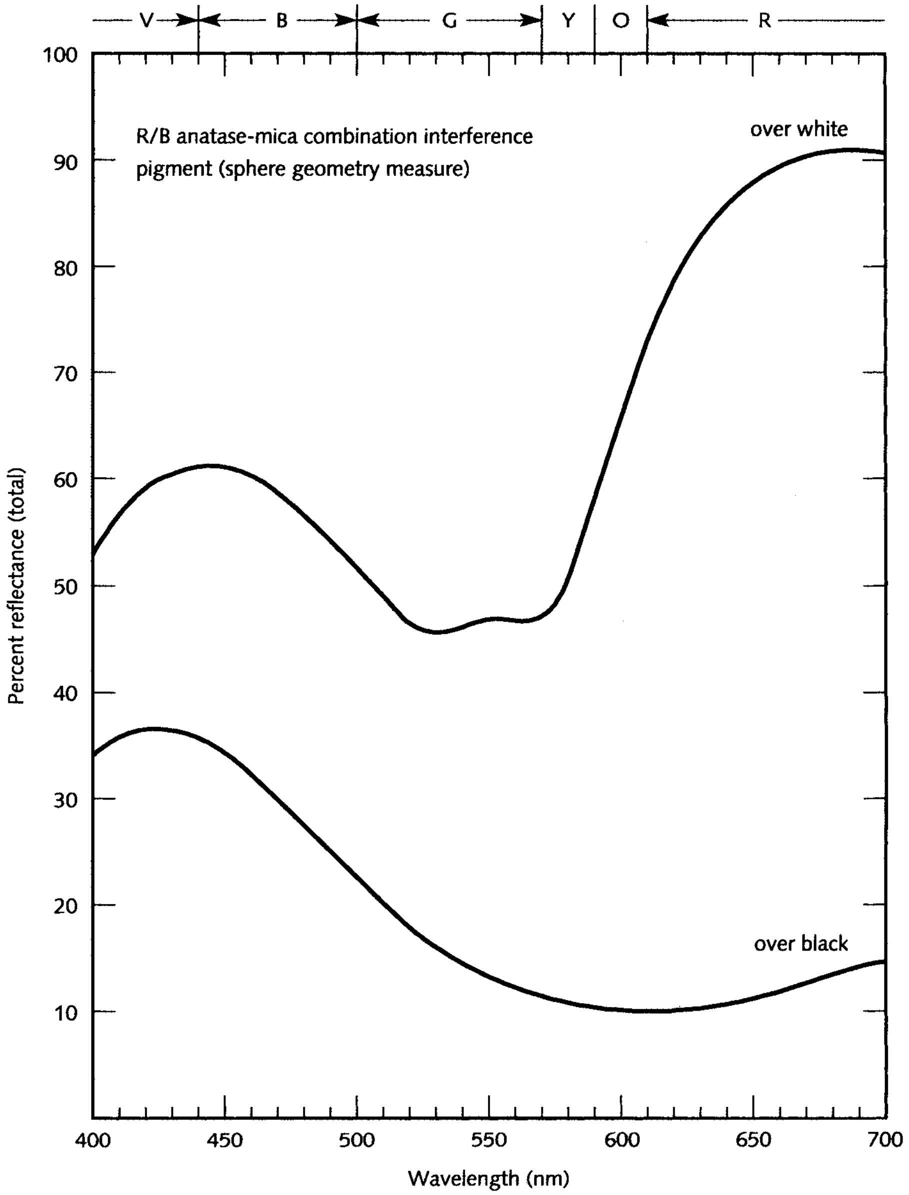

oxide, a beautiful copper is achieved; with a little transparent yellow and a little black, an interesting bronze. That these different optical effects may be of interest to artists is attested to by the current offerings of tube oil colors and acrylic colors by a well-known artists' materials supplier, Daniel Smith (1992). His catalogue offers in oil colors three pearlescent colors, fourteen iridescent colors, and seven interference colors. The iridescent colors and the interference colors, which contain coated mica pigments, cover the visible spectrum. In the spring 1992 Daniel Smith catalogue, an illustrated description of pearlescent and interference pigments is presented by Weingrad (1992); color reprints are available for a small fee from Daniel Smith, Incorporated, in Seattle. Weingrad presents examples that an artist should experiment with to understand these pigments. So, if pearlescent and interference pigments were not extensively used by artists and artisans in the past, they may certainly appear in future objects.

Throughout history, humans have thoroughly appreciated the beauty of pearlescence and iridescence, using shells and pearls, and even beetles and butterflies, to make jewelry and other objects for aesthetic enjoyment. The attempt to use such materials for the artistic creation of objects of beauty and adornment was a natural development. Because so much of color in nature is a result of iridescence (interference), its measurement and characterization may be of particular concern in the care of collections in museums of natural history. Interference colors do not fade in the same sense as dyes and pigments fade—by loss of the colorant chemical compound. The deterioration that *does* affect the stability of interference colors occurs as a result of minute changes in structure due, for example, to shrinkage. Simon (1971) states that "even the most infinitesimal alteration in these structures can lead to the colors' winking out as though a switch had been turned off." Climate control would seem to be critically important, then, in preserving the color of these objects.

It must not be forgotten that many of the colors observed in nature's objects are not attributable to interference phenomena but are, rather, caused by natural pigments and dyes, many of which are extremely fugitive. Control of the intensity and spectral distribution of the illumination of exhibits of such materials is, therefore, vital to their color preservation, in addition to the attention given to the control of climate.

Other Flake Pigments (Metallic Flakes)

Just as metals reflect light specularly (described in the first section of this chapter), so too do flake pigments made from metals. When incorporated into polymer films, they reflect like little mirrors.

For at least four thousand years, flake made from gold, the so-called gold leaf, has been used for decoration. For most of this period, the material was made by hand, with the gold hammered into very thin sheets. Because of the high cost of gold leaf, development of a less-expensive substitute was found in the form of a copper alloy such as brass (copper alloyed primarily with zinc) or bronze (copper alloyed with tin). These substitutes were still hammered by hand, so the products remained relatively expensive, though much less so than gold leaf.

Rogers, Greenawald, and Butters (1973), in their chapter in the *Pigment Handbook,* tell an interesting historical anecdote concerning the mechanization of the preparation of such substitutes. It seems that Bessemer (of steel fame) discovered that gold bronze powder, which he purchased around 1843–44 for his sister's book illustrations at what seemed to him a ridiculously low price, on analysis turned out to be brass. He put his inventive mind to work and developed, around 1845, a mechanized process for making gold bronze powders. Never patented, the secret process was kept within the family for many years. The same process was used to make aluminum flakes until the early 1930s, according to Rolles (1973). He also describes the old "secret" Bessemer hammering process. Small, uniform pieces of metal were fed onto the steel anvil of a stamping mill. A series of steel hammers was raised by action of a cam system and then allowed to fall onto the pieces on the anvil, producing large flakes, called schrodes. The schrodes were then used as the feedstock for smaller hammer mills to further foil out the material. To prevent cold welding, lubricating oils and tallow fats were used. The final step in the process was polishing the foil with rotating brushes. Thus, the "secret" Bessemer process was simply the use of machines to do the work formerly done by hand.

From the days when the imitation gold flakes first appeared, the term *bronze powder* came to be used to describe any metallic flake pigment, regardless of its metal composition. Today the term *bronze pigment* may be preceded by the identification of the metal used, such as "aluminum bronze" or "copper bronze."

Metallic flake pigments may be made from copper, brass, bronze, or aluminum (the last was introduced at about the beginning of the twentieth century) or from stainless steel (introduced around the late 1940s). The brass and then the aluminum flakes, used primarily in artists' materials when first introduced at the turn of the century, are probably those most commonly encountered in addition to the real gold leaf, which is still relatively expensive.

Stainless-steel flake pigments are used in coatings, primarily for their very good durability and corrosion protection. Being of high density, they do not "leaf," as do the other less-dense flake pigments, but tend to form, as described by Hay (1973), a "multilayer structure throughout the paint film." Because of their hardness, stainless-steel flake pigments provide superior abrasion resistance in paint films, becoming "brighter and smoother after several years of weathering" (Hay 1973). Because of their chemical inertness, they provide superior corrosion resistance in extremely antagonistic atmospheres. Also because of their inertness, they may be combined with many types of additives to create desired properties, or combined with other pigments to create desired colors. They may also be formulated in almost any paint vehicle, oil based or water based.

In contrast to what happens with the pearlescent and iridescent flake pigments described in the previous section, the change in color with angle of view of paints pigmented with metallic flake pigments is due simply to the change in the amount of light reflected by the more or less horizontally oriented flakes. Thus, viewing at an angle near to the specular angle, based on the angle of incidence used, results in the brightest color. As the viewing angle increases off the specular, the amount of flake reflectance decreases, and the perceived color darkens.

The 50% cumulative (median) particle size of bronze flake varies from 32 μm for coarse particles to 6 μm for fine particles (Rogers, Greenawald, and Butters 1973); for aluminum flake, from 19 μm for coarse particles to 7 μm for the finest (Rolles 1973); and for stainless steel, the median particle size is about 14 μm (Hay 1973). In contrast, the thickness of the flakes is much less—about 0.1–2.0 μm for aluminum flake, for example (Rolles 1973). The particle size of flake pigments is within the range of a light microscope, making their study reasonably simple.

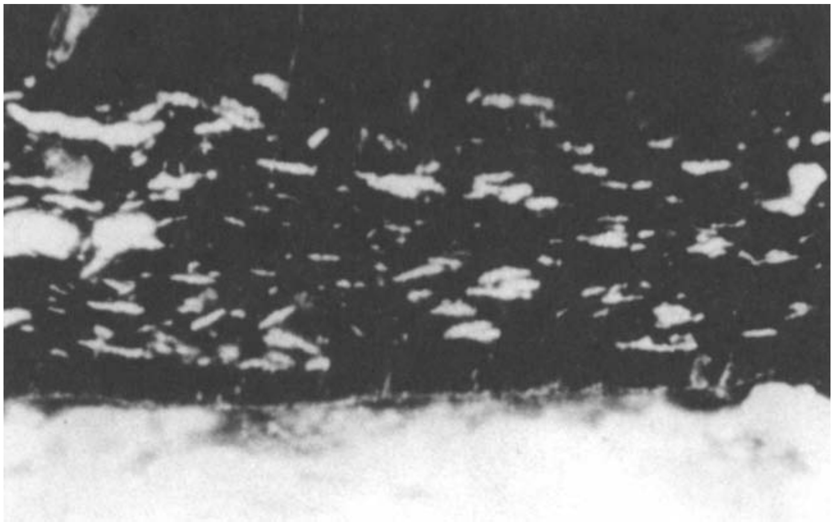

Figure 5.17
Photomicrograph of a cross section of a paint film pigmented with aluminum flakes and phthalocyanine blue pigment. The substrate (white section at the bottom) is metal. The white flakes in the dark field are aluminum flakes. The photograph illustrates how they are typically oriented nearly parallel to the substrate interface.

The amount of metallic aluminum flake used in industrial coatings is generally in the range of 2–3% by weight of the total dry film. Higher concentrations result in an increased loss of gloss of the vehicle surface (Rolles 1973). Today overcoats of clear, transparent pigmented or unpigmented vehicle may be applied to the surface to minimize this loss in gloss. This practice also enables the using of flakes with the largest particle size while still retaining high gloss.

Figure 5.17 is a photomicrograph of a cross section of a film pigmented with aluminum flakes and phthalocyanine blue pigment (Johnston 1967a) applied over a metallic substrate. It can be seen that most of the flakes are oriented primarily parallel to the substrate, as illustrated in the schematic drawing shown in figure 5.18.

Figure 5.19 illustrates the changes in reflectance with angles of illumination and viewing for a film pigmented with aluminum flake. The angles of incidence and viewing are described in degrees, the perpendicular to the surface being designated 0°. The notation used in the

Figure 5.18
Illustration of the orientation of metallic flakes in a paint film, and the reflections and interreflections that can occur at an angle of incidence slightly off the perpendicular.

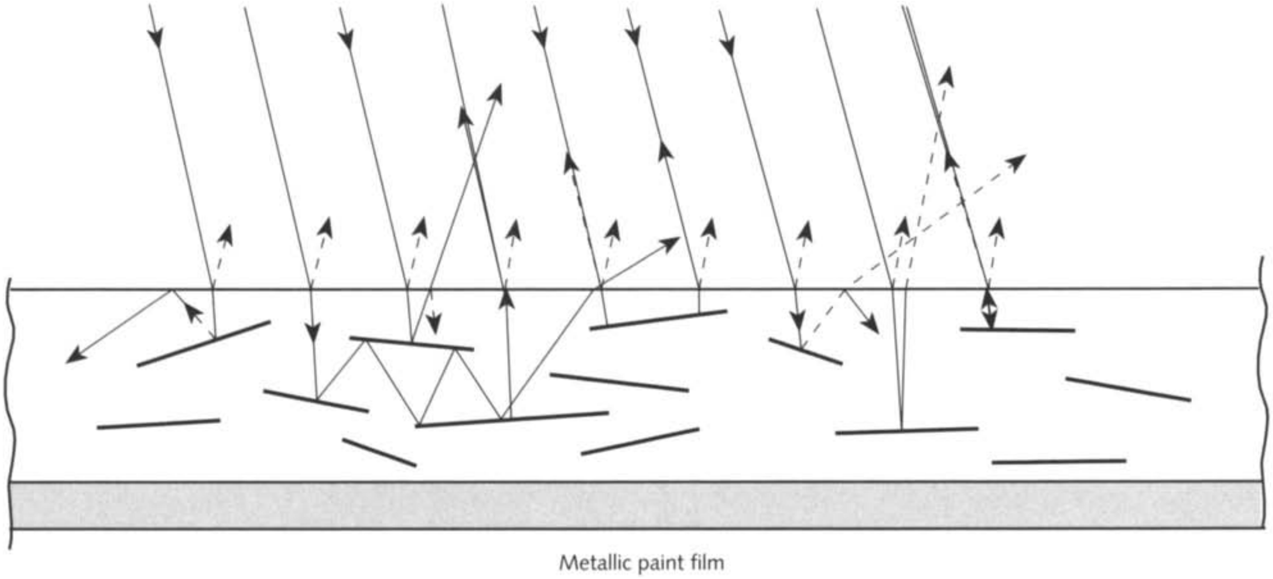

Metallic paint film

Figure 5.19

Variable-angle goniospectrophotometric measurements of a paint film pigmented only with aluminum flake pigment, identified by the composition description 2, 0, 0, 0 (the first number represents the weight percent of aluminum flake, the second number the percent of chromatic pigment, the third number the percent of white pigment, and the fourth number the percent of black). The incident angle in degrees is given first, negative if on the side of the perpendicular opposite the viewing angle (which is always positive), followed by a slash, and then the viewing angle. The number in parentheses is the number of degrees off the specular angle. Note that the measurements made with different numbers of degrees off the specular—that is, the reflectance measurements made at -30°/0° and at 0°/30°—are not identical, as one might expect, because both are measured at 30° off the specular angle. At least part of the explanation is the differences in the light incident (nearly collimated) and the light viewed (subtending an angle of about 15°). The darkest color is observed when the incident and viewing angles are farthest from the specular angle, that is, 0°/75°.

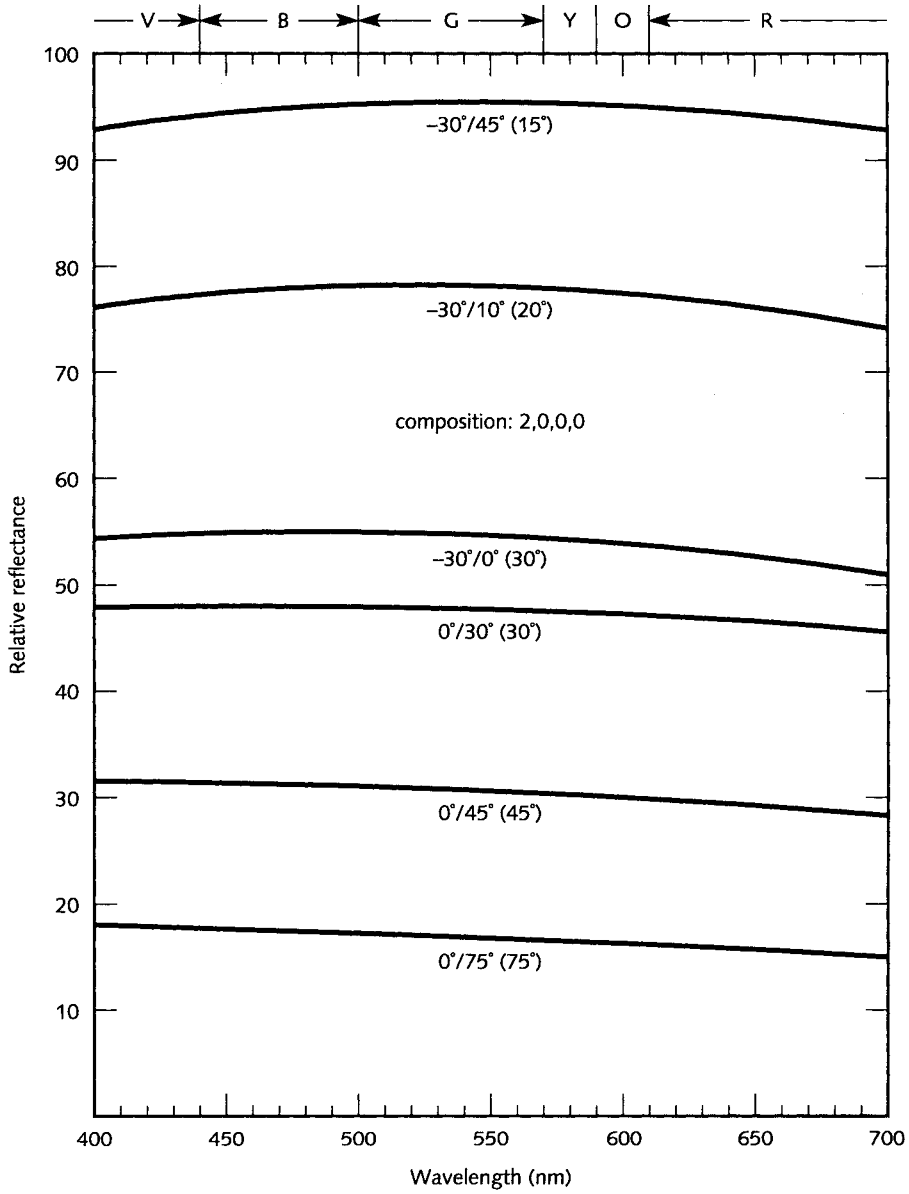

descriptions of the geometrical spectral measurements is described in chapter 1 in the discussion on goniospectrophotometry. The incident angle is noted first, positive if on the same side of the perpendicular (0°) as the viewing angle, and negative if on the opposite side. This number is followed by a slash and then the viewing angle, always positive. The number of degrees off the specular angle is indicated in parentheses, as shown in figures 5.19–5.23 and in table 5.3. The use of parentheses is not standard, however; there is no method of notation generally accepted at this time. Until there is, the notation described provides a convenient shorthand description of the geometrical conditions of measurement.

The goniospectrophotometric measurements on metallic paints illustrated in figure 5.19 and in subsequent figures (figs. 5.20–5.24) were made with the Trilac goniospectrophotometer manufactured by Leres in France (see chap. 6). Measurements were made relative to a pressed $BaSO_4$ white standard. It must be emphasized that the

		Measurement geometry					
Figure	Composition[a] (%) Al, QM, W, Blk	Incident/ viewing angle	Deg. off specular angle	*x*	*y*	*Y*	Comments
5.19	2, 0, 0, 0	-30°/45°	(15°)	0.3096	0.3169	94.74	Al alone
5.19	2, 0, 0, 0	-30°/10°	(20°)	0.3091	0.3168	78.54	Al alone
5.19	2, 0, 0, 0	-30°/0°	(30°)	0.3077	0.3153	56.38	Al alone
5.19	2, 0, 0, 0	0°/30°	(30°)	0.3076	0.3149	47.74	Al alone
5.19	2, 0, 0, 0	0°/45°	(45°)	0.3054	0.3127	30.79	Al alone
5.19	2, 0, 0, 0	0°/75°	(75°)	0.3030	0.3180	17.21	Al alone
5.20	2, 3, 0, 0	-30°/45°	(15°)	0.3109	0.2475	24.90	Al+QM
5.20	2, 3, 0, 0	-30°/10°	(20°)	0.3113	0.2390	21.05	Al+QM
5.20	2, 3, 0, 0	-30°/0°	(30°)	0.3149	0.2330	14.88	Al+QM
5.20	2, 3, 0, 0	0°/30°	(30°)	0.3183	0.2391	12.14	Al+QM
5.20	2, 3, 0, 0	0°/45°	(45°)	0.3281	0.2354	7.90	Al+QM
5.20	2, 3, 0, 0	0°/75°	(75°)	0.3467	0.2326	4.34	Al+QM
5.21	2, 0, 0, 0.1	-30°/45°	(15°)	0.3138	0.3209	72.00	Al+Blk
5.21	2, 0, 0, 0.1	-30°/10°	(20°)	0.3136	0.3211	60.35	Al+Blk
5.21	2, 0, 0, 0.1	-30°/0°	(30°)	0.3132	0.3206	41.97	Al+Blk
5.21	2, 0, 0, 0.1	0°/30°	(30°)	0.3132	0.3203	35.84	Al+Blk
5.21	2, 0, 0, 0.1	0°/45°	(45°)	0.3124	0.3196	22.32	Al+Blk
5.21	2, 0, 0, 0.1	0°/75°	(75°)	0.3125	0.3196	11.68	Al+Blk
5.22	2, 0, 2, 0	-30°/45°	(15°)	0.3065	0.3124	55.40	Al+W
5.22	2, 0, 2, 0	-30°/10°	(20°)	0.3058	0.3115	47.95	Al+W
5.22	2, 0, 2, 0	-30°/0°	(30°)	0.3043	0.3102	38.84	Al+W
5.22	2, 0, 2, 0	0°/30°	(30°)	0.3031	0.3098	35.13	Al+W
5.22	2, 0, 2, 0	0°/45°	(45°)	0.3011	0.3090	29.40	Al+W
5.22	2, 0, 2, 0	0°/75°	(75°)	0.2986	0.3079	23.80	Al+W
5.23	2, 0, 2, 0.1	-30°/45°	(15°)	0.3136	0.3186	45.29	Al+W+Blk
5.23	2, 0, 2, 0.1	-30°/10°	(20°)	0.3115	0.3174	34.04	Al+W+Blk
5.23	2, 0, 2, 0.1	-30°/0°	(30°)	0.3102	0.3166	26.06	Al+W+Blk
5.23	2, 0, 2, 0.1	0°/30°	(30°)	0.3117	0.3171	27.80	Al+W+Blk
5.23	2, 0, 2, 0.1	0°/45°	(45°)	0.3109	0.3178	21.83	Al+W+Blk
5.23	2, 0, 2, 0.1	0°/75°	(75°)	0.3098	0.3178	16.14	Al+W+Blk

[a] Pigment weight concentration in the dried film. Al = aluminum flake; QM = Quinacridone Magenta; Blk = carbon black; W = rutile TiO_2 white.

Table 5.3

CIE notation (illuminant C, 1931 standard observer) for metallic paints.

reflectances measured are *relative* reflectances, valid only for the geometric conditions used in the measurements. It must also be remembered that reflectances (strictly speaking, reflectance factors) as conventionally measured are the ratio of the intensity of the light reflected from the sample, I, to that reflected from the reference white standard, I_0—that is, $R = I/I_0$. In the case of variable-angle measurements, the same is true. However, if measurements are made at the specular angle on flake pigments or on highly reflecting metals, the results will be well above the near 100% reflectance of the white reference standard. For example, the reflectances of the interference flake pigments at the specular angle describing the interference color, as reported by Greenstein (1973a) and in the previous section, required the use of a neutral-density filter in the sample beam, generally one of 10% transmission. Hence, Greenstein's use of the term "relative reflectance" and the author's use of the term correspond here. (For the measurements reported here on the metallic flake pigments, no neutral-density filter was used, because the measurements were made at angles well removed from the specular angle.)

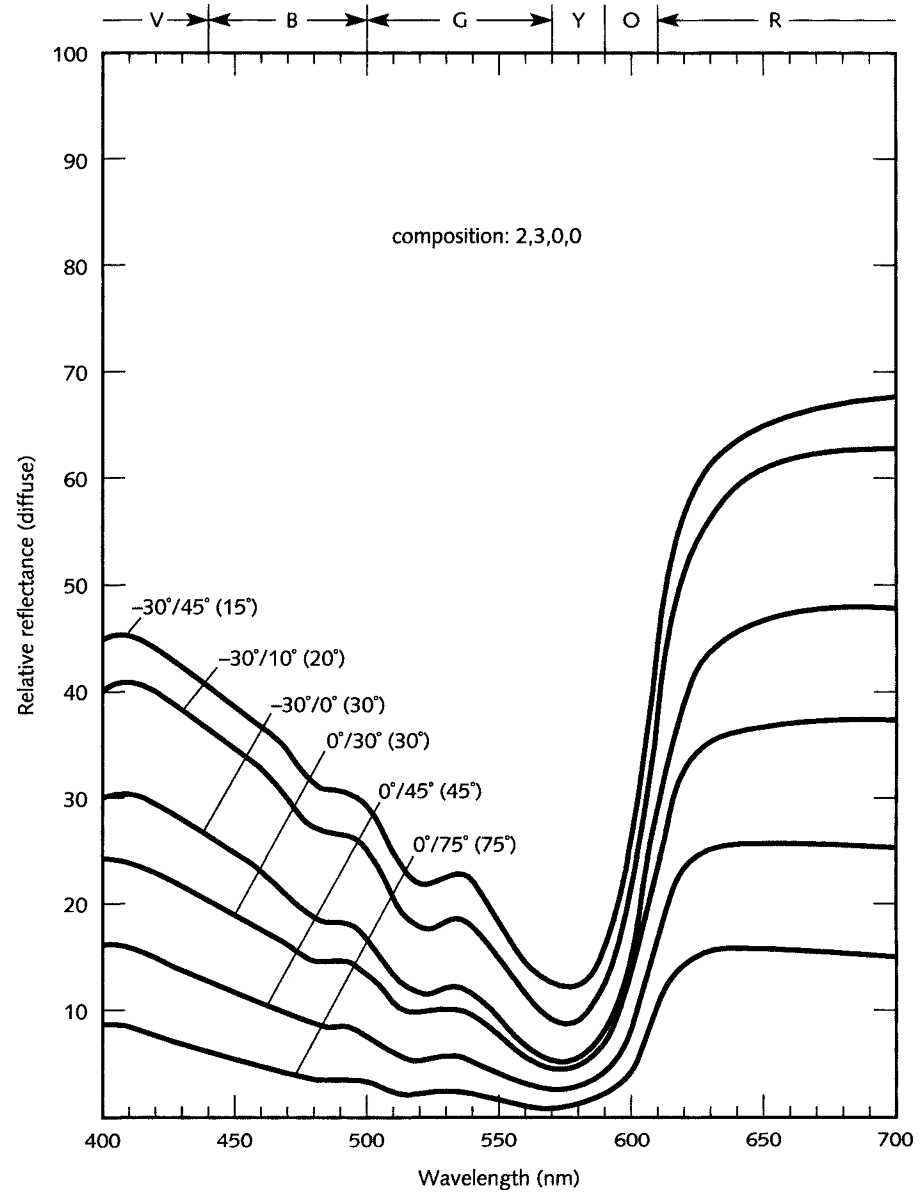

Figure 5.20

Variable-angle goniospectrophotometric measurements of a paint film made with the same aluminum flake pigment in the same amount as in figure 5.19, but with 3% chromatic pigment (Quinacridone Magenta) added. The composition is described as 2, 3, 0, 0 (for explanation, see fig. 5.19). The measurement angles are the same as in figure 5.19.

From an examination of the measurements for aluminum flake alone (without a colored pigment or an inert present), illustrated in figure 5.19, the following observations can be made: (1) the closer the viewing angle is to the specular angle, the higher is the reflectance of the aluminum flake paint; and (2) the magnitude of the reflectance at a specified off-specular viewing angle (30°, as illustrated) varies somewhat with the direction of the incident angle. (The optics of the measuring instrument are not reversible.) The CIE notations (illuminant C, 2° standard observer) for all of the subsequent illustrations of metallic finishes are described in table 5.3.

It should be noted that the CIE color differences calculated for "relative reflectance" measurements do not have the same meaning as those calculated from "absolute reflectance" data for nondirectional samples measured on conventional color-measuring instruments. Corrections can be made for the absorption of the neutral-density filters

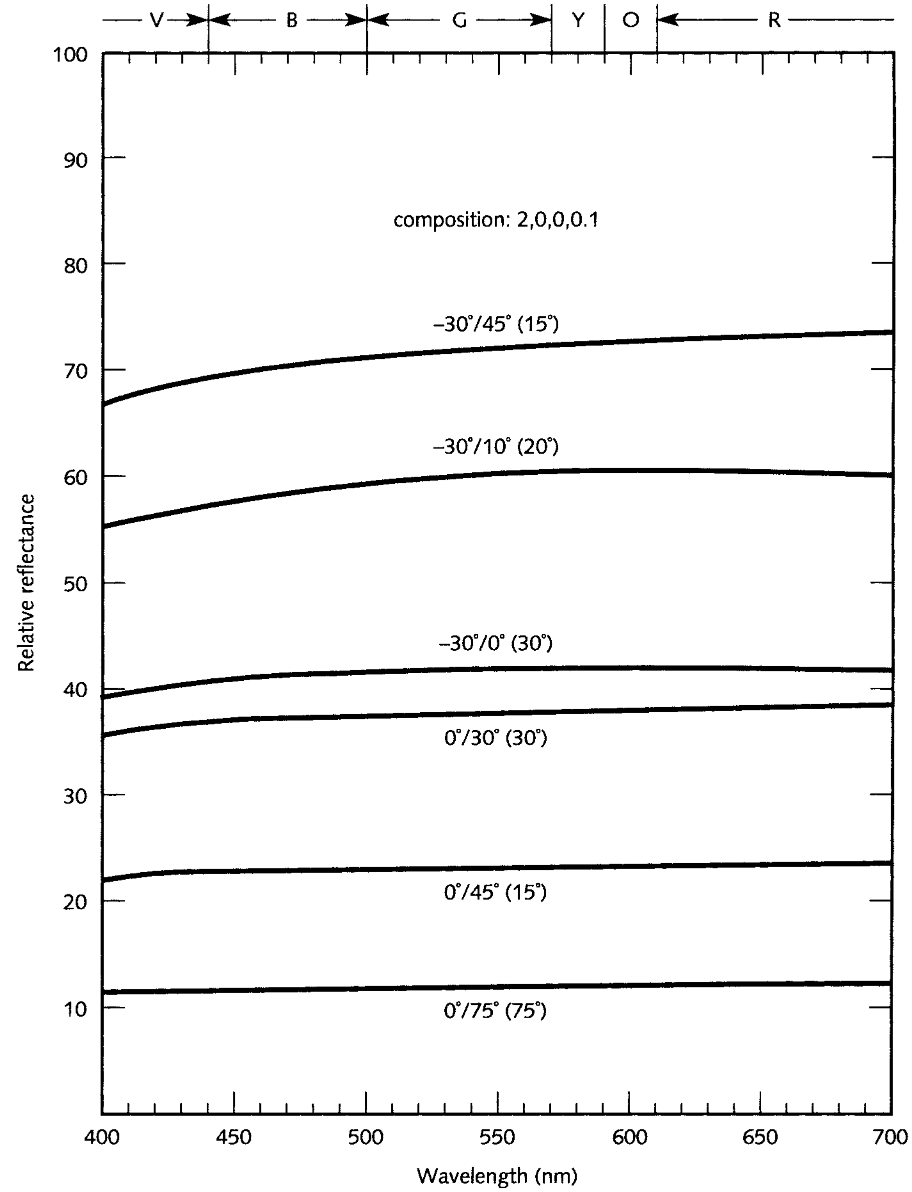

Figure 5.21
Variable-angle goniospectrophotometric measurements of a paint film containing the same aluminum flake pigment as in figures 5.19 and 5.20, but containing only 0.1% carbon black in addition to the aluminum flake. The same angular conditions as in figures 5.19 and 5.20 were used. Note that reflectances at all angles of illumination and viewing are decreased, as would be expected.

used, however. Even without such corrections—but assuming that the neutral-density filter transmission is very flat—the CIE chromaticity coordinates, *x* and *y*, of the metallic finishes still provide useful information for comparison to those of similar samples measured in a similar fashion. In summary, it should be remembered that the relative gonio measurements are not absolute in the normal sense, as are measurements made with conventional color-measuring instruments intended to measure diffuse or total reflectance. Note also that secondary standards for the diffusing reference white, such as white glass or porcelain, should not be used unless they have been calibrated for the particular angular conditions used or are fully described for comparison purposes.

The effect on the reflectance curve resulting from the addition of a relatively transparent absorbing pigment (Quinacridone Magenta) to the same amount of the same aluminum flake in figure 5.19 is illustrated in figure 5.20. The angles of illumination and view are the same as in

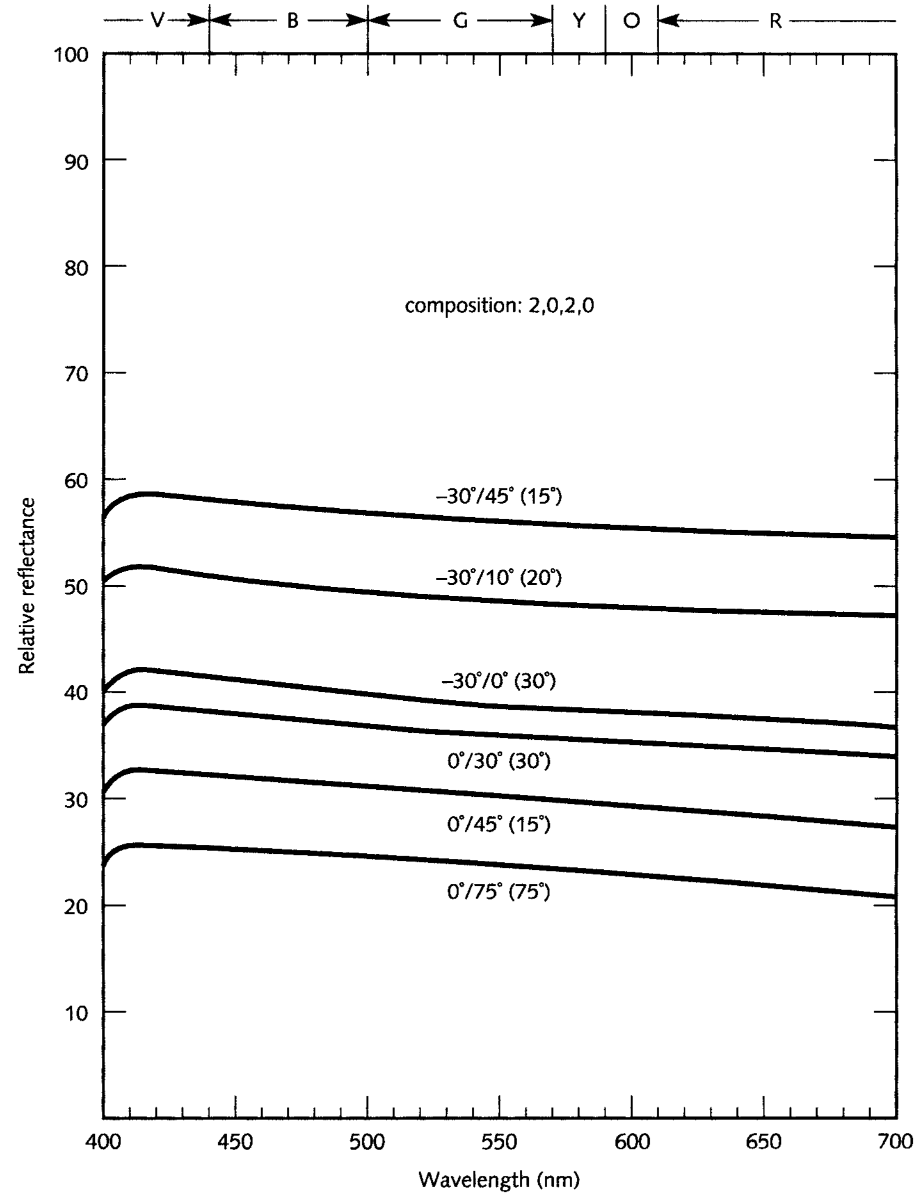

Figure 5.22
Variable-angle goniospectrophotometric measurements of a paint film containing the same aluminum flake in the same amount as in figure 5.19, but also containing 2% rutile TiO_2. Reflectances at near-specular angles are decreased, but at lower angles of view relative to the incident angles, reflectances are increased.

figure 5.19. It can be seen that the addition of a transparent absorbing pigment decreases the reflectance at all angles and that the three characteristic absorption bands of the Quinacridone Magenta remain obvious. (Compare with curves for the closely related Quinacridone Red illustrated in fig. A.16.)

The effect of the addition of carbon black, a transparent, nonselective absorber, is illustrated in figure 5.21. Again the reflectance is lowered (absorption is increased) at all angles of illumination and view. This is as would be expected from Kubelka-Munk theory, described in chapter 4, and from the Beer-Bouguer equation.

However, the effects due to the other constant in the Kubelka-Munk equation—the scattering coefficient, *S*—are far more complex, because light scattering involves so many factors and often gives rise to confusing and unpredictable results. It is particularly puzzling when small amounts of a scattering pigment are added to a metallic flake paint film. The addition of a small amount of TiO_2, representative of a scattering pigment, to an otherwise clear paint made with aluminum flake pigment, results in a *darkening*—as though a black pigment had been added—when the paint is observed near to the specular angle; the addition does not increase the reflectance, as would be expected from Kubelka–Munk theory. At a greater distance from the specular angle, however, the reflectance increases, distinguishing the sample from a film made with black and aluminum flake. This effect is illustrated in figure 5.22 and is summarized in CIE terms in table 5.3.

Figure 5.23 and table 5.3 illustrate the goniospectrophotometric measurements and CIE coordinates of a sample containing both black and white with the same amount of aluminum flake. The effects of each of the pigments, the absorber (black) and the scatterer (TiO_2), are still apparent in the mixture. Figure 5.24 shows a graph of the luminous reflectance, *Y*, versus the various degrees of view off the specular angle.

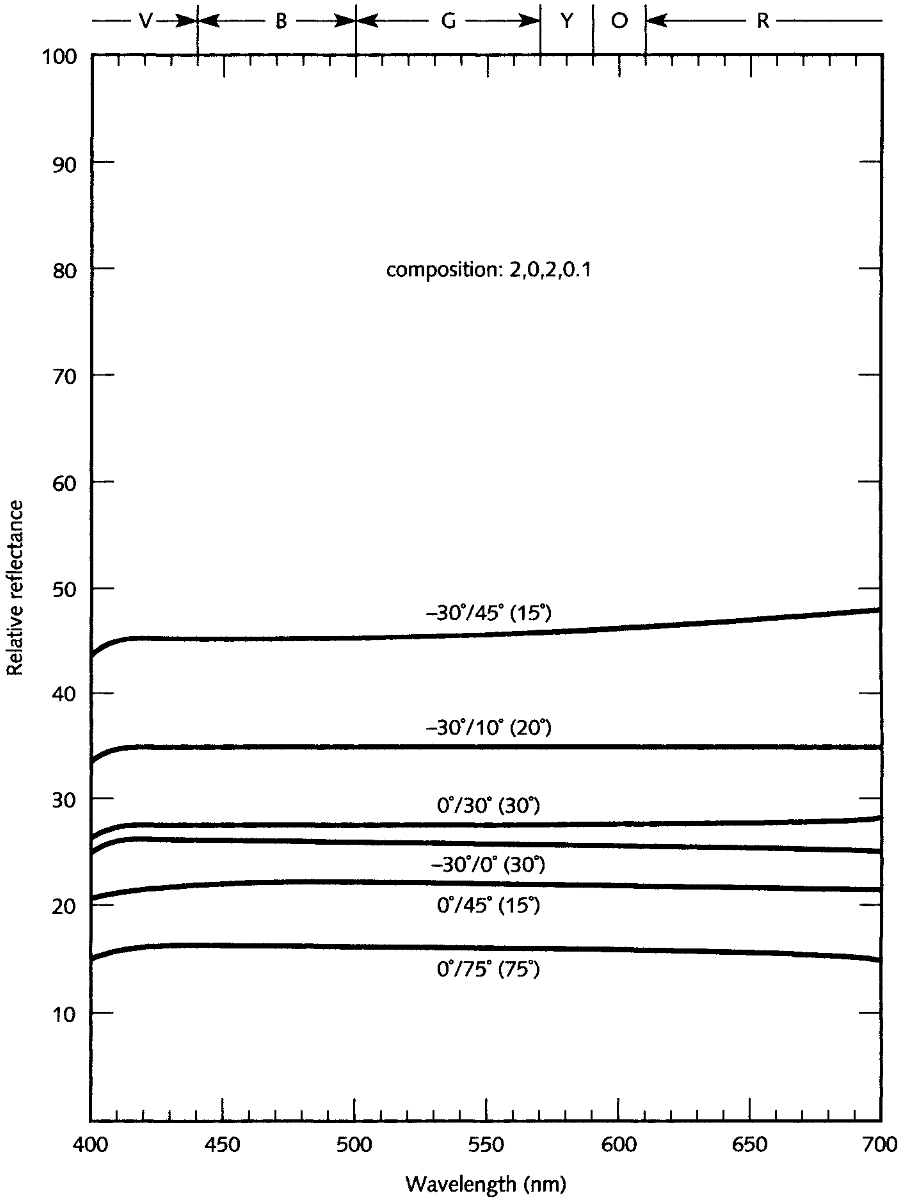

Figure 5.23

Variable-angle goniospectrophotometric measurements of a paint film containing the same aluminum flake in the same amount as in figure 5.19, the same amount of black as in figure 5.21, and the same amount of white as in figure 5.22. The effect of the combination of white TiO_2 with the black is an additive one. At the near-normal viewing angle—for example, 0°/30°—the color is darker than it is when either the black alone, figure 5.21, or the white alone, figure 5.22, is added. However, at low angles of viewing (0°/75°), the color is lighter than it is when only black is added, figure 5.21, but darker than it is when only white is added, figure 5.22. In this case, the lightening effect of white at low angles of viewing is stronger than the darkening effect of black.

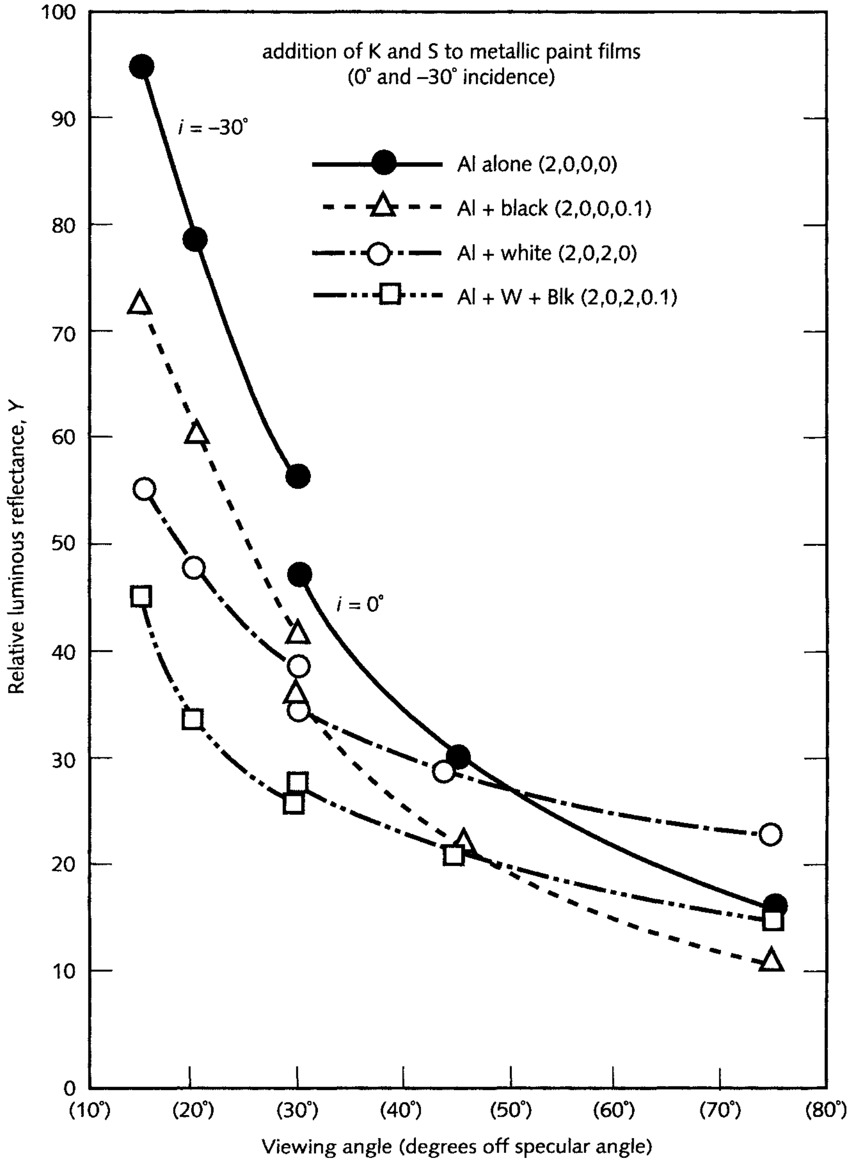

Figure 5.24

Relative luminous reflectance, *Y*, plotted against the degrees of the viewing angle off the specular angle. The addition of K refers to the addition of the black absorbing pigment, and S to the addition of the white scattering pigment. Note that the reflectances measured at different incident angles are different, even when the measurement is made at the same number of degrees off the specular angle, 30°, as illustrated here. Obviously, with this instrument the optics are not reversible.

Thus, the addition of a small amount of a scattering pigment (white) lowers the reflectance near the specular angle but increases the reflectance well off the specular angle of view, even when an absorbing pigment is present. Further increasing the concentration of a scattering pigment, however, results in the more expected behavior of the addition of a scattering pigment—that is, lightening of the color as observed at angles far from the specular angle. But when the concentration of scattering pigment is increased, the specular reflectance of the metallic flake pigment is obscured, and the metallic appearance is decreased.

It should be emphasized that such darkening near the specular angle owing to the addition of a small amount of a scattering pigment occurs whenever any scattering pigment (type I or type III, described in chap. 3) is added, regardless of its hue. Thus, the addition of a small amount of a scattering yellow oxide pigment to a metallic paint film will have a similar effect: darkening of the so-called face color—that is, the color near to the specular angle—and lightening of the so-called flop color, observed well off the specular angle.

The extent of the use of metallic flake pigments in materials of interest in museum collections is not known. However, they may occur in artists' works and in commercial products made since the turn of the last century. Moreover, they may be used increasingly in the future due to their inclusion in artists' tube oil paints by many colorant manufacturers (Smith 1992). One recent catalogue lists eight watercolors varying from silver to gold to copper. Recognizing the possibility of their use is being forewarned.

Chapter 6

Special Topics

The discussion in this chapter involves the description of material characteristics that affect color and appearance but that cannot be attributed to the pigment absorption and scattering described by the Kubelka–Munk theory (chap. 4) or to the special properties of metals and flakes (chap. 5). The characteristics to be considered include surface structure (such as glossiness and matteness), as well as fluorescence, extender pigments, and internal structure, such as microvoids. All of these factors may affect the perceived color and the difference in color between similar objects. It is often difficult to ascertain the cause of observed differences between objects as a result of such factors or to visualize the changes they may induce in color.

Surface Reflection

Objects can exhibit surface reflection that varies between a high gloss and a flat or matte (diffusely reflecting) appearance. Between these two extremes, materials may exhibit a myriad of textures, from "micro" roughness (beyond visual resolution), which is often categorized as semigloss, to various obvious "macro" surface irregularities. In addition to those due to textural roughness, color variations may be encountered that are much more subtle. Mottled color variations will not be considered here (see chaps. 2 and 8).

Refractive index differences: The cause of surface reflection

That surface reflection always occurs when incident light encounters a material of different refractive index has been emphasized previously. For dielectric (nonelectrically conducting) materials, the amount of the surface reflection is described by equation 4.3 and illustrated in figure 4.2. The amount of the incident light reflected depends on the ratio of the refractive indices of the two materials at the interface. In the case of the upper surface reflection, the incident light passes from air, with refractive index n_1 (in eq. 4.3, this is set equal to 1.000), to the surface material, of refractive index n_2. It should be emphasized, however, that interfaces between materials can occur throughout the body of mixtures, not just at the air–material interface. Indeed, the opacity exhibited by pigments is dependent on surface reflection at the interfaces of the pigment particles with the vehicle in which they are suspended. Although most examples presented here refer to pigmented materials such as paints, surface reflection always occurs from objects or we would not be able to see them.

The refractive index of a material changes with wavelength. Commonly cited, so-called characteristic refractive indices of materials are assumed to be those measured at 589 nm, the median wavelength of the sodium D lines, unless specifically designated otherwise. In the case of nonmetallic materials, the refractive index and, therefore, the surface reflection, changes so slightly with wavelength that, for practical purposes, it can be treated as a constant. (An exception occurs in the case of bronzing described in chap. 5.)

When glossy samples are viewed, the specular reflection from the surface is excluded from the visual evaluation of color. To illustrate the effect of this exclusion on the color, consider an off-white glossy sample that reflects 80% diffusely and 4% specularly. The surface reflection of 4% in this case represents 4/84, or 4.8%, of the total reflected light. On a dark glossy material of the same surface composition that has a total reflectance (diffuse plus specular) of 10%, the same 4% now represents 4/10, or 40%, of the reflected light. Thus, small differences in the surface reflection characteristics are far more significant in dark colors than in light colors, a fact well appreciated by artists and conservators. In the case of high-chroma colors (where in one wavelength region the total reflectance is very low, such as the 10% illustrated above, and in another region of the visible spectrum it is very high, such as the 84% for the off-white described above), differences in surface reflection alter the purity or saturation of the perceived color as well as its lightness, but they do not alter its dominant wavelength or hue. When the surface is not glossy, the diffuse surface reflectance is essentially the color of the light source and is additively mixed with the internal diffuse reflectance, which lowers the perceived chroma.

In what follows, the microstructure of surfaces is considered first. When matte surfaces are compared, the structure of this surface is one of the most insidious aspects affecting their appearance—insidious because it is difficult both to identify precisely and to adjust in order to create an identical appearance in two objects. As has been emphasized previously (chap. 4), the nature of the first-surface reflection plays an important role in determining the perceived color that occurs as a result of the selective reflection of the colorants within the object. An extensive, annotated bibliography, *Matte Paint,* has been published by Hansen, Walston, and Bishop (1993).

In this initial discussion of micro surface reflection differences, the assumption is made that the sample surface exhibits rotational symmetry: at each set of incident and viewing angles, the sample may be rotated in its own plane through 360° without exhibiting a significant change in the measured reflectance. The assumption is also made that the pigmentation is the same in the two members of each sample pair.

Matte surfaces that exhibit geometric metamerism

As was pointed out in chapter 2, slight differences in surface structure between pairs of samples of the same pigmentation can lead to geometric metamerism—that is, the pair can appear to be identical in color at one set of illumination and viewing angles but no longer appear to be the same when the viewing or the illumination angle is changed. Figures 6.1 and 6.2 illustrate the variable-angle reflectance measurements, relative to pressed $BaSO_4$ reference white, of two sets of two differently pigmented paint panels—one a violet (light purple), the other a purple—exhibiting surface reflections that seem to be similarly diffuse. The violet and purple samples numbered 1 in figure 6.1 have the same matte surface characteristics. The two samples labeled 2 in figure 6.2 also have the same surface characteristics, with the exception that they also have been coated with a vehicle containing a silica flatting agent. Both appear to be matte surfaces. It can be seen that the samples in figure 6.1 exhibit increasing

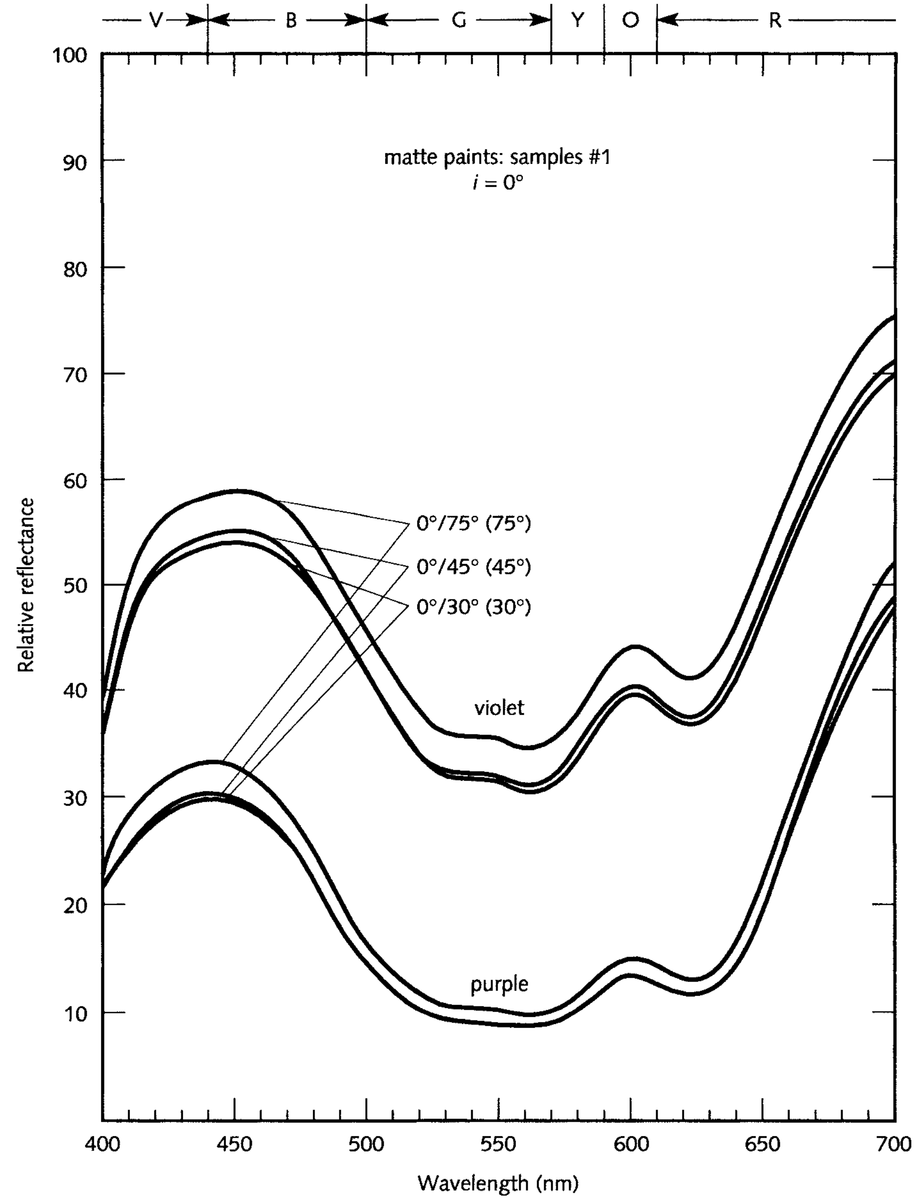

Figure 6.1

Variable-angle reflectances measured on matte paints, a violet and a purple, both pigmented with carbazole dioxazine violet and rutile TiO_2. The measurements were made relative to $BaSO_4$ white standard. Note that the reflectance increases as the angle of viewing increases away from the incident angle, which is also the specular angle; reflectance continues to increase to 75° for both the purple and the violet.

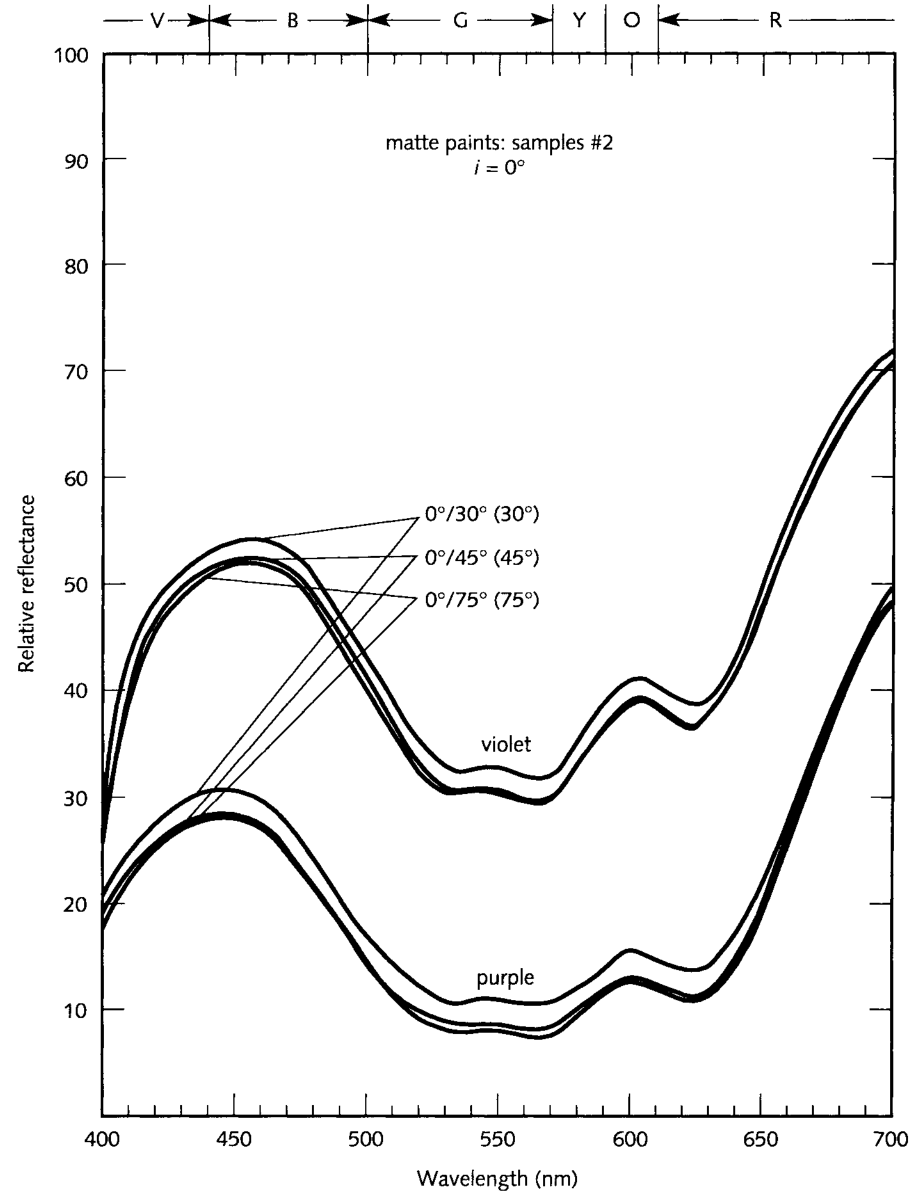

Figure 6.2

Variable-angle reflectances measured on the violet and purple matte paint panels coated with a thin application of vehicle containing a small amount of silica flatting agent. The appearance is still that of a matte paint. Note that the highest reflectance for both the violet and the purple is that made at 30°; reflectance decreases as the viewing angle increases away from the specular angle. In contrast, the maximum reflectance for the uncoated samples in figure 6.1 is farthest away from the specular angle.

reflectance as the viewing angle increases away from the specular angle, 0°. On figure 6.2, however, the samples do the opposite—that is, their reflectances decrease as the viewing angle increases away from the specular angle. The samples were made with carbazole dioxazine violet pigment in mixture with white (see fig. A.25).

Table 6.1 gives the CIE tristimulus data relative to pressed $BaSO_4$ reference white for the variable-angle measurements shown in figures 6.1 and 6.2.

The same Trilac spectrophotometer used for the variable-angle measurements was also used in the sphere mode, with the same pressed $BaSO_4$ white standard. CIE data calculated from these measurements are tabulated in table 6.2.

Comparison of the color differences, ΔE^*_{ab}, calculated from the sphere-mode measurements (table 6.2) and from the variable-angle measurements (table 6.1) illustrates the lack of sensitivity of the

Table 6.1

Variable-angle measurements on violet and purple pairs of matte paints (CIE coordinates; illuminant C; 1931 standard observer; color difference equation, eq. 2.4).

Sample	$i°/v°$	X	Y	Z	x	y	L^*	L^*_2 / L^*_1	ΔE^*_{ab} (Std. = 1)
Violet 1	0°/30°	39.08	35.43	61.18	0.2880	0.2611	66.09	—	
Violet 2	0°/30°	40.27	36.72	60.92	0.2920	0.2662	67.07	1.015	2.2
Purple 1	0°/30°	15.38	11.93	31.72	0.2606	0.2021	41.11	—	—
Purple 2	0°/30°	16.79	13.61	33.15	0.2642	0.2142	43.67	1.062	4.7
Violet 1	0°/45°	40.06	36.22	62.08	0.2895	0.2618	66.69	—	—
Violet 2	0°/45°	38.55	34.84	59.00	0.2912	0.2613	65.63	0.984	1.6
Purple 1	0°/45°	15.61	12.04	32.33	0.2602	0.2008	41.28	—	—
Purple 2	0°/45°	14.58	11.10	30.35	0.2603	0.1980	39.75	0.963	1.4
Violet 1	0°/75°	43.72	39.88	66.92	0.2904	0.2649	69.39	—	—
Violet 2	0°/75°	38.40	34.67	58.62	0.2916	0.2633	65.49	0.944	4.0
Purple 1	0°/75°	17.26	13.52	35.64	0.2599	0.2035	43.54	—	—
Purple 2	0°/75°	14.08	10.55	30.07	0.2575	0.1928	38.82	0.892	5.2

$i°$ = incident angle; $v°$ = viewing angle; 0° = perpendicular to the surface
1 = sample 1 in figure 6.1; 2 = sample 2 in figure 6.2

conventional sphere measurement to the subtle surface angular reflectance differences in these samples. Attempts to reconcile such measurements with visual evaluations can be frustrating indeed.

An additional comment can be made on the sphere-mode measurements: Note in table 6.2 that the total reflectance measurements, SCI, are lower on most of the matte number 1 samples (uncoated) than the diffuse, SCE, measurements. This phenomenon is encountered often on very matte surfaces made with TiO_2. This pigment has a significantly higher refractive index than the pressed $BaSO_4$ standard and hence higher surface reflectance (see Kortüm 1969). In addition, pressed $BaSO_4$ has a slight sheen at angles approaching grazing angle that is not encountered with the most diffuse TiO_2 pigmented matte paints. The effect of TiO_2 on surface characteristics has been discussed by Braun (1991).

The relationships between the angular reflectances of the two types of surfaces described above for samples 1 and 2 can be seen more vividly by plotting their lightness, L^*, against the angle of view (the same as the angle off the specular angle because the incident angle is 0°), as shown in figure 6.3a. At about 38° to 40°, the lightness values cross, as clearly shown by the lightness ratios plotted in figure 6.3b. This measured reversal with angle of viewing is in agreement with visual observation. (It is interesting to note that the angle at which many geometric metamers

Table 6.2

Violet and purple matte paint pairs measured with integrating sphere geometry (CIE coordinates; illuminant C; 1931 standard observer; color difference equation, eq. 2.4).

Sample	Geometry[a]	X	Y	Z	x	y	L^*	L^*_2 / L^*_1	ΔE^*_{ab} (Std. = 1)
Violet 1	SCE	40.31	37.17	62.09	0.2888	0.2663	67.41	—	—
Violet 2	SCE	39.76	36.66	59.99	0.2914	0.2687	67.02	0.994	1.21
Purple 1	SCE	16.28	12.98	34.07	0.2570	0.2050	42.74	—	—
Purple 2	SCE	16.44	13.29	33.03	0.2607	0.2108	43.20	1.011	1.01
Violet 1	SCI	39.74	36.59	61.54	0.2882	0.2654	66.97	—	—
Violet 2	SCI	39.73	36.60	60.26	0.2908	0.2679	66.98	1.000	1.14
Purple 1	SCI	16.06	12.82	33.63	0.2569	0.2050	42.49	—	—
Purple 2	SCI	16.45	13.34	33.25	0.2609	0.2116	43.27	1.018	1.02

[a] SCE = specular component (of the reflectance) excluded; SCI = specular component (of the reflectance) included
1 = sample 1 in figure 6.1; 2 = sample 2 in figure 6.2

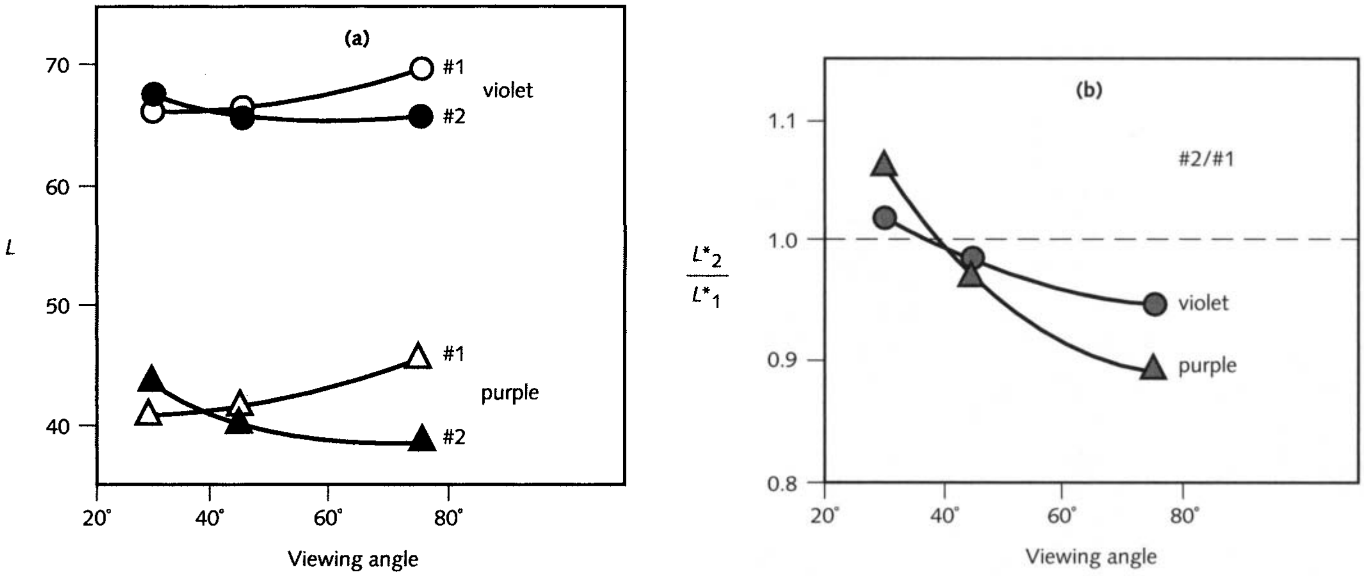

Figure 6.3

(a) Values of L^* for the variable-angle measurements illustrated in figures 6.1 and 6.2, plotted against the viewing angle when the incident angle is 0°. Note that the two types of surfaces match at about 40° viewing. (b) The ratio of the L^* measurements of the violet and purples, based on the data shown in (a).

match is at about 45° when the incident illumination angle is near normal; see the discussion on flake pigments in chap. 5, for example.)

These samples were prepared intentionally to illustrate (1) the phenomenon of geometric metamerism commonly encountered with matte-surface materials, and (2) the effects of changes in micro surface structure on the perceived color of matte surfaces. The two colors were also chosen to illustrate that surface reflection differences are visually more important as the colors become darker. Compare the color differences, ΔE^*_{ab}, of the violets relative to those of the darker purples; the latter exhibit larger color difference when measured at 0°/30° and at 0°/75°. The color differences are similar in magnitude at the angle close to the match angle, 0°/45°. Samples numbered 1 were used as the standard.

In this illustration, sample 2 is the same as sample 1, but the difference between them arises because sample 2 was sprayed with a thin layer of clear vehicle that also contained a small amount of a silica flatting agent. Thus, the samples exemplify a type of problem often encountered when one attempts to consolidate powdery or matte surfaces of museum objects in order to preserve them. An appreciable application of consolidating resin changes the optics of the surface reflection and simultaneously changes the color perceived at various angles.

Figure 6.4 helps explain, in a somewhat simplistic manner, the differences in surfaces that can occur when a clear film of vehicle is applied over a very diffuse surface. Illustration (a) represents the diffuse surface; illustration (b) shows an excellent consolidant application in which the applied vehicle penetrates into the interstices (air spaces) around the pigment on the surface but does not form a film on the upper surface; illustration (c) shows what occurs at the extreme case, in which the applied vehicle does not penetrate into the interstices but stays on top of the surface, forming a smooth, shiny film. A further difficulty can contribute to a less-than-ideal penetration: if the resin solution does not "wet"—that is, it does not adhere to the dry pigment on the surface—the resin can form a film that has poor adhesion to the surface.

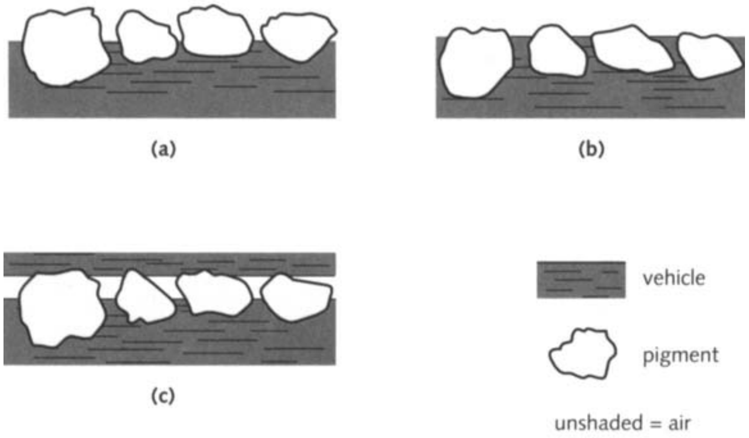

Figure 6.4
(a) Typical matte paint with pigment particles protruding through the surface, causing scattering of the light. (b) Adding a small amount of a vehicle applied to the matte paint fills part of the air interstices between the pigment particles. The result is an increase in the specular reflectance when the angles of incidence and viewing are near to the perpendicular, and a darkening when the angle of incidence is still near to the perpendicular but the viewing angle is closer to the horizontal.
(c) Vehicle is applied over the matte surface but does not penetrate and replace the air in the pigment interstices. A film is formed over the surface, gloss is increased, and the color is thus darkened. Although the surface has become glossy, the entrapped air in the interstices scatters light and partially offsets the darkening. This effect is often the result of inadequate wetting of the surface, which also leads to poor adhesion to the surface.

The film illustrated by (c) in figure 6.4 exhibits some specular gloss, although the color is not as dark as would be expected if there were no air pockets trapped under the film to scatter the light. Even with the rather ideal coating application illustrated in (b), at near-normal illumination and viewing, there is a slight increase in surface reflectance at the angle nearest the specular angle. Such considerations imply that there may be no perfect technique to consolidate powdery surfaces without some change, however slight, in the perceived color.

Hansen, Lowinger, and Sadoff (1993) have developed a technique for achieving good penetration of resin solution into powdery surfaces such as are found on ethnographic objects. This technique involves spraying the object and then keeping it in a closed container filled with solvent vapor. This procedure allows the resin solution time to penetrate into the interstices and replace the air around the protruding particles before the solvent evaporates and a film forms. When the objects are of complex shape or color, or both, the problem of surface alteration of this type may be less acute than when the matte surface is perfectly planar and consists of large areas of a uniform single color. In the latter situation every slight change is obvious.

Matte surfaces are not the only type that exhibit geometric metamerism. Almost any type of surface, short of those with high gloss, may exhibit the phenomenon. Intermediate-gloss surfaces present many possibilities for subtle surface-structure differences.

Surface effects on low-chroma and high-chroma colors

The effects of surface differences on a high-chroma color relative to the same differences on a neutral color can be illustrated by examining the reflectance measurements made on two samples of gel-coated, glass-fiber laminates, one a high-chroma red and the other a neutral gray. The surface characteristics of gel coats, widely used to make glass-fiber laminate boats, are determined by the surface characteristics of the mold employed in their construction and are not attributable to differences in composition. (Gel coats contain no solvent; the liquids are polymerized in the curing process.) If the interior of the mold is very smooth and shiny, the surface cast against it will be glossy; if the mold has a textured surface, so will the object cast in it. The amount of pigment in the plastic gel coat is small relative to that used in paints—often less than 10%—and it does not affect the surfaces.

Three types of mold surfaces were used for each of the red and gray gel coats: a very high gloss; a matte; and a highly textured, wrinkle effect. Figures 6.5 and 6.6 show the reflectance curves of these six samples as measured with the specular component of the reflectance excluded (SCE)—that is, diffuse reflectance. The two glossy samples appear darker than the corresponding matte and textured samples. The red glossy sample is obviously higher in chroma, or saturation, than either of the other two reds. Figures 6.7 and 6.8 depict the reflectances measured with the specular component of the reflectance included (SCI)—that is, total reflectance. All of the measurements were made with the Trilac spectrophotometer operated in the sphere mode relative to pressed $BaSO_4$ reference.

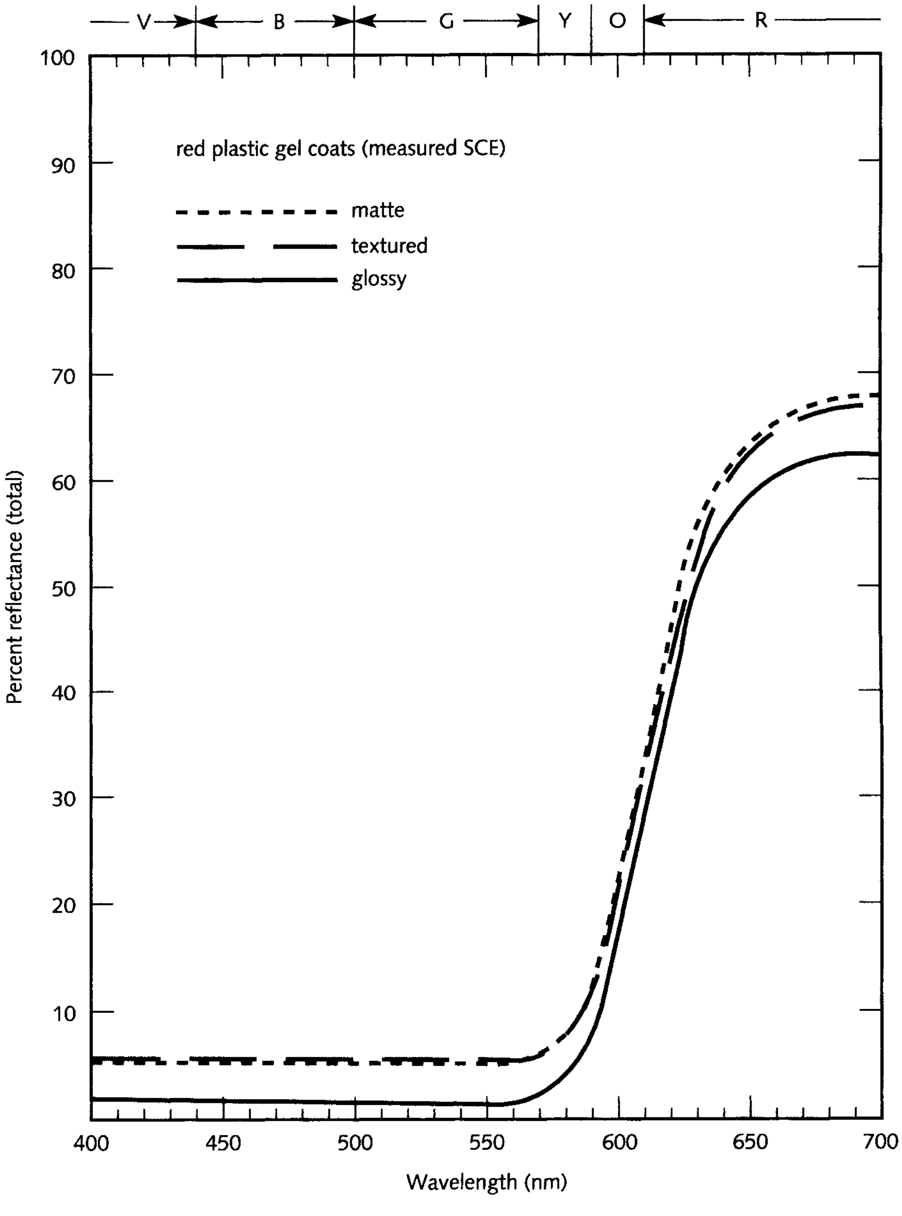

Figure 6.5

Spectral reflectance measurements of three red plastic, gel-coated, glass-fiber laminates exhibiting different surface characteristics. Specular reflectances were excluded. The panels were pigmented with cadmium red medium.

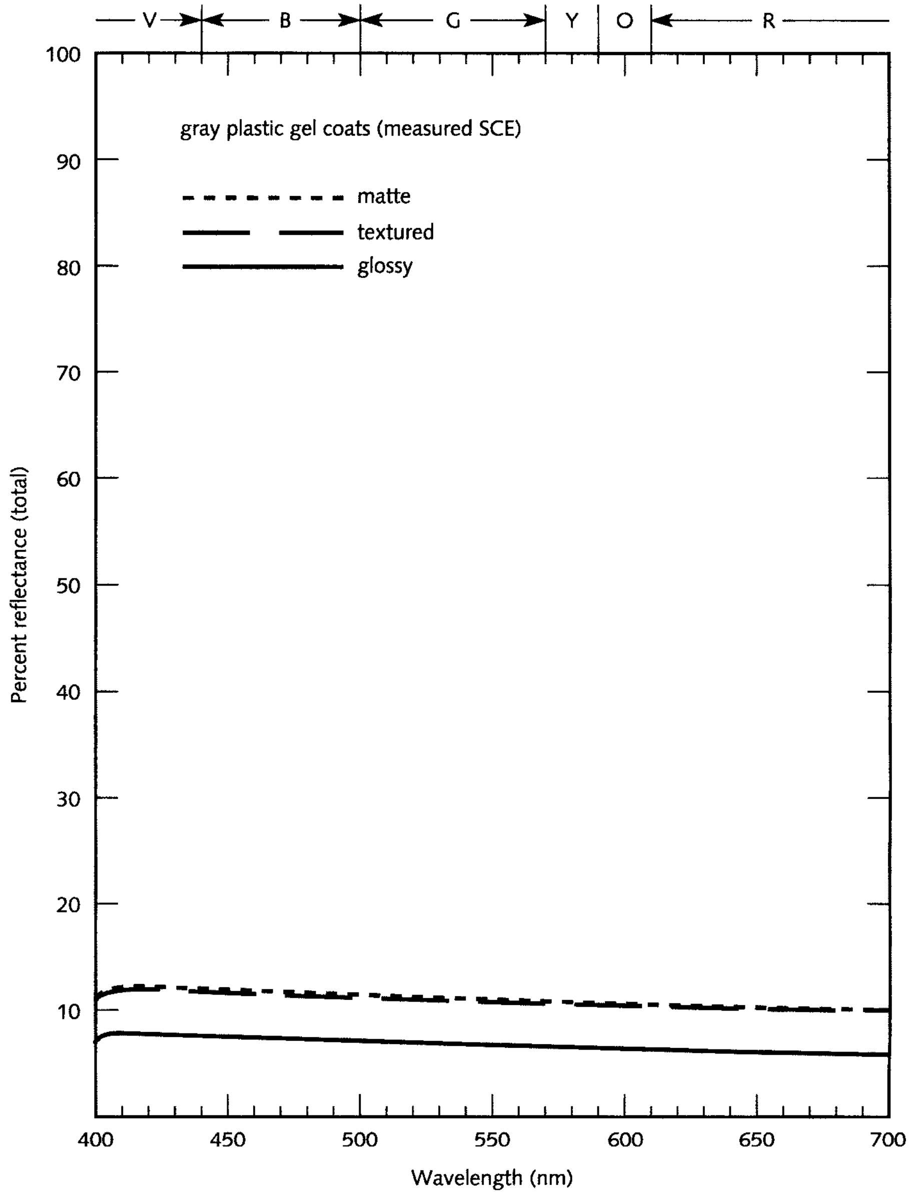

Figure 6.6

Spectral reflectance measurements of three gray plastic, gel-coated, glass-fiber laminates exhibiting the same three surface characteristics as the red panels in figure 6.5. Specular reflectances were excluded. The panels were pigmented with rutile TiO_2 and black.

Figure 6.9 illustrates schematically the angular reflectances for two different surfaces. The glossy surface reflectance illustrated in (a) has a sharp, spiked specular reflectance, marked S in the figure, superposed on the diffuse reflectance, D. When gloss decreases, the width of the specular spike increases, and the height of the spike decreases, as illustrated in (c). One type of integrating sphere, discussed in chapter 1, is illustrated schematically in (b) and (d). The illustrated technique using the spheres is often used with spectrophotometers for measuring separately the total and diffuse reflectances. When the insert in the sphere wall is the same white as the sphere interior wall, all of the light reflected by the sample is included in the measurement (SCI); when the insert is black or is a light trap, then the specular reflectance, S, is absorbed, and only the diffuse reflectance (SCE) is measured. For the high-gloss sample, diagrammed in figure 6.9 as (a), the specular reflectance, S, can be completely absorbed by the black insert and eliminated from the measurement, as illustrated in

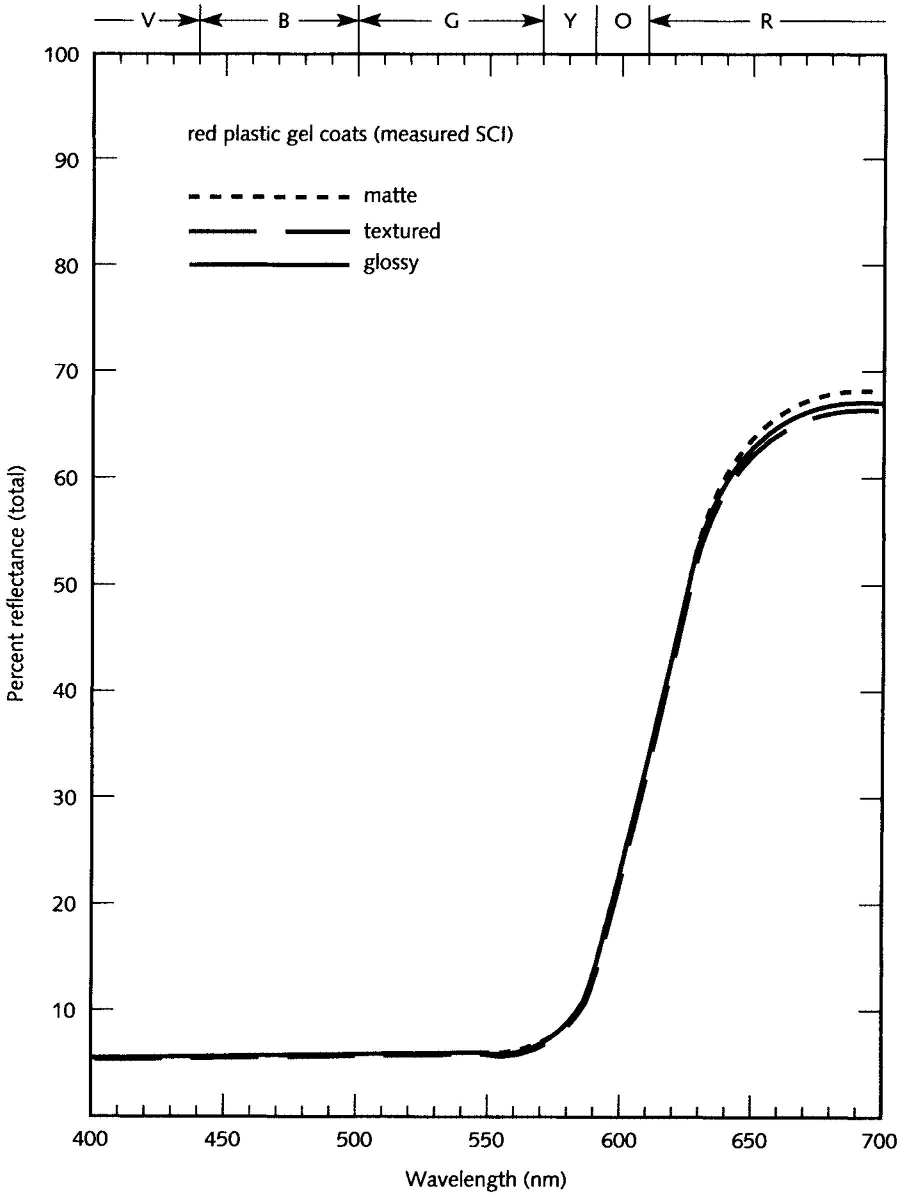

Figure 6.7

Spectral reflectances of the three red plastic, gel-coated, glass-fiber laminates with the different surface characteristics illustrated in figure 6.5, but measured with the specular reflectance included, SCI (total reflectance). Note that the reflectances are very close.

(b). When the gloss is decreased, as illustrated in figure 6.9 as (c), the surface reflectance at the specular angle can no longer be completely eliminated by the black insert and is partially included in the measurement of the diffuse reflectance, as illustrated in (d).

Other designs for including or excluding the specular surface reflection on integrating-sphere spectrophotometers have been used, but basically all give similar results.

Table 6.3 gives a summary of the tristimulus values and chromaticity coordinates (1931 2° standard observer, illuminant C) of the red and gray plastic gel coats whose spectral reflectance curves are illustrated in figures 6.5–6.8. Color differences of the matte and textured samples were calculated relative to the corresponding glossy samples. Note that the luminous reflectances, Y, of the two colors were not identical: for the red (measured SCE), $Y = 8.83$; for the gray (measured SCE), $Y = 6.87$. Nonetheless, they were not in an entirely different range.

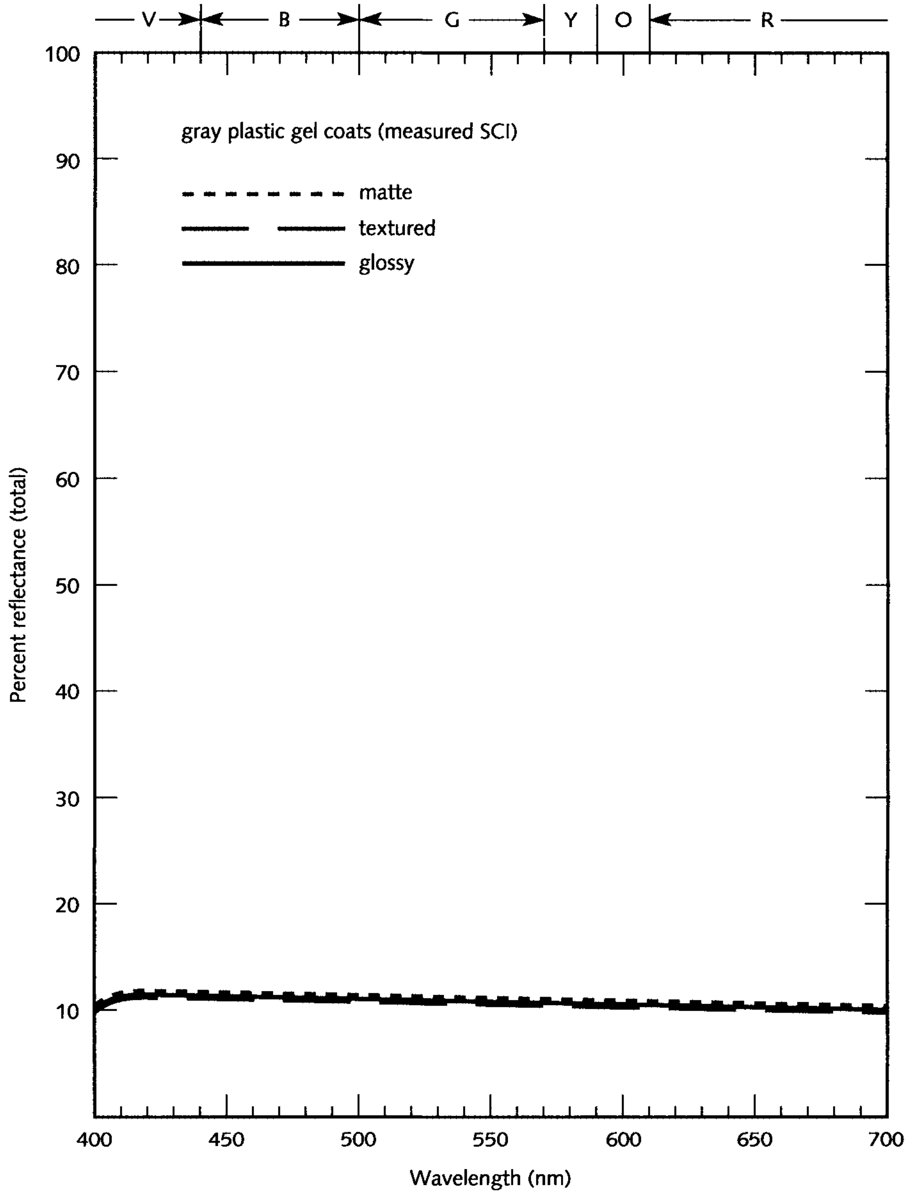

Figure 6.8
Spectral reflectances of the three gray plastic, gel-coated, glass-fiber laminates with the different surface characteristics illustrated in figure 6.6, but measured with the specular reflectance included, SCI (total reflectance). Note that these reflectances are also very close.

Inspection of the curves and the calculations measured with the specular reflectance excluded (SCE) show the effect of surface reflectance dissimilarities on the perceived color of the high-chroma red samples relative to the same surface differences in the achromatic grays. The matte red plastic panel and the glossy red panel are illustrated in color plate 4. For the red panel, the color difference of the matte samples, M, relative to the glossy samples, G, is chiefly due to the chromaticity difference, $\Delta C = 19.0$, with a smaller effect due to the lightness difference, $\Delta L^* = 6.7$. On the other hand, for the achromatic gray panel with the corresponding surfaces, the chromaticity difference, ΔC, is very small on the matte sample (equal to 0.43), whereas the total color difference, $\Delta E^* = 8.0$, is almost completely due to the lightness difference, $\Delta L^* = 8.0$. Note also that the total color difference is much higher for the red samples, $\Delta E^* = 20$, versus $\Delta E^* = 8.0$ for the corresponding achromatic gray samples.

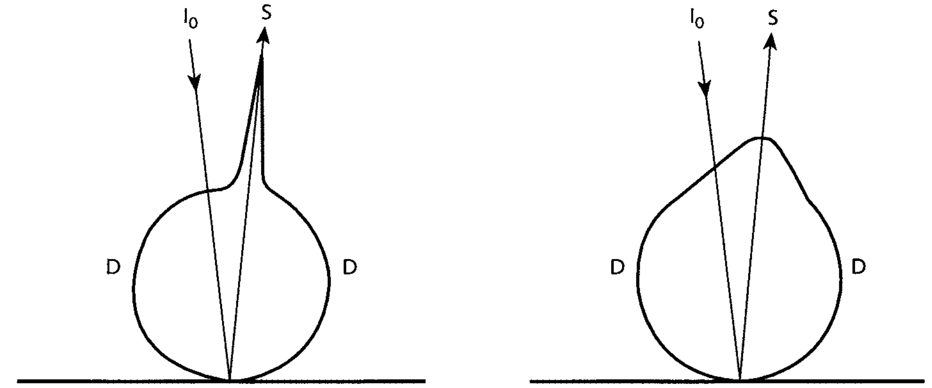

glossy surface

(a)

semimatte surface

(c)

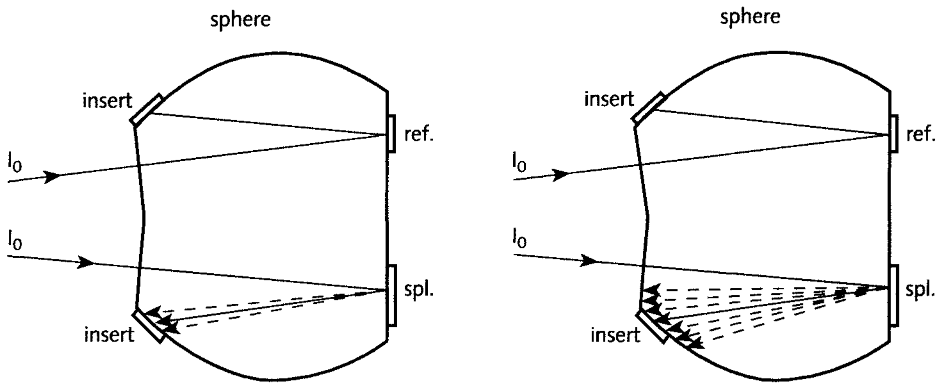

glossy surface

(b)

semimatte surface

(d)

Figure 6.9

Angular distribution of the specular, S, and diffuse, D, reflectances of a high-gloss surface (a) and a semimatte surface (c). I_0 refers to the incident light ray, near to the perpendicular, or normal. Note that for the semimatte surface, the specular peak, S, is broadened and decreased in height. Diagram (b) shows how the specularly reflected light of a glossy surface is measured with an instrument that uses an integrating sphere with the angle of incidence near to the normal. When the sphere insert at the angle equal to and opposite the incident angle is black or a light trap, the specular reflectance is absorbed, and only the diffusely reflected light is reflected onto the white sphere wall and recorded by the detector. See the reflectance curves of the red and the gray glossy, plastic laminates measured with the specular component of the reflectance excluded (SCE) in figures 6.5 and 6.6. Diagram (d) shows how the specularly reflected light is measured for the semimatte surface with an integrating sphere instrument. When a black insert is placed in the sphere wall at the angle equal to and opposite the incident angle, only a portion of the specular reflectance is excluded. When a diffuse white insert that matches the sphere wall is placed in the sphere, all of the reflected light is included in the measurement—that is, the total reflectance is measured. See the curves for the SCI measurements of the red and gray plastic panels in figures 6.7 and 6.8, illustrating that they are the same when all of the light is measured. (Small differences may be due to wear and tear on the panels; they were rather old when these measurements were made.)

Although it is not readily apparent from these data, the chromaticity difference, ΔC, which is so high on the red matte and textured samples relative to the glossy red, is all due to differences in saturation and not to differences in hue. Figure 6.10 shows a portion of the CIE 1931 chromaticity diagram for the red region with the locations of the chromaticity coordinates from table 6.3 for the three red samples (measured SCE). Point C is the illuminant point (0% purity). The lines of constant purity for 60%, 80%, and 100% are indicated on the diagram and illustrate the decrease that takes place as the surface gloss is decreased. Clearly demonstrated is the fact that the dominant wavelength does not change, as illustrated by the straight-line connection of all points for the red samples with the illuminant point. The dominant wavelength for all is 614 nm. This effect has been well documented (Judd and Wyszecki 1975).

At the beginning of this section on surface reflection, it was stated that highly textured samples exhibiting so-called macro surface irregularities would not be the major topic of the initial discussion. The reflectances of the textured gel-coated laminate samples that had been prepared and measured for the previous example can be of interest,

Sample[a]	Geom.[b]	X	Y	Z	x	y	ΔL^*	Δa^*	Δb^*	ΔC	ΔE^*_{ab} (Std. = G_{Spl})
R/g	SCE	17.16	8.83	1.46	0.6249	0.3216	—	—	—	—	—
R/m	SCE	21.27	12.74	5.77	0.5345	0.3203	+6.72	−8.33	−16.826	19.00	20.16
R/t	SCE	20.83	12.68	6.22	0.5242	0.3191	+6.63	−10.00	−18.943	21.42	22.42
G/g	SCE	6.74	6.87	8.87	0.2997	0.3056	—	—	—	—	—
G/m	SCE	10.75	10.97	13.79	0.3027	0.3088	8.025	−0.301	0.305	0.43	8.04
G/t	SCE	10.72	10.92	13.66	0.3035	0.3094	7.935	−0.168	−0.125	0.21	7.94
R/g	SCI	21.55	13.34	6.86	0.5161	0.3196	—	—	—	—	—
R/m	SCI	21.83	13.41	6.67	0.5208	0.3199	0.10	2.74	0.942	2.90	2.92
R/t	SCI	20.82	12.78	6.52	0.5188	0.3186	−0.84	2.07	−0.075	2.07	2.07
G/g	SCI	11.10	11.34	14.18	0.3032	0.3096	—	—	—	—	—
G/m	SCI	11.35	11.58	14.53	0.3030	0.3091	0.390	−0.096	−0.173	0.20	0.44
G/t	SCI	10.82	11.03	13.81	0.3034	0.3092	−0.52	−0.188	−0.024	0.19	0.55
R/t	SCE										
R/t	SCI						+0.15	−0.71	−0.991	1.22	1.23
G/t	SCE										
G/t	SCI						+0.19	0.064	0.056	0.085	0.21

[a] R = red; G = gray; g = glossy; m = matte; t = textured

[b] SCE = gloss excluded; SCI = gloss included

Table 6.3

Red and gray gel-coated plastic laminates measured with integrating sphere geometry (CIE coordinates; illuminant C; 1931 standard observer; color difference equation, eq. 2.4).

however. The textured surfaces resembled rough leather designed for possible use as a nonskid surface. The reflectance measurements and CIE data presented at the bottom of table 6.3 illustrate that there is relatively little difference on the textured samples, T, between the measurements made with the specular reflection included or excluded. Generally, both

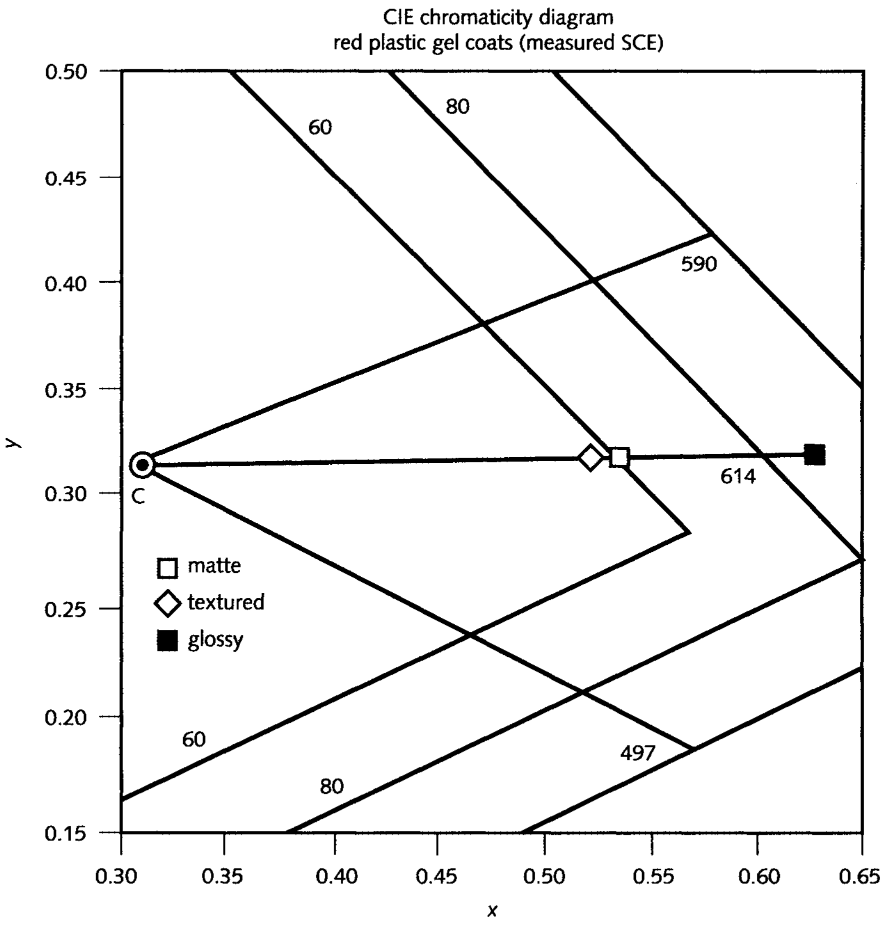

Figure 6.10

CIE 1931 chromaticity diagram of the three red plastic, gel-coated laminates of different surface structure, measured with the specular reflectance excluded (SCE). When surface characteristics alone contribute to the observed color differences, the only change in chromaticity is in the purity (chroma) of the color. The dominant wavelength (hue) remains unchanged.

of these measurements are a little lower than the total reflectances of the other two surfaces—the gloss, G, and matte, M—probably due to light trapping in the irregularities of the surface structure (Ogilvy 1991).

The assumption made for the samples exhibiting micro surface scattering—that the surface reflectances exhibited rotational symmetry—that is, that they did not change as the sample was rotated through 360° in the sample plane—is not a valid assumption in the case of macro textured samples—for example, textiles or surfaces formed by brush marks (Judd and Wyszecki 1975). Such mechanically formed surfaces can exhibit characteristic rotational surface reflectance differences. Thus, at constant illumination and viewing angles, the surface reflectance may change as the sample is rotated in its plane through 360°. The most sensitive measurements of such changes can be made with goniospectrophotometry; the measurements are made at the specular angle, such as –45°/45° incident and viewing angles, and the samples are rotated in the plane through 360°.

Although the interpretation of such goniospectrophotometric measurements may require a high degree of sophisticated knowledge regarding such materials as textiles, which are not cast against a mold, characterization on mechanically created surfaces can be informative. For example, textured papers may exhibit rotational surface reflection that is characteristic of the calender used in their manufacture.

There are many references in the modern literature relating to the characterization of the reflectances of surfaces, a problem independent of the study of color, and no attempt is made here to survey them. Numerous mechanical and optical methods have been devised to provide profiles of the structure of surfaces (Lettieri et al. 1991).

Types of gloss

Attempts to characterize the surface appearance of objects and materials have been carried on for many years, concurrently with attempts to characterize and describe their color. Hunter (1938) and Hunter and Judd (1939)—see also Judd and Wyszecki (1975)—list five different types of gloss: specular, sheen, contrast, distinctness of image, and absence of bloom. All are attributable to aspects of the reflected light basically caused by the effect of the refractive index and the surface characteristics on the surface reflectance.

Special instruments have been designed for the measurement of these various surface reflection factors (Judd and Wyszecki 1975)—as opposed to absolute surface reflectances measured relative to a perfect mirror. These special instruments are called *glossmeters* and are, in effect, abridged goniophotometers. They are designed to measure the relative intensity of the specularly reflected light at fixed angles of illumination and viewing. Each instrument is supplied with reference standards calibrated as unity for the geometrical conditions used. Thus, the measurements are not absolute and so are not relatable to the effect of gloss on observed color. For measuring the specularly reflected light, 20° gloss instruments are used for measuring high-gloss samples; 45° or 60° gloss-measuring instruments are used for intermediate, semigloss materials; and 75° or 85° glossmeters are used for near-matte, diffusely reflecting samples to measure their so-called low-angle sheen (ASTM Standard D 523).

The appearance aspects of the five different types of gloss have been defined in terms of glossmeter measurements. Specular gloss is described as it has been used here: reflectance at the angle equal and opposite to the incident angle (–*i*°/+v°, where *i* = *v*). Sheen is described as the shiny reflectance on matte surfaces when observed near the grazing angle, such as 85° from the perpendicular (–85°/85°). Contrast gloss relates the reflectance at the specular angle to the reflectance well off the specular angle (such as –60° incident angle and +60° viewing angle); *the ratio* relative to a measurement at 0° (–60°/0°, that is, –60°/60°/–60°/0°) is then measured. Distinctness-of-image gloss is measured by viewing the glossy sample at another angle, a few *minutes* of arc away from the specular angle, essentially determining the slope of the change in reflectance at an angle close to the specular. *Bloom* is a term generally associated with a haziness that develops on the surface of high-gloss paint films or plastics, sometimes attributable to the exudation of a plasticizer, for example. Bloom is measured by making one measurement at the specular angle, such as –60°/60°, and a second measurement a few *degrees* of arc away from the specular angle, such as –60°/63°, and is generally described, for example, as the ratio –60°/60°/–60°/63°. In this case, the measurement at the second angle is farther from the specular angle than for distinctness-of-image gloss.

The preferences for an ideal or desired set of characteristics of a glossy surface are highly subjective. In general, in articles of commercial importance, if a surface of higher refractive index, exhibiting high intensity of specular reflectance, is flawed—that is, it exhibits some degree of micro or macro irregularity (like an orange peel)—the imperfect surface has been found to be more objectionable than a more nearly mirrorlike image reflector with no flaws—that is, of better distinctness of image. This is so even though there may be lower intensity in the reflected image because of a lower refractive index in the latter case (Judd and Wyszecki 1975). For example, at one time in the automotive industry, it was thought that the magnitude of the intensity of the surface reflection of a car's finish was paramount. Later, the trend turned toward placing more importance on the distinctness-of-image gloss (Braun 1991).

Determining the subjective preference between two samples, one with sharp distinctness-of-image gloss and the other with higher intensity of reflectance but lower distinctness of reflected image, poses problems. Attempts at ranking samples with varying degrees of the two types of gloss have proved difficult. "In any case the result is dependent on the specific choice of the observer. The situation is similar to the comparison of colored surfaces of the same hue but differing at the same time both in lightness and in saturation. In such cases the samples cannot be ordered on a linear scale. We need at least two dimensions" (Sève 1993). Thus, the problem of ranking samples in terms of their distinctness of image or the intensity of specular reflectance cannot easily be reduced to one simple factor or measurable characteristic. Bartleson (1974), in a report to the CIE, pointed out that gloss and appearance aspects consist not only of the physical aspect but also of physiological and psychological aspects associated with vision and experience.

Surface changes after exposure

Changes in the surface reflection of materials often occur during aging or weathering, or after use (see remarks on surface reflection changes in Johnston and Feller [1967] and Johnston-Feller and Osmer [1977]). The process of change can be so gradual as to be overlooked unless the exposed areas can be compared to an unexposed section of the original material. The general trend of these surface changes is to approach a semimatte surface; on high-gloss materials, the result of exposure is frequently to lower the gloss; while on matte samples the trend is to increase the gloss due to burnishing. Actually, it is extremely difficult to clean most matte, nonglossy surfaces without increasing the gloss. It is essential to remember the importance of surface changes on perceived color changes. In general, it can be stated that the magnitude of any change in the surface must be taken into account before real changes in pigmentation can be accurately determined.

Fluorescence

Fluorescence is a process in which a material absorbs electromagnetic flux of particular wavelengths and emits radiation at other, longer wavelengths. Phosphorescence and fluorescence are two types of the general phenomenon of luminescence. They differ in the length of time that reradiation occurs: phosphorescence continues noticeably after irradiation ceases; fluorescence does not. There are many types of luminescence based on the source of the absorbed energy (Grum 1980; Byler 1973). Here we consider only the fluorescence of organic compounds caused by ultraviolet, visible, or near-infrared radiation. For example, ultraviolet radiation may be absorbed and some of the energy emitted in the visible region; visible radiation may be absorbed and some of it emitted in either the longer-wavelength visible or the near-infrared region. These are the particular situations that will be discussed. For those interested in the origin of such fluorescence in a compound, Voedisch (1973a, 1973b) and de la Rie (1982) present explanations of the molecular structures responsible.

As we emphasize throughout, the color of mixtures of most dyes and pigments is the result of subtractive colorant mixture, dependent on the absorption and scattering coefficients of the systems. In the case of fluorescent colorants, however, the perceived color is the result of the *additive mixture* of the emitted fluorescent radiation with the accompanying normal reflected color of the colorants and, possibly, the substrate (Voedisch 1973a). An illustration of this phenomenon is given in figure 6.11, which shows the spectral curves of a white plastic without a fluorescent blue whitener (fluorescent whitening agent, FWA), curve 1, and the same plastic with an FWA added, curve 2. Curve 3 shows fluoresced radiant energy that is additively mixed with the reflected light of curve 1. The light source used to irradiate the samples was an approximation to CIE illuminant D65 (daylight), which is defined in the ultraviolet region as well as in the visible. All were measured relative to a pressed $BaSO_4$ standard. The term *radiance* is used to describe the

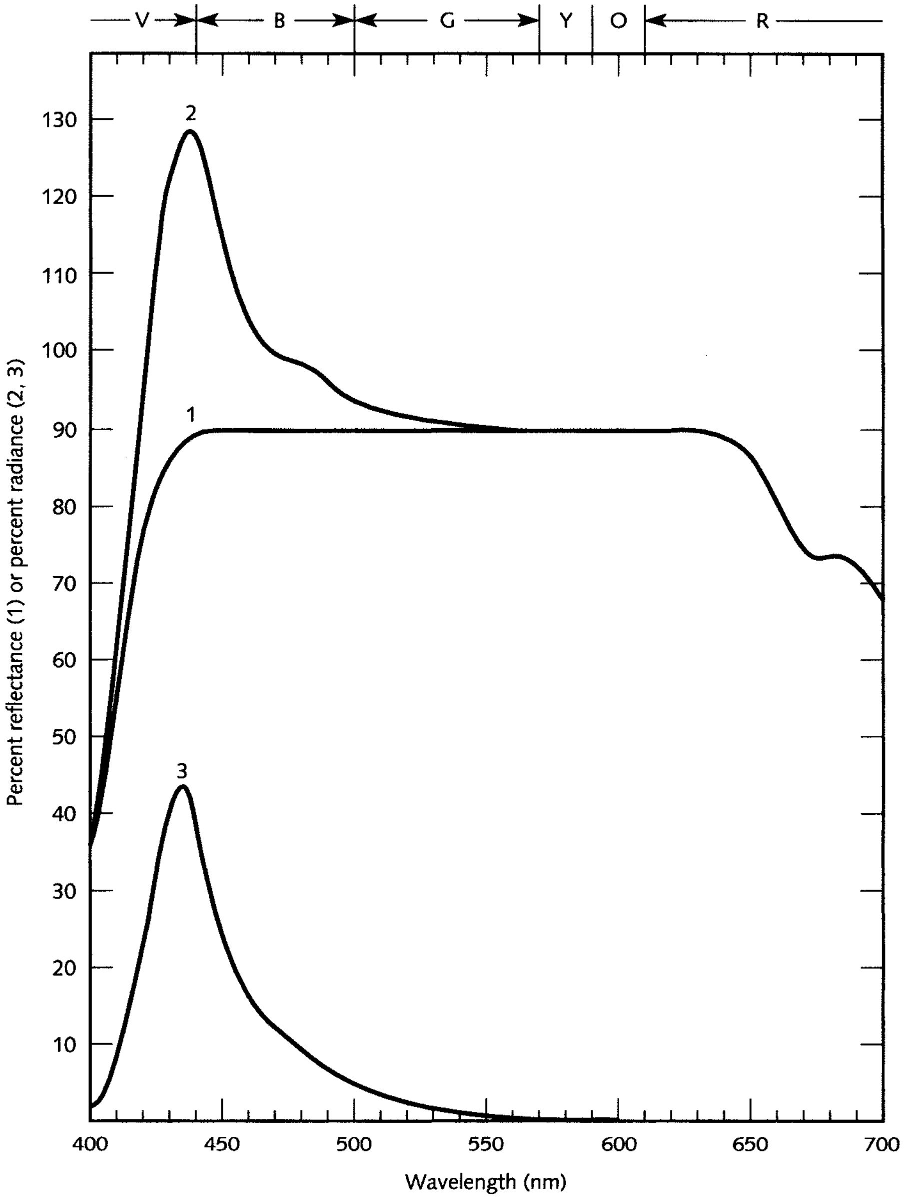

Figure 6.11
Spectral curve measurements of a white plastic: curve 1—without a fluorescent whitening agent (FWA); curve 2—with the addition of an FWA; curve 3—the fluoresced radiant energy from the FWA (after Grum 1980).

fluorescent emission or the reflectance plus the fluorescence, while the nonfluorescent portion is termed simply the *reflectance*. However, in popular usage the simple term *reflectance* is often used instead of *radiance*.

Color measurement of fluorescent materials

Because the observed reflected color is the result of the emittance at wavelengths different from a particular wavelength incident on the material, a special optical arrangement in spectrophotometers or colorimeters must be used for measuring the perceived color of materials that fluoresce. The fluorescent sample must be illuminated by polychromatic light (white light), and the reflected light (or transmitted light in the case of transparent materials) plus the emitted light analyzed with a monochromator or filters (as mentioned in chap. 1). In the past some spectrophotometers illuminated the sample with monochromatic illumination. Illumination of fluorescent materials by monochromatic light results in color measurements very different from the colors observed visually under normal polychromatic light sources. Incident light at the wavelength of excitation is registered by the instrument's detector as reflected light at that particular wavelength and not at the wavelength of the fluorescent emission. It is, therefore, important that the user know whether his instrument uses polychromatic or monochromatic illumination, so that fluorescent samples can be measured in accordance with the visual appearance.

Another special problem when measuring highly fluorescent samples is that the light reflected by these materials is often well over 100% relative to that reflected by the normal white diffusing reference standard. Some measuring instruments, however, may not record over 100% or 120%. In such a case, a neutral-density filter of known transmittance can be inserted into the sample beam to decrease its intensity by a known amount. Thus, a 20% neutral-density filter decreases the intensity to 20% of the actual radiance so that measurements recorded will be on scale. Such decreased reflectances can then be increased by the appropriate factor to establish the actual values of the radiance.

There is one other facet of instrument design that is important in measuring fluorescent colors *accurately:* the use of an integrating sphere compared to the use of a bidirectional, geometric illuminating and viewing arrangement. The latter geometric arrangement is recommended for fluorescent samples because in the sphere arrangement, the color of the fluorescent sample may alter the character of the incident light, thus altering the color of the reference white. The effect decreases as the area of the sample measured is decreased relative to the area of the sphere wall (ASTM Standard E 991). Based on this author's experience with a few good commercial sphere-type color-measuring instruments, the effect is not one of concern for ordinary usefulness. Giving up the ability to either include or exclude the specular reflection, as is possible on most good sphere instruments, is far more important than any small error in accuracy that might occur. However, the author has no experience with instruments utilizing small spheres where the sample size illuminated may be very large relative to the sphere size.

Historical use of fluorescent pigments

A number of organic fluorescent compounds have found their way into museum objects; some are many centuries old, others are of recent vintage. One of the oldest organic fluorescent pigments to be found is natural madder lake, which is based on alizarin (1-2-dihydroxyanthraquinone) from the root of the perennial plant *Rubia tinctorum.* This pigment is a lake of alizarin, generally encountered as the alumina lake but also containing an amount of purpurin (1,2,4-trihydroxyanthraquinone), which fluoresces a bright yellow-red. Feller (1968) has published the curve of the fluorescence of natural madder activated by energy of 400 nm wavelength, as well as the curves for weaker fluorescence activated by 345 nm. Feller's curve of the fluorescence activated by 400 nm incident light is redrawn here as figure 6.12. As can be seen, the peak of the fluoresced radiance is in the 580 nm yellow region. The lake made from pure alizarin, manufactured synthetically since the latter part of the nineteenth century, is not fluorescent since it contains no purpurin.

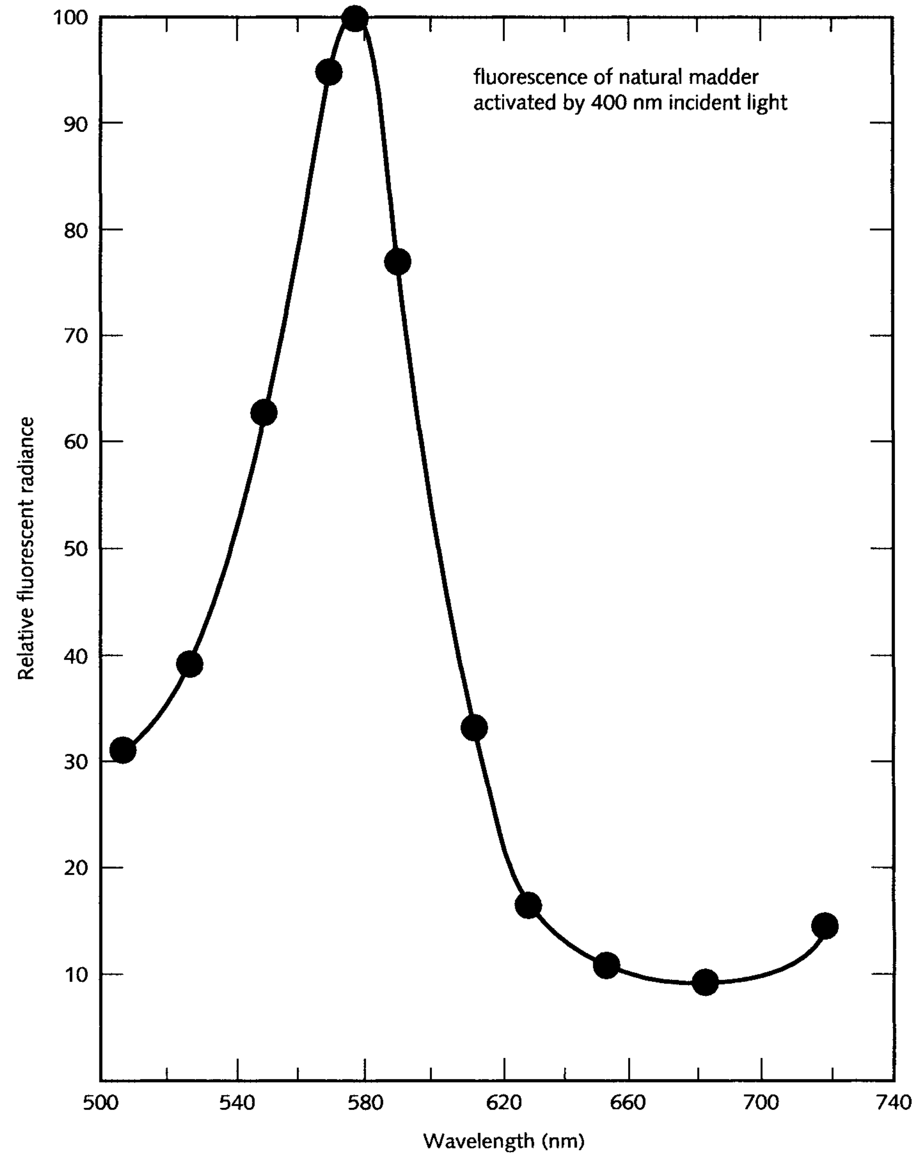

Figure 6.12

Spectral relative fluorescent radiance of natural madder activated by 400 nm radiation (after Feller 1968).

Another traditional organic fluorescent pigment to be found in artworks is Indian Yellow, made from the urine of cows fed mango leaves. The principal component is the yellow, crystalline magnesium salt of euxanthic acid. Baer and coworkers (1986) state that it was used in Indian paintings beginning in the late sixteenth century, and it has been identified in European paintings beginning in the late eighteenth century. Since the early twentieth century, however, manufacture has been prohibited. Feller (1968) and Baer and coworkers (1986) have measured the fluorescence radiance curve of Indian Yellow excited by incident radiation of 436 nm. The fluorescence peaked at 535 nm in the yellowish green region. Figure 6.13 is a redrawing of Feller's fluoresced radiance curve. Figure 6.14 is a redrawing of Feller's total radiance curve as measured on a Model D-1 Color-Eye abridged spectrophotometer. In this instrument, the sample is illuminated with an incandescent lamp, which emits little ultraviolet radiation to be absorbed and reradiated as fluorescence. The

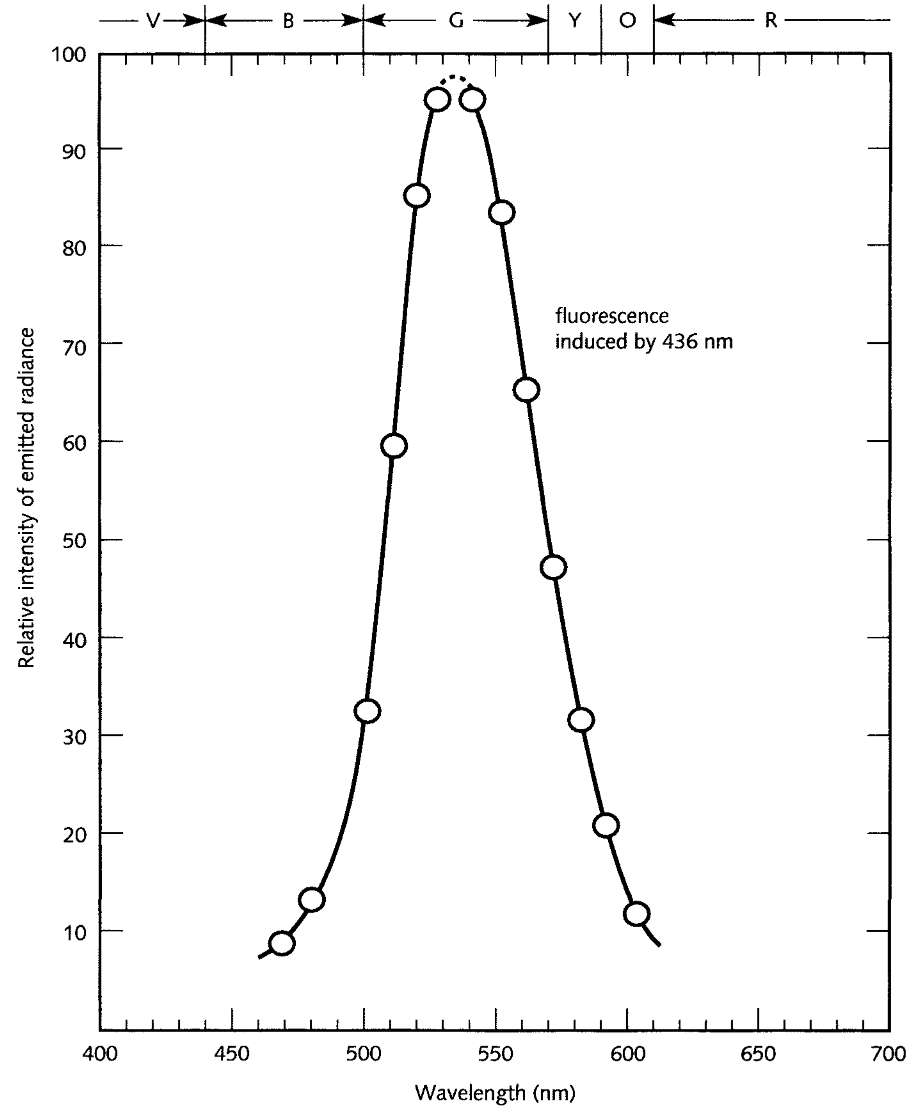

Figure 6.13

Spectral relative fluorescent radiance of Indian Yellow activated by 436 nm radiation (after Feller 1968; Baer et al. 1986).

light reflected is then analyzed by means of narrow band-pass filters. This optical arrangement is the correct one for including the fluorescence in the measurement. Figure 6.15 is a redrawing of Feller's curve of the relative fluoresced radiance at 535 nm as a function of various incident activation wavelengths from 312 nm to 436 nm. It can be seen that wavelengths in this ultraviolet region are not necessary to activate the fluorescence. Strong fluorescence is activated by light in the visible region at 436 nm. Under normal illumination conditions, this fluorescent light is additively mixed with ambient light so the observer is unaware of its occurrence. An ultraviolet light source is normally used to detect the presence of Indian Yellow. Baer and coworkers (1986) show colored photographs of an Indian miniature painting of the early eighteenth century, one illuminated with visible light and another with near-ultraviolet light. The presence of Indian Yellow is immediately suspected because of the greenish color of the fluorescence that is visible in the photograph taken under ultraviolet illumination.

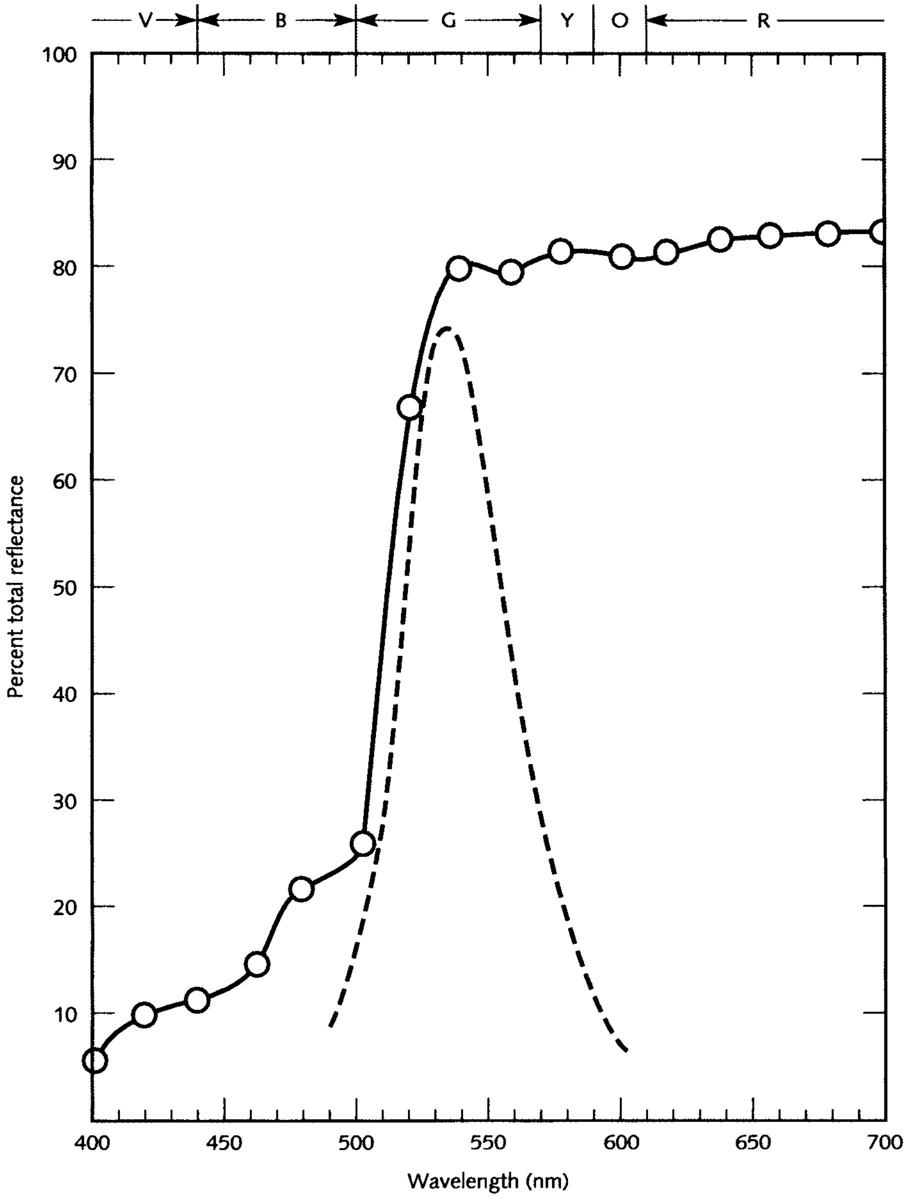

Figure 6.14

Total spectral radiance of Indian Yellow as measured on a Model D-1 Color-Eye with incandescent illumination on the sample.

Development of modern fluorescent, high-visibility pigments

During World War II, the combating countries all made use of fabric signals coated with fluorescent dyes because of their high visibility (Switzer and Switzer 1950). Nearly all of the dyes were extremely fugitive, however. Though pigments had been made by incorporating fluorescent dyes into a resin matrix and grinding the solid mixture into a powder, it was not until Switzer developed the technique of incorporating the fluorescent dyes into urea and melamine resins that their commercial use as pigments began. The patent was issued in 1950 (Switzer and Switzer 1950).

The early pigments had only limited light stability because of the fugitive character of the dyes used; they faded after about one month of exterior exposure. Nevertheless, they were quickly utilized by the advertising industry because of their high visibility. Their value for other uses, particularly for safety signs and directions, was soon realized because of their attention-attracting ability. The value of such applications hastened development by the manufacturers of more light-stable matrices.

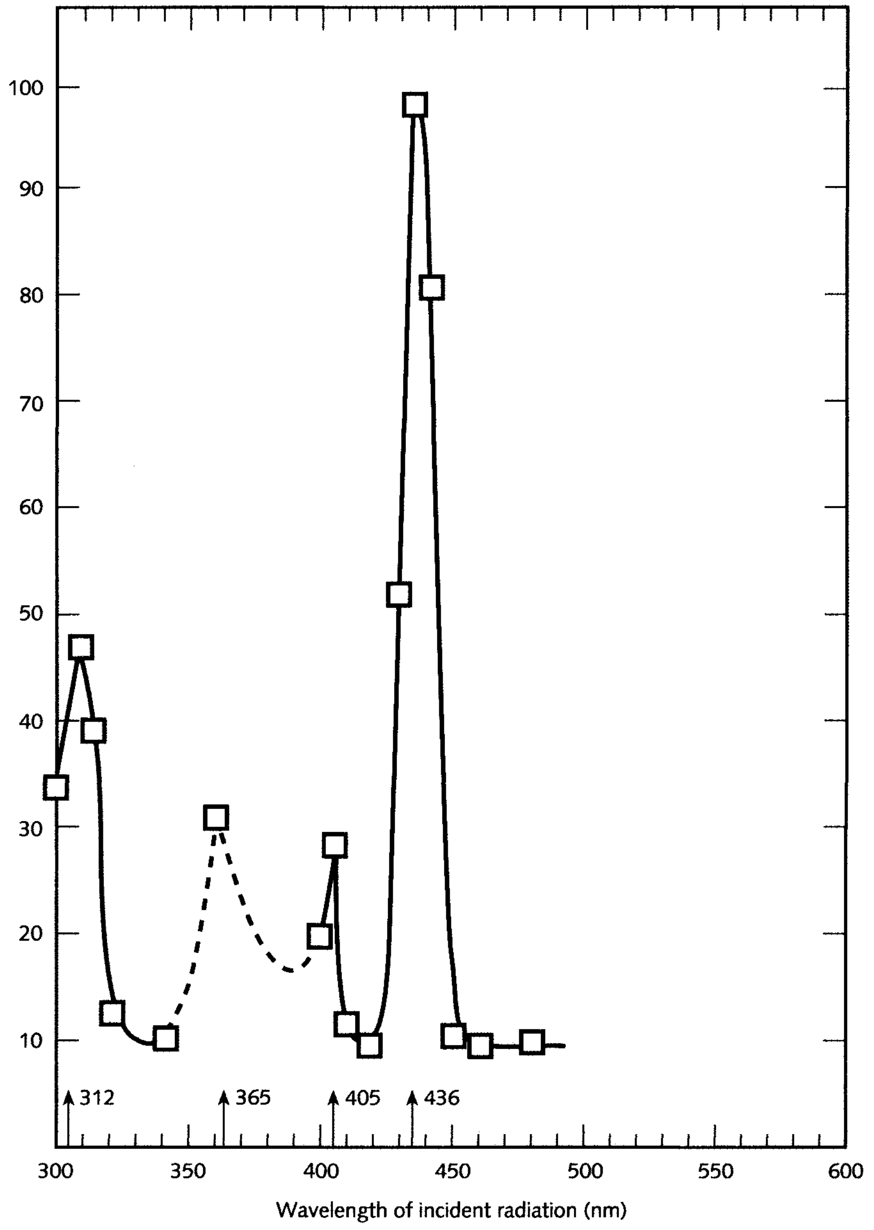

Figure 6.15

Relative fluorescent radiance of Indian Yellow at 535 nm as a function of various incident activation wavelengths from 312 nm to 436 nm.

The improvement in stability was obtained by incorporating ultraviolet absorbers into the resin. One of the first applications was for signs and markings on military aircraft and then on civilian aircraft, using in particular the familiar aircraft orange. Voedisch (1973b) cites and describes military specifications for this material.

Figures 6.16–6.20 illustrate spectral measurements of paper sheets coated with daylight fluorescent pigmented coatings purchased from an artists' supply store. The colors were fluorescent green, yellow-green, orange, pink, and red. Three measurements for each coating are illustrated in the figures. In the two measurements made with the Color-Eye 1500 abridged spectrophotometer, the sample is illuminated with polychromatic illumination, and the total observed light—that is, the reflected plus the fluorescent emitted light (the radiance)—is recorded. The illuminant used is a pulsed xenon lamp filtered to approximate CIE illuminant D65. The instrument is also equipped with an ultraviolet filter

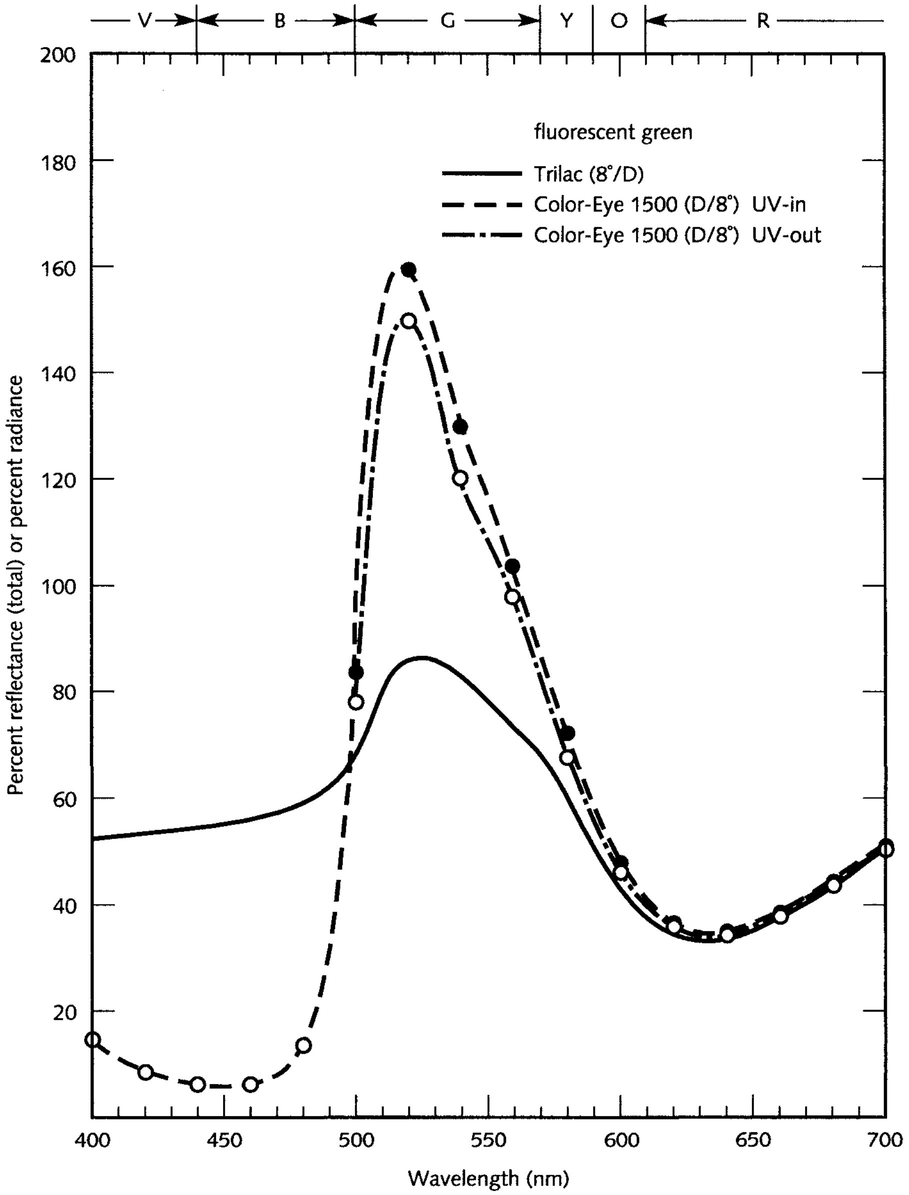

Figure 6.16

Spectral curves of a fluorescent green coating on paper measured in three different ways. The measurement made with the Trilac spectrophotometer, which illuminates the sample with monochromatic light, designated 8°/D, is obviously not correct. The measurements made with the Color-Eye 1500, which illuminates the sample with a polychromatic xenon flash, designated D/8°, indicate the magnitude of the fluorescence. Note that removing most of the ultraviolet wavelengths by means of a filter decreases the fluorescent radiance by a relatively small amount. The CIE tristimulus values and chromaticity coordinates are presented in table 6.4.

(UF-4) to remove all of the ultraviolet portion of the source spectrum below 387 nm (it transmits only 60% at 400 nm). The graphs show the reflectances measured both ways, designated as "UV-in" for the full D65 daylight illumination, and "UV-out" when the UV filter was in place between the light source and the sample. The third measurement on the graphs is the reflectance curves obtained from the Trilac spectrophotometer. This illustrates the situation in which the sample is illuminated with monochromatic (single wavelength) illumination rather than with the polychromatic illumination required to measure both the fluorescence and the normal diffuse reflectance, as used in the Color-Eye 1500.

The CIE notations for the curves illustrated in figures 6.16–6.20 were calculated for illuminant C and the 2° standard observer for each of the three measurements made on each coating. They are presented in table 6.4. The luminous reflectance of the yellow-green is greater than 100%; for others, the reflectance at some wavelengths is also greater than 100% relative to the usual diffuse white standard.

With the monochromatic illumination used in the Trilac, as well as in many older or conventional spectrophotometers and colorimeters, the emitted fluorescent energy is registered by the instrument detector as being reflected at the excitation wavelength (note in figs. 6.16–6.20 the region of maximum absorbance in each case). Reflectance measurements such as these made on the Trilac bear no resemblance to what one would see. The optics of this type of instrument, therefore, are inappropriate for measurements made to describe what we see on materials that exhibit fluorescence in the visible region of the spectrum. (See the section on instrumentation for color measurement in chap. 9.) Most modern instruments designed for color measurement utilize the polychromatic illumination that is correct for fluorescent samples. Some expensive instruments are built with reversible optics, which allow the user to use either polychromatic or monochromatic illumination for spectral measurements.

There is something to be learned by comparing the curves made with monochromatic illumination (the Trilac measurements in figs. 6.16–6.20) to those made using the Color-Eye Model 1500 with polychromatic illumination. The wavelengths of reflectance on the Trilac curves (monochromatic illumination), which are high, relative to those made with the Color-Eye (polychromatic illumination), reveal the wavelengths of importance in the excitation of the fluorescence. For all of these high-visibility pigments, visible wavelengths excite the fluorescence. The presence of ultraviolet wavelengths is not necessary for exciting the fluorescence. Thus, excluding the ultraviolet region from the illuminant does not decrease the brilliance of the emitted fluorescence by a large amount. In addition, the ultraviolet-filtering compounds in the pigment resin matrix absorb most of the ultraviolet. Hence, a museum object containing these daylight fluorescent colorants is not likely to be altered in appearance to a great extent by the use of ultraviolet filters over the light source when it is displayed. Thus, another technique for protecting the fluorescent dyes from fading is the application of a clear varnish containing ultraviolet absorbers over the surface.

Table 6.4

CIE notation for fluorescent samples illustrating measurement differences (illuminant C, 1931 standard observer).

Sample	Optics[a]	*X*	*Y*	*Z*	*x*	*y*
Green	UV-in	53.12	92.57	17.25	0.3260	0.5681
	UV-out	50.78	87.09	16.25	0.3295	0.5650
	Trilac	51.78	66.31	67.12	0.2796	0.3580
Yellow-green	UV-in	86.52	116.40	23.04	0.3829	0.5151
	UV-out	82.55	109.64	22.12	0.3852	0.5116
	Trilac	85.06	89.44	79.74	0.3346	0.3518
Orange	UV-in	107.23	89.63	9.35	0.5200	0.4347
	UV-out	98.95	82.69	9.23	0.5184	0.4332
	Trilac	77.54	74.55	61.27	0.3634	0.3494
Pink	UV-in	78.18	42.02	53.97	0.4488	0.2413
	UV-out	71.97	38.75	53.60	0.4380	0.2358
	Trilac	65.79	54.06	72.19	0.3426	0.2815
Red	UV-in	81.14	48.27	8.47	0.5885	0.3501
	UV-out	75.51	44.98	8.53	0.5852	0.3486
	Trilac	62.63	54.94	45.98	0.3830	0.3359

[a] UV-in and UV-out measurements made on the Color-Eye 1500 abridged spectrophotometer.

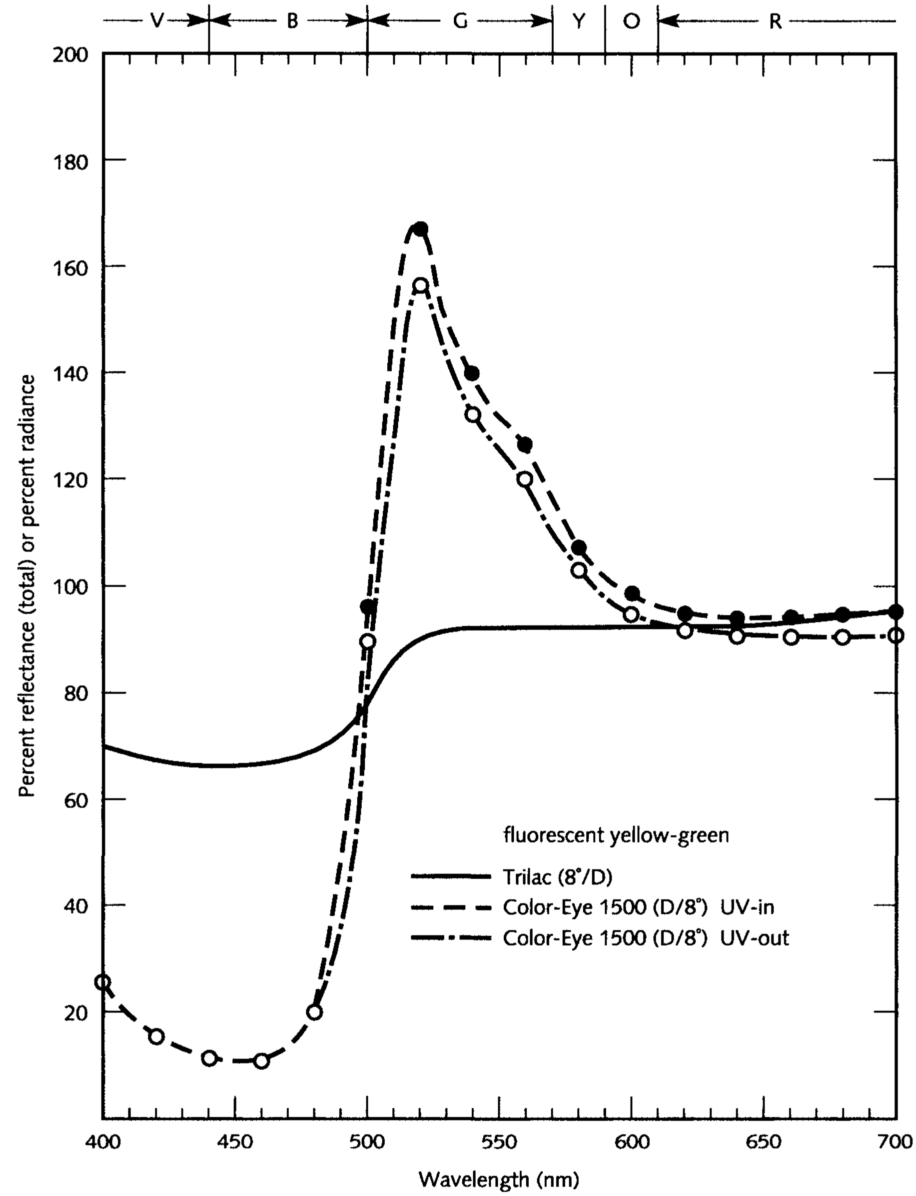

Figure 6.17

Spectral curves of a fluorescent yellow-green coating on paper measured in the three ways as described for figure 6.16.

These comments aren't meant to be misleading: it must be remembered that any fluorescent material, such as those made with natural pigments or dyes, should be protected from prolonged exposure to ultraviolet wavelengths.

Uses of fluorescent, high-visibility pigments by artists

As the use of fluorescent colorants expanded, artists soon became fascinated by these "new" pigments with which they could create innovative and unusual optical effects. By the 1960s artists were using them despite their limited light stability, which was well publicized by scientists as well as by the manufacturers at that time.

The adoption of these pigments by artists necessitated their learning to mix colorants a little differently from mixing absorbing, nonfluorescent pigments. For example, if a fluorescent pigment is mixed with a nonfluorescent pigment that absorbs in the spectral region that

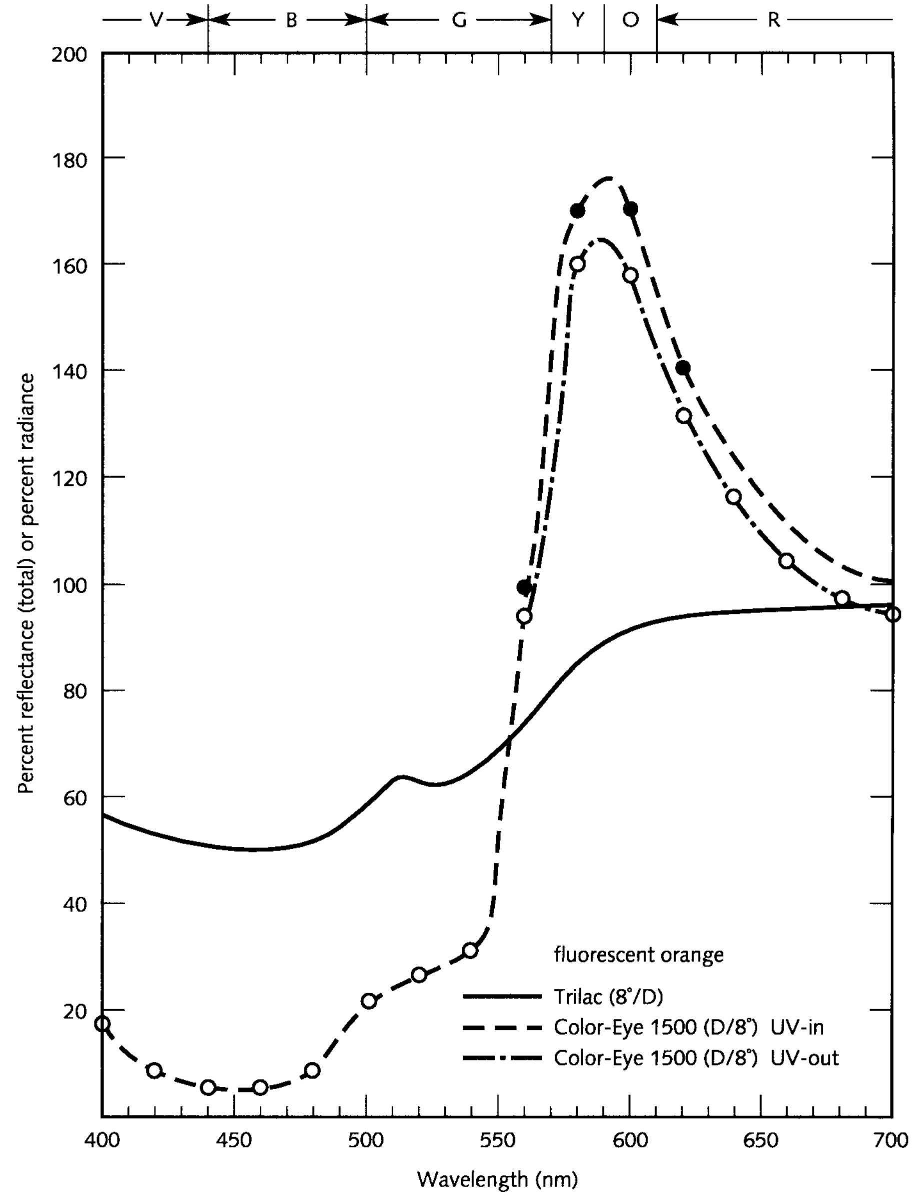

Figure 6.18

Spectral curves of a fluorescent orange coating on paper measured in the three ways as described for figure 6.16.

excites the fluorescence or in the spectral region where the fluorescence is emitted, the fluorescence is decreased or quenched.

In an article describing his use of fluorescent pigments in his paintings, the artist Herbert Aach (1970) wrote, "I have been painting with fluorescent pigments for over five years. Only now do I begin to realize that it took me over three years to relearn color behavior with such pigments." Because the hiding power of these fluorescent pigments is low because of their transparency (they are made with dyes incorporated into a transparent matrix), the reflectance of the substrate, whether neutral or chromatic, as well as the absorption and scattering characteristics of any colorant with which they may be mixed, is of major importance. Aach had to adapt to these factors in relearning colorant behavior.

Because the fluorescent pigments available at that time contained ultraviolet absorbers in the resin matrix, they are not usually activated by black-light illumination (an ultraviolet source filtered to remove

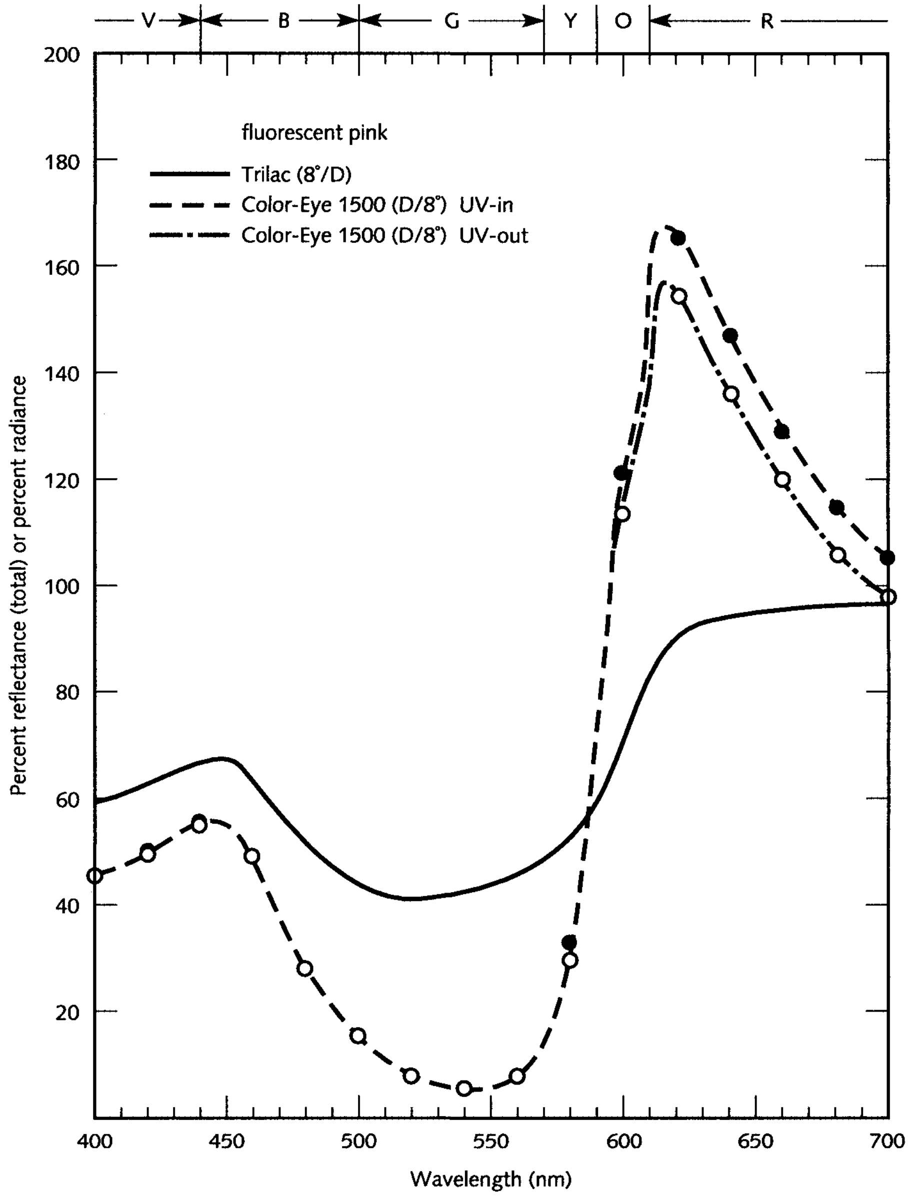

Figure 6.19

Spectral curves of a fluorescent pink coating on paper measured as described for figure 6.16.

visible wavelengths) alone. Aach circumvented this limitation by making up his own fluorescent paints as he needed them, using an extremely high-pigment-volume concentration. Commercial paints cannot be formulated this way because of extreme settling problems in the container. Use of this very highly concentrated pigmentation, however, retained sufficient ultraviolet response to be effective aesthetically; it also resulted in improved light stability.

In a subsequent article, Aach (1972) states, "There are by now a goodly number of us [creative artists] who are working in fluorescent color. Frank Stella, Ralph Humphrey, Al Loving, Frank Bowling come instantly to mind."

The author has a print made by Aach containing fluorescent orange pigment in addition to nonfluorescent pigments. The print, framed under glass, hung on her office wall at Carnegie Mellon Research Institute for seventeen years. The wall on which it hung was illuminated

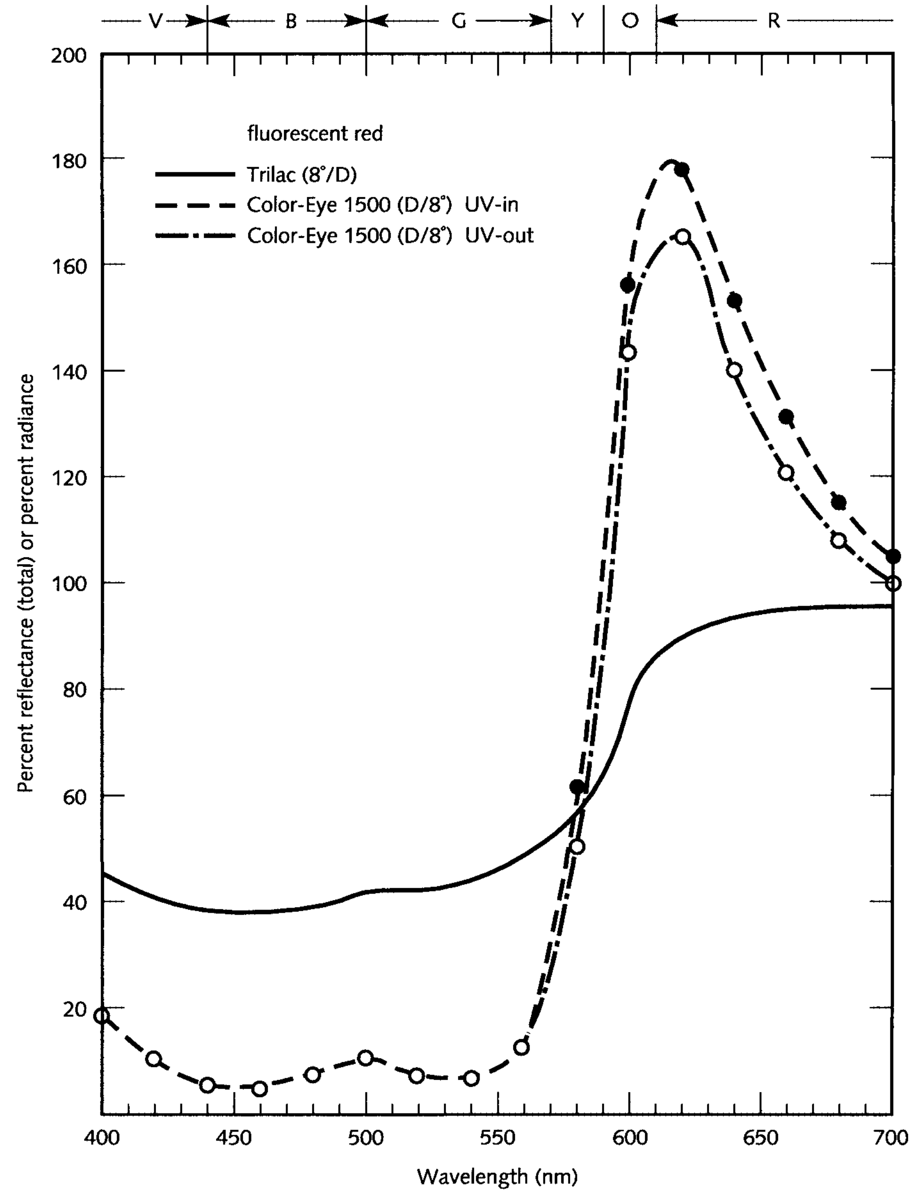

Figure 6.20

Spectral curves of a fluorescent red coating on paper measured as described for figure 6.16.

by diffuse daylight from a nearby window and by ceiling fluorescent luminaires. When the print was recently removed from its frame, the fluorescent paint showed no obvious signs of fading. It was still activated by ultraviolet light alone, as illustrated in color plate 5.

Whether other artists who used fluorescent colorants formulated their paints or inks as well as Aach is not known. Hence, any objects containing fluorescent colorants should be considered to be sensitive to prolonged exposure to light, particularly ultraviolet.

Fluorescent whitening agents (FWAs)

No mention has been made above of blue fluorescent pigments being used for high-visibility applications. Because our eyes have far lower sensitivity to wavelengths of light near the ends of the spectrum—the long-wavelength deep reds and the short-wavelength blues and violets—colorants that fluoresce in these regions are not among the fluorescent dyes and pigments popularly called high-visibility colorants. In the case of the violet-blue fluorescent dyes, their particular and very widespread application is as FWAs to enhance the whiteness appearance of yellowish whites.

Many organic materials become more yellow with age. In other cases, materials such as paper and resins that are intended to be white or colorless are often yellowish. The reader, if too young to remember, will learn from history that one of the most widespread applications for ultramarine blue pigment was as a bluing agent used in laundering and in neutralizing the yellowness in other products. The employment of such a blue pigment, however, lowered the resulting reflectance; it neutralized the yellowness by absorption in the yellow-orange region, resulting in graying rather than in a true whitening effect. Today violet-blue fluorescent dyes produce a neutralizing effect by additive color mixture, actually brightening the color while simultaneously neutralizing the yellowness. Figure 6.11 illustrates the effect: the addition of a blue whitener dye has a significant impact on the color of the white plastic. It can be seen that the total radiance curve of the white plastic plus the fluorescent blue whitener is far higher than the reflectance of the white plastic alone.

Most modern laundry detergents contain these fluorescent brighteners; many white paper products or white plastic materials also contain them. When measuring the discoloration or whiteness of paper, one must take this possibility into consideration. One has only to observe white laundered textiles or white papers under a black-light ultraviolet source to confirm the brilliance contributed by these products. This use of blue-violet fluorescent dyes or pigments is a special and somewhat separate application, certainly very common in recent years. The exciting radiation (for the blue-white fluorescence) is mostly in the ultraviolet region. Hence, eliminating this region by absorption using ultraviolet filters or by mixture with ultraviolet-absorbing pigments such as rutile TiO_2 destroys the fluorescence. One does not find FWAs used in paints or plastics pigmented with TiO_2, either rutile or anatase, which absorbs to a greater or lesser extent some of the violet and most of the ultraviolet region.

The whole subject of whiteness and FWAs has been given an excellent review by Grum (1980). He gives extensive references to other workers who have published on the subject. The reader is referred to the section on single-number color scales in chapter 4 for a brief description of whiteness indices.

Weak fluorescence of resins

No mention has been made up to this point of the fluorescence that occurs as many natural vehicles and varnishes age. Linseed oil, damar, and mastic are examples that not only yellow but also develop fluorescence as they age. Examination of paintings under ultraviolet light is routinely used to detect retouches done at a time later than the original painting, for example. For an informative study of this phenomenon, the articles by de la Rie (1982) should be consulted.

In relation to the degree of fluorescence exhibited by the daylight, high-visibility colorants or the FWAs, the amount of fluorescence of old varnishes and oils is generally extremely small and visible only in a darkened room under black light. Under normal illumination the observer would not be aware of its existence. It is doubtful that it is sufficiently strong to affect the spectral measurements that might be made on the colorants of old oil or varnished paintings, regardless of the type of illumination—monochromatic or polychromatic—used in the color-measuring instrument. For safety's sake with paintings that are old, however, precaution should be taken when they are being measured with an instrument that illuminates the sample with polychromatic light containing ultraviolet wavelengths, such as a xenon source. The instrument should be operated with a filter over the light source to eliminate the wavelengths that activate ultraviolet fluorescence.

It was said at the beginning of this section that the phosphorescence of inorganic materials would not be discussed. However, many objects in museum collections contain these beautiful materials, and it is possible that many more objects of interest containing various phosphors will be preserved. The techniques of spectral measurement described may be of value in establishing identification procedures. Spectral character as well as the decay time of emission may provide identifying parameters.

Microvoids and Vesiculated Beads

Another category of "pigment" deserving special mention may not contain any pigment at all but consists chiefly of air-filled voids suspended in a polymer matrix. It has been mentioned previously that entrapped air can act as a good light scatterer. Figure 4.7 illustrates such a situation. In this example, the development of voids was unwanted. However, air spaces in a polymer matrix can be created intentionally, providing an inexpensive way to introduce desirable scattering in a suspending medium and thus minimizing the need for white pigment.

Many of the white substances encountered in nature do not contain white pigment: snow, clouds, white flowers, foam, and suds (whether on beer or soap solutions) contain no pigment—they contain only air mixed with finely divided particles. Air may not be the only cause of the scattering. Similar scattering phenomena occur in milk and cooked egg white; they contain no white pigment. In his article "Hiding without Pigments," Burrell (1971) gives an excellent explanation of these and similar phenomena and gives a short history of some of the applications of the scattering phenomena created by refractive index differences between particles.

The basic principle stems from the Fresnel equation (eq. 4.3), which relates the mirrorlike reflection, ρ, arising at the interface between two materials of different refractive index, n_1 and n_2, where n_1 is the lower refractive index and n_2 the higher. For light *perpendicular* to the interface,

$$\rho = \frac{(n_2 - n_1)^2}{(n_2 + n_1)^2} \tag{6.1}$$

where ρ is the decimal fraction of the incident light that is reflected at the interface at an angle equal and opposite to the incident angle.

For light not perpendicular to the interface, the angle of incidence in the less dense medium and the angle of refraction in the more dense medium relate to the interfacial reflection in the following way:

$$\rho=\frac{1}{2}\left[\frac{\sin^2(i-r)}{\sin^2(i+r)}+\frac{\tan^2(i-r)}{\tan^2(i+r)}\right] \tag{6.2}$$

where i is the angle of incidence, and r is the angle of refraction.

Here the refractive indices are given by the basic Snell's law relationship, $n_2/n_1 = \sin i/\sin r$. All the above equations assume that the incident light is *not polarized.* For polarized light, see the equations in Judd and Wyszecki (1975).

Ordinary pigments hide (scatter light) largely because of their high refractive index relative to that of the vehicle. Microvoids hide (scatter light) because of the extremely low refractive index of air in the void, relative to that of the vehicle matrix in which they are suspended. If one looks at the ratios of refractive indices of scattering pigments and air-filled microvoids, it can be seen that entrapped air pockets can indeed be very efficient scatterers. By use of 2.5 as an average refractive index for scattering pigments and 1.5 as an average refractive index of organic vehicles, the ratio of the pigment to vehicle (higher to lower refractive index) is 1.7. For the same vehicle with air-filled voids, the ratio of the higher refractive index—the vehicle in this case—to the lower refractive index for air (1.0) is 1.5. It is apparent that air-filled voids are potentially very good scatterers of light. Because the refractive index ratios are so similar, the desired size of pigment particles as well as of voids to achieve maximum scattering is about the same—less than 1 µm in diameter. Recall the universal scattering curve, based on Mie theory, in figure 4.29.

Burrell (1971) describes three methods for making microvoid coatings, only the last of which he considers to be important: formation of a gel structure containing a nonsolvent for the vehicle in the liquid phase. He presents a typical paint formulation and outlines the basic principles for selecting a polymer and the two solvents, a volatile nonsolvent and a less volatile polymer solvent. Many such combinations have been reported; the patent issued to Seiner (1970) and assigned to PPG Industries contains hundreds of formulations.

Microvoids formed in situ as a polymer film dries may not be (and often they are not) the sole scattering source; instead, they are used in combination with TiO_2. In this case, the total scattering may be greater than the sum of that from the two individual scatterers, possibly because of the occurrence of air–TiO_2 interfaces.

An excellent review of the preparation, properties, and uses of microvoids in coatings and in other materials such as paper is given by Rosenthal and McBane (1973). If the comprehensive theory of the optics of microvoid "pigmented" materials is of interest, the articles by Kerker and Cooke (1976); by Kerker, Cooke, and Ross (1975); and by Allen (1973) may be consulted.

It is doubtful that this technology has been utilized in the formulation of artists' materials. However, it certainly may be encountered in commercial products, and artists and artisans who use commercial paints may, albeit inadvertently, be incorporating microvoids in their coatings. The popularity of using this technique to improve hiding (increase scattering) is a strong economic one: air spaces are less expensive than pigments.

The presence of air spaces inside materials may occur unintentionally, for example, due to incomplete wetting of pigments; after the thorough curing of a polymer matrix; or following exposure to deleterious conditions. Michalski (1990) describes the action of solvents, used to clean the surface of a painting (to remove old varnish and so on), that results in the formation of microvoids due to solvent diffusion into the lower layers and subsequent evaporation. He refers to the work of Erhardt and Tsang (1990): "Erhardt and Tsang have measured substantial blanching due solely to solvent application, not *abrasion*. Whether the explanation be micro-voids, surface disruption, granular redeposition or all three remains to be studied."

The monetary value to be realized from using microvoids as pigments led to the development of preformed microvoids in the form of hollow plastic spheres containing air; they are called *vesiculated beads* (Hislop and McGinley 1978). The adjective "vesiculated" is derived from the noun "vesicle," used in the biological sciences to refer to a "fluid-filled pouch, such as a cyst, vacuole, or cell" and in geology to refer to a "cavity in a mineral or rock." Such preformed microscopic beads may be hollow or pigmented. The pigmentation may be incorporated in the vehicle forming the beads, with air in the middle, or it may be encapsulated inside the beads, or both.

One other special product utilizing bead technology is the use of solid plastic beads, either pigmented or clear, to reduce burnishing—that is, the increase in surface gloss of nonglossy (matte) materials. A brief review is presented by Hislop and McGinley (1978).

Although the products and techniques described here may not be encountered in antiquities, they certainly may be found in late-twentieth-century objects and materials.

Extenders, Fillers, Inerts

In the preceding section, solid plastic beads were mentioned, as well as hollow, vesiculated beads. Solid beads can be considered a special type of extender pigment. The Federation of Societies for Coatings Technology's *Coatings Encyclopedic Dictionary* (FSCT 1995) defines "extender pigments" as "a specific group of achromatic pigments of low refractive index (between 1.45 and 1.70) incorporated into a vehicle system whose refractive index is in a range of 1.5 to 1.6." Consequently, extenders do not contribute significantly to the hiding power of paint. They are used in paint to reduce cost, achieve durability, alter appearance (e.g., decrease gloss), control rheology, and influence other desirable properties. If used at sufficiently high concentration, an extender may contribute to dry hiding and increase reflectance.

The *Coatings Encyclopedic Dictionary* states that the word *filler* is synonymous with *extender*. It is in this sense that the word *filler* is used here. Additionally, the term *inert pigment* is defined as being frequently used for *extender*. Based on these definitions of the terms, the most widely used extender pigments are listed in table 6.5; the list, admittedly, is not exhaustive. Patton (1973) presents extensive discussions of the properties and uses of these and a number of other less commonly encountered inerts.

In addition to the extender pigments listed in table 6.5, light aluminum hydrate (Pigment White 24) and gloss white (75% $BaSO_4$ and 25% aluminum hydrate, Pigment White 23) can also be encountered in pigment mixtures. According to Patton (1973), Pigment Whites 23 and 24 are not prepared as independent, dry pigment powders but instead are used primarily as pigment substrates (often prepared in situ) for the manufacture of lake pigments. Alizarin is an example of a pigment that has been laked on aluminum hydrate.

In his book *Artists' Pigments: Lightfastness Tests and Ratings,* Levison (1976), founder in 1933 of the Permanent Pigments Company, discusses the major reasons for the incorporation of extender pigments in artists' oil paints made with organic pigments. Because the book was privately printed and is now out of print, the author will quote many of Levison's remarks verbatim:

> Organic pigments differ considerably in physical properties from the inorganic pigments to which the artist is accustomed. Most inorganic or mineral type pigments are fairly dense and require but a moderate proportion of oil to make a durable and proper working artists' paint. Organic pigments, on the other hand, are light, fluffy and very finely divided so

Table 6.5

Common extender pigments.

Name	Chemical type	Colour Index[a]	Refractive index
Barytes	natural $BaSO_4$	PW 22	1.637
Blanc fixe	synthetic $BaSO_4$	PW 21	1.637
Chalk (whiting)	calcium carbonate	PW 18	1.48–1.65
Dolomite	calcium carbonate and magnesium carbonate	PW 18	1.50–1.68
Precipitated chalk	synthetic calcium carbonate	PW 18	1.53–1.68
Silica (amorphous)	silicon dioxide	PW 27	1.54
Silica (diatomaceous)	hydrous silica	PW 27	1.48
Silica (synthetic)	$(SiO_2)_x - (H_2O)_y$	PW 27	1.46
Silica (pyrogenic)	silicon dioxide		1.45
Gypsum	hydrated calcium sulfate	PW 25	1.52–1.53
Talc	magnesium silicate	PW 26	1.54–1.59
Kaolin clay	hydrated aluminum silicate	PW 19	1.56
Mica	aluminum potassium silicate	PW 20	1.58
Fuller's earth	hydrated aluminum magnesium silicate		1.50–1.55

[a]PW = Pigment White

that it requires considerable oil to "wet" all the pigment particles and make a workable paint.

With the inorganic pigments the percent oil in the total paint will vary from less than 20% in the whites to 24% in the cadmiums, and up to close to 40% for other pigments. With a concentrated organic pigment (called a "toner") the percent oil to make a workable paint can be from 60% to over 70%. Such an excess of oil produces poor drying, a soft film, possible wrinkling and excessive yellowing. With acrylic emulsion paints there is no problem since the pigment is not critical to the properties of the binding vehicle.

A highly durable [oil] paint, however, can be formulated with organic pigments by providing a backbone of dense inorganic "inert" pigment. An inert pigment is one that has little or no coloring power. The ancient and Renaissance artists made their organic colors (obtained from natural sources) by absorbing the color on clays or chalks, which are inerts. Today's oil paints which contain organic pigments can be formulated with more durable inerts, the one most useful being barium sulfate, known as blanc fixe. Alumina, a light form of aluminum hydrate, is also used to make lakes or for transparency. To make Alizarine Crimson, for instance, the madder color is laked with a major proportion of alumina. Most organic colors used, however, are concentrated toners. . . .

Pastes of the inerts ground in linseed oil were applied at .003 inch thickness to aluminum foil, allowed to dry, then exposed for four summer months to the sun in the exposure racks used for the pigment exposure tests. Use of the aluminum [foil] was a test of the stresses set up in the film on accelerated aging and of the flexibility and adhesion. The blanc fixe formed an exceedingly tough, durable and flexible film. It required the least oil and retained color well. The whiting (chalk, calcium carbonate) films behaved quite curiously. The wrinkling stress was so strong that it carried the foil with it into deep wrinkles. The asbestine [magnesium silicate] is usable where it is deliberately desired to create a rough textured paint in not too light a color.

Barium sulfate has all the desired properties to make a durable oil paint having "body" in combination with organic pigments and to reduce the oil proportion considerably. . . . If it is further desired to increase the drying time and hardness of a paint film and at the same time impart opacity, zinc oxide and titanium dioxide in limited amount can be incorporated. By this means the Permanent Green Light pigmented with organic toners could be formulated with but 29% oil and have a paint that is more brilliant and tinctorially much stronger than its inorganic counterpart. The change in color of the organic green on drying was one-fourth that of the inorganic green.

> It was shown . . . that in preparing the panels for test in the oil vehicle most inorganic pigments could not be diluted nearly as far as organic pigments and have a usable tint strength. On a weight basis organic reds can be eight times as strong as cadmiums. That means for a paint of useful strength for artists' use, the organic color pigment content can not only be greatly reduced with an inert, but [this] is frequently necessary so that in mixing the color strength will not be overpowering.
>
> As a result, organic pigments that have a reasonable cost can replace similar hues of inorganic pigments at a lower price per tube. Even many of the moderately expensive and a few of the very expensive organic pigments can be made into artists' colors within the normal price range.

As a brief introduction, Levison's description of the use of extenders leaves little to be added, except to point out their use in substrates of paintings. For example, the grounds of commercially prepared canvases are often treated with formulations containing inerts such as chalk, gypsum, and barytes.

When using the Kubelka–Munk equation to calculate colorant formulations with pigment concentrates that might contain extenders, the pigment calibration data are treated quantitatively as if the extender pigment were a part of the vehicle system, since the refractive indices are similar. If this assumption seems not to be completely successful, a correction factor for the prepared sample in question relative to the same pigment, albeit previously calibrated in a different vehicle system, may be determined. (The use of a correction factor, in effect, allows one to convert the master set of K's and S's for the colorants, determined in a reference vehicle system, to K's and S's that will yield accurate color matches and formulations in a particular, different vehicle system.)

When an extender pigment has been used to prepare the substrate material, its presence can be ignored if hiding is complete. If the hiding of the paint film is incomplete, so that the substrate is visible or partially visible, the hyperbolic form of the Kubelka–Munk equation must be used (see the sections on glazes and opacity in chap. 4).

In Levison's discussion quoted above, he mentions the addition of zinc oxide and titanium dioxide to an organic green pigment (probably phthalocyanine green). Neither of these whites is an extender; they are white pigments with significant scattering characteristics. In essence, such an addition changes the low-scattering phthalocyanine green toner, a type II pigment, into a type III pigment (see definitions in chap. 3), which both absorbs and scatters significantly. A modified organic green of this type would no longer be appropriate for use as a transparent glaze.

Chapter 7

Reflectance Curves of Some Frequently Encountered Chromatic Pigments

This chapter is included to comment on the salient characteristics of reflectance curves for additional pigments; these curves may prove useful for pigment identification. To a limited extent, an attempt has been made to include references to a number of traditional pigments that may have been used in older objects, as well as to a few modern pigments that may be encountered. Unfortunately, this exposition can be only a brief introduction, particularly to the many modern synthetic organic pigments as well as to the many modern synthetic inorganic pigments, which are often tailored to have specific reflection characteristics.

Presented are spectrophotometric reflectance curves of a greater variety of pigments than are described in appendix A. The principal curves, all based on mixtures with rutile TiO_2, are reproduced from the article by Johnston (1967b). They illustrate a collection of recorded and published pigments that, regrettably, encompasses only a fraction of the vast number of pigment reflectance curves that may be encountered. But until a more comprehensive collection of spectral curves is catalogued—and we hope that such a project can be carried out for future reference—these curves offer a brief survey of pigments that may be encountered, particularly from the years after World War II. The discussion also emphasizes and enlarges upon the previously described techniques of spectral curve analysis as an aid in pigment identification.

Primary Colors

The primary colors are described in the following order: blue, red, and yellow, considering wavelengths in the order of long to short.

Blues

Figure 7.1 illustrates a series of blue pigments. The familiar ultramarine blue (see Plesters 1993) and phthalocyanine blue are included as curves A and B. Curve C shows a typical iron blue (Prussian blue); this was widely used for more than two centuries but is in more limited use today. The more or less continuous drop in reflectance in the long-wavelength red region is characteristic of this pigment.

Curves D-1 and D-2 are both cobalt pigments. D-1, labeled "red shade," is cobalt alumina oxide, which is the pigment generally

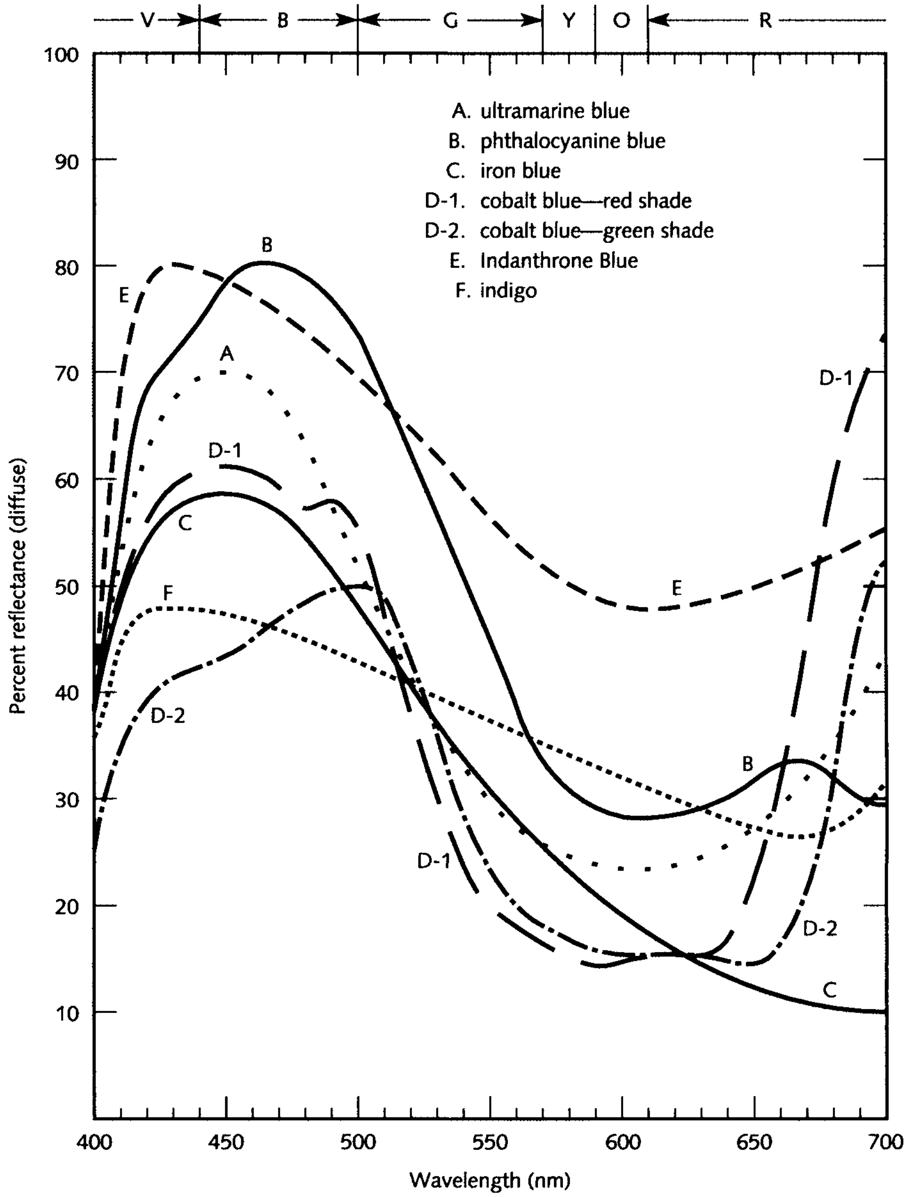

Figure 7.1

Spectral reflectance curves of paints containing various blue pigments in mixture with rutile TiO_2 (after Johnston 1967b; Johnston and Feller 1963).

referred to in artists' paints as cobalt blue. Curve D-2, labeled "green shade," is a cobalt–tin oxide generally referred to in artists' paints as cerulean blue. As can be seen, the curves of both pigments are characteristic. Both exhibit a sharp rise in reflectance in the red region, and both have absorption bands in the orange and red regions. The green shade (cerulean) has bands at 645 and 595 nm; the red shade has its major absorption at 590 nm, with another at about 620 nm. Both have slight bands in the middle of the spectrum, cerulean in the yellow-green region at about 555 nm, and the red shade in the green region at about 540 nm. These cobalt blues represent one class of pigments that have a characteristic curve shape in the region of maximum reflectance, providing another identifying clue. However, if they are mixed with a pigment that absorbs in the blue and violet short-wavelength region, such as a yellow or orange, this characteristic shape may be obscured.

Curve E, which is Indanthrone Blue (see also fig. 4.30), has only one absorption band in the orange region and exhibits gently rising reflectance in the red. Note that this red tail is not as great as that for ultramarine blue, as shown in figure 4.30, and is much less steep than the red tails of the cobalt blues. There is nothing readily characteristic about the curve for this blue, except in terms of pigments it cannot represent.

Curve F shows a typical reflectance curve for indigo. Its flatness relative to most blues describes its low chroma. It has an absorption maximum in the red region at about 660 nm, rising then in a little tail in the longer-wavelength region. Because it is a natural pigment, slight variations may be encountered, but it is generally recognizable as indigo. As this pigment fades under light exposure, it tends to become greener in hue. See, for example, the curve for indigo (called *ai* in Japanese) found in Japanese prints (Feller, Curran, and Bailie 1984). In the same article, the reflectance curve for *aigami* (dayflower blue) is shown to have its own highly characteristic series of absorption bands, unlike any other blue to our knowledge.

A modern blue not illustrated here, but one that could readily be encountered in modern art, is manganese blue. Staniforth (1985) illustrates a reflectance curve of this blue. In older objects, smalt, a pigment made by grinding of blue glass, may be encountered. The color is due to the presence of cobalt, and smalt could therefore be confused with one of the many fired cobalt pigments available today. Staniforth illustrates a curve for smalt, as do Mühlethaler and Thissen (1993). Staniforth also shows a reflectance curve for azurite, which is a natural blue pigment (basic copper carbonate) used for centuries. It exhibits rather flat reflectance in the 610–700 nm region. A curve for azurite is also given by Gettens and FitzHugh (1993a). The blue pigments listed in this paragraph, but not illustrated by the reflectance curves of figure 7.1, contain metals detectable by X-ray fluorescence. This information can be helpful for identification.

Reds

No other group of pigments can serve as well as the reds to emphasize the need for an organized categorization of absorption bands, particularly for the many organic reds developed in the twentieth century or used in pre-twentieth-century classical periods. In figure 7.2, the reds exhibiting a single absorption band include the inorganic reds (the iron oxides—curves 3 and 14; the cadmiums—curves 1 and 2) and the organic reds (see also fig. 4.5, classical alizarin lake). Of the prevalent modern reds exhibiting a single absorption band are some toluidines (curve 9), Lithol Rubine (curve 13), and BON red (curve 12)—all inexpensive, high-chroma reds of great tinting strength. (A few of the other modern organic reds, in certain media, also exhibit a single absorption band.)

Many of the organic reds exhibit two or more characteristic absorption bands, as illustrated in figure 7.2. The number of pigments illustrated is very small compared with the number that has been or is still available. Of the traditional organic reds, one used by artists is carmine lake, which is discussed by Schweppe and Roosen-Runge (1986) in *Artists'*

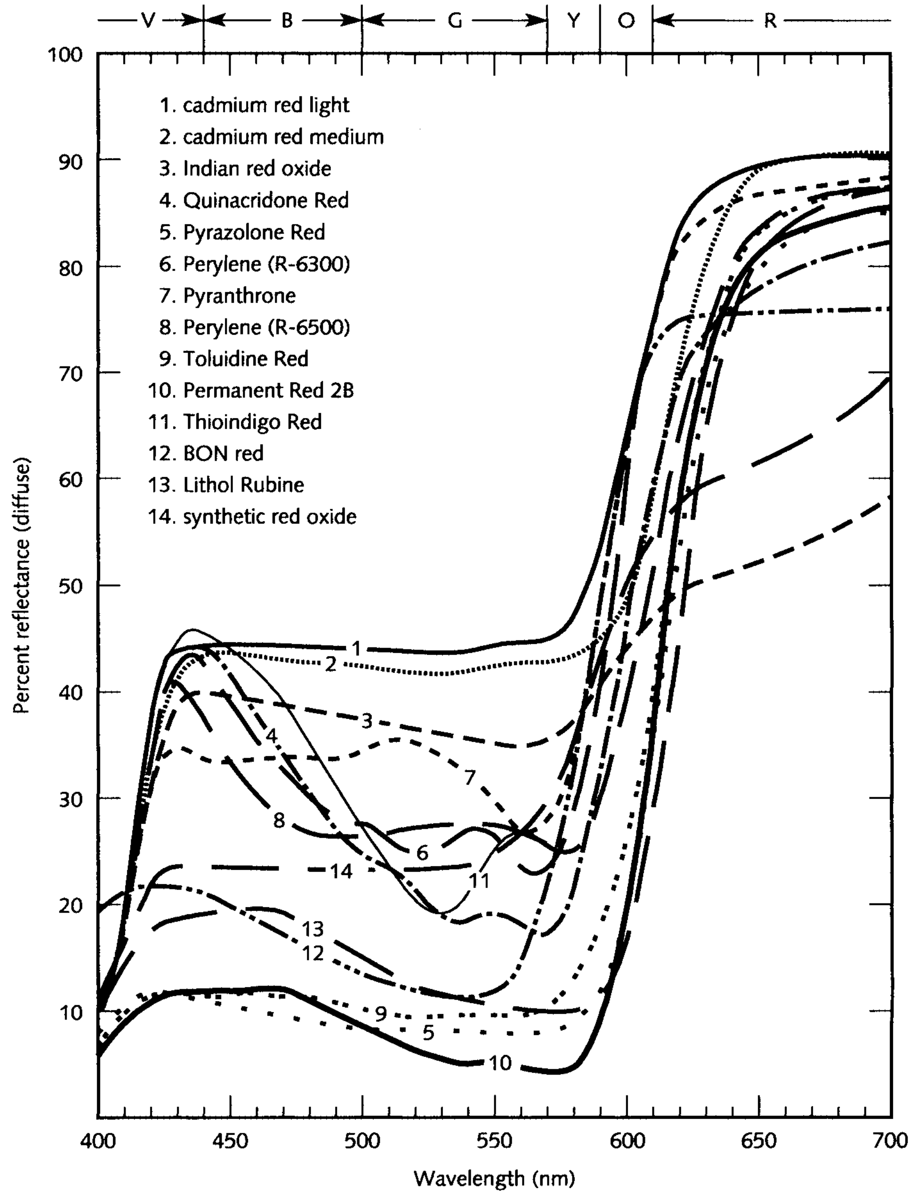

Figure 7.2

Spectral reflectance curves of paints containing various red pigments in mixture with rutile TiO_2 (after Johnston 1967b).

Pigments. The absorption curve for carmine is illustrated by curve 4 in figure 4.19. Note that it exhibits two to three absorption bands.

Of the inorganic reds, the one class of pigments that exhibits a characteristic fingerprint in many situations is that of iron oxide, two forms of which are shown in figure 7.2. Curve 3, Indian red oxide, is a bluish version (natural); curve 14 is a synthetic red oxide, a more-orange pigment that is also illustrated in figure A.12. The curving, rising, long-wavelength tail in both curves is characteristic of iron oxides. We see it again, though it is less pronounced, in the yellow oxide–yellow ocher family, as well as in iron oxides of near-neutral hue, where it is not quite so prominent but still apparent. See also the curve for burnt umber (see fig. A.6). Throughout history, the iron oxides have been staples used in coloring objects of many types. If they are not mixed with a green or blue, which absorb in the long-wavelength region, their curved red reflectance tail is an important aspect to note.

The other classical red pigment used by artists since ancient times is vermilion, illustrated in figure 4.6 (see also Gettens, Feller, and Chase 1993).

A more modern red inorganic pigment extensively used by artists since the early twentieth century is cadmium red, which has largely replaced vermilion (Gettens and Stout 1942). The only characteristic in the absorption region is its flatness. The wavelength at which the reflectance begins its steep rise in the orange and red regions describes the hue. Cadmium red light (curve 1) and cadmium red medium (curve 2) are illustrated in figure 7.2. Note that curve 1 rises at a shorter wavelength than does curve 2. In *Artists' Pigments,* Fiedler and Bayard (1986) provide a series of curves illustrating the masstone reflectance curves for the family of cadmium pigments, from the yellows to the maroons.

Many of the modern organic red pigments have distinctive multiple absorption bands, as illustrated in figure 7.2: the perylenes (curves 6 and 8), Pyranthrone (curve 7), and the thioindigos, one of which is illustrated by curve 11. Appendix D presents a series of red pigment reflectance curves organized in a proposed orderly manner.

Yellows

Because yellows absorb in the short-wavelength violet region, there is not much opportunity to fingerprint their absorption characteristics (they reflect all other wavelengths) unless measurements are made in the ultraviolet spectral region, where they may also absorb selectively. One distinctive organic yellow illustrated in figure 7.3 is Flavanthrone Yellow (curve 5), with its double absorption band; this modern pigment is a very stable transparent yellow. Another recently introduced family of yellow colors of good lightfastness (not shown here) are the azomethines, which are metallic complexes that also have very characteristic absorption bands in the violet region. Although identified by their Colour Index name as Pigment Yellow 129, they are definitely greenish. An isoindolinone cobalt complex has three characteristic absorption bands in the violet region (no Colour Index name), but it is definitely more yellow in hue than the azomethines. Made by Ciba Specialty Chemicals (formerly Ciba-Geigy), these two chemical types are all sold under the trade name Irgazin.

A number of inorganic complexes in the yellow family are also offered by Ciba Specialty Chemicals; they were made by the former Drakenfeld Company, which is now a part of Ciba. Many do not have characteristic absorption in the violet region, but they do exhibit absorptions in the red and near-infrared regions. These pigments are extremely stable to light and heat (they are fired materials) and may be found in ceramic objects as well as in organic media. They are relatively low in tinting strength, so they are selected primarily on the basis of their excellent durability.

Some traditional yellows are cobalt yellow (Aureolin), Indian yellow, lead-tin yellow, and lead antimonate. The only pigment of these four that has striking characteristics in its reflectance curve in the visible region is Indian yellow, which fluoresces strongly. It is described at some

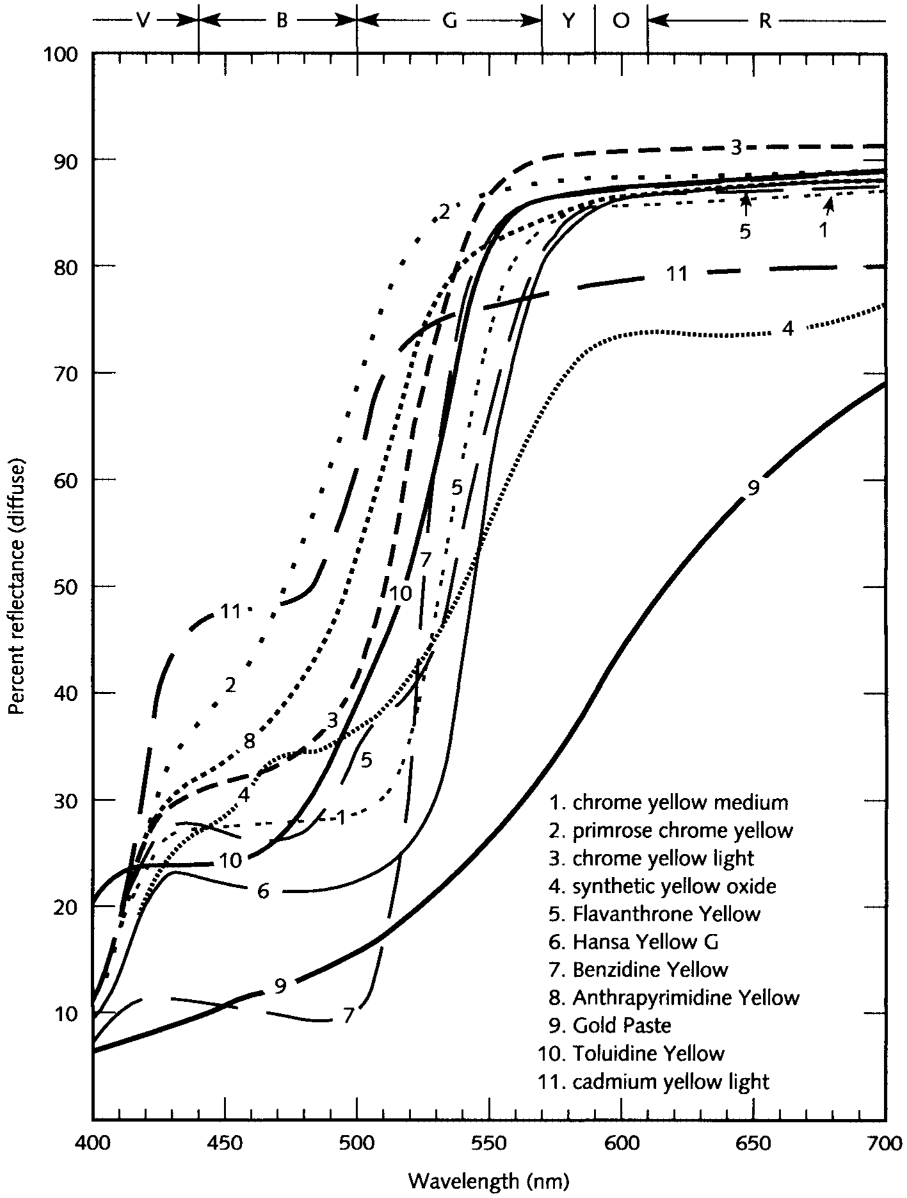

Figure 7.3

Spectral reflectance curves of paints containing various yellow pigments in mixture with rutile TiO_2 (after Johnston 1967b).

length by Baer and coworkers (1986) and discussed earlier in this monograph in the section on fluorescence. The others exhibit no characteristic absorption in the violet region. Reflectance curves for cobalt yellow are illustrated by Cornman (1986) in volume 1 of *Artists' Pigments* and for lead antimonate by Wainwright, Taylor, and Harley (1986); reflection curves for lead-tin yellow are illustrated by Kühn (1993a) in volume 2.

Another traditional yellow colorant used by artists is gamboge, which is highly fugitive. It also has no striking absorption characteristics.

Synthetic yellow iron oxide (curve 4 in fig. 7.3) exhibits the upward curve in the long-wavelength (red) region. The curve shape is more subtle in this region than that of the red oxides, but it is not flat like those of the high-chroma yellows. A further characteristic of yellow oxide is the slight dip, surprisingly persistent, at about 470 nm.

One of the major clues to identifying yellows, oranges, and reds is the wavelength at which the reflectance begins to rise sharply. It describes the hue: the longer the wavelength, the more orange the hue; the shorter the wavelength, the greener the hue. Compare the curves for the three chrome pigments in figure 7.3: Chrome yellow medium (curve 1) is the most orange; chrome yellow light (curve 3) is a true yellow, neither orangish nor greenish; and primrose chrome yellow (curve 2) is perceived as definitely greenish.

Secondary Colors

The secondary colors are those that may be made by the mixture of two primary colorants: green by mixing blue and yellow, purple (sometimes called violet) by mixing blue and red, and orange by mixing red and yellow. These colors may also be achieved with single compounds, not mixtures. The secondary colors illustrated in figure 7.4 (the greens), figure 7.5 (the purples or violets), and figure 7.6 (the oranges) are all single compounds, with the exception of chrome green, which is a mixture of iron blue and chrome yellow. It should be readily apparent why the primary colors should be analyzed first to alert the researcher to the possibility that the secondary colors may be mixtures of the primaries rather than single, distinct pigments. The reader is referred to the mixture curves in appendix A: mixed greens in figure A.24, mixed violets (purples) in figure A.27, and mixed oranges in figure A.30.

Greens

The greens are illustrated in figure 7.4. Chrome green (curve 1) has the distinct absorption in the red region that is characteristic of iron blue (curve C in fig. 7.1); it is a mixture of a chrome yellow and an iron (Prussian) blue. However, since it is traditionally sold as a separate pigment and is given a separate Colour Index name, PG 15, it has been included here in the green category. It may be made by admixture of dry pigments or by coprecipitation. For our purposes, it is immaterial that it be identified as a distinct pigment, since the properties and curves are those of the mixture.

Chrome green should not be confused with the other chromium-containing greens: hydrated chrome oxide (curve 7), which is the artists' Viridian or Vert Emeraude Transparent, and chrome oxide green (curve 2), which is a fired, pure chromium oxide, low in chroma but extremely durable, and known since the early nineteenth century (sometimes referred to by artists as Vert Emeraude Dull). Mixed with a neutral white or gray, each green has its distinctive absorption characteristics: the double absorption bands at 465 nm and 600 nm of the pure chrome oxide are unmistakable. The major absorption of the hydrated chrome oxide at about 625 nm could be confused in shape with the curves of blues, but note that the absorption maximum is at a longer wavelength where greens absorb. One unique characteristic of the hydrated chrome oxide, if it is present without admixture with a yellow, is the little absorption dip in the high-reflection region, at about 435 nm.

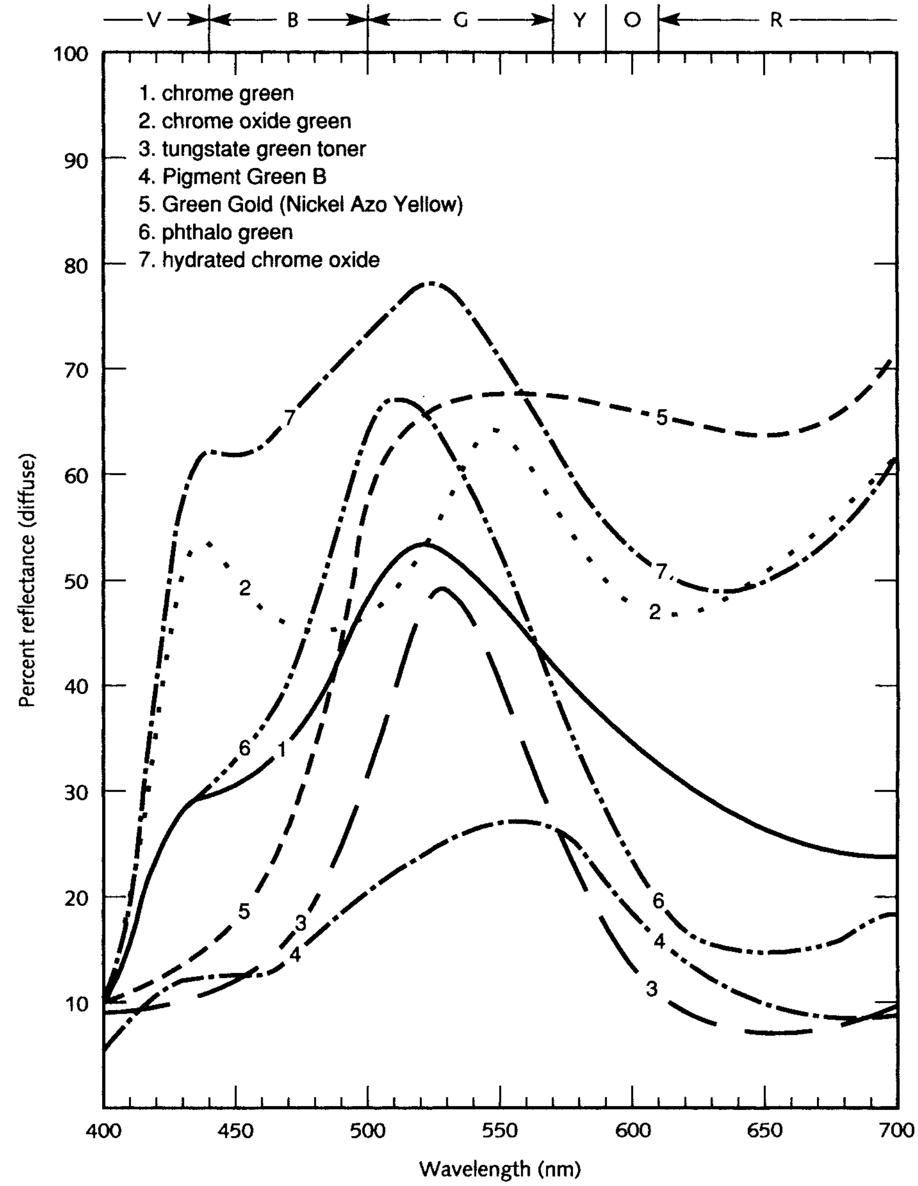

Figure 7.4

Spectral reflectance curves of paints containing various green pigments in mixture with rutile TiO_2 (after Johnston 1967b).

Of the other greens illustrated in figure 7.4, phthalocyanine green (curve 6) is by far the most important green pigment used since about 1950. It is without doubt the most prevalent modern green pigment. Its distinctive tail in the red region is characteristic.

Curve 4 in figure 7.4 is the reflectance curve for Pigment Green B (Pigment Green 8). Since the early twentieth century, the artists' color known as Hooker's Green may have been made with this pigment. According to Levison (1976), Hooker's Green was originally made with iron blue and gamboge. One can assume that since the gamboge faded so rapidly relative to iron blue, trees in some old artworks have become blue. The only characteristic of the Pigment Green B reflectance curve is the very flat absorption in the violet region, 415–440 nm. In the red region, no maximum absorption is exhibited. The dropping off of reflectance is reminiscent of the curve of an iron blue, and, indeed, this pigment is an iron chelate. The chroma is low, with a skewed (nonsymmetrical) reflectance curve. It is still used in watercolors and in polymer-emulsion artists' colors. Unless used singly, it may be difficult to identify this pigment positively from reflectance alone.

Not included in figure 7.4 are several classical green pigments that are found in older works. One of these is Green Earth, whose absorption curve is illustrated in figure 4.9. In *Artists' Pigments,* volume 1, Carol Grissom (1986) discusses its spectral reflectance at some length. The characteristic to be emphasized here is the continuous drop in reflectance in the red region; this could be confused with iron blue's characteristic drop in reflectance in the same region.

Other classical greens are verdigris, which is generally dibasic acetate of copper, and copper resinate, based on verdigris dissolved in a resinous solution. Malachite, which is the natural mineral of basic copper carbonate, and green verditer may also be encountered. Kühn (1993b) has written about and shown reflectance curves for verdigris and copper resinate. Gettens and FitzHugh (1993b) illustrate reflectance curves for malachite and green verditer. Curves of some mixtures of modern blues and yellows are illustrated in figure A.24.

Purples

The purples are sometimes referred to as violets. In Munsell notation, they are designated by the letter P; in the Colour Index, by the letter V. We have chosen to call them purples (P) to emphasize that a similar hue may be obtained by mixing blue and red.

The reader is again referred to the purples made by the mixing of blue and red illustrated in figure A.27.

The reflectance curves of the purples (violets) illustrated in figure 7.5 are highly characteristic; they are all organic in nature, recent twentieth-century developments. Each has a characteristic number and location of its absorption bands, except alizarin maroon. Not included in the figure, but commonly used by artists in the twentieth century, is manganese violet. Introduced at the turn of the century, it also has a unique absorption curve (Patton 1973).

A violet (purple) pigment that might be encountered in artworks is cobalt violet, generally cobalt phosphate (or the arsenate, not generally used because of its toxicity). Its reflectance curve would possibly display the multiple absorption bands characteristic of the cobalt blues, with the absorption peaks shifted to longer wavelengths. No reflectance curve for this pigment has been found.

Oranges

A series of oranges that are not mixtures of reds and yellows is illustrated in figure 7.6. Of those illustrated, only the Halogenated Anthanthrone (curve 1) has a striking fingerprint. The others are more or less flat through the blue region and into the green. The wavelength at which the rise in reflectance occurs determines the hue—the longer the wavelength of the rise, the redder the hue. Many of these oranges can be closely matched by mixtures. For example, cadmium orange (curve 7) could probably be made by admixture of the right pair of cadmium

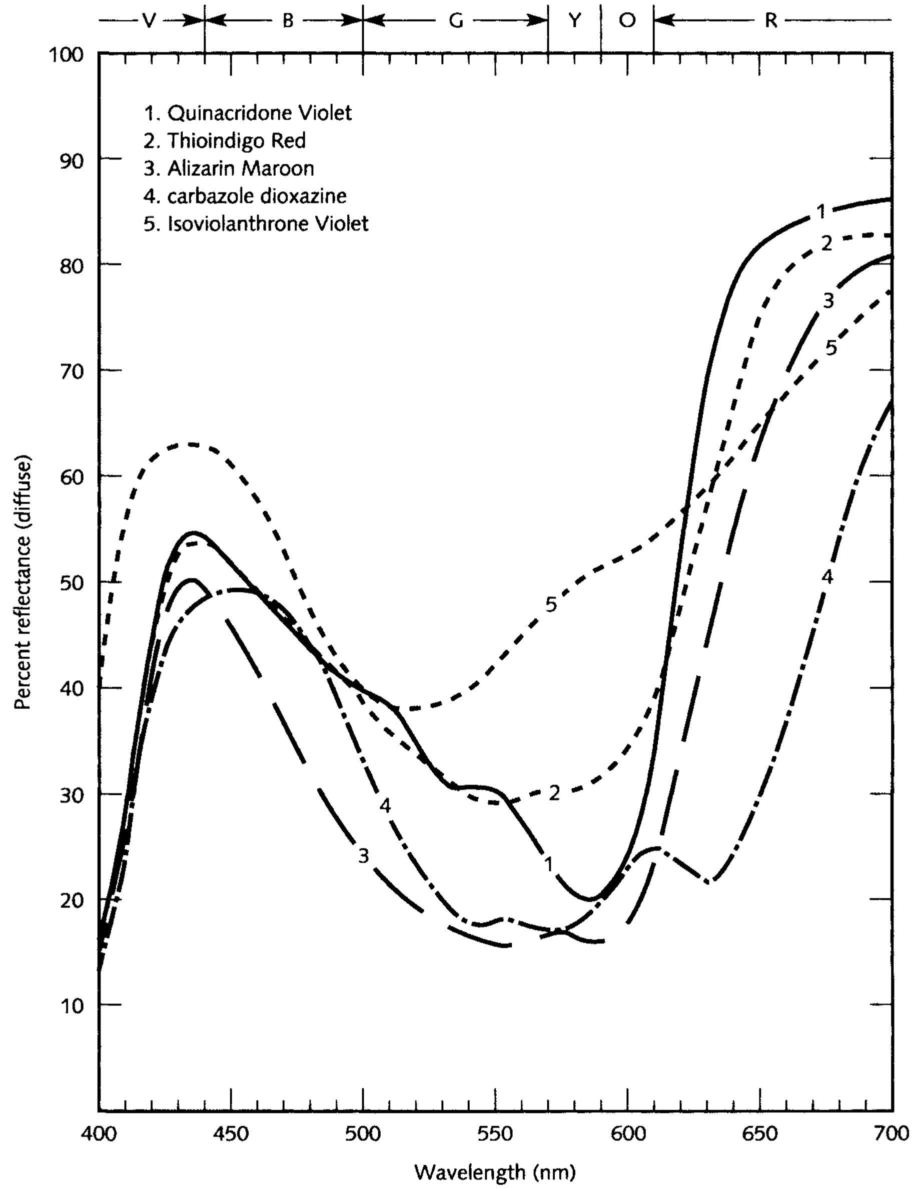

Figure 7.5

Spectral reflectance curves of paints containing various purple pigments in mixture with rutile TiO_2 (after Johnston 1967b).

yellow and cadmium red pigments. Figure A.30 shows the reflectance curves of three oranges made by mixture of a red and a yellow pigment.

Pigment Interactions

There are few interactions among modern pigments. (There are restrictions due to the nature of the medium or vehicle used, and such information is generally supplied by the pigment manufacturer or supplier.) There is, however, one striking exception: phthalocyanine blue appears to "dissolve" in at least one pigment—notably with Benzidine Yellow, one of the diarylide yellows, in which phthalocyanine blue appears to form a solid solution. DiBernardo and Resnick (1959) first pointed out this phenomenon. Figure 7.7 is an illustration of spectral curves of a phthalo blue and a Benzidine Yellow in a textile printing vehicle. The illustration

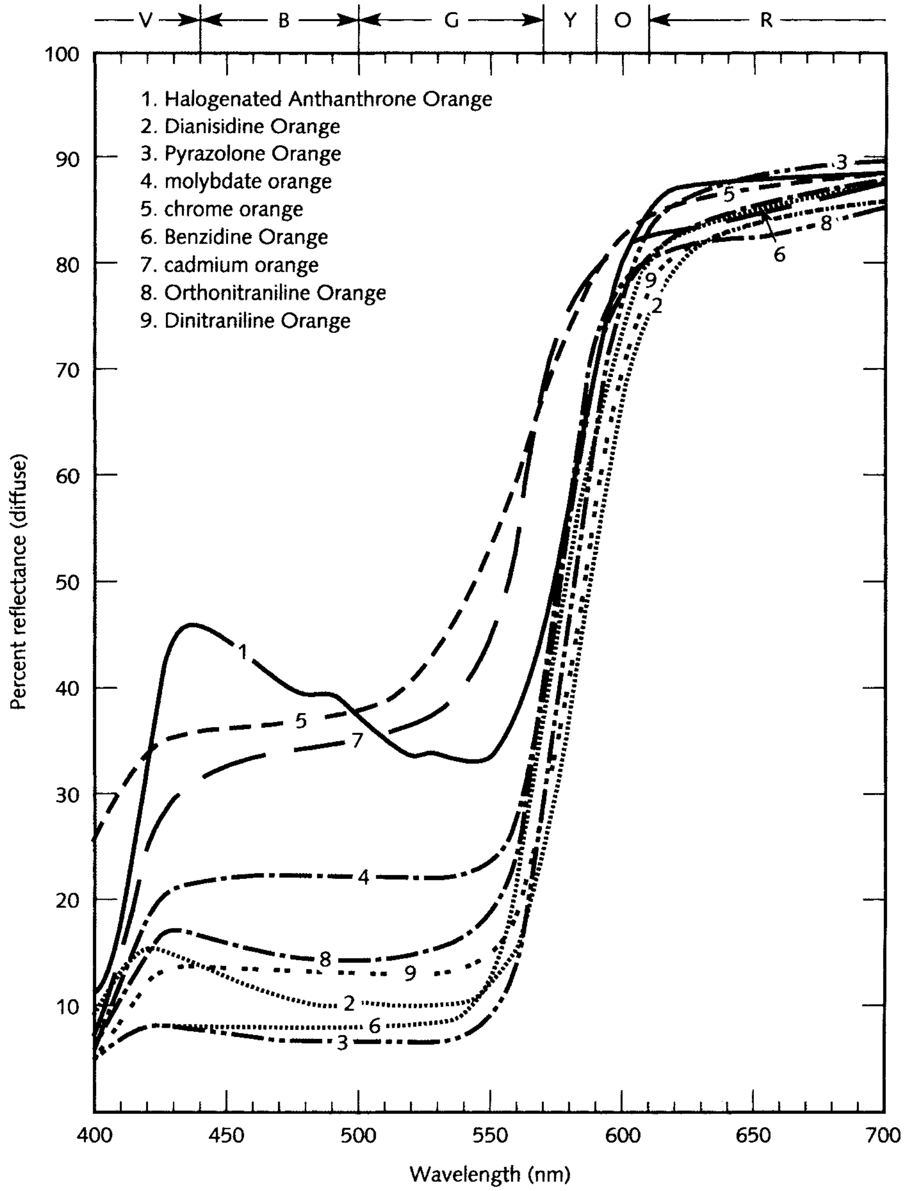

Figure 7.6

Spectral reflectance curves of paints containing various orange pigments in mixture with rutile TiO_2 (after Johnston 1967).

for each pigment shows the normal reflectance curve. Also illustrated is the curve of the combination of the two pigments in the same vehicle. It can be seen that the phthalo blue absorption in the long-wavelength region is very different from the normal curve of phthalo blue illustrated in figures A.10 and 7.1. This "solution" curve occurs as well in the presence of aromaticity in vehicles. For example, the absorption shape beginning at about 540 nm is the only characteristic absorption observed in polystyrene plastics. Many paint vehicles, particularly those containing aromatic groups or involving aromatic solvents, may exhibit curves that dip at about 680 nm, indicating a small amount of phthalocyanine blue in this "soluble" form. (Phthalo blue can often be observed as a contaminant in colors with high reflectance in the long-wavelength region. See the discussion under glazes in chap. 4.)

As mentioned, such interaction between modern pigments is unusual. Most pigments today are very stable and unreactive. However,

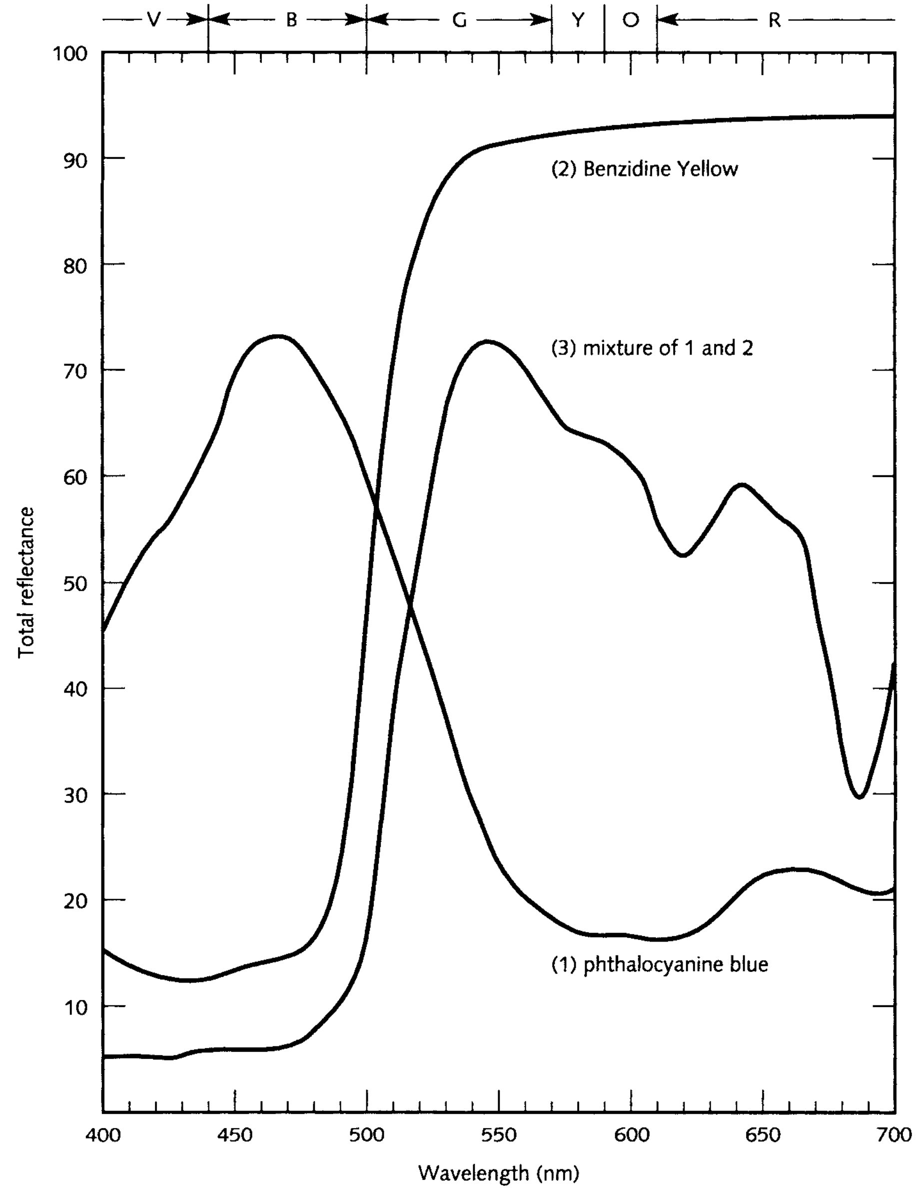

Figure 7.7
Spectral reflectance curve of a phthalo blue and Benzidine Yellow in a textile printing vehicle. The reflectances of the individual pigments in the same vehicle are also shown. The change in reflectance in the long-wavelength region from the typical phthalo blue absorption is characteristic of the absorption of phthalo blue in aromatic paint systems.

they may fade, and they may be unsuitable for certain media. For example, carbazole dioxazine violet is extremely sensitive to peroxides. However, in general, each pigment's unique reflectance curve is not altered by the presence of another, except as would be predicted by overlapping absorptions and reflectances according to the Kubelka–Munk predictions.

This brief summary of reflectance curve characteristics of various pigments can only suggest the information that can be learned from experience and from an extensive reference library of pigment reflectance curves. There is no substitute for learning from the study and measurement of many known pigments. There is no substitute for concentrated effort. There is no substitute for a knowledge of the available pigments and their properties. Of course, the same criteria apply to almost all nonroutine analytical applications of any nondestructive reflection technique, whether it be wavelength dispersive spectrometry in the X-ray region (for metals), in the visible region as described here, in the near-infrared region, in the mid-infrared region, or in the ultraviolet region. The same standards of analytical spectroscopy in the classical sense apply: careful instrument calibration, reliable reference standards, a reference library of known materials, recognition of variant results, and standard analytical knowledge of sensitivity and precision. Most of such expertise is achieved from extensive experience and dedicated continuing study.

Special Technique for Dark or High-Chroma Colors

When colors are very dark, such as a navy blue, or are very high in chroma, such as a bright orange, the characteristic absorption bands are not revealed because the reflectance is very low in the absorption region. Thus, the measurement of the reflectance does not yield the information needed for identification.

If a very small sample can be taken, a dilution in white paint can be made to bring out the characteristic absorption bands. The technique consists of dispersing the very small sample either into white pigment from which paint can be made, or directly into wet white paint. This dispersion can be carried out with a micro ball mill such as is used for grinding micro samples for other analytical methods. McCrone's Micronizing Mill is an example of such a device. A drawdown or paint-out of the white dilution paint is made and dried, and then its reflectance is measured for comparison with the library of curves in the normal way. Although this method requires that a small sample be taken, the sample is not lost—it still exists to be used in solution spectrophotometry or another appropriate analytical procedure. The technique of diluting a dark sample by dispersing it in mixture with a white pigment has proved to be a worthwhile supplement to the arsenal of analytical methods useful for identifying colorants.

Chapter 8

Measured-Data Analysis and Special Measurement Problems

In this chapter a few topics relevant to color measurement and colorimetry, not previously emphasized, are discussed briefly. In general the topics involve the interpretation of multiple measurements, either those made over a short period of time or those made over periods of many months or years. Of particular emphasis is the importance of making multiple measurements on nonhomogeneous or mottled areas. The major points to be made are as follows: (1) Know the reliability of the measurements made on *your* instrument by following a procedure of calibration and measurement mentioned in chapter 1 (see Hemmendinger 1983). (2) Look at the spectral curve shapes of the measured samples and analyze the nature of any differences. (3) Look at the samples. (4) Plot the measured chromaticity coordinates on a chromaticity diagram. Think about what each of these observations is telling you. Analyze—so the total picture can be constructed mentally.

Note that there is no mention above of averaging tristimulus values or chromaticity coordinates. It must be remembered that tristimulus values are *dependent* variables and so should not be averaged. In view of this, how does one select the most representative value from a series of repetitive measurements, sampling, sample preparations, and material preparations? The answer is to *plot the data on a graph* and look at the distribution. For example, plot the chromaticity coordinates on a chromaticity diagram, noting the Y value alongside the points (or plot x against Y), in addition to x against y. Alternatively, the derived uniform chromaticity coordinates, such as a^*, b^*, and L^*, may be employed. On the basis of the plotted data, select the center of the distribution as the best average value. The important point to be emphasized is that one must not simply average thoughtlessly. By doing so, one could get a very false picture or a set of figures that might never even be possible with the particular set of materials being used.

The following illustration, utilizing the concepts outlined in the first paragraph, should help to make the point more lucidly than words alone could do. A new color was being introduced in a polyester gel coat of moderate gloss. It was a turquoise made with 4.9% phthalo green, 0.01% black, 1% yellow iron oxide, and 94.09% TiO_2. The problem was to select the best CIE coordinates to use as the standard in preparing subsequent batches. Table 8.1 shows the data measured on six panel preparations from the same batch of material.

Table 8.1

Panel preparations of turquoise gel coat (illuminant C, 1931 standard observer).

CIE coordinates	Sample number in order of preparation 1	2	3	4	5	6
x	0.2263	0.2276	0.2285	0.2272	0.2247	0.2259
y	0.3483	0.3517	0.3529	0.3484	0.3494	0.3489
Y	31.47	30.94	30.90	31.65	30.79	31.21

All of these measurements were made with the specular reflectance excluded. Three areas of each panel were measured; the panels were very uniform, with negligible deviations over their areas.

Figure 8.1 shows the chromaticity values plotted on a portion of the chromaticity diagram. This turquoise is in the green-blue region, where yellowing is very objectionable, with a dominant wavelength between 495 nm and 496 nm.

After the first three panels were made, a red flag was raised because visual inspection of the panels and their measurements indicated that samples 2 and 3 were increasingly yellow, possibly because of resin yellowing caused by excessive heat. The technician preparing the panels corrected the problem and prepared three more panels, samples 4, 5, and 6. Visual examination of all of the panels suggested that there were slight differences in gloss. Examination of the spectral curves indicated that to be the case. Sample 6 was selected as the sample that was closest to the "normal color," and it was chosen as the best physical standard to use for future preparations. This was in keeping with a policy of selecting measurements made on a real sample close to the center of the distribution.

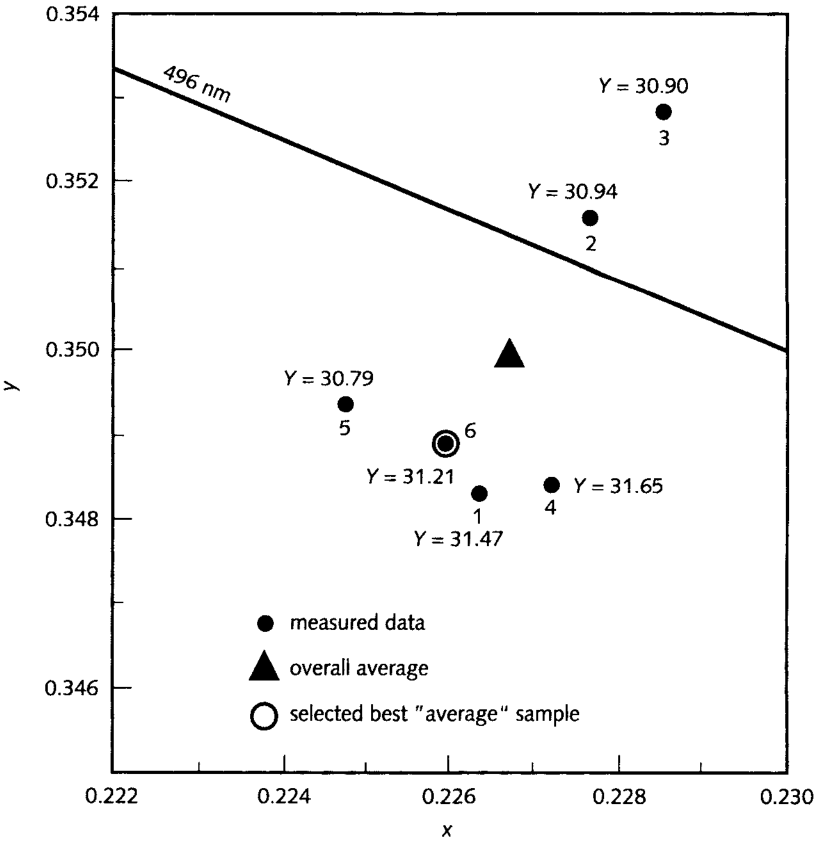

Figure 8.1

Greatly enlarged portion of the CIE 1931 chromaticity diagram, based on data from table 8.1, showing the locations of points, with corresponding Y values, for the six turquoise gel coats, all made from the same batch of original material. The 496 nm dominant wavelength line is shown. Sample 6 was selected as the best standard to use for future preparations. The formulation contained a little yellow oxide, which could be withheld in subsequent manufacture to allow for a vehicle that might be more yellow. Other components were phthalocyanine green, a little black, and rutile TiO_2.

Samples 2 and 3 were rejected as clearly nonrepresentative. Gloss differences in medium-gloss samples, which have somewhat diffuse surfaces, are difficult to control. In general, however, variations of this type are less objectionable than hue differences. In particular, hue differences in the yellow direction in a turquoise are seriously objectionable. In addition, selecting panel 6 provided a real sample to keep as a future reference standard. After subsequent preparations of different batches, the standard could be changed slightly, if that appeared warranted.

Although this is an example from an application in industry, it serves to illustrate the points made in the initial paragraph: look at the spectral curves; look at the samples; plot the data; and think about what all of these observations are telling you. Look and think—the admonition by Billmeyer and Saltzman (1981) presented here in reverse order—sums up the process well. One cannot overemphasize the value of plotting the measured color coordinates and looking at the samples and data, and then thinking about the implications. This is especially true when changes in color are analyzed following exposure (Johnston-Feller and Osmer 1977).

The differences measured over long periods of time must be analyzed in terms of the instrument's repeatability over the same length of time. When changes are small and of the order of magnitude of the instrumental uncertainties, plotting the data can be helpful. One looks for trends: If, in light of the measurement uncertainty, a difference occurs that is within the uncertainty but that in later measurements continues to occur in the same direction, then credence can begin to be placed in the validity of the change.

Does this mean that averaging should not be done? Generally, averaging is improper, as has been pointed out, but it can be used in certain cases. An average is as representative as any other single value (1) when the number of measurements is large and the differences are small—for example, in the evaluation of the repeatability of measurements; (2) when the chroma, or saturation, of the colors is very low; and (3) when the variation in the measurements is large because of the nature of the samples, *and* the number of measurements is also large. Here averaging may be necessary to take into account the large variations in the samples.

An example of this situation is that of measuring the color of coffee beans. A large bag of beans sent to the laboratory was first sorted visually into four groups based on their lightness. Measurements were then made by placing the beans in the lid of a petri dish, about 10 cm (4 in.) in diameter, with the shiny side of each bean against the lid. When the lid was covered, the dish was filled tightly with additional beans and taped shut. The lid side was placed at the port of the sphere on the Trilac spectrophotometer, and measurements were made with the specular reflectance excluded. The dish was rotated 90° and another measurement made; this was repeated until four measurements were taken. The process was repeated with another selection of beans from the pile. Finally, the petri dish was filled with no orientation of the beans, and five more measurements were made as the petri dish was rotated. A total of thirteen measurements was thus made on the darkest beans.

The process was repeated on each pile of beans, although the number of fillings was reduced to one with the beans oriented and one with them randomly oriented, each measured four times and averaged. Figure 8.2 shows typical reflectance curves measured for each of the four categories. Note that the reflectances have been multiplied by 5. There is nothing particularly distinctive about the curves.

In figure 8.3 the chromaticity coordinates for all of the measurements are plotted. The spread in the data is so large, and the reflectance curves are so similar in character, that averages were calculated for each group. Selecting a specific measurement in the center of the distribution would have served just as well, as in the case of the turquoise gel coat. The important point is that one knows much more about the data by plotting and looking at the results. In this situation, every measurement was in one sense an average made by the spectrophotometer.

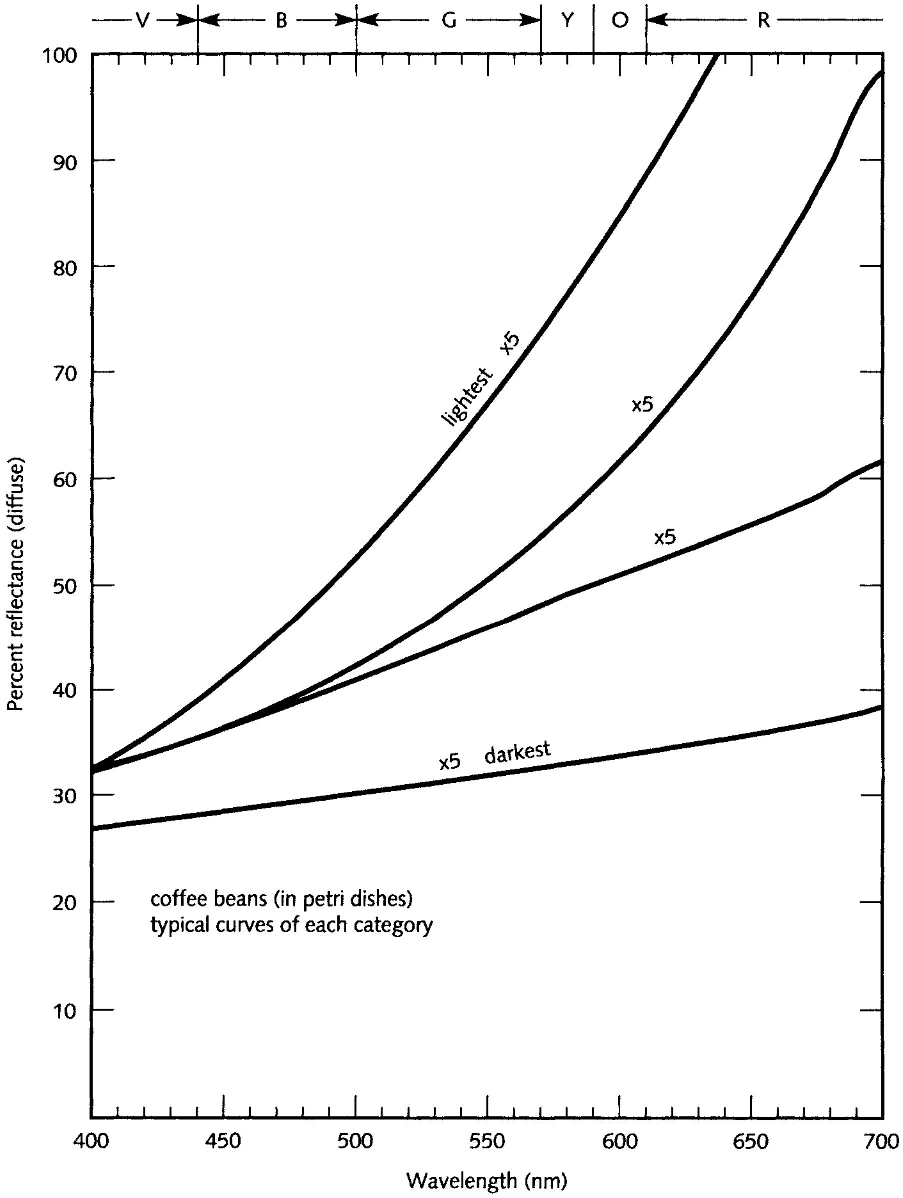

Figure 8.2

Typical spectrophotometric curves of the four groups of visually sorted coffee beans, which were packed into petri dishes and measured with their dark sides facing the Trilac spectrophotometer.

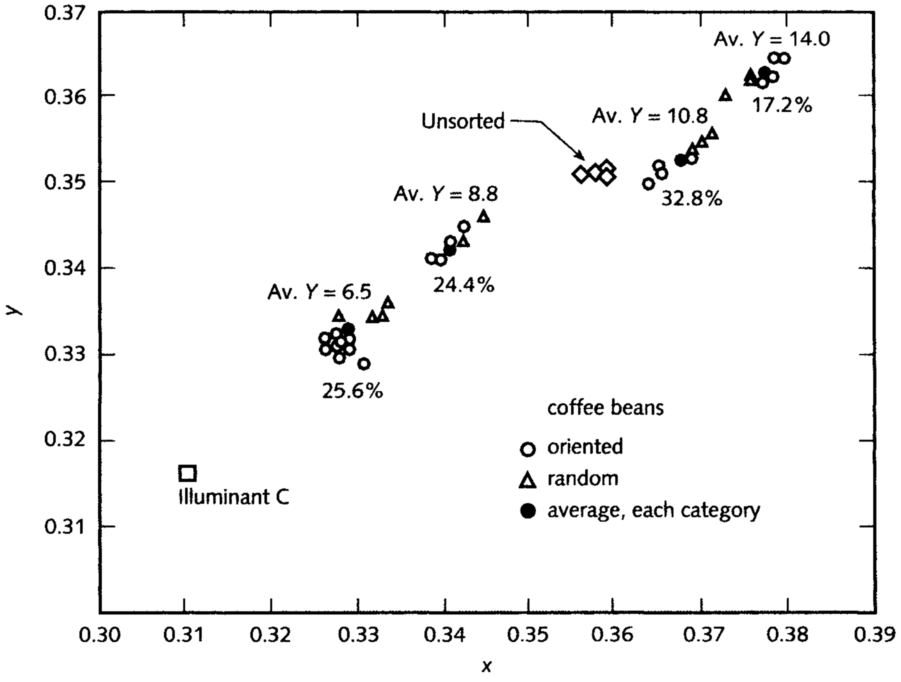

Figure 8.3
Portion of the CIE 1931 chromaticity diagram showing the locations of the measurements made on the four categories of coffee beans. The percentage figures on the diagram are the relative weight amounts of the sorted beans in each category. The average luminous reflectance is indicated alongside the clusters of measurements for each category.

This example is presented for another reason. There are many times when the color of very small objects must be measured; or the color of unevenly colored areas, such as wood with its obvious grain, must be studied. In either of these instances, multiple measurements are essential, and plotting the derived data on a chromaticity diagram can aid tremendously in their interpretation. Blindly averaging the results does not allow for an intelligent interpretation of the measurements.

Once the sample with the best representative color coordinates has been selected as the standard, the total color differences, ΔE, from this chosen standard can be calculated. The total color difference is a *deviation* from the adopted standard and can be treated by standard statistical techniques. For example, in order to determine the significance of measurements, it is useful to calculate the standard deviation, σ or s. It must be remembered that deviations cannot be averaged to determine their statistical significance. The deviations must be converted to variances, the variance being the square of the deviation. The variances can then be averaged. The standard deviation is the square root of the average variance. When the number of measurements, n, is less than about 20, one less than this number, $n - 1$, is used for averaging. Stated as an equation,

$$s = \left[\frac{\Sigma (\Delta E)^2}{n-1} \right]^{\frac{1}{2}} \tag{8.1}$$

In general, s represents the difference that will occur about 67% of the time. Classically, the $2s$ limit, which represents about 95% confidence, is considered a safe limit for the establishment of specifications. Only 5% of the time will results occur that are outside this limit.

An example is the 13 measurements made on the dark coffee beans. The standard deviation calculated using equation 8.1 was $s = 1.63$ $\Delta E^*_{a,b}$; $2s = 3.26$ $\Delta E^*_{a,b}$. One measurement exceeded the $2s$ limit, having a $\Delta E^*_{a,b}$ of 3.6. This procedure was also the statistical method used in adding up the individual color differences of each step in the testing of batches of paints described by Johnston (1963).

The example of the coffee beans represents the problem of measuring mottled or uneven areas, such as the samples of wood mentioned previously. Two approaches can be taken, depending on the nature of the unevenness: (1) if there are patches that are uniform over an area equal to the smallest area of viewing on your instrument, then each of the individual colors in the mottling can be measured separately; (2) if not, measurements can be made with the largest area of view possible. In both cases, take as many measurements as seem necessary to get a picture of the general, overall effect. If measurements are to be made at a later time to determine if any change has occurred, an arrangement must be made to record an accurate location of each area measured. One such arrangement was described by Feller, Curran, and Bailie (1984) for two different instruments used to measure the colors in Japanese prints. Also see the very precise arrangement described by Saunders and Cupitt (1993).

Another difficult color-measuring task is to try to characterize objects that do not have flat, planar surfaces. Curved objects, such as vases, are an example. In general, one should measure total reflectance using the smallest area of view possible and make a number of measurements. If the material has a high gloss and is a dielectric (nonmetal), corrections can be made mathematically for the gloss, as previously described in chapter 4; if it is a metal, the total reflectance is used (see chap. 5).

Many objects present difficult measurement problems when they are nonuniform. Examples are the pointillist dots or the normal streaks and scumbles of many areas in classical painting. This problem was alluded to in the discussion of additive color mixture and subtractive colorant mixture in chapter 2. Just as the human eye integrates such irregularities under certain viewing conditions, so does a color-measuring instrument. The results can be difficult to interpret. Only by making many measurements in the most uniform areas can a possible palette of colorants used by the artist be identified.

Chapter 9

Instrumentation Overview: The Tasks Determine the Selection

The early chapters in this monograph referred to characteristics of instruments used in the study of color problems. The basic design features of spectrophotometers were described in chapter 1, and the calculation of colorimetric descriptions from measured spectrophotometric data was explained in chapter 2. Tristimulus filter colorimeters designed primarily for the measurement of color differences were also mentioned. Later pages dealt with the applications of instrumental measurements of the light reflected or transmitted by objects.

From these discussions, one major conclusion is obvious: the nature of the problem to be solved must first be defined before an instrument appropriate to the task can be selected. Is the problem an analytical problem? Does one wish to measure spectral curves for identification of the colorants used? Does one wish to calculate colorant concentrations for color matching, or to analyze the changes in spectral curves following exposure over periods of time? These are examples of analytical problems. Throughout, it has been emphasized that a spectrophotometric curve in itself is not a description of the color observed. The science of colorimetry derives from the spectral data of the illuminant and standard observers used, as well as from the measured spectral data of the object to be described. Spectral data describing the illuminant and standard observer color-matching functions are necessary to reduce spectral data to terms that may be related to what we see as color. It has been emphasized that both treatments of spectral data—colorimetric and spectrophotometric—are useful and complementary. Thus, three-dimensional colorimetric data, such as tristimulus values, are not very useful in solving analytical problems, and spectral data alone are not generally useful in describing color or color differences. Perhaps it is not necessary to point out that colorimetric data may be obtained from spectral data, but spectral data cannot be determined from colorimetric data.

Spectrophotometry is the fundamental tool used in the study of color. The sensitivities of human visual receptors are described in spectral terms; the sensitivities of other photodetectors, such as the detector used in an instrument, the film in a camera, or the phosphors in a television tube, are also described in spectral terms; so is the light source. And the appearance of the object, the primary aspect discussed in this monograph, is characterized by its spectral reflectance or transmittance.

Spectrophotometry is not, however, an exact science: spectral data depend on the method used to measure them. Factors affecting the measured data depend on the design of the particular instrument used in relation to the characteristics of the material being measured, as well as on the skill and knowledge of the operator. These factors in combination determine the precision of the measurements. The precision of the measurements—that is, their repeatability and reproducibility—must be known. *Repeatability* is here defined as the closeness of the agreement between the results measured successively on the same test specimen by the same operator using the same instrument (ASTM Standard E 284). Thus, repeatability depends on the particular single instrument used, on the skill of the operator, and on the nature of the sample. For measurements made over periods of time, reproducibility is of prime importance. *Reproducibility* is defined as the closeness of agreement of measurements made over periods of time, perhaps by a different operator or by use of a different instrument. Over long periods of time, reproducibility approaching the ability of the human observer to detect small color differences is very difficult to achieve. Careful instrument calibration and a systematic and continuing program of measurement involving stable reference standards (generally ceramics) are required even to approach such a goal. The reference standards need to include samples in various regions of color space and with varying degrees of spectral complexity.

These admonitions apply to tristimulus colorimetric measurements as well as to spectrophotometric measurements. It is absolutely essential that these characteristics of any analytical instrument used, that is, the repeatability and reproducibility, be known before the significance of any measurements can be interpreted meaningfully.

In 1971 a report of the Inter-Society Color Council's Subcommittee for Problem 24, "Color Measuring Instruments: A Guide to Their Selection," was first published (Johnston 1971a). It consisted of a review of instrument characteristics to be considered when an instrument is selected, and it included a basic checklist for analyzing an individual user's problems and needs. In 1983 the report was reprinted by the American Association of Textile Chemists and Colorists as part of their summary publication *Color Technology in the Textile Industry* (Celikiz and Kuehni 1983). Many of the basic ideas presented in this publication are equally valid today. Of particular value is the preparation of a checklist or summary of the purposes for which an instrument is to be used (problems to be solved), and of the various types of instruments, along with their characteristics, that might be used. Thus, a list of available instruments and their characteristics constitutes the second major summary that needs to be made before a logical procedure for solving the color problems at hand can be outlined.

One of the most significant advances in color-measuring instruments made in recent years is the advent of portable colorimeters and spectrophotometers. A summary of the various types was presented by Kettler (1995a) and includes spectrophotometers with 10 nm or 20 nm band intervals, as well as colorimeters. In addition, some "abridged" goniospectrophotometers are described that have fixed angles of illumination and view, generally at three, four, or five angles. Some utilize fiber optics for light transmission.

In a subsequent publication, Kettler (1995b) presented a summary of stationary instruments on the market at the time, including spectrophotometers, colorimeters, and gonio instruments of the abridged type. One goniospectrophotometer, with variable angles of illumination and view over 5° intervals of angle, is described. Made by Carl Zeiss Jena, this instrument measures at 3 nm intervals of wavelength over a 320–720 nm range, using varying angles of illumination and view. Not mentioned in Kettler's review is a goniospectrophotometer manufactured by Murakami Color Research Laboratory in Japan and marketed in the United States by Hunter Associates Laboratory, Incorporated. Both the incident and the viewing angles can be changed. The Trilac goniospectrophotometer, described in chapter 1 and used for the variable-angle measurements reported in chapters 5 and 6, is no longer manufactured, but it may still be in use in some laboratories.

There are several reasons for understanding instrument characteristics, in addition to the need to make a decision concerning the most suitable instrument to purchase. If one already has a color-measuring instrument, or has access to one, there is the need to know exactly what information one can expect to obtain with it. Also, when studying the literature and data reported by previous workers, one must be able to assess the precise meaning of the published data in order to correctly evaluate their significance.

Material (Sample) Characteristics

Of basic importance in defining the problems to be solved and in selecting the best measuring instrument for the task is the consideration of the nature of the materials or samples to be measured. Again, it is advisable to make a list of the types of samples one wishes to study. Throughout this monograph, the types of instruments necessary for measuring various kinds of materials have been described.

If transparent samples—liquids or solids—need to be measured, an instrument capable of making transmission measurements is necessary (see chap. 4). Many of the tristimulus colorimeters using bidirectional geometry have no provisions for making such measurements. In Kettler's lists of color-measuring instruments (Kettler 1995a, b), this feature is not generally included; the specifications obtained from the manufacturer must be consulted.

Translucent samples (liquids or solids) present a difficult measurement problem. (See the section on opacity, translucency, and hiding power in chap. 4.) Because such samples scatter light, an instrument equipped with an integrating sphere that allows for both transmission and reflectance measurements, with a provision for measuring both total and diffuse reflectance, is most desirable.

For the measurement of opaque, uniform, dielectric (nonmetallic) materials, most of the color-measuring instruments are satisfactory, and their selection depends primarily on the purpose of the measurement. If one wishes to measure the color difference of materials of identical colorant composition and surface characteristics, tristimulus filter colorimeters are very satisfactory. There is no need for more elaborate instrumentation. An example of this type of application is quality control in industry.

However, if one wishes to calculate colorant formulations necessary to produce a desired color or to analyze the source of color change (in reality, a colorant composition calculation), then the use of spectrophotometry is essential. (See the section on absorbing and scattering materials in chap. 4.) This task would seem to be a straightforward problem, as some marketers of "push-button" spectrophotometers and computer color-matching systems would have you believe. Although such systems may suffice for many industrial applications, the problems associated with this limited approach largely stem from the small number of wavelengths measured and used for the calculations. If the same colorants can be used to calculate the concentrations necessary to match a given color, such a system may suffice. However, if the same colorants may not be involved in matching a color with a minimum degree of metamerism, as is the case in matching paints to a textile or a ceramic, for example, measurements and computations based on 20 nm intervals may not provide a satisfactory solution. (See the discussion of metamerism in chap. 2.) A larger number of wavelengths, such as those based on 10 nm, 5 nm, or 2 nm intervals, is desirable.

A basic problem to be considered in formulating colorant concentrations to match a standard is the surface reflection characteristics of the reference sample relative to those inherent in the material to be used to make the match. An instrument with an integrating sphere and one that is capable of both including and excluding the specular surface reflection can be helpful. Admittedly, however, there are times when differences in the nature of the surface reflections are a necessary part of the problem, so that visual judgments are often the most satisfactory basis for making a useful compromise.

Throughout these pages, the importance of the surface reflection of dielectrics has been emphasized. Changes in the surface reflection characteristics must be considered, particularly when materials must be evaluated before and after exposure. It is highly desirable to select a color-measuring instrument equipped with an integrating sphere that will measure both the total reflectance (specular component of the reflectance included, SCI) and the diffuse reflectance (specular component of the reflectance excluded, SCE).

For the measurement of the reflectance of metals—that is, nondielectric materials—where the color comes from the reflection at the surface, an instrument capable of measuring the total reflection is essential. If one attempts to measure the color of a highly polished, flat piece of gold, for example, using an instrument with bidirectional geometry or one with an integrating sphere that does not have a provision for including the specular reflection, little or no reflectance will be measured. The proper instrument among those generally used for color measurement is one that measures the total reflectance (SCI). Generally, an instrument equipped with an integrating sphere is used. When the instrument is also capable of excluding the specular reflection—that is, of measuring the diffuse reflectance (SCE)—the specular reflectance (S) alone is then obtained by the difference: S = SCI – SCE. The ratio of the diffuse reflectance to the specular reflectance, SCE/S, provides an indication of the degree to which the polish approaches a perfect mirror surface. (See the section on the color of metals in chap. 5.)

Fluorescent materials have come into common usage today. There are those with obvious fluorescence, such as the fluorescent whitening agents (FWAs) found in most laundry detergents, as well as the high-visibility dyestuffs used in hunters' garb or in warning signs, but others may also be encountered. Many dyes fluoresce; some natural pigments contain fluorescent components; and some modern materials may be made that incorporate fluorescent materials for other reasons. Regardless of the source of the fluorescence, an instrument used for the measurement of such materials must illuminate the sample before separating the reflectances (or transmittances) into the component wavelengths or tristimulus responses. Such an arrangement is generally described as having polychromatic illumination, as opposed to monochromatic illumination. Such an optical arrangement is essential to making measurements that correlate with what one observes. (See the section on fluorescence in chap. 6.) When illuminating materials with the total light from the lamp, the wavelength characteristics of the lamp emission become important in calculating color coordinates. Many of these instruments use xenon flash lamps that include ultraviolet radiation, filtered to approximate the CIE D65 illuminant closely. ASTM Standard E 1247, "Standard Test Method for Identifying Fluorescence in Object-Color Specimens by Spectrophotometry," describes techniques for detecting fluorescence that may not be evident by visual means alone.

The use of metallic flake pigments has become widespread in recent years; the most commonly observed use of aluminum flakes in paints is for automotive finishes. Coated vinyl upholstery fabrics containing metallic flakes have also been used. (See the section on flake pigments in chap. 5.) Because such flakes are relatively large and of low density, they tend to orient primarily parallel to the surface, but they do not completely do so. Thus, these materials change in color intensity depending on the relative orientation of the flakes, and they require goniospectrophotometers to measure the reflectance at various angles of illumination and view. One type of such an instrument was described in chapter 1. Metallic flakes have been used by artists for many years, primarily for simulating silver, gold, bronze, and copper.

Materials that exhibit pearlescence or iridescence also require the use of a goniospectrophotometer to measure their unique color effect. In this case, the critical reflection is specular, which must be measured at an angle equal to and opposite the incident angle. In the use of chromatic interference materials, the reflected color is very high in chroma. Since many such materials are essentially transparent—that is, they scarcely absorb incident light—the wavelengths transmitted are complementary in hue and very much lower in chroma. (See the discussion of pearlescence and iridescence in chap. 5.) The transmitted color can be measured at an angle off the specular angle provided it is reflected by a substrate.

A further application where a goniospectrophotometer is helpful, though less obviously so, is in the characterization of matte or nearly diffuse reflecting surfaces. This elusive aspect was discussed in the section on surface reflection in chapter 6.

Other aspects of the appearance of objects are likewise important, such as the homogeneity of the color in the area to be measured. Nonuniform colored materials can be difficult to measure and describe with certainty. If there are areas where the individual colors can be measured with an available instrument using a very small area of illumination and view corresponding to the size of the areas, such an instrument should be very helpful. If not, an instrument with a very large area of view may be of most value; valuable information can be garnered by making many measurements over the area, then examining the spectral curves (considering both additive color mixture and subtractive colorant mixture), calculating the tristimulus values and chromaticity coordinates and plotting them. An example was presented in chapter 8 describing the measurement of coffee beans. Wood grains are another example where the general color effect of the wood can be characterized using this multiple-measurement technique. Thus, sample size and instrument area of view are important characteristics to be considered in selecting and using an appropriate color-measuring instrument. One may wish to select an instrument that provides several viewing areas, so that the operator can select the smallest for small samples and a larger one for samples where appropriate.

In this monograph no mention has been made of the measurement of the spectral characteristics of light sources or of the intensity of light incident on, transmitted by, or reflected by materials in a display. These measurements require the use of a *spectroradiometer,* an instrument for measuring spectra of colors viewed at a distance away from the instrument. In studying spectroradiometry, a good place to start is ASTM Standard E 1341, "Standard Practice for Obtaining Spectroradiometric Data from Radiant Sources for Colorimetry." In this practice, other sources of basic methods of radiometry are listed: (1) *Radiometric and Photometric Characteristics of Materials and Their Measurement* (CIE 1977); (2) *The Spectroradiometric Measurement of Light Sources* (CIE 1984); (3) "Fundamental Principles of Absolute Radiometry and the Philosophy of the NBS Program," from the National Institute of Standards and Technology (formerly National Bureau of Standards, NBS) (NIST 1968–1971); and (4) *Guide to Spectroradiometric Measurements,* from the Illuminating Engineering Society (IES 1983). A second ASTM standard of interest is E 1336, "Standard Test Method for Obtaining Colorimetric Data from a Video Display Unit by Spectroradiometry." Also referenced in that standard is a technique prescribed by the International Electrochemical Commission (IEC), *Photometric and Colorimetric Methods of Measurement of the Light Emitted by a Cathode-Ray Tube Screen* (IEC 1974).

Because radiometry and spectroradiometry are of such great potential value and importance to those interested in displaying museum objects and in characterizing illumination in museum environments, the above standard methods for their use have been listed. Spectroradiometry and abridged spectroradiometry are far more complex tasks than the spectrophotometry discussed in these pages; they involve many more variables, which must be defined and standardized, such as solid angles, distances, calibrations, and resolutions, in addition to the spectral or colorimetric characteristics.

With modern computers, so-called machine color vision is fast becoming a reality (Novak and Shafer 1992). However, it must be remembered that progress must be based on a fundamental understanding of spectrophotometry and colorimetry and on the factors affecting the appearance of materials, as described in this monograph.

No mention has been made in these pages regarding the study and measurement of retroreflective materials. *Retroreflection* is defined as "reflection in which radiation is returned in directions close to the direction from which it came, this property being maintained over wide variations of the direction of the incident radiation" (ASTM Standard E 284). Retroreflective materials are commonly used for traffic safety markings, license plates, taillights, and so on. Although they may not have been used by artists as yet, thin films of retroreflective material in sheets and tapes are readily available in many colors. For details and information concerning the measurement of retroreflection, consult ASTM Standards E 808, E 809, E 810, and E 811. CIE Publication No. 54 (1982), *Retroreflection: Definition and Measurement,* presents the international standard methods. The measurement of retroreflection incorporates the principles of radiometry and goniophotometry. Special geometric coordinate systems are required and are described in these standards.

Other Instrument Features

The wavelength range of the instrument may offer more versatility in application for analytical purposes. Some spectrophotometers are equipped to be used in the ultraviolet or in the near-infrared regions, for example, in addition to the visible region. Such instruments are generally designed to measure both reflectance and transmittance factors.

The cost of the instrument is always a consideration when making a purchase. As a general rule, the most precise instruments are the most expensive, and the most versatile instruments are also the most expensive. The initial cost may not be the most important factor, however. The importance of the operator and interpreter, and the expense of suitable training and experience for the persons responsible for the instrument's proper usage, ultimately may well be the major cost factor.

Reports

Regardless of the instrumentation used, all reports should include sufficient information about the methods of the instrument's use as well as a precise description—its type, model, serial number, and so on. ASTM Standard E 805, "Standard Practice for Identification of Instrumental Methods of Color or Color-Difference Measurement of Materials," presents an excellent outline of the factors that should be included in a report.

Chapter 10

Suggested Protocol for Recording Spectral Examination Results

The basic nondestructive techniques to be discussed in this chapter—that is, those methods of analysis that do not require samples to be taken from an object—are primarily those based on wavelength-dispersive spectroscopy. They include X-ray fluorescence, which detects most elements, and ultraviolet, visible (the subject primarily dealt with here), and infrared electronic absorptions, which indicate chemical structure. Because many different constituents can exist in any design or depiction of an object, many areas must be examined to achieve insight into the materials that might have been used in its creation. Overlaps of information are common; hence, a systematic scheme of analysis is essential.

It can be helpful, therefore, to prepare an organized procedure (a protocol) to be followed in approaching the analytical problems, so that one is not buried in a random collection of measurements made on many different areas of an object. Fortunately, the number of components used in making any single object is often limited, so that by putting together the information obtained from many measurements, a sense of the artist's medium and palette can be pieced together.

A recommended approach for organizing visible spectrophotometric reflectance data is presented in the following pages. Table 10.1 is an example of a data sheet that could be used in the accumulation of information from spectral reflectance curve measurements on an object.

The following outline provides explanation and suggestions for the item listings on the data sheet. It is keyed to their superscript letters or numbers.

Identification of Object

Object Identification: Use some type of coding that uniquely identifies the object (and its owner).

Artist or Source: If the work is signed, include the name of the artist (if questionable, use a question mark following the name); if the origin of the object is known, record it (if questionable, use a question mark following this designation).

Date of object preparation or creation: If known, record as such; if an estimate, record as such, with a range if possible,

Table 10.1
Data sheet of a protocol for object color analysis by use of spectral reflectance curves.

Object identification:				**Artist or source:**			**Date:**	
Area measured	**Color H, V, C**	**No. abs. bands**	**λ major band**	**λ other abs. bands**	**Positive identification**	**Negative identification**	**Comments**	**Conclusions**
I. Primary colors: B, R, Y								
II. Secondary colors: G, P, O								
III. Near-neutral colors: Gr, Be, nW								

for example, 1940–50, again using a question mark if this range is uncertain.

Working Guide Notes

Area Measured: Assign a number to the measured area and, if possible, identify it by a tracing on the back of the object or on a photocopy of the object or of a picture of the object, and include a description of the area, such as the sky or grass of a landscape painting, or the clothing, drapery, or facial colors of a portrait. Possibly an x and y dimension can be used based on the distance from the lower left corner, as in the usual two-dimensional graph. For a three-dimensional object, provide a location as best as possible.

Color: Include the color name of the hue (H) being measured, for example, the blue (B) in the sky or water, plus an estimate of the lightness or darkness of the measured area (the Munsell Value, V), using the abbreviations of L for light ($V = 6–9$), M for mid-value ($V = 3–5$), and D for dark ($V = 0–2$). To complete the color description, estimate the chroma or saturation: HC for high-chroma colors, MC for medium-chroma colors, and LC for low-chroma colors (near neutrals). Thus, a typical description of the measured color of a painted sky could be B, M, LC, indicating a *blue* (B) of *moderate lightness* (M) and *low chroma* (LC). For additional modifiers, see the remarks that follow the outline.

Number of Absorption Bands: This is important to note; it indicates that pigments exhibiting more than one absorption band may be present or that there may be other colorants present.

λ of Major Absorption Band: The symbol λ is used for wavelength in nanometers (millimicrons in older literature).

λ of Other Absorption Band(s): Present the bands in the order of intensity and, secondarily, on the basis of wavelength—long to short.

Positive Identification: If a unique characteristic is observable in the spectral curves, note it here. For example, phthalo blue and quinacridone structures are often unmistakable.

Negative Identification: Note pigments that are probably *not* present. For example, in a blue region note if phthalo blue with its characteristic red tail, or iron blue with its dropping reflectance in the red region, are not present. To avoid confusion, do this for each color area of the work measured. Do not try to interpret the evidence on the basis of a limited number of measured curves. Facts established step by step eventually reveal a total picture.

Comments: Primarily describe uncertain or questionable results here. It will help with subsequent interpretations.

Conclusions: Include any positive identifications, possible pigments, and recommendations for further measurements, analysis, and testing. If the spectral information is to be used for selecting the least metameric alternate composition for use in reproducing the color, the most suitable colorant or colorant combination could be noted here.

It may be desirable to modify the color designations in column 2 of the data sheet. More specific relative descriptions of the hue, value, and chroma estimates of column 2 may be provided by the use of simple modifiers. Typical hue designations can be B for blue, R for red, Y for Yellow, G for green, P for purple (or violet), and O for orange. For the near neutrals, Gr is used for gray, Be is used for beige, and nW is used for near white. It is a matter of judgment as to when a green becomes a blue or a yellow becomes an orange, and so on. The hue designations selected by one examiner may vary somewhat from those selected by another. Using additional hue modifiers may be of help in avoiding large discrepancies between individuals: differentiations of the basic hue selected may be described by adding a lower-case prefix. For example, measurements made on a blue sky in different areas may be described as rB to indicate a blue area that is redder than the basic blue, or gB to describe a blue area that is greener. Similar descriptors can be used for all of the nine basic hue categories.

Likewise, the relative chroma or lightness can be modified by use of a plus sign (+) or a minus sign (–) after the chroma or lightness designation. Thus, for subsequent measurements of the blue sky illustrated above, a designation could be rB, M+, LC– to describe a blue that is redder than the area designated B; is lighter; and is lower in chroma.

The above descriptors are based on visual evaluations for the convenience of the examiner and are, therefore, relative. They are not defined in any color-order system per se but could be based on reference to the *Munsell Book of Color* if desired.

The data sheet illustrated is abbreviated in length—more data would undoubtedly be needed. However, the important aspect of this abbreviated chart is the systematic approach. A similar but suitably modified protocol could be followed for use with X-ray fluorescence analyses for the metals.

After making many detailed inspections, measurements, and evaluations of the various areas, one should then try to put it all together: enumerate the pigments found with relative certainty; make a record of those not found; note those that may be questionable and subject to further identification techniques if possible; and prepare a summary of the probable palette (selection of pigments) used in creating the object. Further tests that may be required should be noted.

Other regions of absorption are the ultraviolet and the near infrared. Little has been published about pigment absorptions in the ultraviolet. It is probable, however, that only reflectances measured in the near ultraviolet (above 300 nm) would be of value in the case of paints, because of vehicle absorption at shorter wavelengths. The near-infrared region, 700–1000 nm, has been studied more extensively, primarily for camouflage applications. The Colors Division of Ciba Specialty Chemicals (formerly Ciba-Geigy) supplies spectral curves in this region as well as in the visible. For certain pigments, reflectances measured in the near-infrared region can be helpful in identification. The reflectance curves for the α- and β-phthalocyanine blues, for example, differ markedly in this region. Many of the synthetic inorganic pigments tailored for use in camouflage materials likewise have characteristic spectra in the infrared. Whether further study of the regions adjacent to the visible would be helpful is not fully known. Perhaps the near-ultraviolet region would be worthy of further study, especially because of the actinic effect of this shorter-wavelength region.

Finally, it must again be emphasized that in any analytical task, reference material based on known compounds is required. Reference reflectance curves in the visible spectrum of colored compounds are no exception.

Chapter 11

Summary, Conclusions, and Recommendations

The interpretation of spectrophotometric reflectance and transmittance curves in the visible wavelengths encompasses many aspects of color science in addition to the identification of colorants. It is hoped that the material presented in this monograph will prove useful in solving a number of challenging problems encountered in the care of museum objects. The ability to properly interpret spectrophotometric data (the curves) will be a valuable aid in identifying the colorants used in the original work so that the best care and methods of preservation can be instituted. It will contribute to the selection of the colorants most suitable for reproducing the color when necessary. It will provide for the detection and avoidance of metamerism. It will aid in determining when analytical terms of the measured data should be used, or when transformations to trichromatic terms would be more appropriate. It will aid in determining the most meaningful measurement technique for particular materials, such as metals, and for various conditions, such as mottling, streaking, or other irregularities, in the areas to be measured. It will help in determining types and rates of deterioration, and in describing them in analytical terms that can be used for objective interpretation. It will aid in calculating colorant mixture formulations to make desired colors (after suitable reference curves of known pigment concentration are prepared). At the very least, the ability to interpret spectrophotometric data properly contributes to a language that can be used to describe one of our sensations in universally accepted terminology. These points represent the author's principal objectives in preparing this manuscript.

The author's orientation toward the use of pigments led to discussions of the many newer types of pigments and their measurement—fluorescent pigments, pearlescent and interference pigments, and microvoids and vesiculated beads, as well as the more traditional metallic flake pigments. Although these pigments may not occur in antiquities, their presence may occur in post–World War II artifacts or works of art. Most of the examples presented involve pigmented systems; however, the same basic principles apply to materials colored with dyes, such as textiles, paper, and some plastics.

It is hoped that the procedures and guidelines outlined will help the user avoid inappropriate color measurements—measurements made with instruments not carefully standardized; measurements made with instruments not suitable for the task at hand; measurements made with instruments whose reliability and reproducibility are not known; or measurements from which improper conclusions can be drawn out of ignorance. As has been said many times about many specialized analytical applications of instrumentation, the knowledgeable analyst can get a great deal of valid information from the proper use of even the most simple equipment. Conversely, those not experienced in the evaluation of data from elaborate, sophisticated equipment can accumulate considerable information that is meaningless and interpret it with unjustified conclusions.

One cannot understand color and the problems associated with its characterization and description without appreciating its interdisciplinary nature. Color is a psychological response to a physical stimulus. Moreover, object color is but one aspect of appearance. Appearance is affected by many factors: surface characteristics (glossiness, matteness, and uniformity), internal composition, homogeneity, size, shape, and contrast with the surroundings. The attempt to measure and describe human perception requires the application not only of the physical sciences (physics, chemistry, mathematics) but also of the psychology and physiology of vision. Thus, color science requires some knowledge of light and its measurement; some knowledge of the chemistry of the materials that contribute to color; some knowledge of mathematics for treating the measured data; and some knowledge of the visual mechanism and factors that affect the brain's processing of the sensations into a perception.

Because of its interdisciplinary nature, the science of color per se is taught at only a few educational institutions. It is a specialty learned primarily by studying the contributions of previous experts; many of them acquired much of their understanding on their own initiative, helping to create the body of knowledge we have today. The books and selected references listed in appendix E, most of which have already been referred to in the text, provide a useful introduction as well as a means for continuing study. Short courses of a few days to a week, often presented by vendors of instruments, can be helpful if it is remembered that the vendors' primary purpose may be to sell something. A few universities do present short courses, some of an advanced nature and some for a specialized area of application. Nonetheless, the successful acquisition of knowledge about color science depends ultimately on personal pursuit and study.

From the material on spectrophotometry and colorimetry presented in the text, it should be obvious that a reference library of spectrophotometric curves is essential to the application of many of the techniques described. Instead of each laboratory collecting and preparing its own atlas of spectral curves, the information already available in publications or in other laboratories should be collected together for the use of everyone. The development of color-measuring instruments and computer color-matching techniques in the 1950s led to the measurement and publication of numerous reflectance curves, particularly by colorant manufacturers. Before many of the curves become lost due to obsolescence, changes in manufacture, or lack of interest, they should be accumulated into an atlas.

Collections of dyes as well as pigments of known origin and composition should also be accumulated and updated as new materials become available. It would be a shame to lose such a valuable record of the newer colorants that are being used by artists and artisans today—they will be of great value for conservation scientists in the future.

With the expanding use of color-measuring instruments in museum laboratories, collections of both colorants and colorant spectrophotometric curves would aid tremendously in the study of the various problems faced. This is particularly true for the care of relatively modern works, some of which are already in need of restoration and all of which need proper environmental conditions for their preservation.

Organizing the hundreds of curves in a manner that facilitates their use presents a challenge. A protocol for one type of orderly arrangement is presented in appendix D; it is based on hue as well as on the number, location (wavelength), and relative intensity of the absorption bands exhibited in the spectral reflectance curves. The organization of some of the many red pigments available is used as an example. Preparation of such a library may appear initially to be a formidable task, particularly if the curves were to be redrawn to a standard scale. However, if an institution or organization were to take on the work of accumulating and organizing the curves and of offering them simply as reproductions in their original format, it would be carrying out an invaluable service. The author would be happy to turn over her collection as a start in this effort. Many companies and laboratories would be willing to contribute copies of their spectral curves for this undertaking. It is the author's sincere hope that such an atlas of spectrophotometric curves will be made in the near future.

Appendix A

Curves and Data for Pigments Used as Illustrative Problems

The reflectance curves, CIE colorimetric data, and Munsell notations for the colorants used as illustrations in the text are presented for eleven chromatic colorants, four white pigments, and a carbon black at a series of concentrations. All of the samples were prepared in a high gloss thermosetting acrylic automotive enamel. The curves for the eleven chromatic colorants and the carbon black are mixtures with rutile TiO_2 white; curves for one concentration of the eleven chromatic colorants and rutile TiO_2 with carbon black as well as with burnt umber are also included. For the transparent pigments, only the maximum concentrations used in white are illustrated; for scattering pigments, masstones are also illustrated. Masstone curves for the four whites as well as mixtures with carbon black are included. Curves for the whites, black, and burnt umber are presented first. Then the curves for the primary colors, blue, red, and yellow are illustrated, followed by the curves for the secondary colors, green, violet (purple), and orange. Because the secondary colors and the near-neutral colors can be made by admixture of appropriate primary colorants, a few curves of such mixtures are also included.

The reflectance curves illustrated are the total reflectances—that is, the surface specular reflections are included. The CIE colorimetric data for illuminant C and the 2° observer were determined for the diffuse reflectances obtained by subtracting 4% for the specular surface reflections from the total reflectances. The CIE data are illustrated on a chromaticity diagram in figure A.1. For those samples whose masstones are included, they are connected to the highest concentration in white by a dotted line.

The CIE colorimetric data and the Munsell notations calculated from these values are presented in tables that are interspersed with the reflectance curves according to hue.

For simplicity in presenting the CIE and Munsell notations in the tables, abbreviations for the pigments have been used. The following is a list of them:

R. TiO_2 = rutile titanium dioxide; PW 6
A. TiO_2 = anatase titanium dioxide; PW 6
ZnO = zinc oxide; PW 4
Pb white = basic lead carbonate; PW 1
Black = carbon black; Pbk 7

UB = ultramarine blue; PB 29
PB = alpha-phthalocyanine blue (phthalo blue, red shade); α-PB 15
ROX = synthetic red oxide; PR 101
BON = BON red (BON is the abbreviation for beta-oxynaphthoic acid coupling component used in the making of many red pigments. Many red pigments were formerly called BON reds, so the exact composition is not known.)
QR = Quinacridone Red
YOX = synthetic yellow iron oxide; PY 42
FGL = Permanent Yellow FGL; PY 79
PG = phthalocyanine green
CV = carbazole dioxazine violet; PV 23
MO = molybdate orange; PR 104

Colorant names are often misleading; the same name may be applied to different colorants. An example is the BON red described above. Accordingly, the need for a method that would identify colorant chemical composition was recognized long ago. The system most widely used today to accomplish this purpose is the *Colour Index* published under the aegis of the Society of Dyers and Colourists of Great Britain and the American Association of Textile Chemists and Colorists. It is described by Billmeyer and Saltzman. A brief description of the system is given here in appendix C.

In most application laboratories, Colour Index names and numbers were not used extensively when the samples for the reflectance curves in this appendix and those in Chapter 7 were made. At that time, popular color names or trade names were employed in everyday use. Whenever possible, the Colour Index names, such as PW 6 for the TiO_2 white pigments, have been used in the abbreviation list above. Those appearing without Colour Index names cannot be cited with certainty at this late date. This omission is generally not serious, because a Colour Index name alone is not generally sufficiently specific. For example, PW 6 does not distinguish between rutile and anatase TiO_2. The Colour Index number is more specific but also does not characterize all of the variations in pigments that may be dependent on variations in manufacturing and treatments.

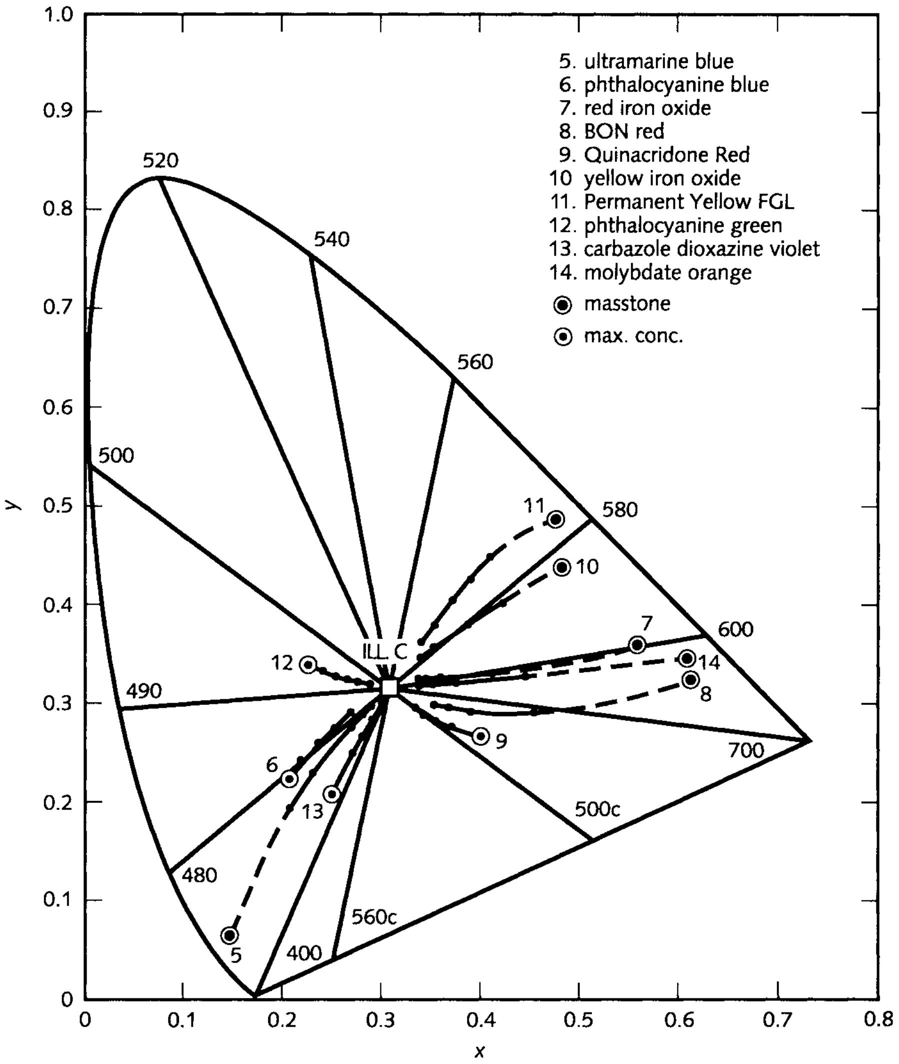

Figure A.1

Chromaticity diagram of colorants in appendix A mixed with rutile TiO_2.

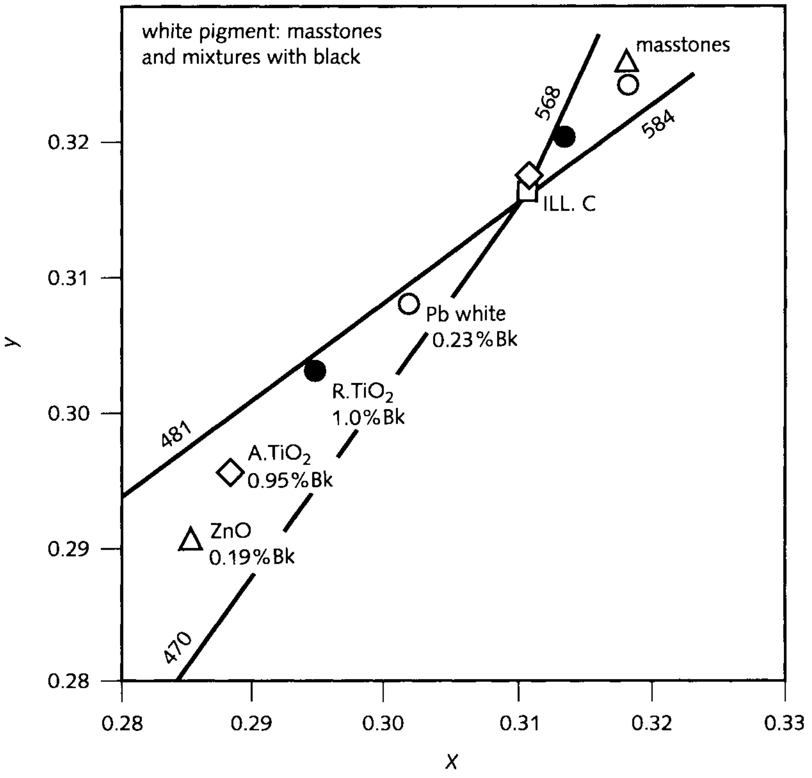

Figure A.2

Portion of the chromaticity diagram for masstone whites and white–black mixtures.

		CIE			Munsell	
Figure	Pigment composition	*x*	*y*	*Y*	Hue	Value/Chroma
A.3	0.10% black, 99.9% R. TiO_2	0.3043	0.3120	68.32	1.61 PB	8.50/0.79
	0.50% black, 99.5% R. TiO_2	0.2982	0.3061	48.45	3.14 PB	7.36/1.54
	2.00% black, 98.0% R. TiO_2	0.2909	0.2990	29.06	3.27 PB	5.92/1.93
	8.00% black, 92.0% R. TiO_2	0.2830	0.2907	13.21	3.08 PB	4.18/1.83
A.4	1.00% black, 99.0% R. TiO_2	0.2947	0.3030	38.65	3.20 PB	6.69/1.78
	0.95% black, 99.05% A. TiO_2	0.2881	0.2952	36.98	4.08 PB	6.56/2.55
	0.19% black, 99.81% ZnO	0.2853	0.2902	39.57	5.32 PB	6.76/3.08
	0.23% black, 99.77% Pb white	0.3016	0.3082	41.34	4.49 PB	6.89/1.09
A.5	100% R. TiO_2	0.3129	0.3203	90.66	8.41 Y	9.53/0.22
	100% A. TiO_2	0.3103	0.3165	91.38	0.00 N	9.56/0.00
	100% ZnO	0.3180	0.3257	86.30	4.37 Y	9.35/0.57
	100% Pb white	0.3178	0.3241	86.16	1.58 Y	9.34/0.53
A.6	0.5% B. umber, 99.5% R. TiO_2	0.3266	0.3286	71.21	7.17 YR	8.65/1.19
	2.5% B. umber, 97.5% R. TiO_2	0.3416	0.3377	52.38	6.63 YR	7.61/2.08
	10.0% B. umber, 90.0% R. TiO_2	0.3620	0.3487	32.30	6.30 YR	6.19/2.83
	40.0% B. umber, 60.0% R. TiO_2	0.3905	0.3594	12.82	6.07 YR	4.13/3.06
	100.0% B. umber, 0.0% R. TiO_2	0.3790	0.3384	1.81	4.09 YR	1.39/1.38

Table A.1

CIE and Munsell notation (diffuse reflectance) for whites, blacks, and burnt umber.

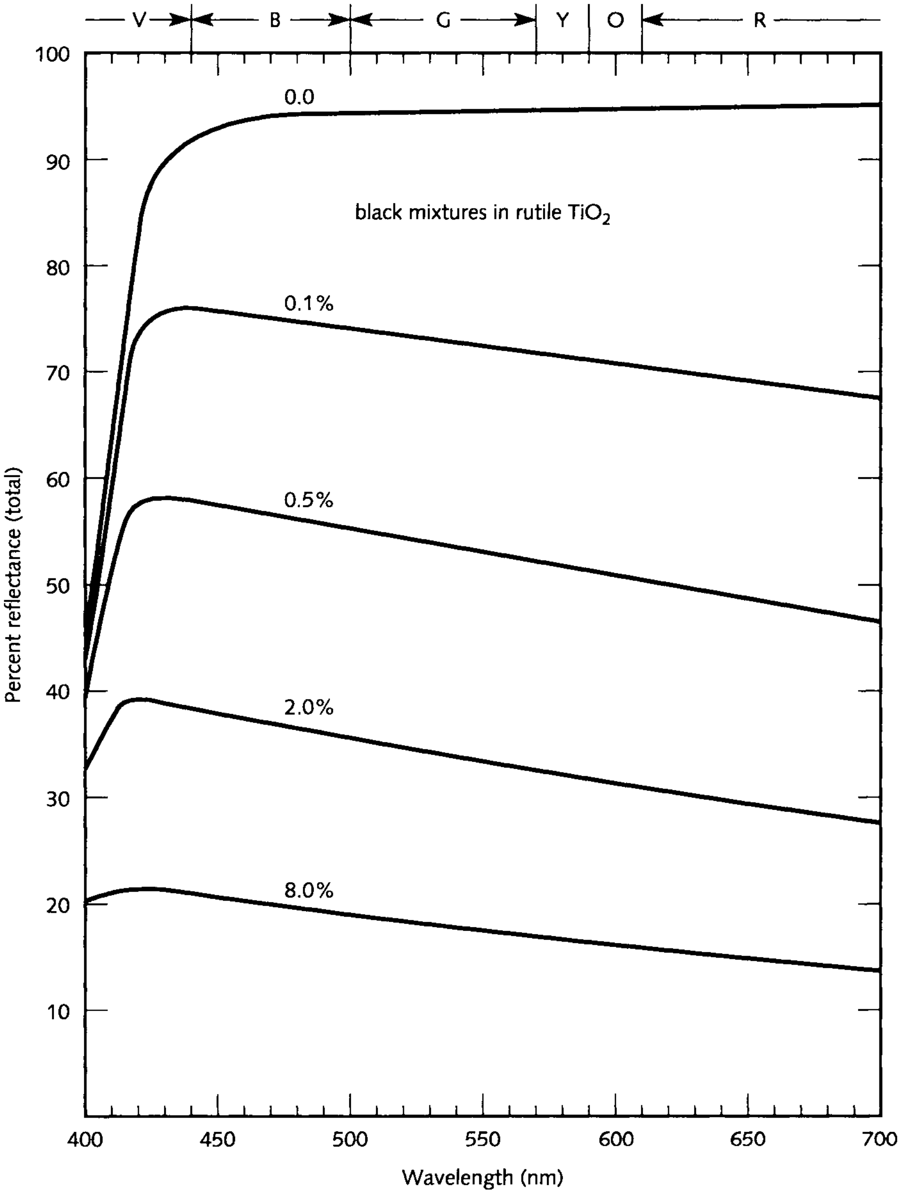

Figure A.3
Carbon black in rutile TiO_2.

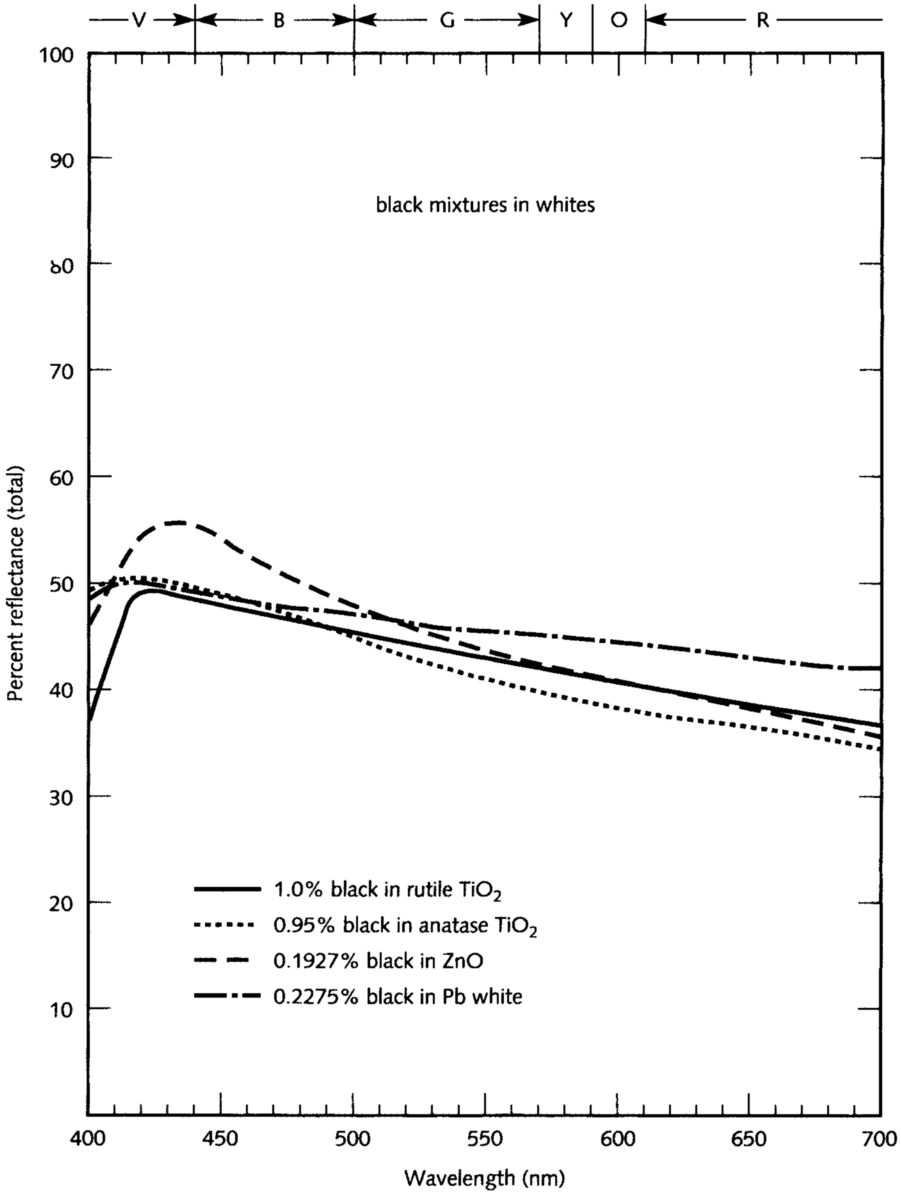

Figure A.4

Carbon black in rutile TiO_2, anatase TiO_2, ZnO, and Pb white.

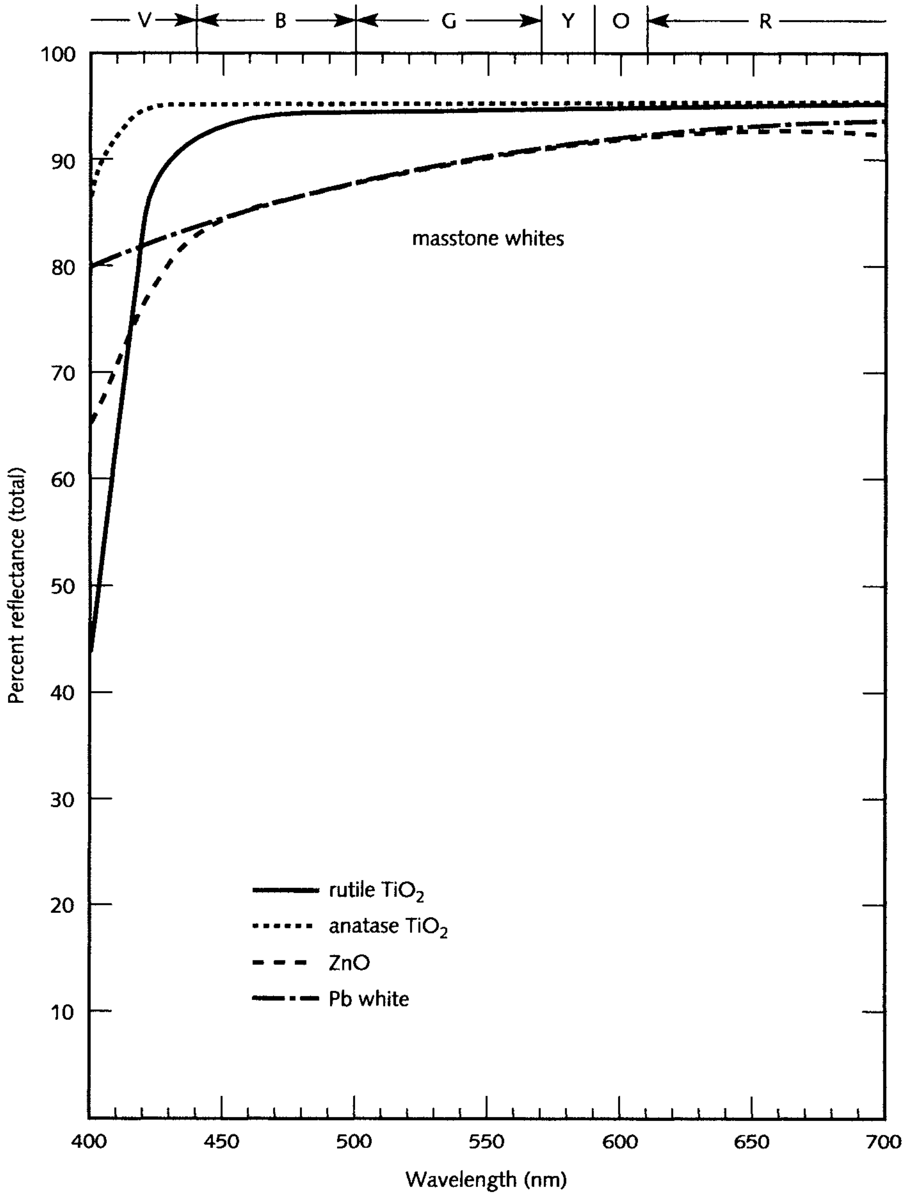

Figure A.5

Masstone whites: rutile TiO_2, anatase TiO_2, ZnO, and Pb white.

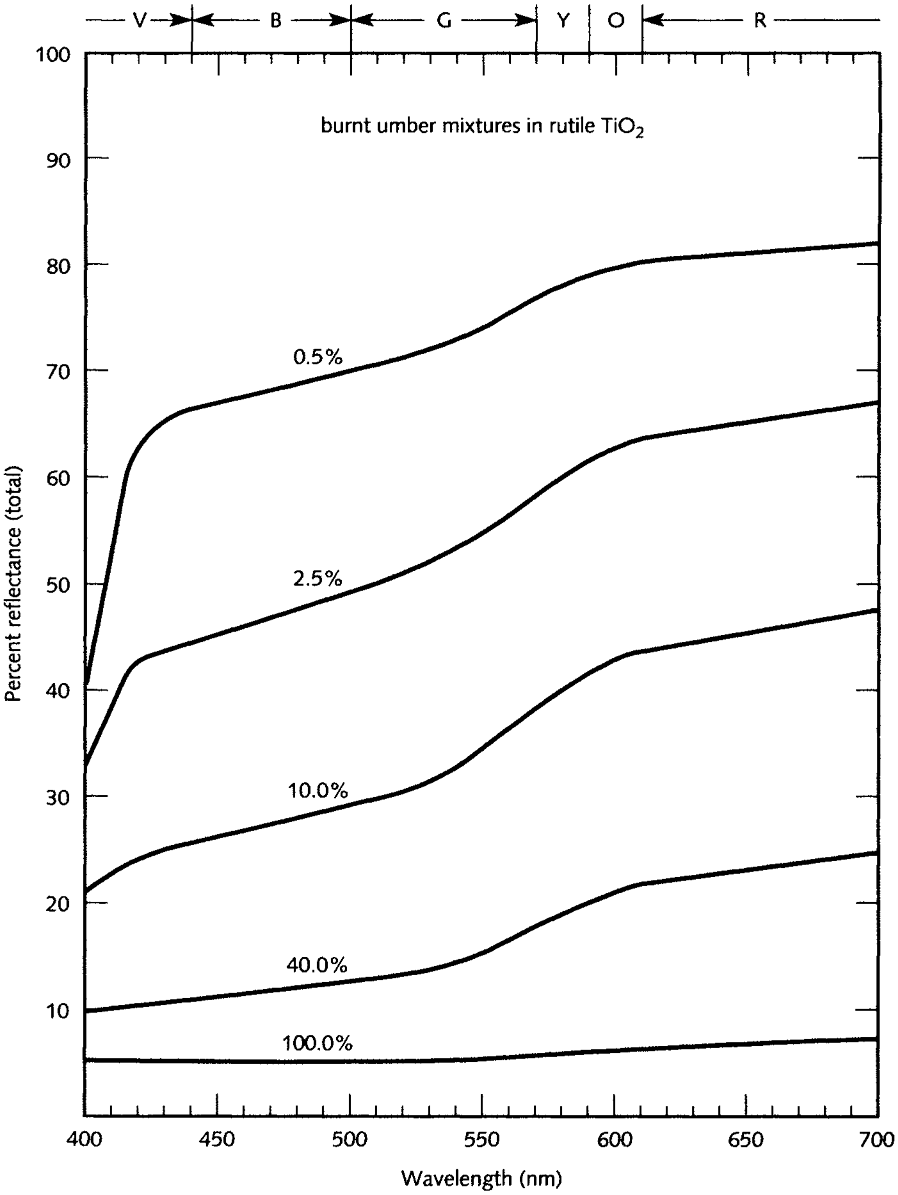

Figure A.6

Burnt umber mixtures in rutile TiO_2.

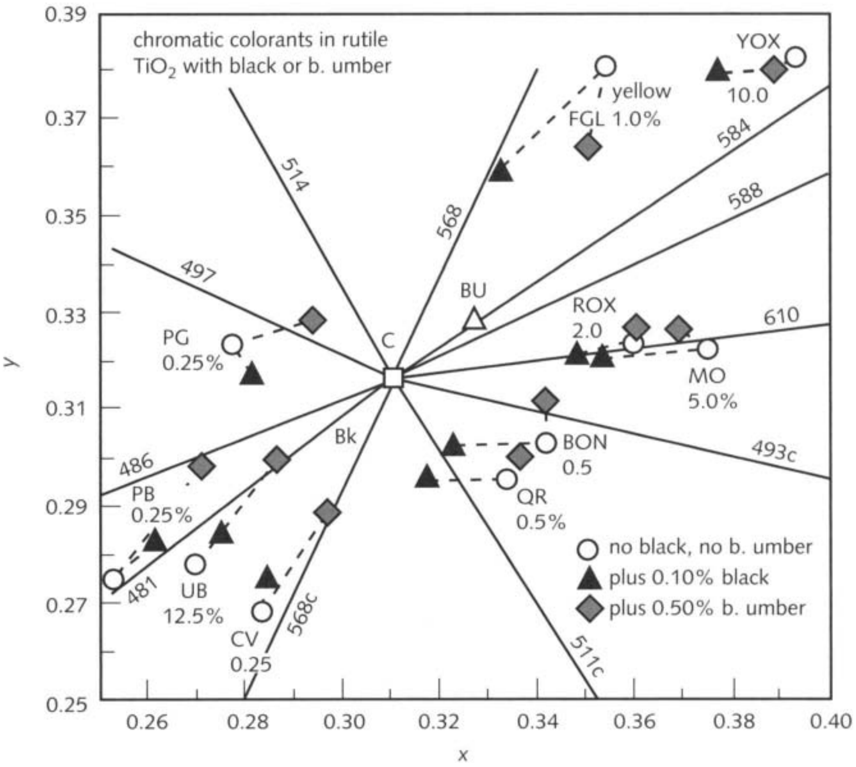

Figure A.7

Portion of the chromaticity diagram for the chromatic colorants mixed with rutile TiO$_2$ and with black or burnt umber added.

		CIE			Munsell	
Figure	**Pigment composition**	***x***	***y***	***Y***	**Hue**	**Value/Chroma**
A.8	3.00% UB, 97.0% R. TiO$_2$	0.2896	0.2990	71.42	2.46 PB	8.66/2.66
	12.50% UB, 87.5% R. TiO$_2$	0.2694	0.2779	54.35	3.82 PB	7.73/4.85
	50.0% UB, 50.0% R. TiO$_2$	0.2313	0.2324	28.56	4.79 PB	5.87/8.33
	75.0% UB, 25.0% R. TiO$_2$	0.2058	0.1951	16.63	5.57 PB	4.64/10.20
	100.0% UB, 0.0% R. TiO$_2$	0.1475	0.0645	2.27	6.28 PB	1.63/17.45
A.9	12.5% UB, 0.02% black, 87.48% R. TiO$_2$	0.2711	0.2800	53.33	3.75 PB	7.67/4.63
	12.5% UB, 0.10% black, 87.40% R. TiO$_2$	0.2750	0.2845	49.97	3.58 PB	7.46/4.10
	12.5% UB, 0.5% B. umber, 87.00% R. TiO$_2$	0.2864	0.2983	50.10	1.33 PB	7.47/2.68
A.10	0.10% PB, 99.9% R. TiO$_2$	0.2703	0.2900	65.26	0.14 PB	8.34/4.13
	0.25% PB, 99.75% R. TiO$_2$	0.2526	0.2747	54.84	0.60 PB	7.76/5.89
	0.50% PB, 99.50% R. TiO$_2$	0.2370	0.2602	46.14	0.73 PB	7.21/7.33
	1.00% PB, 99.00% R. TiO$_2$	0.2201	0.2432	37.27	0.94 PB	6.59/8.72
	2.00% PB, 98.00% R. TiO$_2$	0.2029	0.2242	28.77	1.24 PB	5.89/10.06
A.11	0.25% PB, 0.10% black, 99.65% R.TiO$_2$	0.2614	0.2827	50.19	0.19 PB	7.47/4.87
	0.25% PB, 0.50% B. umber, 99.25% R. TiO$_2$	0.2712	0.2965	49.96	7.45 B	7.46/3.62

Table A.2

CIE and Munsell notation (diffuse reflectance) for ultramarine blue (UB) and phthalo blue (PB).

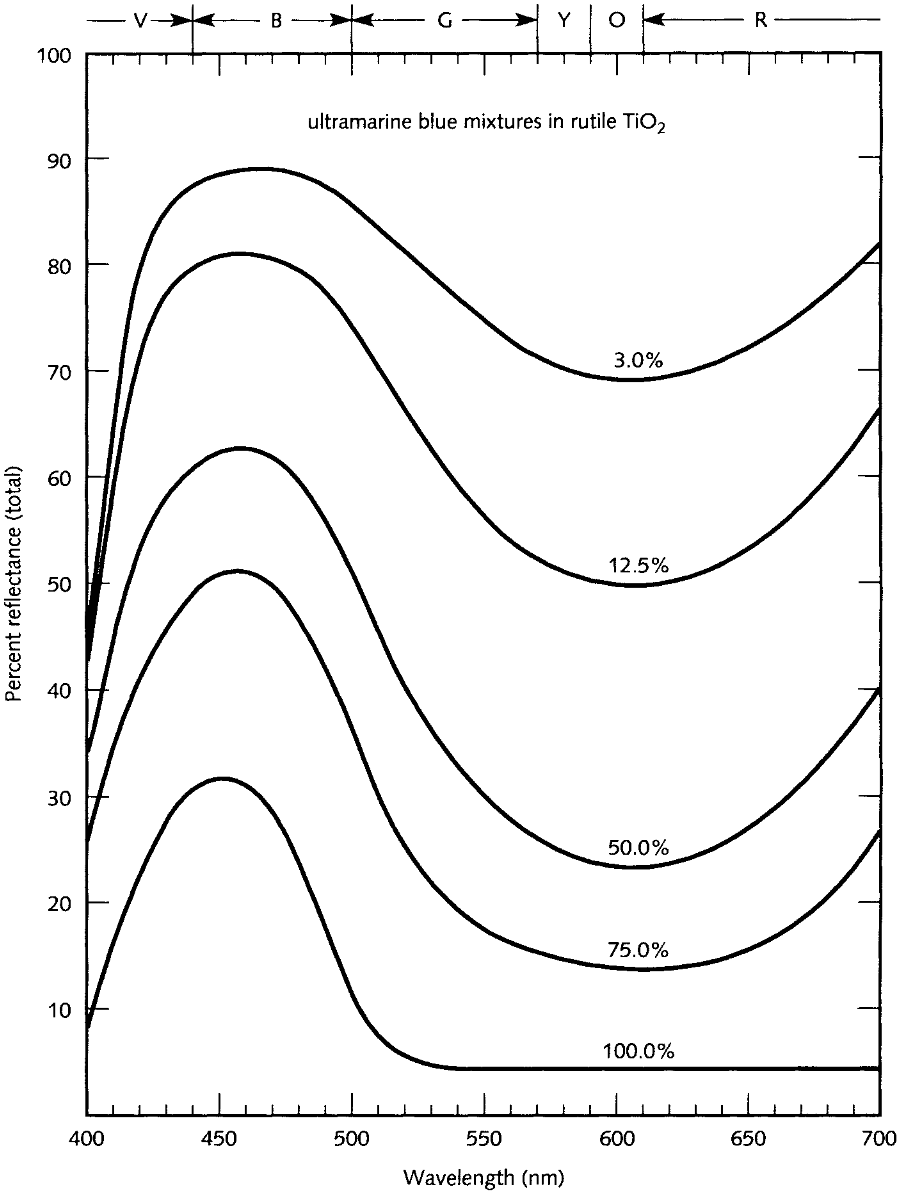

Figure A.8

Ultramarine blue mixtures in rutile TiO_2.

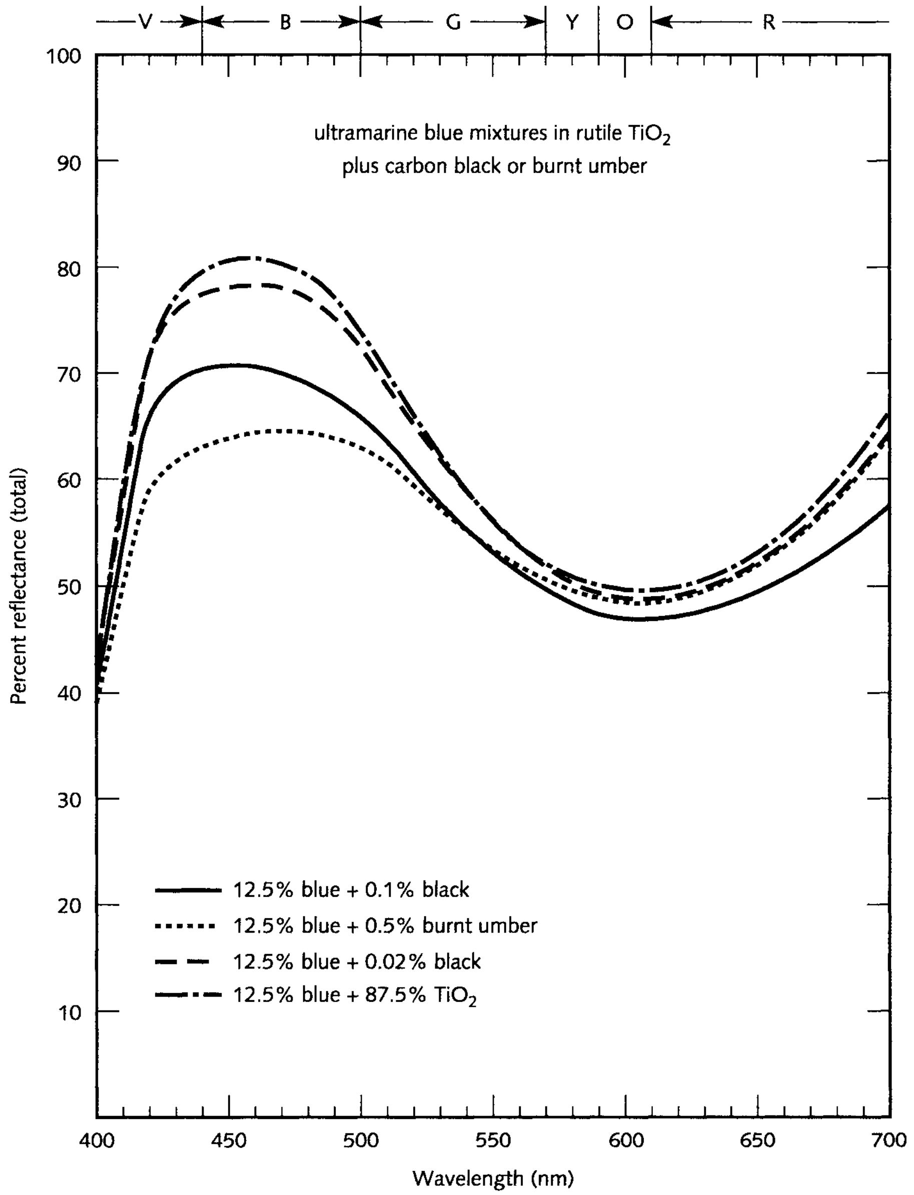

Figure A.9

Ultramarine blue mixtures in rutile TiO_2, and with carbon black or burnt umber added.

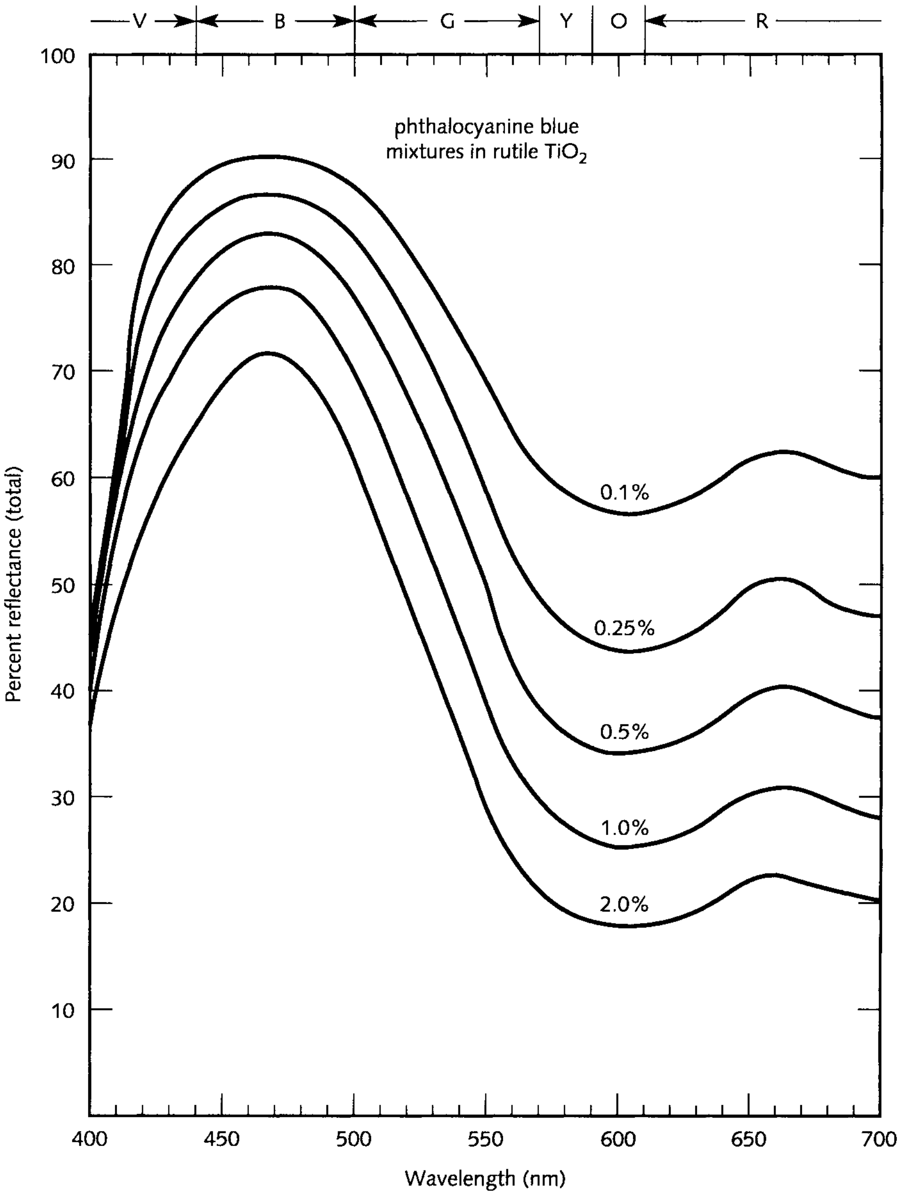

Figure A.10

Phthalocyanine blue mixtures in rutile TiO_2.

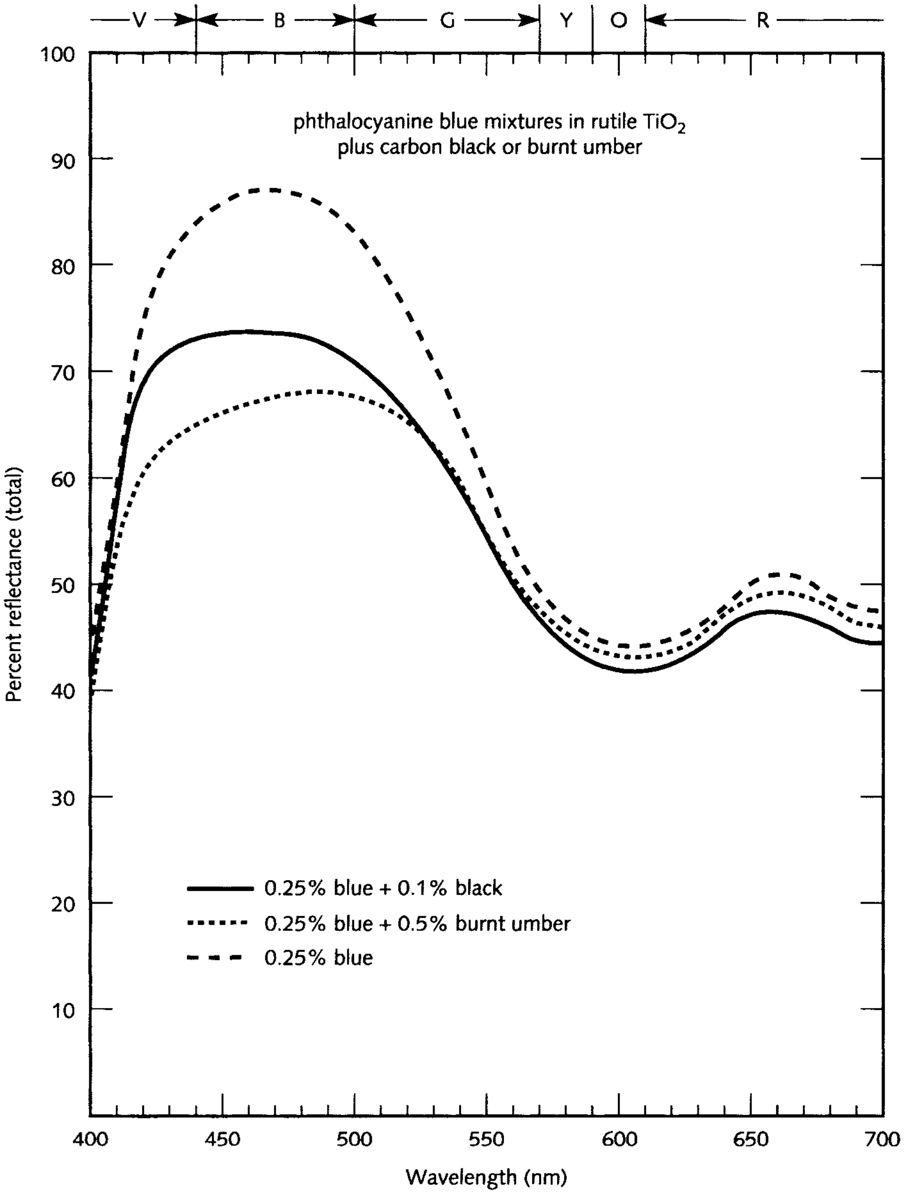

Figure A.11

Phthalocyanine blue mixtures in rutile TiO_2, and with carbon black or burnt umber added.

			CIE			Munsell
Figure	**Pigment composition**	*x*	*y*	*Y*	**Hue**	**Value/Chroma**
A.12	0.50% ROX, 99.5% R. TiO_2	0.3374	0.3209	67.31	4.88 R	8.45/3.05
	2.00% ROX, 98.00% R. TiO_2	0.3595	0.3235	50.89	5.27 R	7.52/4.49
	12.5% ROX, 87.5% R. TiO_2	0.4130	0.3304	26.76	6.20 R	5.71/6.80
	100.00% ROX, 0.00% R. TiO_2	0.5585	0.3595	7.85	0.66 YR	3.28/9.40
A.13	2.00% ROX, 0.10% black, 97.9% R. TiO_2	0.3476	0.3215	47.00	5.05 R	7.27/3.47
	2.00% ROX, 0.50% B. umber, 97.5% R. TiO_2	0.3595	0.3261	48.47	6.42 R	7.36/4.19
A.14	0.25% BON, 99.75% R. TiO_2	0.3320	0.3062	68.80	5.59 RP	8.53/4.06
	0.50% BON, 99.5% R. TiO_2	0.3409	0.3028	61.61	6.00 RP	8.14/5.13
	1.00% BON, 99.00% R. TiO_2	0.3530	0.2990	53.52	6.31 RP	7.68/6.46
	4.00% BON, 96.00% R. TiO_2	0.3918	0.2922	36.36	8.00 RP	6.52/9.62
	15.00% BON, 85.00% R. TiO_2	0.4557	0.2910	21.91	0.58 R	5.24/11.89
	100.00% BON (masstone)	0.6157	0.3248	7.32	8.42 R	3.17/12.28
A.15	0.50% BON, 0.10% black, 99.4% R. TiO_2	0.3225	0.3018	54.44	2.58 RP	7.73/3.52
	0.50% BON, 0.50% B. umber, 99.00% R. TiO_2	0.3407	0.3113	56.60	8.92 RP	7.86/4.14
A.16	0.50% QR, 99.5% R. TiO_2	0.3340	0.2954	63.93	3.34 RP	8.27/5.48
	1.00% QR, 99.00% R. TiO_2	0.3431	0.2890	56.11	3.58 RP	7.83/7.04
	2.00% QR, 98.00% R. TiO_2	0.3553	0.2882	47.65	4.12 RP	7.31/8.41
	4.00% QR, 96.00% R. TiO_2	0.3715	0.2756	39.00	4.73 RP	6.71/10.16
	10.00% QR, 90.00% R. TiO_2	0.4012	0.2685	28.11	6.05 RP	5.83/12.00
A.17	0.50% QR, 0.10% black, 99.40% R. TiO_2	0.3172	0.2960	56.01	9.99 P	7.83/3.83
	0.50% QR, 0.50% B. umber, 99.00% R. TiO_2	0.3366	0.3080	58.29	7.08 RP	7.96/4.17

Table A.3

CIE and Munsell notation (diffuse reflectance) for red iron oxide (ROX), BON red, and Quinacridone Red (QR).

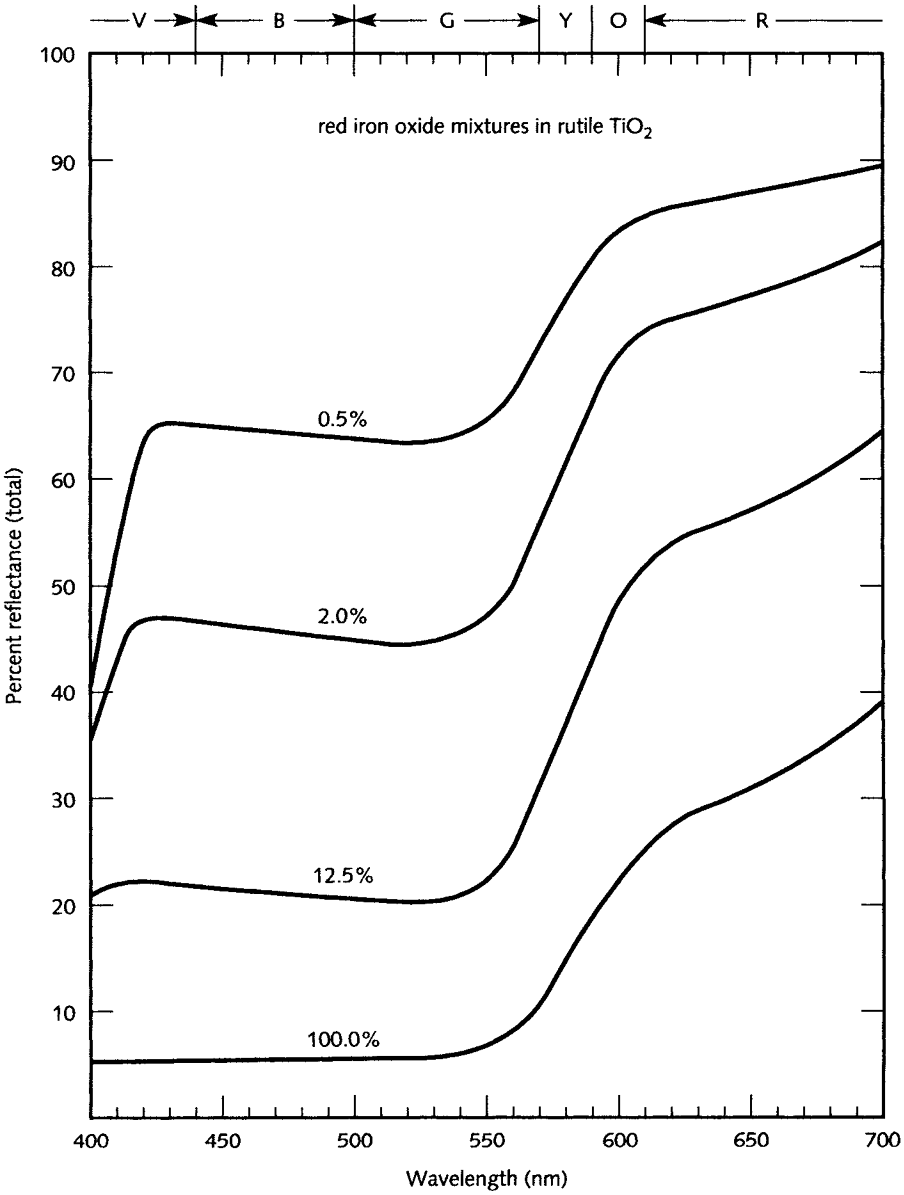

Figure A.12

Red iron oxide mixtures in rutile TiO_2.

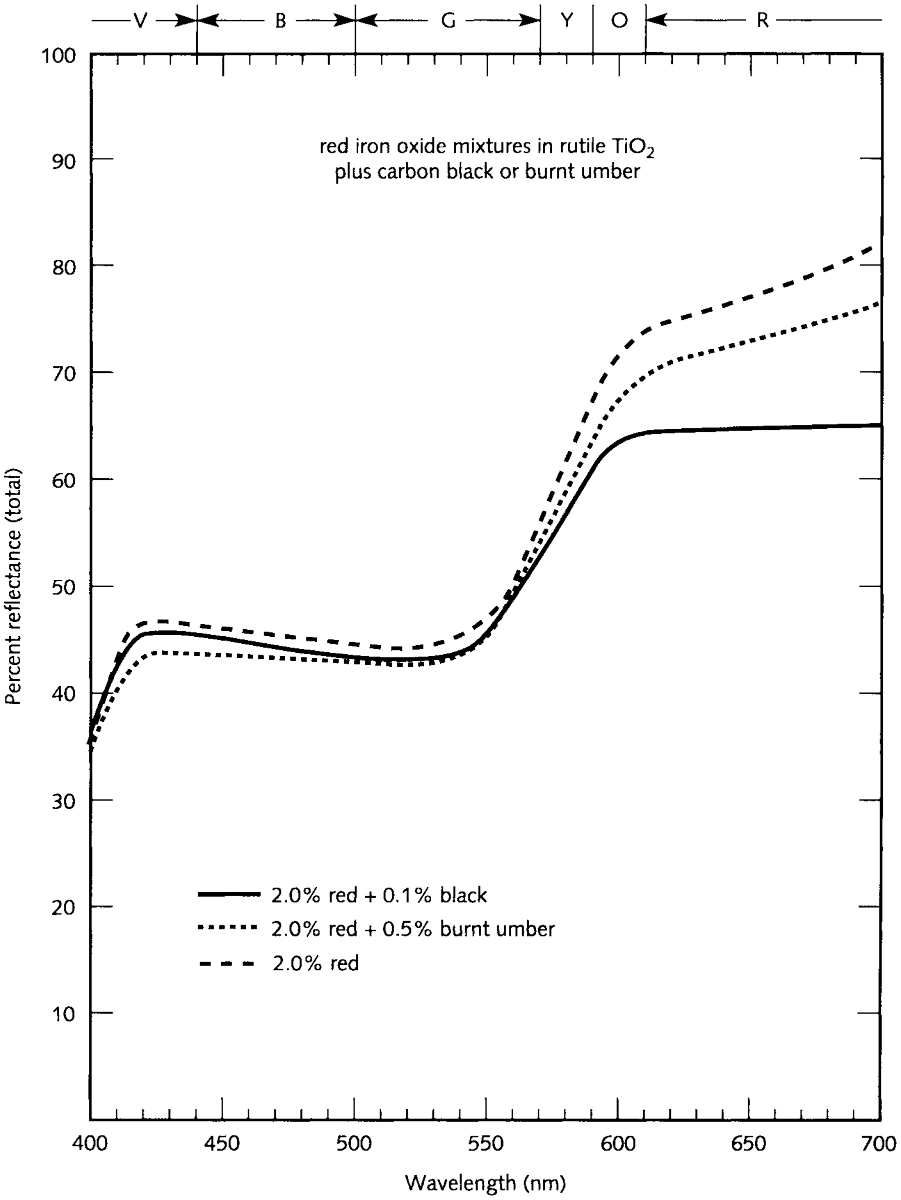

Figure A.13

Red iron oxide mixtures in rutile TiO_2, and with carbon black or burnt umber added.

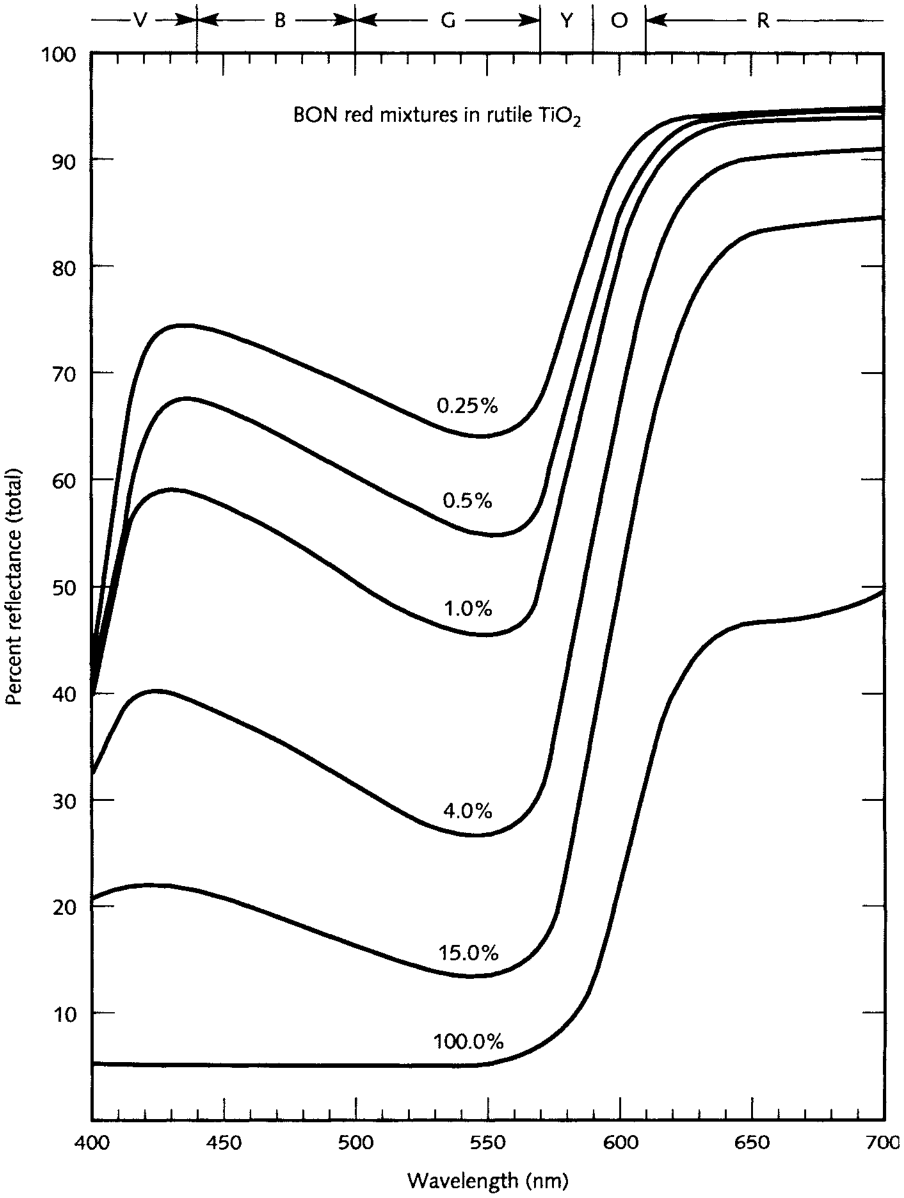

Figure A.14

BON red mixtures in rutile TiO_2.

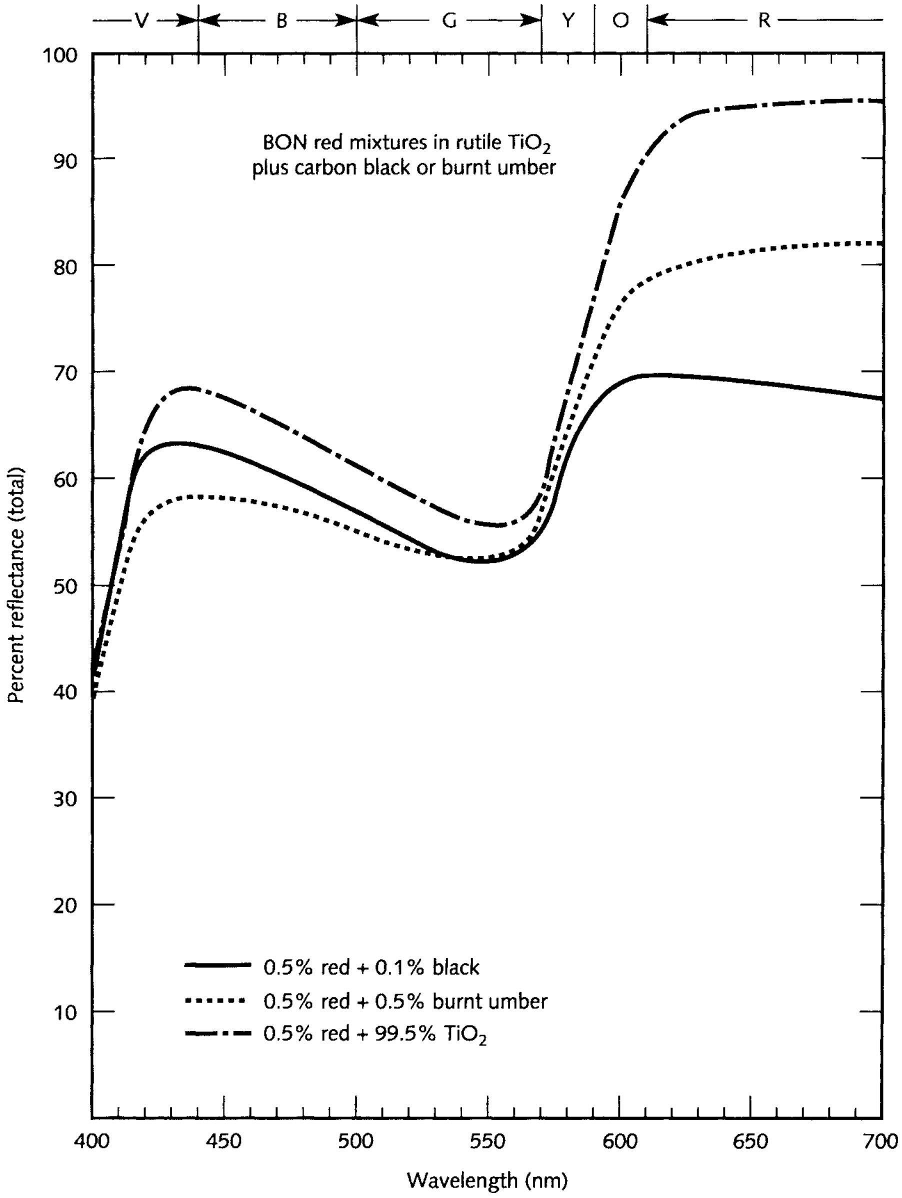

Figure A.15

BON red mixtures in rutile TiO_2, and with carbon black or burnt umber added.

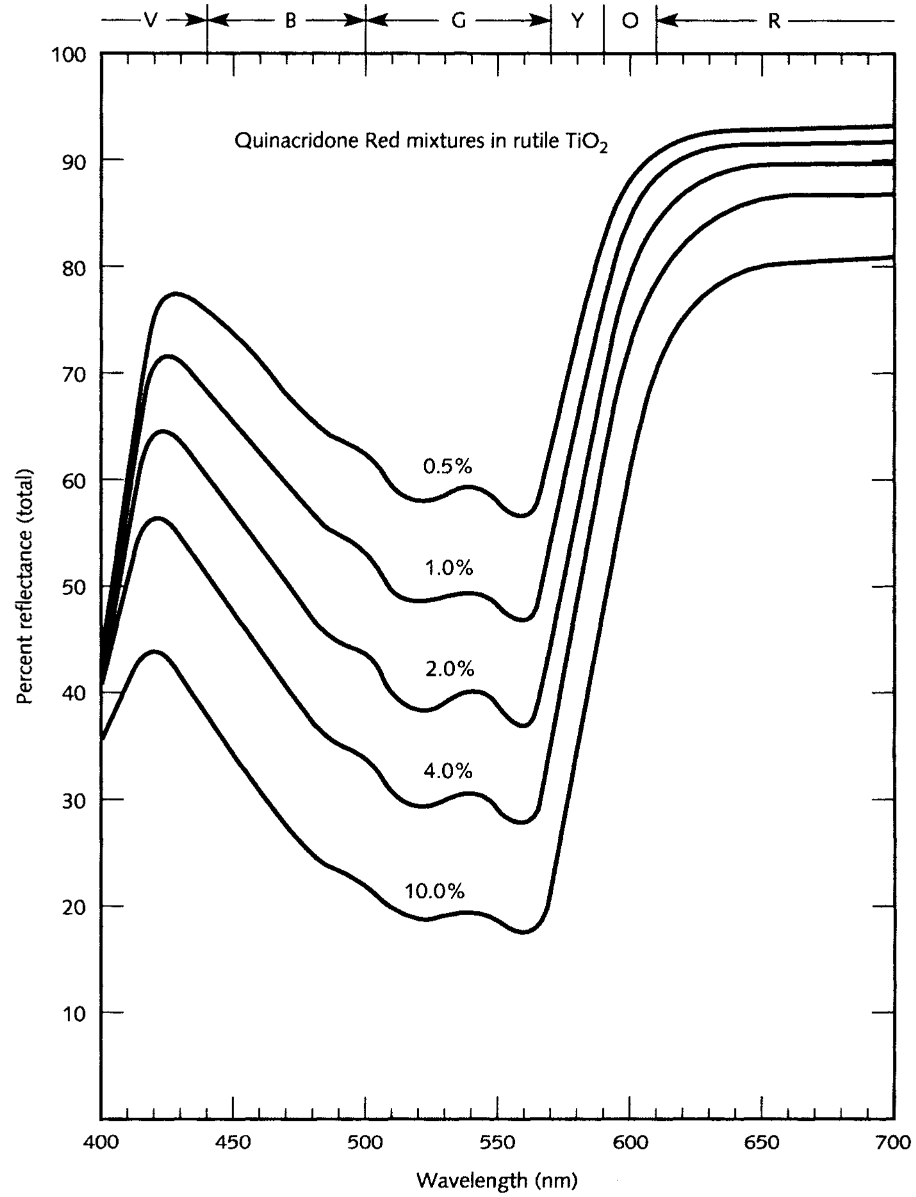

Figure A.16

Quinacridone Red mixtures in rutile TiO_2.

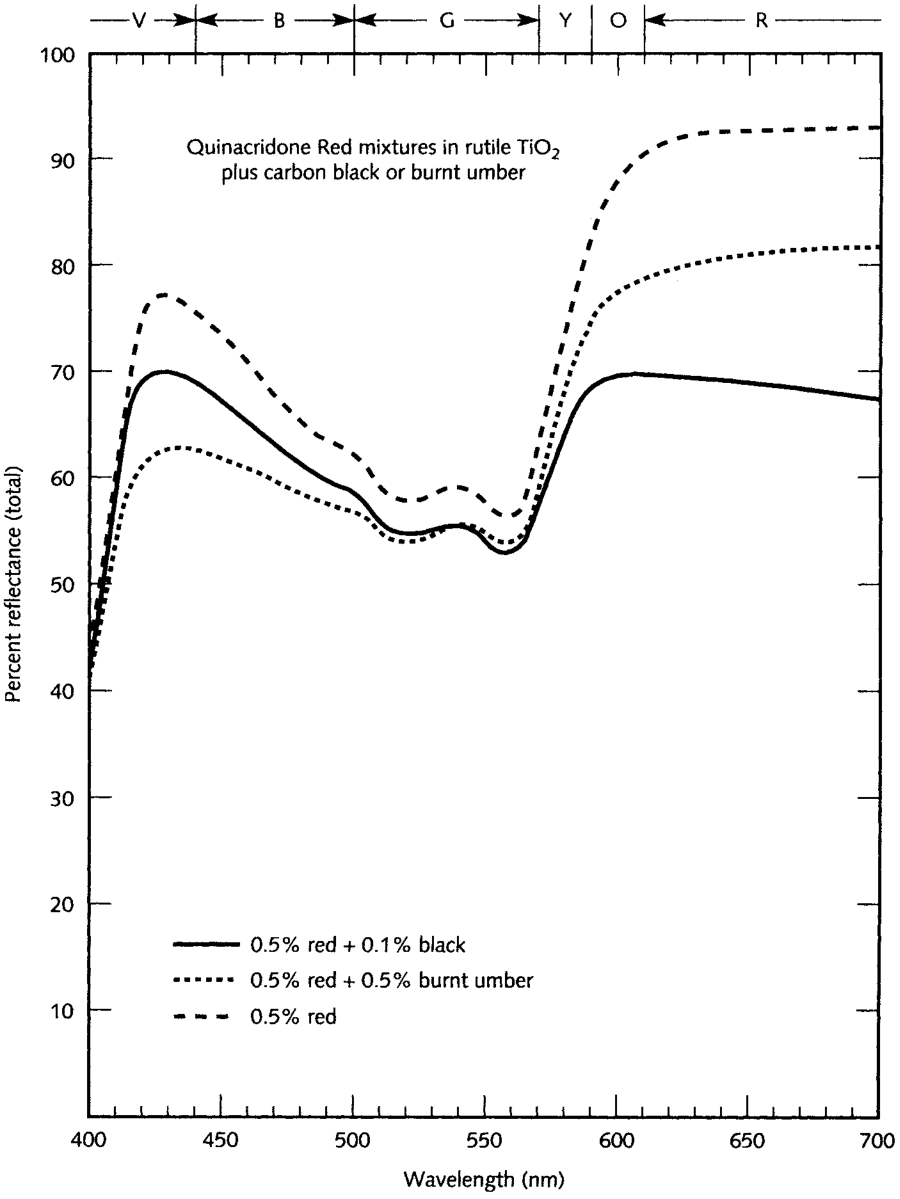

Figure A.17

Quinacridone Red mixtures in rutile TiO_2, and with carbon black or burnt umber added.

Figure	Pigment composition	CIE			Munsell	
		x	*y*	*Y*	Hue	Value/Chroma
A.18	1.00% YOX, 99.00% R. TiO_2	0.3411	0.3453	80.07	0.41 Y	9.07/2.14
	2.50% YOX, 97.50% R. TiO_2	0.3565	0.3577	73.63	0.15 Y	8.77/3.19
	10.00% YOX, 90.00% R. TiO_2	0.3909	0.3823	59.68	9.82 YR	8.04/5.43
	25.00% YOX, 75.00% R. TiO_2	0.4234	0.4017	47.67	9.46 YR	7.31/7.05
	100.00% YOX (masstone)	0.4849	0.4387	24.18	9.86 YR	5.47/9.27
A.19	10.00% YOX, 0.10% black, 89.9% R. TiO_2	0.3756	0.3772	53.00	1.51 Y	7.65/4.27
	10.00% YOX, 0.5% B. umber, 89.5% R. TiO_2	0.3874	0.3793	55.31	9.83 YR	7.79/5.06
	70.00% YOX, 5.00% black, 25.00% R. TiO_2	0.3732	0.4044	10.88	9.09 Y	3.83/3.06
A.20	0.50% FGL, 99.5% R. TiO_2	0.3471	0.3642	88.21	0.13 GY	9.43/2.67
	1.00% FGL, 99.0% R. TiO_2	0.3531	0.3805	87.15	9.71 Y	9.38/3.72
	2.50% FGL, 97.5% R. TiO_2	0.3761	0.4066	85.21	8.91 Y	9.30/5.49
	5.00% FGL, 95.00% R. TiO_2	0.3904	0.4285	83.23	8.25 Y	9.21/7.08
	10.00% FGL, 90.00% R. TiO_2	0.4100	0.4503	80.64	7.66 Y	9.10/8.94
A.21	1.00% FGL, 0.10% black, 98.9% R. TiO_2	0.3317	0.3583	66.79	4.24 GY	8.42/2.25
	1.00% FGL, 0.5% B. umber, 98.5% R. TiO_2	0.3493	0.3637	69.99	4.79 Y	8.59/2.87
	10.00% FGL, 1.00% black, 89.0% R. TiO_2	0.3530	0.4033	35.67	3.69 GY	6.46/4.26

Table A.4

CIE and Munsell notation (diffuse reflectance) for yellow oxide (YOX) and Permanent Yellow FGL.

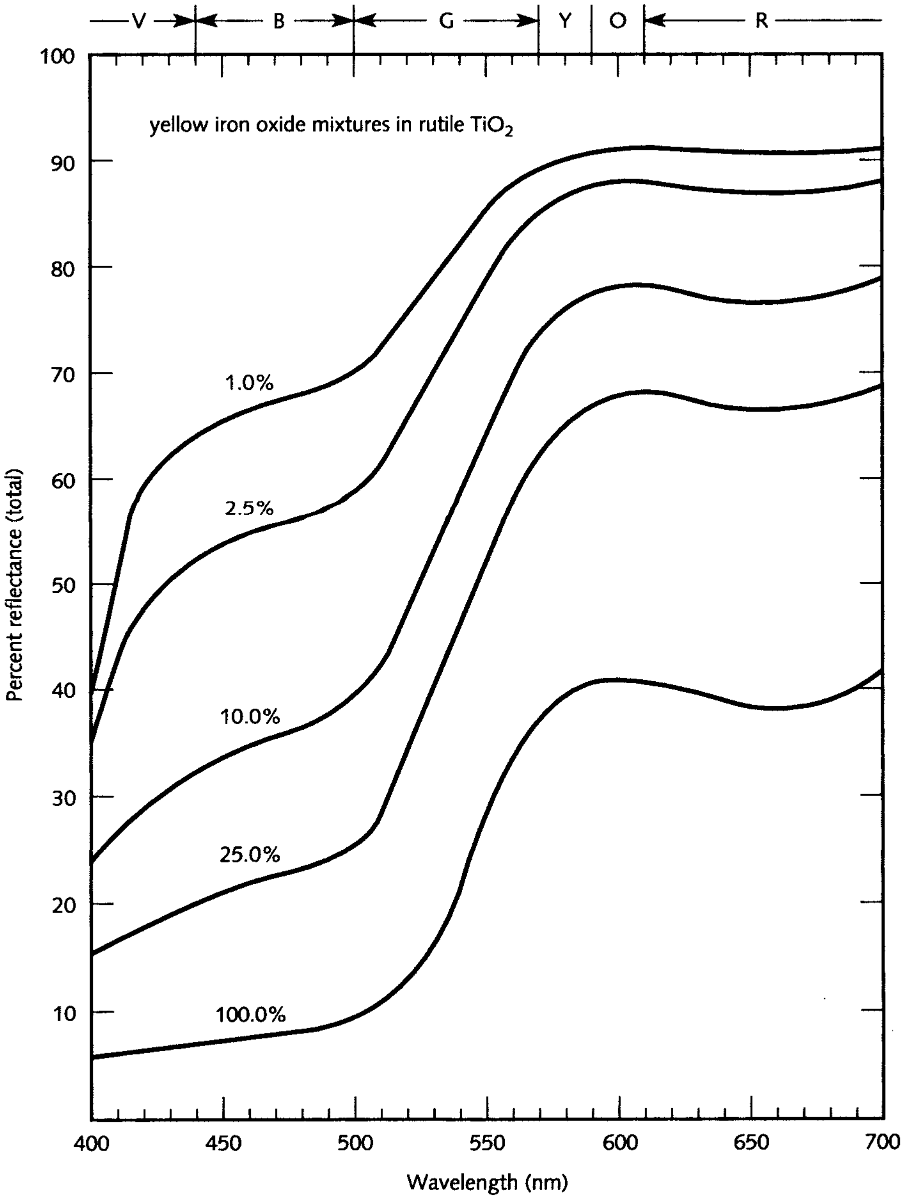

Figure A.18

Yellow iron oxide mixtures in rutile TiO_2.

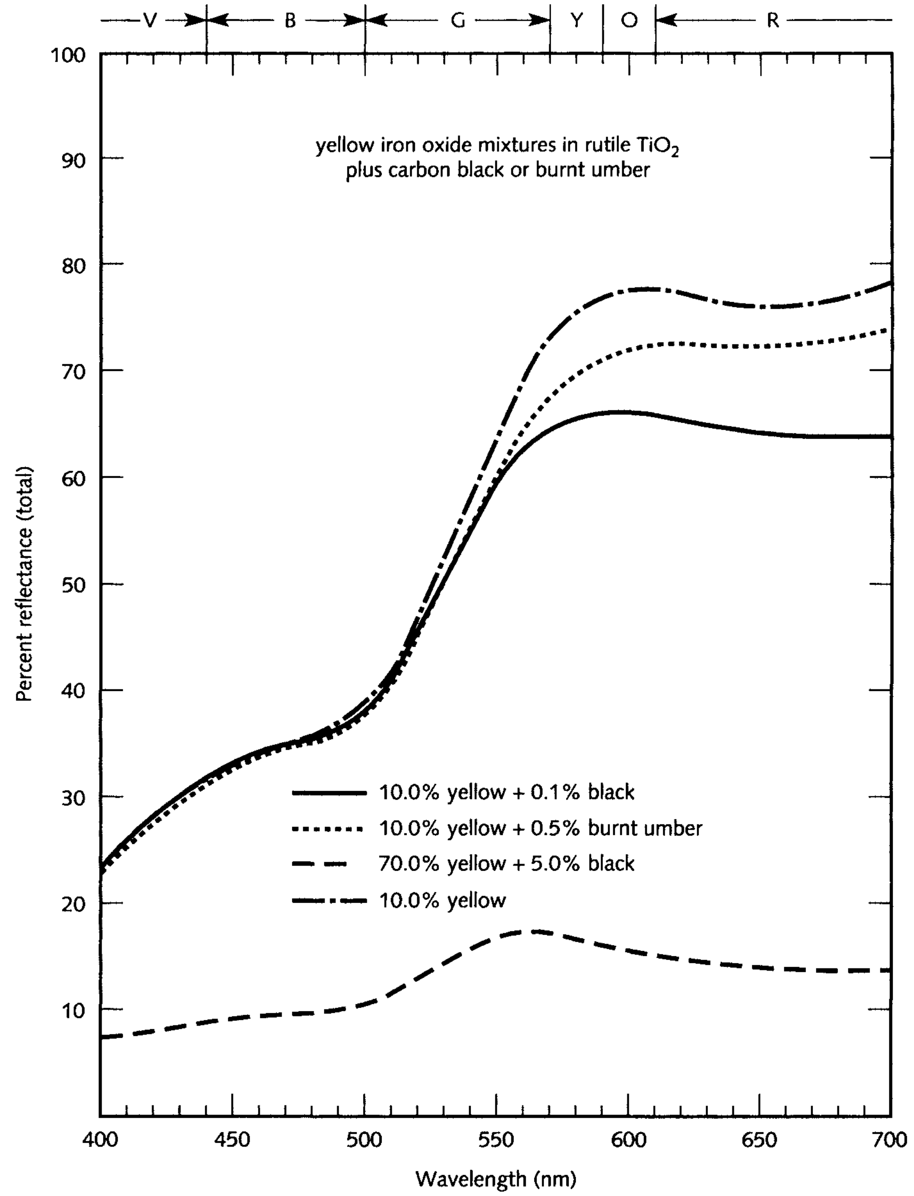

Figure A.19

Yellow iron oxide mixtures in rutile TiO_2, and with carbon black or burnt umber added.

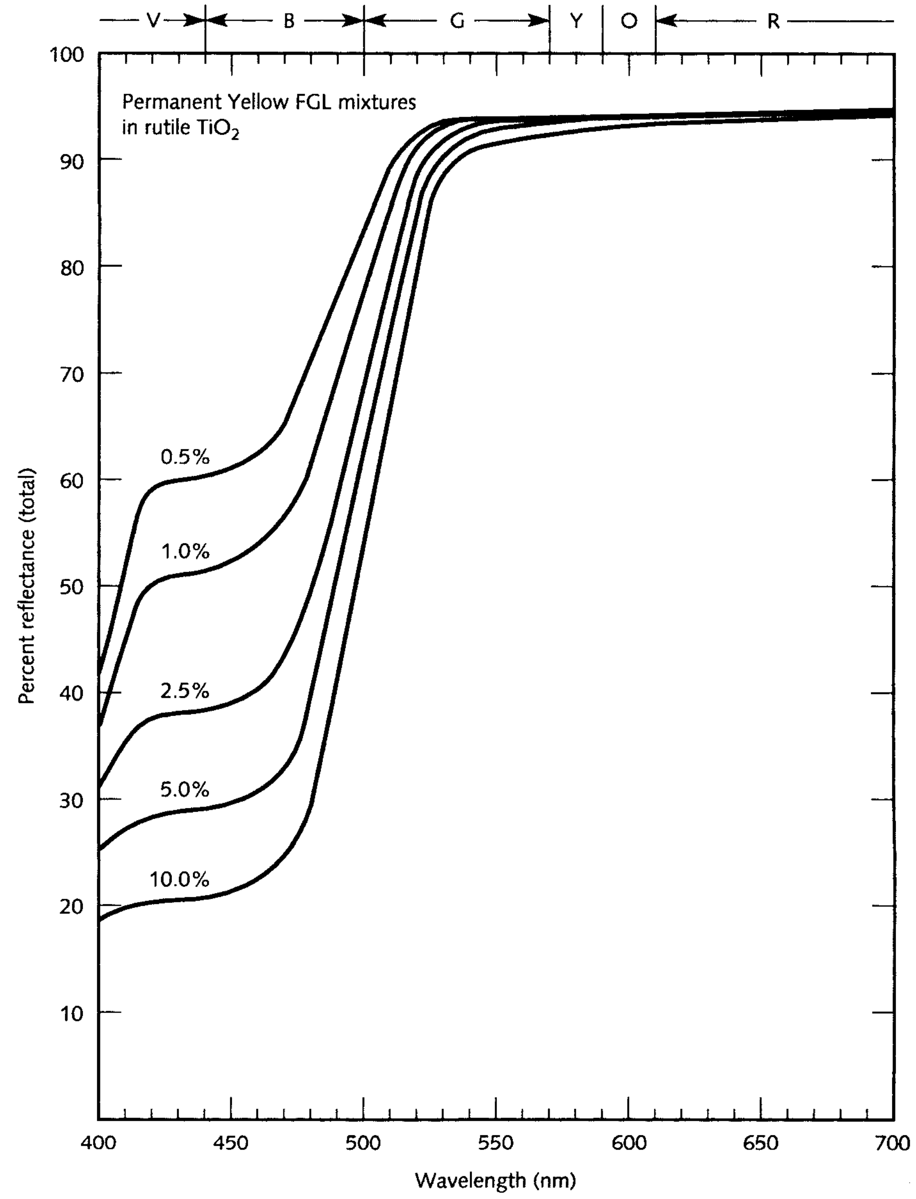

Figure A.20

Permanent Yellow FGL in rutile TiO_2.

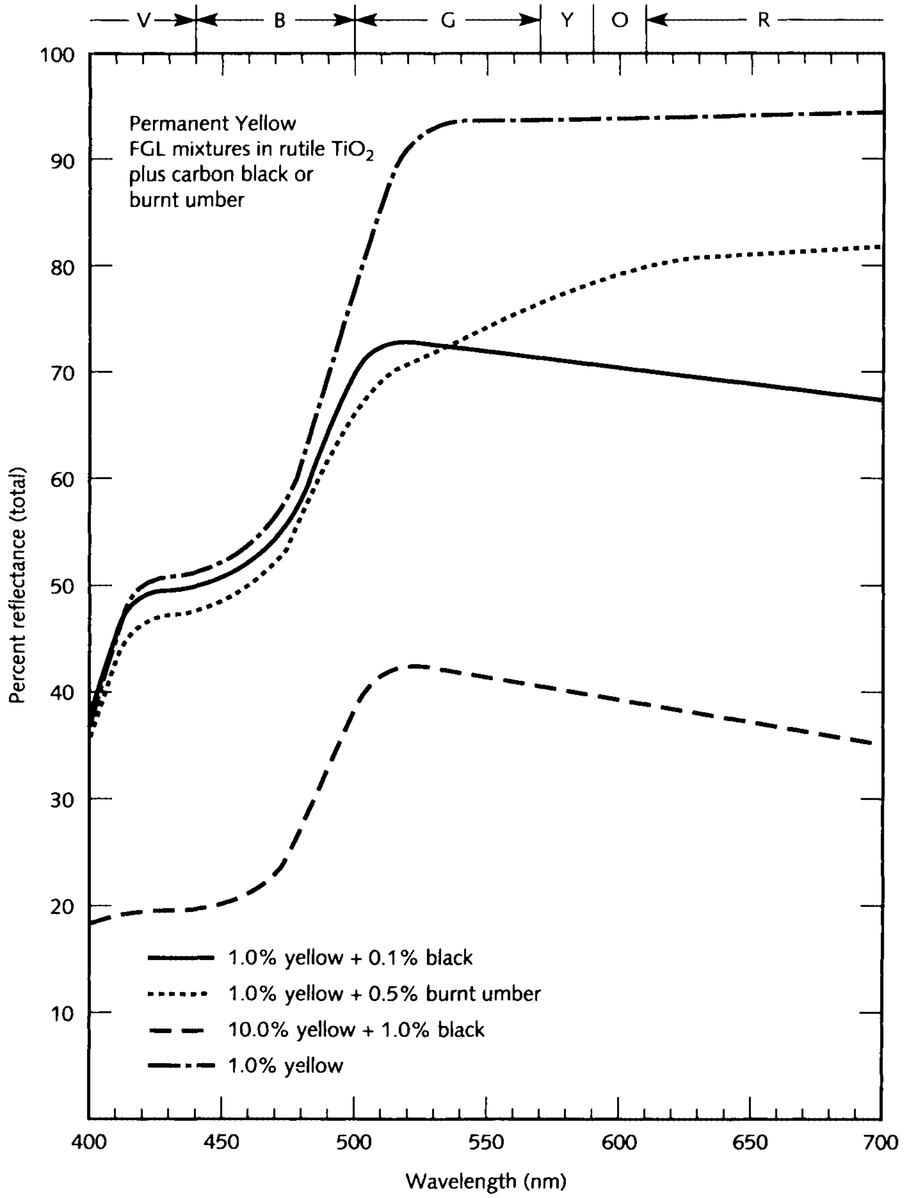

Figure A.21

Permanent Yellow FGL in rutile TiO_2, and with carbon black or burnt umber added.

		CIE			Munsell	
Figure	**Pigment composition**	***x***	***y***	***Y***	**Hue**	**Value/Chroma**
A.22	0.10% PG, 99.9% R. TiO_2	0.2877	0.3216	77.41	6.59 BG	8.95/2.49
	0.25% PG, 99.75% R. TiO_2	0.2768	0.3207	70.28	6.38 BG	8.60/3.66
	0.50% PG, 99.50% R. TiO_2	0.2667	0.3260	63.58	6.13 BG	8.25/4.83
	2.00% PG, 98.00% R. TiO_2	0.2422	0.3341	47.49	4.86 BG	7.30/7.53
	4.00% PG, 96.00% R. TiO_2	0.2284	0.3402	38.72	4.23 BG	6.69/8.67
A.23	0.25% PG, 0.10% black, 99.65% R. TiO_2	0.2825	0.3163	60.52	8.59 BG	8.08/2.70
	0.25% PG, 0.50% B. umber, 99.25% R. TiO_2	0.2934	0.3285	61.02	1.75 BG	8.11/2.18
A.24	0.30% PB, 3.0% FGL, 96.7% R. TiO_2	0.2996	0.3744	48.74	2.07 G	7.38/5.04
	0.20% PB, 5.00% YOX, 94.8% R. TiO_2	0.3140	0.3459	47.59	9.15 GY	7.31/1.86
	25.00% UB, 4.00% FGL, 71.00% R. TiO_2	0.3134	0.3742	39.51	9.91 GY	6.75/3.75
	21.00% UB, 5.00% YOX, 74.00% R. TiO_2	0.3104	0.3333	39.51	0.41 G	6.75/1.12

Table A.5

CIE and Munsell notation (diffuse reflectance) for phthalocyanine green (PG) and green mixtures (with yellow oxide [YOX] and Permanent Yellow FGL).

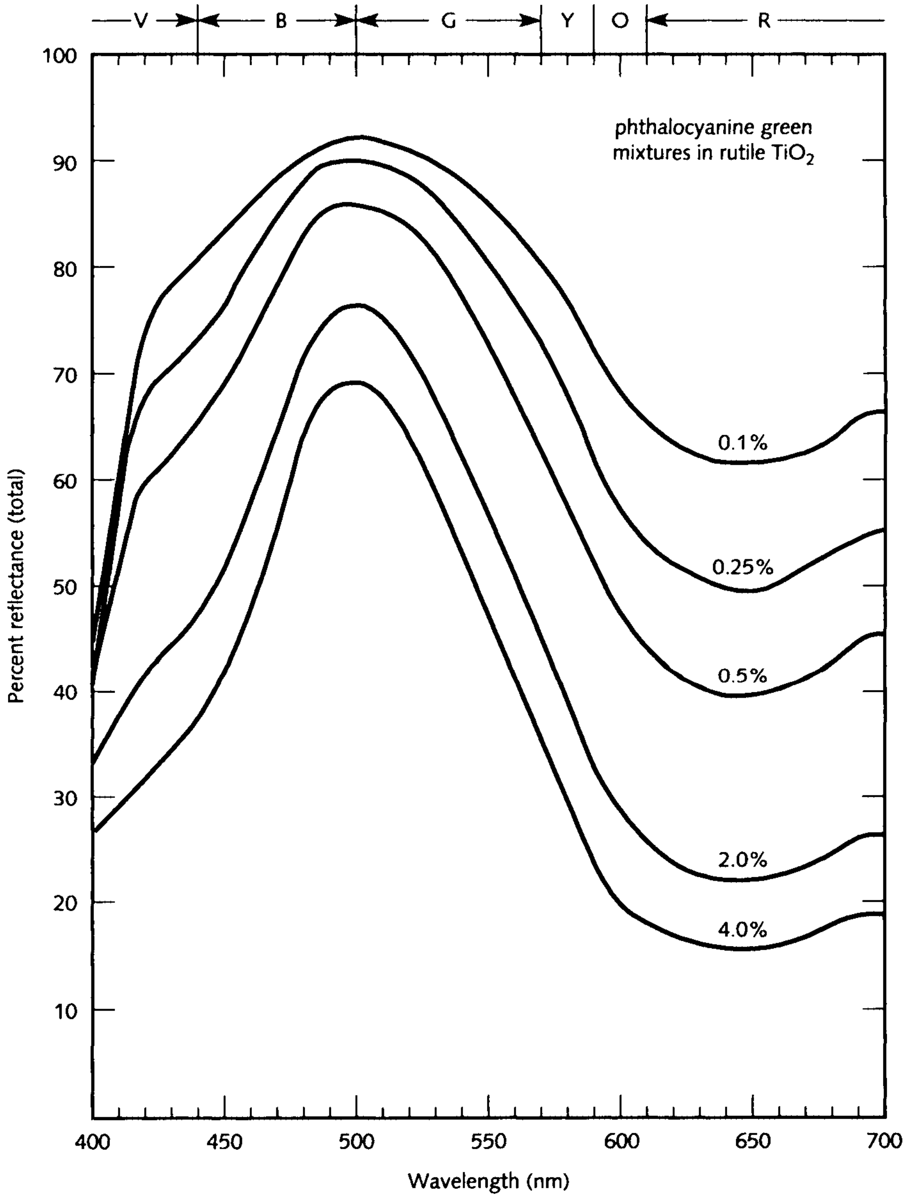

Figure A.22

Phthalocyanine green mixtures in rutile TiO_2.

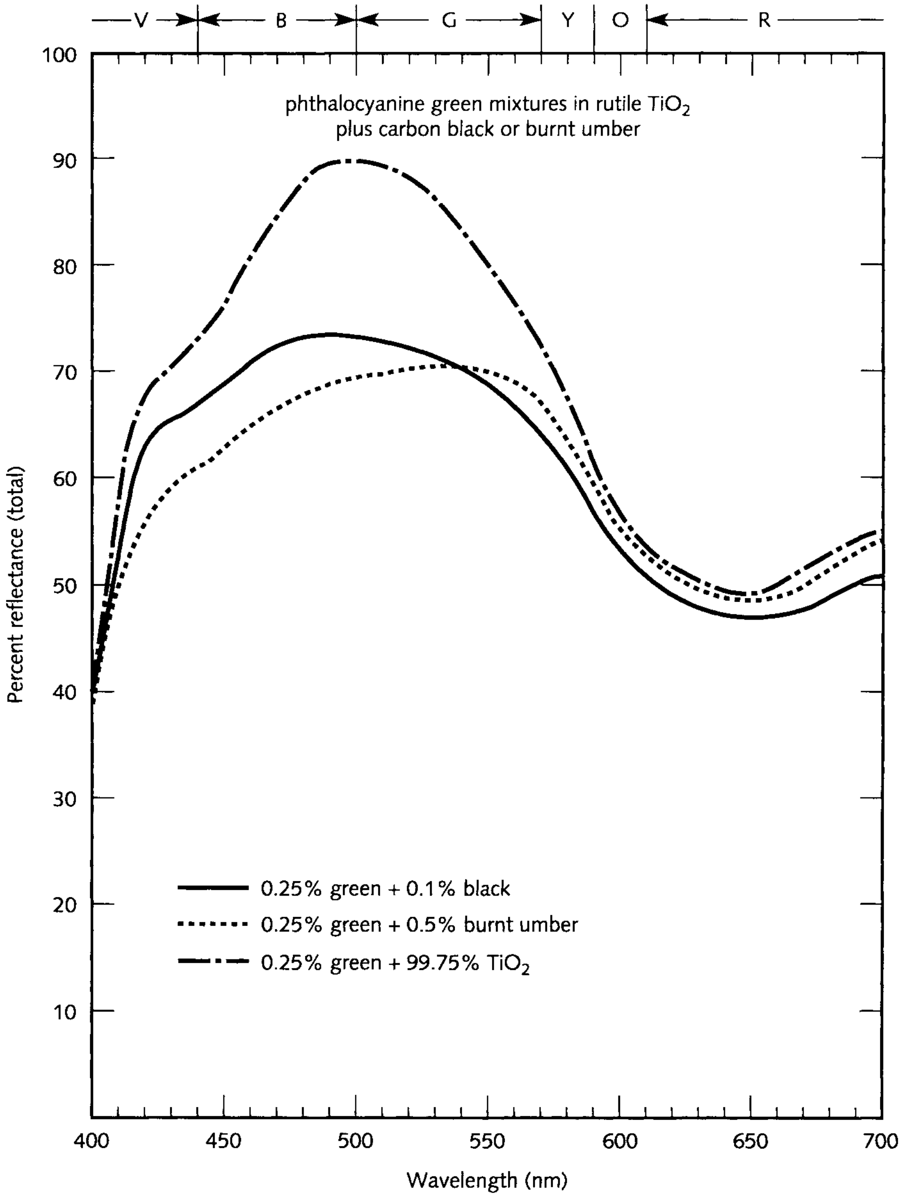

Figure A.23

Phthalocyanine green mixtures in rutile TiO_2, and with carbon black or burnt umber added.

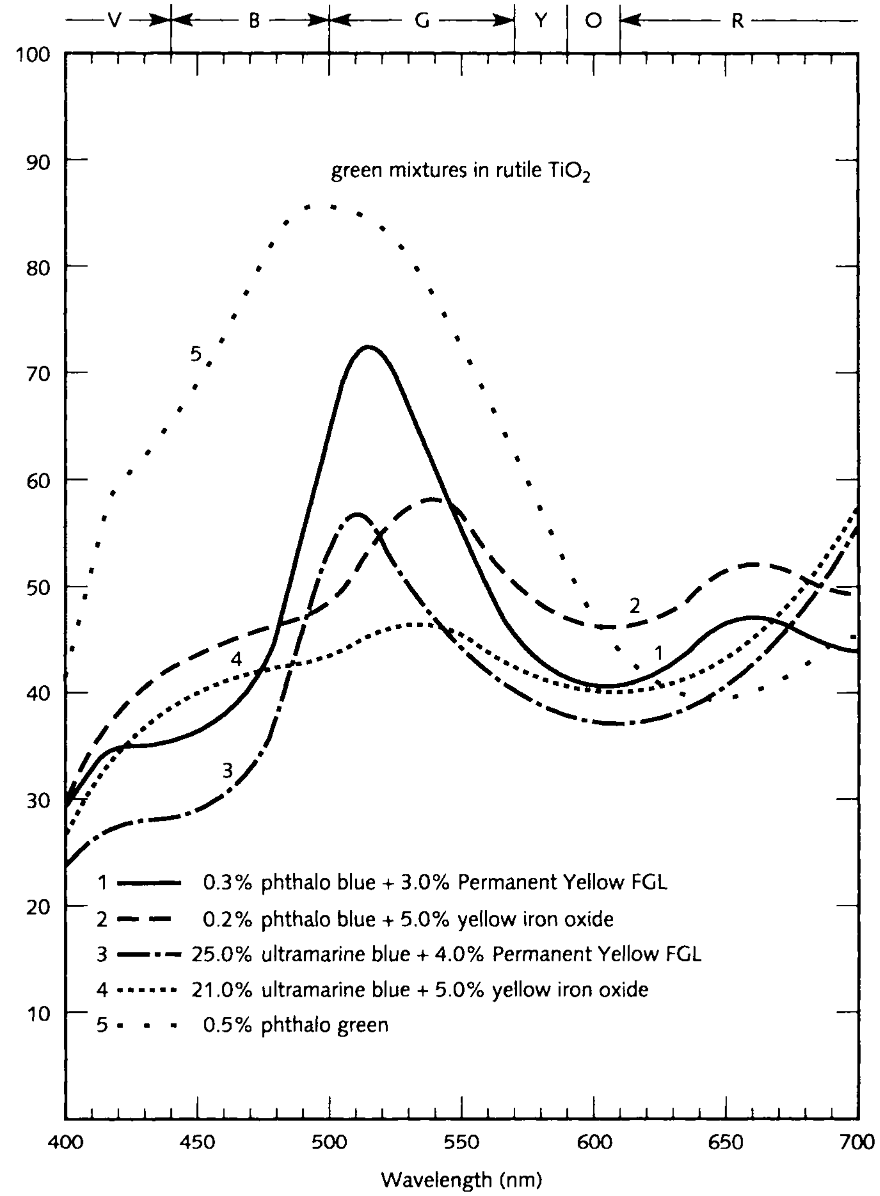

Figure A.24

Green mixtures (blue and yellow mixtures) in rutile TiO_2.

Figure	Pigment composition	CIE			Munsell	
		x	*y*	*Y*	Hue	Value/Chroma
A.25	0.025% CV, 99.975% R. TiO_2	0.3020	0.3018	75.28	0.72 P	8.85/2.31
	0.10% CV, 99.90% R. TiO_2	0.2923	0.2844	61.40	9.54 PB	8.13/3.58
	0.25% CV, 99.75% R. TiO_2	0.2833	0.2680	49.63	0.33 P	7.44/5.34
	0.625% CV, 99.375% R. TiO_2	0.2717	0.2472	36.94	0.39 P	6.56/7.17
	2.50% CV, 97.50% R. TiO_2	0.2502	0.2086	19.44	9.93 PB	4.97/9.31
A.26	0.25% CV, 0.10% black, 99.65% R. TiO_2	0.2854	0.2742	46.76	9.90 PB	7.25/4.64
	0.25% CV, 0.50% B. umber, 99.25% R. TiO_2	0.2963	0.2863	47.08	1.95 P	7.27/3.48
A.27	20.00% UB, 1.5% ROX, 78.5% R. TiO_2	0.3015	0.2973	36.72	2.01 P	6.54/2.09
	16.00% UB, 0.9% BON, 83.10% R. TiO_2	0.2954	0.2786	38.66	3.14 P	6.69/4.16
	0.30% PB, 1.25% QR, 98.45% R. TiO_2	0.2780	0.2637	38.27	9.56 PB	6.66/5.50

Table A.6

CIE and Munsell notation (diffuse reflectance) for carbazole violet (CV) and purple mixtures (with ultramarine blue [UB], red iron oxide [ROX], BON red, and Quinacridone Red [QR]).

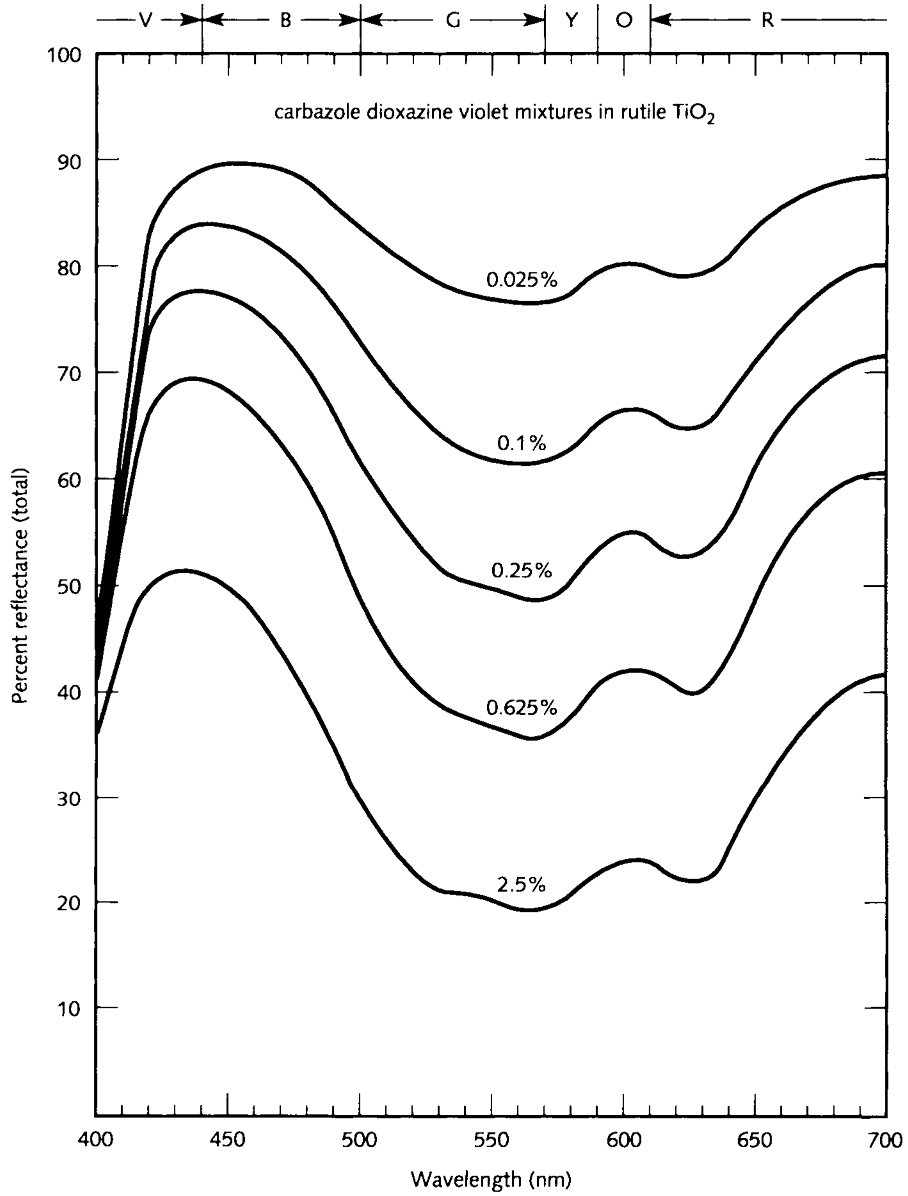

Figure A.25

Carbazole dioxazine violet mixtures in rutile TiO_2.

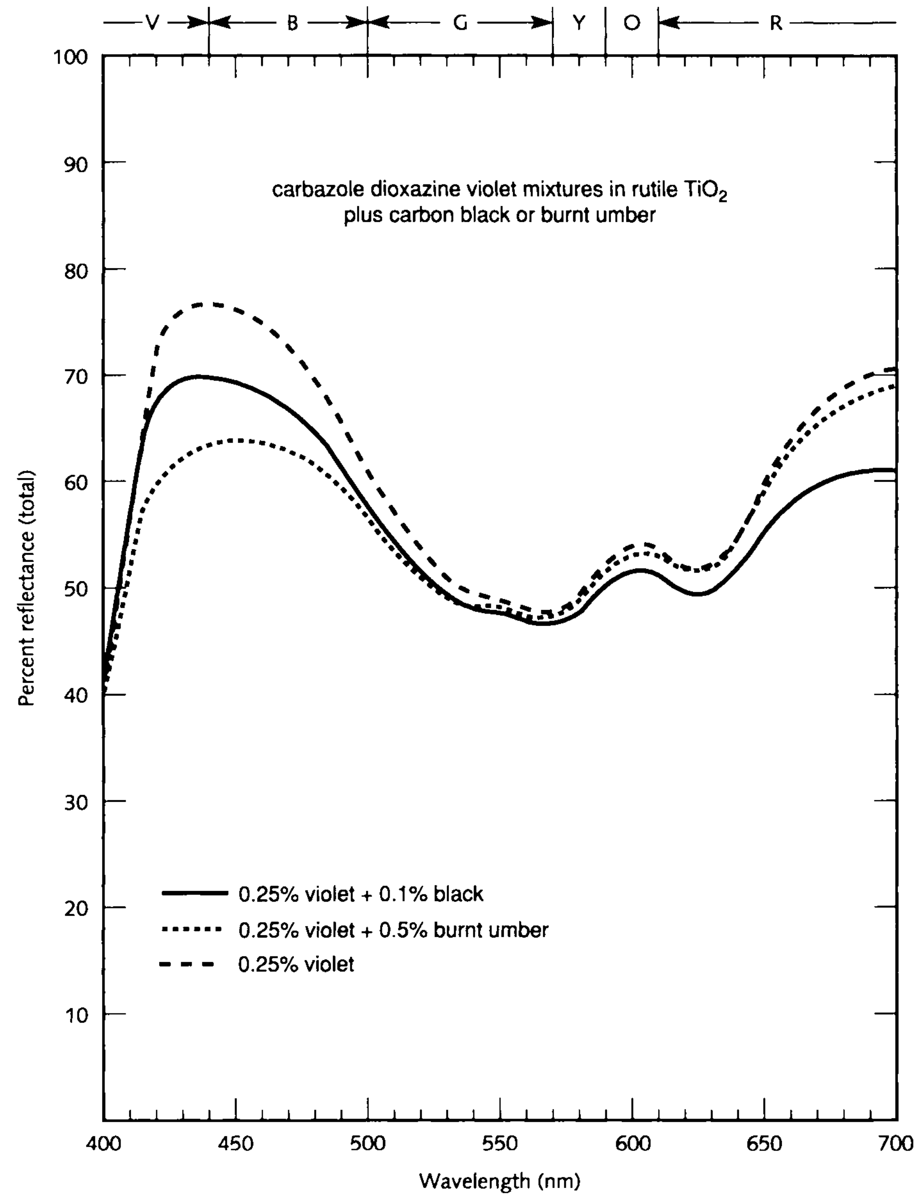

Figure A.26

Carbazole violet mixtures in rutile TiO_2, and with carbon black or burnt umber added.

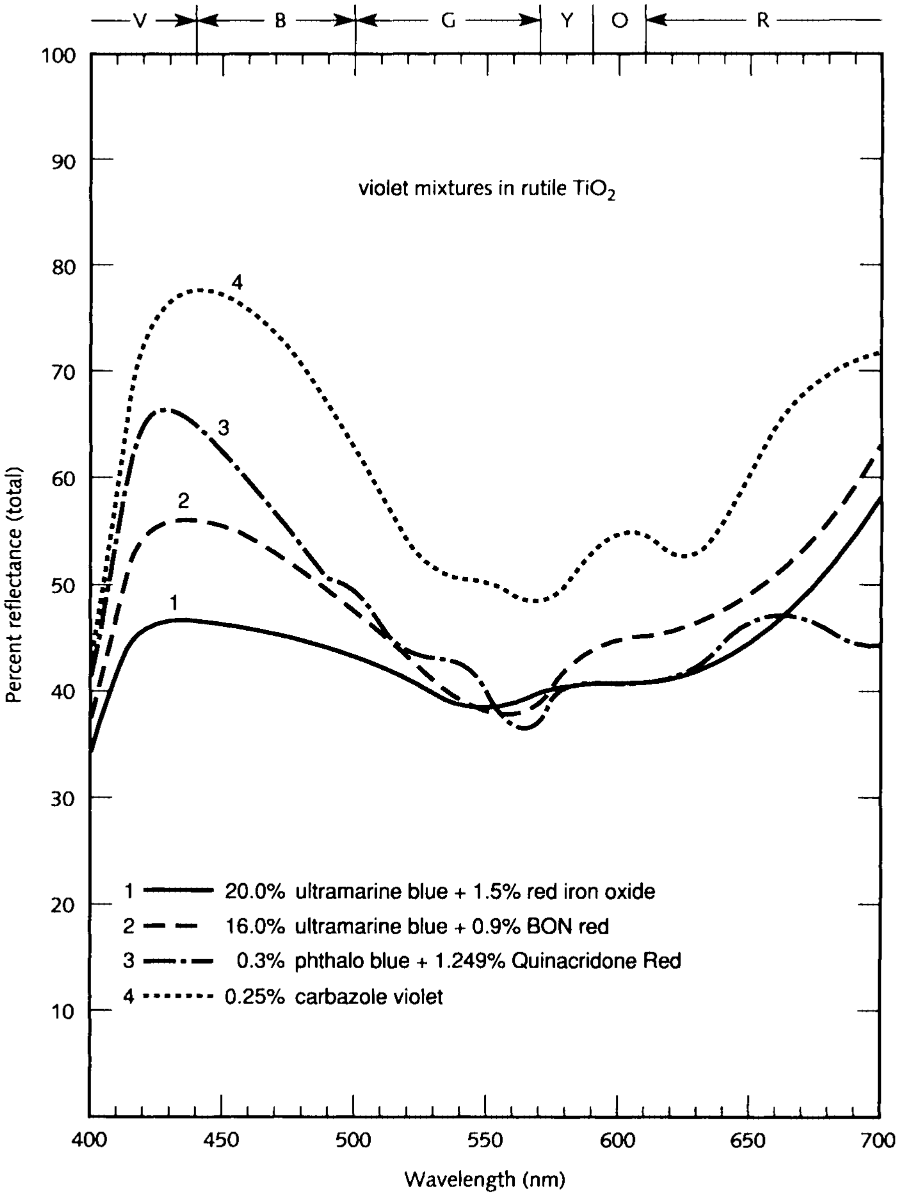

Figure A.27

Violet mixtures (red and blue mixtures) in rutile TiO_2.

			CIE			Munsell
Figure	**Pigment composition**	***x***	***y***	***Y***	**Hue**	**Value/Chroma**
A.28	1.00% MO, 99.00% R. TiO_2	0.3399	0.3202	71.98	4.16 R	8.68/3.32
	5.00% MO, 95.00% R. TiO_2	0.3742	0.3229	54.99	4.40 R	7.77/6.02
	25.00% MO, 75.00% R. TiO_2	0.4454	0.3292	34.03	5.64 R	6.33/9.88
	100.00% MO (masstone)	0.6124	0.3471	15.25	8.90 R	4.46/15.75
A.29	5.0% MO, 0.10% black, 94.9% R. TiO_2	0.3524	0.3206	48.92	4.14 R	7.39/4.06
	5.00% MO, 0.50% B. umber, 94.5% R. TiO_2	0.3685	0.3257	51.17	5.76 R	7.54/5.13
A.30	1.50% BON, 2.5% FGL, 96.00% R. TiO_2	0.3958	0.3375	47.44	8.14 R	7.30/6.43
	1.80% QR, 5.00% FGL, 93.20% R. TiO_2	0.4134	0.3556	47.02	1.32 YR	7.27/6.86
	2.00% ROX, 2.00% YOX, 96.00% R. TiO_2	0.3707	0.3354	49.33	9.15 R	7.42/4.52

Table A.7

CIE and Munsell notation (diffuse reflectance) for molybdate orange (MO) and orange mixtures (with BON red, Permanent Yellow FGL, Quinacridone Red [QR], red iron oxide [ROX], and yellow oxide [YOX]).

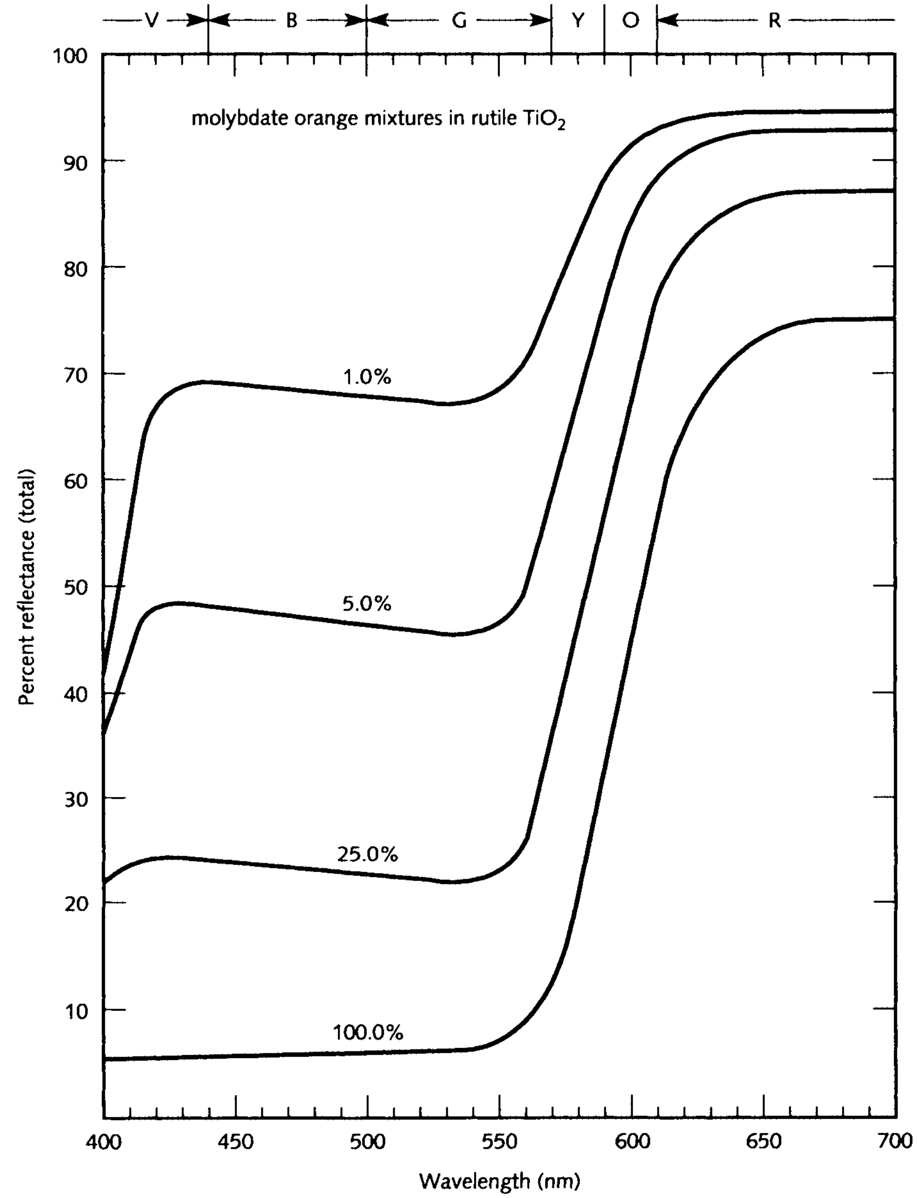

Figure A.28

Molybdate orange mixtures in rutile TiO_2.

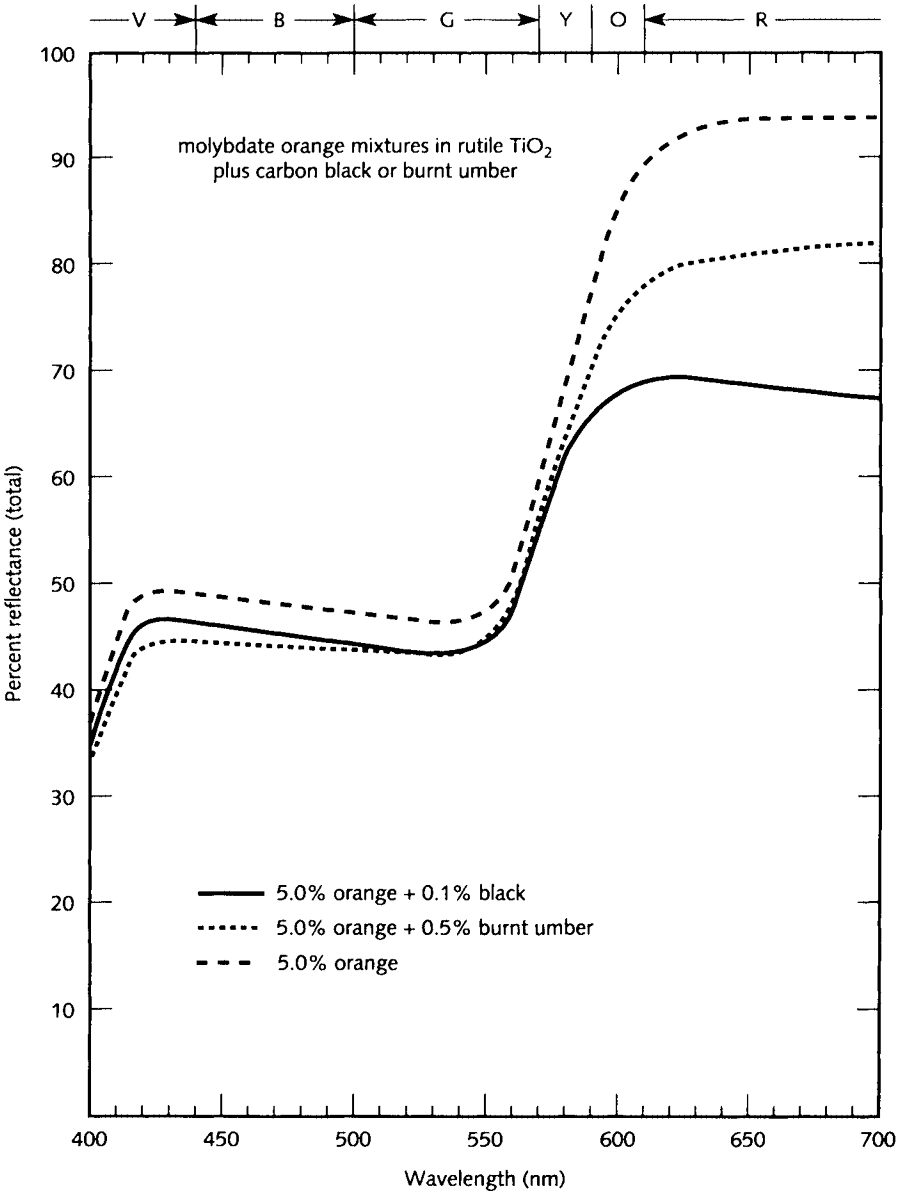

Figure A.29

Molybdate orange mixtures in rutile TiO_2, and with carbon black or burnt umber added.

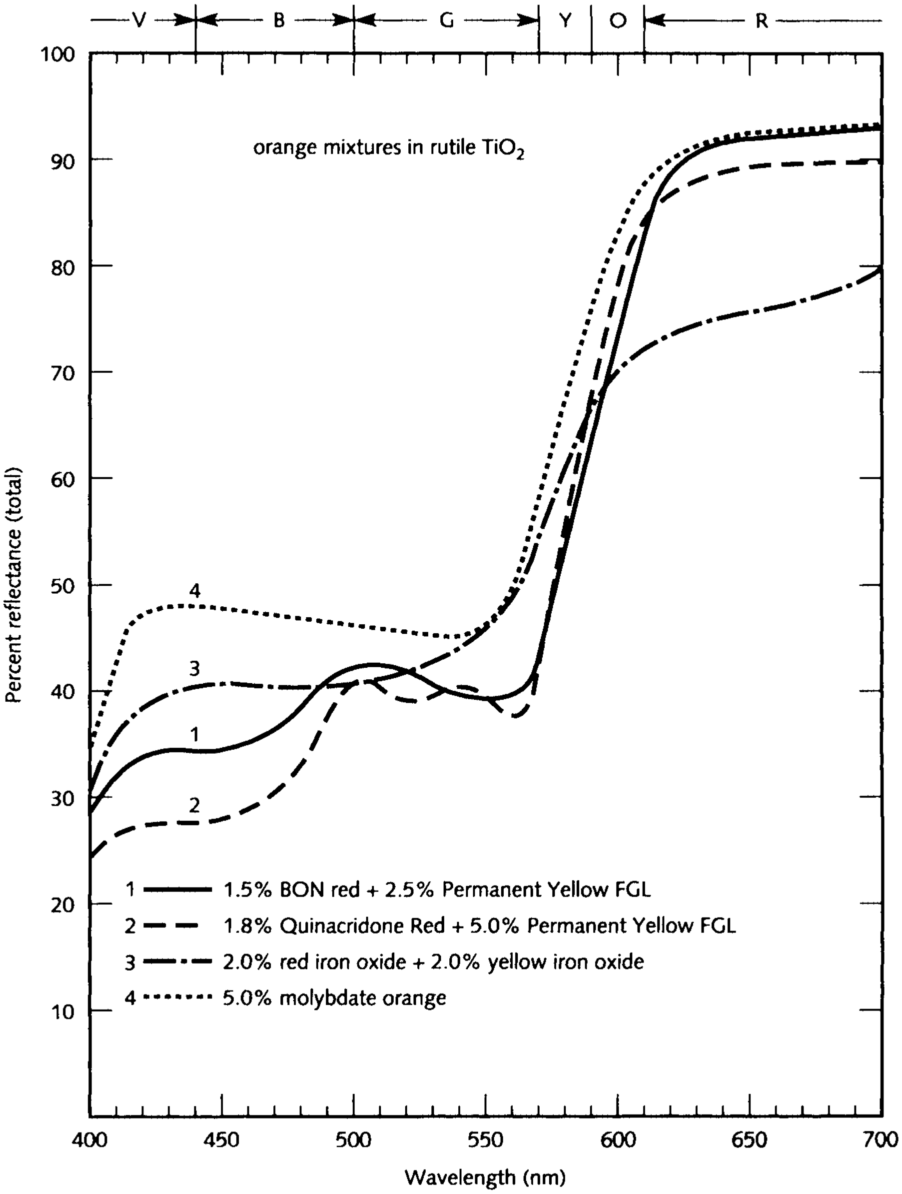

Figure A.30

Orange mixtures (red and yellow mixtures) in rutile TiO_2.

Figure	Pigment composition	CIE x	 y	 Y	Munsell Hue	 Value/Chroma
A.31	0.50% PB, 2.00% ROX, 97.50% R. TiO_2	0.2837	0.2941	34.01	2.43 PB	6.33/2.68
	0.50% PG, 2.00% BON, 97.50% R. TiO_2	0.3089	0.2940	35.53	6.83 P	6.45/2.80
	2.50% YOX, 1.10% ROX, 21.2% UB, 75.2% R. TiO_2	0.3107	0.3154	35.98	2.27 RP	6.49/0.17

Table A.8

CIE and Munsell notation (diffuse reflectance) for neutral mixtures (with phthalo blue [PB], red iron oxide [ROX], phthalo green [PG], BON red, yellow oxide [YOX], and ultramarine blue [UB]).

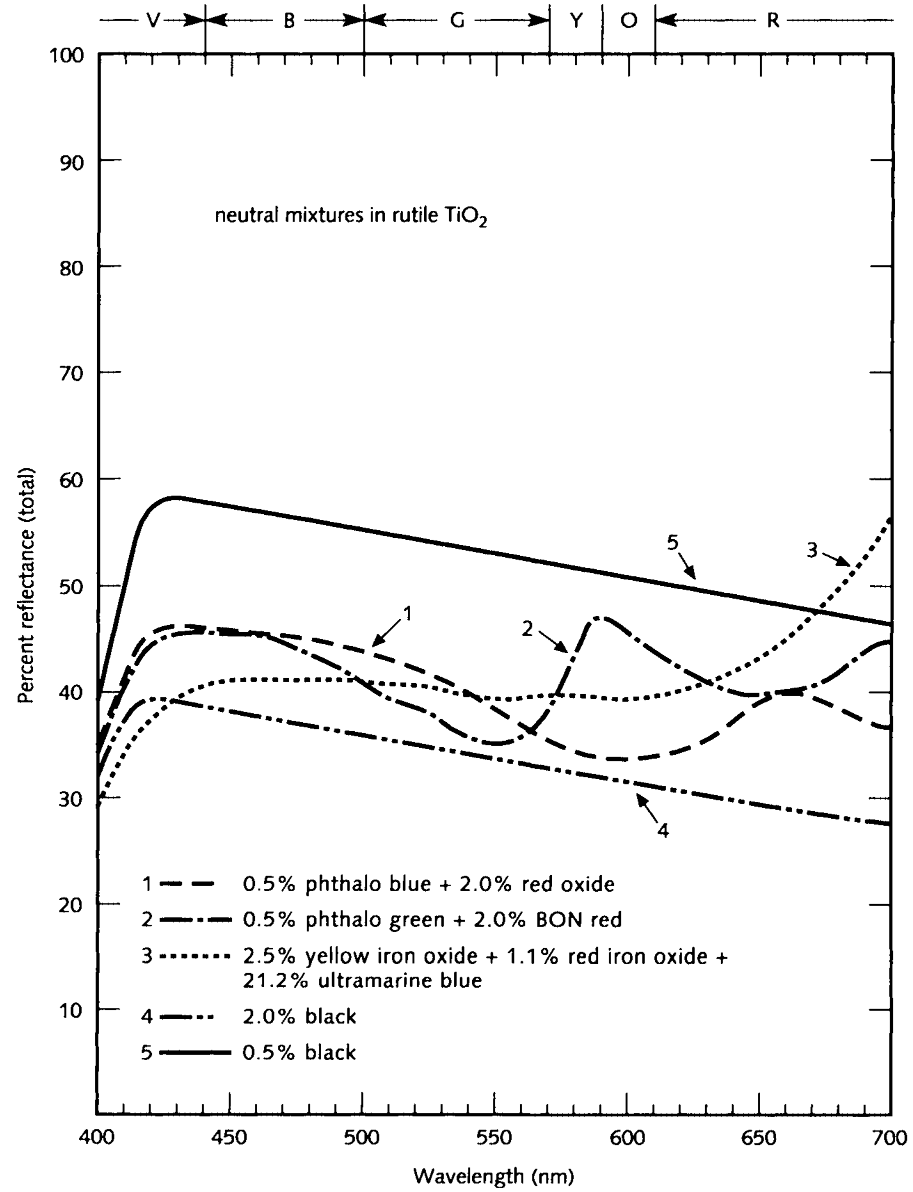

Figure A.31

Neutral mixtures in rutile TiO_2.

Appendix B

K/S versus %*R* Table

%*R*	*K/S*	%*R*	*K/S*	%*R*	*K/S*	%*R*	*K/S*	%*R*	*K/S*	%*R*	*K/S*	%*R*	*K/S*	%*R*	*K/S*	%*R*	*K/S*	%*R*	*K/S*
0.0		5.0	9.02	10.0	4.05	15.0	2.41	20.0	1.600	25.0	1.125	30.0	.817	35.0	.604	40.0	.450	45.0	.336
.1	449.	.1	8.83	.1	4.00	.1	2.39	.1	1.588	.1	1.118	.1	.812	.1	.600	.1	.447	.1	.334
.2	249.	.2	8.64	.2	3.95	.2	2.37	.2	1.576	.2	1.110	.2	.807	.2	.596	.2	.445	.2	.332
.3	166.	.3	8.46	.3	3.91	.3	2.34	.3	1.565	.3	1.103	.3	.802	.3	.593	.3	.442	.3	.330
.4	124.	.4	8.29	.4	3.86	.4	2.32	.4	1.553	.4	1.096	.4	.797	.4	.589	.4	.440	.4	.328
.5	99.0	.5	8.12	.5	3.81	.5	2.30	.5	1.542	.5	1.088	.5	.792	.5	.586	.5	.437	.5	.326
.6	82.3	.6	7.96	.6	3.77	.6	2.28	.6	1.530	.6	1.081	.6	.787	.6	.583	.6	.435	.6	.325
.7	70.4	.7	7.80	.7	3.73	.7	2.26	.7	1.519	.7	1.074	.7	.782	.7	.579	.7	.432	.7	.323
.8	61.5	.8	7.65	.8	3.68	.8	2.24	.8	1.508	.8	1.067	.8	.777	.8	.576	.8	.430	.8	.321
.9	54.6	.9	7.50	.9	3.64	.9	2.22	.9	1.497	.9	1.060	.9	.773	.9	.572	.9	.427	.9	.319
1.0	49.0	6.0	7.36	11.0	3.60	16.0	2.21	21.0	1.486	26.0	1.053	31.0	.768	36.0	.569	41.0	.425	46.0	.317
.1	44.5	.1	7.23	.1	3.56	.1	2.19	.1	1.475	.1	1.046	.1	.763	.1	.566	.1	.422	.1	.315
.2	40.7	.2	7.10	.2	3.52	.2	2.17	.2	1.465	.2	1.039	.2	.759	.2	.562	.2	.420	.2	.313
.3	37.5	.3	6.97	.3	3.48	.3	2.15	.3	1.454	.3	1.033	.3	.754	.3	.559	.3	.417	.3	.311
.4	34.7	.4	6.84	.4	3.44	.4	2.13	.4	1.443	.4	1.026	.4	.749	.4	.556	.4	.415	.4	.310
.5	32.3	.5	6.73	.5	3.41	.5	2.11	.5	1.433	.5	1.019	.5	.745	.5	.552	.5	.412	.5	.308
.6	30.3	.6	6.61	.6	3.37	.6	2.10	.6	1.423	.6	1.013	.6	.740	.6	.549	.6	.410	.6	.306
.7	28.4	.7	6.50	.7	3.33	.7	2.08	.7	1.413	.7	1.006	.7	.736	.7	.546	.7	.408	.7	.304
.8	26.8	.8	6.39	.8	3.30	.8	2.06	.8	1.403	.8	1.000	.8	.731	.8	.543	.8	.405	.8	.302
.9	25.3	.9	6.28	.9	3.26	.9	2.04	.9	1.393	.9	.993	.9	.727	.9	.540	.9	.403	.9	.301
2.0	24.0	7.0	6.18	12.0	3.23	17.0	2.03	22.0	1.383	27.0	.987	32.0	.723	37.0	.536	42.0	.401	47.0	.299
.1	22.8	.1	6.08	.1	3.19	.1	2.01	.1	1.373	.1	.981	.1	.718	.1	.533	.1	.398	.1	.297
.2	21.7	.2	5.98	.2	3.16	.2	1.993	.2	1.363	.2	.974	.2	.714	.2	.530	.2	.396	.2	.295
.3	20.8	.3	5.89	.3	3.13	.3	1.977	.3	1.354	.3	.968	.3	.710	.3	.527	.3	.394	.3	.294
.4	19.85	.4	5.79	.4	3.09	.4	1.961	.4	1.344	.4	.962	.4	.705	.4	.524	.4	.391	.4	.292
.5	19.01	.5	5.70	.5	3.06	.5	1.945	.5	1.335	.5	.956	.5	.701	.5	.521	.5	.389	.5	.290
.6	18.24	.6	5.62	.6	3.03	.6	1.929	.6	1.325	.6	.950	.6	.697	.6	.518	.6	.387	.6	.288
.7	17.53	.7	5.53	.7	3.00	.7	1.913	.7	1.316	.7	.944	.7	.693	.7	.515	.7	.385	.7	.287
.8	16.87	.8	5.45	.8	2.97	.8	1.898	.8	1.307	.8	.938	.8	.688	.8	.512	.8	.382	.8	.285
.9	16.26	.9	5.37	.9	2.94	.9	1.883	.9	1.298	.9	.932	.9	.684	.9	.509	.9	.380	.9	.283
3.0	15.68	8.0	5.29	13.0	2.91	18.0	1.868	23.0	1.289	28.0	.926	33.0	.680	38.0	.506	43.0	.378	48.0	.282
.1	15.14	.1	5.21	.1	2.88	.1	1.853	.1	1.280	.1	.920	.1	.676	.1	.503	.1	.376	.1	.280
.2	14.64	.2	5.14	.2	2.85	.2	1.838	.2	1.271	.2	.914	.2	.672	.2	.500	.2	.373	.2	.278
.3	14.17	.3	5.07	.3	2.83	.3	1.824	.3	1.262	.3	.908	.3	.668	.3	.497	.3	.371	.3	.277
.4	13.72	.4	4.99	.4	2.80	.4	1.809	.4	1.254	.4	.903	.4	.664	.4	.494	.4	.369	.4	.275
.5	13.30	.5	4.93	.5	2.77	.5	1.795	.5	1.245	.5	.897	.5	.660	.5	.491	.5	.367	.5	.273
.6	12.91	.6	4.86	.6	2.74	.6	1.781	.6	1.237	.6	.891	.6	.656	.6	.488	.6	.365	.6	.272
.7	12.53	.7	4.79	.7	2.72	.7	1.767	.7	1.228	.7	.886	.7	.652	.7	.486	.7	.363	.7	.270
.8	12.18	.8	4.73	.8	2.69	.8	1.754	.8	1.220	.8	.880	.8	.648	.8	.483	.8	.361	.8	.269
.9	11.84	.9	4.66	.9	2.67	.9	1.740	.9	1.212	.9	.875	.9	.644	.9	.480	.9	.358	.9	.267
4.0	11.52	9.0	4.60	14.0	2.64	19.0	1.727	24.0	1.203	29.0	.869	34.0	.641	39.0	.477	44.0	.356	49.0	.265
.1	11.22	.1	4.54	.1	2.62	.1	1.713	.1	1.195	.1	.864	.1	.637	.1	.474	.1	.354	.1	.264
.2	10.93	.2	4.48	.2	2.59	.2	1.700	.2	1.187	.2	.858	.2	.633	.2	.472	.2	.352	.2	.262
.3	10.65	.3	4.42	.3	2.57	.3	1.687	.3	1.179	.3	.853	.3	.629	.3	.469	.3	.350	.3	.261
.4	10.39	.4	4.37	.4	2.54	.4	1.674	.4	1.171	.4	.848	.4	.626	.4	.466	.4	.348	.4	.259
.5	10.13	.5	4.31	.5	2.52	.5	1.662	.5	1.163	.5	.842	.5	.622	.5	.463	.5	.346	.5	.258
.6	9.89	.6	4.26	.6	2.50	.6	1.649	.6	1.156	.6	.837	.6	.618	.6	.461	.6	.344	.6	.256
.7	9.66	.7	4.20	.7	2.48	.7	1.637	.7	1.148	.7	.832	.7	.614	.7	.458	.7	.342	.7	.255
.8	9.44	.8	4.15	.8	2.45	.8	1.624	.8	1.140	.8	.827	.8	.611	.8	.455	.8	.340	.8	.253
.9	9.23	.9	4.10	.9	2.43	.9	1.612	.9	1.133	.9	.822	.9	.607	.9	.453	.9	.338	.9	.252

%*R*	*K/S*	%*R*	*K/S*	%*R*	*K/S*	%*R*	*K/S*	%*R*	*K/S*	%*R*	*K/S*	%*R*	*K/S*	%*R*	*K/S*	%*R*	*K/S*	%*R*	*K/S*
50.0	.250	55.0	.1841	60.0	.1333	65.0	.0942	70.0	.0643	75.0	.0417	80.0	.0250	85.0	.0132	90.0	.00556	95.0	.00132
.1	.249	.1	.1829	.1	.1325	.1	.0936	.1	.0638	.1	.0413	.1	.0247	.1	.0130	.1	.00544	.1	.00126
.2	.247	.2	.1818	.2	.1316	.2	.0929	.2	.0633	.2	.0409	.2	.0244	.2	.0129	.2	.00532	.2	.00121
.3	.246	.3	.1807	.3	.1307	.3	.0922	.3	.0627	.3	.0405	.3	.0242	.3	.0127	.3	.00521	.3	.00116
.4	.244	.4	.1795	.4	.1298	.4	.0915	.4	.0622	.4	.0401	.4	.0239	.4	.0125	.4	.00510	.4	.00111
.5	.243	.5	.1784	.5	.1290	.5	.0909	.5	.0617	.5	.0398	.5	.0236	.5	.0123	.5	.00499	.5	.00106
.6	.241	.6	.1773	.6	.1281	.6	.0902	.6	.0612	.6	.0394	.6	.0234	.6	.0121	.6	.00488	.6	.00101
.7	.240	.7	.1762	.7	.1272	.7	.0895	.7	.0607	.7	.0390	.7	.0231	.7	.0119	.7	.00477	.7	.00097
.8	.238	.8	.1751	.8	.1264	.8	.0889	.8	.0602	.8	.0386	.8	.0228	.8	.0118	.8	.00466	.8	.00092
.9	.237	.9	.1740	.9	.1255	.9	.0882	.9	.0597	.9	.0383	.9	.0226	.9	.0116	.9	.00456	.9	.00088
51.0	.235	56.0	.1729	61.0	.1247	66.0	.0876	71.0	.0592	76.0	.0379	81.0	.0223	86.0	.0114	91.0	.00445	96.0	.00083
.1	.234	.1	.1718	.1	.1238	.1	.0869	.1	.0587	.1	.0375	.1	.0220	.1	.0112	.1	.00435	.1	.00079
.2	.233	.2	.1707	.2	.1230	.2	.0863	.2	.0583	.2	.0372	.2	.0218	.2	.0111	.2	.00425	.2	.00075
.3	.231	.3	.1696	.3	.1222	.3	.0857	.3	.0578	.3	.0368	.3	.0215	.3	.0109	.3	.00415	.3	.00071
.4	.230	.4	.1685	.4	.1213	.4	.0850	.4	.0573	.4	.0365	.4	.0213	.4	.0107	.4	.00405	.4	.00067
.5	.228	.5	.1675	.5	.1205	.5	.0844	.5	.0568	.5	.0361	.5	.0210	.5	.0105	.5	.00395	.5	.00064
.6	.227	.6	.1664	.6	.1197	.6	.0838	.6	.0563	.6	.0357	.6	.0208	.6	.0104	.6	.00385	.6	.00060
.7	.226	.7	.1653	.7	.1189	.7	.0831	.7	.0559	.7	.0354	.7	.0205	.7	.0102	.7	.00376	.7	.00056
.8	.224	.8	.1643	.8	.1181	.8	.0825	.8	.0554	.8	.0350	.8	.0203	.8	.0100	.8	.00366	.8	.00053
.9	.223	.9	.1632	.9	.1173	.9	.0819	.9	.0549	.9	.0347	.9	.0200	.9	.00987	.9	.00357	.9	.00050
52.0	.222	57.0	.1622	62.0	.1165	67.0	.0813	72.0	.0544	77.0	.0344	82.0	.0198	87.0	.00971	92.0	.00348	97.0	.00046
.1	.220	.1	.1612	.1	.1157	.1	.0807	.1	.0540	.1	.0340	.1	.0195	.1	.00955	.1	.00339	.1	.00043
.2	.219	.2	.1601	.2	.1149	.2	.0801	.2	.0535	.2	.0337	.2	.0193	.2	.00939	.2	.00330	.2	.00040
.3	.218	.3	.1591	.3	.1141	.3	.0794	.3	.0531	.3	.0333	.3	.0190	.3	.00924	.3	.00321	.3	.00038
.4	.216	.4	.1581	.4	.1133	.4	.0788	.4	.0526	.4	.0330	.4	.0188	.4	.00908	.4	.00313	.4	.00035
.5	.215	.5	.1571	.5	.1125	.5	.0782	.5	.0522	.5	.0327	.5	.0186	.5	.00893	.5	.00304	.5	.00032
.6	.214	.6	.1561	.6	.1117	.6	.0776	.6	.0517	.6	.0323	.6	.0183	.6	.00878	.6	.00296	.6	.00030
.7	.212	.7	.1551	.7	.1110	.7	.0771	.7	.0513	.7	.0320	.7	.0181	.7	.00863	.7	.00287	.7	.00027
.8	.211	.8	.1541	.8	.1102	.8	.0765	.8	.0508	.8	.0317	.8	.0179	.8	.00848	.8	.00279	.8	.00025
.9	.210	.9	.1531	.9	.1094	.9	.0759	.9	.0504	.9	.0314	.9	.0176	.9	.00833	.9	.00271	.9	.00023
53.0	.208	58.0	.1521	63.0	.1087	68.0	.0753	73.0	.0499	78.0	.0310	83.0	.0174	88.0	.00818	93.0	.00263	98.0	.00020
.1	.207	.1	.1511	.1	.1079	.1	.0747	.1	.0495	.1	.0307	.1	.0172	.1	.00804	.1	.00256	.1	.00018
.2	.206	.2	.1501	.2	.1071	.2	.0741	.2	.0491	.2	.0304	.2	.0170	.2	.00789	.2	.00248	.2	.00017
.3	.205	.3	.1491	.3	.1064	.3	.0736	.3	.0486	.3	.0301	.3	.0167	.3	.00775	.3	.00241	.3	.00015
.4	.203	.4	.1482	.4	.1056	.4	.0730	.4	.0482	.4	.0298	.4	.0165	.4	.00761	.4	.00233	.4	.00013
.5	.202	.5	.1472	.5	.1049	.5	.0724	.5	.0478	.5	.0294	.5	.0163	.5	.00747	.5	.00226	.5	.00011
.6	.201	.6	.1462	.6	.1042	.6	.0719	.6	.0474	.6	.0291	.6	.0161	.6	.00733	.6	.00219	.6	.00010
.7	.1996	.7	.1453	.7	.1034	.7	.0713	.7	.0469	.7	.0288	.7	.0159	.7	.00720	.7	.00212	.7	.00009
.8	.1984	.8	.1443	.8	.1027	.8	.0707	.8	.0465	.8	.0285	.8	.0157	.8	.00706	.8	.00205	.8	.00007
.9	.1971	.9	.1434	.9	.1020	.9	.0702	.9	.0461	.9	.0282	.9	.0155	.9	.00693	.9	.00198	.9	.00006
54.0	.1959	59.0	.1425	64.0	.1013	69.0	.0696	74.0	.0457	79.0	.0279	84.0	.0152	89.0	.00680	94.0	.00192	99.0	.00005
.1	.1947	.1	.1415	.1	.1005	.1	.0691	.1	.0453	.1	.0276	.1	.0150	.1	.00667	.1	.00185	.1	.00004
.2	.1935	.2	.1406	.2	.0998	.2	.0685	.2	.0449	.2	.0273	.2	.0148	.2	.00654	.2	.00179	.2	.00003
.3	.1923	.3	.1397	.3	.0991	.3	.0680	.3	.0445	.3	.0270	.3	.0146	.3	.00641	.3	.00172	.3	.00002
.4	.1911	.4	.1388	.4	.0984	.4	.0675	.4	.0440	.4	.0267	.4	.0144	.4	.00628	.4	.00166	.4	.00002
.5	.1899	.5	.1378	.5	.0977	.5	.0669	.5	.0436	.5	.0264	.5	.0142	.5	.00616	.5	.00160	.5	.00001
.6	.1888	.6	.1369	.6	.0970	.6	.0664	.6	.0432	.6	.0261	.6	.0140	.6	.00604	.6	.00154	.6	.00001
.7	.1876	.7	.1360	.7	.0963	.7	.0659	.7	.0428	.7	.0259	.7	.0138	.7	.00591	.7	.00148	.7	.00000
.8	.1864	.8	.1351	.8	.0956	.8	.0653	.8	.0425	.8	.0256	.8	.0136	.8	.00579	.8	.00143	.8	.00000
.9	.1853	.9	.1342	.9	.0949	.9	.0648	.9	.0421	.9	.0253	.9	.0134	.9	.00567	.9	.00137	.9	.00000
																		100.0	0.00000

Appendix C

Colour Index Name

The standard method for naming pigments and dyes worldwide is by means of their Colour Index generic name and number, plus the five-digit constitution number of each pigment or dye. This system for characterizing pigments and dyes is the result of a continuing joint effort of the Society of Dyers and Colourists of Great Britain and the American Association of Textile Chemists and Colorists in the United States. The Colour Index generic name is based on the most common method by which the colorant is applied, such as vat dyes (Vat), acid dyes (Acid), and so on. All pigments are in a single generic class—pigments (P)—with the exception of a few based on vat dyes that may be used in place of the pigment classification. There are twenty generic classes for dyes, assigned depending on their use. The hue description follows the use description. Among pigments there are nine hue descriptions: blue (B), green (G), violet (V), red (R), orange (O), brown (Br), yellow (Y), white (W), and black (Bk). The generic number following the name refers to the particular type of pigment. Thus, the Colour Index generic name and number of natural $BaSO_4$, barytes, is Pigment White 22 (PW 22), whereas the synthetic $BaSO_4$, blanc fixe, has the generic name and number Pigment White 21 (PW 21).

A complete Colour Index designation will also contain a five-digit constitution number after the generic name and number to indicate the chemical constitution of each colorant when it is known. (Some modern pigments have no constitution number because their exact chemical structures are proprietary.) Blocks of numbers have been assigned according to the general chemical character of the colorant. Thus, all natural pigments are given Colour Index constitution numbers from 75000 to 75999; inorganic pigments are assigned numbers from 77000 to 77999; and phthalocyanine colorants are numbered 74000 to 74999. In the case of the barium sulfates, both the barytes and blanc fixe have a constitution number of 77120, because both consist of the compound BaSO4, even though one is of natural origin.

In appendix D, which describes a method for indexing spectrophotometric reflectance curves and gives a representative list of red pigments as an example, the pigments are designated by the generic name

PR (Pigment Red), followed by their generic number. Note that some have a further notation to describe the metallizing ion used: for example, PR 63 Mn and PR 63 Ca describe the particular BON red version (manganese or calcium, respectively).

For a more complete discussion of the Colour Index, Billmeyer and Saltzman (1981) may be consulted.

Appendix D

Compilation of Spectral Reflectance Curves of Pigments: Representative Example

The need for a reference library of pigment reflectance curves in the visible region has been emphasized many times throughout this monograph; its value to the spectrophotometric techniques described in the preceding chapters should be readily apparent. This appendix describes how such a collection could be organized and presents an example in terms of some of the many red pigments available today. The method illustrated here of organizing curves on the basis of the number and the wavelength of the *absorption bands* is an adaptation of the method for providing a curve-shape index for identification outlined by Shurcliff (1942). Ideally, curves plotted as log $1/(K/S)$ versus wavelength, instead of reflectance versus wavelength, would be more useful, as described in the section on colorant calculations and identifications in chapter 4. This derived absorption curve shape is independent of the concentration. However, obtaining such curves would require computation of the values from the reflectances. Hence, collecting the reflectance curves is needed as the first task.

If a complete library were to be done, the first factor forming the basis of the arrangement would be hue: The pigments would be arranged according to their absorption regions, from long to short wavelength—that is, greens (which absorb in the red region), then blues, purples, reds, oranges, and finally yellows (which absorb in the short-wavelength violet region). There would be a separate category for neutrals, whites, and blacks. Each pigment would be identified by its Colour Index name (see appendix C) and by its common chemical-type description. If a curve has been identified by a manufacturer's trade name or product number (or both), that too would be included because of its specificity.

Where available, masstones would be included, but in general, mixtures of all the absorbing pigments with white provide the most information about curve shapes. Their characteristic absorption bands apply to samples at incomplete hiding as well, such as might be seen in watercolors, printing inks, and textile printing.

Familiar historic pigment names may not be included unless their composition is firmly established. The reader is warned again that pigment names used on tubes of artists' colors are not necessarily those of the actual pigments. For example, Johnston and Feller (1963) analyzed four tubes of artists' watercolors labeled "indigo." Only one tube (American) contained the real indigo pigment. The others contained a diversity of pigments such as phthalocyanine blue and black; iron blue plus ultramarine blue and black; and ultramarine blue, phthalocyanine green, phthalocyanine blue, pyrazolone red, and black! Thus, even when artists record the palettes they use, one must beware. The danger of mislabeling, illustrated by this example for indigo, is a valid possibility dating from the times when artists purchased colorants predispersed by the supplier of artists' materials.

Even in previous centuries, when artists often dispersed the pigments themselves, pigment names still cannot be considered to be representative of pigment composition. Feller and Johnston-Feller (1997), for example, found discrepancies in the meaning of the color name Vandyke Brown. To the English and Germans, the name referred to the humic-earth pigment that is mined in peat bogs near Cologne, Germany, and other places, and which is a natural, organic pigment, relatively transparent, and of marginal lightfastness. To the French, however, the name Vandyke Brown referred to an iron oxide pigment that is more opaque and of high lightfastness. For the humic-earth pigment, they used the name Cologne Earth, or some other name derived from the pigment's origin.

In the organizational scheme for a library of reflectance curves illustrated here, the second category is the number of absorption bands present in the curves. The most simple curves—the yellows, for example—may exhibit no absorption maximum in the visible region. Other pigments may exhibit only a single absorption maximum. Even if such cases are encountered, the curve shape can tell the pigment-identification sleuth which pigments may and may not be present.

The number of absorption maxima can range from none (or simply a shoulder—that is, a slight dip in the curve) to one absorption band, then two absorption bands, and so on. When two or more absorption bands are present, the curves are categorized on the basis of the wavelength of the major absorption band.

Table D.1 is an example of this organizational scheme applied to a representative list of red pigments whose curves are found in figures D.1–D.26. The major headings across the table are as follows:

1. Colour Index name
2. Type (the commonly used chemical-type description)
3. Wavelength of absorption bands (entries in the table list the wavelength of the major band first, followed by the wavelengths of any progressively minor absorption bands, and end with the *K/S* ratio relative to the major band; the ratio is in parentheses)
4. Figure (number of the figure illustrating the reflectance curve)

Entries in the table are grouped according to their hue and number of absorption bands—for example, "RED: Three Absorption

Colour Index name	Type	Wavelength of absorption bands[a]	Figure
	RED: One Absorption Band		
PR 48:1	red 2B (barium)	555	D.2
PR 38	pyrazolone in acrylic	540	D.1
PR 101	synthetic red oxide	545	D.4
PR 104	molybdate orange	530	D.3
PR 4	orthochlorparanitraniline	520	D.5
	RED: Two Absorption Bands		
PR 63 Mn	BON maroon (manganese)	585, 540 (0.89)	D.7
PR 49 Ca	lithol maroon (resinated) (calcium)	580, 545 (0.89)	D.6
PR 63 Ca	BON red (calcium)	560, 525 (0.89)	D.7
PR 23	naphthol red	570, 535 (0.82)	D.8
PR 49 Ca	lithol red (resinated) (calcium)	560, 530 (0.88)	D.6
PR 49 Ba	lithol red (resinated) (barium)	560, 530 (0.88)	D.6
PR 48:2	red 2B (calcium)	560, 515 (0.65)	D.9
PR 90	phloxine	555, 510 (0.78)	D.12
PR 49 Na	lithol red (resinated) (sodium)	545, 510 (0.84)	D.6
PR 112	naphthol	550, 512 (0.92)	D.11
PR 22	naphthol	550, 515 (0.88)	D.13
PR 48:3	red 2B (strontium)	550, 515 (0.72)	D.10
PR 166	disazo condensation	545, 512 (0.90)	D.15
PR 38	pyrazolone in nitrocellulose	540, 575 (0.84)	D.14
PR 48:1	red 2B (barium)	540, 505 (0.72)	D.16
PR 63	BON red (Ba-Mn)	530, 570 (0.94)	D.7
PR 41	dianisidine	528, 565 (0.90)	D.17
PR 87	thioindigo	525, 550 (0.61)	D.19
PR 1	paranitraniline	535, 575 (0.76)	D.18
PR 179	perylene maroon	475, 520 (0.82)	D.21
	RED: Three Absorption Bands		
PR 177	anthraquinoid	565, 535 (0.92), 455 (0.48)	D.20
PR 190	perylene	565, 527 (0.85), 480 (0.92)	D.21
Vat R 29	Indofast Brilliant Scarlet	563, 528 (0.85), 483 (0.97)	D.22
PR 197	brominated pyranthrone orange	562, 477 (0.61), 450 (0.59)	D.23
PR 168	brominated anthanthrone orange	545, 520 (0.94), 485 (0.68)	D.24
PR 207	Quinacridone Red	509, 535 (0.91), 475 (0.50)	D.25
	RED: Four Absorption Bands		
PR 123	perylene vermilion	555, 510 (0.81), 480 (0.66), 445 (0.39)	D.26 D.21

[a] The figures in parentheses are the *K/S* ratios of the lower absorptions to the major absorption.

Table D.1

Representative list of red pigments.

Bands." The major absorption bands are ordered *from long to short wavelength,* in keeping with the qualitative identification procedure recommended in chapter 4. This may seem unnatural in view of the left-to-right reading habit generally applied to the interpretation of graphs. However, for the purpose described, and with a little practice, this procedure works best.

All of the curves used for table D.1 are based on manufacturers' literature. They are, therefore, modern pigments manufactured after 1960. A representative entry under the grouping "RED: Three Absorption Bands" is PR 190; perylene; 565, 527 (0.85), 480 (0. 92); D. 21.

One decision that may be subject to question in this organizational scheme is the choice of the hue category. When does a pigment become a red rather than an orange? Or when does a reddish pigment become a violet? Since the categorization of colors close in hue is arbitrary at times, the curves are placed in hue categories according to their assigned Colour Index names. Thus, some "oranges" are classified as reds, and some "reds" are listed with the violets, and so on, in accordance with their designation in the Colour Index.

The reader should be aware that the numbers for the wavelengths and for the reflectances, from which the *K/S* ratios were calculated, were obtained by reading them off the curves shown in this appendix and are, therefore, not precise. The wavelengths were determined only to the nearest 10 nm; the reflectances only to the nearest full percent.

Another part of this organizational scheme that is subjective—and thus open to question—is the choice of the wavelength that should be used to identify broad shoulders and absorption regions. An example is curve D.14 for PR 38. The reader may not agree with the wavelength assignments listed in table D.1. If an atlas of curves is ever prepared, the editors will be confronted with such decisions.

Accumulating a library of spectral reflectance curves must be regarded as an ongoing task, to be added to as additional references or new materials are collected. The accompanying list of red pigments serves only as an introductory demonstration of the possibilities.

In the appendix D figures, the colorant amount in the colorant–TiO_2 ratio is indicated by the letter C—for example, 25 C/75 TiO_2. The curves illustrated in figures D.1, D.5–D.8, D.12–D.14, D.16, D.21, D.23, and D.24 are redrawn from illustrations in volume 1 of the first edition of the *Pigment Handbook* (Patton 1973). The others are redrawn from the manufacturers' literature accumulated by the author and from curves prepared by the author. Sources represented are Ciba Specialty Chemicals (formerly Ciba-Geigy), DuPont, and Harmon Colors.

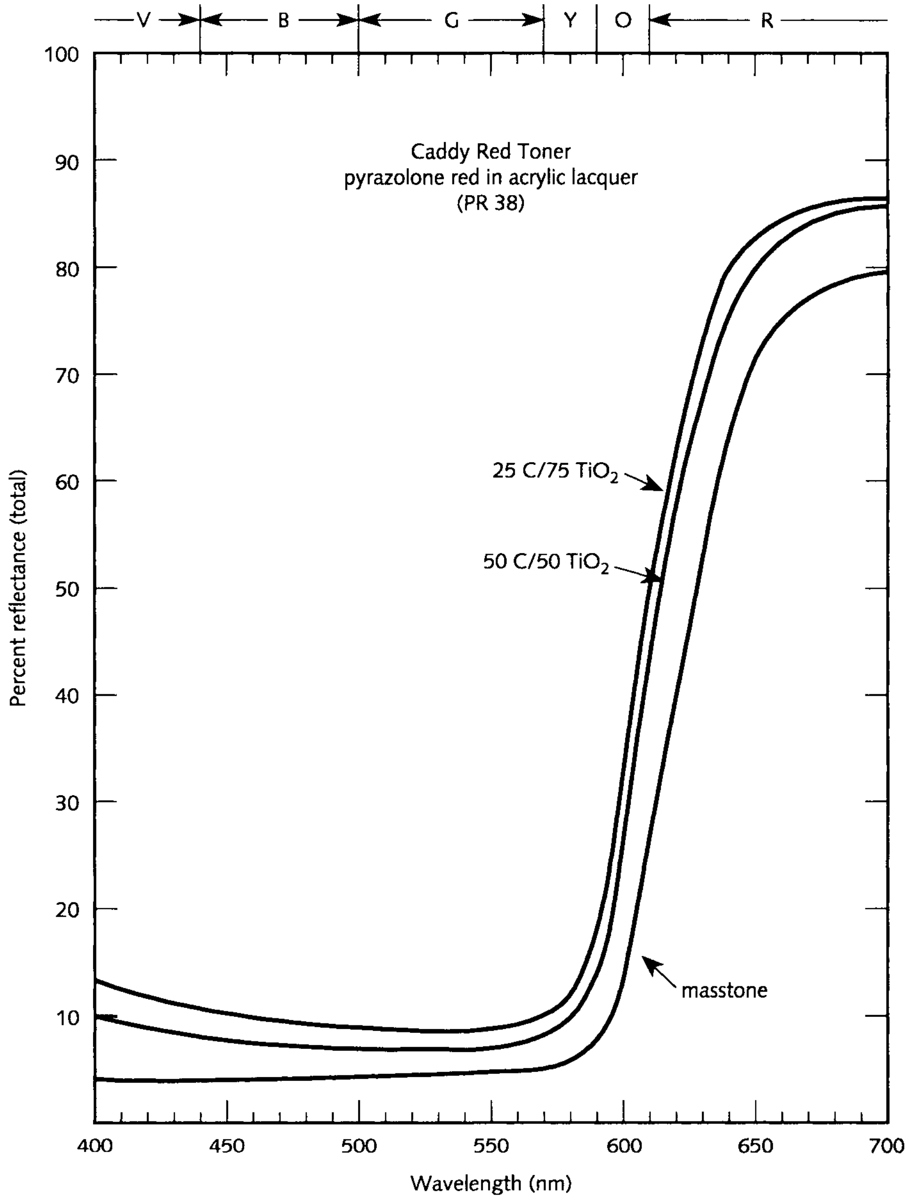

Figure D.1 (from Patton 1973. Copyright © 1973 John Wiley & Sons, Inc. Reprinted by permission).

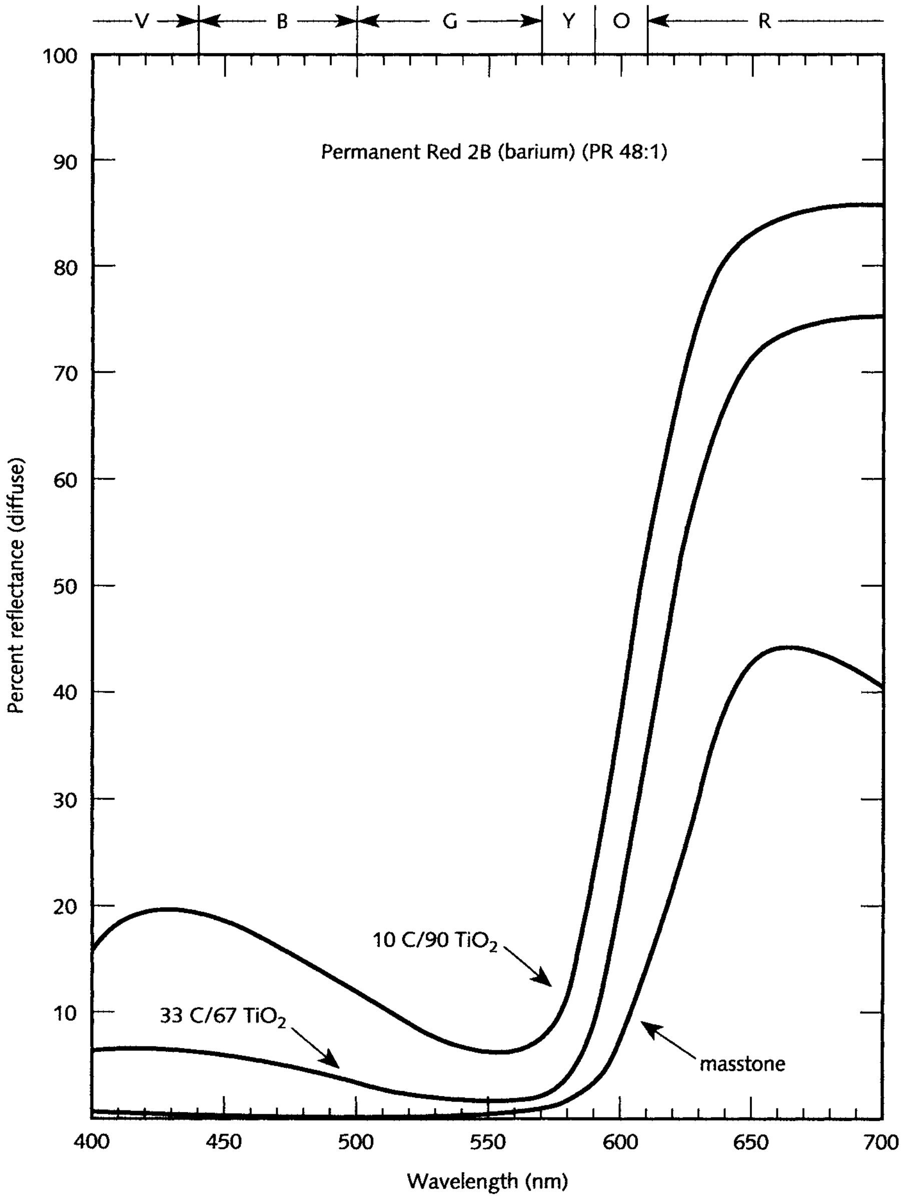
V
B
G
Y
O
R
Permanent Red 2B (barium) (PR 48:1)
10 C/90 TiO2
33 C/67 TiO2
masstone
Percent reflectance (diffuse)
100
90
80
70
60
50
40
30
20
10
400
450
500
550
600
650
700
Wavelength (nm)

Figure D.2

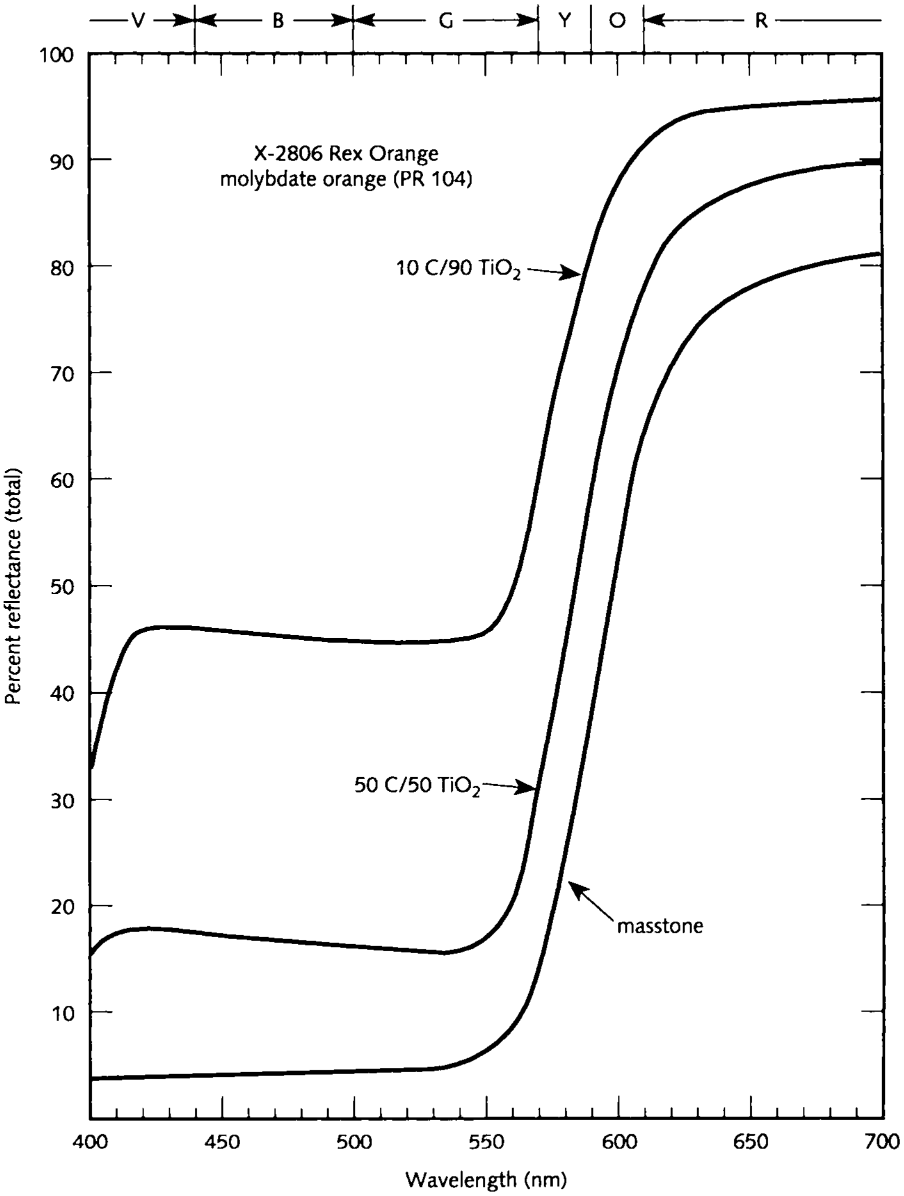
V
B
G
Y
O
R
X-2806 Rex Orange
molybdate orange (PR 104)
10 C/90 TiO2
50 C/50 TiO2
masstone
Percent reflectance (total)
100
90
80
70
60
50
40
30
20
10
400
450
500
550
600
650
700
Wavelength (nm)

Figure D.3

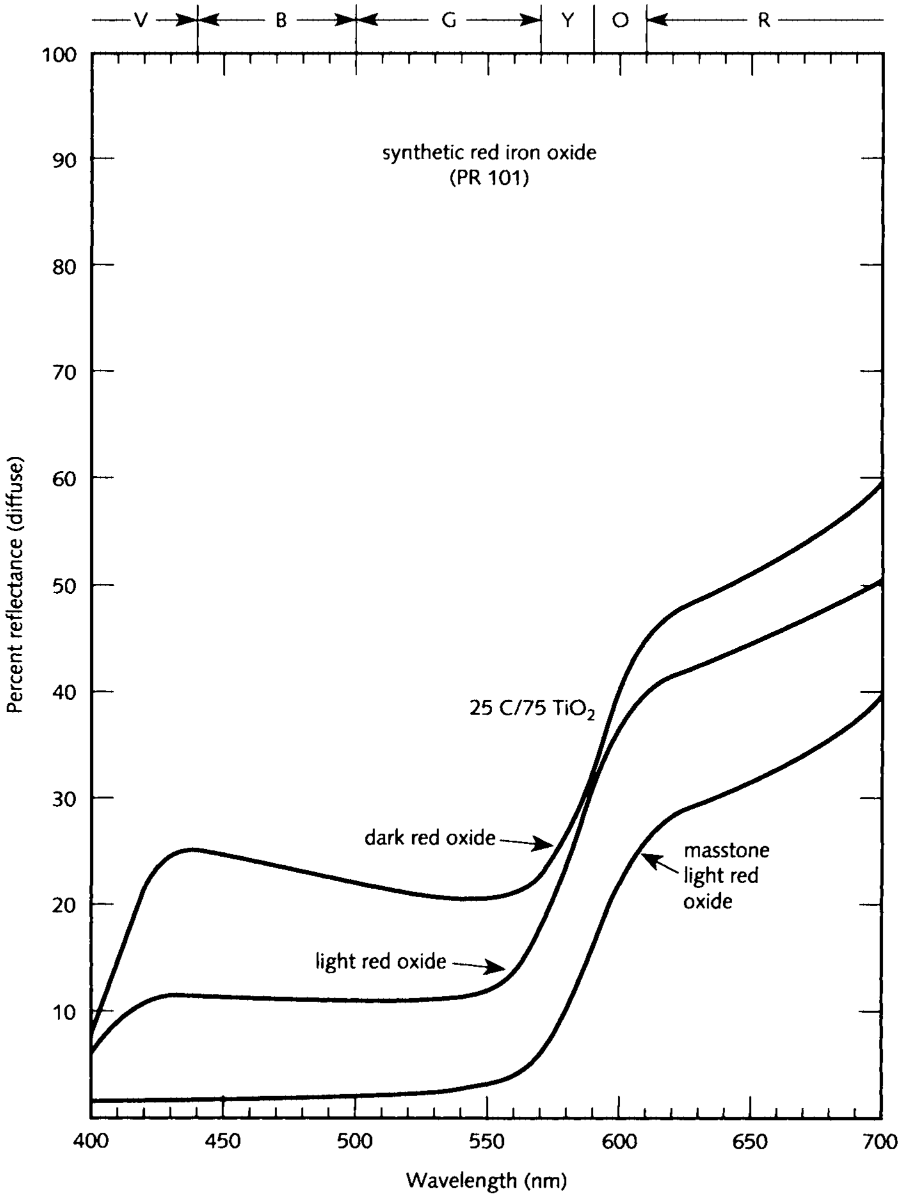
V
B
G
Y
O
R
synthetic red iron oxide
(PR 101)
25 C/75 TiO2
dark red oxide
light red oxide
masstone light red oxide
Percent reflectance (diffuse)
Wavelength (nm)
100
90
80
70
60
50
40
30
20
10
400
450
500
550
600
650
700

Figure D.4

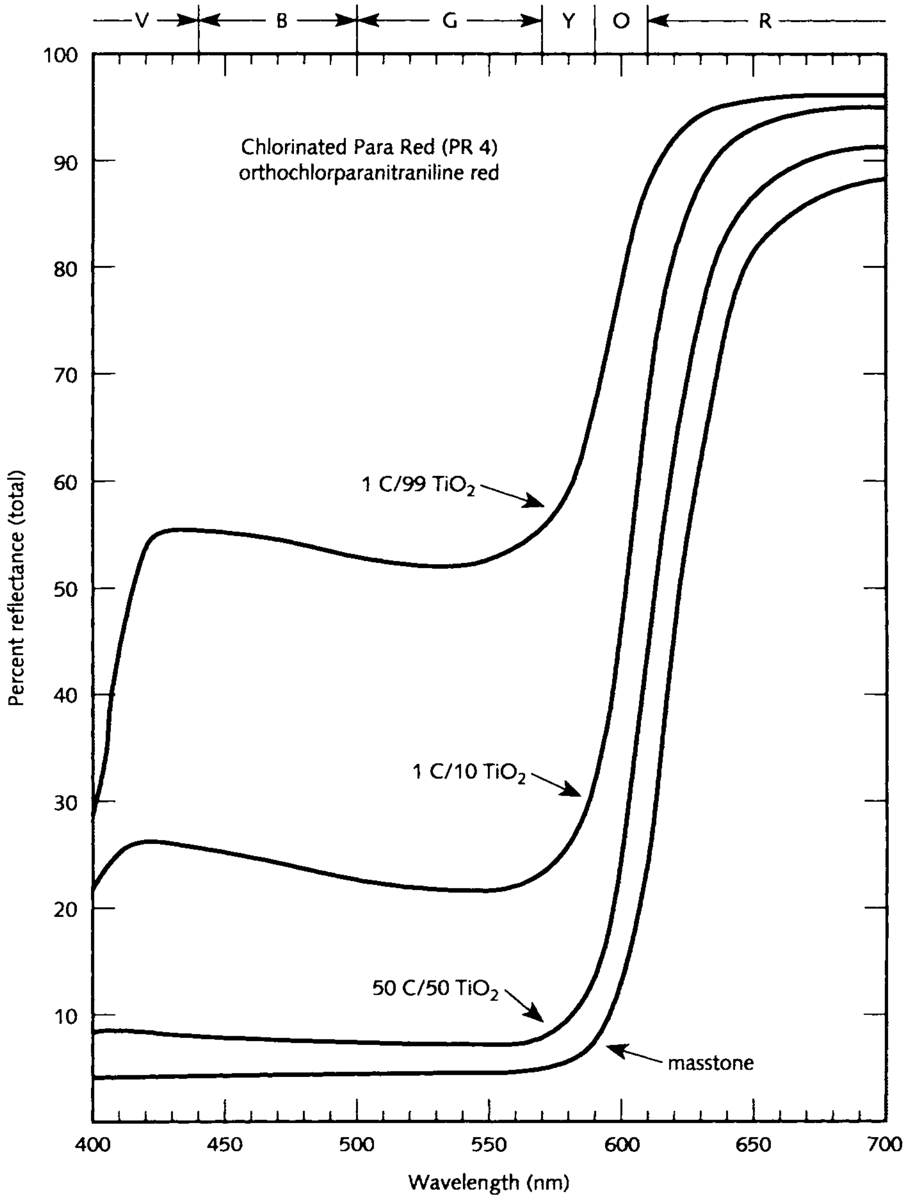

Figure D.5 (from Patton 1973. Copyright © 1973 John Wiley & Sons, Inc. Reprinted by permission).

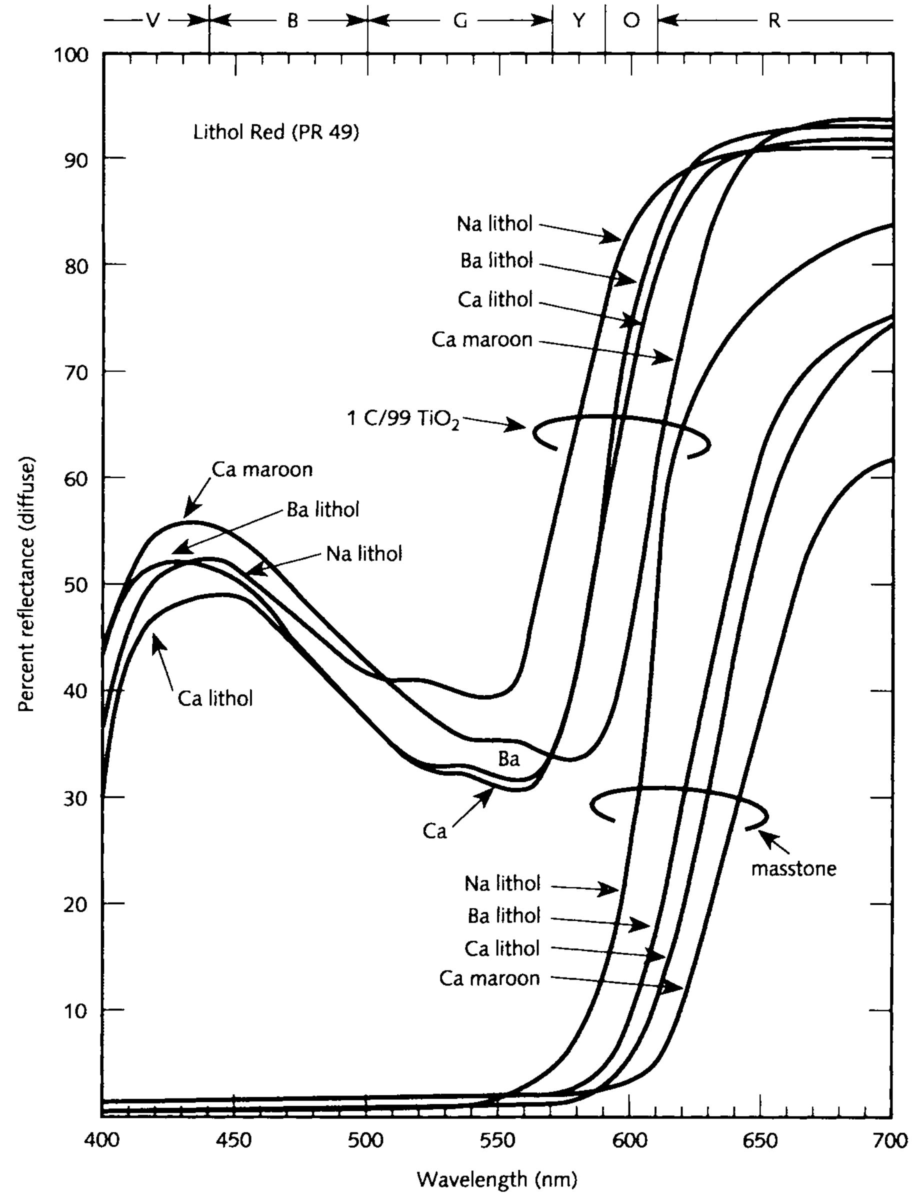

Figure D.6 (from Patton 1973. Copyright © 1973 John Wiley & Sons, Inc. Reprinted by permission).

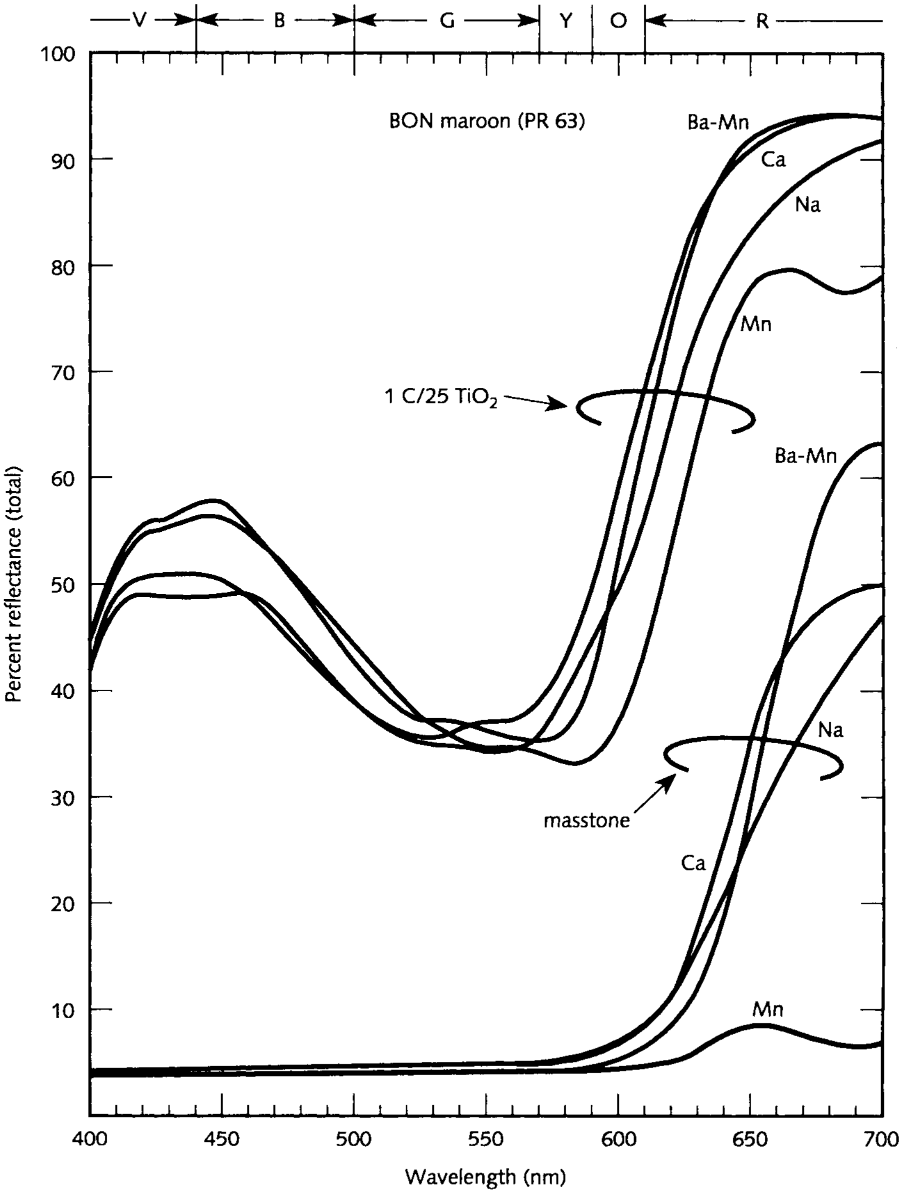

Figure D.7 (from Patton 1973. Copyright © 1973 John Wiley & Sons, Inc. Reprinted by permission).

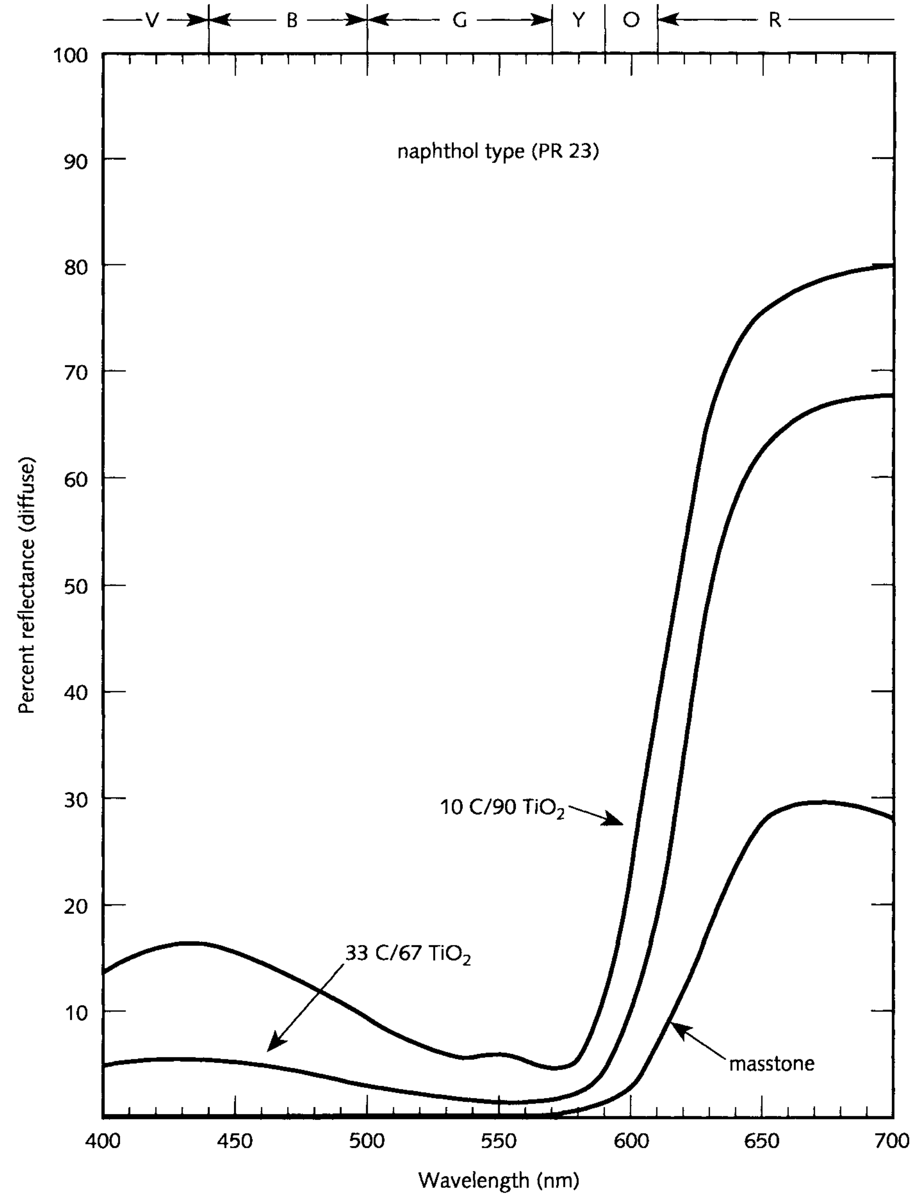

Figure D.8 (from Patton 1973. Copyright © 1973 John Wiley & Sons, Inc. Reprinted by permission).

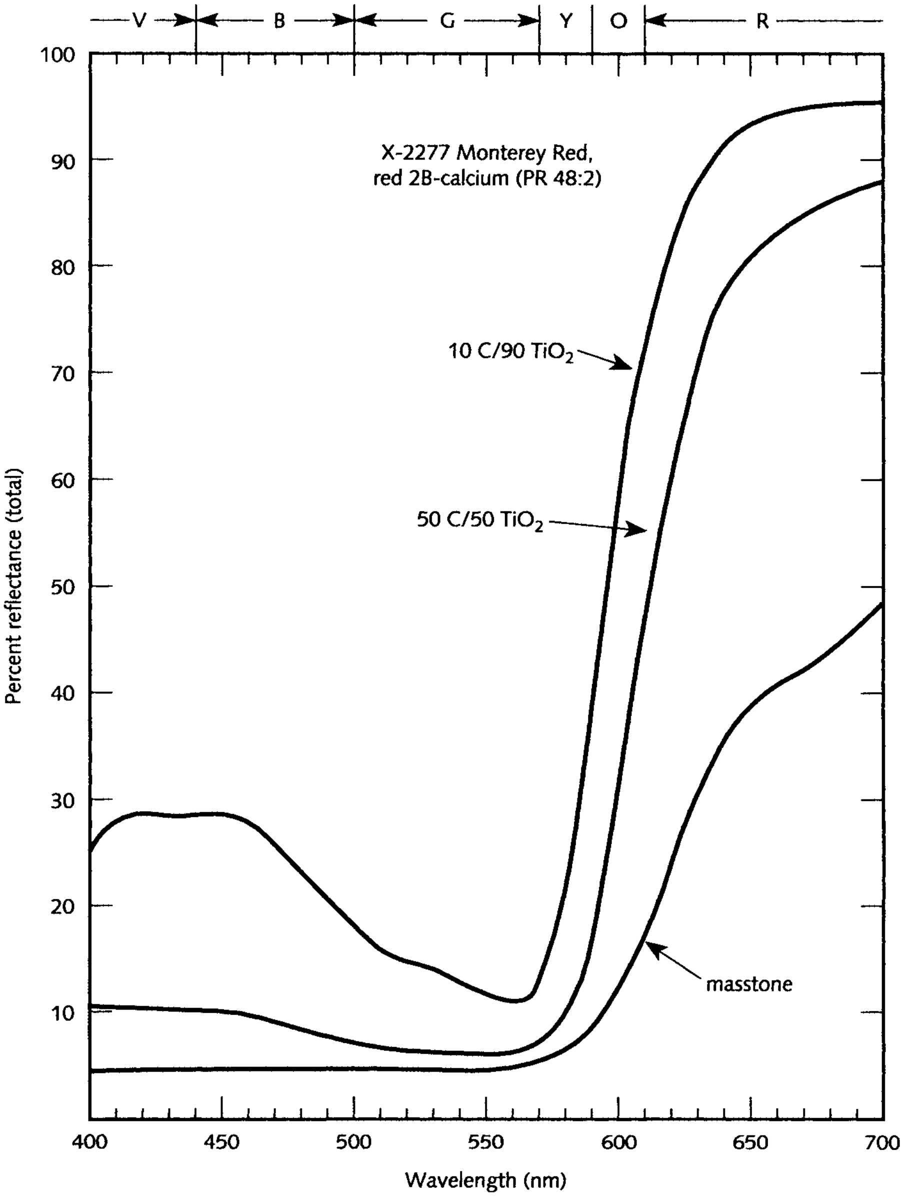
V
B
G
Y
O
R
X-2277 Monterey Red,
red 2B-calcium (PR 48:2)
10 C/90 TiO2
50 C/50 TiO2
masstone
Percent reflectance (total)
100
90
80
70
60
50
40
30
20
10
400
450
500
550
600
650
700
Wavelength (nm)

Figure D.9

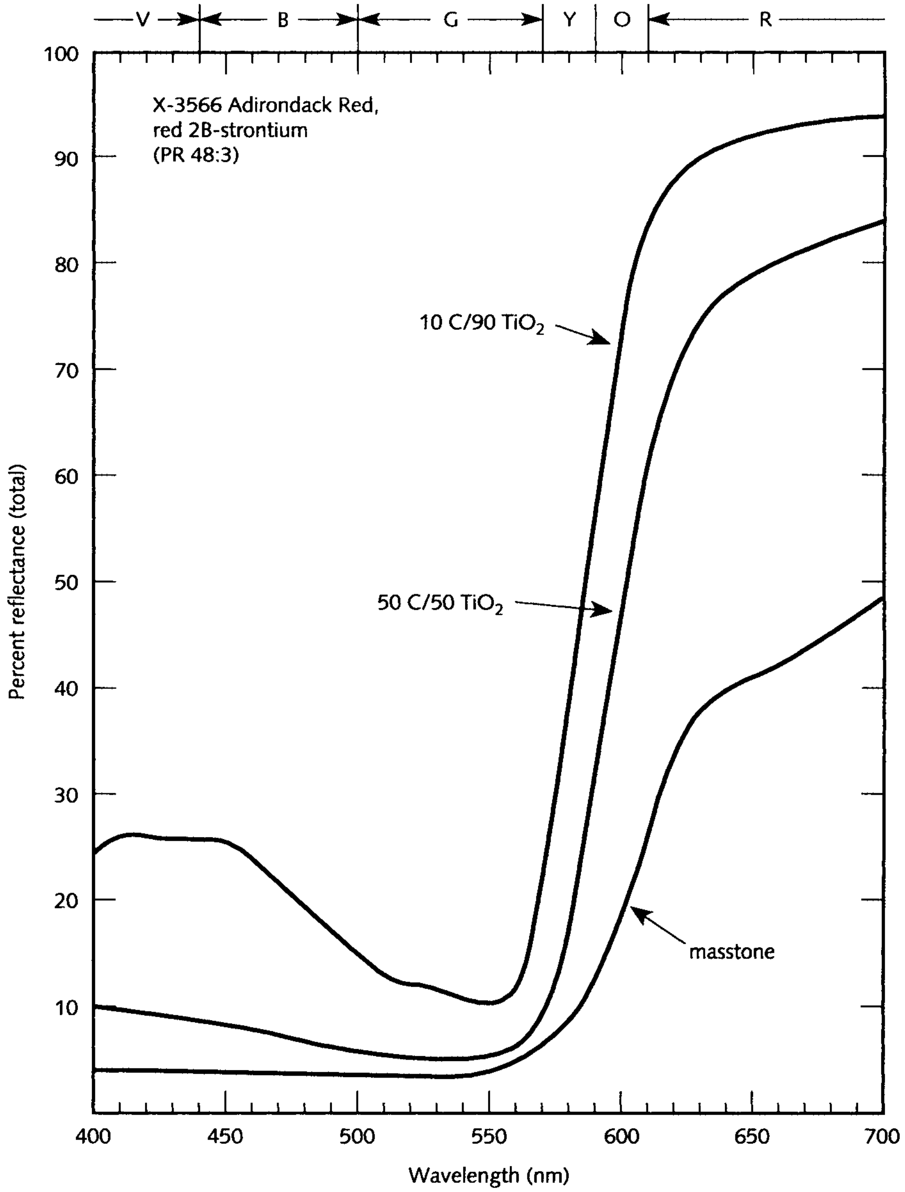
V
B
G
Y
O
R
X-3566 Adirondack Red,
red 2B-strontium
(PR 48:3)
10 C/90 TiO2
50 C/50 TiO2
masstone
Percent reflectance (total)
100
90
80
70
60
50
40
30
20
10
400
450
500
550
600
650
700
Wavelength (nm)

Figure D.10

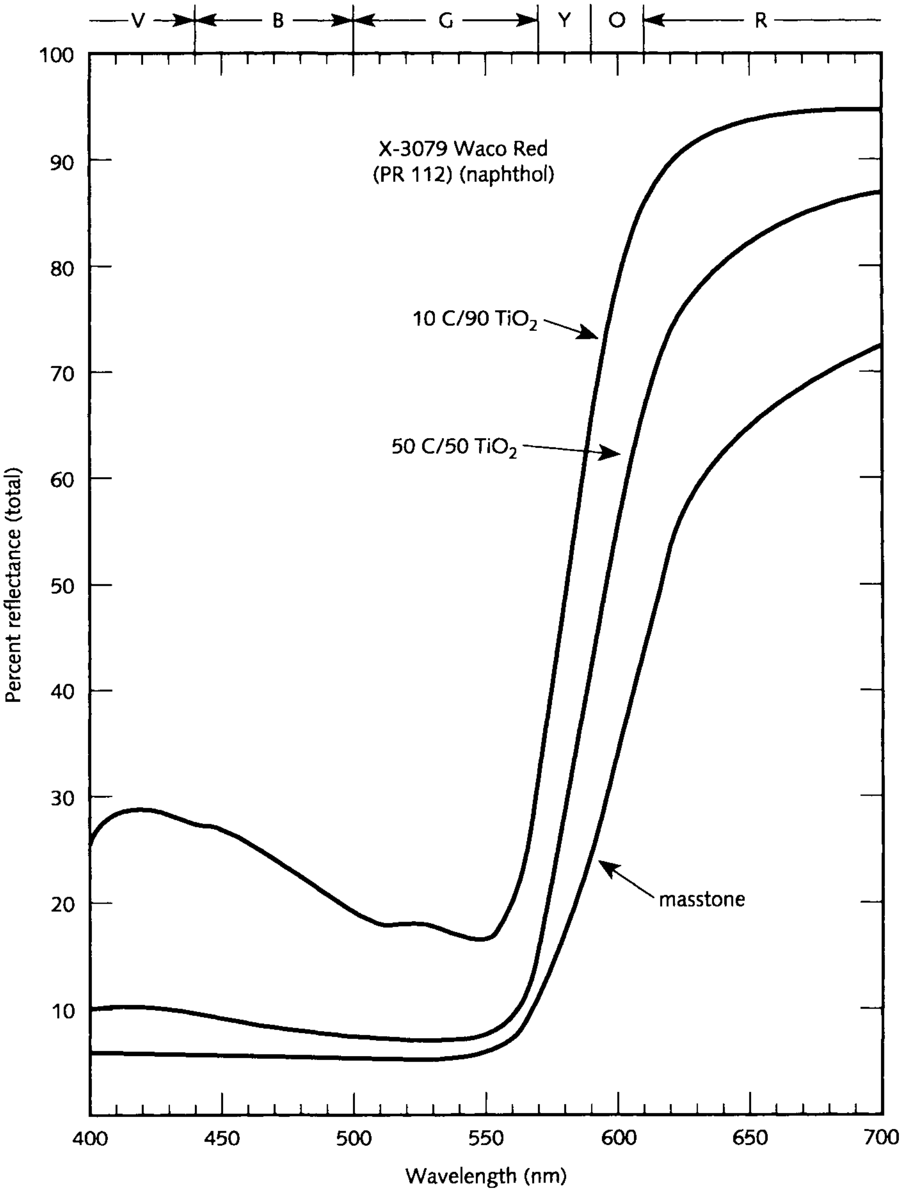
V
B
G
Y
O
R
100
90
80
70
60
50
40
30
20
10
Percent reflectance (total)
X-3079 Waco Red
(PR 112) (naphthol)
10 C/90 TiO_2
50 C/50 TiO_2
masstone
400
450
500
550
600
650
700
Wavelength (nm)

Figure D.11

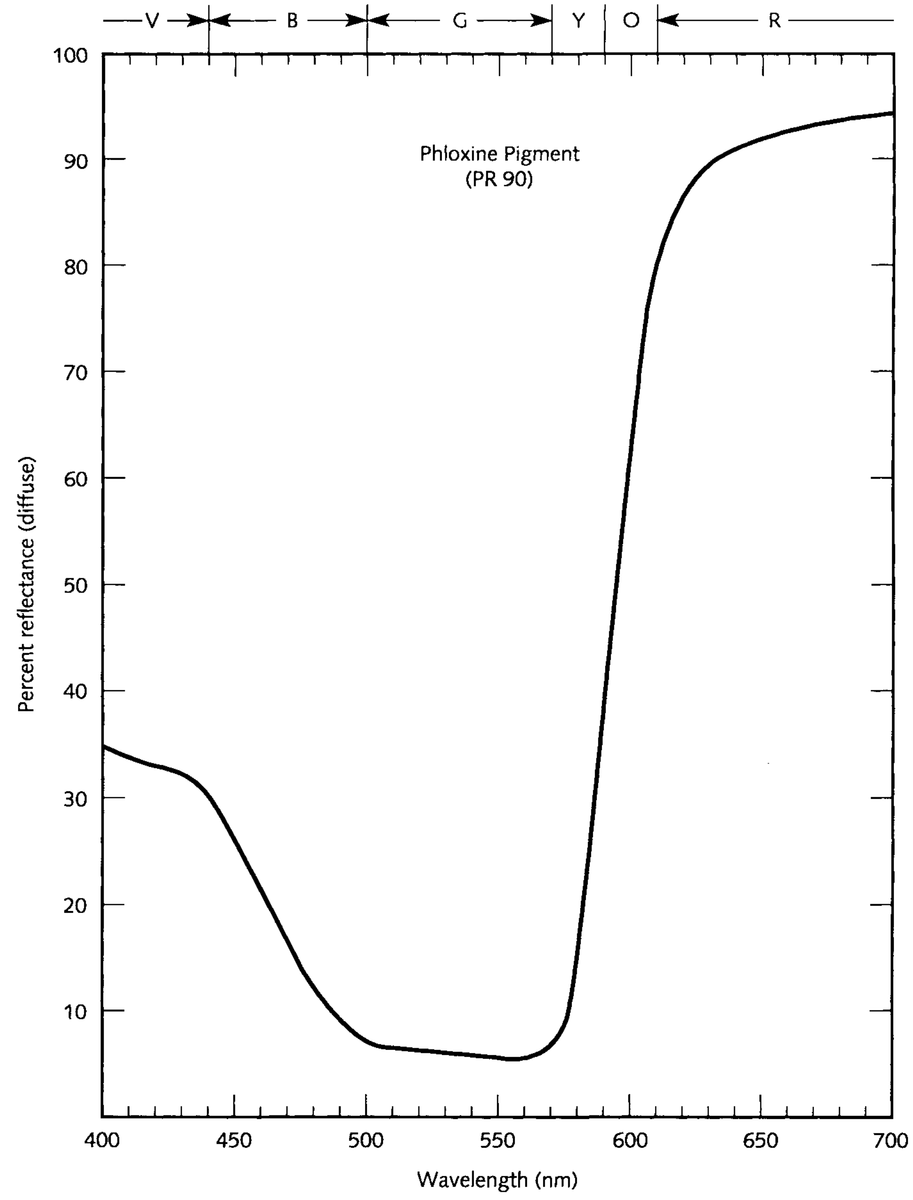

Figure D.12 (from Patton 1973. Copyright © 1973 John Wiley & Sons, Inc. Reprinted by permission).

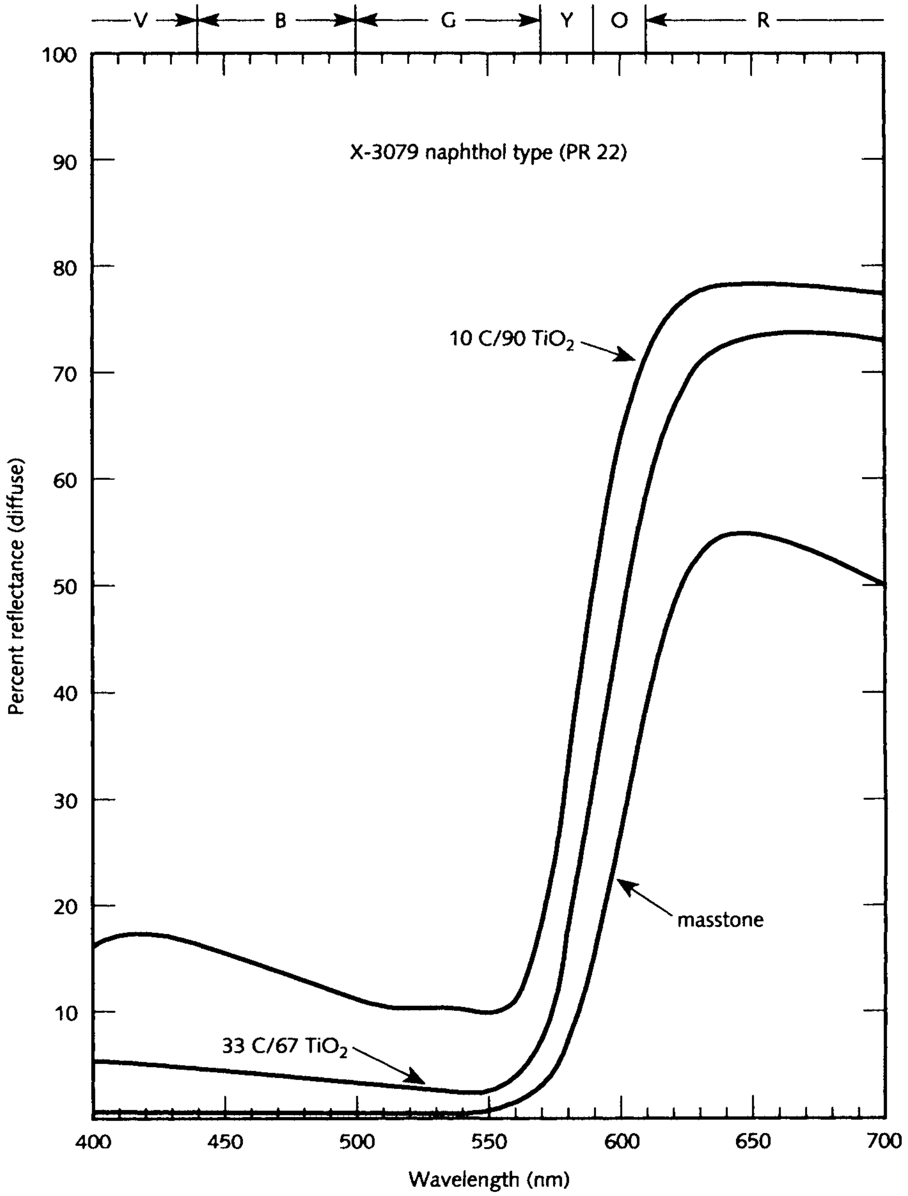

Figure D.13 (from Patton 1973. Copyright © 1973 John Wiley & Sons, Inc. Reprinted by permission).

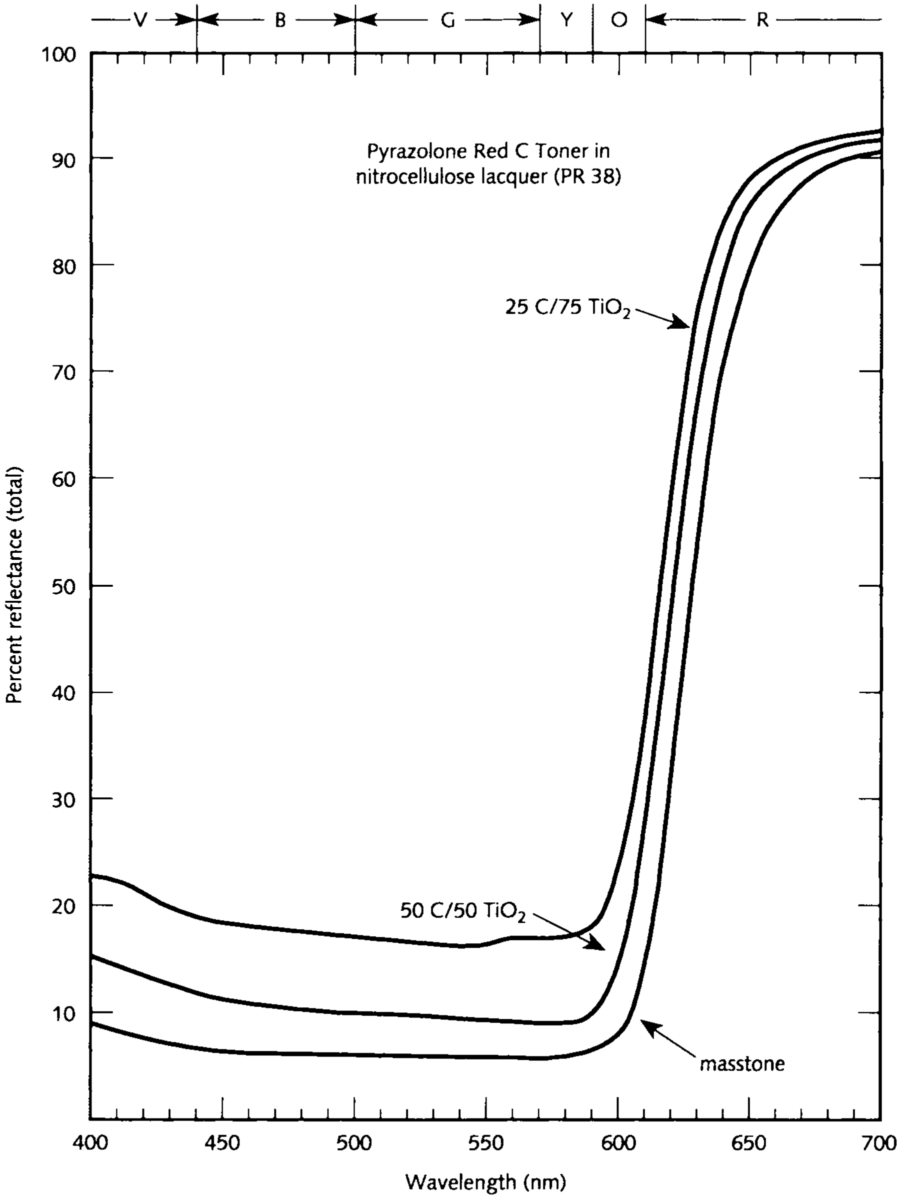

Figure D.14 (from Patton 1973. Copyright © 1973 John Wiley & Sons, Inc. Reprinted by permission).

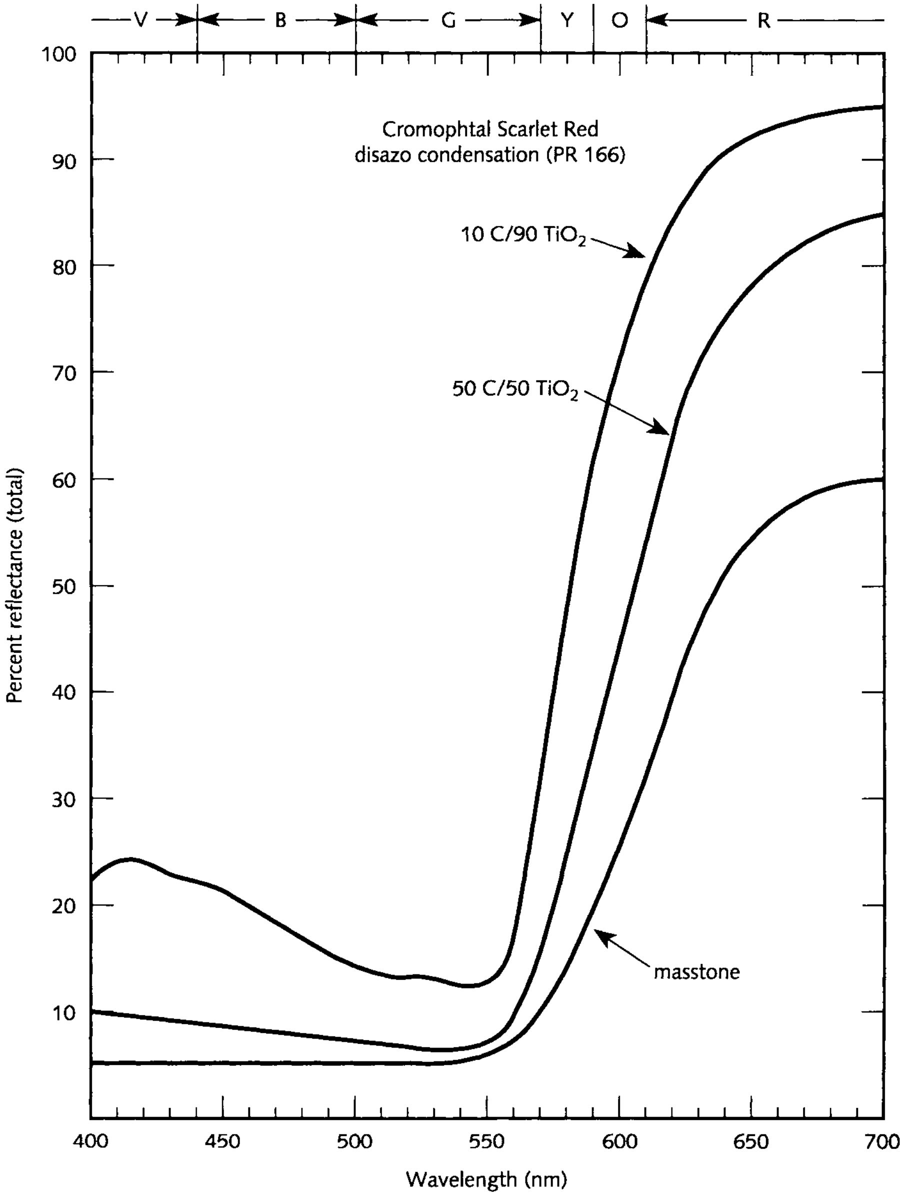
V
B
G
Y
O
R
Cromophtal Scarlet Red
disazo condensation (PR 166)
10 C/90 TiO$_2$
50 C/50 TiO$_2$
masstone
Percent reflectance (total)
100
90
80
70
60
50
40
30
20
10
400
450
500
550
600
650
700
Wavelength (nm)

Figure D.15

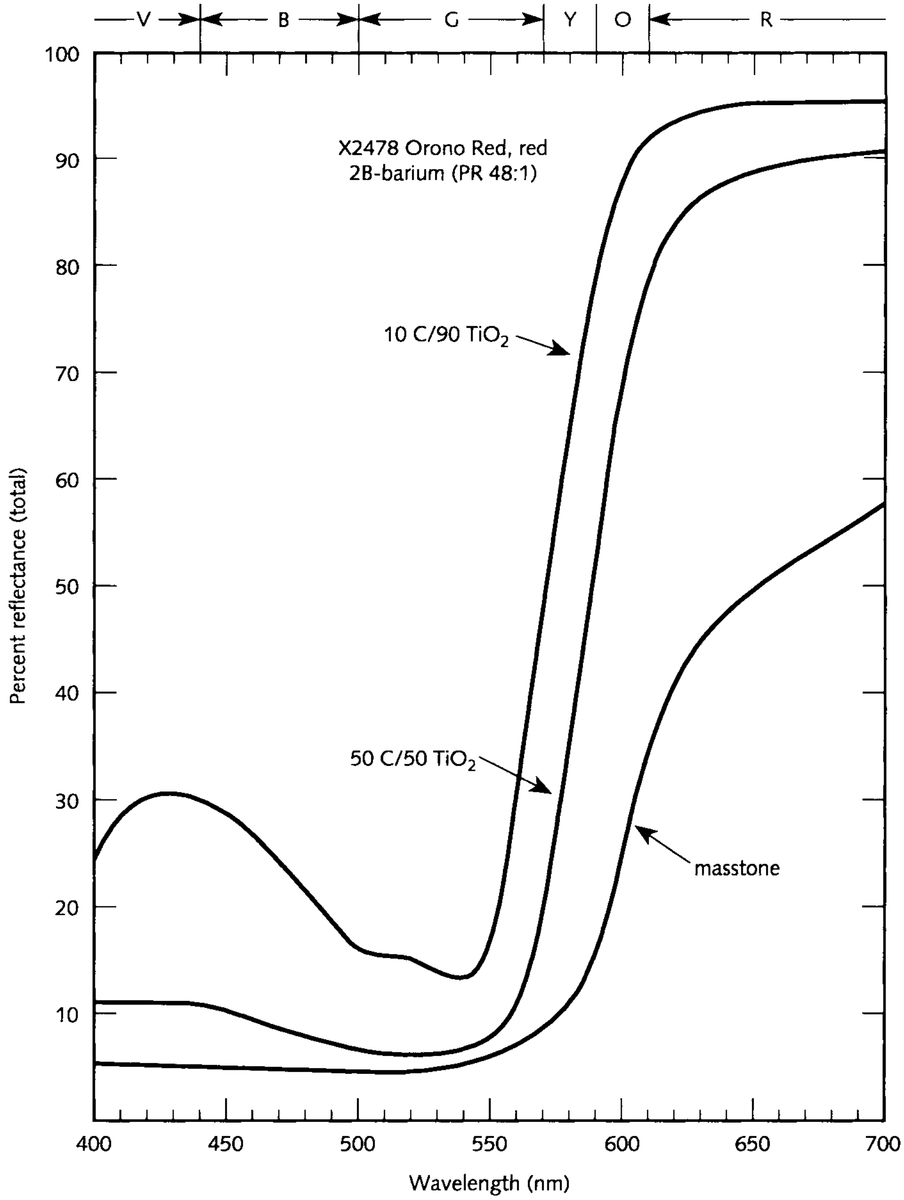

Figure D.16 (from Patton 1973. Copyright © 1973 John Wiley & Sons, Inc. Reprinted by permission).

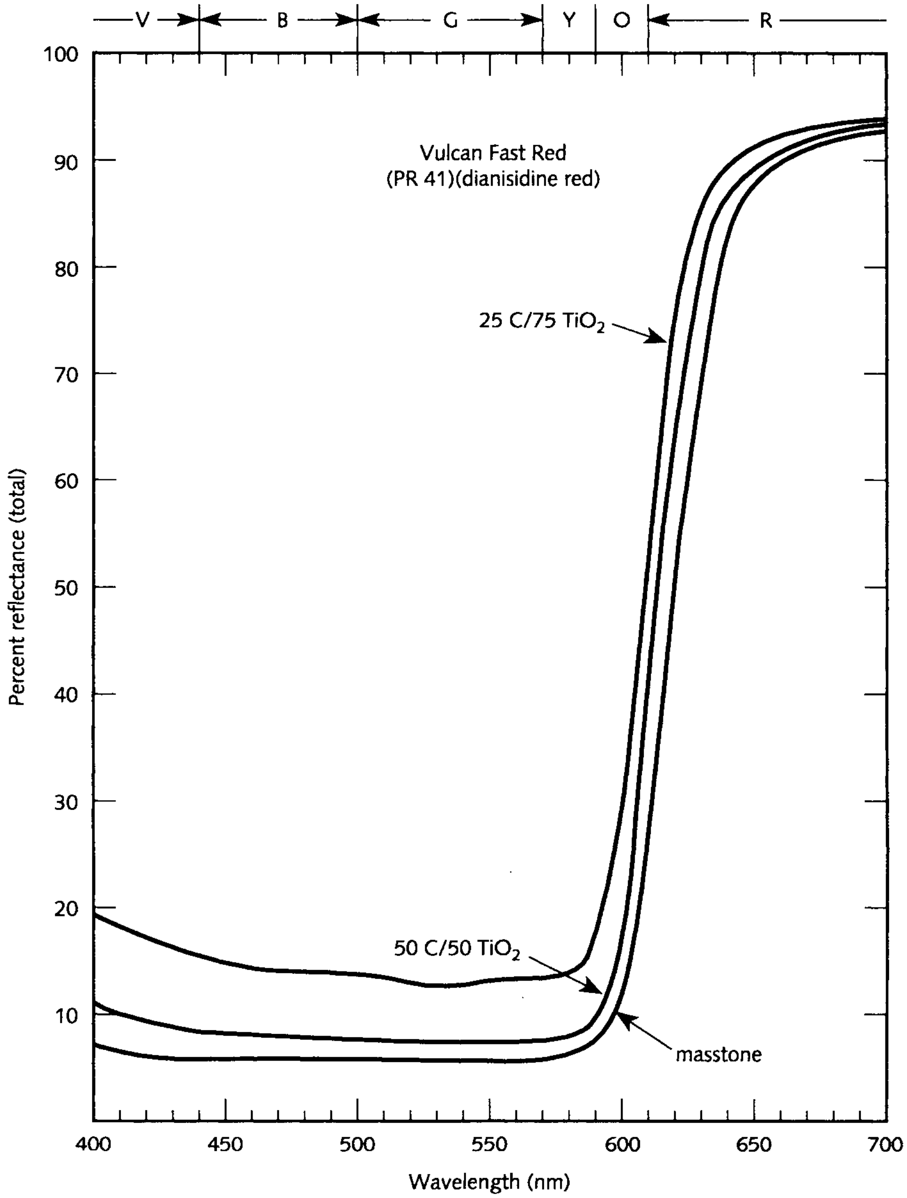
V
B
G
Y
O
R
Vulcan Fast Red
(PR 41)(dianisidine red)
25 C/75 TiO2
50 C/50 TiO2
masstone
Percent reflectance (total)
100
90
80
70
60
50
40
30
20
10
400
450
500
550
600
650
700
Wavelength (nm)

Figure D.17

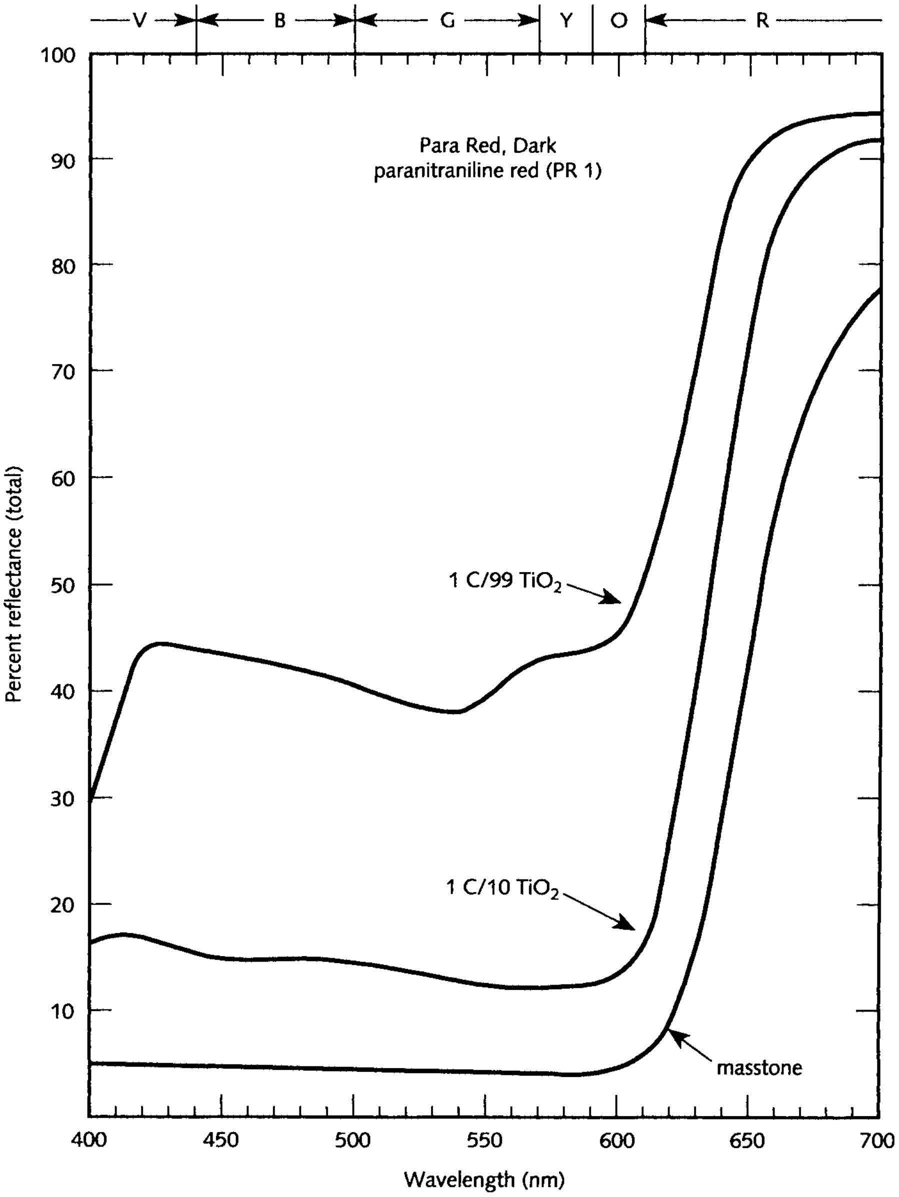
V
B
G
Y
O
R
Para Red, Dark
paranitraniline red (PR 1)
1 C/99 TiO_2
1 C/10 TiO_2
masstone
Percent reflectance (total)
100
90
80
70
60
50
40
30
20
10
400
450
500
550
600
650
700
Wavelength (nm)

Figure D.18

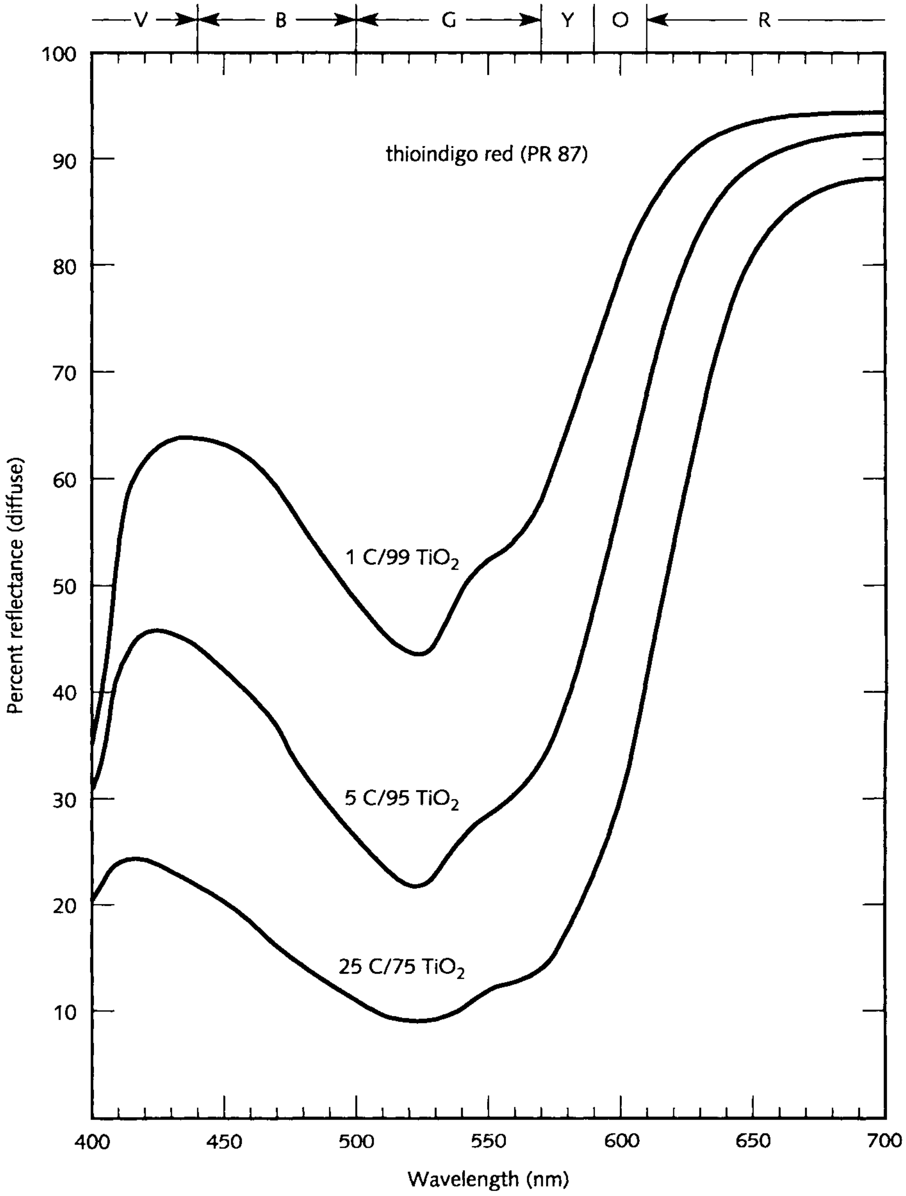
V
B
G
Y
O
R
100
90
80
70
60
50
40
30
20
10
Percent reflectance (diffuse)
thioindigo red (PR 87)
1 C/99 TiO2
5 C/95 TiO2
25 C/75 TiO2
400
450
500
550
600
650
700
Wavelength (nm)

Figure D.19

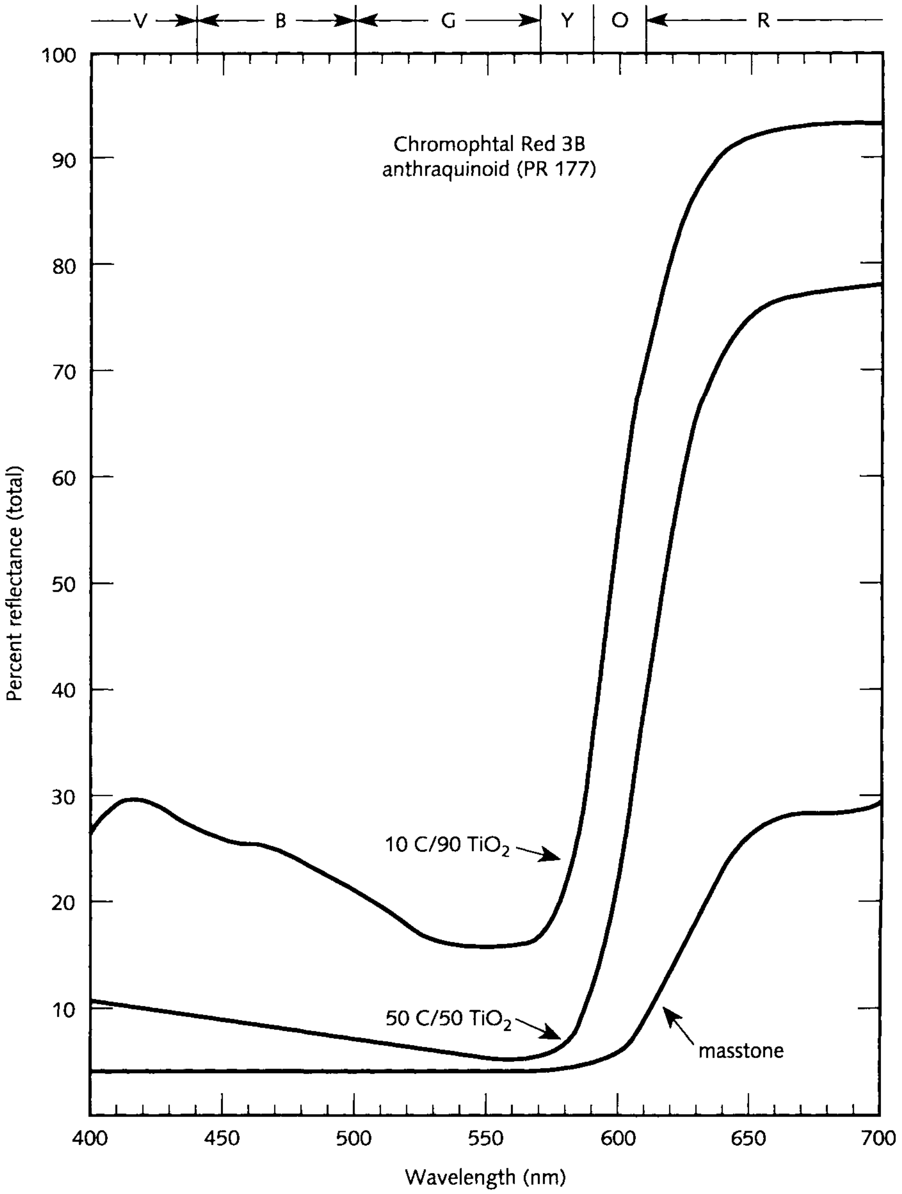
V
B
G
Y
O
R
Chromophtal Red 3B
anthraquinoid (PR 177)
10 C/90 TiO2
50 C/50 TiO2
masstone
Percent reflectance (total)
100
90
80
70
60
50
40
30
20
10
400
450
500
550
600
650
700
Wavelength (nm)

Figure D.20

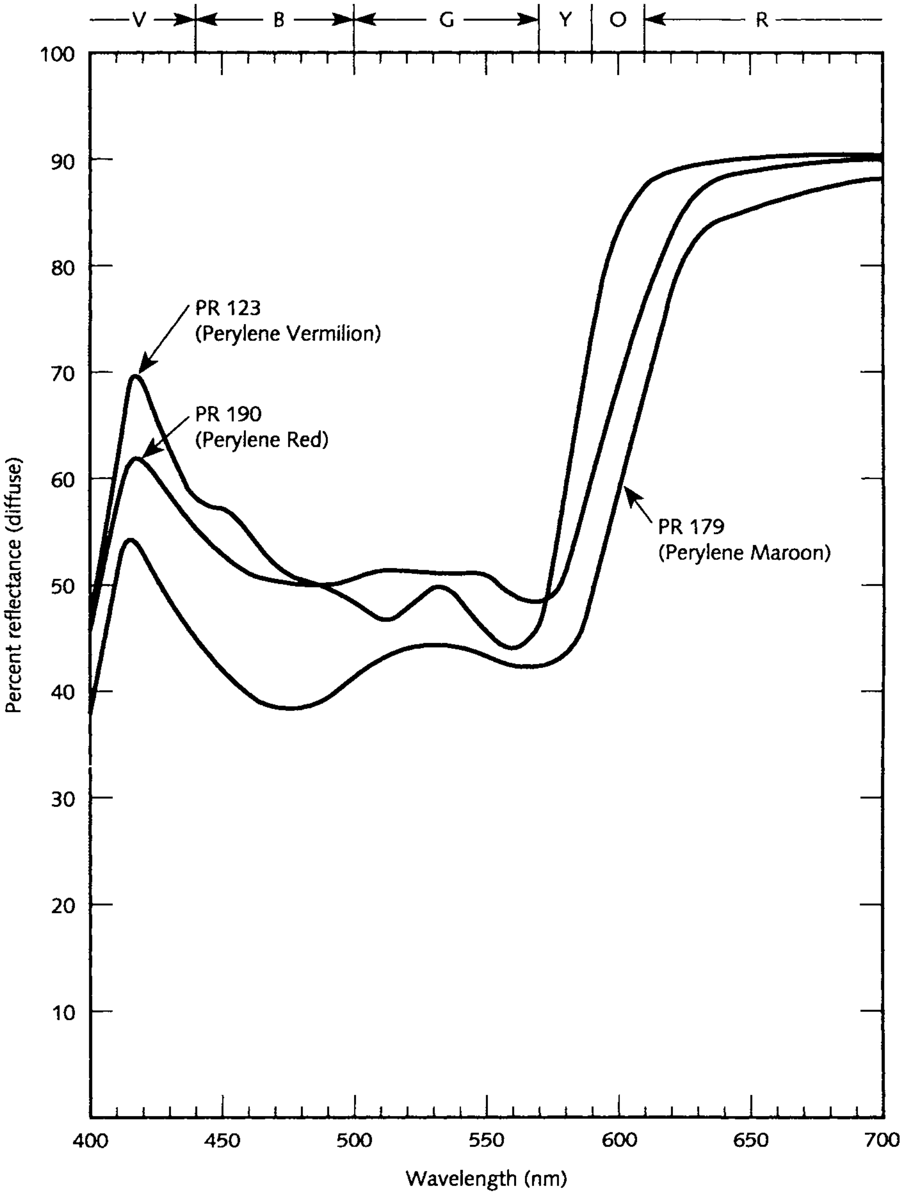

Figure D.21 (from Patton 1973. Copyright © 1973 John Wiley & Sons, Inc. Reprinted by permission).

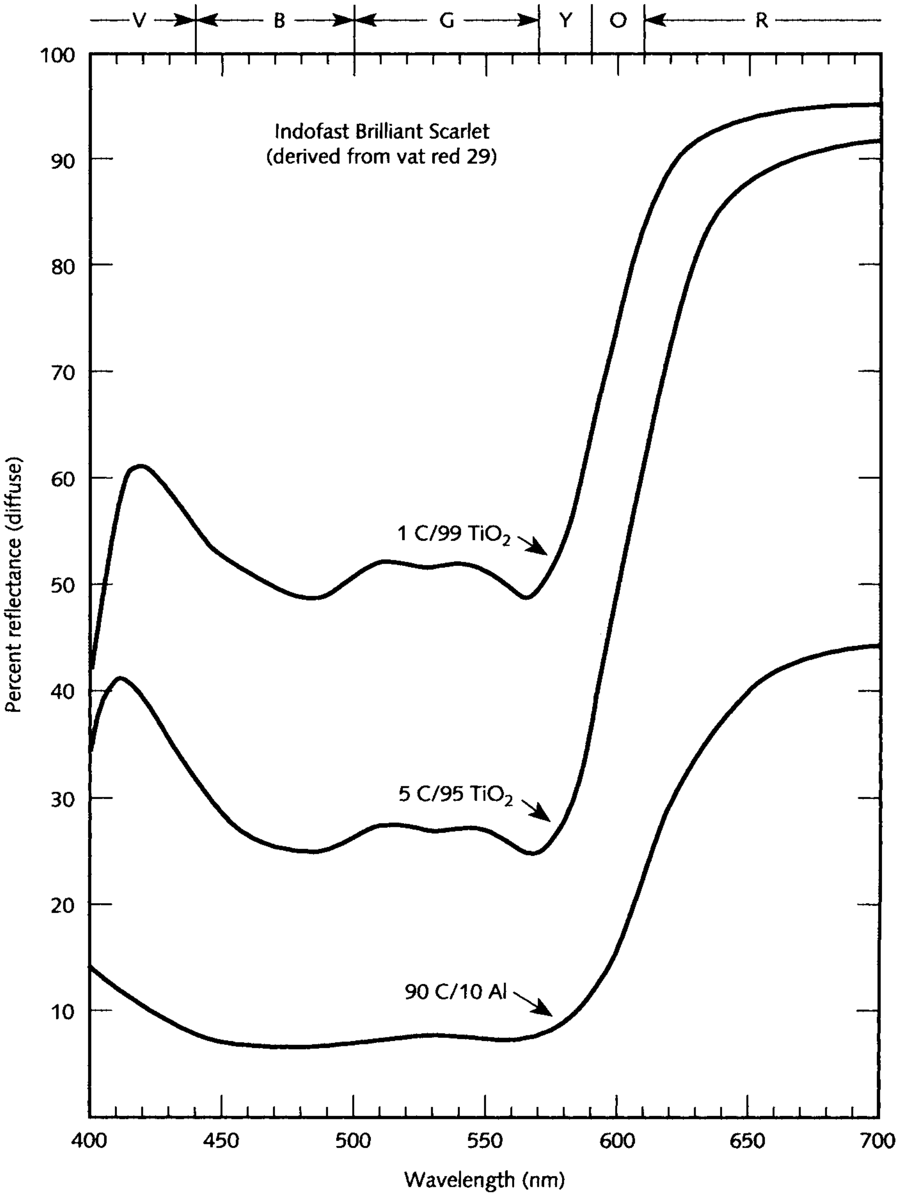
V
B
G
Y
O
R
Indofast Brilliant Scarlet
(derived from vat red 29)
1 C/99 TiO2
5 C/95 TiO2
90 C/10 Al
Percent reflectance (diffuse)
100
90
80
70
60
50
40
30
20
10
400
450
500
550
600
650
700
Wavelength (nm)

Figure D.22

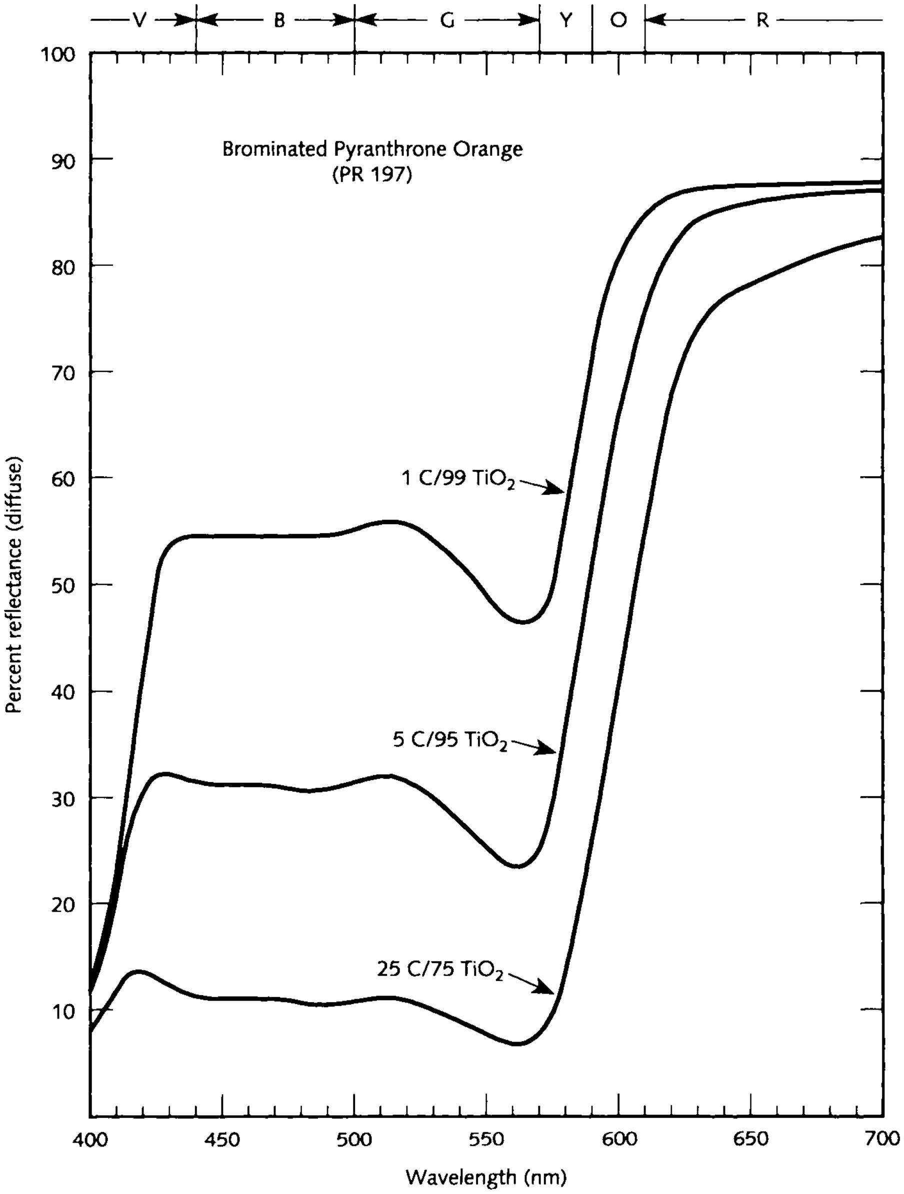

Figure D.23 (from Patton 1973. Copyright © 1973 John Wiley & Sons, Inc. Reprinted by permission).

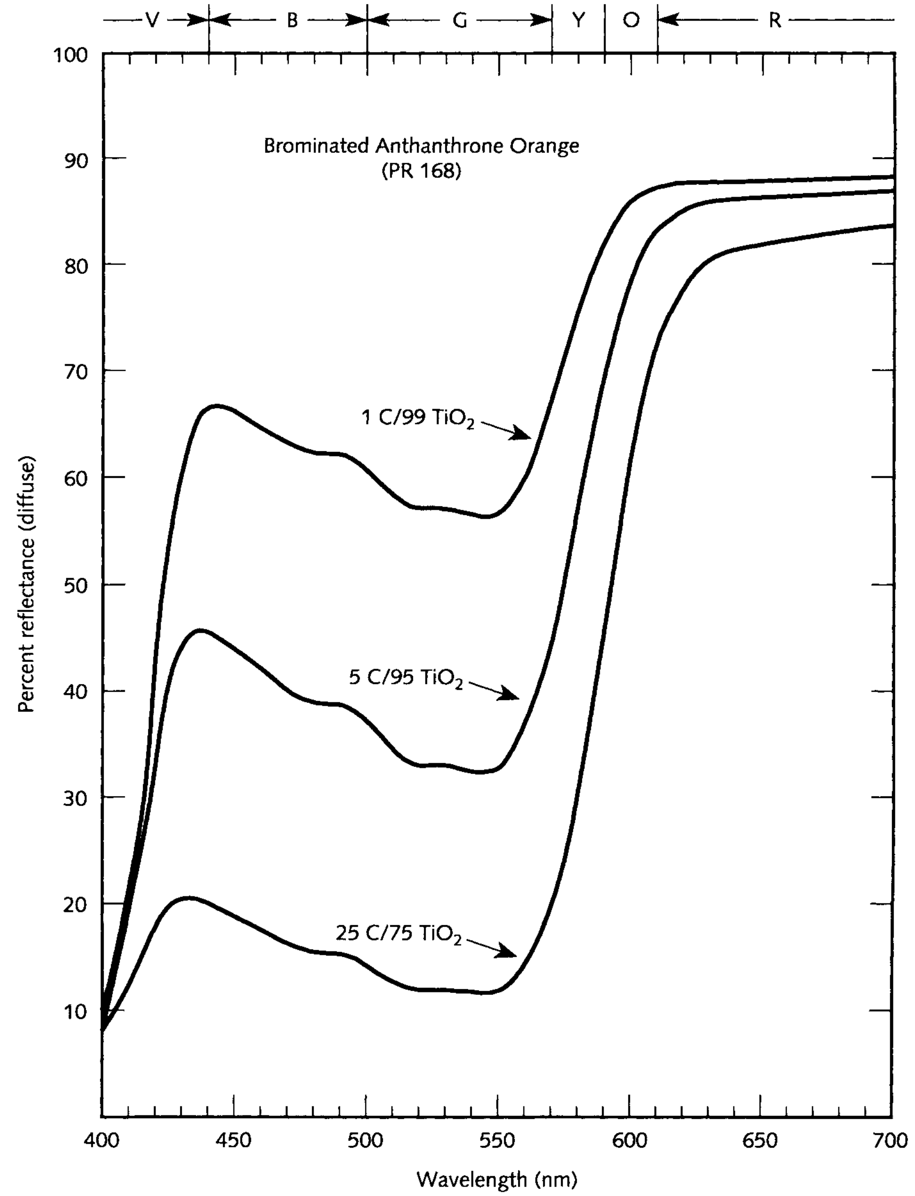

Figure D.24 (from Patton 1973. Copyright © 1973 John Wiley & Sons, Inc. Reprinted by permission).

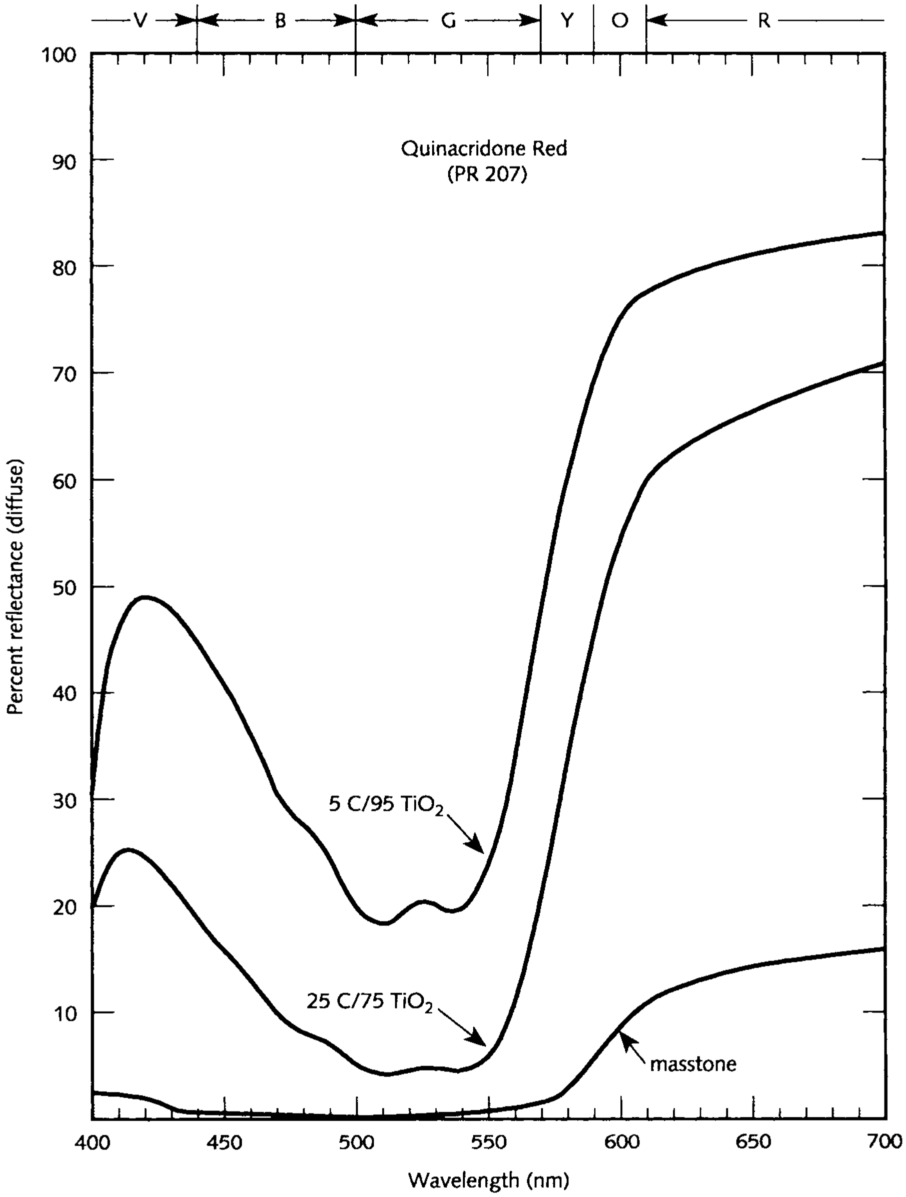
V
B
G
Y
O
R
Quinacridone Red
(PR 207)
5 C/95 TiO$_2$
25 C/75 TiO$_2$
masstone
Percent reflectance (diffuse)
100
90
80
70
60
50
40
30
20
10
400
450
500
550
600
650
700
Wavelength (nm)

Figure D.25

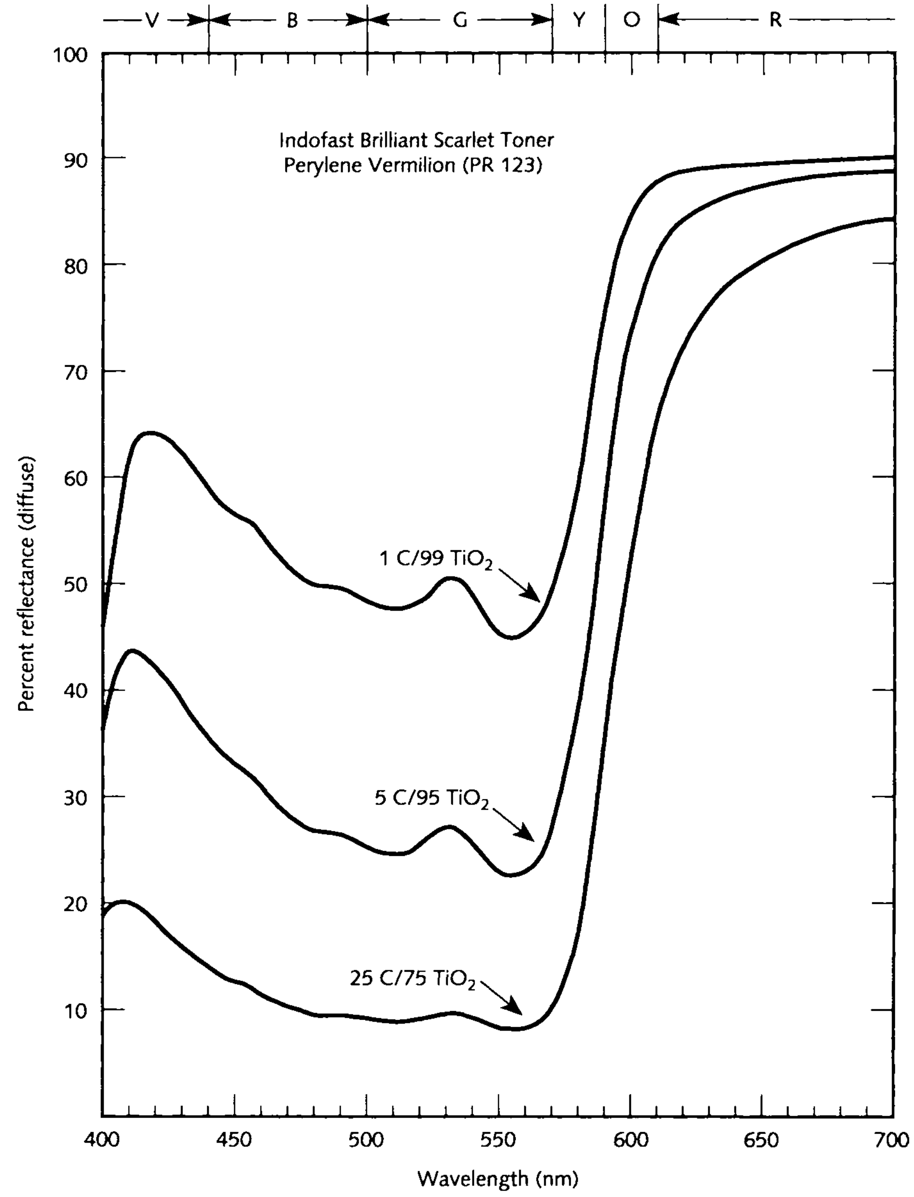
V
B
G
Y
O
R
100
90
80
70
60
50
40
30
20
10
Percent reflectance (diffuse)
Indofast Brilliant Scarlet Toner
Perylene Vermilion (PR 123)
1 C/99 TiO_2
5 C/95 TiO_2
25 C/75 TiO_2
400
450
500
550
600
650
700
Wavelength (nm)

Figure D.26

Appendix E

Recommended Reading

Many of the books and articles listed below have been referred to in the text; a few have not. They are categorized here by subject; notes explain their major emphasis.

General Textbooks on Color Science

Berger-Schunn, A.

1994 *Practical Color Measurement.* Original in German, translated by the author and Max Saltzman. New York: John Wiley and Sons.

Brief coverage of the essentials of color perception, color measurement, correlations between reflectance and colorant concentration, colorant strength, and computer color matching. The stated objective is to describe "only what every user . . . needs to know." The viewpoint is oriented toward textiles.

Billmeyer, F. W., Jr., and M. Saltzman

1981 *Principles of Color Technology,* 2d ed. (1st ed., 1966). New York: John Wiley and Sons.

The best elementary book available. The third edition of this work appeared in 2000 (New York: John Wiley and Sons), revised and updated by Roy S. Berns.

Judd, D. B.

1952 *Color in Business, Science, and Industry,* 1st ed. New York: John Wiley and Sons.

The most comprehensive textbook available. Comparison of this first edition of Judd's with subsequent editions prepared with Wyszecki provides an interesting history of developments in color science and application over nearly twenty-five years of extensive research and application, as well as an appreciation of the constancy of basic ideas.

Judd, D. B., and G. Wyszecki

1975 *Color in Business, Science, and Industry,* 3d ed. (2d ed., 1963). New York: John Wiley and Sons.

Wright, W. D.

1969 *The Measurement of Colour,* 4th ed. New York: Van Nostrand.

A classic.

Wyszecki, G., and W. S. Stiles
1982 *Color Science: Concepts and Methods, Quantitative Data and Formulae,* 2d ed. (1st ed., 1967). New York: John Wiley and Sons.

Both editions are superb sources of the methods, data, and reference materials that make up the science of colorimetry. Encyclopedic in scope.

Spectrophotometry and Its Applications

Frei, R. W., and J. D. MacNeil
1973 *Diffuse Reflectance Spectroscopy in Environmental Problem Solving.* Cleveland: CRC Press, Division of the Chemical Rubber Co.

An interesting book that describes different applications of spectrophotometry and the Kubelka–Munk equation.

Hunt, R. W. G.
1982 *Measuring Colour,* 1st ed. (2d ed., 1991). Chichester, Eng.: Ellis Horwood.

Provides the basic facts needed to measure color. It is lucidly written and eminently suitable as an up-to-date textbook.

Kortüm, G.
1969 *Reflectance Spectroscopy: Principles, Methods, Applications.* Translated from the German by James E. Lohr. New York: Springer-Verlag.

Discusses specular and diffuse reflection, and absorption and light scattering according to Rayleigh, Mie, and Kubelka and Munk.

Stearns, E. I.
1969 *The Practice of Absorption Spectrophotometry.* New York: John Wiley and Sons.

Presents many of the methods and techniques and practical applications of absorption spectrophotometry, particularly of solutions. It is highly worthwhile for its emphasis on the understanding of and logical approach to the analysis of multicomponent materials based on basic principles not requiring elegant computer facilities. Also steps the reader through the preparation of a computer program for color matching. Dyestuffs orientation.

Völz, H. G.
1995 *Industrial Color Testing: Theory and Methods.* English translation. Deerfield Beach, Fla.: VCH.

This is an excellent book on the relation of color to spectra; the theory of light scattering and absorption by pigments; and discussions of the Beer–Bouguer law, the Kubelka–Munk equation, Mie theory, and related measurement and test methods.

Appearance

Hunter, R. S., and R. W. Harold
1987 *The Measurement of Color and Appearance,* 2d ed. New York: John Wiley and Sons.

Colorant Formulation Calculations

Allen, E.
1980 Colorant formulations and shading. In *Optical Radiation Measurements,* ed. F. Grum and C. J. Bartleson, 2:289–336. New York: Academic Press.

An excellent summary and review.

Davidson, H. R., and H. Hemmendinger
1966 Color prediction using the two-constant turbid-media theory. *Journal of the Optical Society of America* 56:1102–9.

Kuehni, R. G.
1975 *Computer Colorant Formulation.* Lexington, Mass.: D. C. Heath and Co.

Oriented toward textiles but includes details for computing Kubelka–Munk two-constant-theory colorant formulations.

Methods and Techniques

American Society for Testing and Materials
ASTM Standards on Color and Appearance Measurements. West Conshohocken, Pa.: American Society for Testing and Materials.

Revised periodically. Contains eighty or more methods for measuring color and appearance attributes, as well as a list of similar length of auxiliary ASTM methods not included but published elsewhere.

Celikiz, G., and R. G. Kuehni, eds.
1983 *Color Technology in the Textile Industry.* Research Triangle Park, N.C.: American Association of Textile Chemists and Colorists.

A collection of articles of general interest, some original and some previously published. Prepared under the aegis of AATCC Committee RA36, Color Measurement Test Methods.

Sensation and Perception

Boynton, R. M.
1979 *Human Color Vision.* New York: Holt, Rinehart and Winston.

An excellent, comprehensive, but very readable text on human vision. The author states in the preface that he hopes it will be of value to nonspecialists, such as "artists, interior decorators, illuminating engineers, architects, graphic arts designers," and many others, as well as to students studying sensation and perception.

Evans, R. M.
1948 *An Introduction to Color.* New York: John Wiley and Sons.

Out of print but worth looking for. Beautifully illustrated camera techniques.

1971 The perception of color. In *Industrial Color Technology*, ed. R. F. Gould, Advances in Chemistry Series 107:43–68. Washington, D.C.: American Chemical Society.

Paper presented at a symposium, arranged by Ruth M. Johnston and Max Saltzman, during the 156th Annual Meeting of the American Chemical Society. It contains beautiful color illustrations, never published elsewhere, of perceptual color effects.

1974 *The Perception of Color*. New York: John Wiley and Sons.

General

Minnaert, M. G. J.

1993 *Light and Color in the Outdoors*. Translated and revised by Len Seymour. New York: Springer-Verlag.

This revision of Minnaert's original book contains 223 figures and 49 color plates in a hard copy that is a delight to read, look at, and enjoy.

O'Neill, M., and L. Weisgard

1961 *Hailstones and Halibut Bones*. Garden City, N.Y.: Doubleday and Co.

A charming book of poems about each color for children of all ages, beautifully illustrated in color by Weisgard.

Optical Society of America, Committee on Colorimetry

1953 *The Science of Color*. New York: Thomas Y. Crowell Co.

A classic still available from the Optical Society of America.

References

Aach, H.

1970 On the use and phenomena of fluorescent pigments in paintings. *Leonardo* 3:135–8.

1972 Fluorescent pigments in art and design. *Journal of Color and Appearance* 1(6):25–28.

Agoston, G. A.

1987 *Color Theory and Its Application in Art and Design*, 2d ed. Berlin: Springer.

Allen, E.

1970 An index of metamerism for observe differences. In *Color 69*, ed. Manfred Richter. Göttingen, Germany: Musterschmidt.

1973 Prediction of optical properties of paints from theory (with special reference to microvoid paints). *Journal of Paint Technology* 45(584):65–72.

American Society for Testing and Materials (ASTM)

ASTM Standard D 156

1994 Standard test method for Saybolt color of petroleum products (Saybolt chromometer method). In *Annual Book of ASTM Standards*. Philadelphia: American Society for Testing and Materials.

ASTM Standard D 523

1989 Standard test method for specular gloss. In *Annual Book of ASTM Standards*. Philadelphia: American Society for Testing and Materials.

ASTM Standard D 985

1993 Standard test method for brightness of pulp, paper, and paperboard (directional reflectance at 457 nm). In *Annual Book of ASTM Standards*. Philadelphia: American Society for Testing and Materials.

ASTM Standard D 1003

1997 Standard test method for haze and luminous transmittance of transparent plastics. In *Annual Book of ASTM Standards*. West Conshohocken, Pa.: American Society for Testing and Materials.

ASTM Standard D 1209

1997 Standard test method for color of clear liquids (platinum–cobalt scale). In *Annual Book of ASTM Standards*. West Conshohocken, Pa.: American Society for Testing and Materials.

ASTM Standard D 1494

1992 Standard test method for diffuse light transmission factor of reinforced plastics panels. In *Annual Book of ASTM Standards*. Philadelphia: American Society for Testing and Materials.

ASTM Standard D 1500
1996 Standard test method for ASTM color of petroleum products (ASTM color scale). In *Annual Book of ASTM Standards*. Philadelphia: American Society for Testing and Materials.

ASTM Standard D 1535
1996 Standard practice for specifying color by the Munsell system. In *Annual Book of ASTM Standards*. Philadelphia: American Society for Testing and Materials.

ASTM Standard D 1544
1998 Standard test method for color of transparent liquids (Gardner color scale). In *Annual Book of ASTM Standards*. West Conshohocken, Pa.: American Society for Testing and Materials.

ASTM Standard D 1746
1997 Standard test method for transparency of plastic sheeting. In *Annual Book of ASTM Standards*. West Conshohocken, Pa.: American Society for Testing and Materials.

ASTM Standard D 1925
(Discontinued in 1995.) Standard test method for yellowness index of plastics. In *Annual Book of ASTM Standards*. Philadelphia: American Society for Testing and Materials.

ASTM Standard D 2244
1993 Standard test method for calculation of color differences from instrumentally measured color coordinates. In *Annual Book of ASTM Standards*. Philadelphia: American Society for Testing and Materials.

ASTM Standard D 2805
1996 Standard test method for hiding power of paints by reflectometry. In *Annual Book of ASTM Standards*. Philadelphia: American Society for Testing and Materials.

ASTM Standard D 4838
1988 Standard test method for determining the relative tinting strength of chromatic paints. In *Annual Book of ASTM Standards*. Philadelphia: American Society for Testing and Materials.

ASTM Standard E 259
1993 Standard practice for preparation of pressed powder white reflectance factor transfer standards for hemispherical geometry. In *Annual Book of ASTM Standards*. Philadelphia: American Society for Testing and Materials.

ASTM Standard E 284
1997 Standard terminology of appearance. In *Annual Book of ASTM Standards*. West Conshohocken, Pa.: American Society for Testing and Materials.

ASTM Standard E 308
1996 Standard practice for computing the colors of objects by using the CIE system. In *Annual Book of ASTM Standards*. Philadelphia: American Society for Testing and Materials.

ASTM Standard E 313
1996 Standard practice for calculating yellowness and whiteness indices from instrumentally measured color coordinates. In *Annual Book of ASTM Standards*. Philadelphia: American Society for Testing and Materials.

ASTM Standard E 805

1994 Standard practice for identification of instrumental methods of color or color-difference measurement of materials. In *Annual Book of ASTM Standards*. Philadelphia: American Society for Testing and Materials.

ASTM Standard E 808

1998 Standard practice for describing retroreflection. In *Annual Book of ASTM Standards*. West Conshohocken, Pa.: American Society for Testing and Materials.

ASTM Standard E 809

1994 Standard practice for measuring photometric characteristics of retroreflectors. In *Annual Book of ASTM Standards*. Philadelphia: American Society for Testing and Materials.

ASTM Standard E 810

1994 Standard test method for coefficient of retroreflection of retroreflective sheeting. In *Annual Book of ASTM Standards*. Philadelphia: American Society for Testing and Materials.

ASTM Standard E 811

1995 Standard practice for measuring colorimetric characteristics of retroreflectors under nighttime conditions. In *Annual Book of ASTM Standards*. Philadelphia: American Society for Testing and Materials.

ASTM Standard E 911

1997 Standard practice for color measurement of fluorescent specimens. In *Annual Book of ASTM Standards*. West Conshohocken, Pa.: American Society for Testing and Materials.

ASTM Standard E 1164

1994 Standard practice for obtaining spectrophotometric data for object-color evaluation. In *Annual Book of ASTM Standards*. Philadelphia: American Society for Testing and Materials.

ASTM Standard E 1247

1992 Standard test method for identifying fluorescence in object-color specimens by spectrophotometry. In *Annual Book of ASTM Standards*. Philadelphia: American Society for Testing and Materials.

ASTM Standard E 1331

1996 Standard test method for reflectance factor and color by spectrophotometry using hemispherical geometry. In *Annual Book of ASTM Standards*. Philadelphia: American Society for Testing and Materials.

ASTM Standard E 1336

1996 Standard test method for obtaining colorimetric data from a video display unit by spectroradiometry. In *Annual Book of ASTM Standards*. Philadelphia: American Society for Testing and Materials.

ASTM Standard E 1341

1996 Standard practice for obtaining spectroradiometric data from radiant sources for colorimetry. In *Annual Book of ASTM Standards*. Philadelphia: American Society for Testing and Materials.

ASTM Standard E 1345

1992 Standard practice for reducing the effect of variability of color measurement by use of multiple measurements. In *Annual Book of ASTM Standards*. Philadelphia: American Society for Testing and Materials.

ASTM Standard E 1348

1990 Standard test method for transmittance and color by spectrophotometry using hemispherical geometry. In *Annual Book of ASTM Standards.* West Conshohocken, Pa.: American Society for Testing and Materials.

ASTM Standard E 1349

(Discontinued in 1997.) Standard test method for reflectance factor and color by spectrophotometry using bidirectional geometry. In *Annual Book of ASTM Standards.* West Conshohocken, Pa.: American Society for Testing and Materials.

ASTM Standard E 1360

1990 Standard practice for specifying color by using the Optical Society of America uniform color scales system. In *Annual Book of ASTM Standards.* Philadelphia: American Society for Testing and Materials.

ASTM Standard E 1541

1994 Standard practice for specifying and matching color using the Colorcurve system. In *Annual Book of ASTM Standards.* Philadelphia: American Society for Testing and Materials.

ASTM Special Technical Publication 478

1970 *Appearance of Metallic Surfaces.* Philadelphia: American Society for Testing and Materials. (Out of print. Authorized facsimile available from University Microfilms International, 300 N. Zeeb Road, Ann Arbor, MI 48106.)

Andrews, C. L.

1960 *Optics of the Electromagnetic Spectrum.* Englewood Cliffs, N.J.: Prentice Hall.

Armstrong, W. G., and W. D. Ross

1966 Anomalous reflectance from films pigmented with titanium dioxide. *Journal of Paint Technology* 38(499):462–68.

Atkins, J. T., and F. W. Billmeyer Jr.

1966 Edge-loss errors in reflectance and transmittance measurement of translucent materials. *Materials Research and Standards* 6:564–70.

1968 On the interaction of light with matter. *Color Engineering* 6(3):40.

Baer, N. S., A. Joel, R. L. Feller, and N. Indictor

1986 Indian Yellow. In *Artists' Pigments: A Handbook of Their History and Characteristics,* vol. 1, ed. R. L. Feller, 17–36. Washington, D.C.: National Gallery of Art.

Bartleson, C. J.

1974 Gloss measurements. *Report to CIE Technical Committee 2.3.* Vienna: CIE Central Bureau.

Beer, A.

1852 Bestimmung der Absorption des rothen Lichts in farbigen Flüssizkeiten (Determination of the absorption of red lights in colored liquids). *Annalen der physikalische Chemie* 86(2):78–88.

Berger-Schunn, A.

1994 *Practical Color Measurement.* New York: John Wiley and Sons.

Berndt, H.

1989 A reexamination of paper yellowing and the Kubelka-Munk theory. In *Historic Textile and Paper Materials*, ed. S. H. Zeronian and H. L. Needles, vol. 2, 81–91. ACS Symposium Series 410. Washington, D.C.: American Chemical Society.

Billmeyer, F. W., Jr., and D. H. Alman

1973 Exact calculation of Fresnel reflection coefficients for diffuse light. *Journal of Color and Appearance* 2(1):36–38.

Billmeyer, F. W., Jr., and D. G. Phillips

1974 Predicting reflectance and color of paint films by Kubelka-Munk analysis. III. Effect of concentration errors on color for mixtures of one chromatic pigment with white. *Journal of Paint Technology* 46(592):36–39.

Billmeyer, F. W., Jr., and M. Saltzman

1981 *Principles of Color Technology*, 2d ed. New York: John Wiley and Sons. (The third edition of this work appeared in 2000 under the title *Billmeyer and Saltzman's Principles of Color Technology*, by Roy S. Berns [New York: Wiley and Sons]).

Bouguer, P.

1729 *Essai d'optique sur la gradation de la lumière* (Essay on the optics of gradation of light). Paris: Claude Tombert.

Braun, J. H.

1991 Gloss of paint films and the mechanism of pigment involvement. *Journal of Coatings Technology* 63(799):43–51.

Brockes, A.

1960 The influence of glossy surfaces on remission measurements. *Farbe* 9(13):53–62.

1964 Der Zusammenhang von Farbstärke und Teilchengrosse von Buntpigmenten nach der Mie-theorie (The dependence of color strength and particle size of colored pigments according to the Mie theory). *Optik* 21(10):550–56.

1969 Vergleich der Metamerie-Indizes bei Lichtartwechsel von Tageslicht zur Glühlampe und zu verschiedenen Leuchstofflampen (Comparison of metameric indices with the change in the kind of light from daylight to incandescent and to various fluorescent lamps). *Farbe* 18:233–39.

1970 Vergleich von berechneten Metamerie-Indizes mit Abmusterungsergebissen (Comparison of calculated metameric indices with the results of the [visual] evaluations of samples). *Farbe* 19:135–44.

Brown, W. R. J., and D. L. MacAdam

1957 Color discriminations of twelve observers. *Journal of the Optical Society of America* 47:137–43.

Buc, G. L., R. H. Kienle, L. A. Melsheimer, and E. I. Stearns

1947 Phenomenon of bronzing and surface coatings. *Industrial and Engineering Chemistry* 39:147–54.

Burnham, R. W., R. M. Hanes, and C. J. Bartleson

1963 *Color: A Guide to Basic Facts and Concepts*. New York: John Wiley and Sons.

Burrell, H.

1971 Hiding without pigments. *Journal of Paint Technology* 43(559):48–53.

Buttignol, V.

1968 Optical behavior of iron oxide pigments. *Journal of Paint Technology* 40(526):480–93.

Byler, W. H.

1973 Luminescent pigments, inorganic. In *Pigment Handbook,* ed. T. C. Patton, vol. 1, 905–23. New York: John Wiley and Sons.

Carr, W.

1973 Pigment powders and dispersions. In *Pigment Handbook,* ed. T. C. Patton, vol. 3, 11–27. New York: John Wiley and Sons.

Celikiz, G., and R. G. Kuehni, eds.

1983 *Color Technology in the Textile Industry.* Research Triangle Park, N.C.: American Association of Textile Chemists and Colorists.

Chase, T.

1982 Poster Session, Washington Congress, International Institute for Conservation of Historic and Artistic Works, September 3–9.

Chickering, K. D.

1967 Optimization of the MacAdam modified 1965 Friele color difference formula. *Journal of the Optical Society of America* 57:537–41.

1971 FMC color-difference formulas: Clarification concerning usage. *Journal of the Optical Society of America* 61:118–22.

Commission Internationale de l'Éclairage (CIE)

1972 Special metamerism index: Change of illuminant. Supplement 1 to *Colorimetry,* CIE publication 15. Vienna: CIE Central Bureau.

1977 *Radiometric and Photometric Characteristics of Materials and Their Measurement.* CIE publication 38. Vienna: CIE Central Bureau.

1982 *Retroreflection: Definition and Measurement.* CIE publication 54. Vienna: CIE Central Bureau.

1984 *The Spectroradiometric Measurement of Light Sources.* CIE Publication 63. Vienna: CIE Central Bureau.

1986 *Colorimetry,* 2d ed. Official Recommendations of the International Commission of Illumination. CIE publication 15.2. Vienna: CIE Central Bureau.

1987 *International Lighting Vocabulary,* 4th ed. CIE publication 17.4. Vienna: CIE Central Bureau.

1995 *Method of Measuring and Specifying Colour Rendering Properties of Light Sources,* 3d ed. CIE publication 13.3. Vienna: CIE Central Bureau.

Cornman, M.

1986 Cobalt yellow (Aureolin). In *Artists' Pigments: A Handbook of Their History and Characteristics,* vol. 1, ed. R. L. Feller, 37–46. Washington, D.C.: National Gallery of Art.

Craker, W. E., and F. D. Robinson

1967 The effect of pigment volume concentration and film thickness on the optical properties of surface coatings. *Journal of the Oil and Colour Chemists Association* 50:111–33.

Davidson, H. R.

1978 Preparation of the OSA uniform color scales committee samples. *Journal of the Optical Society of America* 68:1141–42.

Davidson, H. R., and H. Hemmendinger
1966 Color prediction using the two-constant turbid-media theory. *Journal of the Optical Society of America* 56:1102–9.

Davidson, H. R., H. Hemmendinger, and J. R. R. Landry
1963 A system of instrumental colour control for the textile industry. *Journal of the Society of Dyers and Colourists* 79:577–89.

de la Rie, E. R.
1982 Fluorescence of paint and varnish layers, parts 1, 2, and 3. *Studies in Conservation* 27:1–7; 65–79; 102–8.

Derby, R. E., Jr.
1952 Applied spectrophotometry. I. Color matching with the aid of the 'R' Cam. *American Dyestuff Reporter* 41:550–57.

DeVore, J. R., and A. H. Pfund
1947 Optical scattering by dielectric powders of uniform particle size. *Journal of the Optical Society of America* 37:826–32.

DiBernardo, A., and P. Resnick
1959 Anomalous behavior of copper phthalocyanine–benzidine yellow mixtures. *Journal of the Optical Society of America* 49:480.

Duncan, D. R.
1962 The identification and estimation of pigments in pigmented compositions by reflectance spectrophotometry. *Journal of the Oil and Colour Chemists Association* 45:300–324.

Dunn, E. J.
1973 White hiding lead pigments. In *Pigment Handbook,* ed. T. C. Patton, vol. 1, 65–84. New York: John Wiley and Sons.

Erhardt, D., and J. S. Tsang
1990 The extractable components of oil paint films. In *Cleaning, Retouching, and Coatings: Preprints of the Contributions to the Brussels Congress,* ed. J. S. Mills and P. Smith, 93–97. London: International Institute for Conservation of Historic and Artistic Works.

Evans, R. M.
1948 *An Introduction to Color.* New York: John Wiley and Sons.

1959 *Eye, Film, and Camera in Color Photography.* New York: John Wiley and Sons.

1971 The perception of color. In *Industrial Color Technology,* ed. R. F. Gould, 43–68. Advances in Chemistry Series 107. Washington, D.C.: American Chemical Society.

1974 *The Perception of Color.* New York: John Wiley and Sons.

Federation of Societies for Coatings Technology (FSCT)
1991 *Infrared Spectroscopy Atlas for the Coatings Industry,* 4th ed. Blue Bell, Pa.: Federation of Societies for Coatings Technology.

1995 *Coatings Encyclopedic Dictionary,* ed. Stanley LeSota. Blue Bell, Pa.: Federation of Societies for Coatings Technology.

Feller, R. L.
1967 Studies on the darkening of vermilion by light. In *Report and Studies on the History of Art,* 99–111. Washington, D.C.: National Gallery of Art.

1968 Problems in reflectance spectrophotometry. In *IIC-1967 London Conference on Museum Climatology,* 257–69. London: International Institute for Conservation of Historic and Artistic Works.

Feller, R. L., ed.
1986 *Artists' Pigments: A Handbook of Their History and Characteristics,* vol. 1. Washington, D.C.: National Gallery of Art (softcover); Cambridge: Cambridge University Press (hardcover).

Feller, R. L., M. Curran, and C. W. Bailie
1984 Identification of traditional organic colorants employed in Japanese prints and determination of their rates of fading. In *Japanese Woodblock Prints: A Catalogue of the Mary A. Ainsworth Collection.* Oberlin, Ohio: Allen Memorial Art Museum.

Feller, R. L., and R. M. Johnston-Feller
1997 Vandyke Brown, Cologne and Kassel earth. In *Artists' Pigments, A Handbook of Their History and Characteristics,* vol. 3., ed. Elisabeth West FitzHugh. Washington, D.C.: National Gallery of Art.

Feynman, R. P.
1985 *QED, the Strange Theory of Light and Matter.* Princeton, N.J.: Princeton University Press.

Fiedler, I., and M. Bayard
1986 Cadmium yellows, oranges, and reds. In *Artists' Pigments: A Handbook of Their History and Characteristics,* vol. 1, ed. R. L. Feller, 65–108. Washington, D.C.: National Gallery of Art.

Fraser, I.
1973 Centrifugal sedimentation. In *Pigment Handbook,* ed. T. C. Patton, vol. 3, 53–62. New York: John Wiley and Sons.

Fuller, C. W.
1973 Colored iron oxide pigments, synthetic. In *Pigment Handbook,* ed. T. C. Patton, vol. 1, 333–49. New York: John Wiley and Sons.

Fuller, N. A.
1985 Analysis of thin-layer chromatograms of paint pigments and dyes by direct microspectrophotometry. *Forensic Science International* 27:189–204.

Garland, C. E.
1983 A general procedure for determination of relative dye strength by spectrophotometric measurement of reflectance factor. In *Color Technology in the Textile Industry,* ed. G. Celikiz and R. G. Kuehni, 107–12. Triangle Park, N.C.: American Association of Textile Chemists and Colorists.

Garrett, M. D.
1973 Carbon black, bone black, lamp black. In *Pigment Handbook,* ed. T. C. Patton, vol. 1, 709–43. New York: John Wiley and Sons.

Gerstner, W.
1966 Crystal form and particle size of organic pigments in printing inks and paints. *Journal of the Oil and Colour Chemists Association* 49(11):954. Also reprinted by Badische Anilin+Soda-Fabrik AG, Ludwigshafen am Rhein, Germany.

Gettens, R. J., R. L. Feller, and W. T. Chase
1993 Vermilion and cinnabar. In *Artists' Pigments: A Handbook of Their History and Characteristics,* vol. 2, ed. A. Roy, 159–82. New York: Oxford University Press.

Gettens, R. J., and E. W. FitzHugh

1993a Azurite and blue verditer. In *Artists' Pigments: A Handbook of Their History and Characteristics,* vol. 2, ed. A. Roy, 23–36. New York: Oxford University Press.

1993b Malachite and green verditer. In *Artists' Pigments: A Handbook of Their History and Characteristics,* vol. 2, ed. A. Roy, 183–202. New York: Oxford University Press.

Gettens, R. J., and G. L. Stout

1942 *Painting Materials. A Short Encyclopedia.* New York: D. Van Nostrand Co. (Reprint, New York: Dover, 1966.)

Giovanelli, R. G.

1956 A note on the reflection of internally incident diffuse light. *Optica Acta* 3:127.

Granville, W. C.

1994 The color harmony manual, a color atlas based on the Ostwald system. *Color Research and Application* 19:77–98.

Greenstein, L. M.

1973a Nacreous (pearlescent) pigments. In *Pigment Handbook,* ed. T. C. Patton, vol. 1, 871–90. New York: John Wiley and Sons.

1973b Pearlescence: The optical behavior of nacreous and interference pigments. In *Pigment Handbook,* ed. T. C. Patton, vol. 3, 357–90. New York: John Wiley and Sons.

1988 Nacreous (pearlescent pigments) and interference pigments. *Mearl Technical Bulletin Number* 2. New York: Mearl Corp. (This is a corrected version of the chapter in the 2d ed. of *Pigment Handbook,* ed. T. C. Patton, vol. 1 [New York: John Wiley and Sons].)

Grissom, C. A.

1986 Green Earth. In *Artists' Pigments: A Handbook of Their History and Characteristics,* vol. 1, ed. R. L. Feller, 141–68. Washington, D.C.: National Gallery of Art.

Grum, F.

1980 Colorimetry of fluorescent materials. In *Optical Radiation Measurement.* Vol. 2, *Color Measurement,* ed. F. Grum and C. J. Bartleson, 241–88. New York: Academic Press.

Hansen, E. F., R. Lowinger, and E. Sadoff

1993 Consolidation of porous paint in a vapor-saturated atmosphere: A technique for minimizing changes in the appearance of powdering matte paint. *Journal of the American Institute for Conservation* 32(1):1–14.

Hansen, E. F., S. Walston, and M. H. Bishop, eds.

1993 Matte paint. Bibliographic supplement to *Art and Archeology Technical Abstracts* 30.

Hård, A., and L. Sivik

1981 NCS—natural color system: A Swedish standard for color notation. *Color Research and Application* 6:129–38.

Hardy, A. C.

1936 *Handbook of Colorimetry.* Cambridge, Mass.: Technology Press (Massachusetts Institute of Technology).

Hay, G. N.
1973 Stainless steel flake pigment. In *Pigment Handbook,* ed. T. C. Patton, vol. 1, 833–35. New York: John Wiley and Sons.

Hemmendinger, H.
1983 The calibration of a spectrophotometer for color measurement. In *Color Technology in the Textile Industry,* ed. G. Celikiz and R. G. Kuehni, 35–48. Research Triangle Park, N.C.: American Association of Textile Chemists and Colorists.

Hemmendinger, H., and R. M. Johnston
1970 A goniospectrophotometer for color measurements. In *Proceedings, AIC Color 69,* ed. M. Richter, vol. 1, 509. Göttingen, Germany: Musterschmidt.

Hislop, R. W., and P. L. McGinley
1978 Microvoid coatings: Pigmented, vesiculated beads in flat latex paints. *Journal of Coatings Technology* 50(642):69–77.

Huebner, F. E., and H. N. Monck
1992 Measurement of color in resins and adhesive systems. *Tappi Journal* 75(9):197–204.

Hunter, R. S.
1938 Methods of determining gloss. *Journal of Research, National Bureau of Standards* 18:19.

1942 Photoelectric tristimulus colorimetry with three filters. *National Bureau of Standards Circular C429,* July 30. Washington, D.C.: U.S. Government Printing Office. Reprinted in *Journal of the Optical Society of America* 32:509–38.

1958 Photoelectric color difference meter. *Journal of the Optical Society of America* 48:985–95.

Hunter, R. S., and D. B. Judd
1939 Development of a method of classifying paints according to gloss. *American Society for Testing and Materials Bulletin* 97:11–18.

Illuminating Engineering Society (IES)
1983 *Guide to Spectroradiometric Measurements.* New York: Illuminating Engineering Society (American National Standards Institute).

International Electrochemical Commission (IEC)
1974 *Photometric and Colorimetric Methods of Measurement of the Light Emitted by a Cathode-Ray Tube Screen.* Geneva: International Electrochemical Commission.

Jacobsen, A. E.
1948 Non-adaptability of the ICI system to some near-whites which show absorption in the far-blue region of the spectrum. *Journal of the Optical Society of America* 38:442.

Jacobson, E.
1948 *Basic Color: An Interpretation of the Ostwald Color System.* Chicago: Paul Theobald.

Johnston, R. M.
1963 Pitfalls in color specifications. *Official Digest, Federation of Societies for Paint Technology* 35:259–74.

1967a Geometric metamerism. *Color Engineering* 5(3):42–47, 54.

1967b Spectrophotometry for the analysis and description of color. *Journal of Paint Technology* 39(509):346–54.

1969 Color control in the small paint plant. *Journal of Paint Technology* 41(534):415–21.

1971a Color measuring instruments: A guide to their selection (a report of Inter-Society Color Council). *Journal of Color and Appearance* 1(2):27–30. Reprinted in 1983 with additional prefatory remarks in *Color Technology in the Textile Industry*, ed. G. Celikiz and R. G. Kuehni, 21–33. Research Triangle Park, N.C.: American Association of Textile Chemists and Colorists.

1971b Colorimetry of transparent materials. *Journal of Paint Technology* 43(553):42–50.

1973 Color theory. In *Pigment Handbook*, ed. T. C. Patton, vol. 3, 229–88. New York: John Wiley and Sons.

Johnston, R. M., and R. L. Feller

1963 The use of differential spectral curve analysis in the study of museum objects. *Dyestuffs* 44(9):1–10.

1967 Optics of paint films: Glazes and chalking. In *Application of Science in Examination of Works of Art*, 86–95. Boston: Museum of Fine Arts.

Johnston, R. M., and R. Stanziola

1969 *Angular Color Measurement on Automotive Materials*. Preprint no. 690241. Detroit: International Automotive Engineering Conference.

Johnston-Feller, R. M.

1986 Reflections on the phenomenon of fading. *Journal of Coatings Technology* 58(736):32–50.

Johnston-Feller, R. M., and C. W. Bailie

1982a An analysis of the optics of paint glazes: Fading. In *Science and Technology in the Service of Conservation*, 180–85. Preprints of contributions to the Washington Congress. London: International Institute for Conservation of Historic and Artistic Works.

1982b Determination of the tinting strength of chromatic pigments. *Journal of Coatings Technology* 54(692):43–56.

Johnston-Feller, R. M., R. L. Feller, C. W. Bailie, and M. Curran

1984 The kinetics of fading: Opaque paint films pigmented with alizarin lake and titanium dioxide. *Journal of the American Institute for Conservation* 23:114–29.

Johnston-Feller, R. M., and D. Osmer

1977 Exposure evaluation: Quantification of changes in appearance of pigmented materials. *Journal of Coatings Technology* 49(625):25–36.

1979 Exposure evaluation, part 2—Bronzing. *Journal of Coatings Technology* 51(650):37–44.

Jordan, R. D., and M. A. O'Neill

1991 The whiteness of paper. Colorimetry and visual ranking. *Tappi Journal* 74(5):93–101.

Judd, D. B.

1937 Optical specification of light-scattering materials. *Journal of Research, National Bureau of Standards* 19:287–317.

1939 Specification of color tolerances at the National Bureau of Standards. *American Journal of Psychology* 52:418–28.

1942 Fresnel reflection of diffusely incident light. *Journal of Research, National Bureau of Standards* 29:329–32.

1950 *Colorimetry*. National Bureau of Standards Circular 478. Washington, D.C.: U.S. Government Printing Office.

Judd, D. B., and G. Wyszecki

1963 *Color in Business, Science, and Industry*, 2d ed. New York: John Wiley and Sons.

1975 *Color in Business, Science, and Industry*, 3d ed. New York: John Wiley and Sons.

Kampfer, W. A.

1973 Titanium dioxide. In *Pigment Handbook*, ed. T. C. Patton, vol. 1, 1–36. New York: John Wiley and Sons.

Kelly, K. L., and D. B. Judd

1955 *The ISCC–NBS Method of Designating Colors and a Dictionary of Color Names*. National Bureau of Standards Circular 553. Washington, D.C.: U.S. Government Printing Office (out of print).

1976 *Color: Universal Language and Dictionary of Names*. National Bureau of Standards Special Publication 440. Washington, D.C.: U. S. Government Printing Office. (Available as a photocopy in black and white from the National Technical Information Service, Springfield, VA 22161. Order number PB265225.)

Kerker, M., and D. D. Cooke

1976 Pigmented microvoid coatings II. Luminance and color of the concentric sphere model. *Journal of Coatings Technology* 48(621):35–41.

Kerker, M., D. D. Cooke, and W. D. Ross

1975 Pigmented microvoid coatings. Theoretical study of three models. *Journal of Paint Technology* 47(603):33–42.

Kettler, W.

1995a Color measuring instruments. Part 1: Portable systems. *European Coatings Journal* 1 and 2:210–12, 214, 216.

1995b Color measuring instruments. Part 2: Stationary systems. *European Coatings Journal* 3:59–62.

Kortüm, G.

1969 *Reflectance Spectroscopy: Principles, Methods, Applications*. Translated from German by James E. Lohr. New York: Springer-Verlag.

Kremer Pigments, Inc.

1992 61 East 3d Street, New York, NY 10003. Supplier of artists' pigments, paints, and vehicles; a branch of Dr. George F. Kremer, Farbmühle, D-W-7974 Aichsteiten, Germany.

Kubelka, P.

1948 New contributions to the optics of intensely light scattering materials, part 1. *Journal of the Optical Society of America* 38:448–57, 1067.

1954 New contributions to the optics of intensely light scattering materials, part II. Non-homogeneous layers. *Journal of the Optical Society of America* 44:330–35.

Kubelka, P., and F. Munk
1931 Ein Beitrag zur Optik der Farbanstriche. *Zeitschrift für technische Physik* 12:593–601.

Kuehni, R.
1975 *Computer Colorant Formulation.* Lexington, Mass.: D.C. Heath and Company.

1983 A general procedure for the determination of relative dye strength by spectrophotometric transmittance measurement. In *Color Technology in the Textile Industry,* ed. G. Celikiz and R. G. Kuehni, 77–89. Research Triangle Park, N.C.: American Association of Textile Chemists and Colorists.

Kühn, H.
1993a Lead-tin yellow. In *Artists' Pigments: A Handbook of Their History and Characteristics,* vol. 2, ed. A. Roy, 83–112. New York: Oxford University Press.

1993b Verdigris and copper resinate. In *Artists' Pigments: A Handbook of Their History and Characteristics,* vol. 2, ed. A. Roy, 131–58. New York: Oxford University Press.

Kumar, R.
1981 Analysis for organic pigments using solution spectrophotometry. Ph.D. diss., Rensselaer Polytechnic Institute.

LaFontaine, R. H.
1986 Seeing through a yellow varnish: A compensating illumination system. *Studies in Conservation* 31:97–102.

Lambert, J. H.
1760 *Photometria sine de Mensura et Gradibus Luminis Colorum et Umbrae* (Photometry concerning the measurement and gradation of colored light and shadows). Augsburg, Germany: Eberhard Klett.

LaMer, V. K., J. Q. Umberger, F. Sinclair, and F. E. Buchwalter
1945 OSRD Report 4904, PB32208. U. S. Department of Commerce, Office of Scientific Research and Development.

Laurie, A. P.
1926 *The Painter's Methods and Materials.* London: Seeley Service.

Lettieri, T. R., E. Marx, J.-F. Son, and T. V. Borburger
1991 Light scattering from glossy coatings on paper. *Applied Optics* 30:4439–47.

Levison, H. W.
1976 *Artists' Pigments: Lightfastness Tests and Ratings.* Hallandale, Fla.: Colorlab.

Love, C. H.
1973 Colored iron oxide pigments, natural. In *Pigment Handbook,* ed. T. C. Patton, vol. 1, 323–32. New York: John Wiley and Sons.

MacAdam, D. L.
1942 Visual sensitivities to color differences in daylight. *Journal of the Optical Society of America* 32:247–74.

1943 Specification of small chromaticity differences. *Journal of the Optical Society of America* 33:18–26.

1974 Uniform color scales. *Journal of the Optical Society of America* 64:1619–1702.

1978 Colorimetric data for samples of OSA uniform color scales. *Journal of the Optical Society of America* 68:121–30.

McCarley, J. E., C. E. Green, and K. H. Horowitz

1965 Digital system for converting spectrophotometric data to CIE coordinates, dominant wavelength, and excitation purity. *Journal of the Optical Society of America* 55:355–60.

McCrone, W. C.

1973a Size, shape, and size distribution of pigments. In *Pigment Handbook*, ed. T. C. Patton, vol. 3, 63–69. New York: John Wiley and Sons.

1973b Pigment identification, microscopy. In *Pigment Handbook*, ed. T. C. Patton, vol. 3, 71–76. New York: John Wiley and Sons.

McDonald, R.

1980 Industrial pass-fail colour matching. Part I—Preparation of visual colour-matching data; Part II—Methods of fitting tolerance ellipsoids; Part III—Development of pass-fail formula for use with instrumental measurement of colour difference. *Journal of the Society of Dyers and Colourists* 96:372–76; 418–33; 486–95.

McLaren, K.

1986 *The Colour Science of Dyes and Pigments*, 2d ed. Bristol, Eng.: Adam Hilger.

Maerz, A., and M. R. Paul

1930 *Dictionary of Color*. New York: McGraw-Hill Book Co.

Maxwell, J. C.

1860 On the theory of compound colours and the relations of the colours of the spectrum. *Proceedings of the Royal Society of London* 10:404–9, 484.

Michalski, S.

1990 A physical model of the cleaning of oil paint. In *Cleaning, Retouching, and Coatings: Preprints of the Contributions to the Brussels Congress*, ed. J. S. Mills and P. Smith. London: International Institute for Conservation of Historic and Artistic Works.

Mie, G.

1908 Beiträge zur Optik trüber Medien, speziell kolloidalen Metallösungen (Contributions to the optics of turbid media, especially colloidal metal solutions). *Annalen der Physik* 25:377–445. (A brief presentation in English was made by J. A. Stratton and H. D. Houghton, 1931, Theoretical investigation of light through fog. *Physical Review* 38:159–65.)

Mitton, P. B.

1973 Opacity, hiding power, and tinting strength. In *Pigment Handbook*, ed. T. C. Patton, vol. 3, 289–329. New York: John Wiley and Sons.

Mudgett, P. S., and L. W. Richards

1973 Kubelka-Munk scattering and absorption coefficients for use with glossy opaque objects. *Journal of Paint Technology* 45(586):43–53.

Mühlethaler, B., and J. Thissen

1993 Smalt. In *Artists' Pigments: A Handbook of Their History and Characteristics*, vol. 2, ed. A. Roy, 113–30. New York: Oxford University Press.

Munsell, A. H.

1905 *A Color Notation*. Boston: Ellis.

Munsell Book of Color
Available only from GretagMacbeth, Inc., Munsell Color Dept., 617 Little Britain Road, New Windsor, NY 12553-6148.

Nassau, K.
1983 *The Physics and Chemistry of Color*. New York: John Wiley and Sons.

National Bureau of Standards
1968–71 Fundamental principles of absolute radiometry and the philosophy of the NBS program. In *National Bureau of Standards Technical Note 594-1*. Washington, D.C.: U.S. Government Printing Office.

Newhall, S. M., D. Nickerson, and D. B. Judd
1943 Final report of the O.S.A. subcommittee on the spacing of the Munsell colors. *Journal of the Optical Society of America* 33:385–418.

Nickerson, D.
1940 History of the Munsell color system and its scientific application. *Journal of the Optical Society of America* 30:575–80. Reprinted 1976 in *Color Research and Application* 1:69–77.

1975 Uniform color scales: Munsell conversion of OSA committee selection. *Journal of the Optical Society of America* 65:205–7.

1977 History of the OSA committee on uniform color scales. *Optics News* 3(1):8–17.

1978 Munsell renotations for samples of OSA uniform color scales. *Journal of the Optical Society of America* 68:1343–47.

1981 OSA uniform color scales samples—a unique set. *Color Research and Application* 6:7–33.

Nimeroff, I.
1957 Propagation of errors in tristimulus colorimetry. *Journal of the Optical Society of America* 47:697–702.

1966 Comparison of uncertainty ellipses calculated from two spectrophotometric colorimetry methods by an automatic-computer program. *Journal of the Optical Society of America* 56:230–37.

Nimeroff, I., and J. A. Yurow
1965 Degree of metamerism. *Journal of the Optical Society of America* 55:185–90.

Novak, C. L., and S. A. Shafer
1992 Color vision. In *The Encyclopedia of Artificial Intelligence,* 192–202. New York: John Wiley and Sons.

Ogilvy, J. A.
1991 *Theory of Wave Scattering from Random Rough Surfaces*. Bristol, Eng.: Adam Hilger.

Orchard, S. E.
1968 A new look at pigment optics. *Journal of the Oil and Colour Chemists Association* 51:44–60.

Orr, C., Jr.
1973 Characterization of pigments: Gravity sedimentation techniques. In *Pigment Handbook,* ed. T. C. Patton, vol. 3, 43–51. New York: John Wiley and Sons.

Osmer, D.

1978 The opacity parameter in color matching. *Plastics Engineering* 34:33.

1982 Practical application of Kubelka–Munk theory for the near infrared. *Journal of Coatings Technology* 54(692):35–41.

Ostwald, W.

1931 *Colour Science*. Authorized translation with an introduction by J. Scott Taylor. Part I: Colour theory and colour standardization. Part II: Applied colour science (1933). London: Winsor and Newton Ltd.

1969 *The Colour Primer*. Translated and edited, and with a foreword and evaluation by Faber Birren. New York: Van Nostrand-Rheinhold.

Patton, T. C., ed.

1973 *Pigment Handbook*, vols. 1–3. New York: John Wiley and Sons.

Phillips, D. G., and F. W. Billmeyer Jr.

1976 Predicting reflectance and color of paint films by Kubelka–Munk analysis. IV. Kubelka–Munk scattering coefficient. *Journal of Coatings Technology* 48(616):30–36.

Pierce, P. E., and R. T. Marcus

1994 *Color and Appearance*. Blue Bell, Pa.: Federation of Societies for Coatings Technology.

Plesters, J.

1993 Ultramarine blue, natural and artificial. In *Artists' Pigments: A Handbook of Their History and Characteristics*, vol. 2, ed. A. Roy, 37–54. New York: Oxford University Press.

Raggi, A., and G. Barbiroli

1993 Colour difference measurement: The sensitivity of various instruments compared. *Color Research and Application* 18:11–27.

Rheinboldt, W. C., and J. P. Menard

1960 Mechanized conversion of colorimetric data to Munsell renotation. *Journal of the Optical Society of America* 50:802–7.

Richards, L. W.

1970 The calculation of the optical performance of paint films. *Journal of Paint Technology* 42:276–86.

Richter, M.

1953 Das System der DIN-Farbenkarte. *Farbe* 1:85–98.

1955 The official German standard color chart. *Journal of the Optical Society of America* 45:223–26.

Ridgway, R.

1912 *Color Standards and Color Nomenclature*. Washington, D.C.: Published by author.

Rogers, P. E., F. S. Greenawald, and W. L. Butters

1973 Copper and copper alloy flake powders. In *Pigment Handbook*, ed. T. C. Patton, vol. 1, 807–17. New York: John Wiley and Sons.

Rolles, R.

1973 Aluminum flake pigment. In *Pigment Handbook*, ed. T. C. Patton, vol. 1, 785–806. New York: John Wiley and Sons.

Rosenthal, W. S., and B. N. McBane
1973 Microvoids as light scattering sites in polymer coatings. *Journal of Paint Technology* 45(584):73–80.

Ross, W. D.
1967 Kubelka–Munk formulas adapted for better computation. *Journal of Paint Technology* 39:515–21.

Saltzman, M.
1986 Analysis of dyes in museum textiles. In *Textile Conservation Symposium in Honor of Pat Reeves*, ed. C. C. McLean and P. Connell, 27–39. Los Angeles: Los Angeles County Museum of Art (Conservation Center).

Saltzman, M., and A. M. Keay
1967 Colorant identification. *Journal of Paint Technology* 39(509):360–67.

Saunders, D.
1988 Color change measurement by digital image processing. *National Gallery Technical Bulletin* (London) 12:66–77.

Saunders, D., and J. Cupitt
1993 Image processing at the National Gallery: The VASAR project. *National Gallery Technical Bulletin* (London) 14:72–85.

Saunderson, J. L.
1942 Calculation of the color of pigmented plastics. *Journal of the Optical Society of America* 32:727–36.

Schäfer, H., and G. Wallisch
1981 Obtaining opacity with organic pigments in paint. *Journal of the Oil and Colour Chemists Association* 64:405–14.

Schweppe, H., and H. Roosen-Runge
1986 Carmine. In *Artists' Pigments: A Handbook of Their History and Characteristics*, vol. 1, ed. R. L. Feller, 255–84. Washington, D.C.: National Gallery of Art.

Seiner, J. A.
1970 *Opaque Films*. British Patent 1,178,612. Assigned to PPG Industries, Inc.

Sève, R.
1993 Problems connected with the concept of gloss. *Color Research and Application* 18:240–52.

Shurcliff, W. A.
1942 Curve shape index for identification by means of spectrophotometric curves. *Journal of the Optical Society of America* 32:160–63.

Simon, H.
1971 *The Splendor of Iridescence*. New York: Dodd, Mead and Co.

Smith, D.
1962 Bronze phenomena in pigments and dyes. In *RBH Trends, Interchemical Corporation*, part 1.

1963 Bronze phenomena in pigments and dyes. In *RBH Trends, Interchemical Corporation*, part 2.

1992 *The Catalog of Artists' Materials*. Seattle: Daniel Smith.

Spindel, S.
1973 Coatings for copper. *Paint and Varnish Production* 63(2):21–27.

Staniforth, S.

1985 Retouching and colour matching: The restorer and metamerism. *Studies in Conservation* 30:101–11.

Stanziola, R.

1980 Color differences caused by dye weighing errors. *Color Research and Application* 5:129–32.

1992 The Colorcurve system. *Color Research and Application* 17:262–72.

Stearns, E. I.

1969 *The Practice of Absorption Spectrophotometry*. New York: John Wiley and Sons.

Stenius, A. S.

1951 The application of the Kubelka–Munk theory to the diffuse reflection of light from paper, parts 1 and 2. *Svensk Papperstidning* 54:663–70; 701.

1953 The application of the Kubelka–Munk theory to the diffuse reflection of light from paper, part 3. Surface reflection and light scattering of paper. *Svensk Papperstidning* 56:607–14.

Stiles, W. S., and G. Wyszecki

1968 Intersections of the spectral reflectance curves of metameric object colors. *Journal of the Optical Society of America* 58:32–40.

Switzer, J. L., and R. C. Switzer

1950 *Daylight Fluorescent Pigment Compositions*. U.S. Patent 2,498,592.

Talsky, G., and M. Ristié-Šolajié

1989 Higher order derivative reflectance spectrophotometry of synthetic organic pigments in artists' paints. *Analytica Chimica Acta* 226:293–304.

Technical Association of the Pulp and Paper Industry (TAPPI)

1992a Method T260 om-91. Test to evaluate the aging properties of bleached chemical pulps. In *Tappi Test Methods*. Atlanta: Technical Association of the Pulp and Paper Industry.

1992b Method T425 om-91. Opacity of paper (15° geometry/diffuse Illuminant A, 89% reflectance backing). In *Tappi Test Methods*. Atlanta: Technical Association of the Pulp and Paper Industry.

1992c Method T452 om-92. Brightness of pulp, paper, and paperboard (directional reflectance at 457 nm). In *Tappi Test Methods*. Atlanta: Technical Association of the Pulp and Paper Industry.

1992d Method T519 om-91. Diffuse opacity of paper (D/0° paper backing). In *Tappi Test Methods*. Atlanta: Technical Association of the Pulp and Paper Industry.

Vagias, A. M.

1982 *Thermoplastic Key Face for Pianos or the Like*. U.S. Patent 4,346,639.

Van den Akker, J. A.

1949 Scattering and absorption of light in paper and other diffusing media. A note on the coefficients of the Kubelka–Munk theory. *Tappi* 32:498–500.

Voedisch, R. W.

1973a Luminescent pigments, organic. In *Pigment Handbook*, ed. T. C. Patton, vol. 1, 891–92. New York: John Wiley and Sons.

1973b Pigmentation of fluorescent paints. In *Pigment Handbook*, ed. T. C. Patton, vol. 2, 143–49. New York: John Wiley and Sons.

Wainwright, I. N., J. M. Taylor, and R. D. Harley

1986 Lead antimonate yellow. In *Artists' Pigments: A Handbook of Their History and Characteristics*, vol. 1, ed. R. L. Feller, 219–54. Washington, D.C.: National Gallery of Art.

Walsh, J. W. T.

1926 The reflection factor of a polished glass surface for diffuse light. Appendix of A. K. Taylor and C. J. W. Grieveson, *The Transmission Factor of Commercial Window Glasses*. Department of Scientific and Industrial Research, Illumination Research Technical Paper No. 2. London: Her Majesty's Stationery Office.

Weingrad, C.

1992 Three-dimensional color: Unlocking the mystery of interference pigments. In *Inksmith*, spring: 9, 11–13. Daniel Smith Catalog of Artists' Materials. Seattle: Daniel Smith. (Color reprints available for a small fee.)

Wyszecki, G.

1963 Proposal for a new color difference formula. *Journal of the Optical Society of America* 53:1318–19.

Wyszecki, G., and W. S. Stiles

1982 *Color Science: Concepts and Methods, Quantitative Data, and Formulae*, 2d ed. New York: John Wiley and Sons.

Index

Note: Letters *f* and *t* following page numbers indicate figures and tables, respectively. Letters CP indicate color plates.

Illustration Credits

The following have generously granted permission to reprint previously published material.

Figure 4.5, 4.24, and color plates 1, 2, and 3: From R. M. Johnston-Feller, "Reflections on the phenomenon of fading,"*Journal of Coatings Technology* 58 (1986).

Figure 4.6: From R. L. Feller, "Studies of the darkening of vermilion by light," *Report and Studies on the History of Art* (1967), National Gallery of Art, Washington, D.C.

Figures 4.8, 4.9, 6.12, and 6.13: From R. L. Feller, "Problems in reflectance spectrophotometry," *IIC 1967 London Conference on Museum Climatology* (1968), International Institute for Conservation of Historic and Artistic Works, London.

Figures 4.10 and 4.11: From R. M. Johnston, "Spectrophotometry for the analysis and description of color," *Journal of Paint Technology* 39 (1967).

Figures 4.14, 4.15, 4.16, and 4.17: From R. M Johnston and R. L. Feller, "Optics of paint films: Glazes and chalking," *Application of Science in Examination of Works of Art* (1967), Museum of Fine Arts, Boston.

Figures 4.20 and 4.21: From W. E. Craker and F. D. Robinson, "The effect of pigment volume concentration and film thickness on the optical properties of surface coatings," *Surface Coatings International* 50 (1967).

Figure 4.26: From V. Buttignol, "Optical Behavior of Iron Oxide Pigments," *Journal of Coatings Technology* 40 (1968).

Figures 5.5, 5.6, and 5.7: From R. M. Johnston and D. Osmer, "Exposure evaluation, part II—Bronzing," *Journal of Coatings Technology* 51 (1979).

Figure 6.11: From F. Grum, "Colorimetry of fluorescent materials," *Optical Radiation Measurements,* vol. 2, *Color Measurement*, ed. F. Grum and C. J. Bartleson; reprinted by permission of Academic Press, New York.

Figures 7.1, 7.2, 7.3, 7.4, 7.5, and 7.6: From R. M. Johnston, "Spectrophotometry for the analysis and description of color," *Journal of Paint Technology* 39 (1967).

Other acknowledgments will be found following figure legends.

About the Author

After graduating from the University of Illinois with a degree in chemistry, Ruth Johnston-Feller spent the early years of her career in industry, conducting research in infrared and ultraviolet spectrometry. With the advent of improved measuring instruments and computing devices that made the serious study of color practical in the late 1950s, she shifted her research to the visible part of the spectrum and to the human response to color, areas in which she had a long-standing interest. She joined the Pittsburgh Plate Glass Company, and under her stewardship the company became the first to use instrumental methods for formulating and controlling color in paint and plastics manufacturing facilities. Later she served as director of application services for the Color Systems Division of Kollmorgen Corporation, creators of computer color-matching programs. Her final industrial experience was with the Ciba-Geigy Corporation, Pigments Division (now Ciba Specialty Chemicals, Colors Division).

While at the Pittsburgh Plate Glass Company, she met Robert L. Feller, who introduced her to art conservation research. After their marriage in 1975, she worked part-time with her husband's group at the Research Center on the Materials of the Artist and Conservator at the Carnegie Mellon Research Institute, Carnegie Mellon University. There she devoted her attention principally to the measurement of color and appearance, and to the study of fading of pigmented and dyed materials.

Long active in many technical societies, Ruth Johnston-Feller authored more than fifty technical publications. In 1985 she presented the Mattiello Memorial Lecture of the Federation of Societies for Coatings Technology, an honor given for her distinguished contributions to the coatings industry. She received numerous awards in recognition of her work, including the MacBeth Award, presented by the Inter-Society Color Council for outstanding contributions to the science of color. She died in 2000.